The impact of climate, vegetation and land-use changes on fire regimes during the Holocene

Doctor of Philosophy

School of Archaeology, Geography and Environmental Science

Luke Sweeney

September 2024

Declaration

I confirm that this is my own work and the use of all material from other sources has been properly and fully acknowledged.

Signed

Luke Sweeney

Abstract

The investigation of palaeofire provides the basis for testing the reliability of recognised controls on fire in the present day, but in environmental and social conditions that differ markedly. Whilst present day analysis can make use of comprehensive data at high spatial resolution, palaeodata enables the investigation of controls both spatially and temporally, on time scales that are relevant for longer term processes. Although there are exceptions, the majority of palaeofire research has tended to analyse relationships by visually assessing the synchronicity of time series, and with a focus on a single or limited selection of controls. In this thesis, a number of statistical approaches are tested to identify relationships between palaeofire and its drivers, making use of diverse data proxies.

The relationship between people and palaeofire was first investigated in Iberia during the Holocene. Results from superposed epoch analysis (SEA) show no clear relationship between periods of high population growth or on the time-transgressive spread of farming and fire. To extend this research to the European scale, and to ensure that controls representing humans, vegetation and climate were included in a holistic analysis of palaeofire at a site-level, a new statistical method, with broad-scale applicability, was developed to reconstruct tree cover using sedimentary and modern pollen data. At an aggregate level, the resulting reconstructions broadly matched those published in the literature. These reconstructions were then included within cross-cutting analyses using regression techniques, Granger causality and SEA. Limited evidence of consistent relationships were found at the scale of analysis, emphasising the challenges of drawing regional-level conclusions, and helping to explain contrasting findings from the research literature.

Overall, despite the challenges associated with palaeodata, this research highlights the need for statistically robust, multi-variable analyses of the drivers of palaeofire to improve our understanding of fire in the past, present and future.

Impact statement

- The second chapter of this thesis is published as:

Sweeney, L. F., Harrison, S. P., & Vander Linden, M.: Assessing anthropogenic influence on fire history during the Holocene in the Iberian Peninsula. *Quaternary Science Reviews*, *287*, 107562. https://doi.org/10.1016/j.quascirev.2022.107562, 2022

- The third chapter is a paper currently under (public) review. The version within this thesis is an amended version of the submitted article, taking into account reviewer and community comments. The preprint, reviewer comments and responses are published as:

Sweeney, L. F., Harrison, S. P., and Vander Linden, M.: European forest cover during the Holocene reconstructed from pollen records, EGUsphere [preprint], https://doi.org/10.5194/egusphere-2024-1523, 2024.

- Part of this research led to the publication of the following open-access datasets:

Sweeney, L. F., Harrison, S. P. and Vander Linden, M.: Holocene archaeological radiocarbon data of the Iberian Peninsula. University of Reading. Dataset. https://doi.org/10.17864/1947.000340, 2021.

Harrison, S. P., Villegas-Diaz, R., Lincoln, P., Kesner, D., Cruz-Silva, E., **Sweeney, L. F.**, Shen, Y. and Gallagher, D.: The Reading Palaeofire Database v1b: an expanded global resource to document changes in fire regimes from sedimentary charcoal records. University of Reading. Dataset. https://doi.org/10.17864/1947.000345, 2022.

Harrison, S. P., Shen, Y. and **Sweeney, L. F.**: Pollen data and charcoal data of the Iberian Peninsula (version 3). University of Reading. Dataset. https://doi.org/10.17864/1947.000369, 2022.

Harrison, S. P., Egbudom, M.-A., Liu, M., Cruz-Silva, E. and **Sweeney, L. F.**: The SPECIAL EPD Database: an expanded resource to document changes in vegetation and climate from pollen records from Europe, the Middle East and western Eurasia. University of Reading. Dataset. https://doi.org/10.17864/1947.001295, 2024.

Acknowledgements

I would like to thank my primary supervisor Sandy P. Harrison for her constant support throughout these past 4 years. The depth and breadth of your subject knowledge really is inspiring, and your advice and guidance has helped me to shape my development as a more objective and thorough researcher. I would also like to thank my second supervisor Marc Vander Linden, whose enthusiasm and encouragement for my work has really helped maintain my focus and motivation. Thank you also for being a source of knowledge regarding archaeology and for helping me to think creatively about how to combine the different fields of study within my research.

I would also like to thank the many members of the SPECIAL research group whose positive feedback and support has been invaluable. In particular, I would like to thank Roberto and Mary-Anne for your important assistance with data and programming advice. I would also like to thank the other members of the Leverhulme Centre for Wildfires, Environment and Society, whose incredible and varied work is, and continues to be, a source of inspiration.

I gratefully acknowledge financial support from the Leverhulme Centre for Wildfires, Environment and Society and the University of Reading.

Finally, I would like to thank my family. Casper and Joe, your hugs and smiles have kept me grounded, and I'm sorry if I've been less available than I might have otherwise been during the past few years. And Els, thank you for always being there for me, believing in me and for putting up with my weekend (and sometime-holiday) work schedule. I couldn't have done this without you.

Contents

List of Figures

List of Tables

List of Abbreviations

AIC	Akaike Information Criteria
α	ratio of actual to equilibrium evapotranspiration (representing plant available moisture)
ANOVA	Analysis of Variance
AP	arboreal pollen
ARIMA	autoregressive integrated moving average
BIC	Bayesian information criterion
cal. BP	calibrated years before the present (1950)
DVGM	dynamic global vegetation model
FS	fall speed (of pollen)
fxTWA-PLS	frequency-adjusted tolerance weighted weighted averaging partial least squares
GAM	generalised additive model
GDD_0	growing degree days above 0ºC
GPP	gross primary production
ICC	intraclass correlation
KDE	Kernel Density Estimation
LM	linear model
LMM	linear mixed model
LOESS	locally estimated scatterplot smoothing
LOOCV	leave one out cross validation
LOVE	Local Vegetation Estimates
LRA	landscape reconstruction algorithm
MAE	mean absolute error
MAT	Modern Analogue Technique
MCMC	Markov chain Monte Carlo
MTCO	mean temperature of the coldest month
MTWA	mean temperature of the warmest month
NPP	net primary production
PDF	probability distribution function
PFT	plant functional type
REVEALS	Regional Estimates of Vegetation Abundance from Large Sites
RMSE	root mean squared error

roc	rate of change
RPD	Reading Palaeofire Database
RPP	relative pollen productivity
SEA	Superposed Epoch Analysis
SI	Shannon Index
SP	shrub pollen
SPD	summed probability distribution
TTPS	Total Terrestrial Pollen Sum
VAR	vector autoregressive models
VIF	variance inflation factor
WA-PLS	Weighted averaging partial least squares

1. Introduction

1.1. Overview and thesis structure

The overall goal of this thesis is to test the strength of the relationships between fire and its drivers over the Holocene, particularly considering the uncertainties regarding the role of people in influencing Holocene fire in Europe during the Holocene. Published sedimentary charcoal and pollen records, and archaeological radiocarbon datasets have been used to reconstruct palaeofire, tree cover and infer population change respectively, and to analyse the relationships between these variables. The focus of the research is on Europe to take advantage of the fact that this is a region with relatively large amounts of high quality data. Sedimentary charcoal and pollen records have been used as they provide by the far the best spatiotemporal coverage of datatypes that can be used to reconstruct fire and tree cover. Archaeological radiocarbon data, rather than modelled data, was used to infer population change through time to help identify variable patterns of change throughout the Holocene.

This introductory chapter summarises the importance of wildfire in the earth system (1.2), and the challenges associated with identifying the variable roles of different drivers in space and time in the modern day (1.3). Sub-section 1.4 highlights recent evidence for changes in fire and predictions for fire based on our current understanding. Sub-section 1.5 introduces the potential role for palaeodata to enhance the understanding of drivers of fire, summarising some of the different findings from the research literature. Finally, the main approaches to reconstructing palaeofire and its drivers are discussed in sub-section 1.6.

In addition to this introductory chapter, the thesis is a combination of two papers, formatted in the style of the journal to which they were submitted, and a third chapter, which tests different statistical approaches to investigate palaeofire.

Chapter 2 consists of Sweeney et al. (2022) “Assessing anthropogenic influence on fire history during the Holocene in the Iberian Peninsula”. This paper examines the change in fire during the Holocene in Iberia using sedimentary charcoal records, and related observed changes to inferred population changes reconstructed from archaeological radiocarbon data using a Superposed Epoch Analysis (SEA) framework. The objectives of the paper were to test whether a human signal could be observed within the fire record, based on identified periods of population growth and the time transgressive spread agriculture in the region. Iberia provided a good case study to test this approach, given the availability of data, and the contrasting findings from the literature regarding the role of people in influencing palaeofire there.

Chapter 3 consists of an article currently under review and available as a preprint: “European tree cover during the Holocene reconstructed from pollen records”. The version included within the thesis is an updated version of the submitted article, amended to reflect responses to viewable referee and community comments. This paper introduces a simple calibration approach to reconstruct forest cover, making use of modern maps of tree cover and modern pollen data to build a regression-based model, subsequently applied to fossil pollen data. The basis for this work was the need to reconstruct tree cover at a site-level, using data with up-to-date age models covering the whole of Europe, at a temporal resolution necessary for later composite analysis with climate, population and fire reconstructions. The chapter provides a new method approach builds an alternative method for tree cover reconstruction that could be applied globally and side-steps some of the issues associated with other reconstruction techniques.

In Chapter 4, European-level and sub-regional fire is reconstructed based on sedimentary charcoal data and population change inferred based on archaeological radiocarbon data. Together with reconstructions of tree cover from Chapter 3 and climate (Tang et al., in prep), changes in fire are compared to the variables in concert using different analytical approaches. Firstly, a series of regression models are run, including overlapping spatiotemporal data between fire, tree cover and climate reconstructions. Then time series analysis is performed, running tests of Granger causality at the sub-regional level, including inferred population change, and carrying out SEA analysis based on identified population boom and bust events, also at the sub-regional level.

In the final Chapter (5), the overall implications of the findings are assessed suggestions made for future work.

1.2. The role of fire in the earth system

Although wildfire is typically associated with its destructive potential, especially in relation to direct effects on people (e.g. Paveglio et al., 2011; Doerr and Santín, 2016), fire plays an important role in the earth system. The most recent estimates from the Global Fire Emissions Database (GFED5) covering the period 2001 to 2020 suggests around 774 million hectares per year (Mhayr^{-1}), or 6% of the (non-ice) global land surface burns annually (Chen et al., 2023). This masks substantial spatial variation however, with sub-Saharan Africa accounting for 63% of annual global landscape burning and the USA, Canada, Europe and the Middle East accounting for less than 1% each (Fig.1.1) (Chen et al., 2023). Similarly, these values mask considerable temporal variability: fire return times can vary between 1 to 2 years for some grassland dominated biomes to hundreds of years for boreal forests (Harrison et al., 2021).

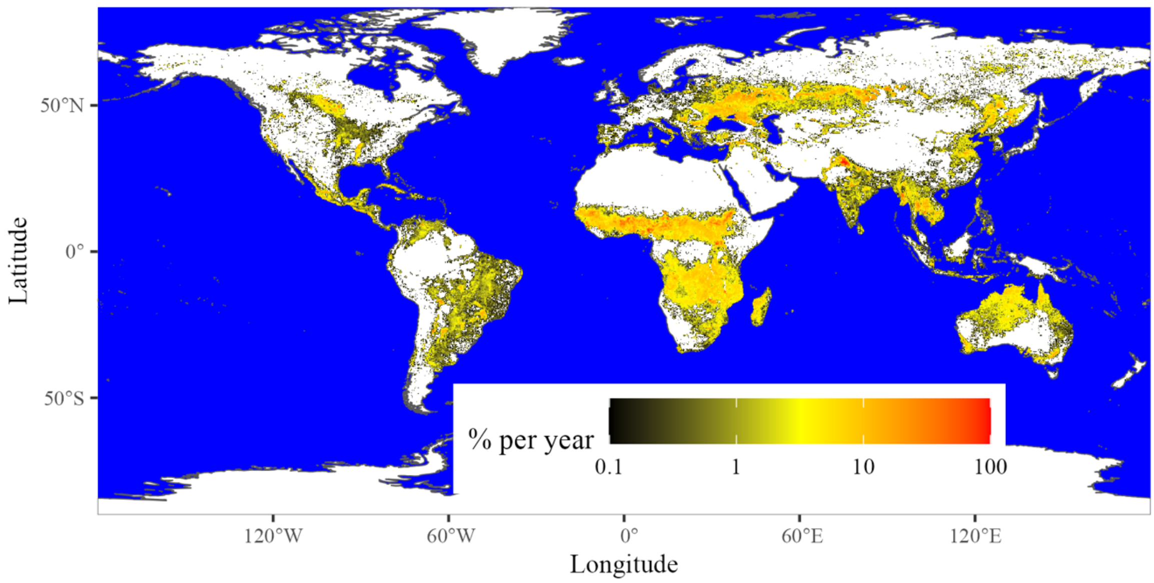

Figure 1.1: Mean annual GFED5 burned area, as a percentage of the burnable land area, from 2001 to 2020. Adapted from Chen et al. (2023; Fig. 4)

Emissions from fire affect the carbon balance, atmospheric conditions, the hydrological cycle and surface albedo (Bowman et al., 2009; Liu et al., 2014). Fire converts stored carbon and nutrients in vegetation into trace gases and aerosols, and through incomplete combustion into charcoal (Ward et al., 2012), acting to increase the natural cycle of primary production and respiration (Bowman et al., 2009). Changes in vegetation resulting from large wildfires can affect the hydrological behaviour of affected catchments, increasing run-off (e.g. Versini et al., 2013; Wine and Cadol, 2016; Soulis et al., 2021) and reducing evapotranspiration rates in the immediate aftermath (e.g. Kang et al., 2006; Soulis et al., 2021). Deposition of black carbon emissions from wildfire onto ice and snow reduces surface albedo (Conway et al., 1996; Aubry-Wake et al., 2022), but overall impacts on surface albedo is dependent on vegetation type burned and the time since wildfire (Gatebe et al., 2014; Quintano et al., 2019; Linares and Ni-Meister, 2024). Although fire may have a detrimental impact on most ecosystem services, for example negatively affecting water and air quality and erosion control (Pereira et al., 2021; Roces-Díaz et al., 2022), fire can also have benefits, in terms of reducing the chance of catastrophic larger fires, regulation of pest populations (Pausas and Keeley, 2019; Pereira et al., 2021), and in terms of water provision (Roces-Díaz et al., 2022).

At a landscape-scale, fire has an important role in influencing vegetation patterns. Simulations of global vegetation patterns in the absence of fire suggest a general increase in tree cover (Bond et al., 2005; Martin Calvo and Prentice, 2015; Lasslop et al., 2020; Harrison et al., 2021), particularly in savanna regions (Harrison et al., 2021). In savannas, fire has a key role in preventing the spread of closed canopy forest tree species (Bond, 2008; Staver et al., 2011; D'Onofrio et al., 2018), which has been demonstrated experimentally (e.g. Swaine et al., 1992; Higgins et al., 2007; Scott et al., 2012; Deklerck et al., 2019; Starns et al., 2020). Similarly, frequent fire has been associated with the maintenance of shrubland in Patagonia (Paritsis et al., 2015) and of open grasslands in the North American Great Plains (Ratajczak et al., 2014).

In ecosystems subject to frequent fire, plants have evolved adaptations to fire. These adaptations vary with the frequency and type of fire. At a species-level, these enhance individual survivability (*resistance*) or community persistence (*resilience*) (Harrison et al., 2021). Species that show resistance to fire have traits such as thick or fast-growing bark, which serve to protect the plant when fire occurs (Pausas, 2015; Charles-Dominique et al., 2017) or the capacity to recover via re-sprouting following fire (Clarke et al., 2013; Pausas et al., 2016). Fire resilient species have traits that enable post-fire recruitment, such as fire-mediated serotiny, post-fire flowering and post-fire seed germination (Lamont and Downes, 2011; Lamont et al., 2019). Species flammability has also been identified as a potentially adaptive trait (Bond and Midgley, 1995; Schwilk and Ackerly, 2001; although see Midgley, 2013), with different aspects of flammability – non-flammability, hot flammability and fast flammability - interacting with other species traits to enhance survivability or persistence (Pausas et al., 2017). The prevalence of species traits is closely related to fire characteristics of the fire-prone ecosystems, with for example, re-sprouting associated with high frequency fires and high intensity crown fires (Shen et al., 2023), and thick bark associated with frequent surface fires (Pausas, 2015). As species are adapted to certain fire characteristics, rather than fire in general (Keeley et al., 2011), changes in fire characteristics then have implications for vegetation community composition if species are not able to respond to these changes (Coop et al., 2020; Tubbesing et al., 2020; Falk et al., 2022). For example, the species composition in conifer forests in some North American regions has been affected by increased fire frequency and severity as a result in recent changes in climate (Cassell et al., 2019; Buma et al., 2022; Dawe et al., 2022). Similarly, although fire has been linked to positive effects on biodiversity in some regions (He et al., 2019; Jones and Tingley, 2022), changes in fire can also threaten species diversity (Bowman and Murphy, 2010; Kelly et al., 2020).

Fire is multifaceted, with many different characteristics including frequency, size, type (crown, surface or ground), power and seasonality (Bowman et al., 2009; Archibald et al., 2018). Typically, these predominant characteristics are conceptualised as the fire regime in an area (Bond and Keeley, 2005; Krebs et al., 2010; Kelly et al., 2023), which illustrate where, when and which types of fire occur (Krebs et al., 2010). Fire regime characteristics can interact, with for example, fire intensity generally constrained when fires are frequent and fire size limited for the longest fire seasons (Archibald et al., 2013). Based on grouping of fire characteristics and the constraints associated with possible combinations of fire regime elements, Archibald et al. (2013) defined five “pyromes”, associated with burned area, fire frequency, fire size, fire intensity and fire season length (Fig. 1.2). Four of these pyromes describe the distinction between crown, litter and grass-fuelled fires, with a fifth primarily associated with human activities such as agriculture and deforestation (Archibald et al., 2013).

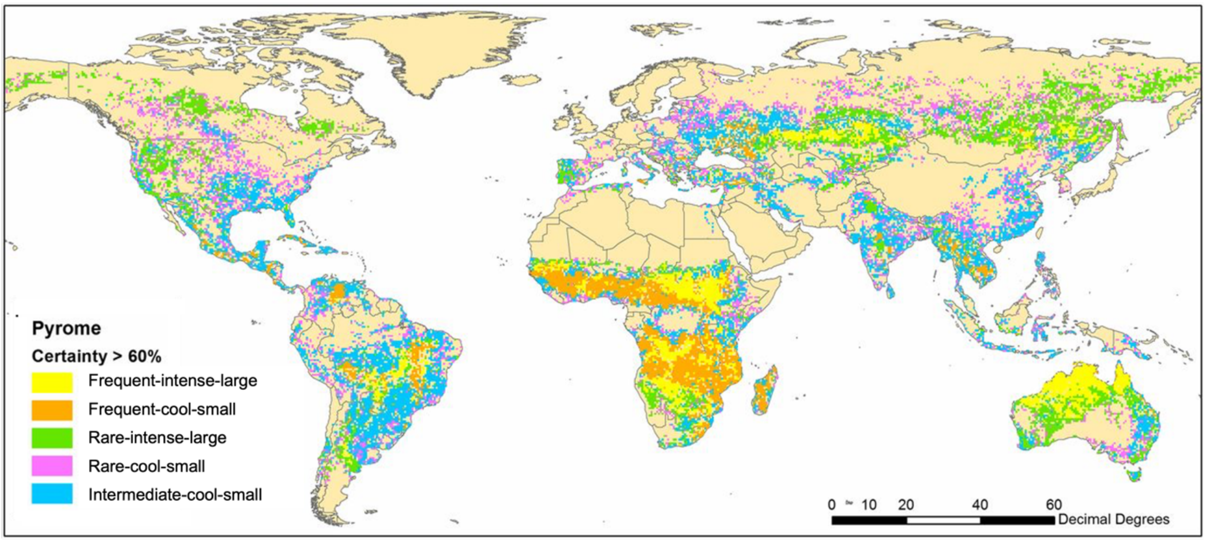

Figure 1.2: Global fire pyromes as defined by Archibald et al. (2013), showing regions with similar fire frequencies, intensities, size, burned areas and fire season lengths. Adapted from Archibald et al. (2013: Fig. 2).

Human involvement in fire is itself varied, affecting different fire regime elements, including fire ignition frequency, landscape transformation affecting fuel type and availability, and direct management of fires (Bowman et al., 2011).

1.3. Drivers of fire

Fire occurs when there is a suitable co-occurrence of various conditions: an ignition source, availability and continuity of material to burn, sufficient flammability of that material and appropriate weather conditions (Pausas and Keeley, 2021). Weather conditions serve to reduce the required thresholds of each of the other conditions, such that, for example, strong winds increase the likelihood of fire given similar conditions (Pausas and Keeley, 2021). Each of these controls on fire is in turn driven by a combination of three factors - climate, vegetation and people – which interact across time and space. Modern satellite observational data has been used to model the relationships between fire and multiple predictors (e.g. Krawchuk et al., 2009; Bistinas et al., 2014; Forkel et al., 2019; Haas et al., 2022), helping to tease out the relationships between fire and its key drivers. Understanding the relationship between fire and its drivers is vital for predictions of future patterns of wildfire.

1.3.1. Climate

At short time scales, the prevailing climate affects fire weather. Meteorological conditions in terms of temperatures, humidity, moisture and wind (influencing evapotranspiration rates) impact fuel dryness, affecting the likelihood of fire (Pausas and Keeley, 2021). High wind speeds increase the chance of successful ignition due to supply of oxygen, and change flame properties and enhance ember dispersal, affecting fire spread rate and allowing fires to bridge fuel discontinuities (Pausas and Keeley, 2021). Natural sources of ignition are almost exclusively lightning. Although the estimated importance of lightning compared to anthropogenic ignitions varies by region, lightning has been estimated to account for 40% of fire counts in North American boreal regions between 2000-2006 (Peterson et al., 2010), 42.1% of known ignition sources in California between 2012 and 2018 (Hantson et al., 2022) and 77% of extratropical burned area in intact forests between 2001 and 2015 (Janssen et al., 2023). Drought and extreme temperatures during the fire season have been shown to increase wildfire in sub-tropical and temperate areas (China (e.g. Yin et al., 2024); the western USA (e.g. Westerling and Swetnam, 2003; Chen, 2022; Richardson et al., 2022); the Mediterranean (e.g. Dimitrakopoulos et al., 2011; Ruffault et al., 2018); and southern Australia (e.g. Mariani et al., 2016; Richardson et al., 2022), and to cause increases in rare wildfires in the Amazon region (e.g. Silva Junior et al., 2019).

As well as fire weather, climate also influences the length and severity of the fire season. The seasonality of rainfall and temperatures influence fire activity, with increased rainfall and temperature seasonality associated with reduced fuel moisture during the dry season and via climate impacts on vegetation, greater fuel growth in the wet season (Holden et al., 2018; Kuhn-Régnier et al., 2021; Swain, 2021). At global scale, increases in monthly maximum number of dry days are associated with increases in burned area (Bistinas et al., 2014; Haas et al., 2022), with antecedent vegetation growth also influencing burned area (Kuhn-Régnier et al., 2021; Haas et al., 2022). Inter-annual variability of rainfall also has implications for wildfires, with around of a third of inter-annual variability in burned area explained by climate variability globally, a relationship which becomes stronger in areas where fire is typically moisture limited (Abatzoglou et al., 2018). In many cases, periodic drought and increasing wildfire is linked to El Niño–Southern Oscillation (e.g. Westerling and Swetnam, 2003; Dong et al., 2021; Fang et al., 2021).

Climate also has in important influence on fuel availability, both in terms of vegetation growth (see 1.3.2. *Vegetation*) and in relation to species extent and landscape vegetation composition (see section 1.3.4. *Relationships between drivers and between drivers and fire*).

1.3.2. Vegetation

Vegetation influences fire in terms of the availability of fuel to burn, the characteristics of that fuel in terms of its flammability, and in relation to the connectivity of the fuel and the ability of fire to spread.

Evidence from modelling studies based on satellite data highlight gross or net primary production (GPP/NPP) as key factors in determining global burned area (Bistinas et al., 2014; Forkel et al., 2019; Haas et al., 2022). As well as the total quantity of fuel, which is in part determined by climate factors, the seasonal production of fuel has also been identified as a key factor for explaining burned area, with increased seasonality (allied with underlying climate conditions) associated with increased burning (Krawchuk and Moritz, 2011; Forkel et al., 2019; Kuhn-Régnier et al., 2021; Haas et al., 2022). Fuel limitation, rather than fuel condition, has been identified as the key constraint to fire in some areas, particularly areas dominated by xeric shrublands and some savanna or grassland systems (Krawchuk and Moritz, 2011; Alvarado et al., 2020).

The pre-dominant plant functional types (PFTs) are important in defining the fire regime in an area. Generally, increasing grass cover is associated with increases in burned area at global level (Bistinas et al., 2014; Haas et al., 2022), and to increases in fire frequency (Archibald et al., 2013). Changes in vegetation, for example in terms of the spread of invasive species, can affect fire regimes (Brooks et al., 2006; Taylor et al., 2017; Fusco et al., 2019). At species level, live leaf traits such as specific leaf area and leaf surface to volume ratio have been positively associated with ignition (Popović et al., 2021). Likewise, leaf litter characteristics have a role in determining fuel flammability, with morphological traits such as higher specific leaf area and higher leaf curl associated with shorter burn duration and increased flame spread rates (Burton et al., 2021). Different species leaf traits can also help explain whether leaf litter rots quickly or is available as fuel (Grootemaat et al., 2015)

The physical structure of the landscape affects fire regimes, with landscape connectivity having important implications for fire spread. Within savanna ecosystems, the relative connectivity of open spaces is linked to an abrupt change in fire frequency (van Nes et al., 2018), and in northeastern Spain, forest connectivity has been linked to increases in burnt area up to a specific threshold, under regular fire weather conditions (Duane et al., 2021). However, the relationship between landscape fragmentation and fire is dependent on the underlying ecosystem (Harrison et al., 2021). In ecosystems adapted to fire, human driven fragmentation decreases burned area through reduced connectivity, whereas landscape fragmentation promotes fire in non-fire adapted ecosystems, based on creating ignitable spaces (Harrison et al., 2021).

1.3.3. People

Humans influence fire directly in terms of ignitions and fire management practices. Although the share of natural and anthropogenic ignitions varies globally and estimates vary, and in many cases due to data limitations the source of ignitions is unknown (Jones et al., 2022), anthropogenic ignitions can account for the majority registered fires in some areas. For example, anthropogenic ignitions are estimated to account for 84% of fires in the USA for the past 20 years (Balch et al., 2017). In Europe, more than 96% of burned area has a human origin (Dijkstra et al., 2022). However, the impact of anthropogenic ignitions on fire regimes is spatially varied. Despite the high proportion of anthropogenic ignitions in the USA, only 44% of burned area is associated with human ignition, as a substantially greater share of these ignitions occur during moister conditions than natural, lightning induced fires (Balch et al., 2017). Human ignitions in some areas may also replace lightning-based ignitions that may have occurred (Keeley et al., 1999). Nevertheless, human ignitions have been associated with an increase in large and extreme fires in the USA (Nagy et al., 2018; Hantson et al., 2022), and with expansion of the fire season (Balch et al., 2017).

Anthropogenic ignitions are more likely to occur near areas of high population or near to infrastructure such as roads (e.g. Syphard et al., 2008; Collins et al., 2015; Syphard and Keeley, 2015; Clarke et al., 2019), and rural population density impacts the probability of fire occurrence more generally (Keeping et al., 2024). Anthropogenic ignitions can take many forms and can be accidental or purposeful. Accidental ignitions include industrial accident, such as powerline failure or mechanical sparks, or negligent behaviour such as escape from campfire, cigarette disposal or fireworks (Ganteaume and Syphard, 2018). Aside from arson, purposeful ignitions also include fire set for the management of habitat, with, for example, prescribed burning in Scottish heathland to encourage red grouse habitat for hunting purposes (Davies et al., 2008) or in the control of invasive weeds or pests (DiTomaso et al., 2006; te Beest et al., 2012). Prescribed burning is also often used as a tool to reduce fuel build up and limit hazardous fires and reduce fire frequency (Penman et al., 2011; Morgan et al., 2020; Santos et al., 2021). In addition, small-scale burning is used for agricultural purposes, in terms of clearing crop residue (Jethva et al., 2018; Nair et al., 2020) - globally cropland burning is estimated to constitute approximately the same burned area as total forest burned area (Chen et al., 2023) - and in terms of traditional fire usage such as swidden agriculture (Fujisaka et al., 1996; Huffman, 2013; Li et al., 2014). Finally, fire is also used in some regions for broad land use change purposes, particularly deforestation in tropical areas (Alencar et al., 2015; Barlow et al., 2020; Brando et al., 2020).

Apart from ignitions associated with prescribed burning, fire management activity is designed to change the likelihood of fire, alter fire extent and type, or more directly extinguish fires when they occur. Fire suppression continues to be the main source of fire management in many areas (Moreira et al., 2020), despite the impacts that this may have on subsequent extreme fires risk due to fuel build up in fuel limited areas (Arno and Brown, 1991; Keeley et al., 1999; Steel et al., 2015; Moreira et al., 2020; Kreider et al., 2024). Other management practices, such as thinning to reduce fuel load, are intended to reduce fire severity; some evidence supporting this shows this is effective (Brodie et al., 2024), but this may depend on the amount of thinning and site conditions (Banerjee, 2020). Herbivory has also been identified as a fire management tool through reduction in fuel load and trampling (Kramer et al., 2003; Nader et al., 2007; Neidermeier et al., 2023) and has been recommended as an approach to reduce wildfire risk in some parts of Europe (Neidermeier et al., 2023).

Humans alter fire regimes indirectly through landscape alteration, affecting the type, continuity and quantity of fuel. In the modern day, the expansion of human activities into spatially contiguous environments, by converting landscapes to agriculture, forest logging, the introduction of roads and the expansion of settlements, leads to landscape fragmentation, with contrasting implications for wildfire driven by whether the underlying environment is already fire-prone (Harrison et al., 2021). In fire-prone environments, fragmentation limits fire by generating artificial fuel breaks and impeding its spread; this impact of land conversion has been associated with reductions in fire in the 20th century in many regions (Marlon et al., 2008), and to reductions in recent decades in sub-Saharan Africa through conversion of savanna into croplands (Andela and van der Werf, 2014). At the same time, human activity increases access to the environment, introducing fire management practices to previously remote landscapes but also exposing the environment to anthropogenic ignitions. Whilst fragmentation can lead to reduced wildfire in these regions, the opening of environments where fires were previously rare provides the opportunity for fuel drying and increasing wind strength, potentially exposing these environments to fire (e.g. Alencar et al., 2015; Silvério et al., 2019; Silva-Junior et al., 2022). Agriculture also impacts the quantity of fuel in rangelands through grazing, potentially impacting wildfire burn probability (Davies et al., 2010; Siegel et al., 2022). Finally, the human introduction of invasive species has implications for fuel continuity, type and quantity. For example, at high densities, the spread of *Pinus contorta* in Patagonia and New Zealand have been associated with increased fuel load (Taylor et al., 2017), and the spread of invasive grasses across the USA have increased fire occurrence and frequency (Fusco et al., 2019).

1.3.4. Relationships between drivers and between drivers and fire

Disentangling the role that individual factors play in driving wildfire is complicated by the different effects that they can have on different aspects of the fire regime. At a global level, Haas et al. (2020) showed that satellite observations of burned area, fire intensity and fire size were controlled by different factors, and that sometimes the direction of influence of a factor varied by fire property. The nature of these relationships is also sometimes spatially differentiated, for example in terms of the influence that landscape fragmentation has on fire in different ecosystems. In part, this is a reflection of different interactions between controls, and feedbacks between fire and the controls at differing spatial and temporal scales.

For example, climate is instrumental in influencing patterns of vegetation, with subsequent influences on fire. Climate extremes can represent boundary conditions where no fire is possible due to insufficient fuel, where moisture or low temperatures for example prohibit vegetation growth (Parisien and Moritz, 2009). But vegetation also affects climate via physical changes to albedo, roughness and water conductivity, and via impacts on the composition of atmospheric gases in the atmosphere (Brovkin, 2002). The nature of these impacts on climate are not straightforward, however. For instance, although forests act as a carbon sink, reducing the impacts of CO_2 on warming, forest cover typically decreases surface albedo compared to more open environments, suggesting in increase in warming due to radiative forcing (e.g. Betts, 2000; Kirschbaum et al., 2011; Bright et al., 2015). Anthropogenic climate change has clear implications for global fires. Future predictions of fires are largely determined by consideration of the impacts of climate change on fire weather and temperature/rainfall patterns, and subsequent changes on vegetation. At the same time, for most of human history, climatic conditions have directly determined human population sizes through impacts on environmental carrying capacity (e.g. Kelly et al., 2013; Manning and Timpson, 2014; Bevan et al., 2017; Palmisano et al., 2021).

At evolutionary times scales, fire has influenced the development of plant traits designed to enable survival, reproduction and competitive advantage in fire prone environments (Keeley et al., 2011). The distribution of plant traits in a given environment is a reflection of this evolutionary past, with, for example, thick bark evolved in tree species such as *P. ponderosa*, which is subject to frequent surface fires in the western USA (Pausas, 2015). In turn, plant distribution influences fire regimes via the quantity and flammability of fuel, and through impacts of climate factors on fire weather and longer-term climate process. At shorter timescales, these fires regimes feedback to species distributions to reinforce system stability. This vegetation-fire feedback can be seen at the species and community level. At the species level, some plants are adapted to certain fire regime. It is therefore beneficial to these plants if that regime is more-or-less stable. At the community level, there are likewise fire-vegetation feedbacks that serve to maintain plant type communities. One of the most studied fire feedbacks relates to the vegetation-fire feedback in tropical savanna ecosystems. In some savanna ecosystems, productive grass growth during the rainy season and subsequent drying of this growth during the dry season combine to provide sufficient dry material for fire. Ground fire then acts to remove tree seedlings and saplings, providing space for future grass growth and maintaining the grass and savanna tree structure (Beckage et al., 2011; Staver et al., 2011; Staver and Levin, 2012;

Accatino and De Michele, 2013). In contrast, the relationship between fuel availability and fire in North American boreal systems is a negative feedback, with fire reducing the prospect of future fires until vegetation has recovered (Heon et al., 2014; Parisien et al., 2014). Changes in fire, through changes in climate or through human action such as fire suppression, therefore act to influence plant species and communities, and can potentially influence fire regimes through modifications in fuel and climate.

Anthropogenic climate change influences global fire weather, as well as having direct influences on fuel availability and flammability. Subsequent changes to fire can in turn alter atmospheric properties, through the short-term impacts of changes to greenhouse gases, albedo and aerosols, and over the long term through changes to carbon burial rates and oxygen concentrations as a result of changes in terrestrial NPP (Archibald et al., 2018). In turn, these changes to atmospheric properties can further impact global fire weather and climate potentially generating a positive feedback loop between fires and climate change in these regions (Janssen et al., 2023). The feedback between fire and climate exemplifies the different spatial and temporal relationships between drivers, with relatively localised and immediate fire affecting longer term and global processes.

Although feedbacks between direct human activities and fire are not systemic in the same way as vegetation-fire and climate-fire feedbacks, there are examples where human activities and fire feedback to each other. For example, fire suppression potentially increases the likelihood of extreme wildfires by increasing future fuel loads (Arno and Brown, 1991; Keeley et al., 1999; Steel et al., 2015; Moreira et al., 2020; Kreider et al., 2024). Increasingly extreme wildfires in turn lead to enhanced suppression effort, given the potential increases in damages associated with larger fires, with subsequent impacts on the extreme fire risk. This feedback is particularly pervasive because suppression effort can only be focussed on suppressing smaller fires, given the relatively limited ability of wildfire management to tackle extreme fire when it does occur (Kreider et al., 2024).

These interlinkages, together with the differing impacts of the individual drivers on fire, imply a need take into account the various factors driving fire in concert.

1.4. Changing fire and predictions for the future

At a global level, satellite observations indicate a general reduction in burned area over the past 30 years (Andela et al., 2017; Chen et al., 2023; Fernández-García and Alonso-González, 2023). However, these reductions are primarily associated with reduced savanna and grassland burning in sub-Saharan Africa, which dominates overall burned area (Andela et al., 2017; Chen et al., 2023;

Fernández-García and Alonso-González, 2023; Zubkova et al., 2023). Declines in African burned area have been attributed to cropland expansion (Andela and van der Werf, 2014; Andela et al., 2017), although there is uncertainty regarding this conclusion given the sensitivity of associated data (Zubkova et al., 2023). In contrast, burned area is increasing in some areas, e.g. boreal Canada and eastern Canada, but the overall share from these regions to global burning is relatively low (Chen et al., 2023). The area burnt from stand replacing forest fires increased between 2001 and 2019 (Tyukavina et al., 2022), and the frequency of extreme wildfires is increasing in boreal and temperate forests (Cunningham et al., 2024). Burn severity, closely associated with fire intensity, increased globally between 2003 and 2019, with areas experiencing significant increases in burn severity outnumbering those with significant decreases (Fernández-García and Alonso-González, 2023).

The spatial heterogeneity in changes to burned area is a partial reflection of competing influences. For example, declines in savanna burned area and number of fires in the Serengeti-Mara system in Tanzania/Kenya between 2001 and 2014 have been associated with increases in livestock farming, changing the quantity of fuel available to burn (Probert et al., 2019). Similarly, the decline in burned area in northern sub-Saharan Africa more generally between 2001 and 2012 has been primarily associated with cropland expansion (Andela and van der Werf, 2014). In contrast, increases in forest burned area, increased likelihood of extreme fires and fire frequency have been linked with anthropogenic climate changes in several regions. For example, warming driven increases in vapour pressure deficit, enhancing fuel drying, has been associated with increases in forest burned area in California between 1972 and 2018 (Williams et al., 2019). Similarly, increases in burned area, reduction in time since last fire and increase in number of megafire years have been observed in east and southern Australia, associated with increasing severity of fire weather conditions and drought occurrence (Canadell et al., 2021; Collins et al., 2022). In Canada, increases in burned area and in large fires, and an earlier fire season have likewise been associated with changes in climate (Hanes et al., 2019). This contrast between increases and decreases in burned area and intensity, and the relative role of climate and humans is not ubiquitous, however. For example, increases in forest fire intensity have resulted from agricultural abandonment in Iberia (Mantero et al., 2020). Likewise, increases in human ignitions and fire suppression have been linked to increased fire season length and wildfire severity in the USA (Steel et al., 2015; Balch et al., 2017; Hantson et al., 2022; Kreider et al., 2024). In the case of increased burn severity in the USA, human actions can act to reinforce changes to climate (which themselves are anthropogenic in origin). Similarly, the impacts of drought and deforestation in the Amazon region act in concert to increase wildfire frequency and burned area (Alencar et al., 2015; Silva Junior et al., 2019; Silveira et al., 2020; Silva-Junior et al., 2022).

Understanding how fire will change in the future has important policy implications. Anthropogenic climate driven changes might be expected to persist, given the predicted 3ºC increase in temperatures by 2100 based on current policies (UNEP, 2023). However, this implies that changes in climate will continue to have the same impacts on fire weather, temperatures and precipitation, only more so, despite the potential systemic feedbacks that exist. For instance, burned area is predicted to increase in the western USA by between 50 to 100% in the period 2020 to 2050, compared to observed burned area between 1990 and 2020, because of increasing fuel aridity (Abatzoglou et al., 2021). Similarly, the number of days with hazardous fire weather is projected to increase in Australia, based on the ensemble outputs of climate projections (Dowdy, 2020). Predictions for fire are heavily dependent on expectations for climate change, which themselves reflect emissions scenarios.

One approach to generate estimates of future fire is to use dynamic global vegetation models (DVGMs), which enable the modelling of the biophysical relationships between fire and vegetation based on climate inputs. The feedbacks between fire and climate can also be included in via the inclusion of atmospheric and climate models, in an earth system model framework (Hantson et al., 2016). The variety of different fire-enabled DVGMs, and the associated outputs, reflect both the complexity of the relationships and the different fire processes and impacts of fire included within each (Hantson et al., 2016) (Tables 1.1 and 1.2).

Table 1.1: Overview summary of fire processes included within selected fire-enabled DVGMs, as described by Hantson et al. (2016). Darker cell shading indicates increasing complexity. Adapted from Hantson et al. (2016; Table 1)

Model	**Fire processes**							
	Overall Complexity	**Fuel moisture**	**Fuel load**	**Fire starts from lightning ignitions**	**Anthro. ignitions**	**Anthro. supression**	**Rate of spread**	**Burnt area**
CASA/ GFED		-	-	-	-	-	-	Simple scaling of number of fires
GLOBFIRM		Empirical/ Fire danger index (FDI) base	Masking threshold	-	-	Fuel manipulation	-	Empirically related to fuel an moisture
MC-FIRE		Mutiple fuel moisture types and modelled/ mutiple FDI	Size classes/ Rate of spread	Moisture based	-	Constant supression	Simplified Rothermel	Entire grid cell affected
CTEM		Mutiple fuel moisture types	Fire function of fuel load	Lightning scaling and weather generator	Deforestation fires	Varies with population density and agricultural masking	Uses rate of spread fire properties	Entire sub-cell
SPITFIRE/ LPX/ Lmfire		Mutiple fuel moisture types and modelled/ mutiple FDI	Complex	Lightning scaling, weather generator and complex weather	Deforestation fires and additional algorithm	Varies with population density, agricultural masking and complex masking	Multiple spread types	Average burnt area multiplied by number of fires

Table 1.2: Overview summary of the impacts of fire in selected fire-enabled DVGMs, as described by Hantson et al. (2016). Darker cell shading indicates increasing complexity. Adapted from Hantson et al. (2016; Table 2)

Model	**Impacts of fire**				
	Overall Complexity	**Carbon emissions**	**Other carbon feedbacks**	**Plant mortality type**	**Plant resistance: survival**
CASA/GFED		Biomass specific	Size classes/ rate of spread	Crown, cambial and root kill	Parameterised mortality
GLOBFIRM		All vegetation consumed	Non combusted carbon becomes litter	Parameterised mortality	Parameterised mortality
MC-FIRE		Proces specific	Size classes/rate of spread	Crown, cambial and root kill	Based on PFT
CTEM		Biomass specific and PFT type specific	Size classes/rate of spread	Parameterised mortality	Based on average plant in grid
SPITFIRE/ LPX/ Lmfire		Process specific and PFT/fuel type specific	Complex	Crown and cambial	Based on PFT, height cohorts and resprouting

The FireMIP model intercomparison project was designed to examine models within a common framework, to ultimately improve performance (Rabin et al., 2017). Generally, models reproduced patterns of burned area (Hantson et al., 2020), but underestimated total burned area compared to the most recent GFED5 observations, and were not able to represent the recent decrease in global burning (Andela et al., 2017). A comparative assessment of the emergent relationships between fire and its drivers showed that the models were able to reproduce data driven relationships between climate variables and burned area (Forkel et al., 2019). However, models were less able to represent the relationships between vegetation and fire, and people and fire (Forkel et al., 2019). At present there are limited examples of published DVGM predictions for future fire. Based on the LPJ-GUESS-SIMFIRE model, (Knorr et al., 2016) estimated continued global declines in burned area until 2050, after which burned area may increase depending upon emissions scenarios until 2100. The JULES-INFERNO model has also been used to project burned area and emissions in South America, with increases in burned area under all scenarios, due to hotter and drier conditions (Burton et al., 2022).

1.5. Palaeodata: relating fire to its drivers using evidence from the past

Remote sensing data has greatly increased the availability of fire information at fine spatial scale and high temporal resolution, improving our ability to test our assumptions regarding earth system processes, but there are limitations associated with these data. In the context of wildfire, there are a variety of satellite-based data products (freely) available, detecting pre-fire conditions, active fires and analysing post fire effects (Chuvieco et al., 2020), but estimates of phenomena can vary substantially between products. For example, recent estimates of average annual global burned area from GFED5 are 774$Mhayr^{-1}$ (Chen et al., 2023), compared to 465$Mhayr^{-1}$ in the earlier GFED4 (Van Der Werf et al., 2017), 478$Mhayr^{-1}$ for 2003-2019 derived from MOSEV (Fernández-García and Alonso-González, 2023), and 463$Mhayr^{-1}$ for 2001-2018 in FireCCI51 (Lizundia-Loiola et al., 2020). Moreover, despite improvements in data resolution, satellite observational data is still relatively coarse – for example the MODIS MCD64A1 data product underpinning the GFED4, GFED5 and MOSEV datasets is at 500m resolution with one-to-two-day temporal resolution (Giglio et al., 2018) – and can be limited during periods of high cloud cover or for assessing changes within the understory (Yang et al., 2023). The temporal coverage of these data are also limited. Processes in ecosystems with longer-term fire return times cannot be captured in the relatively short time covered by the instrumental record (Bowman et al., 2009). Assessment of the strength of various dynamic feedbacks between earth system processes is similarly curtailed given the potentially longer periods associated with these feedbacks.

Palaeodata provides both an alternative means to investigate relationships between fire and its drivers, providing the ability to assess processes at longer time scales, analysing changes in space and time, and allow the testing of assumptions underlying processes for time periods without, or with limited, anthropogenic influence. Analysis of palaeofire can therefore play an important role in enhancing our knowledge of fire in the present day, and in so doing improve our ability to predict and manage fire in the future.

Studies that have looked at palaeofire at a global or continental scale have tended to identify climate as the dominant driver of fire during most the Holocene (e.g. Power et al., 2008; Mooney et al., 2011; Vannière et al., 2011; Daniau et al., 2012; Marlon et al., 2013). This control has been related to general trends in temperatures (Mooney et al., 2011; Daniau et al., 2012; Zennaro et al., 2015), and at a more localised level to specific climate events, such as Bond events (Davis et al., 2003; Davis and Stevenson, 2007; Burjachs and Expósito, 2015), or periods of extreme drought (Higuera et al., 2011).

However, other drivers have been identified as important, particularly since the mid-Holocene. For example, Brown and Giesecke (2014) identified vegetation history in terms of pre-dominant broadleaf or needleleaf tree types as being a key determinant of fire in central Sweden during the mid-Holocene, with increasing fire disturbance linked to increases in *Pinus* prevalence despite a cooling and moistening climate. Similarly, Feurdean et al. (2020) found tree cover percentages were the strongest predictor of biomass burning in central and eastern Europe from 8,000 cal. BP to present, with the threshold level of tree cover after which biomass burning declined dependent on the dominant tree cover type. Blarquez et al. (2010) also attributed increases in reconstructed fire during the mid Holocene to the influence of understorey vegetation production despite cooler and wetter conditions.

Human influence has also been identified as an influence on fire in the early Holocene in some regional studies, for example in the Carpathian regions from 5,500 cal. BP (Feurdean et al., 2012), southern and southwestern Europe from 7,500-6,500 cal. BP (Tinner et al., 2016; Vannière et al., 2016; Connor et al., 2019; Iglesias et al., 2019), and central Europe from 8,500 cal. BP (Dietze et al., 2018). Early to mid-Holocene human influence has been associated with increased fire frequency from landscape clearance (Vannière et al., 2016) but reduced biomass burning due to a reduction fuel availability in southern Europe at regional scale (Vannière et al., 2016; Iglesias et al., 2019). At a sub-regional scale, however, increases in biomass burning have also been attributed to landscape clearance in Sardinia (Tinner et al., 2016) and Iberia (Connor et al., 2019) during the early to mid-Holocene. In central and eastern Europe and the Balkans, potential early human influence is aligned with increases in biomass burning and from landscape clearance (Feurdean et al., 2012; Dietze et al., 2018) and from Mesolithic land use (Dietze et al., 2018). Generally, however, the key role for humans in shaping fire has been more associated with the later part of the Holocene and landscape conversion for farming (e.g. Marlon et al., 2012; Clear et al., 2014; Zennaro et al., 2015; Zhang et al., 2022). However, clearly separating human impacts from prevailing changes in climate is a challenge (e.g. Kaal et al., 2011; Feurdean et al., 2013; López-Sáez et al., 2018). As well as identifying differences in driver impacts through time, several studies have also indicated the impacts vary by location (Blarquez and Carcaillet, 2010; Brossier et al., 2014; Kloster et al., 2015) or elevation (Vannière et al., 2016; Zhang et al., 2022).

Most palaeofire research has focussed on the synchronicity of reconstructed fire with reconstructed or modelled drivers (e.g. Feurdean et al., 2012; Dietze et al., 2018; Iglesias et al., 2019). Other approaches, including correlation analyses (Gobet et al., 2003; Burjachs and Expósito, 2015; Zhang et al., 2022), or generalised additive modelling (GAMs) of time series of drivers to fire (e.g. Daniau et al., 2012; Feurdean et al., 2017, 2020) have been used, but usually only on a subset of the potential drivers. Simulations of fire, driven by climate and vegetation, have been compared to reconstructions based on charcoal at global (Kloster et al., 2015) and European (Zapolska et al., 2023) levels. As well as reconstructions of landscape burning via charcoal reconstructions, recent research focussed on macro-charcoal records has also used decomposition of the charcoal signal to identify fire events and measure fire frequency (Gavin et al., 2007; Blarquez and Carcaillet, 2010; Brown and Giesecke, 2014; Hawthorne and Mitchell, 2016; Feurdean et al., 2019). This approach has also been followed in calibration studies, based on known fire events and fire scar data (Higuera et al., 2005; Brossier et al., 2014; Cui et al., 2020). Human influence is measured in terms of the archaeological context of the site(s), modelled population, the presence of pollen and spore indicators of human activity from sedimentary records, or by changes in forest cover and landscape openness, but the role of humans is usually inferred as the residual explanation of fire change from other drivers (e.g. Clear et al., 2014;

Iglesias and Whitlock, 2014; Iglesias et al., 2019). Whilst this assumption may be more justifiable towards the end of the Holocene, when clear human induced land-use changes are evident with increases in population growth (Klein Goldewijk et al., 2017), earlier inferences of human induced changes to wildfire are more speculative.

Overall, the differing results from the research on the importance of different drivers of palaeofire raises interesting questions about whether the general observed relationships from the modern day are applicable to fire in the past.

1.6. Reconstructing palaeofire and its drivers

Reliable reconstructions based on palaeodata are required to test the relationship between fire and its drivers. The following sub-sections introduce the different methods used to reconstruct fire and its drivers on palaeo-timescales, with a focus on approaches based on using data from sedimentary archives to reconstruct fire, vegetation or climate, and the use of radiocarbon dates on archaeological material to reconstruct human influence.

1.6.1. Reconstructing fire

Several data sources have been used to identify historical fire activity, such as historical written records, dendrochronological fire-scar data, chemical markers in ice-cores, and charcoal in lake sediments and peat bogs (Conedera et al., 2009).

Historical written records give an indication of fire in the past beyond the instrumental record. For example, in California there are written records of wildfires on state and federal lands in some areas from 1910 onwards (Keeley and Syphard, 2015). Historical records of burned area from Australia (from 1950), Canada (from 1985), Chile (from 1980), Europe (from 1980) and the USA (from 1984) have recently been compiled into an online dataset called ONFIRE (Gincheva et al., 2024). Although these historical data are clearly limited in space and scale, they provide a high temporal resolution record of fire activity over the past century.

Dendrochronological fire-scar data provides records of past fires typically spanning centuries to millennia (Margolis et al., 2022), where the longest multi-millennial records are based on the giant sequoia (e.g. Swetnam, 1993). Fire scars have also been identified on fossil trees from the late Triassic, providing fire information for periods further back in time (Byers et al., 2014, 2020). The annual resolution of tree ring data, coupled with the relatively long length of records provide a measure of local fire events. Whilst each measure is essentially only a record of very local fire, multiple measurements can be taken in forest stands, and data can be compiled to represent broader areas. For example, the North American tree-ring fire-scar network is a compilation of forest scar data enabling regional analysis (Margolis et al., 2022; Fig. 1.3). Fire-scar dendrochronological data is limited to fires that are non-lethal (Conedera et al., 2009).

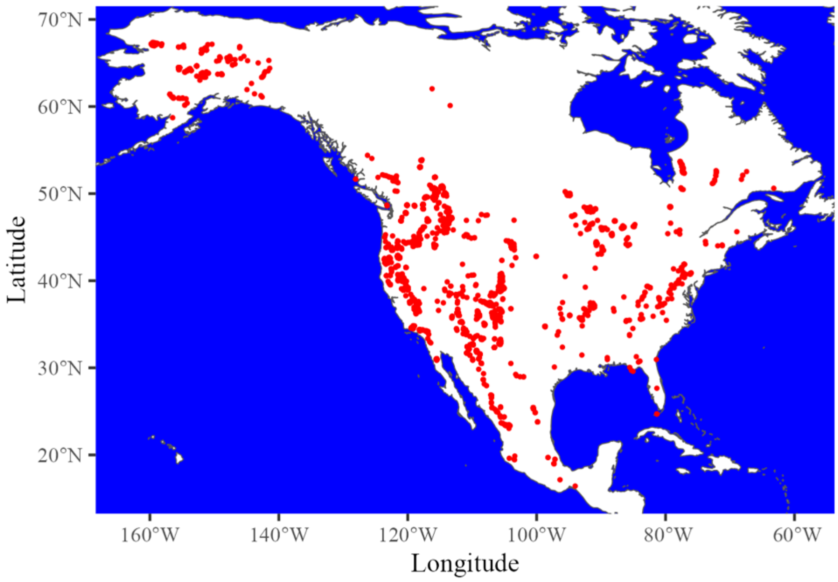

Figure 1.3: Dendroecological fire scar data locations in North America, compiled from the North American tree-ring fire-scar network. Location data from Margolis et al. 2022.

The use of chemical markers within ice-cores makes use of the chemical release of tracers during a fire, their deposition and subsequent storage in ice. There are multiple types of chemical species that have been used to construct vegetation burning, including species with multiple potential sources, such as ammonium or formate, or those specific to biomass burning, such as levoglucosan (Rubino et al., 2016). One weakness of the general approach is the reliance on long-distance transport of the chemical markers from the burning source to the core location which depends on suitable meteorological conditions (Rubino et al., 2016). Most ice-core records of fire only cover the past 2000 years (Rubino et al., 2016), although there are examples of analysis of fire signals for the Holocene period (Zennaro et al., 2015) and for the last glacial interval (Fischer et al., 2015).

Incomplete combustion of organic material produces charcoal, which is then preserved in water bodies, bogs and soils. Whilst the majority of fire records derived from charcoal are from sedimentary cores from water bodies or bogs, charcoal from soils, fluvial deposits and marine sites have also been used to investigate fire at different spatial scales. Soil charcoal, for example, has been used to identify local fire episodes, with individual macrocharcoal samples radiocarbon dated (e.g. Carcaillet, 2001;

Gavin et al., 2003a; Hoffman et al., 2016; Robin & Nelle, 2014). However, it can be challenging to chronologically determine stratified layers in soil because of bioturbation, erosion and uprooting (Carcaillet, 2001; Lertzman et al., 2002; Gavin et al., 2003a). In contrast, due to the relative stability of lake and bog sediment, an assessment of the quantity of charcoal through time can be made , based on counting seasonal layers within the core (varve counting), or by dating material from the core using different dating methods (e.g. radiocarbon, Pb-210, tephra) and by modelling age-depth relationships (e.g. Whitlock and Larsen, 2001; Brenner and Kenney, 2013) (e.g. Fig, 1.4).

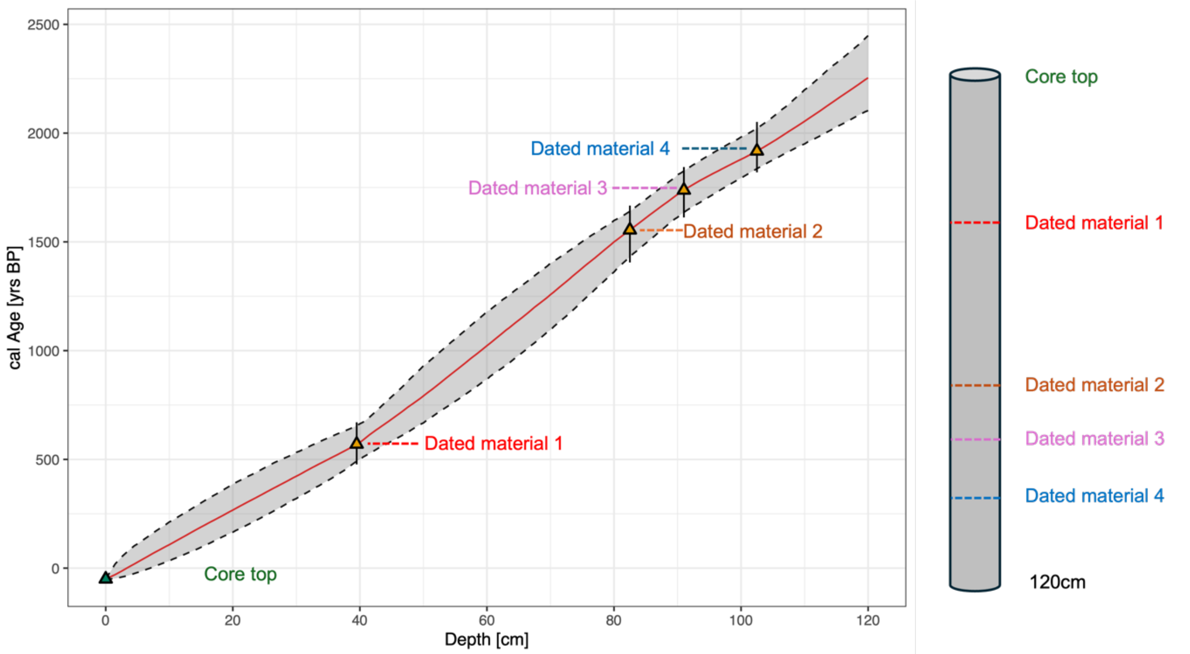

Figure 1.4: Age model example. Calibrated dates through the core are used to construct an age model through time

Changes in charcoal abundance are then taken to represent the fire history of the area. The rate of charcoal accumulation – the count, area, or mass of charcoal per cm per year – depends on both the characteristics of the fires and on the processes that transport charcoal to the site (Whitlock and Larsen, 2001). Whilst charcoal accumulation in relation to airborne deposition can occur during or shortly after a fire based on wind conditions, the record will also include charcoal introduced during non-fire years, from sediment run-off or sediment mixing within the water body (Whitlock and Larsen, 2001). Based on calibration studies of charcoal deposition and known fires, the length of this lag depends on the water body site characteristics. For example, no lag was found in relation to fires in flat or gently rolling landscapes in boreal Canada (Hennebelle et al., 2020) whereas other studies suggest this is a vital element to consider in assessing fire history (e.g. Whitlock and Millspaugh, 1996; Higuera et al., 2005; Duffin et al., 2008).

The timescales for sedimentation can vary dramatically even within a single core, so most charcoal records tend to provide information on fire history at decadal or centennial scales. Further, data also varies between core sites and is influenced by the research design which determines the depth of the core and the sampling resolution. The underlying research question also dictates the type of charcoal being assessed and in turn the method of charcoal analysis. The use of pollen slides, for example, where counts or area of charcoal is calculated within core intervals, is typically used to assess longer periods of change (Whitlock and Larsen, 2001; Conedera et al., 2009). In contrast, sieving, where material is washed and sieved, with counts of charcoal measured per volume; or image analysis, where software is used to identify charcoal particles, is often performed contiguously throughout a core to generate a more detailed temporal record of fire (Whitlock and Larsen, 2001; Conedera et al., 2009). Charcoal is typically measured in terms of concentration (mm^2 per cm^3), charcoal counts per volume, or influx (i.e. cm^2 pieces per year). A distinction is normally drawn between analysis of small pieces of charcoal, with particles less than 100µm in size analysed using pollen slides, and analysis of macroscopic charcoal, although in both cases charcoal is generally assessed as accumulation rates or particle numbers (Whitlock and Larsen, 2001).

Microscopic charcoal is generally used to infer a broad picture of regional fire history due to the potential long-distance deposition of small particles, with, for example, a calibration study by Duffin et al. (2008) finding that more than half of charcoal particles less than 50 µm in length came from more than 15km away from core sites. In contrast, macroscopic charcoal is generally used to identify a more local signal. Recent analysis of sedimentary charcoal for palaeofire research has tended to focus on macroscopic rather than microscopic charcoal (Marlon et al., 2016). Although there is some evidence that macroscopic charcoal can be transported long distances (Tinner et al., 2006; Cui et al., 2020), most macroscopic charcoal is deposited close to the fire edge (Tinner et al., 2006). Despite these expected general differences in transport, there are wide estimates for source location for sedimentary charcoal. As a result, Vachula (2020) suggests a broad measure of $50km^2$ as the source area for fires and particles of all sizes. In practice, regional and global studies have tended to include both micro and macro charcoal, to increase spatiotemporal coverage.

Whilst charcoal analysis has typically been used to identify broad-scale patterns of landscape burning, it can be used to identify fire events, based on identifying particle counts above background levels (Clark and Royall, 1996; Higuera et al., 2010). In order to identify charcoal peaks however, records must have relatively high temporal resolution, have sufficient particle counts to identify these peaks, and relatively stable sedimentation rates (Marlon et al., 2016).

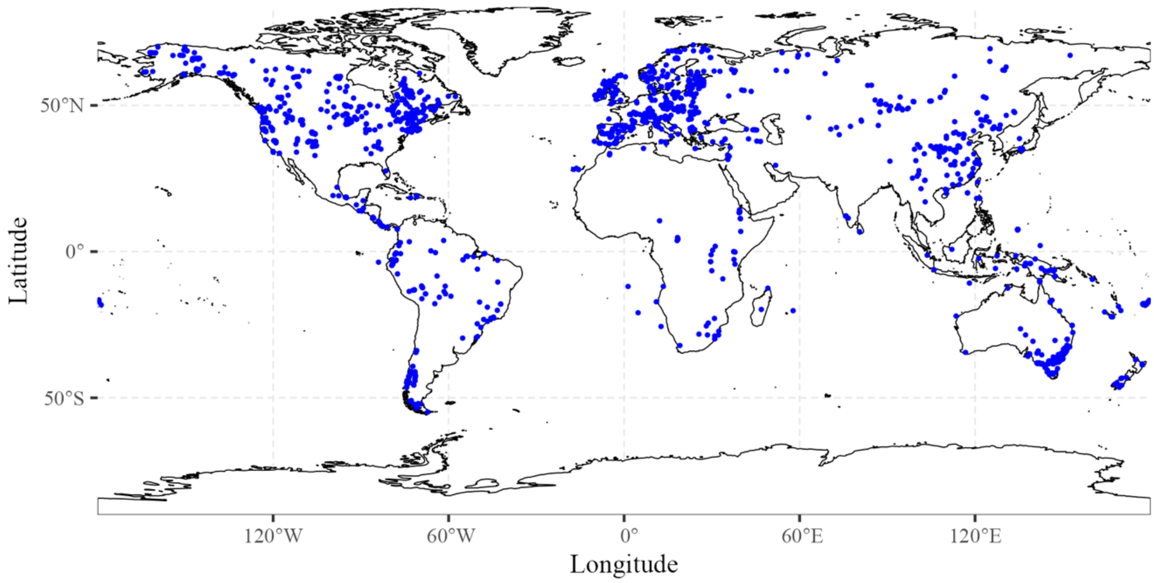

Figure 1.5: Charcoal site locations from the Reading Palaeofire Database (Harrison et al., 2021)

One of the key benefits of using sedimentary charcoal data for global and regional fire reconstructions is the quantity of data available, reflecting the combined efforts and openness of the sedimentary charcoal research community. For example, the Reading Palaeofire Database (RPD) (Harrison et al., 2022), includes 1676 charcoal records from 1480 sites globally, compiled from the Global Paleofire Database (http://paleofire.org/), PANGAEA (https://www.pangaea.de/), NOAA National Centers for Environmental Information (https://www.ncdc.noaa.gov/data-access/paleoclimatology-data), the Neotoma Paleoecology Database (https://www.neotomadb.org/), the European Pollen Database (http://www.europeanpollendatabase.net/index.php,), the Arctic Data Center (https://arcticdata.io/catalog/) and directly from authors. However, despite the number of records, there are spatial gaps (Fig.1.5), reflecting both the lack of suitable lake, bog or wetland sites in typically arid areas and a bias towards sampling in the northern extratropics (Harrison et al., 2022). This limits the ability to reconstruct fire in some regions. The variety of methodological approaches, measurement types and site contexts, such as lake sizes and sedimentation rates, also makes comparison between records challenging. Using data within the RPD, converting different measurements to a standard measure of influx can generate values 14 orders of magnitude in difference between records, reflecting a combination of differences in fire history and also site and environmental characteristics. One widely followed three-step approach proposed by Power et al. (2008) to deal with this issue is normalisation: firstly, charcoal influx values are re-scaled by minmax transformation; these values are then Box-Cox transformed to homogenise variances, and; finally these values are then converted into site-based z-scores. However, comparison between records is still limited to relative changes, and is dependent on the length and timing of core chronologies. Finally, and in common with many of the other approaches to reconstruct fire, the question of what is really being measured from a fire regime context remains difficult to identify. Different authors have used charcoal accumulation as a proxy for various fire regime elements, such as burned area (Higuera et al., 2011; Leys et al., 2017), fire frequency (Power et al., 2006; Prince et al., 2018) or fire intensity (Colombaroli and Gavin, 2010). Furthermore, charcoal itself is an imperfect means to capture the fire record, as very high temperature fires generate soot rather than charcoal, and very low temperature fires may not char vegetation (Whitlock and Larsen, 2001) and thus not be detected at all (Higuera et al., 2005). The variety of factors that can be used to describe a fire regime – the fire frequency, spatial scale, intensity, seasonality etc. – are contained within the charcoal record as a single measure. For example, a fire regime characterised by frequent low intensity fires may generate the same quantity of charcoal as less frequent more intense fires, if the temporal resolution is insufficient to characterise distinct fire events. This lack of precision may confuse the interpretation of charcoal as a fire record, and alternative approaches have been developed, such as assessing the morphology and structure of charcoal to infer fire intensity and type of fuel burnt (Enache and Cumming, 2006; Jensen et al., 2007), or the chemical composition of charcoal fragments to estimate fire intensity (Gosling et al., 2019). These alternative approaches are still in their infancy, however they have been applied to only a relatively limited number of sites.

Although these challenges point to limitations in terms of the use of charcoal in inferring fire history, calibration studies have been able to reconstruct recent fire history using charcoal data (Duffin et al., 2008; Adolf et al., 2018; Hennebelle et al., 2020; Vachula et al., 2020). Additionally, the spatial and temporal coverage of the pool of charcoal records is unmatched compared to other fire reconstruction approaches.

1.6.2. Reconstructing vegetation

Although there are studies that make use of other methods to reconstruct vegetation such as biomarkers (e.g. Hughen et al., 2004; Jansen et al., 2010; Ortiz et al., 2013) or macrofossil remains in sediments (Birks, 2014), most reconstructions are based on the use of pollen (Prentice, 1988; Bunting et al., 2013; Seppä, 2013). Fossil pollen from sedimentary cores represents an archive of vegetation change through time, with age-depth chronology determined by layer counting or dating of core material (see section *1.6.1 Reconstructing fire*).

Pollen samples are typically represented as percentages, based on the relative counts of taxa within the sample. Whilst identification of species from pollen grains is possible in some cases, generally pollen is only identifiable at genus (e.g. *Pinus*), or family (e.g. Poaceae) level (Seppä, 2013). Although early surface sample analysis confirmed the relationship between pollen abundance and vegetation, these same analyses indicated that pollen is biased towards certain taxa (Prentice, 1988).

Well represented taxa are usually wind rather than insect pollinated (Prentice, 1988); additionally, some taxa have pollen that does not necessarily survive the sedimentation process (e.g. *Populus* (Sangster and Dale, 1961; Cushing, 1967). Another finding from early surface sampling studies was that the source area of pollen was dependent on the sampling location characteristics, with larger lakes and mires representing regional vegetation, and samples from smaller lakes, bogs and forest hollows tending to represent more local vegetation (Bradshaw and Webb, 1985; Prentice et al. 1987; Jackson, 1990; Calcote, 1995). Although pollen quantities decline with distance from the source, pollen counts reflect both local and longer distance pollen transport, with pollen dispersal distances varying by taxa due to differences in pollen morphological characteristics (Cain, 1939; Prentice, 1988). As well as differences in transport, the amount of pollen produced by species ("pollen productivity") can be substantially different: recent reconstructions of vegetation for Europe that take account of pollen productivity, for example, use estimates that *Alnus* produces ca. 16 times more pollen than *Acer* (Githumbi et al., 2022; Serge et al., 2023). Pollen represented in surface or sedimentary samples therefore reflects a combination of factors, including taxa abundance, but also the relative quantity of pollen produced and the characteristic pollen dispersal distances by taxa, as well as the source type and size. This implies that care needs to be taken in interpreting fossil-based pollen diagrams as representative of changes in vegetation through time.

There are a variety of quantitative methods that have been applied to sedimentary pollen data. The most widely used include biomisation, the modern analogue technique (MAT), and the landscape reconstruction algorithm (LRA). The following section provides a brief overview of these methods.

Biomisation: The biomisation method was first introduced by Prentice et al. (1996), based on the categorisation of taxa to PFTs, and PFTs to biomes. The first stage of the approach is to assign taxa to PFTs. Although definitions and categorisations differ, PFTs generally represent broad categories containing taxa with similar traits and responses to environmental factors (Harrison et al., 2010), with PFTs constrained by bioclimatic constraints (Prentice et al., 1996). Taxa can be potentially assigned to more than one category, because at the taxon level they may include several species with different responses to the environment, or the species themselves may be highly adaptable to the environment. For example, in the categorisation of European species, Prentice et al. (1996) assign *Abies* to either the "boreal evergreen conifer" or "cool-temperate conifer" PFTs. Re-categorisation of taxa to PFTs after initial assignment is possible at this stage to match target vegetation maps and bioclimatic limits. Following assignment of taxa to PFTs, PFTs are assigned to biomes, based on the bioclimatic range in which they are dominant. Based on these two assignments, taxa can then be assigned to biomes in a presence absence matrix. For the "boreal evergreen conifer" PFT in Europe, Prentice et al. (1996) assign this PFT to "Taiga", "Cool conifer forest", or "cool mixed forest". This then provides the basis for pollen sample categorisation, with affinity scores for each biome calculated based on the sum of each taxa abundance, constrained by the biome/taxa matrix. As shown in Equation 1, a square root transformation of pollen abundances is used to stabilise the variance and to increase the sensitivity to less abundant taxa, and a threshold value θ_j (typically 0.5%) is used to reduce noise in sample assignment.

$$A_{ik} = \Sigma_j \, \delta_{ij} \sqrt{\left\{\max\left[0, \left(p_{jk} - \theta_j\right)\right]\right\}}$$

Equation 1.1: Biomisation affinity calculation. A_{ik} is the affinity of pollen sample k for biome i; summation is over all taxa j; δ_{ij} is the entry in the biome - taxon matrix for biome i and taxon j; p_{jk} are the pollen percentages, and θj is a threshold pollen percentage (Prentice et al., 1996)

The approach has been used extensively since its development (Williams et al., 1998; Pickett et al., 2004; Gotanda et al., 2008; Ortega-Rosas et al., 2008; Tarasov et al., 2013; Marinova et al., 2018; Sun et al., 2020), as it represents an intuitive approach to regional-scale vegetation reconstruction and can make use of pre-existing PFT and biome classifications. The key challenge with this approach is in the classification of taxa to PFTs, which is based on subjective expert opinion, and which may vary based on region of study (Prentice et al., 1996; Prentice and Webb III, 1998). Additionally, the discrete classification of samples to biomes can lead to identical or very close affinity scores. The tie-break rule, which assigns samples with identical affinity scores to the biome defined with less PFTs, helps resolve the issue of identical affinity scores. However, in cases of identical or very close affinity scores, biomes from a single location may alternate rapidly based small changes in taxa abundance (the “flickering switch” problem) (e.g. Allen et al., 2000; Marchant et al. 2001; Allen and Huntley, 2009; Fyfe et al., 2018). For example, Allen et al. (2000) identified potential misclassification of the vegetation for an Italian record during some periods of its history due to small changes in rare tree pollen.

Pseudobiomisation (Fyfe et al., 2010), which classifies pollen taxa into land-cover classes, including pastoral and arable land, rather than PFTs, is a modification of this technique and has been applied to reconstruct land cover in Europe (Fyfe et al., 2010, 2015; Woodbridge et al., 2014a; Roberts et al., 2018). Rules for defining semi-open and mixed classes are based on comparing affinity scores and (for mixed classes) class coverage values (Fyfe et al., 2010; Woodbridge et al., 2014b). Whilst the approach is intuitive and can generally replicate the patterns of vegetation change for other more complex reconstructions (Roberts et al., 2018), the approach is limited to generating broad classifications, and the rules for assigning classes based on affinity scores can appear somewhat arbitrary.

Modern analogues: The MAT (Overpeck et al., 1985; Guiot, 1990; Jackson and Williams, 2004) has been applied to reconstruct vegetation in terms of biomes (Overpeck et al., 1992; Williams et al., 1998; Wang et al., 2020), tree cover (e.g. Williams, 2003; Zanon et al., 2018) and vegetation types (Liu et al., 2021). Vegetation reconstructions using MAT are based on the idea that pollen assemblages are from the same type of vegetation (Jackson and Williams, 2004). Modern pollen samples are classified as discrete classes (as with biomes) or compared with modern tree cover maps, with these classes/values transferred to fossil pollen assemblages most analogous to the modern assemblages. There are a number of distance metrics designed to measure similarity between modern and fossil assemblages (Prentice, 1980; Overpeck et al., 1985), but most typically squared chord distance is applied (Equation 1,2) (Overpeck et al., 1985; Gavin et al., 2003b).

$$d_{ij} = \Sigma_k \left(\sqrt{\rho_{ik}} - \sqrt{p_{jk}}\right)^2$$

Equation 1.2: Squared chord distance calculation. The dissimilarity between samples i and j is calculated as the squared sum of the (root) differences in proportion for each pollen type (k) in each assemblage (Overpeck et al. 1985).

The threshold level of similarity to be considered an analogue depends on the distance metric, the characteristics of the fossil and modern datasets, and the scale of analysis (Jackson and Williams, 2004), and is not straightforward to define. Whilst averaging across the closest analogues has been applied for reconstructing tree cover (e.g. Zanon et al., 2018), for discrete classes such as biomes, ultimately a single class must be selected, with the potential for “flickering switch” issues as for biomisation. The no-analogue situation, where fossil pollen has no modern analogue due to a restricted collection of modern samples or where species combinations occured under climatic conditions that are not found today (Chevalier et al., 2020), can also represent a challenge to the technique. One approach, such as classifying species into similar PFTs has been applied to help reduce this issue (Davis et al., 2003). However, this also raises the same question as with biomisation about the appropriate assignment of taxa to PFTs.

To capitalise on the relative simplicity of the biomisation approach and the rigorous statistical basis of the MAT, a recently developed approach by (Cruz-Silva et al., 2022) combines the techniques and has been applied eastern Mediterranean (Cruz-Silva et al., 2024: Fig. 1.6). With this approach, a map of potential natural vegetation is used to characterise modern pollen assemblages into biomes. The within biome-variability based on modern pollen samples is then calculated for each biome in terms of the mean, range and standard deviation for each taxon in the modern set. These statistics are then used with fossil pollen data to build a dissimilarity index between each pollen sample and biome, which approximates the probability that a given sample would be produced by a particular biome. Non-analogue samples are then identified based on dissimilarity threshold values for each biome using the modern pollen samples. In terms of biome reconstruction, this approach exploits the within-biome variability to avoid the need for subjective assignment of taxa to PFTs with biomisation and minimises the flickering switch issue associated with the MAT by being more robust to minor fluctuations in taxa abundance (Cruz-Silva et al., 2022).

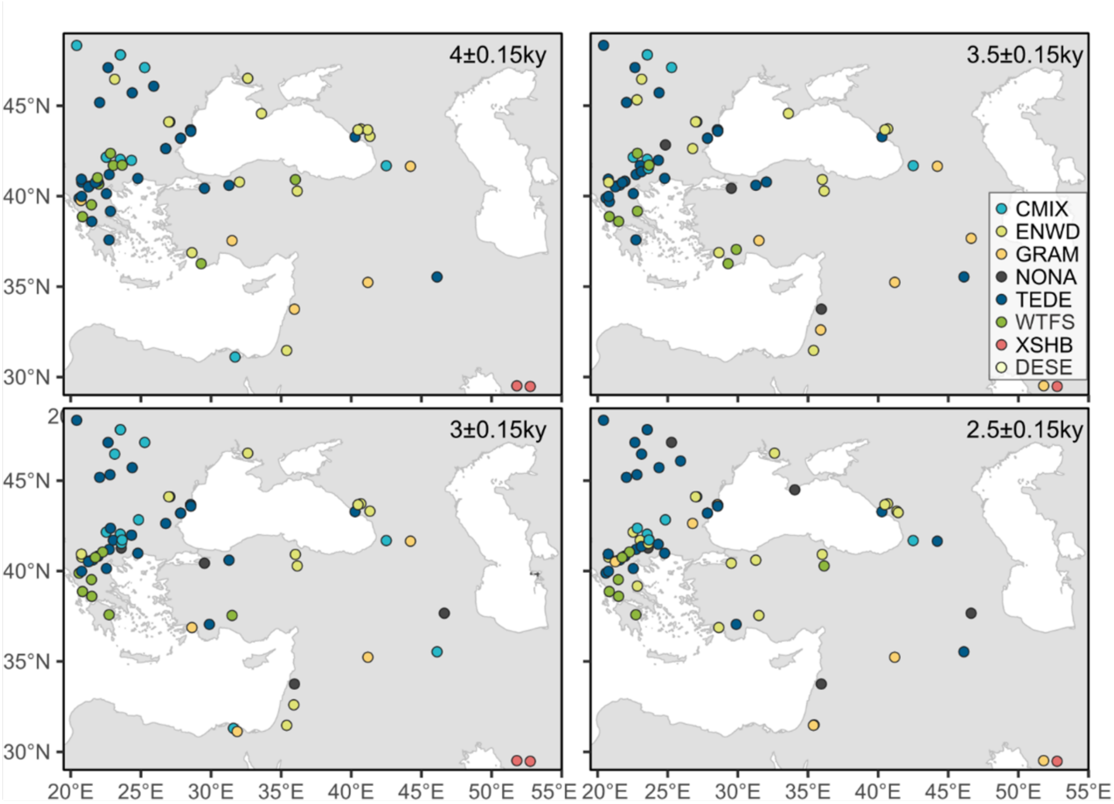

Figure 1.6: Biome reconstructions from Cruz-Silva et al. (2022) at 500-year intervals between 4,000 and 2,500 cal. BP for the Eastern Mediterranean-Black Sea Caspian corridor region. The biome codes are: CMIX, cool mixed evergreen needleleaf and deciduous broadleaf forest; DESE, desert; ENWD, evergreen needleleaf woodland; GRAM, graminoids with forbs; TEDE, temperate deciduous malacophyll broadleaf forest; WTFS, warm-temperate evergreen needleleaf and sclerophyll broadleaf forest; XSHB, xeric shrubland. Adapted from Cruz-Silva et al. (2022: Supplementary Fig. 2).

<u>Landscape reconstruction algorithm:</u> Process-based modelling approaches, which represent the relationship between species vegetation cover and pollen percentages (Davis, 1963), can be used to reconstruct landscape level vegetation quantitatively. Building on the earlier work of Davis (1963), who formalised the R-value framework for adjusting observed pollen species abundances to modern vegetation cover, the Extended R-value (ERV) model allowed estimation of R-values based on multiple sites using either estimations site-specific differences or maximum likelihood, and incorporated background "long distance" pollen within the model (Parsons and Prentice, 1981). In turn, this approach has been developed further into a suit of methods including the Multiple Scenario Approach (Bunting and Middleton, 2009), MARCO POLO (Mrotzek et al., 2016) and the Extended Downscaling Approach (Theuerkauf and Couwenberg, 2017). However, the most widely applied process-based modelling approach is the Landscape Reconstruction Algorithm (Sugita, 2007b, a).

The LRA is a comprehensive modelling approach used to estimate the relative proportion of each type of vegetation, which corrects for differences in pollen productivity, pollen dispersal, and source area (Sugita, 2007b, a). The LRA consists of two models: Regional Estimates of Vegetation Abundance from Large Sites (REVEALS) and Local Vegetation Estimates (LOVE), designed to estimate vegetation at the regional and local scale respectively.

The REVEALS model has been applied in many regions of the Northern Hemisphere (e.g. Hellman et al., 2008a; Sugita et al., 2010; Cui et al., 2013; Li et al., 2020; Githumbi et al., 2022; Serge et al., 2023) to calculate regional vegetation abundance in proportions using fossil pollen counts from large (>50ha.) lakes (Sugita, 2007a). Although REVEALS can also be applied to small lakes and bogs, the estimated standard errors increase, although this can be countered by combining multiple small sites (Trondman et al., 2016). The inputs required to run REVEALS include original pollen counts, relative pollen productivity estimates (RPPs) and their standard deviation to reflect differences in pollen production by taxa, the fall speed (FS) of pollen to reflect difference in pollen dispersal, the basin type (lake or bog), the size of the basin, maximum extent of regional vegetation, wind speed, and atmospheric conditions (Githumbi et al., 2022). Whilst the FS of pollen can be calculated based on diameter and density of pollen using Stokes' Law (Gregory, 1973), and wind speed, atmospheric conditions and maximum extent of regional vegetation are generally assumed as constant, the requirements for basin sizes and RPPs (in particular) can be challenging. The LOVE model is essentially a further step following application of the REVEALS model (Sugita, 2007b). LOVE specifies and then subtracts background pollen, reflecting consistent pollen loading from regional vegetation at similar sites, to estimate a reconstruction of local vegetation within the site source area (Sugita et al., 2010).

Estimates of RPPs of individual species are derived from field data. However, RPPs are only available for a limited number of taxa even in those regions where the REVEALS has been used to reconstruct vegetation patterns (Harrison et al., 2020; Wieczorek & Herzschuh, 2020). Furthermore, RPPs are not available for many regions of the world. Regional variations in species may mean that existing estimates of RPP are inaccurate for specific regions (Wieczorek & Herzschuh, 2020). A recent reconstruction of European vegetation found increasing the number of (mostly entomophilous) included taxa (from 31 to 46 taxa), and changes to RPP estimated values reduced the quality of the reconstruction, showing that the quality rather than the number of RPP estimates is most important (Serge et al., 2023).

1.6.3. Reconstructing climate

Meteorological station data can provide information about historical climates in some areas, with the longest records stretching back hundreds of years (Jones and Bradley, 1992; Jones et al., 1999). However, reconstructions of longer periods of climate assume that climate controls are visible in environmental records, i.e. that changes in a measured record represents a proxy for changes in aspects of the climate. There are many different records that have been used to infer changes in climate.

Dendroclimatology, for example, typically makes use of variations in tree ring width to reconstruct climate variables, with tree ring widths measured and averaged across a site with typically 10 to 20 trees (Fritts et al., 1980; Sheppard, 2010). Cross dating between the measurements of patterns in tree rings is applied to ensure accurate tree ring chronology (Douglass, 1941; Fritts et al., 1980). These widths are then calibrated against meteorological records of climate variables, with a variety of statistical techniques applied (Fritts et al., 1980). Site selection plays a key role in determining the variables to be measured, with tree ring width mainly determined by precipitation or soil moisture limitations in semi-arid areas, by growing season temperature in high elevation or high latitude areas, and a mixture of temperature and precipitation in moist temperate forests (Sheppard, 2010; Anchukaitis, 2017). These variations make combining site measurements a challenge, as different locations may be affected by different climate variables in space and time (Fritts et al., 1980). Additionally, differences in methodology can impact reconstructions (Büntgen et al., 2021). Dendroclimatology is limited to Holocene reconstructions and to areas with long standing tree cover, although the expansion of the approach to non-traditional tree species may increase the future spatial coverage associated with the technique (Pearl et al., 2020).

In contrast to tree-ring data, analysis of ice core records allows very long-term high-resolution analysis of temperature and precipitation, albeit at a regional resolution. Dating of cores is based on a combination of methods, such as annual layer counting based on seasonal cycles of chemical species, and reference horizons (e.g. volcanic eruptions) (Legrand and Mayewski, 1997). Isotopic analysis of (typically) water isotopes within the core provides information about local temperatures (Jouzel et al., 1997; Jouzel, 2013). The ice-core record for the Antarctic (Jouzel et al., 2007) covers the past 800,000 calendar years before 1950 CE (cal. BP) and the past 123,000 cal. BP in Greenland (Andersen et al., 2004). The major challenge with ice core data is the limited spatial coverage of the record.

Speleothems provide a means to reconstruct climate variables based on the slow build-up of mineral deposits in caves, fed by drip water. As their formation is controlled by precipitation and the cave microclimate, they provide a climate record through time, primarily based on measurements of oxygen isotopes (Lechleitner et al., 2018; Parker et al., 2021). Speleothem deposits are normally dated by Uranium-Thorium dating, which allows for dating to ca. 600,000 cal. BP (Spötl and Boch, 2019). The relatively slow accumulation of deposits mean that interval measurements are typically annual to decadal (McDermott, 2004). However, the timing of the climate signal is smoothed by the transport of water through the karst system, the extent of which varies from site to site (Comas-Bru et al., 2019). A major challenge associated with speleothems lies in teasing out the different processes that that may cause variations in oxygen isotope values, including changes in temperature, precipitation, moisture sources and circulation dynamics, and variations in cave conditions (McDermott, 2004).

Climate reconstructions based on chironomids in lake sediments are one of a number of species indicator approaches to reconstructing climate. Community composition of chironomid species is dependent on summer temperature changes, with modern training sets of chironomids used to calibrate composition/temperature relationships based on statistical techniques such as weighted average partial least squares (WA-PLS), or the MAT (Eggermont and Heiri, 2012) (WA-PLS and the MAT are discussed in more detail in relation to pollen in *Pollen-based climate reconstructions*; see below). As with charcoal and pollen deposits in sediments, the depth of the sediment determines the length of the chironomid record, modified by sedimentation rates. One challenge associated with chironomid data is that as well as temperature, assemblages may be influenced by other environmental variables such as lake oxygen or pH levels, thus possibly compromising the underlying reconstruction (Velle et al., 2005). Similarly, chironomid growth may be more dependent on water temperature, rather than air temperature, and so in areas where the relationship between summer water temperature and water temperature is distorted by hydrological effects, the link between chironomids and air temperature may be affected (Eggermont and Heiri, 2012).

<u>Pollen-based climate reconstructions:</u> The long-term preservation of pollen in anoxic environments can be used to generate a record of climate changes through time. Unlike other climate proxies, the spatial coverage of pollen data is near-global, with open access online databases such as Neotoma (Williams et al., 2018), which contains multiple constituent pollen datasets such as the African Pollen Database (Lézine et al., 2021) and European Pollen Database (Fyfe et al., 2009), facilitating quantitative climate reconstructions at regional to continental scales (Bartlein et al., 2011; Chevalier et al., 2020). As well as site-based estimates, the wide dispersal and concentration of pollen sites has also permitted the creation of interpolated gridded surfaces of climate values (e.g. Davis et al., 2003; Sawada et al., 2004; Mauri et al. 2014; Mauri et al., 2015) (Fig.1.7).

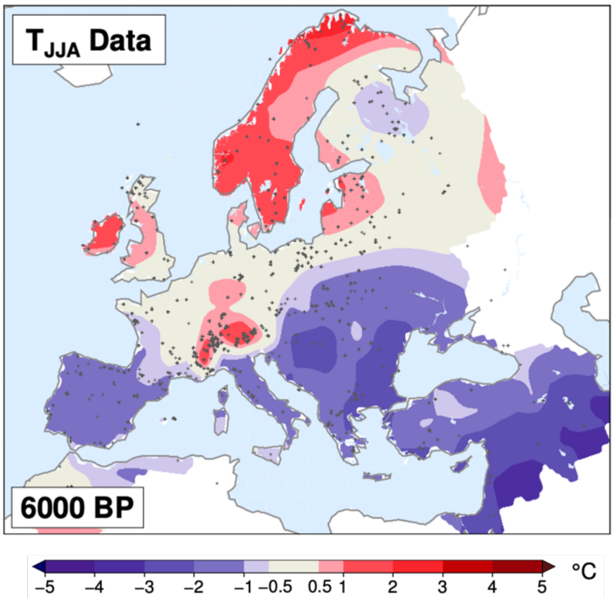

Figure 1.7: Interpolated summer temperature anomalies between 6,000 cal. BP and present, based on pollen data. Adapted from Mauri et al. (2014: Fig. 4).

The use of fossil pollen data to reconstruct climate is based on the principle that plant species distribution patterns are predominantly determined by the prevailing climate space. Bioclimatic variables, which represent specific aspects of the climate that best relate to species physiology such as mean temperature of the warmest month (MTWA) or the ratio of annual actual to equilibrium evapotranspiration (α), place bioclimatic limits on plant taxa ranges (Harrison et al., 2010). Vegetation composition contains information about distinct aspects of climate, based on the different responses of taxa to different bioclimatic variables (Huntley, 1991; Bartlein et al., 2011). This multivariate element separates pollen from (most) other reconstructions of climate, which tend to reflect level climate descriptions (i.e. warmer, more precipitation) (Chevalier et al., 2020).

Most approaches to pollen-based climate reconstruction attempt to model relationships between climate variables and vegetation in the modern day, and apply this relationship to fossil pollen data (Chevalier et al., 2020). Changes in climate are therefore assumed to be reflected in the pollen record, with evidence suggesting the lags between these changes are around 100 years or less (e.g. Williams et al., 2002; Harrison and Sanchez Goñi, 2010). Several general assumptions underlie this approach (e.g. Huntley, 1993; Birks et al., 2010): i) species included within the modern (training) and fossil datasets are systematically related to the climate where they live; ii) climate variables reconstructed determine the vegetation and pollen assemblage; iii) the relationship between climate and species has not changed through time; iv) other environmental variables such as soil properties have a negligible or consistent impact on the fossil data; v) calibration functions have sufficient predictive power to represent the complexity of relationships between species and climate. However, these assumptions can be challenged by, for example, human modification of the landcover changing the modern relationships between pollen and climate, or in terms of changes in CO_2 through time and the affect that this may have on species climatic limits (Chevalier et al., 2020) (although see Prentice et al. (2022) for a way to account for CO_2 variation in reconstructions). Taking these, and other factors into account in the selection of sites, species and methods is an important step in utilising pollen-based reconstruction techniques.

There is a wide range of pollen-based techniques, which, can be grouped following Chevalier et al. (2020) as: indicator species approaches, classification-type approaches, regression approaches, the process-based approach.

Indicator-species approaches construct climate variables based on the bioclimatic envelopes of pollen taxon, with early work using the presence/absence of one or a few species to reconstruct climate (Iversen, 1944). This generalised approach has been extended, with, for example, the probability distribution function (PDF) approach (Kühl et al., 2002) based on overlapping presence/absence of species within climate envelopes, with the probability of observing a climate value conditional on the presence of taxa present. As some climate values are more abundant than others within a given study area, climate values are weighted by the inverse of their abundance so that the PDFs do not inadvertently reflect this frequency (Kühl et al., 2002). Climate reconstructions are then based on the presence of taxa within the record, with the joint PDF providing the most likely climate value. This approach has been found to underestimate past climate variability (Litt et al., 2009; Kühl et al., 2010), in part due to the broad range of bioclimatic envelopes for many species and the limits that presence/absence data provides, whereby a single pollen grain for a taxon can have the same influence on the reconstruction as a more abundant taxon (Birks et al., 2010).

Classification-type approaches compare modern pollen assemblages with fossil pollen assemblages, identifying the most similar analogues. The climate spaces of the modern analogues are then used to reconstruct past climate. MAT (Overpeck et al., 1985; Guiot, 1990; Jackson and Williams, 2004) is an example of this approach (e.g. Cheddadi et al., 1996; Davis et al., 2003; Mauri et al., 2015), and is discussed above in relation to vegetation reconstructions (*1.4.2 Reconstructing vegetation*). The average across multiple analogues can be used to reconstruct climate variables, which helps to prevent potential inaccuracies from relying on selecting the single best match in pollen percentage (Jackson and Williams, 2004; Chevalier et al., 2020). However, the maximum number of potential analogues to include when applying the classification is subjective. As with reconstructing vegetation, MAT-based reconstructions of climate also require decisions regarding thresholds and are subject to non-analogue situations.

Regression-based approaches model the relationships between climate variables and modern pollen, and apply these relationships to fossil pollen assemblages. WA-PLS (ter Braak and Juggins, 1993) is an example of such an approach (e.g. Tonello et al., 2009; Salonen et al., 2012; Wang et al., 2014), which builds on the distinct weighted averaging approach used to reconstruct climate with pollen (ter Braak and Looman, 1986; ter Braak and Juggins, 1993) and partial least squares regression. Based on the assumption that species are more abundant in environments in climates to which they are suited, weighted averaging calculates the average climate conditions suitable for each taxon, weighted by abundance, and then applies this relationship to fossil pollen, weighting climate optima by abundance (ter Braak and Looman, 1986). The use of partial least squares reduces the potential issue of multicollinearity in taxa responses to climate and considers residual correlations in the underlying data when estimating species optima (ter Braak and Juggins, 1993). Cross validation is used to identify the best (minimum) number of components (Chevalier et al., 2020). A recent modification of the technique – frequency adjusted tolerance weighted WA-PLS (fxTWA-PLS) - helps to reduce the tendency for WA-PLS to produce reconstructions that underestimate the amplitude of climate changes, by considering variable climate tolerances by taxa, and the frequency of climate values in the training dataset (Liu et al., 2020, 2023). One of the challenges associated with the WA-PLS approach is that the relationship between species abundance and climate values are assumed to be unimodal, which may not be the case for larger scale studies (Bartlein et al., 2011; Chevalier et al., 2020).

Whereas other approaches seek to link pollen assemblages to the climate, *the process-based* inverse modelling technique (Guiot et al., 2000) seeks to maintain the causality of the relationship from climate to vegetation (e.g. Hatté and Guiot, 2005; Wu et al., 2007). Designed specifically to address the issue of the impact of changing CO_2 concentrations on water-use efficiency and how this might affect vegetation-climate relationships, this approach uses random climate values from modern distributions and feeds these into a process-based vegetation model (e.g. BIOME3: Haxeltine and Prentice, 1996) to generate PFT NPP estimates. These PFT NPPs are compared with the PFT profiles of modern samples to generate a transfer function linking model output to pollen PFTs. The model is then perturbed thousands of times with different changes in climate, and simulated outputs from the model are then compared with fossil pollen PFTs. The reconstruction is based on selecting the climate envelope that best describes the fossil pollen PFT. As well as dealing with the CO_2 concentration issue, this approach is less sensitive than other techniques to non-analogue situations (Chevalier et al., 2020). A weakness relates to the requirement to convert species to PFTs, which is arbitrary (Prentice and Webb III, 1998), as well as the comparability of PFT productivity with pollen percentages (Chevalier et al., 2020). Additionally, the approach is dependent on the underlying model, with different models potentially generating different reconstructions. These model-output differences are evident in the predictions of vegetation change under climate change (e.g. Sitch et al., 2008).

1.6.4. Reconstructing human influences on fire

Humans influence fire regimes in the modern day though anthropogenic climate change, land use change and direct fire activities such as ignitions, crop fire and fire management activities that modify the characteristics of wildfires. In general, the impact of early hunter-gathers on fire, through lighting fires and resource use is expected to be have been localised and sporadic (Scharf, 2010; Innes et al., 2013; Gajewski et al., 2019), although evidence from Australia suggests that indigenous fire management may have had a broader impact (e.g. Adeleye et al., 2021; Bird et al., 2024). However, more regional-scale influences on the fire regime are more likely to have been associated with more comprehensive land use changes following the spread of agriculture (Vannière et al., 2011; Zennaro et al., 2015). The differences in timing of the Neolithic across Europe - e.g. ca. 9,100 to 8,100 cal. BP for southern Greece compared to after ca. 6,400 for Great Britain and Ireland (Silva and Vander Linden, 2017) -together with different regional farming practices mean it is important to reconstruct potential human influence in time and space.

There are two main approaches for directly estimating anthropogenic land use change over time. One approach is based on the principle that land use changes can be closely tied to human population, and per capita land use. The second approach aims to reconstruct vegetation patterns using sedimentary records of pollen or other indicators, with these records highlighting changes in landcover.

<u>Landcover changes as a function of population and per capita land use:</u> The shift from foraging to agriculture increased the potential carrying capacity of the land, leading to changes in human settlement patterns and to population growth (Bocquet-Appel and Bar-Yosef, 2008). Prior to the spread of agriculture, population size was likely to have been dependent on climatic conditions, whereas this dependency was reduced once agriculture had become widespread (Palmisano et al., 2021b). As populations increased over time, more land would have been converted to agricultural use, except where technological development allowed more food to be grown in a given area, thus reducing land-use per capita.

There are several modelled estimates of how land cover may have changed based on population and per capita land use in Europe. Most approaches based on this method used a fixed or near constant land use per capita through time (Pongratz et al., 2008; Klein Goldewijk et al., 2011, 2017), although the KK10 estimates (Kaplan et al., 2009) increase land use per capita as a function of population density. Land cover use estimates are therefore almost wholly reliant on population density estimates (e.g. McEvedy and Jones, 1978), with the location of those changes based on assumptions regarding the suitability of land for different types of agriculture. Underlying this approach is remote sensing data from the present, and historical records of land use and population change. The relationship between population and land use is then hindcasted through time. A key source of uncertainty is the change in population through time, with population prior to 1700 essentially an educated guess (Klein Goldewijk et al., 2010). The different methodological approaches generate substantial differences in pre-industrial land use. For example, global estimates of anthropogenic land use in 1,000 cal. BP vary from 18Mkm^2 in KK10 (Kaplan et al., 2011); 5.27Mkm^2 in HYDE 3.2 (Klein Goldewijk et al., 2017); 2.96Mkm^2 in HYDE 3.1 (n.b. 950 cal. BP) (Klein Goldewijk et al., 2010); and 3.95 Mkm^2 in the estimates by Pongratz et al. (2008) (n.b. 900 cal. BP). This has implications for estimates of anthropogenic climate change during the Holocene based on land use and land use change (Harrison et al., 2020).

Pollen and spore-based indicators of human impact: Pollen (and spore) data from sedimentary records have been used to identify human impacts on the environment. In some instances, indicator species have been used in pollen diagrams to provide evidence of the intensity of past land use. For example, Behre (1981a, 1988) identified a range of pollen indicators that have been used in central and western Europe to identify human impact, including cultivars, other species not native to a specific area ("anthropochores"), and native species favoured by human activities (e.g. disturbance, "apophyts"). Cultivar pollen identified included: *Secale,* which is readily identifiable but was only introduced in Europe as a cultivar at a late period and existed as a weed at earlier times; *Triticum*, *Hordeum* and *Avena,* which are identifiable but poorly dispersed; *Linum usitatissimum* and *Vicia faba*, both of which are identifiable; and *Cannabis*, which can be confused with *Humulus* (Behre, 1981). A range of secondary indicators include: *Plantago lanceolata*, which is seen as indicating disturbed grassland and also potentially an indicator of fallow land, but which may be absent in some areas with grazing; *Rumex spp.* which occur in weed communities, but which can also appear in fen vegetation; and Chenopodiaceae, *Artemesia* and *Urtica,* which are associated with nitrogen rich areas in and around habitations, but will also occur naturally in areas rich in nitrogen (Behre, 1981). As well as these primary and secondary indicators, Deza-Araujo et al. (2020) identified a range of semi-quantitative indicators that have been used to identify human pressure, which mostly include groups of species, such as Cultural Indicators - *Plantago lanceolata*-type and Cerealia-type (excluding *Secale*) (Tinner et al., 2003), OJCV - *Olea, Juglans, Castanea, Vitis* (Bevan et al., 2019; Roberts et al., 2019), and the relative abundance of arboreal pollen with respect to non-arboreal pollen (Favre et al., 2008). The performance of these indicators based on archaeological evidence across a range of sites in Europe was mixed, with primary indicators performing well in the areas for which they were developed, but secondary indicators occasionally providing evidence for increasing human impact that was inconsistent with archaeological evidence (Deza-Araujo et al., 2020). In addition to pollen, spores from coprophilous fungi (e.g. *Sporormiella*) have been used to represent grazing in sedimentary records (van Geel et al., 2003; Etienne et al., 2015; Zhang et al., 2021). One of the challenges in the use of spores is separating wildlife and livestock signals (Feranec et al., 2011). Additionally, the number of sedimentary pollen records where measure coprophilous fungi have been measured is limited, making it difficult to apply this indicator at a regional scale.

In general, the use of indicator species to reconstruct human activity is limited by the ability to identify cultivars in the pollen assemblage, the challenge of identifying a human signal from secondary indicators such as fungal spores, and by the inconsistent and limited inclusion of indicator pollen or spores within pollen diagrams.

Vegetation reconstruction approaches have also been used to reconstruct anthropogenic land cover changes using the full pollen assemblage. For instance, the biomisation approach has been adapted to reflect land cover classes rather than biomes ("pseudobiomisation": Fyfe et al., 2010, 2015), and the REVEALS approach used to map open land and Cerealia through time (e.g. Githumbi et al., 2022). However, the amount of agricultural land may be mis-estimated in these approaches because of the difficulty of identifying cultivars other than cereals, the under-representation of cereals in pollen assemblages, or where wild grasses are erroneously identified as cereals. Recently, REVEALS-based vegetation reconstructions have also been used indirectly to infer cumulative human influence through time, by comparing landscape reconstructions to DGVM-generated potential natural vegetation estimates based on climate simulations (Zapolska et al., 2023). However, this approach is dependent on the accuracy of the modelled potential natural vegetation and the ability of the REVEALS reconstructions to accurately reflect the landscape.

<u>Human influence and archaeological radiocarbon:</u> Data-based estimates of population change have been used to identify increasing pressure on the landscape. One approach for inferring population change makes use of radiocarbon dates on archaeological material, with large-scale open-source datasets facilitating analysis (e.g. p3k14c: Bird et al., 2022; XRONOS: Hinz and Roe, 2024). The "dates as data" approach relies on three assumptions in an inferential chain: 1) a larger population would leave a larger quantity of archaeological material; 2) a larger quantity of material would lead to a greater quantity of that material being preserved; and 3) the greater quantity of material would lead to a greater chance that this would be discovered through archaeological study (Rick, 1987). At one level, spatially independent site counts based on available archaeological (radiocarbon) data provide an indication of the relative population in an area, with more sites at a given time implying higher population levels (e.g. Bocquet-Appel et al., 2005, 2009; Mellars and French, 2011). Although the size of the settlement is assumed to be consistent and unchanging through time (Palmisano et al., 2017), this simple metric is intuitive and can be used as a first means of assessing environmental pressure. Alternatively, the use of summed probability distributions (SPDs) of calibrated radiocarbon dates is gaining popularity in archaeology (Williams, 2012). The approach combines radiocarbon

calibration curves into a single summed curve, with peaks taken to represent relatively higher population levels, and troughs representing lower populations (e.g. Fig. 1.8).

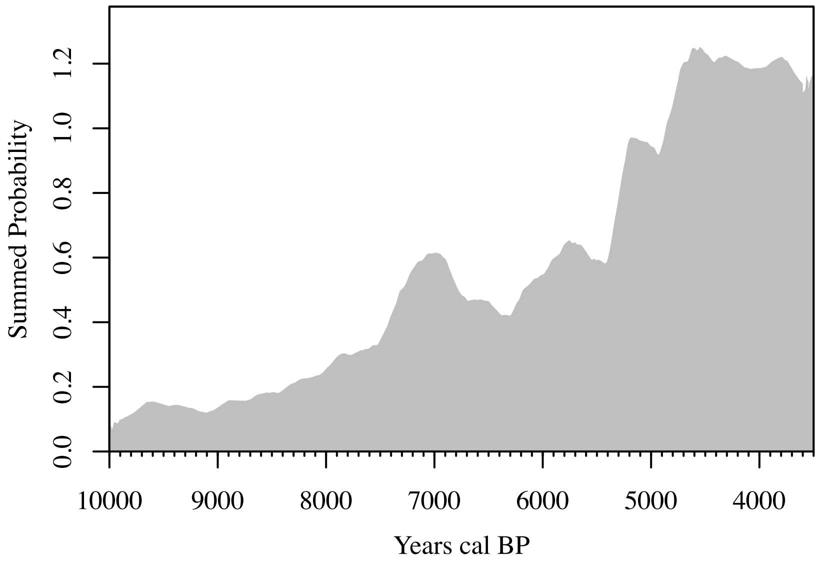

Figure 1.8: Summed probability distribution for Iberia between 10,000 and 3,500 cal. BP, with a running mean of 200 years. Archaeological data from multiple sources (see Sweeney et al. 2021 for details)

Over time there have been multiple methodological developments associated with this approach, and alternative approaches suggested, principally based on addressing potential recognised biases. These biases are mostly associated with direct interpretation of the SPD as a population measure, and include sampling error, heterogeneity in sampling intensity, spatial averaging and non-stationarity, taphonomic loss, and calibration error (Crema, 2022).

Sampling error refers to the question of whether the available radiocarbon data is representative of the population of dates, irrespective of certainty of the relationship between the dates as data approach and populations (Crema, 2022). Whilst the possibility of sampling error is reduced by ensuring sufficient sample numbers – analysis by Williams (2012) suggested a minimum of 500 dates to confidently reproduce SPD population plots – what constitutes a minimum number of samples is dependent on the level of precision required, with a small number of samples sufficient to identify broad trends confidently, but larger numbers needed to address specific spatiotemporal changes (Crema, 2022).

Differences in *sampling intensity* are a function of bias in research effort at a site level. For example, the interest in precisely dating the period of Neolithisation at a site may mean substantially greater numbers radiocarbon dated material from this period (Crema, 2022). Taken as a whole, an SPD for a region may then see a peak in density reflecting this research interest, rather than a true reflection of the underlying population density (Mithen and Wicks, 2021). Although there are approaches to dealing with this bias - binning radiocarbon dates for a site within a certain data range to limit oversampling of an individual site (Shennan et al., 2013; Timpson et al., 2014) is now standard practice – this issue persists in relation to SPD edge effects approaching the present day. Alternative practices that are cheaper and more accurate for dating material, such as cultural dating, are more likely to be employed closer to the present, leading to a sudden reduction in radiocarbon dates (Crema, 2022). This limits the use of SPD-based population analysis towards the present, with different research traditions by region affecting the timing of this artificial drop-off. To counter this issue, the use of actual archaeological site counts, rather than counts based on radiocarbon data, has been used to reflect later changes in population (e.g. Roberts et al., 2019; Kolář et al., 2022).

Whilst heterogeneity in sampling intensity refers to differences in radiocarbon dating effort through time, the challenge associated with *spatial averaging and non-stationarity* refers to differences by location. Due to different research traditions in different regions, associated with differences in wealth, sample design or research interest, the quantity of radiocarbon dates by location can vary substantially, independently from underlying population trends (Crema, 2022). Large-region analysis, combining locations with fundamentally different research histories in terms of radiocarbon, can mean that population signals are dominated by certain areas. Similarly, analysing population trends with SPDs over larger regions assumes population trajectories are essentially the same across the region, potentially obscuring information regarding very different trends (Crema, 2022).

The issue of *taphonomic loss*, such that younger items are more likely to be preserved than older items, has implications for the use of SPDs. Correction formula to take taphonomic loss into account when assessing population changes based on radiocarbon have been proposed (e.g. Surovell et al., 2009; Contreras and Codding, 2024). However, Williams (2012) cautions against the blind application of a correction, which may obscure legitimate trends in occupation.

The final major issue relates to the issue of *calibration effects*. Plateaus within the calibration curve – periods where the radiocarbon age remains relatively stable over a period of calendar years – have been shown to smooth out legitimate peaks within an SPD, as dates falling within these plateaus have flattened probability distributions (Williams, 2012). Alternatively, steeper portions of the calibration curve have the effect of amplifying peaks within the SPD (Williams, 2012). Methods designed to reduce the potential impact of this effect, such as smoothing the SPD through time, do not fundamentally address this issue (Crema, 2022).

A range of different approaches to tackle these issues have been proposed (Crema, 2022). For example, to counter issues with calibration effects and sampling error, the *OxCal* Kernel Density Estimation (KDE) approach presents an alternative to SPDs, displaying uncertainty measures based on different Markov chain Monte Carlo (MCMC) states of sampled radiocarbon data (Ramsey, 2017). The general approach: 1) samples the radiocarbon data; 2) calibrates the sampled dates; 3) samples a calendar date from each calibrated probability distribution; 4) runs a KDE with defined shape (i.e. normal, exponential etc.) and bandwidth defined by Bayesian inference and; 5) repeats the process multiple times to develop an envelope of possible KDEs (Ramsey, 2017). Another approach, developed by Shennan et al. (2013) and refined by Timpson et al. (2014), tests specific hypotheses regarding the shape of the population growth function. This approach simulates radiocarbon dates under a predicted null model of demographic change, calibrates these radiocarbon dates, and then compares this to the generated SPD to test the quality of the fitted model, and identify periods of rapid population growth and decline above or below the generated envelope of simulated SPDs. This approach helps with calibration and sampling effects, by emulating these consequences within the MCMC routine (Crema, 2022) and will by definition account for the issue of taphonomic loss in testing for an exponential null model (Timpson et al., 2014). A final example approach, described within the R package *nimbleCarbon* (Crema and Shoda, 2021), forgoes the explicit testing of a modelled growth rate under the null hypothesis, using Bayesian inference to construct a model of population change based on maximum likelihood. Under this approach, the population growth rate is estimated by the fitted model, with each calibration date having a posterior probability (Crema and Shoda, 2021)

Spatial estimates of population change and the spread of agriculture: Radiocarbon dates can also be used as a means to identify population changes spatially, using bivariate KDE (e.g. Collard et al., 2010; Crombé et al., 2011; Grove, 2011; Manning and Timpson, 2014; Chaput et al., 2015). Although regional SPD analysis can help provide a spatial dimension to population analysis, smaller sample sizes from dividing the data increases the chance of sampling error, as well as raising questions as to where the appropriate border for each region should be (Manning & Timpson, 2014). Under this approach, first formally described by Collard et al., (2010) for radiocarbon dates in Britain, each sample is assumed to represent an undefined level of population density across space and time, with a kernel around the point representing spatial extent of the population density. The spatial data is then binned into defined periods or time-slices, to identify spatial changes in population, and by extension, "hot-spots" for land-use change through time. However, in practice the level of data required to generate high resolution spatiotemporal maps limits the range of this approach.

Radiocarbon dates have also been used to explicitly identify the start of agriculture, based on the dating of materials from Neolithic contexts (e.g. Isern et al., 2012; Silva and Vander Linden, 2017). As the start of agriculture might reasonably be assumed to represent the feasible start point in time of broad-scale land-use changes, this approach also has value in investigating human influences.

1.6.5. Limitations associated with reconstructions based on empirical data

Subsequent analysis in this thesis brings together differing approaches to reconstructing variables though time, based on the sedimentary charcoal and pollen data, and archaeological radiocarbon data used. However, it is important to acknowledge and re-emphasise some of the general limitations associated with reconstructions of this nature. These limitations can be grouped into chronological uncertainties, data interpretation issues, spatial uncertainties and dataset quality issues.

Both the sedimentary data and archaeological data are subject to uncertainty regarding the specific chronology of samples. The age-depth modelling process for sedimentary samples (generally) relies on dated material within the sediment core, which itself is subject to dating uncertainty inherent to both the measurement process (e.g. radiocarbon dating error) and subsequent calibration of dates to calendar years. Additionally, despite the application of complex models utilising Bayesian statistics (e.g. Ramsey, 2008; Blaauw and Christen, 2011), sedimentation rates are estimates, limiting the chronological precision throughout the core. Whilst models can provide error estimates, typically composites of records are based on median estimated ages. Finally, the nature of the sampling process, whereby small sections of each core is sampled to assess charcoal or pollen, inherently reflects a period rather than a moment in time. The length of this period is dependent on both the measurement interval and sedimentation rate, and affects the chronological precision of the sample. However, when longer term trends are of interest, or sufficient record numbers are available to smooth out chronological uncertainty, this issue may be less problematic. Although archaeological radiocarbon data is individually measured, the same issues of radiocarbon dating error and calibration uncertainty apply.

Reconstructions based on empirical data are dependent on the interpretation of the data and underlying methodological approaches. Relationships between "proxies" utilised to represent reconstructed variables are inherently uncertain, due to stochasticity, uncertain relationships, methological assumptions or noise within the data. Sedimentary charcoal data, for example, is a broad measure of landscape burning through time, reflecting a combination of fire regime elements: charcoal production varies depending on fire size, intensity and vegetation types (e.g. Patterson et al., 1987; Higuera et al., 2011). Interpreting charcoal data in relation to fire is then challenging, as changes in the record may reflect multiple fire regime elements changing in concert. Non-contiguous sampling of the sedimentary core, as is often the case for pollen slide analysis, can pose particular problems for fire reconstructions, where periods of higher or lower fire activity may be missed. As such, the record of fire may be incomplete, despite sampling at regular intervals. The link between pollen data and vegetation depends upon the methodology applied, and the assumptions utilised. For example, estimates of RPP used in the LRA generally assume that the RPP value is consistent for each taxon, but differences by species mixes (e.g. *Quercus* includes *Quercus robur* vs *Quercus petrea*) and by geographical location even for the same species may yield different RPP values (Li, 2018; Bunting and Farrell, 2022), impacting subsequent reconstructions. For population change reconstructions based on archaeological data, some researchers caution against the use of the "dates as data" method in general because of the challenges mentioned above, despite widespread application within the archaeological community (see, e.g. Attenbrow and Hiscock, 2015; Carleton and Groucutt, 2021). For each dataset, differences in record lengths potentially affect the consistency of record composites. For example, particular research interest in the Neolithic may artificially lead to increased quantities of radiocarbon dates for this period in a given location, giving the impression of a boost population in a region (Torfing, 2015). Similarly, z-score composite values of charcoal influx may be impacted by the inclusion or exclusion of records through time, especially when the region in question contains few records.

Spatial uncertainty refers to the applicable area associated with each record. For sedimentary charcoal, long distance transport, particularly over open areas can muddy the accumulation signal (Whitlock and Larsen, 2001). Although methods to correct for pollen transport differences help reduce the issue of long-distance transport for vegetation reconstructions, the source area for vegetation reconstructions is never completely known. Similarly, the quantity of archaeological radiocarbon data gives an indication of the population change at a given site, but the extent to which sites can be pooled in space to give sub-regional or regional population changes is uncertain. This issue of pooling records is also a challenge for charcoal data, where measurement differences affect the ability to compare absolute values of fire between sites.

Finally, there are issues associated with the spatiotemporal coverage of the datasets. As previously alluded to, both the sedimentary charcoal and pollen have comparatively broad spatial coverage in Europe. Nevertheless, there are inevitably gaps in the data, with, for example, limited lake and bog sites available for northern France and the Benelux within the RPD (Harrison et al, 2022). The availability and consistency of archaeological radiocarbon data has greatly improved with the publication of the p3k14c (Bird et al., 2022) and XRONOS (Hinz and Roe, 2024) datasets, but there are clear gaps in data in eastern Europe. These gaps reflect differences in research effort and suitable sites (e.g. lakes) for sedimentary records. Additionally, gaps may reflect the comprehensiveness of the datasets: each record reflects substantial research effort, and whilst it is a credit to contributing authors that their data has been made available in comprehensive open-access datasets, not all data are included in such complications. As the quantity of data can minimise some of the aforementioned uncertainties - although note that composites of data can reduce the ability to detect legitimate changes – periods or locations with data gaps are therefore more subject to these issues.

1.7. References

Abatzoglou, J. T., Williams, A. P., Boschetti, L., Zubkova, M., and Kolden, C. A.: Global patterns of interannual climate–fire relationships, Glob Chang Biol, 24, 5164–5175, https://doi.org/10.1111/gcb.14405, 2018.

Abatzoglou, J. T., Battisti, D. S., Williams, A. P., Hansen, W. D., Harvey, B. J., and Kolden, C. A.: Projected increases in western US forest fire despite growing fuel constraints, Commun Earth Environ, 2, 227, https://doi.org/10.1038/s43247-021-00299-0, 2021.

Accatino, F. and De Michele, C.: Humid savanna–forest dynamics: A matrix model with vegetation–fire interactions and seasonality, Ecol Modell, 265, 170–179, https://doi.org/10.1016/j.ecolmodel.2013.05.022, 2013.

Adeleye, M. A., Haberle, S. G., Connor, S. E., Stevenson, J., and Bowman, D. M. J. S.: Indigenous Fire-Managed Landscapes in Southeast Australia during the Holocene—New Insights from the Furneaux Group Islands, Bass Strait, Fire, 4, 17, https://doi.org/10.3390/fire4020017, 2021.

Adolf, C., Wunderle, S., Colombaroli, D., Weber, H., Gobet, E., Heiri, O., van Leeuwen, J. F. N., Bigler, C., Connor, S. E., Gałka, M., La Mantia, T., Makhortykh, S., Svitavská-Svobodová, H., Vannière, B., and Tinner, W.: The sedimentary and remote-sensing reflection of biomass burning in Europe, Global Ecol Biogeogr, 27, 199–212, https://doi.org/10.1111/geb.12682, 2018.

Alencar, A. A., Brando, P. M., Asner, G. P., and Putz, F. E.: Landscape fragmentation, severe drought, and the new Amazon forest fire regime, Ecol Appl, 25, https://doi.org/10.1890/14-1528.1, 2015.

Allen, J. R. M. and Huntley, B.: Last Interglacial palaeovegetation, palaeoenvironments and chronology: a new record from Lago Grande di Monticchio, southern Italy, Quat Sci Rev, 28, 1521–1538, https://doi.org/10.1016/j.quascirev.2009.02.013, 2009.

Allen, J. R. M., Watts, W. A., and Huntley, B.: Weichselian palynostratigraphy, palaeovegetation and palaeoenvironment; the record from Lago Grande di Monticchio, southern Italy, Quat Int, 73–74, 91–110, https://doi.org/10.1016/S1040-6182(00)00067-7, 2000.

Alvarado, S. T., Andela, N., Silva, T. S. F., and Archibald, S.: Thresholds of fire response to moisture and fuel load differ between tropical savannas and grasslands across continents, Global Ecol Biogeogr, 29, 331–344, https://doi.org/10.1111/geb.13034, 2020.

Anchukaitis, K. J.: Tree Rings Reveal Climate Change Past, Present, and Future, Proc Am Philos Soc, 161, 244–263, 2017.

Andela, N. and van der Werf, G. R.: Recent trends in African fires driven by cropland expansion and El Niño to La Niña transition, Nat Clim Chang, 4, 791–795, https://doi.org/10.1038/nclimate2313, 2014.

Andela, N., Morton, D. C., Giglio, L., Chen, Y., van der Werf, G. R., Kasibhatla, P. S., DeFries, R. S., Collatz, G. J., Hantson, S., Kloster, S., Bachelet, D., Forrest, M., Lasslop, G., Li, F., Mangeon, S., Melton, J. R., Yue, C., and Randerson, J. T.: A human-driven decline in global burned area, Science, 356, 1356–1362, https://doi.org/10.1126/science.aal4108, 2017.

Andersen, K. K., Azuma, N., Barnola, J. M., Bigler, M., Biscaye, P., Caillon, N., Chappellaz, J., Clausen, H. B., Dahl-Jensen, D., Fischer, H., Flückiger, J., Fritzsche, D., Fujii, Y., Goto-Azuma, K., Grønvold, K., Gundestrup, N. S., Hansson, M., Huber, C., Hvidberg, C. S., Johnsen, S. J., Jonsell, U., Jouzel, J., Kipfstuhl, S., Landais, A., Leuenberger, M., Lorrain, R., Masson-Delmotte, V., Miller, H., Motoyama, H., Narita, H., Popp, T., Rasmussen, S. O., Raynaud, D., Rothlisberger, R., Ruth, U., Samyn, D., Schwander, J., Shoji, H., Siggard-Andersen, M. L., Steffensen, J. P., Stocker, T., Sveinbjörnsdóttir, A. E., Svensson, A., Takata, M., Tison, J. L., Thorsteinsson, T., Watanabe, O., Wilhelms, F., and White, J. W. C.: High-resolution record of Northern Hemisphere climate extending into the last interglacial period, Nature, https://doi.org/10.1038/nature02805, 2004.

Archibald, S., Lehmann, C. E. R., Gómez-Dans, J. L., and Bradstock, R. A.: Defining pyromes and global syndromes of fire regimes, Proc Natl Acad Sci U S A, 110, 6442–6447, https://doi.org/10.1073/pnas.1211466110, 2013.

Archibald, S., Lehmann, C. E. R., Belcher, C. M., Bond, W. J., Bradstock, R. A., Daniau, A.-L., Dexter, K. G., Forrestel, E. J., Greve, M., He, T., Higgins, S. I., Hoffmann, W. A., Lamont, B. B., McGlinn, D. J., Moncrieff, G. R., Osborne, C. P., Pausas, J. G., Price, O., Ripley, B. S., Rogers, B. M., Schwilk, D. W., Simon, M. F., Turetsky, M. R., Van der Werf, G. R., and Zanne, A. E.: Biological and geophysical feedbacks with fire in the Earth system, Environ Res Lett, 13, 33003, https://doi.org/10.1088/1748-9326/aa9ead, 2018.

Arno, S. F. and Brown, J. K.: Overcoming the paradox in managing wildland fire, Western Wildlands, 17, 40–46, 1991.

Attenbrow, V. and Hiscock, P.: Dates and demography: are radiometric dates a robust proxy for long-term prehistoric demographic change?, Archaeology in Oceania, 50, 30–36, https://doi.org/10.1002/arco.5052, 2015.

Aubry-Wake, C., Bertoncini, A., and Pomeroy, J. W.: Fire and Ice: The Impact of Wildfire-Affected Albedo and Irradiance on Glacier Melt, Earths Future, 10, https://doi.org/10.1029/2022EF002685, 2022.

Balch, J. K., Bradley, B. A., Abatzoglou, J. T., Nagy, R. C., Fusco, E. J., and Mahood, A. L.: Human-started wildfires expand the fire niche across the United States, P Natl Acad Sci USA, 114, https://doi.org/10.1073/pnas.1617394114, 2017.

Banerjee, T.: Impacts of Forest Thinning on Wildland Fire Behavior, Forests, 11, 918, https://doi.org/10.3390/f11090918, 2020.

Barlow, J., Berenguer, E., Carmenta, R., and França, F.: Clarifying Amazonia's burning crisis, Glob Chang Biol, 26, https://doi.org/10.1111/gcb.14872, 2020.

Bartlein, P. J., Harrison, S. P., Brewer, S., Connor, S., Davis, B. A. S., Gajewski, K., Guiot, J., Harrison-Prentice, T. I., Henderson, A., Peyron, O., Prentice, I. C., Scholze, M., Seppä, H., Shuman, B., Sugita, S., Thompson, R. S., Viau, A. E., Williams, J., and Wu, H.: Pollen-based continental climate reconstructions at 6 and 21 ka: A global synthesis, Clim Dyn, 37, 775–802, https://doi.org/10.1007/s00382-010-0904-1, 2011.

Beckage, B., Gross, L. J., and Platt, W. J.: Grass feedbacks on fire stabilize savannas, Ecol Modell, 222, 2227–2233, https://doi.org/10.1016/j.ecolmodel.2011.01.015, 2011.

te Beest, M., Cromsigt, J. P. G. M., Ngobese, J., and Olff, H.: Managing invasions at the cost of native habitat? An experimental test of the impact of fire on the invasion of Chromolaena odorata in a South African savanna, Biol Invasions, 14, 607–618, https://doi.org/10.1007/s10530-011-0102-z, 2012.

Behre, K.-E.: The interpretation of anthropogenic indicators in pollen diagrams, Pollen et spores, 23(2), 225–245, 1981.

Behre, K.-E.: The rôle of man in European vegetation history, in: Vegetation history, Springer Netherlands, Dordrecht, 633–672, https://doi.org/10.1007/978-94-009-3081-0_17, 1988.

Betts, R. A.: Offset of the potential carbon sink from boreal forestation by decreases in surface albedo, Nature, 408, 187–190, https://doi.org/10.1038/35041545, 2000.

Bevan, A., Colledge, S., Fuller, D., Fyfe, R. M., Shennan, S., and Stevens, C.: Holocene fluctuations in human population demonstrate repeated links to food production and climate, Proc Natl Acad Sci USA, 114, E10524–E10531, https://doi.org/10.1073/pnas.1709190114, 2017.

Bevan, A., Palmisano, A., Woodbridge, J., Fyfe, R. M., Roberts, C. N., and Shennan, S.: The changing face of the Mediterranean – Land cover, demography and environmental change: Introduction and overview, Holocene, 29, https://doi.org/10.1177/0959683619826688, 2019.

Bird, D., Miranda, L., Vander Linden, M., Robinson, E., Bocinsky, R. K., Nicholson, C., Capriles, J. M., Finley, J. B., Gayo, E. M., Gil, A., d'Alpoim Guedes, J., Hoggarth, J. A., Kay, A., Loftus, E., Lombardo, U., Mackie, M., Palmisano, A., Solheim, S., Kelly, R. L., and Freeman, J.: p3k14c, a synthetic global database of archaeological radiocarbon dates, Sci Data, 9, 27, https://doi.org/10.1038/s41597-022-01118-7, 2022.

Bird, M. I., Brand, M., Comley, R., Fu, X., Hadeen, X., Jacobs, Z., Rowe, C., Wurster, C. M., Zwart, C., and Bradshaw, C. J. A.: Late Pleistocene emergence of an anthropogenic fire regime in Australia's tropical savannahs, Nat Geosci, 17, 233–240, https://doi.org/10.1038/s41561-024-01388-3, 2024.

Birks, H. J. B.: Challenges in the presentation and analysis of plant-macrofossil stratigraphical data, Veg Hist Archaeobot, 23, 309–330, https://doi.org/10.1007/s00334-013-0430-2, 2014.

Birks, H. J. B., Heiri, O., Seppä, H., and Bjune, A. E.: Strengths and Weaknesses of Quantitative Climate Reconstructions Based on Late-Quaternary Biological Proxies, The Open Ecology Journal, 3, 68–110, https://doi.org/10.2174/1874213001003020068, 2010.

Bistinas, I., Harrison, S. P., Prentice, I. C., and Pereira, J. M. C.: Causal relationships versus emergent patterns in the global controls of fire frequency, Biogeosciences, 11, 5087–5101, https://doi.org/10.5194/bg-11-5087-2014, 2014.

Blaauw, M. and Christen, J. A.: Flexible paleoclimate age-depth models using an autoregressive gamma process, Bayesian Anal, 6, https://doi.org/10.1214/11-BA618, 2011.

Blarquez, O. and Carcaillet, C.: Fire, fuel composition and resilience threshold in subalpine ecosystem, PLoS One, 5, https://doi.org/10.1371/journal.pone.0012480, 2010.

Blarquez, O., Bremond, L., and Carcaillet, C.: Holocene fires and a herb-dominated understorey track wetter climates in subalpine forests, J Ecol, 98, 1358–1368, https://doi.org/10.1111/j.1365-2745.2010.01721.x, 2010.

Bocquet-Appel, J.-P. and Bar-Yosef, O.: The Neolithic Demographic Transition and its Consequences, Springer Netherlands, Dordrecht, https://doi.org/10.1007/978-1-4020-8539-0, 2008.

Bocquet-Appel, J.-P., Demars, P.-Y., Noiret, L., and Dobrowsky, D.: Estimates of Upper Palaeolithic meta-population size in Europe from archaeological data, J Archaeol Sci, 32, 1656–1668, https://doi.org/10.1016/j.jas.2005.05.006, 2005.

Bocquet-Appel, J.-P., Naji, S., Linden, M. Vander, and Kozlowski, J. K.: Detection of diffusion and contact zones of early farming in Europe from the space-time distribution of 14C dates, J Archaeol Sci, 36, 807–820, https://doi.org/10.1016/j.jas.2008.11.004, 2009.

Bond, W. J.: What Limits Trees in C 4 Grasslands and Savannas?, Annu Rev Ecol Evol Syst, 39, 641–659, https://doi.org/10.1146/annurev.ecolsys.39.110707.173411, 2008.

Bond, W. J. and Keeley, J. E.: Fire as a global "herbivore": The ecology and evolution of flammable ecosystems, Trends Ecol Evol, 20, 387–394, https://doi.org/10.1016/j.tree.2005.04.025, 2005.

Bond, W. J. and Midgley, J. J.: Kill Thy Neighbour: An Individualistic Argument for the Evolution of Flammability, Oikos, 73, 79, https://doi.org/10.2307/3545728, 1995.

Bond, W. J., Woodward, F. I., and Midgley, G. F.: The global distribution of ecosystems in a world without fire, New Phytol, https://doi.org/10.1111/j.1469-8137.2004.01252.x, 2005.

Bowman, D. M. J. S. and Murphy, B. P.: Fire and biodiversity, in: Conservation Biology for All, edited by: Sodhi, N. S. and Ehrlich, P. R., Oxford University Press, Oxford, 163–180, https://doi.org/10.1093/acprof:oso/9780199554232.003.0010, 2010.

Bowman, D. M. J. S., Balch, J. K., Artaxo, P., Bond, W. J., Carlson, J. M., Cochrane, M. A., D'Antonio, C. M., DeFries, R. S., Doyle, J. C., Harrison, S. P., Johnston, F. H., Keeley, J. E., Krawchuk, M. A., Kull, C. A., Marston, J. B., Moritz, M. A., Prentice, I. C., Roos, C. I., Scott, A. C., Swetnam, T. W., van der Werf, G. R., and Pyne, S. J.: Fire in the Earth System, Science, 324, 481–484, https://doi.org/10.1126/science.1163886, 2009.

Bowman, D. M. J. S., Balch, J., Artaxo, P., Bond, W. J., Cochrane, M. A., D'Antonio, C. M., DeFries, R., Johnston, F. H., Keeley, J. E., Krawchuk, M. A., Kull, C. A., Mack, M., Moritz, M. A., Pyne, S., Roos, C. I., Scott, A. C., Sodhi, N. S., and Swetnam, T. W.: The human dimension of fire regimes on Earth, J Biogeogr, 38, 2223–2236, https://doi.org/10.1111/j.1365-2699.2011.02595.x, 2011.

ter Braak, C. J. F. and Juggins, S.: Weighted averaging partial least squares regression (WA-PLS): an improved method for reconstructing environmental variables from species assemblages, Hydrobiologia, 269–270, 485–502, https://doi.org/10.1007/BF00028046, 1993.

ter Braak, C. J. F. and Looman, C. W. N.: Weighted averaging, logistic regression and the Gaussian response model, Vegetatio, 65, 3–11, https://doi.org/10.1007/BF00032121, 1986.

Bradshaw, R. H. W. and Webb, T.: Relationships between Contemporary Pollen and Vegetation Data from Wisconsin and Michigan, USA, Ecology, 66, 721–737, https://doi.org/10.2307/1940533, 1985.

Brando, P., Macedo, M., Silvério, D., Rattis, L., Paolucci, L., Alencar, A., Coe, M., and Amorim, C.: Amazon wildfires: Scenes from a foreseeable disaster, Flora, 268, https://doi.org/10.1016/j.flora.2020.151609, 2020.

Brenner, M. and Kenney, W.F: Dating wetland sediment cores, in: Methods in biogeochemistry of wetlands, Soil Science Society of America, Madison, Wisconsin, USA, 2013.

Bright, R. M., Zhao, K., Jackson, R. B., and Cherubini, F.: Quantifying surface albedo and other direct biogeophysical climate forcings of forestry activities, Glob Chang Biol, 21, 3246–3266, https://doi.org/10.1111/gcb.12951, 2015.

Brodie, E. G., Knapp, E. E., Brooks, W. R., Drury, S. A., and Ritchie, M. W.: Forest thinning and prescribed burning treatments reduce wildfire severity and buffer the impacts of severe fire weather, Fire Ecol, 20, 17, https://doi.org/10.1186/s42408-023-00241-z, 2024.

Brooks, M. L., D'Antonio, C. M., Richardson, D. M., Grace, J. B., Keeley, J. E., DiTomaso, J. M., Honns, Ri. J., Pellant, M., and Pyke, D.: Effects of Invasive Alien Plants on Fire Regimes, Bioscience, 54, 677, https://doi.org/10.1641/0006-3568(2004)054[0677:eoiapo]2.0.co;2, 2006.

Brossier, B., Oris, F., Finsinger, W., Asselin, H., Bergeron, Y., and Ali, A. A.: Using tree-ring records to calibrate peak detection in fire reconstructions based on sedimentary charcoal records, Holocene, 24, 635–645, https://doi.org/10.1177/0959683614526902, 2014.

Brovkin, V.: Climate-vegetation interaction, Journal de Physique IV (Proceedings), 12, 57–72, https://doi.org/10.1051/jp4:20020452, 2002.

Brown, K. J. and Giesecke, T.: Holocene fire disturbance in the boreal forest of central Sweden, Boreas, 43, 639–651, https://doi.org/10.1111/bor.12056, 2014.

Buma, B., Hayes, K., Weiss, S., and Lucash, M.: Short-interval fires increasing in the Alaskan boreal forest as fire self-regulation decays across forest types, Sci Rep, 12, 4901, https://doi.org/10.1038/s41598-022-08912-8, 2022.

Büntgen, U., Allen, K., Anchukaitis, K. J., Arseneault, D., Boucher, É., Bräuning, A., Chatterjee, S., Cherubini, P., Churakova, O. V., Corona, C., Gennaretti, F., Grießinger, J., Guillet, S., Guiot, J., Gunnarson, B., Helama, S., Hochreuther, P., Hughes, M. K., Huybers, P., Kirdyanov, A. V., Krusic, P. J., Ludescher, J., Meier, W. J.-H., Myglan, V. S., Nicolussi, K., Oppenheimer, C., Reinig, F., Salzer, M. W., Seftigen, K., Stine, A. R., Stoffel, M., St. George, S., Tejedor, E., Trevino, A., Trouet, V., Wang, J., Wilson, R., Yang, B., Xu, G., and Esper, J.: The influence of decision-making in tree ring-based climate reconstructions, Nat Commun, 12, 3411, https://doi.org/10.1038/s41467-021-23627-6, 2021.

Bunting, M. J. and Farrell, M.: Do Local Habitat Conditions Affect Estimates of Relative Pollen Productivity and Source Area in Heathlands?, Front Ecol Evol, 10, https://doi.org/10.3389/fevo.2022.787345, 2022.

Bunting, M. J. and Middleton, R.: Equifinality and uncertainty in the interpretation of pollen data: the Multiple Scenario Approach to reconstruction of past vegetation mosaics, Holocene, 19, 799–803, https://doi.org/10.1177/0959683609105304, 2009.

Bunting, M. J., Farrell, M., Broström, A., Hjelle, K. L., Mazier, F., Middleton, R., Nielsen, A. B., Rushton, E., Shaw, H., and Twiddle, C. L.: Palynological perspectives on vegetation survey: a critical step for model-based reconstruction of Quaternary land cover, Quat Sci Rev, 82, 41–55, https://doi.org/10.1016/j.quascirev.2013.10.006, 2013.

Burjachs, F. and Expósito, I.: Charcoal and pollen analysis: Examples of Holocene fire dynamics in Mediterranean Iberian Peninsula, Catena (Amst), 135, 340–349, https://doi.org/10.1016/j.catena.2014.10.006, 2015.

Burton, C., Kelley, D. I., Jones, C. D., Betts, R. A., Cardoso, M., and Anderson, L.: South American fires and their impacts on ecosystems increase with continued emissions, Climate Resilience and Sustainability, 1, https://doi.org/10.1002/cli2.8, 2022.

Burton, J. E., Cawson, J. G., Filkov, A. I., and Penman, T. D.: Leaf traits predict global patterns in the structure and flammability of forest litter beds, J Ecol, 109, 1344–1355, https://doi.org/10.1111/1365-2745.13561, 2021.

Byers, B. A., Ash, S. R., Chaney, D., and DeSoto, L.: First known fire scar on a fossil tree trunk provides evidence of Late Triassic wildfire, Palaeogeogr Palaeoclimatol Palaeoecol, 411, 180–187, https://doi.org/10.1016/j.palaeo.2014.06.009, 2014.

Byers, B. A., DeSoto, L., Chaney, D., Ash, S. R., Byers, A. B., Byers, J. B., and Stoffel, M.: Fire-scarred fossil tree from the Late Triassic shows a pre-fire drought signal, Sci Rep, 10, 20104, https://doi.org/10.1038/s41598-020-77018-w, 2020.

Cain, S. A.: Pollen analysis as a paleo-ecological research method, The Botanical Review, 5, 627–654, https://doi.org/10.1007/BF02871650, 1939.

Calcote, R.: Pollen Source Area and Pollen Productivity: Evidence from Forest Hollows, J Ecol, 83, 591, https://doi.org/10.2307/2261627, 1995.

Canadell, J. G., Meyer, C. P., Cook, G. D., Dowdy, A., Briggs, P. R., Knauer, J., Pepler, A., and Haverd, V.: Multi-decadal increase of forest burned area in Australia is linked to climate change, Nat Commun, 12, 6921, https://doi.org/10.1038/s41467-021-27225-4, 2021.

Carcaillet, C.: Are Holocene wood-charcoal fragments stratified in alpine and subalpine soils? Evidence from the Alps based on AMS 14C dates, Holocene, 11, 231–242, https://doi.org/10.1191/095968301674071040, 2001.

Carleton, W. C. and Groucutt, H. S.: Sum things are not what they seem: Problems with point-wise interpretations and quantitative analyses of proxies based on aggregated radiocarbon dates, Holocene, 31, 630–643, https://doi.org/10.1177/0959683620981700, 2021.

Cassell, B. A., Scheller, R. M., Lucash, M. S., Hurteau, M. D., and Loudermilk, E. L.: Widespread severe wildfires under climate change lead to increased forest homogeneity in dry mixed-conifer forests, Ecosphere, 10, https://doi.org/10.1002/ecs2.2934, 2019.

Chaput, M. A., Kriesche, B., Betts, M., Martindale, A., Kulik, R., Schmidt, V., and Gajewski, K.: Spatiotemporal distribution of Holocene populations in North America, P Natl Acad Sci USA, 112, https://doi.org/10.1073/pnas.1505657112, 2015.

Charles-Dominique, T., Midgley, G. F., and Bond, W. J.: Fire frequency filters species by bark traits in a savanna–forest mosaic, J Veg Sci, 28, 728–735, https://doi.org/10.1111/jvs.12528, 2017.

Cheddadi, R., Yu, G., Guiot, J., Harrison, S. P., and Prentice, I. C.: The climate of Europe 6000 years ago, Clim Dyn, 13, 1–9, https://doi.org/10.1007/s003820050148, 1996.

Chen, A.: Evaluating the relationships between wildfires and drought using machine learning, Int J Wildland Fire, 31, 230–239, https://doi.org/10.1071/WF21145, 2022.

Chen, Y., Hall, J., van Wees, D., Andela, N., Hantson, S., Giglio, L., van der Werf, G. R., Morton, D. C., and Randerson, J. T.: Multi-decadal trends and variability in burned area from the fifth version of the Global Fire Emissions Database (GFED5), Earth Syst Sci Data, 15, 5227–5259, https://doi.org/10.5194/essd-15-5227-2023, 2023.

Chevalier, M., Davis, B. A. S., Heiri, O., Seppä, H., Chase, B. M., Gajewski, K., Lacourse, T., Telford, R. J., Finsinger, W., Guiot, J., Kühl, N., Maezumi, S. Y., Tipton, J. R., Carter, V. A., Brussel, T., Phelps, L. N., Dawson, A., Zanon, M., Vallé, F., Nolan, C., Mauri, A., de Vernal, A., Izumi, K., Holmström, L., Marsicek, J., Goring, S., Sommer, P. S., Chaput, M., and Kupriyanov, D.: Pollen-based climate reconstruction techniques for late Quaternary studies, Earth Sci Rev, 210, https://doi.org/10.1016/j.earscirev.2020.103384, 2020.

Chuvieco, E., Aguado, I., Salas, J., García, M., Yebra, M., and Oliva, P.: Satellite Remote Sensing Contributions to Wildland Fire Science and Management, Current Forestry Reports, 6, 81–96, https://doi.org/10.1007/s40725-020-00116-5, 2020.

Clark, J. S. and Royall, P. D.: Local and Regional Sediment Charcoal Evidence for Fire Regimes in Presettlement North-Eastern North America, J Ecol, 84, 365, https://doi.org/10.2307/2261199, 1996.

Clarke, H., Gibson, R., Cirulis, B., Bradstock, R. A., and Penman, T. D.: Developing and testing models of the drivers of anthropogenic and lightning-caused wildfire ignitions in south-eastern Australia, J Environ Manage, 235, 34–41, https://doi.org/10.1016/j.jenvman.2019.01.055, 2019.

Clarke, P. J., Lawes, M. J., Midgley, J. J., Lamont, B. B., Ojeda, F., Burrows, G. E., Enright, N. J., and Knox, K. J. E.: Resprouting as a key functional trait: How buds, protection and resources drive persistence after fire, New Phytol, 197, 19–35, https://doi.org/10.1111/nph.12001, 2013.

Clear, J. L., Molinari, C., and Bradshaw, R. H. W.: Holocene fire in Fennoscandia and Denmark, Int J Wildland Fire, 23, 781, https://doi.org/10.1071/WF13188, 2014.

Collard, M., Edinborough, K., Shennan, S., and Thomas, M. G.: Radiocarbon evidence indicates that migrants introduced farming to Britain, J Archaeol Sci, 37, https://doi.org/10.1016/j.jas.2009.11.016, 2010.

Collins, K. M., Price, O. F., and Penman, T. D.: Spatial patterns of wildfire ignitions in south-eastern Australia, Int J Wildland Fire, 24, 1098, https://doi.org/10.1071/WF15054, 2015.

Collins, L., Clarke, H., Clarke, M. F., McColl Gausden, S. C., Nolan, R. H., Penman, T., and Bradstock, R.: Warmer and drier conditions have increased the potential for large and severe fire seasons across south-eastern Australia, Global Ecol Biogeogr, 31, 1933–1948, https://doi.org/10.1111/geb.13514, 2022.

Colombaroli, D. and Gavin, D. G.: Highly episodic fire and erosion regime over the past 2,000 y in the Siskiyou Mountains, Oregon, Proc Natl Acad Sci USA, 107, 18909–18914, https://doi.org/10.1073/pnas.1007692107, 2010.

Comas-Bru, L., Harrison, S. P., Werner, M., Rehfeld, K., Scroxton, N., and Veiga-Pires, C.: Evaluating model outputs using integrated global speleothem records of climate change since the last glacial, Clim Past, 15, 1557–1579, https://doi.org/10.5194/cp-15-1557-2019, 2019.

Conedera, M., Tinner, W., Neff, C., Meurer, M., Dickens, A. F., and Krebs, P.: Reconstructing past fire regimes: methods, applications, and relevance to fire management and conservation, Quat Sci Rev, 28, 555–576, https://doi.org/10.1016/j.quascirev.2008.11.005, 2009.

Connor, S. E., Vannière, B., Colombaroli, D., Anderson, R. S., Carrión, J. S., Ejarque, A., Gil Romera, G., González-Sampériz, P., Hoefer, D., Morales-Molino, C., Revelles, J., Schneider, H., van der Knaap, W. O., van Leeuwen, J. F., and Woodbridge, J.: Humans take control of fire-driven diversity changes in Mediterranean Iberia's vegetation during the mid–late Holocene, Holocene, 29, 886–901, https://doi.org/10.1177/0959683619826652, 2019.

Contreras, D. A. and Codding, B. F.: Landscape Taphonomy Predictably Complicates Demographic Reconstruction, J Archaeol Method Theory, 31, 1102–1128, https://doi.org/10.1007/s10816-023-09634-5, 2024.

Conway, H., Gades, A., and Raymond, C. F.: Albedo of dirty snow during conditions of melt, Water Resour Res, 32, 1713–1718, https://doi.org/10.1029/96WR00712, 1996.

Coop, J. D., Parks, S. A., Stevens-Rumann, C. S., Crausbay, S. D., Higuera, P. E., Hurteau, M. D., Tepley, A., Whitman, E., Assal, T., Collins, B. M., Davis, K. T., Dobrowski, S., Falk, D. A., Fornwalt, P. J., Fulé, P. Z., Harvey, B. J., Kane, V. R., Littlefield, C. E., Margolis, E. Q., North, M., Parisien, M.-A., Prichard, S., and Rodman, K. C.: Wildfire-Driven Forest Conversion in Western North American Landscapes, Bioscience, 70, 659–673, https://doi.org/10.1093/biosci/biaa061, 2020.

Crema, E. R.: Statistical Inference of Prehistoric Demography from Frequency Distributions of Radiocarbon Dates: A Review and a Guide for the Perplexed, J Archaeol Method Theory, 29, 1387–1418, https://doi.org/10.1007/s10816-022-09559-5, 2022.

Crema, E. R. and Shoda, S.: A Bayesian approach for fitting and comparing demographic growth models of radiocarbon dates: A case study on the Jomon-Yayoi transition in Kyushu (Japan), PLoS One, 16, e0251695, https://doi.org/10.1371/journal.pone.0251695, 2021.

Crombé, P., Sergant, J., Robinson, E., and De Reu, J.: Hunter–gatherer responses to environmental change during the Pleistocene–Holocene transition in the southern North Sea basin: Final Palaeolithic–Final Mesolithic land use in northwest Belgium, J Anthropol Archaeol, 30, https://doi.org/10.1016/j.jaa.2011.04.001, 2011.

Cruz-Silva, E., Harrison, S. P., Marinova, E., and Prentice, I. C.: A new method based on surface-sample pollen data for reconstructing palaeovegetation patterns, J Biogeogr, 49, 1381–1396, https://doi.org/10.1111/jbi.14448, 2022.

Cruz-Silva, E., Harrison, S. P., Prentice, I. C., and Marinova, E.: Holocene vegetation dynamics of the Eastern Mediterranean region: Old controversies addressed by a new analysis, J Biogeogr, 51, 294–310, https://doi.org/10.1111/jbi.14749, 2024.

Cui, Q. Y., Gaillard, M. J., Vannière, B., Colombaroli, D., Lemdahl, G., Olsson, F., Benito, B., and Zhao, Y.: Evaluating fossil charcoal representation in small peat bogs: Detailed Holocene fire records from southern Sweden, Holocene, 30, 1540–1551, https://doi.org/10.1177/0959683620941069, 2020a.

Cui, Q.-Y., Gaillard, M.-J., Lemdahl, G., Sugita, S., Greisman, A., Jacobson, G. L., and Olsson, F.: The role of tree composition in Holocene fire history of the hemiboreal and southern boreal zones of southern Sweden, as revealed by the application of the Landscape Reconstruction Algorithm: Implications for biodiversity and climate-change issues, Holocene, 23, 1747–1763, https://doi.org/10.1177/0959683613505339, 2013.

Cunningham, C. X., Williamson, G. J., and Bowman, D. M. J. S.: Increasing frequency and intensity of the most extreme wildfires on Earth, Nat Ecol Evol, https://doi.org/10.1038/s41559-024-02452-2, 2024.

Cushing, E. J.: Evidence for differential pollen preservation in late quaternary sediments in Minnesota, Rev Palaeobot Palynol, 4, 87–101, https://doi.org/10.1016/0034-6667(67)90175-3, 1967.

Daniau, A.-L., Bartlein, P. J., Harrison, S. P., Prentice, I. C., Brewer, S., Friedlingstein, P., Harrison-Prentice, T. I., Inoue, J., Izumi, K., Marlon, J. R., Mooney, S., Power, M. J., Stevenson, J., Tinner, W., Andrič, M., Atanassova, J., Behling, H., Black, M., Blarquez, O., Brown, K. J., Carcaillet, C., Colhoun, E. A., Colombaroli, D., Davis, B. A. S., D'Costa, D., Dodson, J., Dupont, L., Eshetu, Z., Gavin, D. G., Genries, A., Haberle, S., Hallett, D. J., Hope, G., Horn, S. P., Kassa, T. G., Katamura, F., Kennedy, L. M., Kershaw, P., Krivonogov, S., Long, C., Magri, D., Marinova, E., McKenzie, G. M., Moreno, P. I., Moss, P., Neumann, F. H., Norström, E., Paitre, C., Rius, D., Roberts, N., Robinson, G. S., Sasaki, N., Scott, L., Takahara, H., Terwilliger, V., Thevenon, F., Turner, R., Valsecchi, V. G., Vannière, B., Walsh, M., Williams, N., and Zhang, Y.: Predictability of biomass burning in response to climate changes, Global Biogeochem Cycles, 26, 2011GB004249, https://doi.org/10.1029/2011GB004249, 2012.

Davies, K. W., Bates, J. D., Svejcar, T. J., and Boyd, C. S.: Effects of Long-Term Livestock Grazing on Fuel Characteristics in Rangelands: An Example From the Sagebrush Steppe, Rangel Ecol Manag, 63, 662–669, https://doi.org/10.2111/REM-D-10-00006.1, 2010.

Davies, M. G., Gray, A., Hamilton, A., and Legg, C. J.: The future of fire management in the British uplands, International Journal of Biodiversity Science & Management, 4, https://doi.org/10.3843/Biodiv.4.3:1, 2008.

Davis, B. A. S. and Stevenson, A. C.: The 8.2 ka event and Early-Mid Holocene forests, fires and flooding in the Central Ebro Desert, NE Spain, Quat Sci Rev, 26, 1695–1712, https://doi.org/10.1016/j.quascirev.2007.04.007, 2007.

Davis, B. A. S., Brewer, S., Stevenson, A. C., and Guiot, J.: The temperature of Europe during the Holocene reconstructed from pollen data, Quat Sci Rev, 22, 1701–1716, https://doi.org/10.1016/S0277-3791(03)00173-2, 2003.

Dawe, D. A., Parisien, M.-A., Van Dongen, A., and Whitman, E.: Initial succession after wildfire in dry boreal forests of northwestern North America, Plant Ecol, 223, 789–809, https://doi.org/10.1007/s11258-022-01237-6, 2022.

Deklerck, V., De Mil, T., Ilondea, B. A., Nsenga, L., De Caluwé, C., Van den Bulcke, J., Van Acker, J., Beeckman, H., and Hubau, W.: Rate of forest recovery after fire exclusion on anthropogenic savannas in the Democratic Republic of Congo, Biol Conserv, 233, 118–130, https://doi.org/10.1016/j.biocon.2019.02.027, 2019.

Deza-Araujo, M., Morales-Molino, C., Tinner, W., Henne, P. D., Heitz, C., Pezzatti, G. B., Hafner, A., and Conedera, M.: A critical assessment of human-impact indices based on anthropogenic pollen indicators, Quat Sci Rev, 236, https://doi.org/10.1016/j.quascirev.2020.106291, 2020.

Dietze, E., Theuerkauf, M., Bloom, K., Brauer, A., Dörfler, W., Feeser, I., Feurdean, A., Gedminienė, L., Giesecke, T., Jahns, S., Karpińska-Kołaczek, M., Kołaczek, P., Lamentowicz, M., Latałowa, M., Marcisz, K., Obremska, M., Pędziszewska, A., Poska, A., Rehfeld, K., Stančikaitė, M., Stivrins, N., Święta-Musznicka, J., Szal, M., Vassiljev, J., Veski, S., Wacnik, A., Weisbrodt, D., Wiethold, J., Vannière, B., and Słowiński, M.: Holocene fire activity during low-natural flammability periods reveals scale-dependent cultural human-fire relationships in Europe, Quat Sci Rev, 201, 44–56, https://doi.org/10.1016/j.quascirev.2018.10.005, 2018.

Dijkstra, J., Durrant, T., San-Miguel-Ayanz, J., and Veraverbeke, S.: Anthropogenic and Lightning Fire Incidence and Burned Area in Europe, Land (Basel), 11, 651, https://doi.org/10.3390/land11050651, 2022.

Dimitrakopoulos, A. P., Vlahou, M., Anagnostopoulou, Ch. G., and Mitsopoulos, I. D.: Impact of drought on wildland fires in Greece: implications of climatic change?, Clim Change, 109, 331–347, https://doi.org/10.1007/s10584-011-0026-8, 2011.

DiTomaso, J. M., Brooks, M. L., Allen, E. B., Minnich, R., Rice, P. M., and Kyser, G. B.: Control of Invasive Weeds with Prescribed Burning, Weed Technol, 20, 535–548, https://doi.org/10.1614/wt-05-086r1.1, 2006.

Doerr, S. H. and Santín, C.: Global trends in wildfire and its impacts: perceptions versus realities in a changing world, Phil Trans of the R Soc B, 371, 20150345, https://doi.org/10.1098/rstb.2015.0345, 2016.

Dong, X., Li, F., Lin, Z., Harrison, S. P., Chen, Y., and Kug, J.-S.: Climate influence on the 2019 fires in Amazonia, Sci Total Environ, 794, 148718, https://doi.org/10.1016/j.scitotenv.2021.148718, 2021.

D'Onofrio, D., von Hardenberg, J., and Baudena, M.: Not only trees: Grasses determine African tropical biome distributions via water limitation and fire, Global Ecol Biogeogr, 27, 714–725, https://doi.org/10.1111/geb.12735, 2018.

Douglass, A. E.: Crossdating in Dendrochronology, J For, 39, 825–831, 1941.

Dowdy, A. J.: Seamless climate change projections and seasonal predictions for bushfires in Australia, Journal of Southern Hemisphere Earth Systems Science, 70, 120–138, https://doi.org/10.1071/ES20001, 2020.

Duane, A., Miranda, M. D., and Brotons, L.: Forest connectivity percolation thresholds for fire spread under different weather conditions, For Ecol Manage, 498, 119558, https://doi.org/10.1016/j.foreco.2021.119558, 2021.

Duffin, K. I., Gillson, L., and Willis, K. J.: Testing the sensitivity of charcoal as an indicator of fire events in savanna environments: Quantitative predictions of fire proximity, area and intensity, Holocene, 18, 279–291, https://doi.org/10.1177/0959683607086766, 2008.

Eggermont, H. and Heiri, O.: The chironomid-temperature relationship: expression in nature and palaeoenvironmental implications, Biol Rev, 87, 430–456, https://doi.org/10.1111/j.1469-185X.2011.00206.x, 2012.

Enache, M. D. and Cumming, B. F.: Tracking recorded fires using charcoal morphology from the sedimentary sequence of Prosser Lake, British Columbia (Canada), Quat Res, 65, 282–292, https://doi.org/10.1016/j.yqres.2005.09.003, 2006.

Etienne, D., Destas, M., Lyautey, E., Marti, R., Ruffaldi, P., Georges-Leroy, M., Dambrine, E., and Topp, E.: Two thousand–year reconstruction of livestock production intensity in France using sediment-archived fecal *Bacteroidales* and source-specific mitochondrial markers, Holocene, 25, 1384–1393, https://doi.org/10.1177/0959683615585836, 2015.

Falk, D. A., van Mantgem, P. J., Keeley, J. E., Gregg, R. M., Guiterman, C. H., Tepley, A. J., JN Young, D., and Marshall, L. A.: Mechanisms of forest resilience, For Ecol Manage, 512, 120129, https://doi.org/10.1016/j.foreco.2022.120129, 2022.

Fang, K., Yao, Q., Guo, Z., Zheng, B., Du, J., Qi, F., Yan, P., Li, J., Ou, T., Liu, J., He, M., and Trouet, V.: ENSO modulates wildfire activity in China, Nat Commun, 12, 1764, https://doi.org/10.1038/s41467-021-21988-6, 2021.

Favre, E., Escarguel, G., Suc, J.-P., Vidal, G., and Thévenod, L.: A contribution to deciphering the meaning of AP/NAP with respect to vegetation cover, Rev Palaeobot Palynol, 148, 13–35, https://doi.org/10.1016/j.revpalbo.2007.08.003, 2008.

Feranec, R. S., Miller, N. G., Lothrop, J. C., and Graham, R. W.: The Sporormiella proxy and end-Pleistocene megafaunal extinction: A perspective, Quat Int, 245, 333–338, https://doi.org/10.1016/j.quaint.2011.06.004, 2011.

Fernández-García, V. and Alonso-González, E.: Global Patterns and Dynamics of Burned Area and Burn Severity, Remote Sens (Basel), 15, 3401, https://doi.org/10.3390/rs15133401, 2023.

Feurdean, A., Spessa, A., Magyari, E. K., Willis, K. J., Veres, D., and Hickler, T.: Trends in biomass burning in the Carpathian region over the last 15,000 years, Quat Sci Rev, 45, 111–125, https://doi.org/10.1016/j.quascirev.2012.04.001, 2012.

Feurdean, A., Liakka, J., Vannière, B., Marinova, E., Hutchinson, S. M., Mosburgger, V., and Hickler, T.: 12,000-Years of fire regime drivers in the lowlands of Transylvania (Central-Eastern Europe): a data-model approach, Quat Sci Rev, 81, 48–61, https://doi.org/10.1016/j.quascirev.2013.09.014, 2013.

Feurdean, A., Florescu, G., Vannière, B., Tanţău, I., O‘Hara, R. B., Pfeiffer, M., Hutchinson, S. M., Gałka, M., Moskal-del Hoyo, M., and Hickler, T.: Fire has been an important driver of forest dynamics in the Carpathian Mountains during the Holocene, For Ecol Manage, 389, 15–26, https://doi.org/10.1016/j.foreco.2016.11.046, 2017.

Feurdean, A., Tonkov, S., Pfeiffer, M., Panait, A., Warren, D., Vannière, B., and Marinova, E.: Fire frequency and intensity associated with functional traits of dominant forest type in the Balkans during the Holocene, Eur J For Res, 138, 1049–1066, https://doi.org/10.1007/s10342-019-01223-0, 2019.

Feurdean, A., Vannière, B., Finsinger, W., Warren, D., Connor, S. C., Forrest, M., Liakka, J., Panait, A., Werner, C., Andrič, M., Bobek, P., Carter, V. A., Davis, B., Diaconu, A.-C., Dietze, E., Feeser, I., Florescu, G., Gałka, M., Giesecke, T., Jahns, S., Jamrichová, E., Kajukało, K., Kaplan, J., Karpińska-Kołaczek, M., Kołaczek, P., Kuneš, P., Kupriyanov, D., Lamentowicz, M., Lemmen, C., Magyari, E. K., Marcisz, K., Marinova, E., Niamir, A., Novenko, E., Obremska, M., Pędziszewska, A., Pfeiffer, M., Poska, A., Rösch, M., Słowiński, M., Stančikaitė, M., Szal, M., Święta-Musznicka, J., Tanţău, I., Theuerkauf, M., Tonkov, S., Valkó, O., Vassiljev, J., Veski, S., Vincze, I., Wacnik, A., Wiethold, J., and Hickler, T.: Fire hazard modulation by long-term dynamics in land cover and dominant forest type in eastern and central Europe, Biogeosciences, 17, 1213–1230, https://doi.org/10.5194/bg-17-1213-2020, 2020.

Fischer, H., Schüpbach, S., Gfeller, G., Bigler, M., Röthlisberger, R., Erhardt, T., Stocker, T. F., Mulvaney, R., and Wolff, E. W.: Millennial changes in North American wildfire and soil activity over the last glacial cycle, Nat Geosci, 8, 723–727, https://doi.org/10.1038/ngeo2495, 2015.

Forkel, M., Andela, N., Harrison, S. P., Lasslop, G., van Marle, M., Chuvieco, E., Dorigo, W., Forrest, M., Hantson, S., Heil, A., Li, F., Melton, J., Sitch, S., Yue, C., and Arneth, A.: Emergent relationships with respect to burned area in global satellite observations and fire-enabled vegetation models, Biogeosciences, 16, 57–76, https://doi.org/10.5194/bg-16-57-2019, 2019.

Fritts, H. C., Lofgren, G. R., and Gordon, G. A.: Past Climate Reconstructed from Tree Rings, J Interdiscip Hist, 10, 773–793, https://doi.org/10.2307/203070, 1980.

Fujisaka, S., Hurtado, L., and Uribe, R.: A working classification of slash-and-burn agricultural systems, Agroforest Syst, 34, 151–169, https://doi.org/10.1007/BF00148159, 1996.

Fusco, E. J., Finn, J. T., Balch, J. K., Nagy, R. C., and Bradley, B. A.: Invasive grasses increase fire occurrence and frequency across US ecoregions, P Natl Acad Sci USA, 116, https://doi.org/10.1073/pnas.1908253116, 2019.

Fyfe, R. M., de Beaulieu, J.-L., Binney, H., Bradshaw, R. H. W., Brewer, S., Le Flao, A., Finsinger, W., Gaillard, M.-J., Giesecke, T., Gil-Romera, G., Grimm, E. C., Huntley, B., Kunes, P., Kühl, N., Leydet, M., Lotter, A. F., Tarasov, P. E., and Tonkov, S.: The European Pollen Database: past efforts and current activities, Veg Hist Archaeobot, 18, 417–424, https://doi.org/10.1007/s00334-009-0215-9, 2009.

Fyfe, R. M., Roberts, N., and Woodbridge, J.: A pollen-based pseudobiomisation approach to anthropogenic land-cover change, Holocene, 20, 1165–1171, https://doi.org/10.1177/0959683610369509, 2010.

Fyfe, R. M., Woodbridge, J., and Roberts, N.: From forest to farmland: pollen-inferred land cover change across Europe using the pseudobiomization approach, Glob Chang Biol, 21, 1197–1212, https://doi.org/10.1111/gcb.12776, 2015.

Fyfe, R. M., Woodbridge, J., and Roberts, C. N.: Trajectories of change in Mediterranean Holocene vegetation through classification of pollen data, Veg Hist Archaeobot, 27, 351–364, https://doi.org/10.1007/s00334-017-0657-4, 2018.

Gajewski, K., Kriesche, B., Chaput, M. A., Kulik, R., and Schmidt, V.: Human–vegetation interactions during the Holocene in North America, Veg Hist Archaeobot, 28, https://doi.org/10.1007/s00334-019-00721-w, 2019.

Ganteaume, A. and Syphard, A. D.: Ignition Sources, in: Encyclopedia of Wildfires and Wildland-Urban Interface (WUI) Fires, Springer International Publishing, Cham, 1–17, https://doi.org/10.1007/978-3-319-51727-8_43-1, 2018.

Gatebe, C. K., Ichoku, C. M., Poudyal, R., Román, M. O., and Wilcox, E.: Surface albedo darkening from wildfires in northern sub-Saharan Africa, Environ Res Lett, 9, 065003, https://doi.org/10.1088/1748-9326/9/6/065003, 2014.

Gavin, D. G., Brubaker, L. B., and Lertzman, K. P.: Holocene fire history of a coastal temperate rain forest based on soil charcoal radiocarbon dates, Ecology, 84, 186–201, https://doi.org/https://doi.org/10.1890/0012-9658(2003)084[0186:HFHOAC]2.0.CO;2, 2003a.

Gavin, D. G., Oswald, W. W., Wahl, E. R., and Williams, J. W.: A statistical approach to evaluating distance metrics and analog assignments for pollen records, Quat Res, 60, 356–367, https://doi.org/10.1016/S0033-5894(03)00088-7, 2003b.

Gavin, D. G., Hallett, D. J., Feng, S. H., Lertzman, K. P., Prichard, S. J., Brown, K. J., Lynch, J. A., Bartlein, P., and Peterson, D. L.: Forest fire and climate change in western North America: Insights from sediment charcoal records, Front Ecol Environ, 5, 499–506, https://doi.org/10.1890/060161, 2007.

van Geel, B., Buurman, J., Brinkkemper, O., Schelvis, J., Aptroot, A., van Reenen, G., and Hakbijl, T.: Environmental reconstruction of a Roman Period settlement site in Uitgeest (The Netherlands), with special reference to coprophilous fungi, J Archaeol Sci, 30, 873–883, https://doi.org/10.1016/S0305-4403(02)00265-0, 2003.

Giglio, L., Boschetti, L., Roy, D. P., Humber, M. L., and Justice, C. O.: The Collection 6 MODIS burned area mapping algorithm and product, Remote Sens Environ, 217, 72–85, https://doi.org/10.1016/j.rse.2018.08.005, 2018.

Gincheva, A., Pausas, J. G., Edwards, A., Provenzale, A., Cerdà, A., Hanes, C., Royé, D., Chuvieco, E., Mouillot, F., Vissio, G., Rodrigo, J., Bedía, J., Abatzoglou, J. T., Senciales González, J. M., Short, K. C., Baudena, M., Llasat, M. C., Magnani, M., Boer, M. M., González, M. E., Torres-Vázquez, M. Á., Fiorucci, P., Jacklyn, P., Libonati, R., Trigo, R. M., Herrera, S., Jerez, S., Wang, X., and Turco, M.: A monthly gridded burned area database of national wildland fire data, Sci Data, 11, 352, https://doi.org/10.1038/s41597-024-03141-2, 2024.

Githumbi, E., Fyfe, R., Gaillard, M.-J., Trondman, A.-K., Mazier, F., Nielsen, A.-B., Poska, A., Sugita, S., Woodbridge, J., Azuara, J., Feurdean, A., Grindean, R., Lebreton, V., Marquer, L., Nebout-Combourieu, N., Stančikaitė, M., Tanţău, I., Tonkov, S., and Shumilovskikh, L.: European pollen-based REVEALS land-cover reconstructions for the Holocene: methodology, mapping and potentials, Earth Syst Sci Data, 14, 1581–1619, https://doi.org/10.5194/essd-14-1581-2022, 2022.

Gobet, E., Tinner, W., Hochuli, P. A., van Leeuwen, J. F. N., and Ammann, B.: Middle to Late Holocene vegetation history of the Upper Engadine (Swiss Alps): the role of man and fire, Veg Hist Archaeobot, 12, 143–163, https://doi.org/10.1007/s00334-003-0017-4, 2003.

Gosling, W. D., Cornelissen, H. L., and McMichael, C. N. H.: Reconstructing past fire temperatures from ancient charcoal material, Palaeogeogr Palaeoclimatol Palaeoecol, 520, 128–137, https://doi.org/10.1016/j.palaeo.2019.01.029, 2019.

Gotanda, K., Nakagawa, T., Tarasov, P. E., and Yasuda, Y.: Disturbed vegetation reconstruction using the biomization method from Japanese pollen data: Modern and Late Quaternary samples, Quat Int, 184, 56–74, https://doi.org/10.1016/j.quaint.2007.09.030, 2008.

Gregory, P.: Spores: their properties and sedimentation in still air, in: A plant science monograph, Leonard Hill, Aylesbury, 1973.

Grootemaat, S., Wright, I. J., van Bodegom, P. M., Cornelissen, J. H. C., and Cornwell, W. K.: Burn or rot: leaf traits explain why flammability and decomposability are decoupled across species, Funct Ecol, 29, 1486–1497, https://doi.org/10.1111/1365-2435.12449, 2015.

Grove, M.: A Spatio-Temporal Kernel Method For Mapping Changes In Prehistoric Land-Use Patterns, Archaeometry, 53, 1012–1030, https://doi.org/10.1111/j.1475-4754.2010.00578.x, 2011.

Guiot, J.: Methodology of the last climatic cycle reconstruction in France from pollen data, Palaeogeogr Palaeoclimatol Palaeoecol, 80, 49–69, https://doi.org/10.1016/0031-0182(90)90033-4, 1990.

Guiot, J., Torre, F., Jolly, D., Peyron, O., Boreux, J. J., and Cheddadi, R.: Inverse vegetation modeling by Monte Carlo sampling to reconstruct palaeoclimates under changed precipitation seasonality and CO2 conditions: application to glacial climate in Mediterranean region, Ecol Modell, 127, 119–140, https://doi.org/10.1016/S0304-3800(99)00219-7, 2000.

Haas, O., Prentice, I. C., and Harrison, S. P.: Global environmental controls on wildfire burnt area, size, and intensity, Environ Res Lett, 17, 065004, https://doi.org/10.1088/1748-9326/ac6a69, 2022.

Hanes, C. C., Wang, X., Jain, P., Parisien, M.-A., Little, J. M., and Flannigan, M. D.: Fire-regime changes in Canada over the last half century, Can J Forest Res, 49, 256–269, https://doi.org/10.1139/cjfr-2018-0293, 2019.

Hantson, S., Arneth, A., Harrison, S. P., Kelley, D. I., Colin Prentice, I., Rabin, S. S., Archibald, S., Mouillot, F., Arnold, S. R., Artaxo, P., Bachelet, D., Ciais, P., Forrest, M., Friedlingstein, P., Hickler, T., Kaplan, J. O., Kloster, S., Knorr, W., Lasslop, G., Li, F., Mangeon, S., Melton, J. R., Meyn, A., Sitch, S., Spessa, A., Van Der Werf, G. R., Voulgarakis, A., and Yue, C.: The status and challenge of global fire modelling, Biogeosciences, 13, 3359–3375, https://doi.org/10.5194/bg-13-3359-2016, 2016.

Hantson, S., Kelley, D. I., Arneth, A., Harrison, S. P., Archibald, S., Bachelet, D., Forrest, M., Hickler, T., Lasslop, G., Li, F., Mangeon, S., Melton, J. R., Nieradzik, L., Rabin, S. S., Prentice, I. C., Sheehan, T., Sitch, S., Teckentrup, L., Voulgarakis, A., and Yue, C.: Quantitative assessment of fire and vegetation properties in simulations with fire-enabled vegetation models from the Fire Model Intercomparison Project, Geosci Model Dev, 13, 3299–3318, https://doi.org/10.5194/gmd-13-3299-2020, 2020.

Hantson, S., Andela, N., Goulden, M. L., and Randerson, J. T.: Human-ignited fires result in more extreme fire behavior and ecosystem impacts, Nat Commun, 13, 2717, https://doi.org/10.1038/s41467-022-30030-2, 2022.

Harrison, S. P. and Sanchez Goñi, M. F.: Global patterns of vegetation response to millennial-scale variability and rapid climate change during the last glacial period, Quat Sci Rev, 29, 2957–2980, https://doi.org/10.1016/j.quascirev.2010.07.016, 2010.

Harrison, S. P., Prentice, I. C., Barboni, D., Kohfeld, K. E., Ni, J., and Sutra, J.-P.: Ecophysiological and bioclimatic foundations for a global plant functional classification, J Veg Sci, 21, 300–317, https://doi.org/10.1111/j.1654-1103.2009.01144.x, 2010.

Harrison, S. P., Gaillard, M.-J., Stocker, B. D., Vander Linden, M., Klein Goldewijk, K., Boles, O., Braconnot, P., Dawson, A., Fluet-Chouinard, E., Kaplan, J. O., Kastner, T., Pausata, F. S. R., Robinson, E., Whitehouse, N. J., Madella, M., and Morrison, K. D.: Development and testing scenarios for implementing land use and land cover changes during the Holocene in Earth system model experiments, Geosci Model Dev, 13, 805–824, https://doi.org/10.5194/gmd-13-805-2020, 2020.

Harrison, S. P., Prentice, I. C., Bloomfield, K. J., Dong, N., Forkel, M., Forrest, M., Ningthoujam, R. K., Pellegrini, A., Shen, Y., Baudena, M., Cardoso, A. W., Huss, J. C., Joshi, J., Oliveras, I., Pausas, J. G., and Simpson, K. J.: Understanding and modelling wildfire regimes: an ecological perspective, Environ Res Lett, 16, 125008, https://doi.org/10.1088/1748-9326/ac39be, 2021.

Harrison, S. P., Villegas-Diaz, R., Cruz-Silva, E., Gallagher, D., Kesner, D., Lincoln, P., Shen, Y., Sweeney, L., Colombaroli, D., Ali, A., Barhoumi, C., Bergeron, Y., Blyakharchuk, T., Bobek, P., Bradshaw, R., Clear, J. L., Czerwiński, S., Daniau, A.-L., Dodson, J., Edwards, K. J., Edwards, M. E., Feurdean, A., Foster, D., Gajewski, K., Gałka, M., Garneau, M., Giesecke, T., Gil Romera, G., Girardin, M. P., Hoefer, D., Huang, K., Inoue, J., Jamrichová, E., Jasiunas, N., Jiang, W., Jiménez-Moreno, G., Karpińska-Kołaczek, M., Kołaczek, P., Kuosmanen, N., Lamentowicz, M., Lavoie, M., Li, F., Li, J., Lisitsyna, O., López-Sáez, J. A., Luelmo-Lautenschlaeger, R., Magnan, G., Magyari, E. K., Maksims, A., Marcisz, K., Marinova, E., Marlon, J. R., Mensing, S., Miroslaw-Grabowska, J., Oswald, W., Pérez-Díaz, S., Pérez-Obiol, R., Piilo, S., Poska, A., Qin, X., Remy, C. C., Richard, P. J. H., Salonen, S., Sasaki, N., Schneider, H., Shotyk, W., Stancikaite, M., Šteinberga, D., Stivrins, N., Takahara, H., Tan, Z., Trasune, L., Umbanhowar, C. E., Väliranta, M., Vassiljev, J., Xiao, X., Xu, Q., Xu, X., Zawisza, E., Zhao, Y., Zhou, Z., and Paillard, J.: The Reading Palaeofire Database: an expanded global resource to document changes in fire regimes from sedimentary charcoal records, Earth Syst Sci Data, 14, 1109–1124, https://doi.org/10.5194/essd-14-1109-2022, 2022.

Hatté, C. and Guiot, J.: Palaeoprecipitation reconstruction by inverse modelling using the isotopic signal of loess organic matter: application to the Nußloch loess sequence (Rhine Valley, Germany), Clim Dyn, 25, 315–327, https://doi.org/10.1007/s00382-005-0034-3, 2005.

Hawthorne, D. and Mitchell, F. J. G.: Identifying past fire regimes throughout the Holocene in Ireland using new and established methods of charcoal analysis, Quat Sci Rev, 137, 45–53, https://doi.org/10.1016/j.quascirev.2016.01.027, 2016.

Haxeltine, A. and Prentice, I. C.: BIOME3: An equilibrium terrestrial biosphere model based on ecophysiological constraints, resource availability, and competition among plant functional types, Global Biogeochem Cycles, 10, 693–709, https://doi.org/10.1029/96GB02344, 1996.

He, T., Lamont, B. B., and Pausas, J. G.: Fire as a key driver of Earth's biodiversity, Biol Rev, 94, 1983–2010, https://doi.org/10.1111/brv.12544, 2019.

Hellman, S. E. V., Gaillard, M. J., Broström, A., and Sugita, S.: Effects of the sampling design and selection of parameter values on pollen-based quantitative reconstructions of regional vegetation: A case study in southern Sweden using the REVEALS model, Veg Hist Archaeobot, 17, 445–459, https://doi.org/10.1007/s00334-008-0149-7, 2008.

Hennebelle, A., Aleman, J. C., Ali, A. A., Bergeron, Y., Carcaillet, C., Grondin, P., Landry, J., and Blarquez, O.: The reconstruction of burned area and fire severity using charcoal from boreal lake sediments, Holocene, 30, 1400–1409, https://doi.org/10.1177/0959683620932979, 2020.

Heon, J., Arseneault, D., and Parisien, M.-A.: Resistance of the boreal forest to high burn rates, P Natl Acad Sci USA, 111, 13888–13893, https://doi.org/10.1073/pnas.1409316111, 2014.

Higgins, S. I., Bond, W. J., February, E. C., Bronn, A., Euston-Brown, D. I. W., Enslin, B., Govender, N., Rademan, L., O’Regan, S., Potgieter, A. L. F., Scheiter, S., Sowry, R., Trollope, L., and Trollope, W. S. W.: Effects of four decades of fire manipulation on woody vegetation structure in savanna, Ecology, 88, 1119–1125, https://doi.org/10.1890/06-1664, 2007.

Higuera, P. E., Sprugel, D. G., and Brubaker, L. B.: Reconstructing fire regimes with charcoal from small-hollow sediments: A calibration with tree-ring records of fire, Holocene, 15, 238–251, https://doi.org/10.1191/0959683605hl789rp, 2005.

Higuera, P. E., Gavin, D. G., Bartlein, P. J., and Hallett, D. J.: Peak detection in sediment - charcoal records: impacts of alternative data analysis methods on fire-history interpretations, Int J Wildland Fire, 19, 996, https://doi.org/10.1071/WF09134, 2010.

Higuera, P. E., Whitlock, C., and Gage, J. A.: Linking tree-ring and sediment-charcoal records to reconstruct fire occurrence and area burned in subalpine forests of Yellowstone National Park, USA, Holocene, 21, https://doi.org/10.1177/0959683610374882, 2011.

Hinz, M. and Roe, J.: xronos: Client for the “XRONOS” Chronological Database, 2024.

Hoffman, K. M., Gavin, D. G., Lertzman, K. P., Smith, D. J., and Starzomski, B. M.: 13,000 years of fire history derived from soil charcoal in a British Columbia coastal temperate rain forest, Ecosphere, 7, https://doi.org/10.1002/ecs2.1415, 2016.

Holden, Z. A., Swanson, A., Luce, C. H., Jolly, W. M., Maneta, M., Oyler, J. W., Warren, D. A., Parsons, R., and Affleck, D.: Decreasing fire season precipitation increased recent western US forest wildfire activity, P Natl Acad Sci USA, 115, https://doi.org/10.1073/pnas.1802316115, 2018.

Huffman, M. R.: The Many Elements of Traditional Fire Knowledge: Synthesis, Classification, and Aids to Cross-cultural Problem Solving in Fire-dependent Systems Around the World, Ecol Soc, 18, art3, https://doi.org/10.5751/ES-05843-180403, 2013.

Hughen, K. A., Eglinton, T. I., Xu, L., and Makou, M.: Abrupt Tropical Vegetation Response to Rapid Climate Changes, Science, 304, 1955–1959, https://doi.org/10.1126/science.1092995, 2004.

Huntley, B.: How Plants Respond to Climate Change: Migration Rates, Individualism and the Consequences for Plant Communities, Ann Bot, 67, 15–22, 1991.

Huntley, B.: The use of climate response surfaces to reconstruct palaeoclimate from Quaternary pollen and plant macrofossil data, Philos Trans R Soc Lond B Biol Sci, 341, 215–224, https://doi.org/10.1098/rstb.1993.0106, 1993.

Iglesias, V. and Whitlock, C.: Fire responses to postglacial climate change and human impact in northern Patagonia (41–43°S), P Natl Acad Sci USA, 111, E5545–E5554, https://doi.org/10.1073/pnas.1410443111, 2014.

Iglesias, V., Vannière, B., and Jouffroy-Bapicot, I.: Emergence and Evolution of Anthropogenic Landscapes in the Western Mediterranean and Adjacent Atlantic Regions, Fire, 2, 53, https://doi.org/10.3390/fire2040053, 2019.

Innes, J. B., Blackford, J. J., and Rowley-Conwy, P. A.: Late Mesolithic and early Neolithic forest disturbance: a high resolution palaeoecological test of human impact hypotheses, Quat Sci Rev, 77, https://doi.org/10.1016/j.quascirev.2013.07.012, 2013.

Isern, N., Fort, J., and Vander Linden, M.: Space Competition and Time Delays in Human Range Expansions. Application to the Neolithic Transition, PLoS One, 7, e51106, https://doi.org/10.1371/journal.pone.0051106, 2012.

Iversen, J.: Viscum, Hedera and Ilex as Climate Indicators, Geologiska Föreningen i Stockholm Förhandlingar, 66, https://doi.org/10.1080/11035894409445689, 1944.

Jackson, S. T.: Pollen source area and representation in small lakes of the northeastern United States, Rev Palaeobot Palynol, 63, 53–76, https://doi.org/10.1016/0034-6667(90)90006-5, 1990.

Jackson, S. T. and Williams, J. W.: Modern Analogs in Quaternary Paleoecology: Here Today, Gone Yesterday, Gone Tomorrow?, Annu Rev Earth Planet Sci, 32, 495–537, https://doi.org/10.1146/annurev.earth.32.101802.120435, 2004.

Jansen, B., van Loon, E. E., Hooghiemstra, H., and Verstraten, J. M.: Improved reconstruction of palaeo-environments through unravelling of preserved vegetation biomarker patterns, Palaeogeogr Palaeoclimatol Palaeoecol, 285, 119–130, https://doi.org/10.1016/j.palaeo.2009.10.029, 2010.

Janssen, T. A. J., Jones, M. W., Finney, D., van der Werf, G. R., van Wees, D., Xu, W., and Veraverbeke, S.: Extratropical forests increasingly at risk due to lightning fires, Nat Geosci, 16, 1136–1144, https://doi.org/10.1038/s41561-023-01322-z, 2023.

Jensen, K., Lynch, E. A., Calcote, R., and Hotchkiss, S. C.: Interpretation of charcoal morphotypes in sediments from Ferry Lake, Wisconsin, USA: Do different plant fuel sources produce distinctive charcoal morphotypes?, Holocene, 17, 907–915, https://doi.org/10.1177/0959683607082405, 2007.

Jethva, H., Chand, D., Torres, O., Gupta, P., Lyapustin, A., and Patadia, F.: Agricultural Burning and Air Quality over Northern India: A Synergistic Analysis using NASA's A-train Satellite Data and Ground Measurements, Aerosol Air Qual Res, 18, https://doi.org/10.4209/aaqr.2017.12.0583, 2018.

Jones, G. M. and Tingley, M. W.: Pyrodiversity and biodiversity: A history, synthesis, and outlook, Divers Distrib, 28, 386–403, https://doi.org/10.1111/ddi.13280, 2022.

Jones, M. W., Abatzoglou, J. T., Veraverbeke, S., Andela, N., Lasslop, G., Forkel, M., Smith, A. J. P., Burton, C., Betts, R. A., van der Werf, G. R., Sitch, S., Canadell, J. G., Santín, C., Kolden, C., Doerr, S. H., and Le Quéré, C.: Global and Regional Trends and Drivers of Fire Under Climate Change, Rev Geophys, 60, https://doi.org/10.1029/2020RG000726, 2022.

Jones, P. D. and Bradley, R. S.: Climatic variations in the longest instrumental records, in: Climate since AD 1500, edited by: Bradley, R. D. and Jones, P. D., Routledge, London, 246–268, 1992.

Jones, P. D., New, M., Parker, D. E., Martin, S., and Rigor, I. G.: Surface air temperature and its changes over the past 150 years, Rev Geophys, 37, 173–199, https://doi.org/10.1029/1999RG900002, 1999.

Jouzel, J.: A brief history of ice core science over the last 50 yr, Clim Past, 9, 2525–2547, https://doi.org/10.5194/cp-9-2525-2013, 2013.

Jouzel, J., Alley, R. B., Cuffey, K. M., Dansgaard, W., Grootes, P., Hoffmann, G., Johnsen, S. J., Koster, R. D., Peel, D., Shuman, C. A., Stievenard, M., Stuiver, M., and White, J.: Validity of the temperature reconstruction from water isotopes in ice cores, J Geophys Res Oceans, 102, 26471–26487, https://doi.org/10.1029/97JC01283, 1997.

Jouzel, J., Masson-Delmotte, V., Cattani, O., Dreyfus, G., Falourd, S., Hoffmann, G., Minster, B., Nouet, J., Barnola, J. M., Chappellaz, J., Fischer, H., Gallet, J. C., Johnsen, S., Leuenberger, M., Loulergue, L., Luethi, D., Oerter, H., Parrenin, F., Raisbeck, G., Raynaud, D., Schilt, A., Schwander, J., Selmo, E., Souchez, R., Spahni, R., Stauffer, B., Steffensen, J. P., Stenni, B., Stocker, T. F., Tison, J. L., Werner, M., and Wolff, E. W.: Orbital and millennial antarctic climate variability over the past 800,000 years, Science, 317, 793–796, https://doi.org/10.1126/science.1141038, 2007.

Kaal, J., Carrión Marco, Y., Asouti, E., Martín Seijo, M., Martínez Cortizas, A., Costa Casáis, M., and Criado Boado, F.: Long-term deforestation in NW Spain: linking the Holocene fire history to vegetation change and human activities, Quat Sci Rev, 30, 161–175, https://doi.org/10.1016/j.quascirev.2010.10.006, 2011.

Kang, S., Kimball, J. S., and Running, S. W.: Simulating effects of fire disturbance and climate change on boreal forest productivity and evapotranspiration, Sci Total Environ, 362, 85–102, https://doi.org/10.1016/j.scitotenv.2005.11.014, 2006.

Kaplan, J. O., Krumhardt, K. M., and Zimmermann, N.: The prehistoric and preindustrial deforestation of Europe, Quat Sci Rev, 28, 3016–3034, https://doi.org/10.1016/j.quascirev.2009.09.028, 2009.

Keeley, J. E. and Syphard, A. D.: Different fire–climate relationships on forested and non-forested landscapes in the Sierra Nevada ecoregion, Int J Wildland Fire, 24, 27, https://doi.org/10.1071/WF14102, 2015.

Keeley, J. E., Fotheringham, C. J., and Morais, M.: Reexamining Fire Suppression Impacts on Brushland Fire Regimes, Science, 284, 1829–1832, https://doi.org/10.1126/science.284.5421.1829, 1999.

Keeley, J. E., Pausas, J. G., Rundel, P. W., Bond, W. J., and Bradstock, R. A.: Fire as an evolutionary pressure shaping plant traits, Trends Plant Sci, 16, 406–411, https://doi.org/10.1016/j.tplants.2011.04.002, 2011.

Keeping, T., Harrison, S. P., and Prentice, I. C.: Modelling the daily probability of wildfire occurrence in the contiguous United States, Environ Res Lett, 19, 024036, https://doi.org/10.1088/1748-9326/ad21b0, 2024.

Kelly, L. T., Giljohann, K. M., Duane, A., Aquilué, N., Archibald, S., Batllori, E., Bennett, A. F., Buckland, S. T., Canelles, Q., Clarke, M. F., Fortin, M.-J., Hermoso, V., Herrando, S., Keane, R. E., Lake, F. K., McCarthy, M. A., Morán-Ordóñez, A., Parr, C. L., Pausas, J. G., Penman, T. D., Regos, A., Rumpff, L., Santos, J. L., Smith, A. L., Syphard, A. D., Tingley, M. W., and Brotons, L.: Fire and biodiversity in the Anthropocene, Science, 370, https://doi.org/10.1126/science.abb0355, 2020.

Kelly, L. T., Fletcher, M.-S., Oliveras Menor, I., Pellegrini, A. F. A., Plumanns-Pouton, E. S., Pons, P., Williamson, G. J., and Bowman, D. M. J. S.: Understanding Fire Regimes for a Better Anthropocene, Annu Rev Environ Resour, 48, 207–235, https://doi.org/10.1146/annurev-environ-120220-055357, 2023.

Kelly, R. L., Surovell, T. A., Shuman, B. N., and Smith, G. M.: A continuous climatic impact on Holocene human population in the Rocky Mountains, P Natl Acad Sci USA, 110, 443–447, https://doi.org/10.1073/pnas.1201341110, 2013.

Kirschbaum, M. U. F., Whitehead, D., Dean, S. M., Beets, P. N., Shepherd, J. D., and Ausseil, A.-G. E.: Implications of albedo changes following afforestation on the benefits of forests as carbon sinks, Biogeosciences, 8, 3687–3696, https://doi.org/10.5194/bg-8-3687-2011, 2011.

Klein Goldewijk, K., Beusen, A., and Janssen, P.: Long-term dynamic modeling of global population and built-up area in a spatially explicit way: HYDE 3.1, Holocene, 20, 565–573, https://doi.org/10.1177/0959683609356587, 2010.

Klein Goldewijk, K., Beusen, A., Van Drecht, G., and De Vos, M.: The HYDE 3.1 spatially explicit database of human-induced global land-use change over the past 12,000 years, Global Ecol Biogeogr, 20, 73–86, https://doi.org/10.1111/j.1466-8238.2010.00587.x, 2011.

Klein Goldewijk, K., Beusen, A., Doelman, J., and Stehfest, E.: Anthropogenic land use estimates for the Holocene – HYDE 3.2, Earth Syst Sci Data, 9, 927–953, https://doi.org/10.5194/essd-9-927-2017, 2017.

Kloster, S., Brücher, T., Brovkin, V., and Wilkenskjeld, S.: Controls on fire activity over the Holocene, Clim Past, 11, 781–788, https://doi.org/10.5194/cp-11-781-2015, 2015.

Knorr, W., Arneth, A., and Jiang, L.: Demographic controls of future global fire risk, Nat Clim Chang, 6, 781–785, https://doi.org/10.1038/nclimate2999, 2016.

Kolář, J., Macek, M., Tkáč, P., Novák, D., and Abraham, V.: Long-term demographic trends and spatio-temporal distribution of past human activity in Central Europe: Comparison of archaeological and palaeoecological proxies, Quat Sci Rev, 297, 107834, https://doi.org/10.1016/j.quascirev.2022.107834, 2022.

Kramer, K., Groen, T. A., and van Wieren, S. E.: The interacting effects of ungulates and fire on forest dynamics: an analysis using the model FORSPACE, For Ecol Manage, 181, 205–222, https://doi.org/10.1016/S0378-1127(03)00134-8, 2003.

Krawchuk, M. A. and Moritz, M. A.: Constraints on global fire activity vary across a resource gradient, Ecology, 92, 121–132, https://doi.org/10.1890/09-1843.1, 2011.

Krawchuk, M. A., Moritz, M. A., Parisien, M. A., Van Dorn, J., and Hayhoe, K.: Global pyrogeography: The current and future distribution of wildfire, PLoS One, 4, https://doi.org/10.1371/journal.pone.0005102, 2009.

Krebs, P., Pezzatti, G. B., Mazzoleni, S., Talbot, L. M., and Conedera, M.: Fire regime: History and definition of a key concept in disturbance ecology, Theor Biosci, 129, 53–69, https://doi.org/10.1007/s12064-010-0082-z, 2010.

Kreider, M. R., Higuera, P. E., Parks, S. A., Rice, W. L., White, N., and Larson, A. J.: Fire suppression makes wildfires more severe and accentuates impacts of climate change and fuel accumulation, Nat Commun, 15, 2412, https://doi.org/10.1038/s41467-024-46702-0, 2024.

Kühl, N., Gebhardt, C., Litt, T., and Hense, A.: Probability Density Functions as Botanical-Climatological Transfer Functions for Climate Reconstruction, Quat Res, 58, 381–392, https://doi.org/10.1006/qres.2002.2380, 2002.

Kühl, N., Moschen, R., Wagner, S., Brewer, S., and Peyron, O.: A multiproxy record of late Holocene natural and anthropogenic environmental change from the *Sphagnum* peat bog Dürres Maar, Germany: implications for quantitative climate reconstructions based on pollen, J Quat Sci, 25, 675–688, https://doi.org/10.1002/jqs.1342, 2010.

Kuhn-Régnier, A., Voulgarakis, A., Nowack, P., Forkel, M., Prentice, I. C., and Harrison, S. P.: The importance of antecedent vegetation and drought conditions as global drivers of burnt area, Biogeosciences, 18, 3861–3879, https://doi.org/10.5194/bg-18-3861-2021, 2021.

Lamont, B. B. and Downes, K. S.: Fire-stimulated flowering among resprouters and geophytes in Australia and South Africa, Plant Ecol, 212, 2111–2125, https://doi.org/10.1007/s11258-011-9987-y, 2011.

Lamont, B. B., He, T., and Yan, Z.: Evolutionary history of fire-stimulated resprouting, flowering, seed release and germination, Biol Rev, 94, 903–928, https://doi.org/10.1111/brv.12483, 2019.

Lasslop, G., Hantson, S., Harrison, S. P., Bachelet, D., Burton, C., Forkel, M., Forrest, M., Li, F., Melton, J. R., Yue, C., Archibald, S., Scheiter, S., Arneth, A., Hickler, T., and Sitch, S.: Global ecosystems and fire: Multi-model assessment of fire-induced tree-cover and carbon storage reduction, Glob Chang Biol, 26, 5027–5041, https://doi.org/10.1111/gcb.15160, 2020.

Lechleitner, F., Amirnezhad-Mozhdehi, S., Columbu, A., Comas-Bru, L., Labuhn, I., Pérez-Mejías, C., and Rehfeld, K.: The Potential of Speleothems from Western Europe as Recorders of Regional Climate: A Critical Assessment of the SISAL Database, Quaternary, 1, 30, https://doi.org/10.3390/quat1030030, 2018.

Legrand, M. and Mayewski, P.: Glaciochemistry of polar ice cores: A review, Rev Geophys, 35, 219–243, https://doi.org/10.1029/96RG03527, 1997.

Lertzman, K., Gavin, D., Hallett, D., Brubaker, L., Lepofsky, D., and Mathewes, R.: Long-Term Fire Regime Estimated from Soil Charcoal in Coastal Temperate Rainforests, Conservation Ecology, 6, art5, https://doi.org/10.5751/ES-00432-060205, 2002.

Leys, B. A., Commerford, J. L., and McLauchlan, K. K.: Reconstructing grassland fire history using sedimentary charcoal: Considering count, size and shape, PLoS One, 12, https://doi.org/10.1371/journal.pone.0176445, 2017.

Lézine, A.-M., Ivory, S. J., Gosling, W. D., and Scott, L.: The African Pollen Database (APD) and tracing environmental change: State of the Art, in: Quaternary Vegetation Dynamics – The African Pollen Database, CRC Press, London, 5–12, https://doi.org/10.1201/9781003162766-2, 2021.

Li, F., Gaillard, M.-J., Xu, Q., Bunting, M. J., Li, Y., Li, J., Mu, H., Lu, J., Zhang, P., Zhang, S., Cui, Q., Zhang, Y., and Shen, W.: A Review of Relative Pollen Productivity Estimates From Temperate China for Pollen-Based Quantitative Reconstruction of Past Plant Cover, Front Plant Sci, 9, https://doi.org/10.3389/fpls.2018.01214, 2018.

Li, F., Gaillard, M.-J., Cao, X., Herzschuh, U., Sugita, S., Tarasov, P. E., Wagner, M., Xu, Q., Ni, J., Wang, W., Zhao, Y., An, C., Beusen, A. H. W., Chen, F., Feng, Z., Goldewijk, C. G. M. K., Huang, X., Li, Y., Li, Y., Liu, H., Sun, A., Yao, Y., Zheng, Z., and Jia, X.: Towards quantification of Holocene anthropogenic land-cover change in temperate China: A review in the light of pollen-based REVEALS reconstructions of regional plant cover, Earth Sci Rev, 203, 103119, https://doi.org/10.1016/j.earscirev.2020.103119, 2020.

Li, P., Feng, Z., Jiang, L., Liao, C., and Zhang, J.: A Review of Swidden Agriculture in Southeast Asia, Remote Sens (Basel), 6, 1654–1683, https://doi.org/10.3390/rs6021654, 2014.

Linares, M. and Ni-Meister, W.: Impact of Wildfires on Land Surface Cold Season Climate in the Northern High-Latitudes: A Study on Changes in Vegetation, Snow Dynamics, Albedo, and Radiative Forcing, Remote Sens (Basel), 16, 1461, https://doi.org/10.3390/rs16081461, 2024.

Litt, T., Schölzel, C., Kühl, N., and Brauer, A.: Vegetation and climate history in the Westeifel Volcanic Field (Germany) during the past 11 000 years based on annually laminated lacustrine maar sediments, Boreas, 38, 679–690, https://doi.org/10.1111/j.1502-3885.2009.00096.x, 2009.

Liu, M., Prentice, I. C., ter Braak, C. J. F., and Harrison, S. P.: An improved statistical approach for reconstructing past climates from biotic assemblages, P Roy Soc A-Math Phy, 476, https://doi.org/10.1098/rspa.2020.0346, 2020.

Liu, M., Shen, Y., González-Sampériz, P., Gil-Romera, G., ter Braak, C. J. F., Prentice, I. C., and Harrison, S. P.: Holocene climates of the Iberian Peninsula: pollen-based reconstructions of changes in the west–east gradient of temperature and moisture, Clim Past, 19, 803–834, https://doi.org/10.5194/cp-19-803-2023, 2023.

Liu, S., Li, K., Jia, W., Stoof-Leichsenring, K. R., Liu, X., Cao, X., and Herzschuh, U.: Vegetation Reconstruction From Siberia and the Tibetan Plateau Using Modern Analogue Technique–Comparing Sedimentary (Ancient) DNA and Pollen Data, Front Ecol Evol, 9, https://doi.org/10.3389/fevo.2021.668611, 2021.

Liu, Y., Goodrick, S., and Heilman, W.: Wildland fire emissions, carbon, and climate: Wildfire–climate interactions, For Ecol Manage, 317, https://doi.org/10.1016/j.foreco.2013.02.020, 2014.

Lizundia-Loiola, J., Otón, G., Ramo, R., and Chuvieco, E.: A spatio-temporal active-fire clustering approach for global burned area mapping at 250 m from MODIS data, Remote Sens Environ, 236, 111493, https://doi.org/10.1016/j.rse.2019.111493, 2020.

López-Sáez, J. A., Vargas, G., Ruiz-Fernández, J., Blarquez, O., Alba-Sánchez, F., Oliva, M., Pérez-Díaz, S., Robles-López, S., and Abel-Schaad, D.: Paleofire Dynamics in Central Spain during the Late Holocene: The Role of Climatic and Anthropogenic Forcing, Land Degrad Dev, 29, 2045–2059, https://doi.org/10.1002/ldr.2751, 2018.

Manning, K. and Timpson, A.: The demographic response to Holocene climate change in the Sahara, Quat Sci Rev, 101, 28–35, https://doi.org/10.1016/j.quascirev.2014.07.003, 2014.

Mantero, G., Morresi, D., Marzano, R., Motta, R., Mladenoff, D. J., and Garbarino, M.: The influence of land abandonment on forest disturbance regimes: a global review, Landsc Ecol, 35, https://doi.org/10.1007/s10980-020-01147-w, 2020.

Margolis, E. Q., Guiterman, C. H., Chavardès, R. D., Coop, J. D., Copes-Gerbitz, K., Dawe, D. A., Falk, D. A., Johnston, J. D., Larson, E., Li, H., Marschall, J. M., Naficy, C. E., Naito, A. T., Parisien, M., Parks, S. A., Portier, J., Poulos, H. M., Robertson, K. M., Speer, J. H., Stambaugh, M., Swetnam, T. W., Tepley, A. J., Thapa, I., Allen, C. D., Bergeron, Y., Daniels, L. D., Fulé, P. Z., Gervais, D., Girardin, M. P., Harley, G. L., Harvey, J. E., Hoffman, K. M., Huffman, J. M., Hurteau, M. D., Johnson, L. B., Lafon, C. W., Lopez, M. K., Maxwell, R. S., Meunier, J., North, M., Rother, M. T., Schmidt, M. R., Sherriff, R. L., Stachowiak, L. A., Taylor, A., Taylor, E. J., Trouet, V., Villarreal, M. L., Yocom, L. L., Arabas, K. B., Arizpe, A. H., Arseneault, D., Tarancón, A. A., Baisan, C., Bigio, E., Biondi, F., Cahalan, G. D., Caprio, A., Cerano-Paredes, J., Collins, B. M., Dey, D. C., Drobyshev, I., Farris, C., Fenwick, M. A., Flatley, W., Floyd, M. L., Gedalof, Z., Holz, A., Howard, L. F., Huffman, D. W., Iniguez, J., Kipfmueller, K. F., Kitchen, S. G., Lombardo, K., McKenzie, D., Merschel, A. G., Metlen, K. L., Minor, J., O'Connor, C. D., Platt, L., Platt, W. J., Saladyga, T., Stan, A. B., Stephens, S., Sutheimer, C., Touchan, R., and Weisberg, P. J.: The North American tree-ring fire-scar network, Ecosphere, 13, https://doi.org/10.1002/ecs2.4159, 2022.

Mariani, M., Fletcher, M. -S., Holz, A., and Nyman, P.: ENSO controls interannual fire activity in southeast Australia, Geophys Res Lett, 43, https://doi.org/10.1002/2016GL070572, 2016.

Marinova, E., Harrison, S. P., Bragg, F., Connor, S., de Laet, V., Leroy, S. A. G., Mudie, P., Atanassova, J., Bozilova, E., Caner, H., Cordova, C., Djamali, M., Filipova-Marinova, M., Gerasimenko, N., Jahns, S., Kouli, K., Kotthoff, U., Kvavadze, E., Lazarova, M., Novenko, E., Ramezani, E., Röpke, A., Shumilovskikh, L., Tanţău, I., and Tonkov, S.: Pollen-derived biomes in the Eastern Mediterranean–Black Sea–Caspian-Corridor, J Biogeogr, 45, 484–499, https://doi.org/10.1111/jbi.13128, 2018.

Marlon, J. R., Bartlein, P. J., Carcaillet, C., Gavin, D. G., Harrison, S. P., Higuera, P. E., Joos, F., Power, M. J., and Prentice, I. C.: Climate and human influences on global biomass burning over the past two millennia, Nat Geosci, 1, 697–702, https://doi.org/10.1038/ngeo313, 2008.

Marlon, J. R., Bartlein, P. J., Gavin, D. G., Long, C. J., Anderson, R. S., Briles, C. E., Brown, K. J., Colombaroli, D., Hallett, D. J., Power, M. J., Scharf, E. A., and Walsh, M. K.: Long-term perspective on wildfires in the western USA, P Natl Acad Sci USA, 109, E535–E543, https://doi.org/10.1073/pnas.1112839109, 2012.

Marlon, J. R., Bartlein, P. J., Daniau, A.-L., Harrison, S. P., Maezumi, S. Y., Power, M. J., Tinner, W., and Vannière, B.: Global biomass burning: a synthesis and review of Holocene paleofire records and their controls, Quat Sci Rev, 65, 5–25, https://doi.org/10.1016/j.quascirev.2012.11.029, 2013.

Marlon, J. R., Kelly, R., Daniau, A.-L., Vannière, B., Power, M. J., Bartlein, P., Higuera, P., Blarquez, O., Brewer, S., Brücher, T., Feurdean, A., Romera, G. G., Iglesias, V., Maezumi, S. Y., Magi, B., Courtney Mustaphi, C. J., and Zhihai, T.: Reconstructions of biomass burning from sediment-charcoal records to improve data–model comparisons, Biogeosciences, 13, 3225–3244, https://doi.org/10.5194/bg-13-3225-2016, 2016.

Martin Calvo, M. and Prentice, I. C.: Effects of fire and CO_2 on biogeography and primary production in glacial and modern climates, New Phytol, 208, 987–994, https://doi.org/10.1111/nph.13485, 2015.

Mauri, A., Davis, B. A. S., Collins, P. M., and Kaplan, J. O.: The influence of atmospheric circulation on the mid-Holocene climate of Europe: a data–model comparison, Climate of the Past, 10, 1925–1938, https://doi.org/10.5194/cp-10-1925-2014, 2014.

Mauri, A., Davis, B. A. S., Collins, P. M., and Kaplan, J. O.: The climate of Europe during the Holocene: A gridded pollen-based reconstruction and its multi-proxy evaluation, Quat Sci Rev, 112, 109–127, https://doi.org/10.1016/j.quascirev.2015.01.013, 2015.

McDermott, F.: Palaeo-climate reconstruction from stable isotope variations in speleothems: a review, Quat Sci Rev, 23, https://doi.org/10.1016/j.quascirev.2003.06.021, 2004.

McEvedy, C. and Jones, Richard.: Atlas of World Population History, Penguin Books Ltd, Harmondsworth, Middlesex, England, 1978.

Mellars, P. and French, J. C.: Tenfold Population Increase in Western Europe at the Neandertal—to—Modern Human Transition, Science, 333, 623–627, 2011.

Midgley, J. J.: Flammability is not selected for, it emerges, Aust J Bot, 61, 102, https://doi.org/10.1071/BT12289, 2013.

Mithen, S. and Wicks, K.: Population level models for testing hunter-gatherer resilience and settlement response to the combined impact of abrupt climatic events and sea level change: A case study from the Holocene of northern Britain, Quat Sci Rev, 265, 107027, https://doi.org/10.1016/j.quascirev.2021.107027, 2021.

Mooney, S. D., Harrison, S. P., Bartlein, P. J., Daniau, A.-L., Stevenson, J., Brownlie, K. C., Buckman, S., Cupper, M., Luly, J., Black, M., Colhoun, E., D'Costa, D., Dodson, J., Haberle, S., Hope, G. S., Kershaw, P., Kenyon, C., McKenzie, M., and Williams, N.: Late Quaternary fire regimes of Australasia, Quat Sci Rev, 30, 28–46, https://doi.org/10.1016/j.quascirev.2010.10.010, 2011.

Moreira, F., Ascoli, D., Safford, H., Adams, M. A., Moreno, J. M., Pereira, J. M. C., Catry, F. X., Armesto, J., Bond, W., González, M. E., Curt, T., Koutsias, N., McCaw, L., Price, O., Pausas, J. G., Rigolot, E., Stephens, S., Tavsanoglu, C., Vallejo, V. R., Van Wilgen, B. W., Xanthopoulos, G., and Fernandes, P. M.: Wildfire management in Mediterranean-type regions: paradigm change needed, Environ Res Lett, 15, 011001, https://doi.org/10.1088/1748-9326/ab541e, 2020.

Morgan, G. W., Tolhurst, K. G., Poynter, M. W., Cooper, N., McGuffog, T., Ryan, R., Wouters, M. A., Stephens, N., Black, P., Sheehan, D., Leeson, P., Whight, S., and Davey, S. M.: Prescribed burning in south-eastern Australia: history and future directions, Aust For, 83, 4–28, https://doi.org/10.1080/00049158.2020.1739883, 2020.

Mrotzek, A., Couwenberg, J., Theuerkauf, M., and Joosten, H.: MARCO POLO – A new and simple tool for pollen-based stand-scale vegetation reconstruction, Holocene, 27, 321–330, https://doi.org/10.1177/0959683616660171, 2017.

Nader, G., Henkin, Z., Smith, E., Ingram, R., and Narvaez, N.: Planned Herbivory in the Management of Wildfire Fuels, Rangelands, 29, 18–24, https://doi.org/10.2111/1551-501X(2007)29[18:PHITMO]2.0.CO;2, 2007.

Nagy, R. C., Fusco, E., Bradley, B., Abatzoglou, J. T., and Balch, J.: Human-Related Ignitions Increase the Number of Large Wildfires across U.S. Ecoregions, Fire, 1, 4, https://doi.org/10.3390/fire1010004, 2018.

Nair, M., Bherwani, H., Kumar, S., Gulia, S., Goyal, S., and Kumar, R.: Assessment of contribution of agricultural residue burning on air quality of Delhi using remote sensing and modelling tools, Atmos Environ, 230, https://doi.org/10.1016/j.atmosenv.2020.117504, 2020.

Neidermeier, A. N., Zagaria, C., Pampanoni, V., West, T. A. P., and Verburg, P. H.: Mapping opportunities for the use of land management strategies to address fire risk in Europe, J Environ Manage, 346, 118941, https://doi.org/10.1016/j.jenvman.2023.118941, 2023.

van Nes, E. H., Staal, A., Hantson, S., Holmgren, M., Pueyo, S., Bernardi, R. E., Flores, B. M., Xu, C., and Scheffer, M.: Fire forbids fifty-fifty forest, PLoS One, 13, e0191027, https://doi.org/10.1371/journal.pone.0191027, 2018.

Ortega-Rosas, C. I., Guiot, J., Peñalba, M. C., and Ortiz-Acosta, M. E.: Biomization and quantitative climate reconstruction techniques in northwestern Mexico—With an application to four Holocene pollen sequences, Glob Planet Change, 61, 242–266, https://doi.org/10.1016/j.gloplacha.2007.10.006, 2008.

Ortiz, J. E., Moreno, L., Torres, T., Vegas, J., Ruiz-Zapata, B., García-Cortés, Á., Galán, L., and Pérez-González, A.: A 220 ka palaeoenvironmental reconstruction of the Fuentillejo maar lake record

(Central Spain) using biomarker analysis, Org Geochem, 55, 85–97, https://doi.org/10.1016/j.orggeochem.2012.11.012, 2013.

Overpeck, J. T., Webb, T., and Prentice, I. C.: Quantitative Interpretation of Fossil Pollen Spectra: Dissimilarity Coefficients and the Method of Modern Analogs, Quat Res, 23, 87–108, https://doi.org/10.1016/0033-5894(85)90074-2, 1985.

Overpeck, J. T., Webb, R. S., and Webb III, T.: Mapping eastern North American vegetation change of the past 18 ka: No-analogs and the future, Geology, 20, 1071, https://doi.org/10.1130/0091-7613(1992)020<1071:MENAVC>2.3.CO;2, 1992.

Palmisano, A., Bevan, A., and Shennan, S.: Comparing archaeological proxies for long-term population patterns: An example from central Italy, J Archaeol Sci, 87, 59–72, https://doi.org/10.1016/j.jas.2017.10.001, 2017.

Palmisano, A., Lawrence, D., de Gruchy, M. W., Bevan, A., and Shennan, S.: Holocene regional population dynamics and climatic trends in the Near East: A first comparison using archaeo-demographic proxies, Quat Sci Rev, 252, 106739, https://doi.org/10.1016/j.quascirev.2020.106739, 2021a.

Palmisano, A., Lawrence, D., de Gruchy, M. W., Bevan, A., and Shennan, S.: Holocene regional population dynamics and climatic trends in the Near East: A first comparison using archaeo-demographic proxies, Quat Sci Rev, 252, https://doi.org/10.1016/j.quascirev.2020.106739, 2021b.

Parisien, M.-A. and Moritz, M. A.: Environmental controls on the distribution of wildfire at multiple spatial scales, Ecol Monogr, 79, 127–154, https://doi.org/10.1890/07-1289.1, 2009.

Parisien, M.-A., Parks, S. A., Krawchuk, M. A., Little, J. M., Flannigan, M. D., Gowman, L. M., and Moritz, M. A.: An analysis of controls on fire activity in boreal Canada: comparing models built with different temporal resolutions, Ecol Appl, 24, 1341–1356, https://doi.org/10.1890/13-1477.1, 2014.

Paritsis, J., Veblen, T. T., and Holz, A.: Positive fire feedbacks contribute to shifts from *Nothofagus pumilio* forests to fire-prone shrublands in Patagonia, J Veg Sci, 26, 89–101, https://doi.org/10.1111/jvs.12225, 2015.

Parker, S. E., Harrison, S. P., Comas-Bru, L., Kaushal, N., LeGrande, A. N., and Werner, M.: A data–model approach to interpreting speleothem oxygen isotope records from monsoon regions, Clim Past, 17, 1119–1138, https://doi.org/10.5194/cp-17-1119-2021, 2021.

Parsons, R. W. and Prentice, I. C.: Statistical approaches to R-values and the pollen- vegetation relationship, Rev Palaeobot Palynol, https://doi.org/10.1016/0034-6667(81)90001-4, 1981.

Patterson, W. A., Edwards, K. J., and Maguire, D. J.: Microscopic charcoal as a fossil indicator of fire, Quat Sci Rev, 6, 3–23, https://doi.org/10.1016/0277-3791(87)90012-6, 1987.

Pausas, J. G.: Bark thickness and fire regime, Funct Ecol, 29, 315–327, https://doi.org/10.1111/1365-2435.12372, 2015.

Pausas, J. G. and Keeley, J. E.: Wildfires as an ecosystem service, Front Ecol Environ, 17, 289–295, https://doi.org/10.1002/fee.2044, 2019.

Pausas, J. G. and Keeley, J. E.: Wildfires and global change, Front Ecol Environ, 19, 387–395, https://doi.org/10.1002/fee.2359, 2021.

Pausas, J. G., Pratt, R. B., Keeley, J. E., Jacobsen, A. L., Ramirez, A. R., Vilagrosa, A., Paula, S., Kaneakua-Pia, I. N., and Davis, S. D.: Towards understanding resprouting at the global scale, New Phytol, 209, 945–954, https://doi.org/10.1111/nph.13644, 2016.

Pausas, J. G., Keeley, J. E., and Schwilk, D. W.: Flammability as an ecological and evolutionary driver, J Ecol, 105, 289–297, https://doi.org/10.1111/1365-2745.12691, 2017.

Paveglio, T., Norton, T., and Carroll, M. S.: Fanning the Flames? Media Coverage during Wildfire Events and its Relation to Broader Societal Understandings of the Hazard, Human Ecology Review, 18, 41–52, 2011.

Pearl, J. K., Keck, J. R., Tintor, W., Siekacz, L., Herrick, H. M., Meko, M. D., and Pearson, C. L.: New frontiers in tree-ring research, Holocene, 30, 923–941, https://doi.org/10.1177/0959683620902230, 2020.

Penman, T. D., Christie, F. J., Andersen, A. N., Bradstock, R. A., Cary, G. J., Henderson, M. K., Price, O., Tran, C., Wardle, G. M., Williams, R. J., and York, A.: Prescribed burning: how can it work to conserve the things we value?, Int J Wildland Fire, 20, https://doi.org/10.1071/WF09131, 2011.

Pereira, P., Bogunovic, I., Zhao, W., and Barcelo, D.: Short-term effect of wildfires and prescribed fires on ecosystem services, Curr Opin Environ Sci Health, 22, 100266, https://doi.org/10.1016/j.coesh.2021.100266, 2021.

Peterson, D., Wang, J., Ichoku, C., and Remer, L. A.: Effects of lightning and other meteorological factors on fire activity in the North American boreal forest: implications for fire weather forecasting, Atmos Chem Phys, 10, 6873–6888, https://doi.org/10.5194/acp-10-6873-2010, 2010.

Pickett, E. J., Harrison, S. P., Hope, G., Harle, K., Dodson, J. R., Peter Kershaw, A., Colin Prentice, I., Backhouse, J., Colhoun, E. A., D'Costa, D., Flenley, J., Grindrod, J., Haberle, S., Hassell, C., Kenyon, C., Macphail, M., Martin, H., Martin, A. H., McKenzie, M., Newsome, J. C., Penny, D., Powell, J., Ian Raine, J., Southern, W., Stevenson, J., Sutra, J., Thomas, I., van der Kaars, S., and Ward, J.: Pollen-based reconstructions of biome distributions for Australia, Southeast Asia and the Pacific (SEAPAC region) at 0, 6000 and 18,000 14 C yr BP, J Biogeogr, 31, 1381–1444, https://doi.org/10.1111/j.1365-2699.2004.01001.x, 2004.

Pongratz, J., Reick, C., Raddatz, T., and Claussen, M.: A reconstruction of global agricultural areas and land cover for the last millennium, Global Biogeochem Cycles, 22, GB3018, https://doi.org/10.1029/2007GB003153, 2008.

Popović, Z., Bojović, S., Marković, M., and Cerdà, A.: Tree species flammability based on plant traits: A synthesis, Sci Total Environ, 800, 149625, https://doi.org/10.1016/j.scitotenv.2021.149625, 2021.

Power, M. J., Whitlock, C., Bartlein, P., and Stevens, L. R.: Fire and vegetation history during the last 3800 years in northwestern Montana, Geomorphology, 75, https://doi.org/10.1016/j.geomorph.2005.07.025, 2006.

Power, M. J., Marlon, J. R., Ortiz, N., Bartlein, P. J., Harrison, S. P., Mayle, F. E., Ballouche, A., Bradshaw, R. H. W., Carcaillet, C., Cordova, C., Mooney, S., Moreno, P. I., Prentice, I. C., Thonicke, K., Tinner, W., Whitlock, C., Zhang, Y., Zhao, Y., Ali, A. A., Anderson, R. S., Beer, R., Behling, H., Briles, C., Brown, K. J., Brunelle, A., Bush, M., Camill, P., Chu, G. Q., Clark, J., Colombaroli, D., Connor, S., Daniau, A.-L., Daniels, M., Dodson, J., Doughty, E., Edwards, M. E., Finsinger, W., Foster, D., Frechette, J., Gaillard, M.-J., Gavin, D. G., Gobet, E., Haberle, S., Hallett, D. J., Higuera, P., Hope, G., Horn, S., Inoue, J., Kaltenrieder, P., Kennedy, L., Kong, Z. C., Larsen, C., Long, C. J., Lynch, J., Lynch, E. A., McGlone, M., Meeks, S., Mensing, S., Meyer, G., Minckley, T., Mohr, J., Nelson, D. M., New, J., Newnham, R., Noti, R., Oswald, W., Pierce, J., Richard, P. J. H., Rowe, C., Sanchez Goñi, M. F., Shuman, B. N., Takahara, H., Toney, J., Turney, C., Urrego-Sanchez, D. H., Umbanhowar, C., Vandergoes, M., Vannière, B., Vescovi, E., Walsh, M., Wang, X., Williams, N., Wilmshurst, J., and Zhang, J. H.: Changes in fire regimes since the Last Glacial Maximum: an assessment based on a global synthesis and analysis of charcoal data, Clim Dyn, 30, 887–907, https://doi.org/10.1007/s00382-007-0334-x, 2008.

Prentice, C.: Records of vegetation in time and space: the principles of pollen analysis, in: Vegetation history, Springer Netherlands, Dordrecht, 17–42, https://doi.org/10.1007/978-94-009-3081-0_2, 1988.

Prentice, C., Guiot, J., Huntley, B., Jolly, D., and Cheddadi, R.: Reconstructing biomes from palaeoecological data: a general method and its application to European pollen data at 0 and 6 ka, Clim Dyn, 12, https://doi.org/10.1007/BF00211617, 1996.

Prentice, I. C.: Multidimensional scaling as a research tool in quaternary palynology: A review of theory and methods, Rev Palaeobot Palynol, 31, 71–104, https://doi.org/10.1016/0034-6667(80)90023-8, 1980.

Prentice, I. C. and Webb III, T.: BIOME 6000: reconstructing global mid-Holocene vegetation patterns from palaeoecological records, J Biogeogr, 25, 997–1005, https://doi.org/10.1046/j.1365-2699.1998.00235.x, 1998.

Prentice, I. C., Berglund, B. E., and Olsson, T.: Quantitative forest-composition sensing characteristics of pollen samples from Swedish lakes, Boreas, 16, 43–54, https://doi.org/10.1111/j.1502-3885.1987.tb00753.x, 1987.

Prentice, I. C., Villegas-Diaz, R., and Harrison, S. P.: Accounting for atmospheric carbon dioxide variations in pollen-based reconstruction of past hydroclimates, Glob Planet Change, 211, 103790, https://doi.org/10.1016/j.gloplacha.2022.103790, 2022.

Prince, T. J., Pisaric, M. F. J., and Turner, K. W.: Postglacial Reconstruction of Fire History Using Sedimentary Charcoal and Pollen From a Small Lake in Southwest Yukon Territory, Canada, Front Ecol Evol, 6, https://doi.org/10.3389/fevo.2018.00209, 2018.

Probert, J. R., Parr, C. L., Holdo, R. M., Anderson, T. M., Archibald, S., Courtney Mustaphi, C. J., Dobson, A. P., Donaldson, J. E., Hopcraft, G. C., Hempson, G. P., Morrison, T. A., and Beale, C. M.: Anthropogenic modifications to fire regimes in the wider Serengeti-Mara ecosystem, Glob Chang Biol, 25, 3406–3423, https://doi.org/10.1111/gcb.14711, 2019.

Quintano, C., Fernandez-Manso, A., Marcos, E., and Calvo, L.: Burn Severity and Post-Fire Land Surface Albedo Relationship in Mediterranean Forest Ecosystems, Remote Sens (Basel), 11, 2309, https://doi.org/10.3390/rs11192309, 2019.

Rabin, S. S., Melton, J. R., Lasslop, G., Bachelet, D., Forrest, M., Hantson, S., Kaplan, J. O., Li, F., Mangeon, S., Ward, D. S., Yue, C., Arora, V. K., Hickler, T., Kloster, S., Knorr, W., Nieradzik, L., Spessa, A., Folberth, G. A., Sheehan, T., Voulgarakis, A., Kelley, D. I., Prentice, I. C., Sitch, S., Harrison, S., and Arneth, A.: The Fire Modeling Intercomparison Project (FireMIP), phase 1: experimental and analytical protocols with detailed model descriptions, Geosci Model Dev, 10, 1175–1197, https://doi.org/10.5194/gmd-10-1175-2017, 2017.

Ramsey, C. B.: Deposition models for chronological records, Quat Sci Rev, 27, 42–60, https://doi.org/10.1016/j.quascirev.2007.01.019, 2008.

Ramsey, C. B.: Methods for Summarizing Radiocarbon Datasets, Radiocarbon, 59, 1809–1833, https://doi.org/10.1017/RDC.2017.108, 2017.

Ratajczak, Z., Nippert, J. B., Briggs, J. M., and Blair, J. M.: Fire dynamics distinguish grasslands, shrublands and woodlands as alternative attractors in the Central Great Plains of North America, J Ecol, 102, 1374–1385, https://doi.org/10.1111/1365-2745.12311, 2014.

Richardson, D., Black, A. S., Irving, D., Matear, R. J., Monselesan, D. P., Risbey, J. S., Squire, D. T., and Tozer, C. R.: Global increase in wildfire potential from compound fire weather and drought, NPJ Clim Atmos Sci, 5, 23, https://doi.org/10.1038/s41612-022-00248-4, 2022.

Rick, J. W.: Dates as Data: An Examination of the Peruvian Preceramic Radiocarbon Record, Am Antiq, 52, 55, https://doi.org/10.2307/281060, 1987.

Roberts, N., Fyfe, R. M., Woodbridge, J., Gaillard, M.-J., Davis, B. A. S., Kaplan, J. O., Marquer, L., Mazier, F., Nielsen, A. B., Sugita, S., Trondman, A.-K., and Leydet, M.: Europe's lost forests: a pollen-based synthesis for the last 11,000 years, Sci Rep, 8, 716, https://doi.org/10.1038/s41598-017-18646-7, 2018.

Roberts, C. N., Woodbridge, J., Palmisano, A., Bevan, A., Fyfe, R., and Shennan, S.: Mediterranean landscape change during the Holocene: Synthesis, comparison and regional trends in population, land cover and climate, Holocene, 29, 923–937, https://doi.org/10.1177/0959683619826697, 2019.

Robin, V. and Nelle, O.: Contribution to the reconstruction of central European fire history, based on the soil charcoal analysis of study sites in northern and central Germany, Veg Hist Archaeobot, 23, 51–65, https://doi.org/10.1007/s00334-014-0438-2, 2014.

Roces-Díaz, J. V, Santín, C., Martínez-Vilalta, J., and Doerr, S. H.: A global synthesis of fire effects on ecosystem services of forests and woodlands, Front Ecol Environ, 20, 170–178, https://doi.org/10.1002/fee.2349, 2022.

Rubino, M., D'Onofrio, A., Seki, O., and Bendle, J. A.: Ice-core records of biomass burning, The Anthropocene Review, 3, 140–162, https://doi.org/10.1177/2053019615605117, 2016.

Ruffault, J., Curt, T., Martin-StPaul, N. K., Moron, V., and Trigo, R. M.: Extreme wildfire events are linked to global-change-type droughts in the northern Mediterranean, Natural Hazards and Earth System Sciences, 18, 847–856, https://doi.org/10.5194/nhess-18-847-2018, 2018.

Salonen, J. S., Ilvonen, L., Seppä, H., Holmström, L., Telford, R. J., Gaidamavičius, A., Stančikaitė, M., and Subetto, D.: Comparing different calibration methods (WA/WA-PLS regression and Bayesian modelling) and different-sized calibration sets in pollen-based quantitative climate reconstruction, Holocene, 22, 413–424, https://doi.org/10.1177/0959683611425548, 2012.

Sangster, A. G. and Dale, H. M.: A preliminary study of differential pollen grain preservation, Canadian Journal of Botany, 39, 35–43, https://doi.org/10.1139/b61-004, 1961.

Santos, F. L. M., Nogueira, J., Souza, R. A. F. de, Falleiro, R. M., Schmidt, I. B., and Libonati, R.: Prescribed Burning Reduces Large, High-Intensity Wildfires and Emissions in the Brazilian Savanna, Fire, 4, 56, https://doi.org/10.3390/fire4030056, 2021.

Sawada, M., Viau, A. E., Vettoretti, G., Peltier, W. R., and Gajewski, K.: Comparison of North-American pollen-based temperature and global lake-status with CCCma AGCM2 output at 6ka, Quat Sci Rev, 23, 225–244, https://doi.org/10.1016/j.quascirev.2003.08.005, 2004.

Scharf, E. A.: A statistical evaluation of the relative influences of climate, vegetation, and prehistoric human population on the charcoal record of Five Lakes, Washington (USA), Quat Int, 215, 74–86, https://doi.org/10.1016/j.quaint.2009.09.021, 2010.

Schwilk, D. W. and Ackerly, D. D.: Flammability and serotiny as strategies: correlated evolution in pines, Oikos, 94, 326–336, https://doi.org/10.1034/j.1600-0706.2001.940213.x, 2001.

Scott, K., Setterfield, S. A., Douglas, M. M., Parr, C. L., Schatz, J., and Andersen, A. N.: Does long-term fire exclusion in an Australian tropical savanna result in a biome shift? A test using the reintroduction of fire, Austral Ecol, 37, 693–711, https://doi.org/10.1111/j.1442-9993.2012.02379.x, 2012.

Seppä, H.: Pollen analysis, principles, in: Encyclopedia of Quaternary Science, Elsevier, 794–804, https://doi.org/10.1016/B978-0-444-53643-3.00171-0, 2013.

Serge, M., Mazier, F., Fyfe, R., Gaillard, M.-J., Klein, T., Lagnoux, A., Galop, D., Githumbi, E., Mindrescu, M., Nielsen, A., Trondman, A.-K., Poska, A., Sugita, S., Woodbridge, J., Abel-Schaad, D., Åkesson, C., Alenius, T., Ammann, B., Andersen, S., Anderson, R., Andrič, M., Balakauskas, L., Barnekow, L., Batalova, V., Bergman, J., Birks, H., Björkman, L., Bjune, A., Borisova, O., Broothaerts, N., Carrion, J., Caseldine, C., Christiansen, J., Cui, Q., Currás, A., Czerwiński, S., David, R., Davies, A., De Jong, R., Di Rita, F., Dietre, B., Dörfler, W., Doyen, E., Edwards, K., Ejarque, A., Endtmann, E., Etienne, D., Faure, E., Feeser, I., Feurdean, A., Fischer, E., Fletcher, W., Franco-Múgica, F., Fredh, E., Froyd, C., Garcés-Pastor, S., García-Moreiras, I., Gauthier, E., Gil-Romera, G., González-Sampériz, P., Grant, M., Grindean, R., Haas, J., Hannon, G., Heather, A.-J., Heikkilä, M., Hjelle, K., Jahns, S., Jasiunas, N., Jiménez-Moreno, G., Jouffroy-Bapicot, I., Kabailienė, M., Kamerling, I., Kangur, M., Karpińska-Kołaczek, M., Kasianova, A., Kołaczek, P., Lagerås, P., Latalowa, M., Lechterbeck, J., Leroyer, C., Leydet, M., Lindbladh, M., Lisitsyna, O., López-Sáez, J.-A., Lowe, J., Luelmo-Lautenschlaeger, R., Lukanina, E., Macijauskaitė, L., Magri, D., Marguerie, D., Marquer, L., Martinez-Cortizas, A., Mehl, I., Mesa-Fernández, J., Mighall, T., Miola, A., Miras, Y., Morales-Molino, C., et al.: Testing the Effect of Relative Pollen Productivity on the REVEALS Model: A Validated Reconstruction of Europe-Wide Holocene Vegetation, Land (Basel), 12, 986, https://doi.org/10.3390/land12050986, 2023.

Shen, Y., Cai, W., Prentice, I. C., and Harrison, S. P.: Community Abundance of Resprouting in Woody Plants Reflects Fire Return Time, Intensity, and Type, Forests, 14, 878, https://doi.org/10.3390/f14050878, 2023.

Shennan, S., Downey, S. S., Timpson, A., Edinborough, K., Colledge, S., Kerig, T., Manning, K., and Thomas, M. G.: Regional population collapse followed initial agriculture booms in mid-Holocene Europe, Nat Commun, 4, 31–34, https://doi.org/10.1038/ncomms3486, 2013.

Sheppard, P. R.: Dendroclimatology: extracting climate from trees, WIREs Climate Change, 1, 343–352, https://doi.org/10.1002/wcc.42, 2010.

Siegel, K. J., Macaulay, L., Shapero, M., Becchetti, T., Larson, S., Mashiri, F. E., Waks, L., Larsen, L., and Butsic, V.: Impacts of livestock grazing on the probability of burning in wildfires vary by region and vegetation type in California, J Environ Manage, 322, 116092, https://doi.org/10.1016/j.jenvman.2022.116092, 2022.

Silva, F. and Vander Linden, M.: Amplitude of travelling front as inferred from 14C predicts levels of genetic admixture among European early farmers, Sci Rep, 7, 11985, https://doi.org/10.1038/s41598-017-12318-2, 2017.

Silva Junior, C. H. L., Anderson, L. O., Silva, A. L., Almeida, C. T., Dalagnol, R., Pletsch, M. A. J. S., Penha, T. V., Paloschi, R. A., and Aragão, L. E. O. C.: Fire Responses to the 2010 and 2015/2016 Amazonian Droughts, Front Earth Sci (Lausanne), 7, https://doi.org/10.3389/feart.2019.00097, 2019.

Silva-Junior, C. H. L., Buna, A. T. M., Bezerra, D. S., Costa, O. S., Santos, A. L., Basson, L. O. D., Santos, A. L. S., Alvarado, S. T., Almeida, C. T., Freire, A. T. G., Rousseau, G. X., Celentano, D., Silva, F. B., Pinheiro, M. S. S., Amaral, S., Kampel, M., Vedovato, L. B., Anderson, L. O., and Aragão, L. E. O. C.: Forest Fragmentation and Fires in the Eastern Brazilian Amazon–Maranhão State, Brazil, Fire, 5, 77, https://doi.org/10.3390/fire5030077, 2022.

Silveira, M. V. F., Petri, C. A., Broggio, I. S., Chagas, G. O., Macul, M. S., Leite, C. C. S. S., Ferrari, E. M. M., Amim, C. G. V., Freitas, A. L. R., Motta, A. Z. V., Carvalho, L. M. E., Silva Junior, C. H. L., Anderson, L. O., and Aragão, L. E. O. C.: Drivers of Fire Anomalies in the Brazilian Amazon: Lessons Learned from the 2019 Fire Crisis, Land (Basel), 9, 516, https://doi.org/10.3390/land9120516, 2020.

Silvério, D. V., Brando, P. M., Bustamante, M. M. C., Putz, F. E., Marra, D. M., Levick, S. R., and Trumbore, S. E.: Fire, fragmentation, and windstorms: A recipe for tropical forest degradation, J Ecol, 107, 656–667, https://doi.org/10.1111/1365-2745.13076, 2019.

Sitch, S., Huntingford, C., Gedney, N., Levy, P. E., Lomas, M., Piao, S. L., Betts, R., Ciais, P., Cox, P., Friedlindstein, P., Jones, C. D., Prentice, I. C., and Woodward, F. I.: Evaluation of the terrestrial carbon cycle, future plant geography and climate-carbon cycle feedbacks using five Dynamic Global Vegetation Models (DGVMs), Glob Chang Biol, 14, 2015–2039, https://doi.org/10.1111/j.1365-2486.2008.01626.x, 2008.

Soulis, K. X., Generali, K. A., Papadaki, C., Theodoropoulos, C., and Psomiadis, E.: Hydrological Response of Natural Mediterranean Watersheds to Forest Fires, Hydrology, 8, 15, https://doi.org/10.3390/hydrology8010015, 2021.

Spötl, C. and Boch, R.: Uranium series dating of speleothems, in: Encyclopedia of Caves, Elsevier, 1096–1102, https://doi.org/10.1016/B978-0-12-814124-3.00128-X, 2019.

Starns, H. D., Taylor, C. A., Garza, N. E., and Tolleson, D. R.: Effects of Fire Exclusion on Previously Fire-Managed Semiarid Savanna Ecosystem, Rangel Ecol Manag, 73, 93–96, https://doi.org/10.1016/j.rama.2019.09.006, 2020.

Staver, A. C. and Levin, S. A.: Integrating Theoretical Climate and Fire Effects on Savanna and Forest Systems, Am Nat, 180, 211–224, https://doi.org/10.1086/666648, 2012.

Staver, A. C., Archibald, S., and Levin, S. A.: The global extent and determinants of savanna and forest as alternative biome states, Science, 334, 230–232, https://doi.org/10.1126/science.1210465, 2011.

Steel, Z. L., Safford, H. D., and Viers, J. H.: The fire frequency-severity relationship and the legacy of fire suppression in California forests, Ecosphere, 6, 1–23, https://doi.org/10.1890/ES14-00224.1, 2015.

Sugita, S.: Theory of quantitative reconstruction of vegetation I: Pollen from large sites REVEALS regional vegetation composition, Holocene, https://doi.org/10.1177/0959683607075837, 2007a.

Sugita, S.: Theory of quantitative reconstruction of vegetation II: all you need is LOVE, Holocene, 17, 243–257, https://doi.org/10.1177/0959683607075838, 2007b.

Sugita, S., Parshall, T., Calcote, R., and Walker, K.: Testing the Landscape Reconstruction Algorithm for spatially explicit reconstruction of vegetation in northern Michigan and Wisconsin, Quat Res, 74, 289–300, https://doi.org/10.1016/j.yqres.2010.07.008, 2010.

Sun, A., Luo, Y., Wu, H., Chen, X., Li, Q., Yu, Y., Sun, X., and Guo, Z.: An updated biomization scheme and vegetation reconstruction based on a synthesis of modern and mid-Holocene pollen data in China, Glob Planet Change, 192, 103178, https://doi.org/10.1016/j.gloplacha.2020.103178, 2020.

Surovell, T. A., Byrd Finley, J., Smith, G. M., Brantingham, P. J., and Kelly, R.: Correcting temporal frequency distributions for taphonomic bias, J Archaeol Sci, 36, https://doi.org/10.1016/j.jas.2009.03.029, 2009.

Swain, D. L.: A Shorter, Sharper Rainy Season Amplifies California Wildfire Risk, Geophys Res Lett, 48, https://doi.org/10.1029/2021GL092843, 2021.

Swaine, M. D., Hawthorne, W. D., and Orgle, T. K.: The Effects of Fire Exclusion on Savanna Vegetation at Kpong, Ghana, Biotropica, 24, 166, https://doi.org/10.2307/2388670, 1992.

Sweeney, L. F., Harrison, S. P. and Vander Linden, M.: Holocene archaeological radiocarbon data of the Iberian Peninsula. University of Reading. Dataset. https://doi.org/10.17864/1947.000340, 2021.

Swetnam, T. W.: Fire history and climate change in giant sequoia groves, Science, 262, 885–889, https://doi.org/10.1126/science.262.5135.885, 1993.

Syphard, A. D. and Keeley, J. E.: Location, timing and extent of wildfire vary by cause of ignition, Int J Wildland Fire, 24, 37, https://doi.org/10.1071/WF14024, 2015.

Syphard, A. D., Radeloff, V. C., Keuler, N. S., Taylor, R. S., Hawbaker, T. J., Stewart, S. I., and Clayton, M. K.: Predicting spatial patterns of fire on a southern California landscape, Int J Wildland Fire, 17, 602, https://doi.org/10.1071/WF07087, 2008.

Tang, M., Liu, M., Harrison S. P. and Prentice, I. C. European tree migrations during the Holocene, [Manuscript in preparation].

Tarasov, P. E., Andreev, A. A., Anderson, P. M., Lozhkin, A. V., Leipe, C., Haltia, E., Nowaczyk, N. R., Wennrich, V., Brigham-Grette, J., and Melles, M.: A pollen-based biome reconstruction over the last 3.562 million years in the Far East Russian Arctic – new insights into climate–vegetation relationships at the regional scale, Clim Past, 9, 2759–2775, https://doi.org/10.5194/cp-9-2759-2013, 2013.

Taylor, K. T., Maxwell, B. D., McWethy, D. B., Pauchard, A., Nuñez, M. A., and Whitlock, C.: Pinus contorta invasions increase wildfire fuel loads and may create a positive feedback with fire, Ecology, 98, 678–687, https://doi.org/10.1002/ecy.1673, 2017.

Timpson, A., Colledge, S., Crema, E., Edinborough, K., Kerig, T., Manning, K., Thomas, M. G., and Shennan, S.: Reconstructing regional population fluctuations in the European Neolithic using radiocarbon dates: A new case-study using an improved method, J Archaeol Sci, 52, 549–557, https://doi.org/10.1016/j.jas.2014.08.011, 2014.

Tinner, W., Lotter, A. F., Ammann, B., Conedera, M., Hubschmid, P., van Leeuwen, J. F. N., and Wehrli, M.: Climatic change and contemporaneous land-use phases north and south of the Alps 2300 BC to 800 AD, Quat Sci Rev, 22, 1447–1460, https://doi.org/10.1016/S0277-3791(03)00083-0, 2003.

Tinner, W., Hofstetter, S., Zeugin, F., Conedera, M., Wohlgemuth, T., Zimmermann, L., and Zweifel, R.: Long-distance transport of macroscopic charcoal by an intensive crown fire in the Swiss Alps - Implications for fire history reconstruction, Holocene, 16, 287–292, https://doi.org/10.1191/0959683606hl925rr, 2006.

Tinner, W., Vescovi, E., van Leeuwen, J. F. N., Colombaroli, D., Henne, P. D., Kaltenrieder, P., Morales-Molino, C., Beffa, G., Gnaegi, B., van der Knaap, W. O., La Mantia, T., and Pasta, S.: Holocene vegetation and fire history of the mountains of Northern Sicily (Italy), Veg Hist Archaeobot, 25, 499–519, https://doi.org/10.1007/s00334-016-0569-8, 2016.

Theuerkauf, M. and Couwenberg, J.: The extended downscaling approach: A new R-tool for pollen-based reconstruction of vegetation patterns, Holocene, 27, 1252–1258, https://doi.org/10.1177/0959683616683256, 2017.

Tonello, M. S., Mancini, M. V., and Seppä, H.: Quantitative reconstruction of Holocene precipitation changes in southern Patagonia, Quat Res, 72, 410–420, https://doi.org/10.1016/j.yqres.2009.06.011, 2009.

Torfing, T.: Neolithic population and summed probability distribution of 14C-dates, J Archaeol Sci, 63, 193–198, https://doi.org/10.1016/j.jas.2015.06.004, 2015.

Trondman, A.-K., Gaillard, M.-J., Sugita, S., Björkman, L., Greisman, A., Hultberg, T., Lagerås, P., Lindbladh, M., and Mazier, F.: Are pollen records from small sites appropriate for REVEALS model-based quantitative reconstructions of past regional vegetation? An empirical test in southern Sweden, Veg Hist Archaeobot, 25, 131–151, https://doi.org/10.1007/s00334-015-0536-9, 2016.

Tubbesing, C. L., York, R. A., Stephens, S. L., and Battles, J. J.: Rethinking fire-adapted species in an altered fire regime, Ecosphere, 11, https://doi.org/10.1002/ecs2.3091, 2020.

Tyukavina, A., Potapov, P., Hansen, M. C., Pickens, A. H., Stehman, S. V., Turubanova, S., Parker, D., Zalles, V., Lima, A., Kommareddy, I., Song, X.-P., Wang, L., and Harris, N.: Global Trends of Forest Loss Due to Fire From 2001 to 2019, Frontiers in Remote Sensing, 3, https://doi.org/10.3389/frsen.2022.825190, 2022.

UNEP: Emissions Gap Report 2023: Broken Record – Temperatures hit new highs, yet world fails to cut emissions (again), United Nations Environment Programme, https://doi.org/10.59117/20.500.11822/43922, 2023.

Vachula, R. S.: A meta-analytical approach to understanding the charcoal source area problem, Palaeogeogr Palaeoclimatol Palaeoecol, 562, 110111, https://doi.org/10.1016/j.palaeo.2020.110111, 2020.

Vachula, R. S., Sae-Lim, J., and Russell, J. M.: Sedimentary charcoal proxy records of fire in Alaskan tundra ecosystems, Palaeogeogr Palaeoclimatol Palaeoecol, 541, 109564, https://doi.org/10.1016/j.palaeo.2019.109564, 2020.

Vannière, B., Power, M. J., Roberts, N., Tinner, W., Carrión, J., Magny, M., Bartlein, P., Colombaroli, D., Daniau, A.-L., Finsinger, W., Gil-Romera, G., Kaltenrieder, P., Pini, R., Sadori, L., Turner, R., Valsecchi, V., and Vescovi, E.: Circum-Mediterranean fire activity and climate changes during the mid-Holocene environmental transition (8500-2500 cal. BP), Holocene, 21, 53–73, https://doi.org/10.1177/0959683610384164, 2011.

Vannière, B., Blarquez, O., Rius, D., Doyen, E., Brücher, T., Colombaroli, D., Connor, S., Feurdean, A., Hickler, T., Kaltenrieder, P., Lemmen, C., Leys, B., Massa, C., and Olofsson, J.: 7000-year human legacy of elevation-dependent European fire regimes, Quat Sci Rev, 132, 206–212, https://doi.org/10.1016/j.quascirev.2015.11.012, 2016.

Velle, G., Brooks, S. J., Birks, H. J. B., and Willassen, E.: Chironomids as a tool for inferring Holocene climate: an assessment based on six sites in southern Scandinavia, Quat Sci Rev, 24, 1429–1462, https://doi.org/10.1016/j.quascirev.2004.10.010, 2005.

Versini, P.-A., Velasco, M., Cabello, A., and Sempere-Torres, D.: Hydrological impact of forest fires and climate change in a Mediterranean basin, Natural Hazards, 66, 609–628, https://doi.org/10.1007/s11069-012-0503-z, 2013.

Wang, Y., Herzschuh, U., Shumilovskikh, L. S., Mischke, S., Birks, H. J. B., Wischnewski, J., Böhner, J., Schlütz, F., Lehmkuhl, F., Diekmann, B., Wünnemann, B., and Zhang, C.: Quantitative reconstruction of precipitation changes on the NE Tibetan Plateau since the Last Glacial Maximum – extending the concept of pollen source area to pollen-based climate reconstructions from large lakes, Clim Past, 10, 21–39, https://doi.org/10.5194/cp-10-21-2014, 2014.

Wang, Y., Shipley, B. R., Lauer, D. A., Pineau, R. M., and McGuire, J. L.: Plant biomes demonstrate that landscape resilience today is the lowest it has been since end-Pleistocene megafaunal extinctions, Glob Chang Biol, 26, 5914–5927, https://doi.org/10.1111/gcb.15299, 2020.

Ward, D. S., Kloster, S., Mahowald, N. M., Rogers, B. M., Randerson, J. T., and Hess, P. G.: The changing radiative forcing of fires: global model estimates for past, present and future, Atmos Chem Phys, 12, 10857–10886, https://doi.org/10.5194/acp-12-10857-2012, 2012.

Van Der Werf, G. R., Randerson, J. T., Giglio, L., Van Leeuwen, T. T., Chen, Y., Rogers, B. M., Mu, M., Van Marle, M. J. E., Morton, D. C., Collatz, G. J., Yokelson, R. J., and Kasibhatla, P. S.: Global fire emissions estimates during 1997-2016, Earth Syst Sci Data, 9, 697–720, https://doi.org/10.5194/essd-9-697-2017, 2017.

Westerling, A. L. and Swetnam, T. W.: Interannual to decadal drought and wildfire in the western United States, Eos, 84, 545–555, https://doi.org/10.1029/2003EO490001, 2003.

Whitlock, C. and Larsen, C.: Charcoal as a Fire Proxi. In: Smol J.P., Birks H.J.B., Last W.M., Bradley R.S., Alverson K. (eds) Tracking Environmental Change Using Lake Sediments. Developments in Paleoenvironmental Research, vol 3., 5, 75–97, https://doi.org/10.1007/0-306-47668-1, 2001.

Whitlock, C. and Millspaugh, S. H.: Testing the assumptions of fire-history studies: An examination of modern charcoal accumulation in Yellowstone National Park, USA, Holocene, 6, 7–15, https://doi.org/10.1177/095968369600600102, 1996.

Williams, A. N.: The use of summed radiocarbon probability distributions in archaeology: a review of methods, J Archaeol Sci, 39, 578–589, https://doi.org/10.1016/j.jas.2011.07.014, 2012.

Williams, A. P., Abatzoglou, J. T., Gershunov, A., Guzman-Morales, J., Bishop, D. A., Balch, J. K., and Lettenmaier, D. P.: Observed Impacts of Anthropogenic Climate Change on Wildfire in California, Earths Future, 7, https://doi.org/10.1029/2019EF001210, 2019.

Williams, J. W.: Variations in tree cover in North America since the last glacial maximum, Glob Planet Change, 35, 1–23, https://doi.org/10.1016/S0921-8181(02)00088-7, 2003.

Williams, J. W., Summers, R. L., and Webb III, T.: Applying plant functional types to construct biome maps from eastern North American pollen data, Quat Sci Rev, 17, 607–627, https://doi.org/10.1016/S0277-3791(98)00014-6, 1998.

Williams, J. W., Post, D. M., Cwynar, L. C., Lotter, A. F., and Levesque, A. J.: Rapid and widespread vegetation responses to past climate change in the North Atlantic region, Geology, 30, 971, https://doi.org/10.1130/0091-7613(2002)030<0971:RAWVRT>2.0.CO;2, 2002.

Williams, J. W., Grimm, E. C., Blois, J. L., Charles, D. F., Davis, E. B., Goring, S. J., Graham, R. W., Smith, A. J., Anderson, M., Arroyo-Cabrales, J., Ashworth, A. C., Betancourt, J. L., Bills, B. W., Booth, R. K., Buckland, P. I., Curry, B. B., Giesecke, T., Jackson, S. T., Latorre, C., Nichols, J., Purdum, T., Roth, R. E., Stryker, M., and Takahara, H.: The Neotoma Paleoecology Database, a multiproxy, international, community-curated data resource, Quat Res, 89, 156–177, https://doi.org/10.1017/qua.2017.105, 2018.

Wine, M. L. and Cadol, D.: Hydrologic effects of large southwestern USA wildfires significantly increase regional water supply: fact or fiction?, Environ Res Lett, 11, 085006, https://doi.org/10.1088/1748-9326/11/8/085006, 2016.

Woodbridge, J., Fyfe, R. M., and Roberts, N.: A comparison of remotely sensed and pollen-based approaches to mapping Europe’s land cover, J Biogeogr, 41, 2080–2092, https://doi.org/10.1111/jbi.12353, 2014a.

Woodbridge, J., Fyfe, R. M., Roberts, N., Downey, S., Edinborough, K., and Shennan, S.: The impact of the Neolithic agricultural transition in Britain: a comparison of pollen-based land-cover and archaeological 14C date-inferred population change, J Archaeol Sci, 51, 216–224, https://doi.org/10.1016/j.jas.2012.10.025, 2014b.

Wu, H., Guiot, J., Brewer, S., and Guo, Z.: Climatic changes in Eurasia and Africa at the last glacial maximum and mid-Holocene: reconstruction from pollen data using inverse vegetation modelling, Clim Dyn, 29, 211–229, https://doi.org/10.1007/s00382-007-0231-3, 2007.

Yang, X., Qiu, S., Zhu, Z., Rittenhouse, C., Riordan, D., and Cullerton, M.: Mapping understory plant communities in deciduous forests from Sentinel-2 time series, Remote Sens Environ, 293, 113601, https://doi.org/10.1016/j.rse.2023.113601, 2023.

Yin, J., He, B., Fan, C., Chen, R., Zhang, H., and Zhang, Y.: Drought-related wildfire accounts for one-third of the forest wildfires in subtropical China, Agric For Meteorol, 346, 109893, https://doi.org/10.1016/j.agrformet.2024.109893, 2024.

Zanon, M., Davis, B. A. S., Marquer, L., Brewer, S., and Kaplan, J. O.: European forest cover during the past 12,000 years: A palynological reconstruction based on modern analogs and remote sensing, Front Plant Sci, 9, 1–25, https://doi.org/10.3389/fpls.2018.00253, 2018.

Zapolska, A., Serge, M. A., Mazier, F., Quiquet, A., Renssen, H., Vrac, M., Fyfe, R., and Roche, D. M.: More than agriculture: Analysing time-cumulative human impact on European land-cover of second half of the Holocene, Quat Sci Rev, 314, 108227, https://doi.org/10.1016/j.quascirev.2023.108227, 2023.

Zennaro, P., Kehrwald, N., Marlon, J. R., Ruddiman, W. F., Brücher, T., Agostinelli, C., Dahl-Jensen, D., Zangrando, R., Gambaro, A., and Barbante, C.: Europe on fire three thousand years ago: Arson or climate?, Geophys Res Lett, 42, 5023–2033, https://doi.org/10.1002/2015GL064259, 2015.

Zhang, D., Huang, X., Liu, Q., Chen, X., and Feng, Z.: Holocene fire records and their drivers in the westerlies-dominated Central Asia, Sci Total Environ, 833, 155153, https://doi.org/10.1016/j.scitotenv.2022.155153, 2022.

Zhang, J., Huang, X., Zhang, S., Ren, X., Xiao, Y., Wang, J., Xiang, L., Xu, Q., and Birks, H. J. B.: Cycles of grazing and agricultural activity during the historical period and its relationship with climatic and societal changes in northern China, Land Degrad Dev, 32, 3315–3325, https://doi.org/10.1002/ldr.4007, 2021.

Zubkova, M., Humber, M. L., and Giglio, L.: Is global burned area declining due to cropland expansion? How much do we know based on remotely sensed data?, Int J Remote Sens, 44, 1132–1150, https://doi.org/10.1080/01431161.2023.2174389, 2023.

2. Assessing anthropogenic influence on fire history during the Holocene in the Iberian Peninsula

The following chapter is a paper published in Quaternary Science Reviews and is available to read online (https://doi.org/10.1016/j.quascirev.2022.107562). It has been written and referenced in the style guidelines of this journal. The authors were Luke F. Sweeney, Sandy P. Harrison and Marc Vander Linden. The study was designed by all authors. LS carried out the analyses. The first draft of the manuscript was written by LS and SPH, and all authors contributed to the final article. Estimated contributions are LS: 65%, SPH: 20% and MVL: 15%.

2.1. Abstract

The relative importance of climate change and human activities in influencing regional fire regimes during the Holocene is still a matter of debate. The introduction of agriculture during the Neolithic provides an opportunity to examine the impact of human activities on fire regimes. Here, we examine changes in fire regimes across Iberia between 10,000 and 3,500 cal. BP, reconstructed using sedimentary charcoal records. We compare the regional fire history with estimates of changes in population size, reconstructed based on summed probability distributions of radiocarbon dates on archaeological material. We also compare the fire records and population reconstructions with the timing of the onset of agriculture across the region as indicated by archaeological data. For Iberia as a whole, there are two intervals of rapid population increase centred on ca. 7,400 and ca. 5,400 cal. BP. Periods of rapid population growth, either for the region as a whole or more locally, do not closely align with changes in charcoal accumulation. Charcoal accumulation had already begun to increase ca. 400 years prior to the onset of the Neolithic and continued to increase for ca. 750 years afterwards, indicating that changes in fire are not directly associated with the introduction of agriculture. Similarly, there is no direct relationship between changes in charcoal accumulation and later intervals of rapid population growth. There is also no significant relationship between population size and charcoal accumulation across the period of analysis. Our analyses show that the introduction of agriculture and subsequent increases in population are not directly linked with changes in fire regimes in Iberia and support the idea that changes in fire are largely driven by other factors such as climate.

2.2. Introduction

People affect modern fire regimes in various ways, directly by altering the timing and number of ignitions or suppressing fires, and indirectly by altering fuel types, and through changing fuel structure and fuel continuity (Bowman et al., 2011; Archibald, 2016). Land use changes, for example, have been linked to increased frequency of forest fires in the Brazilian Amazon as a result of deforestation (Brando et al., 2020; Cardil et al., 2020), and to an increasing likelihood of larger more intense wildfires in Iberia following agricultural abandonment (Lloret et al., 2002; Pausas and Fernández-Muñoz, 2012). The magnitude of human influence on fire regimes before the recent period is, however, still debated. Several global and regional studies have shown that climate was the dominant driver of changes in fire regimes during the Holocene (e.g. Marlon et al., 2006, 2008, 2013; Power et al., 2008, 2010; Mooney et al., 2011; Daniau et al., 2012). However, human influence has been identified as an important factor in determining Holocene fire history at a local or regional scale (e.g. Scharf, 2010; Vannière et al., 2011; Feurdean et al., 2013; Innes et al., 2013; Zennaro et al., 2015; Dietze et al., 2018; Connor et al., 2019; Gajewski et al., 2019). There are also contrasting conclusions about the influence of people on fire history in Iberia during the early and middle Holocene, with some studies pointing to a limited influence (e.g. Gil-Romera et al., 2010; Burjachs and Expósito, 2015) and others suggesting humans had a major role, particularly through the introduction of agriculture during the Neolithic (e.g. Carracedo et al., 2018; Connor et al., 2019). Although there are several tools to reconstruct fire history, including historical written records, dendrochronological fire-scar data and chemical markers (Conedera et al., 2009), charcoal preserved in sedimentary sequences is the most widely used approach to investigate fire over millennial timescales and at different spatial scales. However, research that has made use of sedimentary charcoal together with other lines of palaeo-evidence to reconstruct and investigate changes to fire history in Iberia has either focused on individual sites (e.g. Abel-Schaad and López-Sáez, 2013), small regions (e.g. Gil-Romera et al., 2010; García-Alix et al., 2013; Burjachs and Expósito, 2015) or have only used a limited number of records to represent the whole peninsula (e.g. Connor et al., 2019), thus raising the concern that they may not provide a complete picture of the regional fire history.

Human influence on the environment during the Holocene is reflected in changes in land use. These land use changes have been reconstructed in Iberia using pollen data (e.g. Mighall et al., 2006; Revelles et al., 2015; Fyfe et al., 2019), with the appearance of cereal pollen being considered a marker of Neolithic agriculture (e.g. Peña-Chocarro et al., 2005; López-Merino et al., 2010; Cortés Sánchez et al., 2012). However, most pollen records have a limited representation of non-cereal crops and thus may not provide a complete picture of agricultural activities (Trondman et al., 2015). Although fungal spores associated with animal faeces have been used to identify the presence of domesticated animals (e.g. López Sáez and López Merino, 2007; Revelles et al., 2018), land-use transformations as a result of grazing are often identified by the presence of weed plants (e.g. Palmisano et al., 2019; Woodbridge et al., 2019), which can also indicate non-anthropogenic disturbances (Trondman et al., 2015; Roberts et al., 2019). As a result, there can be large uncertainties associated with pollen-based reconstructions of anthropogenic land-use changes.

An alternative approach to reconstruct land-use changes though time involves modelling land use as a function of historical population change and estimates of per capita land use (e.g. Kaplan et al., 2011; Klein Goldewijk et al., 2011; Klein Goldewijk et al., 2017), where increases in population density are assumed to reflect increasing human influence on the environment. However, establishing absolute historical population levels is challenging and estimates before the 1700s are extremely uncertain (Klein Goldewijk et al., 2010). An alternative method is to estimate relative changes in population size based on fluctuations in the quantity of radiocarbon-dated archaeological material (Rick, 1987). This technique has been used extensively to reconstruct changes in population size for Iberia as a whole (e.g. Balsera et al., 2015; Blanco-González et al., 2018; Fernandez-Lopez de Pablo et al., 2019) and for smaller regions of the peninsula (Drake et al., 2017; Fyfe et al., 2019; McLaughlin et al., 2021) for different time periods.

Radiocarbon-dated archaeological material has the additional advantage that the dates are normally associated with particular cultures and can thus be used, for example, to identify the start of Neolithic agriculture at a specific site. This is particularly important because the introduction of agriculture was not a single event. The earliest evidence of Neolithic agriculture in Iberia is dated to ca. 7,600 calendar years before 1950 CE (cal. BP) (Zapata et al., 2004; Bernabeu Aubán et al., 2015; Silva and Vander Linden, 2017; Fyfe et al., 2019). Agriculture was established initially in the south and east of the peninsula and spread from there, with the earliest evidence of farming in the northwestern part of the region dated to around 6,000 cal. BP (Isern et al., 2012, 2014; Drake et al., 2017). This long and spatially uneven dispersal provides a further means to assess human influence, as the introduction of agriculture has been linked to significant land-use changes in several areas of Europe (e.g. Lechterbeck et al., 2014; Marquer et al., 2014; Woodbridge et al., 2014; Revelles et al., 2018).

In this paper, we investigate the relationship between humans and fire during the Holocene period, using a dataset of 32 sedimentary charcoal sites from the Iberian Peninsula and a reconstruction of changes in human population based on more than 6,300 published radiocarbon samples. We focus on the early to middle Holocene, between 10,000 and 3,500 cal. BP, because of constraints in the amount of radiocarbon data after this time. We focus on relationships at a regional scale, accounting for the fact that the start of the Neolithic was asynchronous, in order to evaluate relationships statistically and reduce the noise associated with site-level differences in registration. We do not assume that the relationship between human population changes and fire is necessarily the same everywhere or consistent through time, only that some impact will be apparent in the fire records if there is a causal link between the two. Through comparison of the sedimentary charcoal and archaeological radiocarbon date records, we address the following questions: 1) Are rapid changes in population reflected in changes in fire? 2) Is there a relationship between fire and the onset of agriculture in Iberia? 3) Is there a relationship between population size and changes in fire?

2.3. Materials and method

2.3.1. Fire history

We used sedimentary charcoal extracted from the Reading Palaeofire Database (Harrison et al., 2022) to reconstruct the fire history of Iberia. The RPD provides Bayesian age-depth models for each of the records using the INTCAL20 Northern Hemisphere (Reimer et al., 2020) and Marine20 (Heaton et al., 2020) calibration curves as appropriate (see Harrison et al., 2022). There are 54 records from 39 sites across Iberia with charcoal data covering some part of the period between 10,000 and 3,500 cal. BP. Multiple records are available from some sites, either because different charcoal size factions were counted to distinguish local from regional fires or, for one site, because multiple sedimentary cores were taken. We selected a single record to represent each site. For the single site with multiple sedimentary cores, we selected the record with the greatest number of sampled radiocarbon ages for age-depth modelling purposes. For the other sites with multiple records, we gave preference firstly to records with the greatest number of charcoal samples and secondly to macro-charcoal records, which are believed to be more likely to indicate local fires (Clark and Patterson, 1997). However, analysis of charcoal composites for sites with multiple records shows no substantial differences when including either micro- or macro-charcoal sites (see Supplementary Information, S1). We subsequently excluded four sites at elevations above 2000m because there are relatively few archaeological sites above this elevation and the amount of both charcoal and radiocarbon data is thus insufficient to draw conclusions about the relationship between fire and human influence. For data quality control purposes, we additionally excluded a further three sites that contained less than five charcoal samples within the time range of analysis, as they provide a limited record of fire history. Thus, the final analyses were based on 32 records (Fig. 2.1A and Table 2.1). We imposed no limit on the minimum length or sampling resolution of each record since we use binned data in our subsequent analysis, but every record provided information for a minimum of six 100-year bins and the average number of 100-year bins per record was 28. Each record had at least one dating tie-point per 3000 years for the construction of the age model, with 70% having a dating tie-point every 1500 years on average.

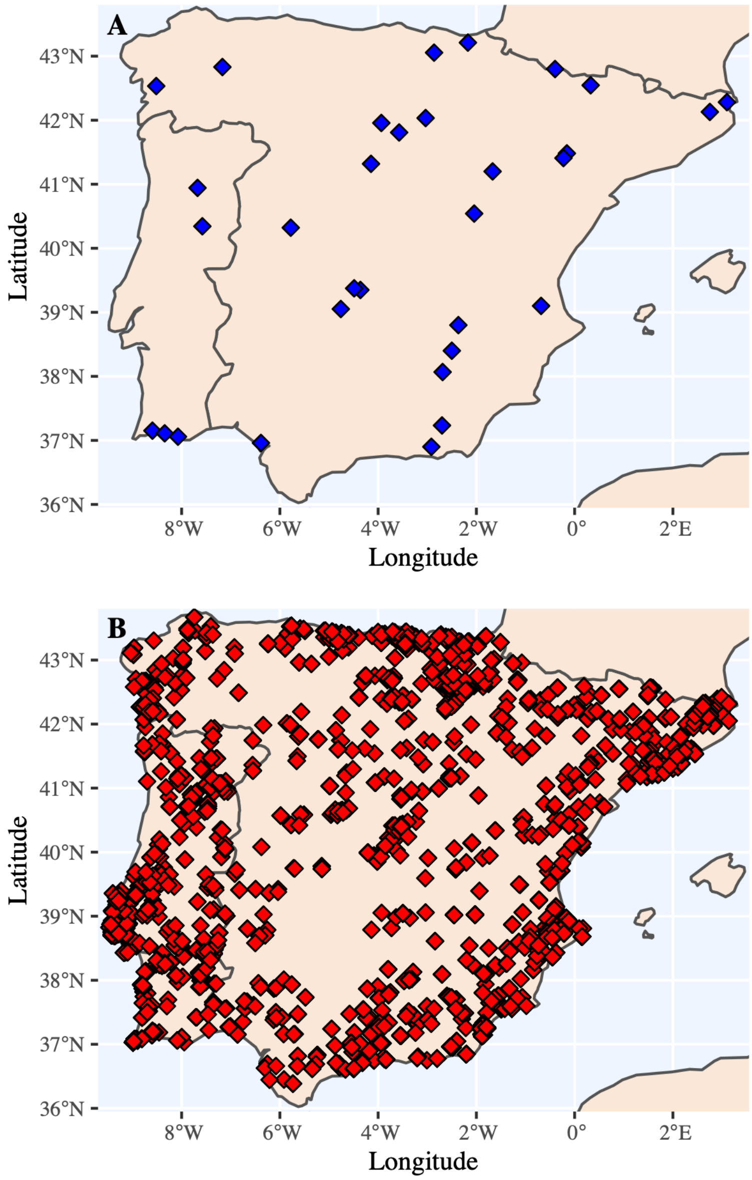

Figure 2.1: Maps of Iberia showing the locations of the charcoal (A) and archaeological (B) sites

Table 2.1: Information about the charcoal sites used for analyses. Latitude and longitude are given in decimal degrees where N and E are positive, and W is negative

Site name	Lat. (°)	Lon. (°)	Elevation (m a.s.l.)	Depositional context	Charcoal methods	Record length between 10-3.5k (age ka)	Resolution (samples/age ka)	No. of 100-year bins represented between 10-3.5k (age ka)	Citation
Alvor Estuary Ribeira do Farelo Ribeira da Torre	37.15	-8.59	1	estuarine sediment	macro, pollen slide	4.36	7.57	29	Schneider et al. (2016, 2010)
Arbarrain Mire	43.21	-2.17	1004	bog sediment	macro, sieved	3.35	11.34	31	Pérez-Díaz et al. (2018)
Armacao de Pera Ribeira de Alcantarilha	37.11	-8.34	2	estuarine sediment	macro, pollen slide	4.16	1.68	7	Schneider et al. (2016, 2010)
Basa de la Mora	42.55	0.33	1906	lake sediment	micro, pollen slide	6.36	15.72	54	Pérez-Sanz et al. (2013)
Campo Lameiro	42.53	-8.52	295	soil	micro, sieved	6.37	3.45	22	Kaal et al. (2008)
Canada de la Cruz	38.07	-2.69	1595	lake sediment	micro, pollen slide	5.88	2.72	14	Carrión et al. (2001b)
Canada del Gitano_Sierra de Baza	37.23	-2.7	1900	bog sediment	micro, pollen slide	4.98	12.65	48	Carrión et al. (2007)
Castello Lagoon	42.28	3.1	2	other	macro, sieved	1.29	12.40	9	Ejarque et al. (2016)
Cha das Lameiras	40.94	-7.68	950	soil	macro, other	5.28	2.84	15	López-Sáez et al. (2017)
Charco da Candieira	40.34	-7.58	1409	lake sediment	micro, pollen slide	6.57	17.81	65	Connor et al. (2012); van der Knaap and van Leeuwen (1997, 1995)
Cubelles	41.2	-1.67	2	other	macro, not known	2.46	5.28	12	Riera-Mora and Esteban-Amat (1994)
El Brezosa	39.35	-4.36	733	bog sediment	macro, sieved	0.52	125.00	6	Morales-Molino et al. (2018)
El Carrizal	41.32	-4.14	860	lake sediment	micro, pollen slide	4.57	3.50	16	Franco-Múgica et al. (2005)

El Perro mire	39.05	-4.76	690	bog sediment	macro, sieved	1.17	15.38	13	Luelmo-Lautenschlaeger et al. (2019a, 2019b)
El Portalet	42.8	-0.4	1802	bog sediment	macro, sieved	2.64	70.08	27	González-Sampériz et al. (2006)
Espinosa de Cerrato	41.96	-3.94	885	other	micro, pollen slide	6.55	12.82	65	Morales-Molino et al. (2017)
Hinojos Marsh	36.96	-6.39	2	bog sediment	macro, pollen slide	1.28	22.66	13	López-Sáez et al. (2018a)
Hoya del Castillo	41.48	-0.16	258	lake sediment	micro, other	4.37	18.08	41	Davis and Stevenson (2007)
Laguna Guallar	41.41	-0.23	336	lake sediment	macro, sieved	1.97	24.87	20	Davis and Stevenson (2007; Davies, unpublished data)
Lake Banyoles	42.13	2.75	174	lake sediment	macro, sieved	5.34	18.54	53	Revelles et al. (2015)
Las Pardillas	42.03	-3.03	1850	lake sediment	macro, sieved	6.40	5.62	35	Sánchez Goñi and Hannon (1999)
Las Vinuelas	39.37	-4.49	761	bog sediment	macro, sieved	0.71	11.27	8	Morales-Molino et al. (2019)
Navamuno	40.32	-5.78	1505	bog sediment	macro, sieved	3.38	8.28	20	López-Sáez et al. (2020)
Navarres	39.1	-0.68	225	bog sediment	micro, sieved	6.48	8.95	53	Carrión and Van Geel (1999)
Ojos del Tremendal	40.54	-2.04	1650	bog sediment	micro, pollen slide	6.41	5.15	32	Stevenson (2000)
Pena da Cadela	42.83	-7.17	970	bog sediment	micro, pollen slide	1.76	11.26	18	Martínez Cortizas et al. (2002)
Sierra de Gador	36.9	-2.92	1530	bog sediment	micro, pollen slide	2.75	13.82	28	Carrión et al. (2003)
Siles Lake	38.4	-2.5	1320	lake sediment	micro, pollen slide	6.42	5.61	33	Carrión (2002)
Tubilla del Lago	41.81	-3.57	900	bog sediment	micro, pollen slide	3.93	11.20	36	Morales-Molino et al. (2017)
Valle do Lobo Ribeira de Carcavai	37.06	-8.07	2	estuarine sediment	macro, pollen slide	4.85	9.90	26	Schneider et al. (2016, 2010)

Verdeospesoa	43.06	-2.86	1015	bog sediment	macro, sieved	5.97	1.01	6	Pérez-Díaz and López-Sáez (2017; Pérez Díaz and López Sáez (2021)
Villaverde	38.8	-2.37	870	bog sediment	micro, pollen slide	5.72	12.06	45	Carrión et al. (2001a)
High elevation sites									
Laguna de la Mosca	37.06	-3.32	2889	lake sediment	macro, sieved	4.86	27.16	34	Manzano et al. (2019)
Laguna de la Mula	37.06	-3.42	2497	lake sediment	macro, sieved	1.13	22.12	11	Jiménez-Moreno et al. (2013)
Laguna de Rio Seco	37.05	-3.35	3020	lake sediment	macro, sieved	6.56	25.04	66	Anderson et al. (2011)
Marbore	42.7	0.04	2612	lake sediment	micro, pollen slide	6.45	8.68	47	Leunda et al. (2017)

We constructed a regional composite curve from the individual sedimentary charcoal records. This curve was constructed in three steps, following a modified version of the protocol described by Power et al. (2008). Firstly, individual samples were converted into influx (i.e. particles/cm^2/year), re-scaled by site using a max transformation, Box-Cox transformed to homogenise inter-site variance, and then converted to z-scores using a base period of 200 - 8,200 cal. BP, to ensure that each site has a common mean and variance. We used a max transformation rather than the minimax transformation used by Power et al. (2008) to take account of zero values of charcoal accumulation; the impact of this difference on the composite charcoal curve is almost imperceptible (see *2.9. Supplement: S2*). The base period was chosen to maximise the number of cores used for analysis; previous research has shown that the length of the base period does not significantly affect the composite curve (Power et al., 2010). Secondly, data from individual records were binned into 100-year bins. This reduces the potential impact of high-resolution sampling at individual sites on the composite curve (Marlon et al., 2008). The 100-year bin width was chosen as a compromise between maximising the temporal resolution of the composite curve and ensuring sufficient data coverage. Since choice of bin width could affect the final composite curve, we investigated the impact of using different bin widths (see S3). Finally, a locally fitted regression ("LOCFIT": Loader, 2020) with a 500-year smoothing (half) window was fitted to the data. This step reduces the potential impact of outliers on the shape of the composite curve (e.g. Daniau et al., 2012). The 500-year smoothing window was chosen to emphasise the millennial trends in the data; the influence of using a shorter 250-year (half) window and a longer 1000-year (half) window width was investigated. Bootstrap resampling (with replacement) of individual records 1000 times was performed to generate 95% confidence intervals for the composite curve (Marlon et al., 2008; Mooney et al., 2011).

The code and general approach used in this data treatment was based on amendments of R scripts developed by Bartlein (see https://pjbartlein.github.io/GCDv3Analysis/index.html) for analysis of the Global Charcoal Database v3 (Marlon et al., 2016), available for the R statistical language (R Core Team, 2021) (see *2.7. Data and code availability*).

2.3.2. Population change and the spread of Neolithic agriculture

We used the quantity of radiocarbon dated material to reconstruct changes in population size. The use of radiocarbon dated material in this way is based on a chain of inference whereby 1) a larger population would leave a larger amount of radiocarbon datable material; 2) a larger amount of material would lead to a greater amount of that material being preserved; and 3) the greater amount of material would lead to a greater chance that this would be discovered through archaeological study and then processed for radiocarbon dating (Rick, 1987). Relative changes in population size are then estimated through the creation of a summed probability distribution (SPD) of the aggregated calibrated radiocarbon dates through time.

The robustness of this "dates as data" approach is largely dependent on using the maximum amount of data available for a region (Williams, 2012). We assembled data from recently published sources (Table 2.2) to create a dataset for analysis. The dataset was cleaned to remove duplicates, to correct errors e.g. in geographic location, to remove dates with standard errors > 200 years (following e.g. Fernandez-Lopez de Pablo et al., 2019; McLaughlin et al., 2021) and to remove dates on marine shells where no local marine reservoir correction was provided. To align with the charcoal data, any dates from sites above 2000m were removed. Where discrepancies between the datasets were apparent, we tried as far possible to use the most recently published dataset. The final consolidated dataset consisted of 6,343 radiocarbon samples from 1,615 sites (Table 2.2, see *2.7. Data and code availability*). Analyses were not performed for the period after 3,500 cal. BP because of the limited number of radiocarbon dates available after this time from Iberia, as site chronologies for the late Holocene are generally established using cultural dating techniques such as typo-chronology (Fyfe et al., 2019) (see *2.9. Supplement: S4* for details of the quantity of radiocarbon material available through time).

Table 2.2: Details of published archaeological radiocarbon data used for population analysis. Focus period refers to actual radiocarbon years BP.

Reference	**Title**	**Dataset region**	**Approx. focus period (uncal. BP)**
Balsera et al. (2015)	Approaching the demography of late prehistoric Iberia through summed calibrated date probability distributions (7000-2000 cal. BC)	Iberia	7k – 2k
Capuzzo et al. (2014) *	EUBAR: A database of 14 C measurements for the European Bronze Age. A Bayesian analysis of 14 C-dated archaeological contexts from Northern Italy and Southern France	Western Europe	4k – 2k
d'Errico et al. (2011) *	PACEA geo-referenced radiocarbon database	Europe	40k – 8k
Drake et al. (2017)	Regional demographic dynamics in the Neolithic transition in Iberia: results from summed calibrated date analysis	Iberia	9k – 6k
Hinz et al. (2012) *	RADON - Radiocarbon dates online 2012. Central European database of 14 C dates for the Neolithic and the Early Bronze Age	Europe	40k – 0k

Kniesel et al. (2014) *	Radon-B	Europe	4.5k – 2.5k
Manning et al. (2016) *	The cultural evolution of Neolithic Europe. EUROEVOL Dataset 1: sites, phases and radiocarbon data	Western Europe	8k – 4k
McLaughlin et al. (2021)	Late Glacial and Early Holocene human demographic responses to climatic and environmental change in Atlantic Iberia	West / Southwest Coast Portugal	20k – 5k
Pardo-Gordó et al. (2019)	Timing the Mesolithic-Neolithic transition in the Iberian Peninsula: The radiocarbon dataset	Iberia	8k – 5.5k
Vermeersch (2020) *	Radiocarbon Palaeolithic Europe database: A regularly updated dataset of the radiometric data regarding the Palaeolithic of Europe, Siberia included	Europe	From palaeolithic to modern

* Datasets accessed via R package *c14bazAAR* (Schmid et al., 2019)

An SPD was constructed using the radiocarbon data and the R package *rcarbon* (v1.4.2: Crema & Bevan, 2021). Radiocarbon date calibration was performed using the calibration curve IntCal2020 (Reimer et al., 2020) and the Marine20 curve (Heaton et al., 2020) for marine shell samples with the associated local marine offset value adjustment. The site data were binned using 100-year bins to create a single probability value to prevent site oversampling (Shennan et al., 2013). Dates were not normalised; this avoids spurious spikes in the data linked to the shape of the calibration curve (Weninger et al., 2015). The SPD was smoothed using a 200-year running mean, to limit both the potential for sampling error and for the calibration process to create spurious spikes (Shennan et al., 2013), whilst at the same time proving sufficient detail to identify key trends. The *rcarbon* package was used to construct a fitted exponential model of population growth based on a Monte Carlo conditional simulation. This was used to identify periods of growth (and decline) within the SPD significantly different from the fitted model (Timpson et al., 2014). The rate of change of the SPD was constructed using *rcarbon* based on change over a 50-year period, with statistical testing of the observed growth rates against fitted null model growth rates. Both exponential and logistic growth curves have been used as null models in previous work on Iberia (e.g. Balsera et al., 2015; Drake et al., 2017; Fernandez-Lopez de Pablo et al., 2019; Fyfe et al., 2019; McLaughlin et al., 2021). As the focus of our analysis is on deviations from longer-term population growth rather than testing variations in growth associated with the density dependent maximum or carrying capacity threshold, we used an exponential model. Furthermore, this specific model also takes into account, from a theoretical point of view, constant homogeneous taphonomic loss of archaeological sites, without having to resort to any other correction bias (Timpson et al., 2014).

Some 1,343 radiocarbon samples from 430 sites that were explicitly tagged as associated with Neolithic material were used to identify the spatial pattern of the onset of agriculture across Iberia, on the assumption that evidence of the Neolithic represents the start of agriculture in an area, using kriging interpolation. This kriged Neolithic surface was then used to assign the first date of agriculture at each charcoal site. The kriging interpolation was necessary because (a) there are some charcoal sites that are not close to archaeological sites with Neolithic dates, and (b) the incomplete nature of the sampled archaeological record means the earliest Neolithic date at a particular site may not be coherent with that of other sites in the area. For example, the oldest Neolithic date from one site may be several thousands of years younger than for a neighbouring site. We pre-processed the data as follows. Where several dates from an archaeological site were identified as Neolithic, the oldest calibrated date was used except when a tagged sample had an age earlier than 7,600 cal. BP, which is the generally accepted earliest date for the Neolithic in Iberia (Zapata et al., 2004; Bernabeu Aubán et al., 2015; Silva and Vander Linden, 2017; Fyfe et al., 2019). The site ages were compared to all sites within a 50km radius, and only retained if they were the oldest date within this buffer zone. This approach filters out spatially unrealistic Neolithic dates, which is necessary to produce a non-singular fitted variogram model. The choice of a buffer size was based on balancing data inclusivity against spatial coherence: 50km was the smallest buffer, and hence the largest number of surface points, that could produce a fitted model. The degree of spatial autocorrelation between the remaining 59 Neolithic surface points was then described using a variogram, using the R package *gstat* (v2.0-7) (Pebesma, 2004; Gräler et al., 2016) and a variogram model fitted based on the (weighted) mean squared difference between the model and variogram using the *gstat* default. The choice of model was however constrained by the accepted earliest start of the Neolithic in Iberia of 7,600 cal. BP; there were several better fitting models that were excluded because of this constraint. An *Exponential* – type model was fitted to the variogram and used in the ordinary kriging interpolation. Although the general interpolation shape remains relatively coherent despite the choice of variogram model, there are small differences in the interpolated surface (see *2.9. Supplement: S5*).

2.3.3. Analysis of fire, population and the onset of agriculture

<u>General approach</u>

To assesses the potential influence of people on fire regimes, we performed three statistical tests: Superposed Epoch Analysis (SEA) of the regional charcoal z-score composite focusing on times of rapid population change and associated with the time-transgressive start of the Neolithic, and correlation analysis on segmented data. In each case, we used appropriate tools to assess the impact of uncertainty in the data sources and to determine whether a signal emerged from the noise inherent in the records. These methods were designed to investigate relationships in a more robust manner than possible through simple visual comparison of the records. Our approach is to determine whether a relationship between fire and either rapid population growth, the spread of agriculture or population levels can be detected at a regional level to avoid possible differences between individual sites. Although we assume that a strong enough signal would be detectable at the regional scale, no assumptions have been made about the nature of any relationship.

Concurrent changes in rapid population growth and fire

Periods of rapid growth in population were identified as times when either the SPD was greater than the fitted null model, or the rate of change of the SPD was substantially different from the null model. These periods were compared with the timings of significant changes in mean values for the SPD, based on changepoint analysis. Changepoint analysis was performed using the R package *changepoint* (v2.2.2: Killick & Eckley, 2014), with the binary segmentation approach (Edwards and Cavalli-Sforza, 1965) used to identify the mean values of the SPD where changes occurred. We used Superposed Epoch Analysis (SEA) to examine the charcoal z-score time series in a 750-year time window before and after each key date. This approach identifies whether there are consistent relationships between the fire history and specific events (see e.g. Arneth et al., 2010; Daniau et al., 2010). To test whether a longer-term trend in the resulting composite curve could influence the results, we also detrended the z-score composite by fitting a simple linear regression to the composite curve and extracting the residuals. We generated a 95% confidence interval by making 1000 runs where the time point was randomly selected within a ±200-year window around each key date. This window was chosen to align with that used for the Neolithic analysis, which was itself determined by the maximum permitted dating error for radiocarbon samples within the archaeological radiocarbon dataset.

We ran an intervention analysis using autoregressive integrated moving average (ARIMA) modelling (Box and Tiao, 1975) to test whether there was an association between the key population dates and z-scores of charcoal accumulation, with post-epoch model forecasting compared to actual z-score values. ARIMA model forecasting was performed with R package *fable* (v0.3.1: O'Hara-Wild et al., 2021), with 750 years of annualised z-score composite values informing the auto generated model. Annualising the z-score composite was performed using cubic spline interpolation, with R package *zoo* (v1.8-9: Zeileis and Grothendieck, 2005).

Assessing the impact of the Neolithic

The interpolated surface of the timing of the start of the Neolithic was used to assign a date for the onset of agriculture at each charcoal site. For each site, the sample dates were then aligned to the associated Neolithic date. Z-score composites were then constructed based on these centred dates using the binning and smoothing procedures discussed above. Detrended composites were also constructed from simple linear regression of the composite, to test whether a longer-term trend in the curves affected the results. We tested the influence of the Neolithic surface on the shape of this curve by running the kriging interpolation 1000 times, with random ±200-year adjustments to the median calibrated dates of archaeological samples with Neolithic cultural tags. This 200-year adjustment was chosen because it was the maximum permitted error for the radiocarbon dates in the dataset. A Neolithic z-score charcoal composite was then re-calculated, and 95% confidence intervals assessed. Intervention analysis was performed on this Neolithic z-score charcoal composite curve using ARIMA forecasting, comparing the forecasted post-Neolithic curve to the actual z-score curve to assess whether an immediate significant change in the time series followed the spread of agriculture, using 750 years pre-epoch annualised data to inform the ARIMA model.

<u>Changes in population size and fire</u>

The SPD reconstructions provide an approximate measure of changes in population size through time. We assessed the relationship between population size and fire by comparing the SPD and the z-score of charcoal influx, both through visual inspection of the smoothed curves and through correlation analysis using unsmoothed data. Correlations were made by binning both the charcoal and the SPD data using 100-year bins. We then examined the correlations when values of the SPD and charcoal composite were above the 75% value, between the 75% and 25% value and below the 25% value, and also for the intervals identified by changepoint analysis as corresponding to significant changes in the mean values of the SPD.

2.4. Results

2.4.1. Fire and population change through time

<u>Fire</u>

The z-score composite of charcoal influx for the whole of Iberia (Fig. 2.2, 500-year smoothing window) shows an initial increase in fire between 10,000 and 9,500 cal. BP, a decline in fire until 8,800 cal. BP, followed by an increase and peak in fire around 8,200 cal. BP. Fire then declines until 7,600 cal. BP, after which it increases until 7,000 cal. BP. Fire then declines once more until around 6,500 cal. BP, after which there is a period of stability in fire until around 6,100 cal. BP. Fire then declines further to a minimum around 5,800 cal. BP. There is an increase in fire up to 4,700 cal. BP, with a more rapid increase from 5,800 cal. BP to 5,200 cal. BP followed by a more gradual increase. Fire declines to a minimum around 3,800 cal. BP, and the last part of the record is characterised by an increase in fire. This broad pattern is not affected by the choice of charcoal site bin width (see *2.9. Supplement: S3*) or smoothing window (half) width (Fig. 2.2). However, the inclusion of high elevation sites has a small but visible impact on the shape of the curve, suggesting these high-elevation sites had a different trend in charcoal accumulation (see *2.9. Supplement: S6*). Changepoint analysis detected no differences in mean values across the period covered by the composite curve. However, the 95% confidence intervals generated by bootstrap re-sampling become slightly narrower through time, as a result of the increasing number of records included (see *2.9. Supplement: S7* for details of the number of records contributing to the composite curve through time). Across the period of analysis there is a marginal upwards trend in fire (see *2.9. Supplement: S8*).

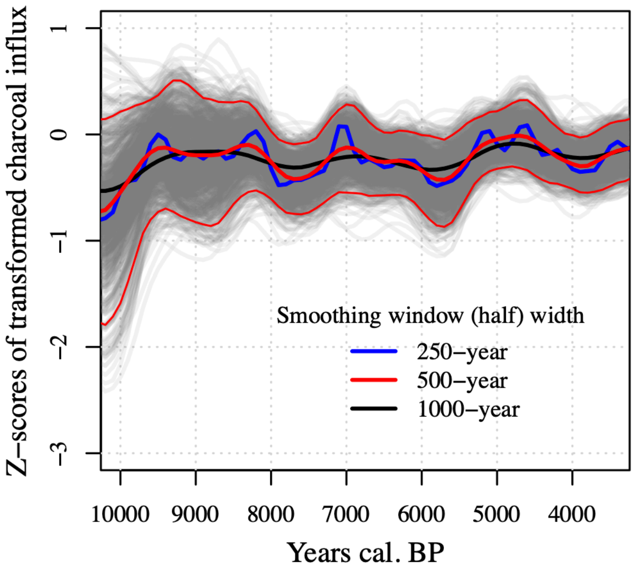

Figure 2.2: Z-score composite of charcoal influx for Iberia, 10,000 to 3,500 cal. BP. The solid lines show the median value, with smoothing windows of 500 (red), 250 (blue) and 1000 (black) years, the thin red lines show the 95% confidence intervals of 1000 bootstrap resample runs.

<u>Population change</u>

The SPD for Iberia between in 10,000 and 3,500 cal. BP (Fig. 2.3) shows a general trend of increasing population through time, with changepoint analysis of the mean of the SPD identifying changes at ca. 7,490 cal. BP and ca. 5,320 cal. BP. The first episode of high growth occurs between ca. 7,400 cal. BP and ca. 6,880 cal. BP. This change broadly corresponds to the start of the Neolithic period in Iberia. Two periods of population decline in comparison to the exponential model occur from ca. 6,400 to ca. 6,220 cal. BP and from ca. 5,560 to ca. 5,370 cal. BP. Another period of higher growth occurs between ca. 4,750 and ca. 4,460 cal. BP, followed by a period of significant population decline between ca. 3,720 cal. BP and the end of the record at 3,500 cal. BP. The rate of change of the SPD likewise identified periods of high growth and population decline, the most important of which is the high rate of change between ca. 5,370 to ca. 5,160 cal. BP. This is the fastest rate of change in the record, but is not reflected in the SPD because it follows the decline in population that occurred between ca. 5,370 to ca. 5,170 cal. BP. The interval of growth at ca. 4,730 cal. BP in the SPD is in part a reflection of this interval of high rate of change in population.

Given the broad consistency of the dates at ca. 7,400 and ca. 5,370 cal. BP with those identified by the changepoint analysis, these dates were used in the SEA analysis. The impact of using an exponential growth model rather than a logistic growth model had little impact on the identification on periods of rapid growth (see *2.9. Supplement: S9*).

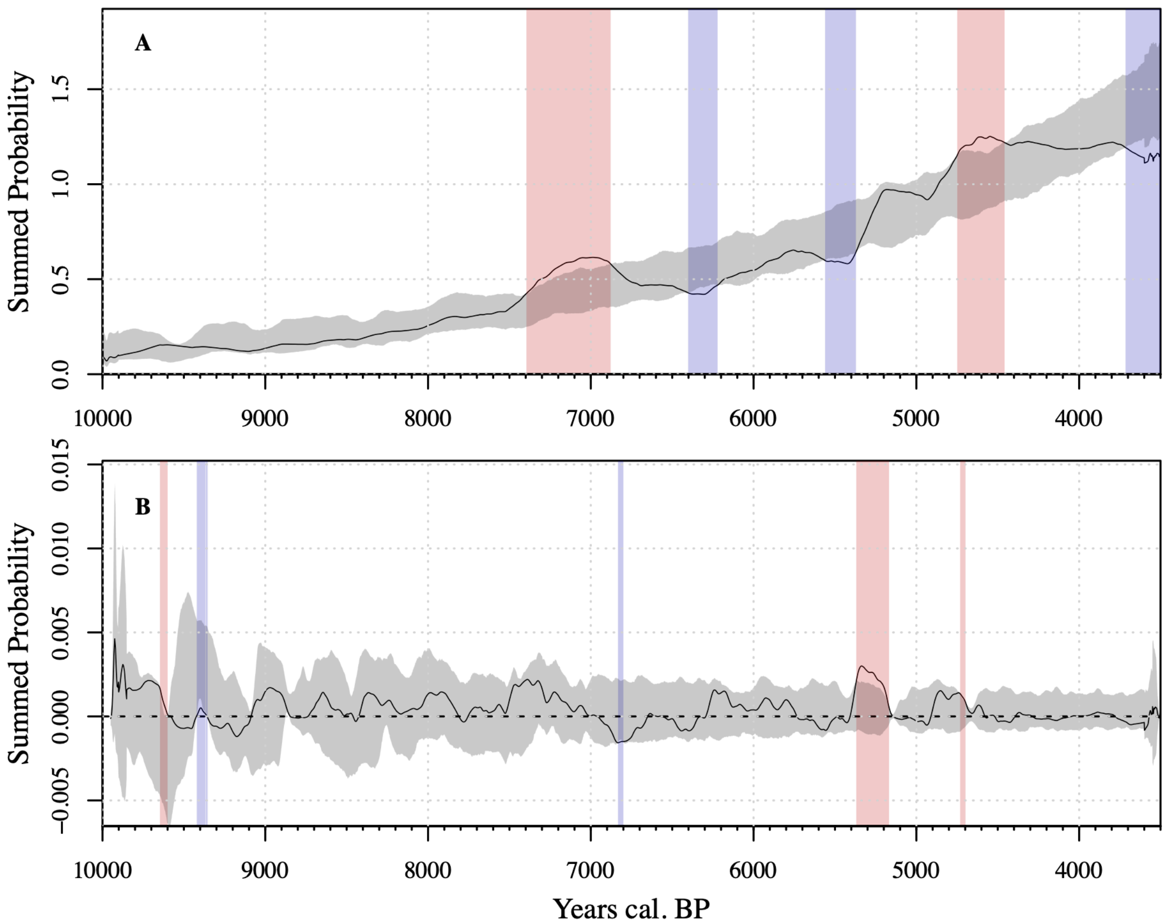

Figure 2.3: (A) Summed probability distribution (black line) and exponential null model for Iberia (grey envelope) (10,000 – 3500 cal. BP) (B) Summed probability distribution rate of change and exponential null model for Iberia (10,000 – 3500 cal. BP), both constructed from radiocarbon data from archaeological sites; Deviations from simulated growth models are shown in red (positive deviation) and blue (negative deviation).

<u>Relationship between changes in population and fire</u>

While there is no obvious relationship between the SPD and the z-score composite curve of charcoal influx across the entire period of analysis (Fig. 2.4), there are some time periods when peaks in the two records appear to align, most noticeably the peaks at ca. 7,000 cal. BP. There are no significant correlations between population and fire activity across the whole record, or when the population data are segmented, either by quartiles or by time intervals between periods of rapid change (Table 2.3), and the sign of the relationship is inconsistent. Similarly, segmenting the dataset by charcoal quartiles generates no significant relationships (Table 2.3).

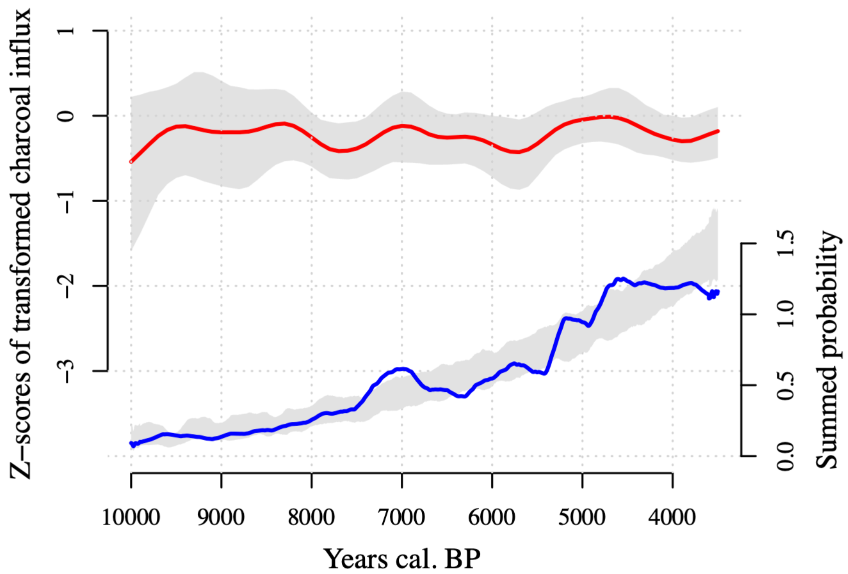

Figure 2.4: Temporal comparison between z-scores of transformed charcoal influx and summed probability distribution for Iberia (10 – 3.5k cal. BP). Grey shading on the z-score composite curve shows the 95% confidence intervals of 1000 bootstrap resample runs; grey shading on the summed probability curve shows the exponential null model

Table 2.3: Correlations between the SPD and z-score composite of charcoal influx for different segments of SPD and charcoal data

Segmentation		**Correlation (R)**	**P-value (sig ≤0.05)**
All data		0.16	0.21
SPD	Below 25% value	0.33	0.20
	Between 25% and 75% value	-0.01	0.94
	Above 75% value	-0.28	0.28
	Prior to first changepoint at 7469 BP	-0.20	0.32
	Between first changepoint and second changepoint at 5324 BP	-0.01	0.95
	After second changepoint at 5324 BP	-0.08	0.74
Charcoal z-scores	Below 25% value	0.31	0.22
	Between 25% and 75% value	-0.08	0.67
	Above 75% value	0.14	0.58

Relationship between changes in population and fire during key growth periods

The SEA analysis shows that fire was increasing ca. 275 years before the intervals of rapid growth at 7,400 and 5,370 cal. BP (Fig. 2.5) following a period of earlier decline. Fire reaches a maximum ca. 275 years after these periods of rapid population growth and then remains relatively stable thereafter. Detrending the charcoal z-score composite does not affect these overall findings (see *2.9. Supplement: S10*).

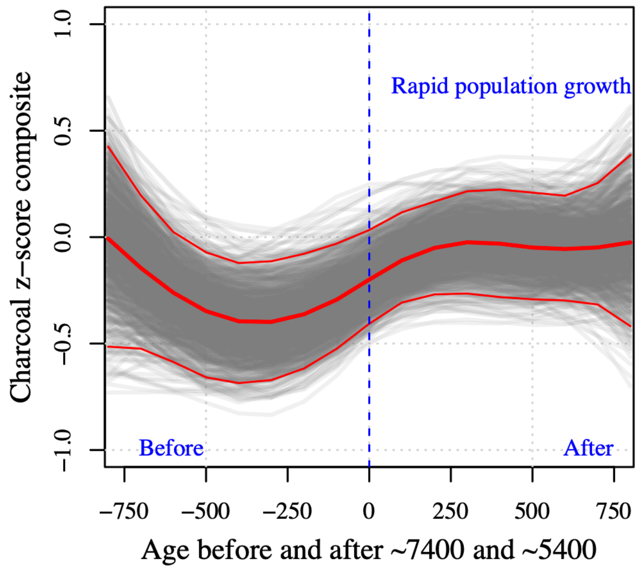

Figure 2.5: Superposed epoch analysis of z-score composite of charcoal influx for Iberia, with dates aligned before and after SPD key growth periods at 7,400 and 5,370 cal. BP. Grey lines indicate 1000 bootstrap re-samples of records, with replacement. The solid red line shows the median z-score values, and the fine red lines are the 95% confidence intervals.

The precise specification of the timings of these rapid population growth periods does not substantially alter this pattern (see *2.9. Supplement: S11*) and intervention analysis through ARIMA modelling (see *2.9. Supplement: S12*) confirms that the influence of population growth on charcoal influx is negligible.

2.4.2. The impact of the Neolithic on fire history

The start of the Neolithic was time-transgressive (Fig. 2.6), with the earliest dates registered in the east and in coastal regions. The latest start of the Neolithic was registered in the northwest of the peninsula, in southern Portugal and in relatively mountainous inland regions of eastern Spain.

The analysis of regional fire history with respect to the site-specific dating of the Neolithic transition (Fig. 2.7) shows that fire is generally declining prior to the local onset of agriculture, starting from ca. 750 years to ca. 450 years before. However, as in the previous analysis, fire starts to increase before the site-specific onset of the Neolithic. As with the SEA analysis, detrending the resulting z-score composite curve does not affect these overall findings (see *2.9. Supplement: S13*). The increase in fire begins ca. 450 years prior to the onset of the Neolithic and continues after the onset of agriculture. This pre-Neolithic trend is robust to minor adjustments in underlying radiocarbon cultural data (see *2.9. Supplement: S14*). ARIMA modelling forecasts (see *2.9. Supplement: S15*) also indicate no obvious change in the charcoal composite for the following 200 years after the site-specific Neolithic start date.

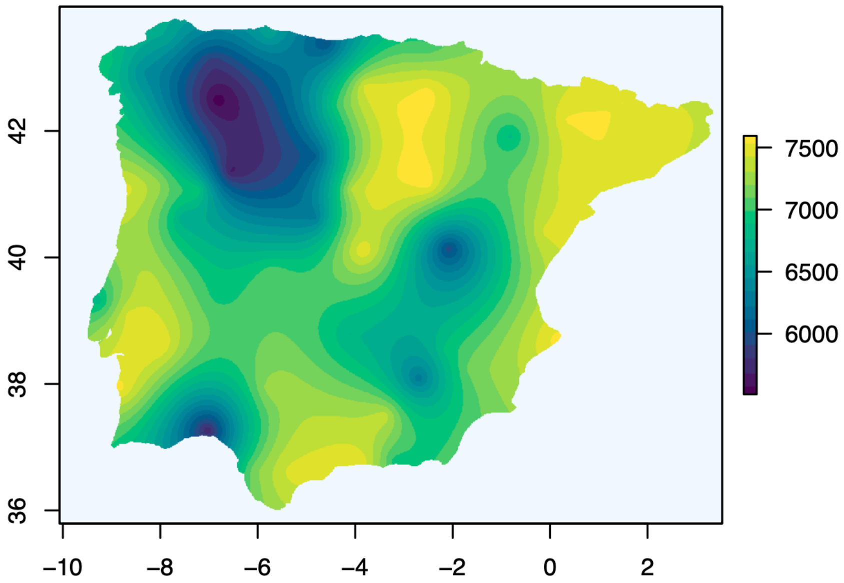

Figure 2.6: Ordinary kriging interpolated spread of the Neolithic across Iberia in cal. BP

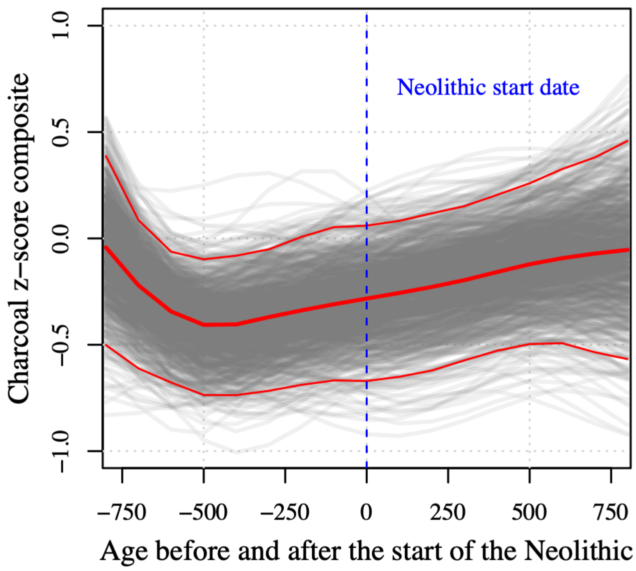

Figure 2.7: Superposed epoch analysis of z-score composite of charcoal influx for Iberia, based on spatially heterogenous dates relative to the start of the Neolithic across Iberia. Grey lines indicate 1000 bootstrap re-samples of core sites, with replacement. The solid red line shows the median z-score values, and the fine red lines are the 95% confidence intervals

2.5. Discussion

Our results show that the population of Iberia grew at an exponential rate between 10,000 and 3,500 cal. BP, punctuated by periods of rapid population growth and decline. This general increase in population is consistent with the other reconstructions for Iberia covering overlapping time periods (Balsera et al., 2015; Fernández-López de Pablo et al., 2019) and with different spatial foci (Lillios et al., 2016; Drake et al., 2017; Fyfe et al., 2019; Pardo-Gordó and Carvalho, 2020). This similarity between our results and prior studies is not surprising since they are based on the same or similar datasets. The first period of rapid growth identified between ca. 7,400 and ca. 6,880 cal. BP coincides with a period of population growth identified between 7,250 and 7,100 cal. BP by Balsera et al. (2015) for Iberia as a whole, and broadly aligns with periods of rapid growth identified by Drake et al. (2017) for their “southwest” and “inner Mediterranean” regions of Iberia between 7,250 and 6,750 cal. BP and 7,400 and 6,900 cal. BP respectively. However, this period of rapid growth is not present in the “north-western” region analysed by Drake et al. (2017) or in Portugal (Pardo-Gordó and Carvalho, 2020). The second period of rapid growth between ca. 5,370 to ca. 5,170 cal. BP coincides with an increase at ca. 5,350 cal. BP in the SPD curve developed by Balsera et al. (2015) for Iberia as a whole, and has also been identified for Portugal (5,351 to 4934 cal. BP; Pardo-Gordó and Carvalho, 2020) and for southwestern Iberia (ca. 5,300 to ca. 4,500 cal. BP; Lillios et al., 2016). However, it has not been recognised in analyses of population changes in northwestern or southeastern Iberia (Lillios et al., 2016). These differences suggest regional variation in population growth, with implications for local land-use change.

Our reconstruction of regional fire shows periods of increase and decline throughout the composite record. There are two other comparable regional-scale reconstructions of fire history that largely focus on Iberia and these show limited similarity with our z-score composite curve. Connor et al. (2019), for example, shows a steady increase in fire for Iberia as a whole from ca. 6,700 to ca. 4,700 cal. BP, whereas our composite curve shows a decrease in fire from ca. 6,100 to ca. 5,800, followed by a subsequent increase until ca. 4,700 cal. BP. However, the reconstructed decrease in fire between ca. 5,000 and ca. 3,800 cal. BP is seen in the composite curve of Connor et al. (2019). Iberia is included in the z-score curves for the "Mediterranean West" and "Mediterranean West South" regions produced by Vannière et al. (2011), but again there is limited similarity with our reconstructions. However, the reconstructed increase in fire from ca. 5,800 to ca. 4,700 cal. BP is seen in the "Mediterranean West South" region. Shen et al. (2021) have reconstructed the fire history of the Iberian Peninsula over the Holocene using pollen data and a calibration that relates charcoal abundance directly to burnt area. Although the burnt area reconstruction is not strictly comparable to the z-score composite curve of fire activity, and indeed the two records differ in several respects, nevertheless there are some common features including a peak in fire before 7000 cal. BP and an interval of lower fire after 7000 cal. BP (Shen et al., 2021).

Both Connor et al. (2019) and Vannière et al. (2011) use fewer individual records to reconstruct their regional curves: Connor et al. (2019) uses 13 records and Vannière et al. (2011) uses 11 records for the Mediterranean West region (including 7 non-Iberian records) and 9 records for the Mediterranean West South region (including 3 non-Iberian records). Our analysis includes all of the Iberian sites from Vannière et al. (2011) and 11 of the sites from Connor et al. (2019). The differences in site numbers, the different regions used by Vannière et al. (2011) and our application of the updated INTCAL20 calibration curves, likely underpin the differences with our reconstructions. Differences in the criteria used for site selection could also contribute to differences in the regional curves. Connor et al. (2019), for example, only used records with greater than 5,000 cal. years of data, an average sampling resolution < 100 cal. years, with an average interval of < 1500 cal. years between dating samples, and excluded records with sedimentary hiatuses. The absolute length of the record is not important for our analyses since we used binned data to minimise the impact of different sampling frequencies on the composite curve and all of the records provide information for at least 6 of the 100-year bins between 10000 and 3500 cal. BP. Although we include three records with an hiatus, we constructed separate age models before and after the hiatus. The sampling resolution of each record was always > 1 sample per 1000 years and 55% of the records had an average sampling resolution of <100 years for the 10,000 to 3,500 cal. BP interval. Furthermore, all of the records had age models constructed with at least one dating tie-point per 3000 cal. years on average, with most (> 70%) having at least one dating tie-point per 1500 cal. years on average. Thus, it seems unlikely that the inclusion of a greater number of sites in our analyses has significantly compromised the data quality, and this is confirmed by the confidence intervals generated by bootstrap resampling, but the better spatial coverage provides a more robust region-wide assessment of changes in fire regimes.

Although increases (or decreases) in anthropogenic burning to either create or maintain open landscapes as populations grow more rapidly (or decline) have been considered important during the Holocene (e.g. Gobet et al., 2003; Kaal et al., 2011; Vannière et al., 2016; Dietze et al., 2018), there is no consistent correlation between rapid changes in the rate of population growth and the occurrence of fire in Iberia. Both the correlation analysis and the SEA analysis show no relationship between fire and periods of high population growth, or, in the case of the correlation analysis, for periods of rapid population decline. Furthermore, we detected no significant relationship between population size, as indexed by SPD values, and fire activity. These analyses suggest that the influence of human activities on Iberian fire regimes during the period between 10,000 and 3,500 cal. BP was limited.

Although there are differences in methodology and data used, our reconstructions of the spread of the Neolithic show similar patterns to previous research, particularly that the earliest Neolithic locations are found in the south, east and northeast of Iberia suggesting multiple start locations as shown by Bernabeu Aubán et al. (2015) and the later spread of the Neolithic to the northwest of Iberia indicated by Isern et al. (2014). Our analyses do not identify a clear relationship between the timing of the Neolithic transition and the fire record, in contrast with other studies that suggest that fires in Iberia at this time were closely linked to land cover burning associated with Neolithic agriculture (Carracedo et al., 2018; Connor et al., 2019). However, other regional and site-level studies indicate that the widespread use of fire to create open spaces for agriculture often occurred much later than the first introduction of Neolithic culture (e.g. Morales-Molino and García-Antón, 2014; Iglesias et al., 2019). Whilst the spread of agriculture may have had an impact on fire regimes in the longer term or a site-specific level, our results suggest that the initial spread of the Neolithic had limited direct implications for region-wide fire regimes.

Our research conclusions are based on several assumptions. These include: 1) the ability to reconstruct fire, population change and the spread of the Neolithic; 2) the use of estimated population and the spread of agriculture to approximate human influence on fire; 3) the temporal correspondence of changes in fire with population changes as evidence of a causal link between them; and 4) the ability to detect this relationship at a regional scale.

We assume that our estimates of fire, population change and the spread of agriculture through time are sufficiently robust, despite uncertainties inherent to each reconstruction approach. The use of sedimentary charcoal records to reconstruct fire is widespread in palaeofire research, but it is recognised that uncertainties in the accuracy of the age depth model (e.g. Trachsel and Telford, 2016; Blaauw et al., 2018; Zimmerman and Wahl, 2020) or the stability of site characteristics through time (e.g. Whitlock and Anderson, 2003; Allen et al., 2008; Iglesias et al., 2015) could influence reconstructed fire at individual sites. These uncertainties underpin our focus on broad-scale, rather than site-based, patterns in fire, which are less likely to be affected by individual site uncertainty. Composite charcoal accumulation curves rarely reflect individual charcoal records (e.g. Marlon et al., 2009; Daniau et al., 2010), but are designed to minimise the impact of local conditions and to draw attention to broadscale patterns in the data. Composite charcoal records provide an indication of fire activity but may not reflect other aspects of the fire regime (Conedera et al., 2009), such as fire intensity or duration, which could be influenced by human actions.

Despite their widespread use, there are acknowledged limitations associated with the SPD approach to estimating population including biases in sampling of identified archaeological sites (e.g. Torfing, 2015), variation in the sampling intensity of radiocarbon dates through time (Crema and Bevan, 2021), and the creation of artificial peaks or smooth periods in the SPD produced by radiocarbon calibration (Crema and Bevan, 2021). Furthermore, SPDs do not provide information about variations in settlement sizes, which could affect the picture of population growth. Methodological developments designed to reduce potential bias, including the use of model fitting and hypothesis testing (e.g. Shennan et al., 2013; Timpson et al., 2014) underlie our approach to detecting periods of rapid population change. Our focus on regional rather than local change, which would rely on fewer radiocarbon dates and thus potentially produce less reliable SPDs, is also a way of reducing potential bias. The ability to assess the spread of the Neolithic across Iberia using radiocarbon dates relies on the availability of items from this cultural period. Assessing the degree to which missing dates affect the interpolated surface, and the use of composite charcoal curves rather than site-level information, mitigates the degree to which these inaccuracies affect our conclusions.

Our second assumption is that population changes and the start of agriculture can be used as a measure of human influence on fire regimes via changes in land use. Other sources of evidence of human impacts on land use, such as the presence of taxa indicative of farming such as cereals (e.g. Zapata et al., 2004; Peña-Chocarro et al., 2005; López-Merino et al., 2010; Cortés Sánchez et al., 2012), the presence of species indicating open landscapes and disturbance such as *Plantago* (e.g. López-Merino et al., 2010; Kaal et al., 2011), or the presence of fungi found in the faeces of grazing animals (e.g. López Sáez and López Merino, 2007; Abel-Schaad and López-Sáez, 2013; Morales-Molino and García-Antón, 2014; Revelles et al., 2018), could potentially be compared with charcoal records to determine whether the inferred changes in land use correlate with changes in fire regimes. However, these alternatives also have inherent uncertainties and do not provide a direct measure of human impact on fire regimes.

Thirdly, we assume that changes in population and fire would occur at the same time and focus on periods of rapid population growth and the start of agriculture as periods when landscape change might be expected to be large and hence changes in fire most visible. There could be lags between population changes and changes in fire, such that an increase in fire may occur sometime after population has started to increase. However, our analysis shows that increases in fire precede periods of rapid population growth by several centuries, which is more difficult to explain. There may be non-linear population dynamics that could explain the absence of rapid population growth following land clearance and increases human-induced burning, but we are unable to plausibly explain this result based on the data available.

Finally, we assume that a human influence on fire is detectable at regional scale and is not obscured by local variation. Other studies of the relationships between people and fire in Iberia using multiple records (e.g. López-Sáez et al., 2018b; Connor et al., 2019), have only used sites where the fire record could be compared directly with evidence of human impact based on other types of palaeo-records. However, the geographic distribution of the charcoal sites aligns well with the archaeological site data. Our SEA analysis focuses on changes in fire at two time periods, and any potential human impact may be obscured if the signal is not consistent between these time periods. However, the analysis of the impact of the Neolithic on fire regimes is spatially and temporally precise. Given that neither analysis shows an immediate effect on fire regimes, this suggests that the conclusion that there is no obvious relationship between humans and fire is robust.

At the region-wide scale, the temporal consistency of the changes in fire with respect to population changes in different time intervals, and in relationship to the asynchronous Neolithisation of the Iberian Peninsula, suggests that neither rapid changes in population nor the introduction of agriculture had a noticeable impact on fire in Iberia during the early and middle Holocene. This suggests that other drivers of fire, such as climate and climate-induced environmental changes, may have been a more important influence during this period. Climate influences fire directly through controlling fire weather and fuel moisture and indirectly through influencing vegetation type and productivity and hence fuel availability (Bowman et al., 2009; Bradstock, 2010; Harrison et al., 2010; Archibald et al., 2013). Today, fuel availability limits fire in the relatively dry regions of southeastern Iberia and climate conditions limit fire in the wetter regions of northern Iberia (Pausas and Paula, 2012). Changes in climate through time affect fire regimes through changing vegetation type and productivity, influencing fuel dryness and controlling the occurrence of lightning ignitions. The direct influence of climate conditions on fire regimes can be amplified or dampened depending on post-fire vegetation regrowth (Gil-Romera et al., 2010; Tepley et al., 2018; Hurteau et al., 2019). Furthermore, changes in the fire regime can also influence vegetation type (Baudena et al., 2010; D'Onofrio et al., 2018; Halofsky et al., 2020; Pausas and Bond, 2020). There is a considerable body of evidence from Iberia that provides insight into the dynamics of climate and vegetation during the Holocene, including changes in lake levels (e.g. Morellón et al., 2008; González-Sampériz et al., 2017; Morellón et al., 2018; Schröder et al., 2018), isotopic records from speleothems (e.g. Moreno et al., 2017; Baldini et al., 2019; Budsky et al., 2019; Thatcher et al., 2020; Benson et al., 2021), pollen assemblages (e.g. Broothaerts et al., 2018; López-Sáez et al., 2020) and sea-surface temperatures from adjacent ocean regions (e.g. Rodrigues et al. 2009; Chabaud et al., 2014; Schirrmacher et al., 2019; Gomes et al., 2020). However, it is difficult to use these types of record to separate out the influence of potential individual drivers of changes in fire regimes. Statistical approaches have been used to disentangle the multivariate impacts of different drivers on fire in the recent past (e.g. Bistinas et al., 2014; Andela et al., 2017; Forkel et al., 2019; Harrison et al., 2021) and similar techniques could be applied to palaeofires given sufficient independent quantitative reconstructions of climate variables and vegetation characteristics. Although there are a limited number of site-based quantitative reconstructions of temperature or moisture changes during the Holocene based on pollen (e.g. Kaufman et al., 2020; Ilvonen et al. 2022) and chironomid data (Muñoz Sobrino et al., 2013; Tarrats et al., 2018), the only large-scale mapped reconstructions of climate variables (Mauri et al., 2015) are based on interpolation from a geographically biased set of sites concentrated in northern mountain or coastal regions. Similarly, the available quantitative reconstructions of vegetation characteristics for the region (Zanon et al., 2018; Githumbi et al., 2021) have limited spatial coverage or temporal resolution and focus on a limited range of vegetation types. Thus, a thorough statistical analysis of the interacting drivers of fire over the Holocene period is currently not possible.

Our results suggest that human activities had little impact on fire during the interval from 10,000 to 3,500 cal. BP. This does not preclude a role for humans in the later Holocene, and indeed other studies have suggested that human influences are more recognisable in the last few millennia (e.g. Fletcher et al., 2007; Gil-Romera et al., 2010; Anderson et al., 2011). The role of other factors, such as climate or climate-induced changes in vegetation, during the earlier part of the Holocene could be investigated using the statistical approaches that have previously been used to analyse and disentangle the multivariate drivers of fire in the recent past (e.g. Bistinas et al., 2014; Andela et al., 2017; Forkel et al., 2019). These methods could also be used to identify when a strong regional signal of human influence on fire emerges. Further insights could be gained through the calibration of the charcoal data to provide quantitative reconstructions of the fire regime (see e.g. Hennebelle et al., 2020; Shen et al., 2021) or the use of alternative data sources that might provide information on other aspects of the fire regime, such as charcoal morphology or anatomy (e.g. Umbanhowar and McGrath, 1998;

Iglesias and Whitlock, 2014) or combustion biomarkers (e.g. Argiriadis et al., 2018; Kong et al., 2021). Radiocarbon-based reconstructions of population changes could also be compared with and complemented by alternative approaches to reconstruct anthropogenic land-use changes (e.g. Gaillard et al., 2010; Pirzamanbein et al., 2014; Fyfe et al., 2015). Further research using other sources of data on human impact and the application of emerging techniques to enhance coverage of fire history (see e.g. Shen et al., 2021) would help test the reliability of our results. Similarly, the application of the techniques used in this research to other areas could help assess the general applicability of our findings.

2.6. Conclusions

We have used sedimentary charcoal and radiocarbon dates on archaeological material to reconstruct changes in fire and human populations between 10,000 and 3,500 cal. BP for Iberia and examined the impact of the spread of the Neolithic on fire regimes. Whilst region-wide fire and population changes are evident from our reconstructions, these changes do not occur in concert. Correlation and SEA analyses indicate that rapid population changes are not associated with changes in fire regimes. Furthermore, there are no changes in fire regime associated with the immediate influence of the spread of Neolithic agriculture and the resulting change in land use. There is also no significant relationship between population size and fire activity. While further research to disentangle the multivariate drivers of fire regimes is necessary to quantify the precise nature of human influence during this time, at a region-wide scale our research indicates that human influence is likely of less importance to fire regimes than other environmental influences during the early and middle Holocene in Iberia.

2.7. Data and code availability

The charcoal data is available from the University of Reading Research Data Archive (https://doi.org/10.17864/1947.000369). See S16 for plots of the 32 individual records of charcoal influx through time utilised in this analysis.
The radiocarbon data is available from the University of Reading Research Data Archive (http://doi.org/10.17864/1947.000340).
The code utilised in generating fire and population reconstructions, as well as cross-analysis of the data is available at (https://github.com/sweeney-l/Iberian_fire_history)

2.8. References

Abel-Schaad, D., López-Sáez, J.A., 2013. Vegetation changes in relation to fire history and human activities at the Peña Negra mire (Bejar Range, Iberian Central Mountain System, Spain) during the past 4,000 years. Veg. Hist. Archaeobot. 22, 199–214. https://doi.org/10.1007/s00334-012-0368-9

Allen, C.D., Anderson, R.S., Jass, R.B., Toney, J.L., Baisan, C.H., 2008. Paired charcoal and tree-ring records of high-frequency Holocene fire from two New Mexico bog sites. Int. J. Wildl. Fire 17, 115–130. https://doi.org/10.1007/WF07165.

Andela, N., Morton, D.C., Giglio, L., Chen, Y., van der Werf, G.R., Kasibhatla, P.S., DeFries, R.S., Collatz, G.J., Hantson, S., Kloster, S., Bachelet, D., Forrest, M., Lasslop, G., Li, F., Mangeon, S., Melton, J.R., Yue, C., Randerson, J.T., 2017. A human-driven decline in global burned area. Science. 356, 1356–1362. https://doi.org/10.1126/science.aal4108

Anderson, R.S., Jiménez-Moreno, G., Carrión, J.S., Pérez-Martínez, C., 2011. Postglacial history of alpine vegetation, fire, and climate from Laguna de Río Seco, Sierra Nevada, southern Spain. Quat. Sci. Rev. 30, 1615–1629. https://doi.org/10.1016/j.quascirev.2011.03.005

Archibald, S., 2016. Managing the human component of fire regimes: lessons from Africa. Philos. Trans. R. Soc. B Biol. Sci. 371, 20150346. https://doi.org/10.1098/rstb.2015.0346

Archibald, S., Lehmann, C.E.R., Gomez-Dans, J.L., Bradstock, R.A., 2013. Defining pyromes and global syndromes of fire regimes. Proc. Natl. Acad. Sci. 110, 6442–6447. https://doi.org/10.1073/pnas.1211466110

Argiriadis, E., Battistel, D., McWethy, D.B., Vecchiato, M., Kirchgeorg, T., Kehrwald, N.M., Whitlock, C., Wilmshurst, J.M., Barbante, C., 2018. Lake sediment fecal and biomass burning biomarkers provide direct evidence for prehistoric human-lit fires in New Zealand. Sci. Rep. 8, 12113. https://doi.org/10.1038/s41598-018-30606-3

Arneth, A., Lehsten, V., Spessa, A., Thonicke, K., 2010. Climate-fire interactions and savanna ecosystems: a dynamic vegetation modelling study for the African continent, in: Hill, M.J., Hanan, N.P. (Eds.), Ecosystem Function in Savannas: Measurement and Modeling at Landscape to Global Scales. CRC Press, pp. 463-479.

Baldini, L.M., Baldini, J.U.L., McDermott, F., Arias, P., Cueto, M., Fairchild, I.J., Hoffmann, D.L., Mattey, D.P., Müller, W., Nita, D.C., Ontañón, R., Garciá-Moncó, C., Richards, D.A., 2019. North Iberian temperature and rainfall seasonality over the Younger Dryas and Holocene. Quat. Sci. Rev. 226, 105998. https://doi.org/10.1016/j.quascirev.2019.105998

Balsera, V., Díaz-del-Río, P., Gilman, A., Uriarte, A., Vicent, J.M., 2015. Approaching the demography of late prehistoric Iberia through summed calibrated date probability distributions (7000–2000 cal BC). Quat. Int. 386, 208–211. https://doi.org/10.1016/j.quaint.2015.06.022

Bartlein, P.J., n.d. Analysis of the Global Charcoal Database – GCDv3 [WWW Document]. URL https://pjbartlein.github.io/GCDv3Analysis/index.html (accessed 11.1.21).

Baudena, M., D'Andrea, F., Provenzale, A., 2010. An idealized model for tree-grass coexistence in savannas: The role of life stage structure and fire disturbances. J. Ecol. 98, 74–80. https://doi.org/10.1111/j.1365-2745.2009.01588.x

Benson, A., Hoffmann, D.L., Daura, J., Sanz, M., Rodrigues, F., Souto, P., Zilhão, J., 2021. A speleothem record from Portugal reveals phases of increased winter precipitation in western Iberia during the Holocene. The Holocene 31, 1339–1350. https://doi.org/10.1177/09596836211011666

Bernabeu Aubán, J., Michael Barton, C., Pardo Gordó, S., Bergin, S.M., 2015. Modeling initial Neolithic dispersal. The first agricultural groups in West Mediterranean. Ecol. Modell. 307, 22–31. https://doi.org/10.1016/j.ecolmodel.2015.03.015

Bistinas, I., Harrison, S.P., Prentice, I.C., Pereira, J.M.C., 2014. Causal relationships versus emergent patterns in the global controls of fire frequency. Biogeosciences 11, 5087–5101. https://doi.org/10.5194/bg-11-5087-2014

Blaauw, M., Christen, J.A., Bennett, K.D., Reimer, P.J., 2018. Double the dates and go for Bayes — Impacts of model choice, dating density and quality on chronologies. Quat. Sci. Rev. 188, 58–66. https://doi.org/https://doi.org/10.1016/j.quascirev.2018.03.032

Blanco-González, A., Lillios, K.T., López-Sáez, J.A., Drake, B.L., 2018. Cultural, Demographic and Environmental Dynamics of the Copper and Early Bronze Age in Iberia (3300–1500 BC): Towards an Interregional Multiproxy Comparison at the Time of the 4.2 ky BP Event. J. World Prehistory 31, 1–79. https://doi.org/10.1007/s10963-018-9113-3

Bowman, D.M.J.S., Balch, J.K., Artaxo, P., Bond, W.J., Cochrane, M.A., D'Antonio, C.M.D., DeFrie s, R., Johnston, F.H., Keeley, J.E., Krawchuk, M.A., Kull, C.A., Mack, M., Moritz, M.A., Pyne, S.J., Roos, C.I., Scott, A.C., Sodhi, N.S., Swetnam, T.W., 2011. The human dimension of fire regimes on Earth. J. Biogeogr. 38, 2223–2236. doi:10.1111/j.1365-2699.2011.02595.x.

Bowman, D.M.J.S., Balch, J.K., Artaxo, P., Bond, W.J., Carlson, J.M., Cochrane, M.A., Antonio, C. M.D., Defries, R.S., Doyle, J.C., Harrison, S.P., Johnston, F.H., Keeley, J.E., Krawchuk, M.A., Kull, C.A., Marston, J., Moritz, M.A., Prentice, I.C., Roos, C.I., Scott, A.C., Swetnam, T.W., van der Werf, G.R., Pyne, S.J., 2009. Fire in the earth system. Science 481, 481–
484 80- doi:10.1126/science.1163886.

Box, G.E.P., Tiao, G.C., 1975. Intervention Analysis with Applications to Economic and Environmental Problems. J. Am. Stat. Assoc. 70, 70–79. https://doi.org/10.1080/01621459.1975.10480264

Bradstock, R.A., 2010. A biogeographic model of fire regimes in Australia: current and future implications. Glob. Ecol. Biogeogr. 19. https://doi.org/10.1111/j.1466-8238.2009.00512.x

Brando, P., Macedo, M., Silvério, D., Rattis, L., Paolucci, L., Alencar, A., Coe, M., Amorim, C., 2020. Amazon wildfires: Scenes from a foreseeable disaster. Flora 268, 151609. https://doi.org/10.1016/j.flora.2020.151609

Broothaerts, N., Robles-López, S., Abel-Schaad, D., Pérez-Díaz, S., Alba-Sánchez, F., Luelmo-Lautenschlaeger, R., Glais, A., López-Sáez, J.A., 2018. Reconstructing past arboreal cover based on modern and fossil pollen data: A statistical approach for the Gredos Range (Central Spain). Rev. Palaeobot. Palynol. 255, 1–13. https://doi.org/10.1016/j.revpalbo.2018.04.007

Budsky, A., Scholz, D., Wassenburg, J.A., Mertz-Kraus, R., Spötl, C., Riechelmann, D.F., Gibert, L., Jochum, K.P., Andreae, M.O., 2019. Speleothem δ^{13} C record suggests enhanced spring/summer drought in south-eastern Spain between 9.7 and 7.8 ka – A circum-Western Mediterranean anomaly? The Holocene 29, 1113–1133. https://doi.org/10.1177/0959683619838021

Burjachs, F., Expósito, I., 2015. Charcoal and pollen analysis: Examples of Holocene fire dynamics in Mediterranean Iberian Peninsula. CATENA 135, 340–349. https://doi.org/10.1016/j.catena.2014.10.006

Capuzzo, G., Boaretto, E., Barceló, J.A., 2014. EUBAR: A Database of ^{14}C Measurements for the European Bronze Age. A Bayesian Analysis of ^{14}C-Dated Archaeological Contexts from Northern Italy and Southern France. Radiocarbon 56, 851–869. https://doi.org/10.2458/56.17453

Cardil, A., de-Miguel, S., Silva, C.A., Reich, P.B., Calkin, D., Brancalion, P.H.S., Vibrans, A.C., Gamarra, J.G.P., Zhou, M., Pijanowski, B.C., Hui, C., Crowther, T.W., Hérault, B., Piotto, D., Salas-Eljatib, C., Broadbent, E.N., Almeyda Zambrano, A.M., Picard, N., Aragão, L.E.O.C., Bastin, J.-F., Routh, D., van den Hoogen, J., Peri, P.L., Liang, J., 2020. Recent deforestation drove the spike in Amazonian fires. Environ. Res. Lett. 15, 121003. https://doi.org/10.1088/1748-9326/abcac7

Carracedo, V., Cunill, R., García-Codron, J.C., Pèlachs, A., Pérez-Obiol, R., Soriano, J.M., 2018. History of fires and vegetation since the Neolithic in the Cantabrian Mountains (Spain). L. Degrad. Dev. 29, 2060–2072. https://doi.org/10.1002/ldr.2891

Carrión, J.S., 2002. Patterns and processes of Late Quaternary environmental change in a montane region of southwestern Europe. Quat. Sci. Rev. 21. https://doi.org/10.1016/S0277-3791(02)00010-0

Carrión, J.S., Andrade, A., Bennett, K.D., Navarro, C., Munuera, M., 2001a. Crossing forest thresholds: inertia and collapse in a Holocene sequence from south-central Spain. The Holocene 11. https://doi.org/10.1191/09596830195672

Carrión, J.S., Fuentes, N., González-Sampériz, P., Sánchez Quirante, L., Finlayson, J.C., Fernández, S., Andrade, A., 2007. Holocene environmental change in a montane region of southern Europe with a long history of human settlement. Quat. Sci. Rev. 26. https://doi.org/10.1016/j.quascirev.2007.03.013

Carrión, J.S., Munuera, M., Dupré, M., Andrade, A., 2001b. Abrupt vegetation changes in the Segura Mountains of southern Spain throughout the Holocene. J. Ecol. 89. https://doi.org/10.1046/j.0022-0477.2001.00601.x

Carrión, J.S., Sánchez-Gómez, P., Mota, J.F., Yll, R., Chaín, C., 2003. Holocene vegetation dynamics, fire and grazing in the Sierra de Gádor, southern Spain. The Holocene 13. https://doi.org/10.1191/0959683603hl662rp

Carrión, J.S., Van Geel, B., 1999. Fine-resolution Upper Weichselian and Holocene palynological record from Navarrés (Valencia, Spain) and a discussion about factors of Mediterranean forest succession. Rev. Palaeobot. Palynol. 106. https://doi.org/10.1016/S0034-6667(99)00009-3

Chabaud, L., Sánchez Goñi, M.F., Desprat, S., Rossignol, L., 2014. Land–sea climatic variability in the eastern North Atlantic subtropical region over the last 14,200 years: Atmospheric and oceanic processes at different timescales. The Holocene 24, 787–797. https://doi.org/10.1177/0959683614530439

Clark, J.S., Patterson, W.A., 1997. Background and Local Charcoal in Sediments: Scales of Fire Evidence in the Paleorecord, in: Sediment Records of Biomass Burning and Global Change. Springer Berlin Heidelberg, Berlin, Heidelberg, pp. 23–48. https://doi.org/10.1007/978-3-642-59171-6_3

Conedera, M., Tinner, W., Neff, C., Meurer, M., Dickens, A.F., Krebs, P., 2009. Reconstructing past fire regimes: methods, applications, and relevance to fire management and conservation. Quat. Sci. Rev. 28, 555–576. https://doi.org/10.1016/j.quascirev.2008.11.005

Connor, S.E., Araújo, J., van der Knaap, W.O., van Leeuwen, J.F.N., 2012. A long-term perspective on biomass burning in the Serra da Estrela, Portugal. Quat. Sci. Rev. 55. https://doi.org/10.1016/j.quascirev.2012.08.007

Connor, S.E., Vannière, B., Colombaroli, D., Anderson, R.S., Carrión, J.S., Ejarque, A., Gil Romera, G., González-Sampériz, P., Hoefer, D., Morales-Molino, C., Revelles, J., Schneider, H., van der Knaap, W.O., van Leeuwen, J.F., Woodbridge, J., 2019. Humans take control of fire-driven diversity changes in Mediterranean Iberia's vegetation during the mid–late Holocene. The Holocene 29, 886–901. https://doi.org/10.1177/0959683619826652

Cortés Sánchez, M., Jiménez Espejo, F.J., Simón Vallejo, M.D., Gibaja Bao, J.F., Carvalho, A.F., Martinez-Ruiz, F., Gamiz, M.R., Flores, J.-A., Paytan, A., López Sáez, J.A., Peña-Chocarro, L., Carrión, J.S., Muñiz, A.M., Izquierdo, E.R., Riquelme Cantal, J.A., Dean, R.M., Salgueiro, E., Martínez Sánchez, R.M., De la Rubia de Gracia, J.J., Lozano Francisco, M.C., Vera Peláez, J.L., Rodríguez, L.L., Bicho, N.F., 2012. The Mesolithic–Neolithic transition in southern Iberia. Quat. Res. 77, 221–234. https://doi.org/10.1016/j.yqres.2011.12.003

Crema, E.R., Bevan, A., 2021. Inference from large sets of radiocarbon dates: software and methods. Radiocarbon 63, 23–39. https://doi.org/10.1017/RDC.2020.95

d'Errico, F., Banks, W.E., Vanhaeren, M., Laroulandie, V., Langlais, M., 2011. PACEA geo-referenced radiocarbon database. PaleoAnthropology 2011, 1–12. https://doi.org/doi:10.4207/PA.2011.ART40

D'Onofrio, D., von Hardenberg, J., Baudena, M., 2018. Not only trees: Grasses determine African tropical biome distributions via water limitation and fire. Glob. Ecol. Biogeogr. 27, 714–725. https://doi.org/10.1111/geb.12735

Daniau, A.-L., Bartlein, P.J., Harrison, S.P., Prentice, I.C., Brewer, S., Friedlingstein, P., Harrison-Prentice, T.I., Inoue, J., Izumi, K., Marlon, J.R., Mooney, S., Power, M.J., Stevenson, J., Tinner, W., Andrič, M., Atanassova, J., Behling, H., Black, M., Blarquez, O., Brown, K.J., Carcaillet, C., Colhoun, E.A., Colombaroli, D., Davis, B.A.S., D'Costa, D., Dodson, J., Dupont, L., Eshetu, Z., Gavin, D.G., Genries, A., Haberle, S., Hallett, D.J., Hope, G., Horn, S.P., Kassa, T.G., Katamura, F., Kennedy, L.M., Kershaw, P., Krivonogov, S., Long, C., Magri, D., Marinova, E., McKenzie, G.M., Moreno, P.I., Moss, P., Neumann, F.H., Norström, E., Paitre, C., Rius, D., Roberts, N., Robinson, G.S., Sasaki, N., Scott, L., Takahara, H., Terwilliger, V., Thevenon, F., Turner, R., Valsecchi, V.G., Vannière, B., Walsh, M., Williams, N., Zhang, Y., 2012. Predictability of biomass burning in response to climate changes. Global Biogeochem. Cycles 26, 2011GB004249. https://doi.org/10.1029/2011GB004249

Daniau, A.-L., Harrison, S.P., Bartlein, P.J., 2010. Fire regimes during the Last Glacial. Quat. Sci. Rev. 29, 2918–2930. https://doi.org/10.1016/j.quascirev.2009.11.008

Davis, B.A.S., Stevenson, A.C., 2007. The 8.2 ka event and Early-Mid Holocene forests, fires and flooding in the Central Ebro Desert, NE Spain. Quat. Sci. Rev. 26, 1695–1712. https://doi.org/10.1016/j.quascirev.2007.04.007

Dietze, E., Theuerkauf, M., Bloom, K., Brauer, A., Dörfler, W., Feeser, I., Feurdean, A., Gedminienė, L., Giesecke, T., Jahns, S., Karpińska-Kołaczek, M., Kołaczek, P., Lamentowicz, M., Latałowa, M., Marcisz, K., Obremska, M., Pędziszewska, A., Poska, A., Rehfeld, K., Stančikaitė, M., Stivrins, N., Święta-Musznicka, J., Szal, M., Vassiljev, J., Veski, S., Wacnik, A., Weisbrodt, D., Wiethold, J., Vannière, B., Słowiński, M., 2018. Holocene fire activity during low-natural flammability periods reveals scale-dependent cultural human-fire relationships in Europe. Quat. Sci. Rev. 201, 44–56. https://doi.org/10.1016/j.quascirev.2018.10.005

Drake, B.L., Blanco-González, A., Lillios, K.T., 2017. Regional Demographic Dynamics in the Neolithic Transition in Iberia: Results from Summed Calibrated Date Analysis. J. Archaeol. Method Theory 24, 796–812. https://doi.org/10.1007/s10816-016-9286-y

Edwards, A.W.F., Cavalli-Sforza, L.L., 1965. A method for cluster analysis. Biometrics 21, 362. https://doi.org/10.2307/2528096

Ejarque, A., Julià, R., Reed, J.M., Mesquita-Joanes, F., Marco-Barba, J., Riera, S., 2016. Coastal Evolution in a Mediterranean Microtidal Zone: Mid to Late Holocene Natural Dynamics and Human Management of the Castelló Lagoon, NE Spain. PLoS One 11. https://doi.org/10.1371/journal.pone.0155446

Fernández-López de Pablo, J., Gutiérrez-Roig, M., Gómez-Puche, M., McLaughlin, R., Silva, F., Lozano, S., 2019. Palaeodemographic modelling supports a population bottleneck during the Pleistocene-Holocene transition in Iberia. Nat. Commun. 10, 1872. https://doi.org/10.1038/s41467-019-09833-3

Feurdean, A., Liakka, J., Vannière, B., Marinova, E., Hutchinson, S.M., Mosburgger, V., Hickler, T., 2013. 12,000-Years of fire regime drivers in the lowlands of Transylvania (Central-Eastern Europe): a data-model approach. Quat. Sci. Rev. 81, 48–61. https://doi.org/10.1016/j.quascirev.2013.09.014

Fletcher, W.J., Boski, T., Moura, D., 2007. Palynological evidence for environmental and climatic change in the lower Guadiana valley, Portugal, during the last 13 000 years. The Holocene 17, 481–494. https://doi.org/10.1177/0959683607077027

Forkel, M., Andela, N., Harrison, S.P., Lasslop, G., van Marle, M., Chuvieco, E., Dorigo, W., Forrest, M., Hantson, S., Heil, A., Li, F., Melton, J., Sitch, S., Yue, C., Arneth, A., 2019. Emergent relationships with respect to burned area in global satellite observations and fire-enabled vegetation models. Biogeosciences 16, 57–76. https://doi.org/10.5194/bg-16-57-2019

Franco-Múgica, F., García-Antón, M., Maldonado-Ruiz, J., Morla-Juaristi, C., Sainz-Ollero, H., 2005. Ancient pine forest on inland dunes in the Spanish northern meseta. Quat. Res. 63, 1–14. https://doi.org/10.1016/j.yqres.2004.08.004

Fyfe, R.M., Woodbridge, J., Palmisano, A., Bevan, A., Shennan, S., Burjachs, F., Legarra Herrero, B., García Puchol, O., Carrión, J.S., Revelles, J., Roberts, C.N., 2019. Prehistoric palaeodemographics and regional land cover change in eastern Iberia. Holocene 29, 799–815. https://doi.org/10.1177/0959683619826643

Fyfe, R.M., Woodbridge, J., Roberts, N., 2015. From forest to farmland: pollen-inferred land cover change across Europe using the pseudobiomization approach. Glob. Chang. Biol. 21, 1197–1212. https://doi.org/10.1111/gcb.12776

Gaillard, M.-J., Sugita, S., Mazier, F., Trondman, A.-K., Broström, A., Hickler, T., Kaplan, J.O., Kjellström, E., Kokfelt, U., Kuneš, P., Lemmen, C., Miller, P., Olofsson, J., Poska, A., Rundgren, M., Smith, B., Strandberg, G., Fyfe, R., Nielsen, A.B., Alenius, T., Balakauskas, L., Barnekow, L., Birks, H.J.B., Bjune, A., Björkman, L., Giesecke, T., Hjelle, K., Kalnina, L., Kangur, M., van der Knaap, W.O., Koff, T., Lagerås, P., Latałowa, M., Leydet, M., Lechterbeck, J., Lindbladh, M., Odgaard, B., Peglar, S., Segerström, U., von Stedingk, H., Seppä, H., 2010. Holocene land-cover reconstructions for studies on land cover-climate feedbacks. Clim. Past 6, 483–499. https://doi.org/10.5194/cp-6-483-2010

Gajewski, K., Kriesche, B., Chaput, M.A., Kulik, R., Schmidt, V., 2019. Human–vegetation interactions during the Holocene in North America. Veg. Hist. Archaeobot. 28, 635–647. https://doi.org/10.1007/s00334-019-00721-w

García-Alix, A., Jimenez-Espejo, F.J., Lozano, J.A., Jiménez-Moreno, G., Martinez-Ruiz, F., García Sanjuán, L., Aranda Jiménez, G., García Alfonso, E., Ruiz-Puertas, G., Anderson, R.S., 2013. Anthropogenic impact and lead pollution throughout the Holocene in Southern Iberia. Sci. Total Environ. 449, 451–460. https://doi.org/10.1016/j.scitotenv.2013.01.081

Gil-Romera, G., Carrión, J.S., Pausas, J.G., Sevilla-Callejo, M., Lamb, H.F., Fernández, S., Burjachs, F., 2010. Holocene fire activity and vegetation response in South-Eastern Iberia. Quat. Sci. Rev. 29, 1082–1092. https://doi.org/10.1016/j.quascirev.2010.01.006

Githumbi, E., Fyfe, R.M., Gaillard, M.-J., Trondman, A.-K., Mazier, F., Nielsen, A.-B., Poska, A., Sugita, S., Theuerkauf, M., Woodbridge, J., Azuara, J., Feurdean, A., Grindean, R., Lebreton, V., Marquer, L., Nebout-Combourieu, N., Stančikaitė, M., Tanţău, I., Tonkov, S., Shumilovskikh, L., 2022. European pollen-based REVEALS land-cover reconstructions for the Holocene: methodology, mapping and potentials. Earth Syst. Sci. Data 14 (4,), 1581–619. doi:10.5194/ essd-14-1581-2022.

Gobet, E., Tinner, W., Hochuli, P.A., van Leeuwen, J.F.N., Ammann, B., 2003. Middle to Late Holocene vegetation history of the Upper Engadine (Swiss Alps): the role of man and fire. Veg. Hist. Archaeobot. 12, 143–163. https://doi.org/10.1007/s00334-003-0017-4

Gomes, S.D., Fletcher, W.J., Rodrigues, T., Stone, A., Abrantes, F., Naughton, F., 2020. Time-transgressive Holocene maximum of temperate and Mediterranean forest development across the Iberian Peninsula reflects orbital forcing. Palaeogeogr. Palaeoclimatol. Palaeoecol. 550, 109739. https://doi.org/10.1016/j.palaeo.2020.109739

González-Sampériz, P., Aranbarri, J., Pérez-Sanz, A., Gil-Romera, G., Moreno, A., Leunda, M., Sevilla-Callejo, M., Corella, J.P., Morellón, M., Oliva, B., Valero-Garcés, B., 2017. Environmental and climate change in the southern Central Pyrenees since the Last Glacial Maximum: A view from the lake records. CATENA 149, 668–688. https://doi.org/10.1016/j.catena.2016.07.041

González-Sampériz, P., Valero-Garcés, B.L., Moreno, A., Jalut, G., García-Ruiz, J.M., Martí-Bono, C., Delgado-Huertas, A., Navas, A., Otto, T., Dedoubat, J.J., 2006. Climate variability in the Spanish Pyrenees during the last 30,000 yr revealed by the El Portalet sequence. Quat. Res. 66, 38–52. https://doi.org/10.1016/j.yqres.2006.02.004

Gräler, B., Pebesma, E., Heuvelink, G., 2016. Spatio-Temporal Interpolation using gstat. R J. 8, 204. https://doi.org/10.32614/RJ-2016-014

Halofsky, J.E., Peterson, D.L., Harvey, B.J., 2020. Changing wildfire, changing forests: the effects of climate change on fire regimes and vegetation in the Pacific Northwest, USA. Fire Ecol. 16, 4. https://doi.org/10.1186/s42408-019-0062-8

Harrison, S.P., Prentice, I.C., Barboni, D., Kohfeld, K.E., Ni, J., Sutra, J.-P., 2010. Ecophysiological and bioclimatic foundations for a global plant functional classification. J. Veg. Sci. 21, 300–317. https://doi.org/10.1111/j.1654-1103.2009.01144.x

Harrison, S.P., Prentice, I.C., Bloomfield, K., Dong, N., Forkel, M., Forrest, M., Ningthoujam, R.K., Pellegrini, A., Shen, Y., Baudena, M., Cardoso, A.W., Huss, J.C., Joshi, J., Oliveras, I., Pausas, J.G., Simpson, K.J., 2021. Understanding and modelling wildfire regimes: an ecological perspective. Environ. Res. Lett. 16: 125008, https://doi.org/10.1088/1748-9326/ac39be

Harrison, S.P., Villegas-Diaz, R., Cruz-Silva, E., Gallagher, D., Kesner, D., Lincoln, P., Shen, Y., Sweeney, L., Colombaroli, D., Ali, A., Barhoumi, C., Bergeron, Y., Blyakharchuk, T., Bobek, P., Bradshaw, R., Clear, J.L., Czerwiński, S., Daniau, A.-L., Dodson, J., Edwards, K.J., Edwards, M.E., Feurdean, A., Foster, D., Gajewski, K., Gałka, M., Garneau, M., Giesecke, T., Gil Romera, G., Girardin, M.P., Hoefer, D., Huang, K., Inoue, J., Jamrichová, E., Jasiunas, N., Jiang, W., Jiménez-Moreno, G., Karpińska-Kołaczek, M., Kołaczek, P., Kuosmanen, N., Lamentowicz, M., Lavoie, M., Li, F., Li, J., Lisitsyna, O., López-Sáez, J.A., Luelmo-Lautenschlaeger, R., Magnan, G., Magyari, E.K., Maksims, A., Marcisz, K., Marinova, E., Marlon, J.R., Mensing, S., Miroslaw-Grabowska, J., Oswald, W., Pérez-Díaz, S., Pérez-Obiol, R., Piilo, S., Poska, A., Qin, X., Remy, C.C., Richard, P.J.H., Salonen, S., Sasaki, N., Schneider, H., Shotyk, W., Stancikaite, M., Šteinberga, D., Stivrins, N., Takahara, H., Tan, Z., Trasune, L., Umbanhowar, C.E., Väliranta, M., Vassiljev, J., Xiao, X., Xu, Q., Xu, X., Zawisza, E., Zhao, Y., Zhou, Z., Paillard, J., 2022. The Reading Palaeofire Database: an expanded global resource to document changes in fire regimes from sedimentary charcoal records. Earth Syst. Sci. Data 14, 1109–1124. https://doi.org/10.5194/essd-14-1109-2022

Heaton, T.J., Köhler, P., Butzin, M., Bard, E., Reimer, R.W., Austin, W.E.N., Bronk Ramsey, C., Grootes, P.M., Hughen, K.A., Kromer, B., Reimer, P.J., Adkins, J., Burke, A., Cook, M.S., Olsen, J., Skinner, L.C., 2020. Marine20—The Marine Radiocarbon Age Calibration Curve (0–55,000 cal BP). Radiocarbon 62, 779–820. https://doi.org/10.1017/RDC.2020.68

Hennebelle, A., Aleman, J.C., Ali, A.A., Bergeron, Y., Carcaillet, C., Grondin, P., Landry, J., Blarquez, O., 2020. The reconstruction of burned area and fire severity using charcoal from boreal lake sediments. The Holocene 30, 1400–1409. https://doi.org/10.1177/0959683620932979

Hinz, M., Furholt, M., Müller, J., Raetzel-fabian, D., 2012. RADON - Radiocarbon dates online 2012. Central European database of 14 C dates for the Neolithic and the Early Bronze Age. www.jungsteinSITE.de 0, 0–5. https://doi.org/10.12766/jna.2012.65

Hurteau, M.D., Liang, S., Westerling, A.L.R., Wiedinmyer, C., 2019. Vegetation-fire feedback reduces projected area burned under climate change. Sci. Rep. 9, 1–6. https://doi.org/10.1038/s41598-019-39284-1

Iglesias, V., Vannière, B., Jouffroy-Bapicot, I., 2019. Emergence and Evolution of Anthropogenic Landscapes in the Western Mediterranean and Adjacent Atlantic Regions. Fire 2, 53. https://doi.org/10.3390/fire2040053

Iglesias, V., Whitlock, C., 2014. Fire responses to postglacial climate change and human impact in northern Patagonia (41–43°S). Proc. Natl. Acad. Sci. 111, E5545–E5554. https://doi.org/10.1073/pnas.1410443111

Iglesias, V., Yospin, G.I., Whitlock, C., 2015. Reconstruction of fire regimes through integrated paleoecological proxy data and ecological modeling. Front. Plant Sci. 5. https://doi.org/10.3389/fpls.2014.00785

Ilvonen, L., López-Sáez, J.A., Holmström, L., Alba-Sánchez, F., Pérez-Díaz, S., Carrión, J.S., Ramos-Román, M.J., Camuera, J., Jiménez-Moreno, G., Ruha, L., Seppä, H., 2022. Spatial and temporal patterns of Holocene precipitation change in the Iberian Peninsula. Boreas. https://doi.org/10.1111/bor.12586

Innes, J.B., Blackford, J.J., Rowley-Conwy, P.A., 2013. Late Mesolithic and early Neolithic forest disturbance: a high resolution palaeoecological test of human impact hypotheses. Quat. Sci. Rev. 77, 80–100. https://doi.org/10.1016/j.quascirev.2013.07.012

Isern, N., Fort, J., Carvalho, A.F., Gibaja, J.F., Ibañez, J.J., 2014. The Neolithic Transition in the Iberian Peninsula: Data Analysis and Modeling. J. Archaeol. Method Theory 21, 447–460. https://doi.org/10.1007/s10816-013-9193-4

Isern, N., Fort, J., Vander Linden, M., 2012. Space Competition and Time Delays in Human Range Expansions. Application to the Neolithic Transition. PLoS One 7, e51106. https://doi.org/10.1371/journal.pone.0051106

Jiménez-Moreno, G., García-Alix, A., Hernández-Corbalán, M.D., Anderson, R.S., Delgado-Huertas, A., 2013. Vegetation, fire, climate and human disturbance history in the southwestern Mediterranean area during the late Holocene. Quat. Res. 79. https://doi.org/10.1016/j.yqres.2012.11.008

Kaal, J., Carrión Marco, Y., Asouti, E., Martín Seijo, M., Martínez Cortizas, A., Costa Casáis, M., Criado Boado, F., 2011. Long-term deforestation in NW Spain: linking the Holocene fire history to vegetation change and human activities. Quat. Sci. Rev. 30, 161–175. https://doi.org/10.1016/j.quascirev.2010.10.006

Kaal, J., Costa-Casais, M., Ferro-Vázquez, C., Pontevedra-Pombal, X., Martínez-Cortizas, A., 2008. Soil Formation of “Atlantic Rankers” from NW Spain—A High Resolution Aluminium and Iron Fractionation Study. Pedosphere 18, 441–453. https://doi.org/10.1016/S1002-0160(08)60035-1

Kaplan, J.O., Krumhardt, K.M., Ellis, E.C., Ruddiman, W.F., Lemmen, C., Goldewijk, K.K., 2011. Holocene carbon emissions as a result of anthropogenic land cover change. Holocene 21, 775–791. https://doi.org/10.1177/0959683610386983

Kaufman, D., McKay, N., Routson, C., Erb, M., Dätwyler, C., Sommer, P.S., Heiri, O., Davis, B., 2020. Holocene global mean surface temperature, a multi-method reconstruction approach. Sci. Data. https://doi.org/10.1038/s41597-020-0530-7

Killick, R., Eckley, I.A., 2014. changepoint : An R Package for Changepoint Analysis. J. Stat. Softw. 58, 1–19. https://doi.org/10.18637/jss.v058.i03

Klein Goldewijk, K., Beusen, A., Doelman, J., Stehfest, E., 2017. Anthropogenic land use estimates for the Holocene – HYDE 3.2. Earth Syst. Sci. Data 9, 927–953. https://doi.org/10.5194/essd-9-927-2017

Klein Goldewijk, K., Beusen, A., Janssen, P., 2010. Long-term dynamic modeling of global population and built-up area in a spatially explicit way: HYDE 3.1. The Holocene 20, 565–573. https://doi.org/10.1177/0959683609356587

Klein Goldewijk, K., Beusen, A., Van Drecht, G., De Vos, M., 2011. The HYDE 3.1 spatially explicit database of human-induced global land-use change over the past 12,000 years. Glob. Ecol. Biogeogr. 20, 73–86. https://doi.org/10.1111/j.1466-8238.2010.00587.x

Kniesel, J., Hinz, M., Rinne, C., 2014. Radon-B. In: http://radon-b.ufg.uni-kiel.de.

Kong, S.-R., Yamamoto, M., Shaari, H., Hayashi, R., Seki, O., Mohd Tahir, N., Fadzil, M.F., Sulaiman, A., 2021. The significance of pyrogenic polycyclic aromatic hydrocarbons in Borneo peat core for the reconstruction of fire history. PLoS One 16, e0256853. https://doi.org/10.1371/journal.pone.0256853

Lechterbeck, J., Edinborough, K., Kerig, T., Fyfe, R., Roberts, N., Shennan, S., 2014. Is Neolithic land use correlated with demography? An evaluation of pollen-derived land cover and radiocarbon-inferred demographic change from Central Europe. The Holocene 24, 1297–1307. https://doi.org/10.1177/0959683614540952

Leunda, M., González-Sampériz, P., Gil-Romera, G., Aranbarri, J., Moreno, A., Oliva-Urcia, B., Sevilla-Callejo, M., Valero-Garcés, B., 2017. The Late-Glacial and Holocene Marboré Lake sequence (2612 m a.s.l., Central Pyrenees, Spain): Testing high altitude sites sensitivity to millennial scale vegetation and climate variability. Glob. Planet. Change 157. https://doi.org/10.1016/j.gloplacha.2017.08.008

Lillios, K.T., Blanco-González, A., Drake, B.L., López-Sáez, J.A., 2016. Mid-late Holocene climate, demography, and cultural dynamics in Iberia: A multi-proxy approach. Quat. Sci. Rev. 135, 138–153. https://doi.org/10.1016/j.quascirev.2016.01.011

Lloret, F., Calvo, E., Pons, X., Díaz-Delgado, R., 2002. Wildfires and landscape patterns in the Eastern Iberian Peninsula. Landsc. Ecol. 17, 745–759. https://doi.org/10.1023/A:1022966930861

Loader, C., 2020. Locfit: Local regression, likelihood and density estimation. R Packag. version 1.5-9.4. https://CRAN.R-project.org/package=locfit

López-Merino, L., Cortizas, A.M., López-Sáez, J.A., 2010. Early agriculture and palaeoenvironmental history in the North of the Iberian Peninsula: a multi-proxy analysis of the Monte Areo mire (Asturias, Spain). J. Archaeol. Sci. 37, 1978–1988. https://doi.org/10.1016/j.jas.2010.03.003

López-Sáez, J.A., Carrasco, R.M., Turu, V., Ruiz-Zapata, B., Gil-García, M.J., Luelmo-Lautenschlaeger, R., Pérez-Díaz, S., Alba-Sánchez, F., Abel-Schaad, D., Ros, X., Pedraza, J., 2020. Late Glacial-early holocene vegetation and environmental changes in the western Iberian Central System inferred from a key site: The Navamuño record, Béjar range (Spain). Quat. Sci. Rev. 230, 106167. https://doi.org/10.1016/j.quascirev.2020.106167

López-Sáez, J.A., Figueiral, I., Cruz, D.J., 2017. Palaeoenvironment and vegetation dynamics in Serra da Nave (Alto Paiva, Beira Alta, Portugal) during the Late Pleistocene and the Holocene, in: Actas Da Mesa-Redonda "A Pré-História e a Proto-História No Centro de Portugal: Avaliação e Perspectivas de Futuro."

López-Sáez, J.A., Pérez-Díaz, S., Rodríguez-Ramírez, A., Blanco-González, A., Villarías-Robles, J.J.R., Luelmo-Lautenschlaeger, R., Jiménez-Moreno, G., Celestino-Pérez, S., Cerrillo-Cuenca, E., Pérez-Asensio, J.N., León, Á., 2018a. Mid-late Holocene environmental and cultural dynamics at the south-west tip of Europe (Doñana National Park, SW Iberia, Spain). J. Archaeol. Sci. Reports 22, 58–78. https://doi.org/10.1016/j.jasrep.2018.09.014

López-Sáez, J.A., Vargas, G., Ruiz-Fernández, J., Blarquez, O., Alba-Sánchez, F., Oliva, M., Pérez-Díaz, S., Robles-López, S., Abel-Schaad, D., 2018b. Paleofire Dynamics in Central Spain during the Late Holocene: The Role of Climatic and Anthropogenic Forcing. L. Degrad. Dev. 29, 2045–2059. https://doi.org/10.1002/ldr.2751

López-Sáez, J., López Merino, L., 2007. Coprophilous fungi as a source of information of anthropic activities during the Prehistory in the Amblés Valley (Avila, Spain): the archaeopalynological record. Rev. española Micropaleontol. 39, 103–116.

Luelmo-Lautenschlaeger, R., Blarquez, O., Pérez-Díaz, S., Morales-Molino, C., López-Sáez, J.A., 2019a. The iberian peninsula's burning heart-long-term fire history in the toledo mountains (central Spain). Fire 2, 1–23. https://doi.org/10.3390/fire2040054

Luelmo-Lautenschlaeger, R., Pérez-Díaz, S., Blarquez, O., Morales-Molino, C., López-Sáez, J.A., 2019b. The Toledo Mountains: A Resilient Landscape and a Landscape for Resilience? Hazards and Strategies in a Mid-Elevation Mountain Region in Central Spain. Quaternary 2. https://doi.org/10.3390/quat2040035

Manning, K., Colledge, S., Crema, E.R., Shennan, S., Timpson, A., 2016. The Cultural Evolution of Neolithic Europe. EUROEVOL Dataset 1: Sites, Phases and Radiocarbon Data. J. Open Archaeol. Data 5. https://doi.org/10.5334/joad.40

Manzano, S., Carrión, J.S., López-Merino, L., Jiménez-Moreno, G., Toney, J.L., Amstrong, H., Anderson, R.S., García-Alix, A., Pérez, J.L.G., Sánchez-Mata, D., 2019. A palaeoecological approach to understanding the past and present of Sierra Nevada, a Southwestern European biodiversity hotspot. Glob. Planet. Change 175. https://doi.org/10.1016/j.gloplacha.2019.02.006

Marlon, J.R., Bartlein, P.J., Carcaillet, C., Gavin, D.G., Harrison, S.P., Higuera, P.E., Joos, F., Power, M.J., Prentice, I.C., 2008. Climate and human influences on global biomass burning over the past two millennia. Nat. Geosci. 1, 697–702. https://doi.org/10.1038/ngeo313

Marlon, J.R., Bartlein, P.J., Daniau, A.-L., Harrison, S.P., Maezumi, S.Y., Power, M.J., Tinner, W., Vannière, B., 2013. Global biomass burning: a synthesis and review of Holocene paleofire records and their controls. Quat. Sci. Rev. 65, 5–25. https://doi.org/10.1016/j.quascirev.2012.11.029

Marlon, J.R., Bartlein, P.J., Walsh, M.K., Harrison, S.P., Brown, K.J., Edwards, M.E., Higuera, P.E., Power, M.J., Anderson, R.S., Briles, C., Brunelle, A., Carcaillet, C., Daniels, M., Hu, F.S., Lavoie, M., Long, C., Minckley, T., Richard, P.J.H., Scott, A.C., Shafer, D.S., Tinner, W., Umbanhowar, C.E., Whitlock, C., 2009. Wildfire responses to abrupt climate change in North America. Proc. Natl. Acad. Sci. 106, 2519–2524. https://doi.org/10.1073/pnas.0808212106

Marlon, J.R., Bartlein, P.J., Whitlock, C., 2006. Fire-fuel-climate linkages in the northwestern USA during the Holocene. The Holocene 16, 1059–1071. https://doi.org/10.1177/0959683606069396

Marlon, J.R., Kelly, R., Daniau, A.-L., Vannière, B., Power, M.J., Bartlein, P., Higuera, P., Blarquez, O., Brewer, S., Brücher, T., Feurdean, A., Romera, G.G., Iglesias, V., Maezumi, S.Y., Magi, B., Courtney Mustaphi, C.J., Zhihai, T., 2016. Reconstructions of biomass burning from sediment-charcoal records to improve data–model comparisons. Biogeosciences 13, 3225–3244. https://doi.org/10.5194/bg-13-3225-2016

Marquer, L., Gaillard, M.-J., Sugita, S., Trondman, A.-K., Mazier, F., Nielsen, A.B., Fyfe, R.M., Odgaard, B.V., Alenius, T., Birks, H.J.B., Bjune, A.E., Christiansen, J., Dodson, J., Edwards, K.J., Giesecke, T., Herzschuh, U., Kangur, M., Lorenz, S., Poska, A., Schult, M., Seppä, H., 2014. Holocene changes in vegetation composition in northern Europe: why quantitative pollen-based vegetation reconstructions matter. Quat. Sci. Rev. 90, 199–216. https://doi.org/10.1016/j.quascirev.2014.02.013

Martínez Cortizas, A., García-Rodeja, E., Pontevedra Pombal, X., Nóvoa Muñoz, J.C., Weiss, D., Cheburkin, A., 2002. Atmospheric Pb deposition in Spain during the last 4600 years recorded by two ombrotrophic peat bogs and implications for the use of peat as archive. Sci. Total Environ. 292. https://doi.org/10.1016/S0048-9697(02)00031-1

Mauri, A., Davis, B.A.S., Collins, P.M., Kaplan, J.O., 2015. The climate of Europe during the Holocene: A gridded pollen-based reconstruction and its multi-proxy evaluation. Quat. Sci. Rev. 112, 109–127. https://doi.org/10.1016/j.quascirev.2015.01.013

McLaughlin, T.R., Gómez-Puche, M., Cascalheira, J., Bicho, N., Fernández-López de Pablo, J., 2021. Late Glacial and Early Holocene human demographic responses to climatic and environmental change in Atlantic Iberia. Philos. Trans. R. Soc. B Biol. Sci. 376, 20190724. https://doi.org/10.1098/rstb.2019.0724

Mighall, T.M., Martínez Cortizas, A., Biester, H., Turner, S.E., 2006. Proxy climate and vegetation changes during the last five millennia in NW Iberia: Pollen and non-pollen palynomorph data from two ombrotrophic peat bogs in the North Western Iberian Peninsula. Rev. Palaeobot. Palynol. 141, 203–223. https://doi.org/10.1016/j.revpalbo.2006.03.013

Mooney, S.D., Harrison, S.P., Bartlein, P.J., Daniau, A.-L., Stevenson, J., Brownlie, K.C., Buckman, S., Cupper, M., Luly, J., Black, M., Colhoun, E., D'Costa, D., Dodson, J., Haberle, S., Hope, G.S., Kershaw, P., Kenyon, C., McKenzie, M., Williams, N., 2011. Late Quaternary fire regimes of Australasia. Quat. Sci. Rev. 30, 28–46. https://doi.org/10.1016/j.quascirev.2010.10.010

Morales-Molino, C., Colombaroli, D., Tinner, W., Perea, R., Valbuena-Carabaña, M., Carrión, J.S., Gil, L., 2018. Vegetation and fire dynamics during the last 4000 years in the Cabañeros National Park (central Spain). Rev. Palaeobot. Palynol. 253, 110–122. https://doi.org/10.1016/j.revpalbo.2018.04.001

Morales-Molino, C., García-Antón, M., 2014. Vegetation and fire history since the last glacial maximum in an inland area of the western Mediterranean Basin (Northern Iberian Plateau, NW Spain). Quat. Res. 81, 63–77. https://doi.org/10.1016/j.yqres.2013.10.010

Morales-Molino, C., Tinner, W., García-Antón, M., Colombaroli, D., 2017. The historical demise of *Pinus nigra* forests in the Northern Iberian Plateau (south-western Europe). J. Ecol. 105, 634–646. https://doi.org/10.1111/1365-2745.12702

Morales-Molino, C., Tinner, W., Perea, R., Carrión, J.S., Colombaroli, D., Valbuena-Carabaña, M., Zafra, E., Gil, L., 2019. Unprecedented herbivory threatens rear-edge populations of *Betula* in southwestern Eurasia. Ecology 100 (11). https://doi.org/10.1002/ecy.2833

Morellón, M., Aranbarri, J., Moreno, A., González-Sampériz, P., Valero-Garcés, B.L., 2018. Early Holocene humidity patterns in the Iberian Peninsula reconstructed from lake, pollen and speleothem records. Quat. Sci. Rev. 181, 1–18. https://doi.org/10.1016/j.quascirev.2017.11.016

Morellón, M., Valero-Garcés, B., Moreno, A., González-Sampériz, P., Mata, P., Romero, O., Maestro, M., Navas, A., 2008. Holocene palaeohydrology and climate variability in northeastern Spain: The sedimentary record of Lake Estanya (Pre-Pyrenean range). Quat. Int. 181, 15–31. https://doi.org/10.1016/j.quaint.2007.02.021

Moreno, A., Pérez-Mejías, C., Bartolomé, M., Sancho, C., Cacho, I., Stoll, H., Delgado-Huertas, A., Hellstrom, J., Edwards, R.L., Cheng, H., 2017. New speleothem data from Molinos and Ejulve caves reveal Holocene hydrological variability in northeast Iberia. Quat. Res. 88, 223–233. https://doi.org/10.1017/qua.2017.39

Muñoz Sobrino, C., Heiri, O., Hazekamp, M., van der Velden, D., Kirilova, E.P., García-Moreiras, I., Lotter, A.F., 2013. New data on the Lateglacial period of SW Europe: a high resolution multiproxy record from Laguna de la Roya (NW Iberia). Quat. Sci. Rev. 80, 58–77. https://doi.org/https://doi.org/10.1016/j.quascirev.2013.08.016

O'Hara-Wild, M., Hyndman, R., Wang, E., 2021. fable: Forecasting Models for Tidy Time Series. R Packag. version 0.3.1. https://CRAN.R-project.org/package=fable

Palmisano, A., Woodbridge, J., Roberts, C.N., Bevan, A., Fyfe, R., Shennan, S., Cheddadi, R., Greenberg, R., Kaniewski, D., Langgut, D., Leroy, S.A., Litt, T., Miebach, A., 2019. Holocene landscape dynamics and long-term population trends in the Levant. The Holocene 29, 708–727. https://doi.org/10.1177/0959683619826642

Pardo-Gordó, S., Carvalho, A.F., 2020. Population dynamics during the Neolithic transition and the onset of megalithism in Portugal according to summed probability distribution of radiocarbon determinations. Archaeol. Anthropol. Sci. 12, 129. https://doi.org/10.1007/s12520-020-01086-2

Pardo-Gordó, S., García Puchol, O., Bernabeu Aubán, J., Diez Castillo, A., 2019. Timing the Mesolithic-Neolithic Transition in the Iberian Peninsula: The Radiocarbon Dataset. J. Open Archaeol. Data 7. https://doi.org/10.5334/joad.49

Pausas, J.G., Bond, W.J., 2020. On the Three Major Recycling Pathways in Terrestrial Ecosystems. Trends Ecol. Evol. 35, 767–775. https://doi.org/https://doi.org/10.1016/j.tree.2020.04.004

Pausas, J.G., Fernández-Muñoz, S., 2012. Fire regime changes in the Western Mediterranean Basin: from fuel-limited to drought-driven fire regime. Clim. Change 110, 215–226. https://doi.org/10.1007/s10584-011-0060-6

Pausas, J.G., Paula, S., 2012. Fuel shapes the fire-climate relationship: Evidence from Mediterranean ecosystems. Glob. Ecol. Biogeogr. 21, 1074–1082. https://doi.org/10.1111/j.1466-8238.2012.00769.x

Pebesma, E.J., 2004. Multivariable geostatistics in S: the gstat package. Comput. Geosci. 30, 683–691. https://doi.org/10.1016/j.cageo.2004.03.012

Peña-Chocarro, L., Peña, L.Z., Gazólaz, J.G., Morales, M.G., Sesma, J.S., Straus, L.G., 2005. The spread of agriculture in northern Iberia: new archaeobotanical data from El Mirón cave (Cantabria) and the open-air site of Los Cascajos (Navarra). Veg. Hist. Archaeobot. 14, 268–278. https://doi.org/10.1007/s00334-005-0078-7

Pérez-Díaz, S., López Sáez, J.A., 2019. The Western Pyrenean (Northern Iberian Peninsula) during the Upper Paleolithic: a palaeoenvironmental approach.
In: Schmidt, I., Cascalheira, J., Bicho, N., Wenige, G.-C. (Eds.), Human adaptations to the Last Glacial Maximum: the Solutrean and its neighbors. Cambridge Scholars Publishing, Newcastle.

Pérez-Díaz, S., López-Sáez, J.A., 2017. 33. Verdeospesoa mire (Basque Country, Northern Iberian Peninsula, Spain). Grana 56. https://doi.org/10.1080/00173134.2016.1271824

Pérez-Díaz, S., López-Sáez, J.A., Núñez de la Fuente, S., Ruiz-Alonso, M., 2018. Early farmers, megalithic builders and the shaping of the cultural landscapes during the Holocene in Northern Iberian mountains. A palaeoenvironmental perspective. J. Archaeol. Sci. Reports 18, 463–474. https://doi.org/10.1016/j.jasrep.2018.01.043

Pérez-Sanz, A., González-Sampériz, P., Moreno, A., Valero-Garcés, B., Gil-Romera, G., Rieradevall, M., Tarrats, P., Lasheras-Álvarez, L., Morellón, M., Belmonte, A., Sancho, C., Sevilla-Callejo, M., Navas, A., 2013. Holocene climate variability, vegetation dynamics and fire regime in the central

Pyrenees: the Basa de la Mora sequence (NE Spain). Quat. Sci. Rev. 73. https://doi.org/10.1016/j.quascirev.2013.05.010

Pirzamanbein, B., Lindström, J., Poska, A., Sugita, S., Trondman, A.-K., Fyfe, R.M., Mazier, F., Nielsen, A.B., Kaplan, J.O., Bjune, A.E., Birks, H.J.B., Giesecke, T., Kangur, M., Latałowa, M., Marquer, L., Smith, B., Gaillard, M.-J., 2014. Creating spatially continuous maps of past land cover from point estimates: A new statistical approach applied to pollen data. Ecol. Complex. 20, 127–141. https://doi.org/10.1016/j.ecocom.2014.09.005

Power, M.J., Marlon, J.R., Bartlein, P.J., Harrison, S.P., 2010. Fire history and the Global Charcoal Database: A new tool for hypothesis testing and data exploration. Palaeogeogr. Palaeoclimatol. Palaeoecol. 291, 52–59. https://doi.org/10.1016/j.palaeo.2009.09.014

Power, M.J., Marlon, J.R., Ortiz, N., Bartlein, P.J., Harrison, S.P., Mayle, F.E., Ballouche, A., Bradshaw, R.H.W., Carcaillet, C., Cordova, C., Mooney, S., Moreno, P.I., Prentice, I.C., Thonicke, K., Tinner, W., Whitlock, C., Zhang, Y., Zhao, Y., Ali, A.A., Anderson, R.S., Beer, R., Behling, H., Briles, C., Brown, K.J., Brunelle, A., Bush, M., Camill, P., Chu, G.Q., Clark, J., Colombaroli, D., Connor, S., Daniau, A.-L., Daniels, M., Dodson, J., Doughty, E., Edwards, M.E., Finsinger, W., Foster, D., Frechette, J., Gaillard, M.-J., Gavin, D.G., Gobet, E., Haberle, S., Hallett, D.J., Higuera, P., Hope, G., Horn, S., Inoue, J., Kaltenrieder, P., Kennedy, L., Kong, Z.C., Larsen, C., Long, C.J., Lynch, J., Lynch, E.A., McGlone, M., Meeks, S., Mensing, S., Meyer, G., Minckley, T., Mohr, J., Nelson, D.M., New, J., Newnham, R., Noti, R., Oswald, W., Pierce, J., Richard, P.J.H., Rowe, C., Sanchez Goñi, M.F., Shuman, B.N., Takahara, H., Toney, J., Turney, C., Urrego-Sanchez, D.H., Umbanhowar, C., Vandergoes, M., Vannière, B., Vescovi, E., Walsh, M., Wang, X., Williams, N., Wilmshurst, J., Zhang, J.H., 2008. Changes in fire regimes since the Last Glacial Maximum: an assessment based on a global synthesis and analysis of charcoal data. Clim. Dyn. 30, 887–907. https://doi.org/10.1007/s00382-007-0334-x

R Core Team, 2021. R: A Language and Environment for Statistical Computing. R Foundation for Statistical Computing, Vienna, Austria. https://www.R-project.org/.

Reimer, P.J., Austin, W.E.N., Bard, E., Bayliss, A., Blackwell, P.G., Bronk Ramsey, C., Butzin, M., Cheng, H., Edwards, R.L., Friedrich, M., Grootes, P.M., Guilderson, T.P., Hajdas, I., Heaton, T.J., Hogg, A.G., Hughen, K.A., Kromer, B., Manning, S.W., Muscheler, R., Palmer, J.G., Pearson, C., van der Plicht, J., Reimer, R.W., Richards, D.A., Scott, E.M., Southon, J.R., Turney, C.S.M., Wacker, L., Adolphi, F., Büntgen, U., Capano, M., Fahrni, S.M., Fogtmann-Schulz, A., Friedrich, R., Köhler, P., Kudsk, S., Miyake, F., Olsen, J., Reinig, F., Sakamoto, M., Sookdeo, A., Talamo, S., 2020. The IntCal20 Northern Hemisphere Radiocarbon Age Calibration Curve (0–55 cal kBP). Radiocarbon 62, 1–33. https://doi.org/10.1017/rdc.2020.41

Revelles, J., Burjachs, F., Palomo, A., Piqué, R., Iriarte, E., Pérez-Obiol, R., Terradas, X., 2018. Human-environment interaction during the Mesolithic- Neolithic transition in the NE Iberian Peninsula. Vegetation history, climate change and human impact during the Early-Middle Holocene in the Eastern Pre-Pyrenees. Quat. Sci. Rev. 184, 183–200. https://doi.org/10.1016/j.quascirev.2017.08.025

Revelles, J., Cho, S., Iriarte, E., Burjachs, F., van Geel, B., Palomo, A., Piqué, R., Peña-Chocarro, L., Terradas, X., 2015. Mid-Holocene vegetation history and Neolithic land-use in the Lake Banyoles area (Girona, Spain). Palaeogeogr. Palaeoclimatol. Palaeoecol. 435, 70–85. https://doi.org/10.1016/j.palaeo.2015.06.002

Rick, J.W., 1987. Dates as Data: An Examination of the Peruvian Preceramic Radiocarbon Record. Am. Antiq. 52, 55. https://doi.org/10.2307/281060

Riera-Mora, S., Esteban-Amat, A., 1994. Vegetation history and human activity during the last 6000 years on the central Catalan coast (northeastern Iberian Peninsula). Veg. Hist. Archaeobot. 3, 7–23. https://doi.org/10.1007/BF00208885

Roberts, C.N., Woodbridge, J., Palmisano, A., Bevan, A., Fyfe, R., Shennan, S., 2019. Mediterranean landscape change during the Holocene: Synthesis, comparison and regional trends in population, land cover and climate. The Holocene 29, 923–937. https://doi.org/10.1177/0959683619826697

Rodrigues, T., Grimalt, J.O., Abrantes, F.G., Flores, J.A., Lebreiro, S.M., 2009. Holocene interdependences of changes in sea surface temperature, productivity, and fluvial inputs in the Iberian continental shelf (Tagus mud patch). Geochemistry, Geophys. Geosystems 10 (7). https://doi.org/10.1029/2008GC002367

Sánchez Goñi, M.F., Hannon, G.E., 1999. High-altitude vegetational pattern on the Iberian Mountain Chain (north-central Spain) during the Holocene. Holocene 9, 39–57. https://doi.org/10.1191/095968399671230625

Scharf, E.A., 2010. A statistical evaluation of the relative influences of climate, vegetation, and prehistoric human population on the charcoal record of Five Lakes, Washington (USA). Quat. Int. 215, 74–86. https://doi.org/10.1016/j.quaint.2009.09.021

Schirrmacher, J., Weinelt, M., Blanz, T., Andersen, N., Salgueiro, E., Schneider, R.R., 2019. Multi-decadal atmospheric and marine climate variability in southern Iberia during the mid- to late-Holocene. Clim. Past 15, 617–634. https://doi.org/10.5194/cp-15-617-2019

Schmid, C., Seidensticker, D., Hinz, M., 2019. c14bazAAR: An R package for downloading and preparing C14 dates from different source databases. J. Open Source Softw. 4, 1914. https://doi.org/10.21105/joss.01914

Schneider, H., Höfer, D., Trog, C., Busch, S., Schneider, M., Baade, J., Daut, G., Mäusbacher, R., 2010. Holocene estuary development in the Algarve Region (Southern Portugal) – A reconstruction of sedimentological and ecological evolution. Quat. Int. 221 (1-2), 141-158. https://doi.org/10.1016/j.quaint.2009.10.004

Schneider, H., Höfer, D., Trog, C., Mäusbacher, R., 2016. Holocene landscape development along the Portuguese Algarve coast - A high resolution palynological approach. Quat. Int. 407, 47–63. https://doi.org/10.1016/j.quaint.2016.02.039

Schröder, T., van't Hoff, J., López-Sáez, J.A., Viehberg, F., Melles, M., Reicherter, K., 2018. Holocene climatic and environmental evolution on the southwestern Iberian Peninsula: A high-resolution multi-proxy study from Lake Medina (Cádiz, SW Spain). Quat. Sci. Rev. 198, 208–225. https://doi.org/10.1016/j.quascirev.2018.08.030

Shen, Y., Sweeney, L., Liu, M., Lopez Saez, J.A., Pérez-Díaz, S., Luelmo-Lautenschlaeger, R., Gil-Romera, G., Hoefer, D., Jiménez-Moreno, G., Schneider, H., Prentice, I.C., Harrison, S., 2021. Reconstructing burnt area during the Holocene: an Iberian case study. Clim. Past Discuss. 1–23. https://doi.org/10.5194/cp-2021-36

Shennan, S., Downey, S.S., Timpson, A., Edinborough, K., Colledge, S., Kerig, T., Manning, K., Thomas, M.G., 2013. Regional population collapse followed initial agriculture booms in mid-Holocene Europe. Nat. Commun. 4, 2486. https://doi.org/10.1038/ncomms3486

Silva, F., Vander Linden, M., 2017. Amplitude of travelling front as inferred from 14C predicts levels of genetic admixture among European early farmers. Sci. Rep. 7, 11985. https://doi.org/10.1038/s41598-017-12318-2

Stevenson, A.C., 2000. The Holocene forest history of the Montes Universales, Teruel, Spain. Holocene 10, 603–610. https://doi.org/10.1191/095968300670543500

Tarrats, P., Heiri, O., Valero-Garcés, B., Cañedo-Argüelles, M., Prat, N., Rieradevall, M., González-Sampériz, P., 2018. Chironomid-inferred Holocene temperature reconstruction in Basa de la Mora Lake (Central Pyrenees). The Holocene 28, 1685–1696. https://doi.org/10.1177/0959683618788662

Tepley, A.J., Thomann, E., Veblen, T.T., Perry, G.L.W., Holz, A., Paritsis, J., Kitzberger, T., Anderson-Teixeira, K.J., 2018. Influences of fire–vegetation feedbacks and post-fire recovery rates on forest landscape vulnerability to altered fire regimes. J. Ecol. 106, 1925–1940. https://doi.org/10.1111/1365-2745.12950

Thatcher, D.L., Wanamaker, A.D., Denniston, R.F., Asmerom, Y., Polyak, V.J., Fullick, D., Ummenhofer, C.C., Gillikin, D.P., Haws, J.A., 2020. Hydroclimate variability from western Iberia (Portugal) during the Holocene: Insights from a composite stalagmite isotope record. The Holocene 30, 966–981. https://doi.org/10.1177/0959683620908648

Timpson, A., Colledge, S., Crema, E.R., Edinborough, K., Kerig, T., Manning, K., Thomas, M.G., Shennan, S., 2014. Reconstructing regional population fluctuations in the European Neolithic using radiocarbon dates: a new case-study using an improved method. J. Archaeol. Sci. 52, 549–557. https://doi.org/10.1016/j.jas.2014.08.011

Torfing, T., 2015. Neolithic population and summed probability distribution of 14C-dates. J. Archaeol. Sci. 63, 193–198. https://doi.org/10.1016/j.jas.2015.06.004

Trachsel, M., Telford, R.J., 2016. All age–depth models are wrong, but are getting better. The Holocene 27, 860–869. https://doi.org/10.1177/0959683616675939

Trondman, A. -K., Gaillard, M. -J., Mazier, F., Sugita, S., Fyfe, R.M., Nielsen, A.B., Twiddle, C., Barratt, P., Birks, H.J.B., Bjune, A.E., Björkman, L., Broström, A., Caseldine, C., David, R., Dodson, J., Dörfler, W., Fischer, E., Geel, B., Giesecke, T., Hultberg, T., Kalnina, L., Kangur, M., Knaap, P., Koff, T., Kuneš, P., Lagerås, P., Latałowa, M., Lechterbeck, J., Leroyer, C., Leydet, M., Lindbladh, M., Marquer, L., Mitchell, F.J.G., Odgaard, B. V., Peglar, S.M., Persson, T., Poska, A., Rösch, M., Seppä, H., Veski, S., Wick, L., 2015. Pollen-based quantitative reconstructions of Holocene regional vegetation cover (plant-functional types and land-cover types) in Europe suitable for climate modelling. Glob. Chang. Biol. 21, 676–697. https://doi.org/10.1111/gcb.12737

Umbanhowar, C.E., McGrath, M.J., 1998. Experimental production and analysis of microscopic charcoal from wood, leaves and grasses. The Holocene 8, 341–346. https://doi.org/10.1191/095968398666496051

van der Knaap, W.O., van Leeuwen, J.F.N., 1997. Late Glacial and early Holocene vegetation succession, altitudinal vegetation zonation, and climatic change in the Serra da Estrela, Portugal. Rev. Palaeobot. Palynol. 97. https://doi.org/10.1016/S0034-6667(97)00008-0

van der Knaap, W.O., van Leeuwen, J.F.N., 1995. Holocene vegetation succession and degradation as responses to climatic change and human activity in the Serra de Estrela, Portugal. Rev. Palaeobot. Palynol. 89. https://doi.org/10.1016/0034-6667(95)00048-0

Vannière, B., Blarquez, O., Rius, D., Doyen, E., Brücher, T., Colombaroli, D., Connor, S., Feurdean, A., Hickler, T., Kaltenrieder, P., Lemmen, C., Leys, B., Massa, C., Olofsson, J., 2016. 7000-year human legacy of elevation-dependent European fire regimes. Quat. Sci. Rev. 132, 206–212. https://doi.org/10.1016/j.quascirev.2015.11.012

Vannière, B., Power, M.J., Roberts, N., Tinner, W., Carrión, J., Magny, M., Bartlein, P., Colombaroli, D., Daniau, A.-L., Finsinger, W., Gil-Romera, G., Kaltenrieder, P., Pini, R., Sadori, L., Turner, R., Valsecchi, V., Vescovi, E., 2011. Circum-Mediterranean fire activity and climate changes during the mid-Holocene environmental transition (8500-2500 cal. BP). The Holocene 21, 53–73. https://doi.org/10.1177/0959683610384164

Vermeersch, P.M., 2020. Radiocarbon Palaeolithic Europe database: A regularly updated dataset of the radiometric data regarding the Palaeolithic of Europe, Siberia included. Data Br. 31, 105793. https://doi.org/10.1016/j.dib.2020.105793

Weninger, B., Clare, L., Jöris, O., Jung, R., Edinborough, K., 2015. Quantum theory of radiocarbon calibration. World Archaeol. 47, 543–566. https://doi.org/10.1080/00438243.2015.1064022

Whitlock, C., Anderson, R.S., 2003. Fire History Reconstructions Based on Sediment Records from Lakes and Wetlands, in: Veblen, T.T., Baker, W.L., Montenegro, G., Swetnam, T.W. (Eds.), Fire and Climatic Change in Temperate Ecosystems of the Western Americas. Springer New York, New York, NY, pp. 3–31. https://doi.org/10.1007/0-387-21710-X_1

Williams, A.N., 2012. The use of summed radiocarbon probability distributions in archaeology: a review of methods. J. Archaeol. Sci. 39, 578–589. https://doi.org/10.1016/j.jas.2011.07.014

Woodbridge, J., Fyfe, R.M., Roberts, N., Downey, S., Edinborough, K., Shennan, S., 2014. The impact of the Neolithic agricultural transition in Britain: a comparison of pollen-based land-cover and archaeological 14C date-inferred population change. J. Archaeol. Sci. 51, 216–224. https://doi.org/10.1016/j.jas.2012.10.025

Woodbridge, J., Roberts, C.N., Palmisano, A., Bevan, A., Shennan, S., Fyfe, R.M., Eastwood, W.J., Izdebski, A., Çakırlar, C., Woldring, H., Broothaerts, N., Kaniewski, D., Finné, M., Labuhn, I., 2019. Pollen-inferred regional vegetation patterns and demographic change in Southern Anatolia through the Holocene. The Holocene 29, 728–741. https://doi.org/10.1177/0959683619826635

Zanon, M., Davis, B.A.S., Marquer, L., Brewer, S., Kaplan, J.O., 2018. European forest cover during the past 12,000 years: A palynological reconstruction based on modern analogs and remote sensing. Front. Plant Sci. 9, 1–25. https://doi.org/10.3389/fpls.2018.00253

Zapata, L., Peña-Chocarro, L., Pérez-Jordá, G., Stika, H.-P., 2004. Early Neolithic Agriculture in the Iberian Peninsula. J. World Prehistory 18, 283–325. https://doi.org/10.1007/s10963-004-5621-4

Zeileis, A., Grothendieck, G., 2005. **zoo** : *S3* Infrastructure for Regular and Irregular Time Series. J. Stat. Softw. 14. https://doi.org/10.18637/jss.v014.i06

Zennaro, P., Kehrwald, N., Marlon, J.R., Ruddiman, W.F., Brücher, T., Agostinelli, C., Dahl-Jensen, D., Zangrando, R., Gambaro, A., Barbante, C., 2015. Europe on fire three thousand years ago: Arson or climate? Geophys. Res. Lett. 42, 5023–2033. https://doi.org/10.1002/2015GL064259

Zimmerman, S.R.H., Wahl, D.B., 2020. Holocene paleoclimate change in the western US: The importance of chronology in discerning patterns and drivers. Quat. Sci. Rev. 246, 106487. https://doi.org/https://doi.org/10.1016/j.quascirev.2020.106487

2.9. Supplement

This supplement contains the following sections: (1) the influence of the selection of macro or micro charcoal on the charcoal z-score composite; (2) the influence of max transformation compared with minmax transformation on the charcoal z-score composite; (3) the impact of the choice of variogram model and kriging interpolated Neolithic surface; (4) the raw quantity of radiocarbon dated archaeological material available through time; (5) the influence of bin width choice on the charcoal z-score composite; (6) the influence of the exclusion or inclusion of high elevation sites (>2000m) on the charcoal z-score composite; (7) the number of charcoal records contributing to the z-score composite curve through time; (8) long-term trend of the z-score composite of charcoal influx; (9) the implications of exponential compared to logistic model choice in the summed probability distribution (SPD) null model selection; (10) detrended superposed epoch analysis of charcoal z-score composite; (11) superposed epoch analysis of charcoal z-score composite with randomly adjusted "key population growth dates"; (12) superposed epoch analysis of charcoal z-score composites using AutoRegressive Integrated Moving Average (ARIMA) analysis; (13) detrended Neolithic charcoal z-score composite; (14) Neolithic charcoal z-score composite with randomly adjusted radiocarbon Neolithic dates; (15) Neolithic charcoal z-score composite ARIMA analysis; (16) charcoal influx through time of utilised Iberian records.

This supplement includes the following Figures and Tables:

- Supplementary Figure 2.1: Influence of the selection of macro or micro charcoal on charcoal z-score composite
- Supplementary Figure 2.2: Z-score composites of charcoal influx for Iberia, 10,000 to 3,500 cal. BP. The curves show the impact of max (red) or minmax (blue) transformation.
- Supplementary Figure 2.3: Z-score composite of charcoal influx for Iberia, 10,000 to 3,500 cal. BP.
- Supplementary Figure 2.4: Number of radiocarbon dated archaeological samples, per 100 year bin. 10,000 to 3,500 cal. BP
- Supplementary Figure 2.5: Variogram and variogram models associated with the Neolithic radiocarbon dates (N.B. Matern and Stein Matern models overlap)Supplementary Figure 2.5: Kriging interpolated Neolithic surfaces, based on different variogram fitted models: A) Exponential; B) Stein Matern; C) Matern; D) Spherical
- Supplementary Figure 2.6: Z-score composites of charcoal influx for Iberia, 10,000 to 3,500 cal. BP. Curves represent the sites below 2000m (red) or those sites above 2000m (blue)
- Supplementary Figure 2.7: Number of records contributing to each 100 year bin used in the construction of the z-score composite of charcoal influx, 10,000 to 3,500 cal. BP

- Supplementary Figure 2.8: Z-score composite of charcoal influx for Iberia, 10,000 to 3,500 cal. BP (red) and fitted linear model representing longer-term trend in fire (black)
- Supplementary Figure 2.9: Detrended z-score composite of charcoal influx for Iberia, 10,000 to 3,500 cal. BP
- Supplementary Figure 2.10: (A) Summed probability distribution and exponential null model for Iberia (10 – 3.5k cal. BP.) (B) Summed probability distribution rate of change and exponential null model for Iberia (10 – 3.5k cal. BP.); (C) Summed probability distribution and logistic null model for Iberia (10 – 3.5k cal. BP.) (D) Summed probability distribution rate of change and logistic null model for Iberia (10 – 3.5k cal. BP.) Deviations from simulated growth models are shown in red and blue
- Supplementary Figure 2.11: Superposed epoch analysis of detrended z-score composite of charcoal influx for Iberia, with dates aligned before and after SPD key growth periods at 7,383 and 5,371 cal. BP. Grey lines indicate 1000 bootstrap re-samples of records, with replacement. The solid red lines shows the median z-score values, and the fine red lines are the 95% confidence intervals.
- Supplementary Figure 2.12: Superposed epoch analysis of z-score composite of charcoal influx for Iberia, with dates adjusted before and after SPD key growth periods at 7,395 and 5,369 cal. BP. Grey lines indicate 1000 re-runs of the SEA with randomly adjusted key growth periods
- Supplementary Figure 2.13: Superposed epoch analysis of z-score composite of charcoal influx for Iberia, with dates adjusted before and after SPD key growth periods at 7,395 and 5,369 cal. BP. ARIMA model forecast post-epoch dates in blue, with forecast confidence intervals shown
- Supplementary Figure 2.14: Superposed epoch analysis of detrended z-score composite of charcoal influx for Iberia, based on spatially heterogenous dates relative to the start of the Neolithic across Iberia. Grey lines indicate 1000 bootstrap re-samples of core sites, with replacement. The solid red line shows the median z-score values, and the fine red lines are the 95% confidence intervals
- Supplementary Figure 2.15: Neolithic detrended z-score composite of charcoal influx for Iberia, based on spatially heterogenous dates relative to the start of the Neolithic across Iberia. The yellow line represents the detrended adjusted composite; grey lines represent alternative detrended adjusted composites based on randomised changes to the Neolithic interpolation; blue lines represent 95% confidence intervals of the detrended adjusted composite
- Supplementary Figure 2.16: Neolithic z-score composite of charcoal influx for Iberia, based on spatially heterogenous dates relative to the start of the Neolithic across Iberia. ARIMA model forecast post-Neolithic dates overlayed by actual influx, with forecast confidence intervals shown

- Supplementary Figure 2.17: Charcoal influx associated with records included within the analysis of fire history for Iberia; complete record shown, with macro or micro charcoal type indicated. Records 1-8 of 32
- Supplementary Figure 2.18: Charcoal influx associated with records included within the analysis of fire history for Iberia; complete record shown, with macro or micro charcoal type indicated. Records 9-16 of 32
- Supplementary Figure 2.19: Charcoal influx associated with records included within the analysis of fire history for Iberia; complete record shown, with macro or micro charcoal type indicated. Records 17-24 of 32
- Supplementary Figure 2.20: Charcoal influx associated with records included within the analysis of fire history for Iberia; complete record shown, with macro or micro charcoal type indicated. Records 25-32 of 32

S1. Influence of the selection of macro or micro charcoal on charcoal z-score composite

To prevent individual site overrepresentation within the composite curve, a single record has been selected for each site. Of the 32 records included within the charcoal z-score composite, 11 sites contain both macro- or micro-charcoal records. After first selecting for records with the maximum number of charcoal samples, we then selected macro-charcoal records for our analysis. The impact of this selection on the shape of the overall composite curve is, however, minimal (Sup. Fig. 2.1)

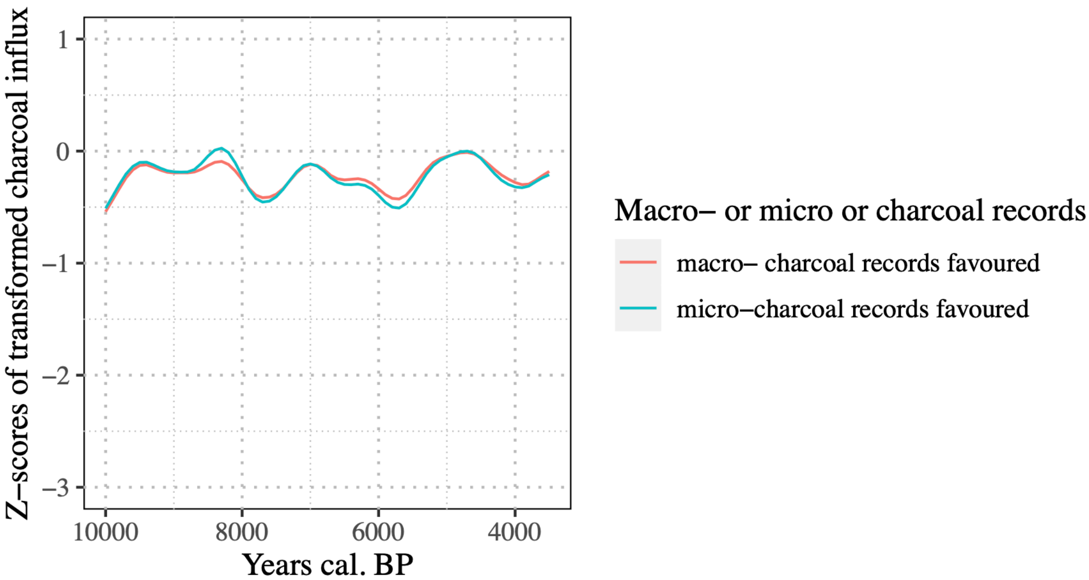

Supplementary Figure 2.1: Z-score composites of charcoal influx for Iberia, 10,000 to 3,500 cal. BP. The curves show the impact of including macro- (red) or micro-charcoal (blue) for sites with multiple types of record

S2.	Influence of max compared with minmax transformation on charcoal z-score composite

One of the steps in standardising the charcoal records so that they can be both comparable and composited is transformation of site influx values to a common range of 0-1. In order to take into account zero values of charcoal accumulation, we performed a max transformation (Eq. (1)), rather than the minimax transformation (Eq. (2)) suggested by Power et al. (2008). The influence of this change on the shape of the charcoal z-score composite is almost imperceptible, with only minor differences visible at ca. 5,000 and 4,000 cal. BP (Sup. Fig. 2.2). Note that the scale in Sup. Fig. 2.2 is narrower than other charcoal z-score figures (e.g. Sup. Fig. 2.3), in order to visualise these minor differences.

Max transformation: $$x'_{i,j} = \frac{x_{i,j}}{x_{j,max}} \quad (1)$$

Minimax transformation: $$x'_{i,j} = \frac{x_{i,j} - x_{j,min}}{x_{j,\max} - x_{j,min}} \quad (2)$$

where $x'_{i,j}$ is the transformed influx value of the i-th sample in the j-th record, $x_{j,max}$ is the maximum influx value for the j-th record, and $x_{j,min}$ is the minimum influx value for the j-th record.

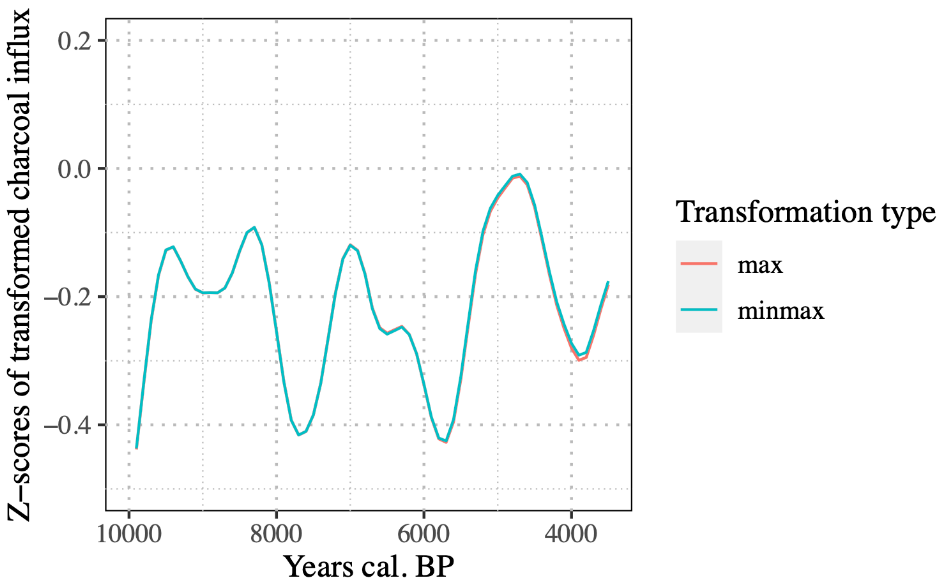

Supplementary Figure 2.2: Z-score composites of charcoal influx for Iberia, 10,000 to 3,500 cal. BP. The curves show the impact of max (red) or minmax (blue) transformation.

S3. Influence of bin width choice on charcoal z-score composite

The choice of bin width affects the z-score composite curve in terms of the magnitude of variations (Sup. Fig. 2.3). The differences in the curve using different bin widths are more apparent prior to ca. 7,800 cal. BP, due to the more limited numbers of charcoal records used (see S8). The increase in fire at ca. 9,500 cal. BP becomes more pronounced with shorter bin widths. The shape of the curves is very similar after 7,800 cal. BP, with the exception of the 500-yr bin width where variability is muted, indicating that bin width choice has a limited impact on the construction of fire history.

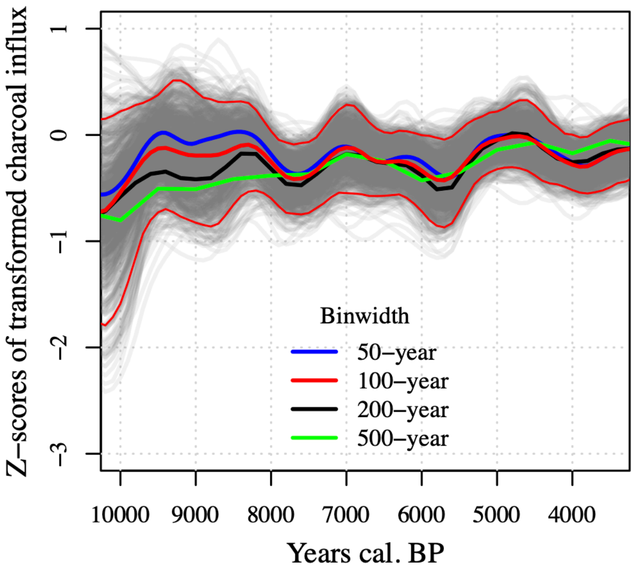

Supplementary Figure 2.3: Z-score composite of charcoal influx for Iberia, 10,000 to 3,500 cal. BP. The solid lines show the median value, with smoothing windows of 50 (blue), 100 (red), 200 (black) and 500 (green) years, the thin red lines show the 95% confidence intervals of the 1000 bootstrap resample (shown in pale grey).

S4. The raw quantity of radiocarbon dated archaeological material through time

The number of radiocarbon dates archaeological samples increases through time (Sup. Fig. 2.4), and broadly mirrors the shape of the SPD curve (Sup. Fig. 2.11). The differences in the shape of this curve with the SPD reflects both the site binning procedure and the 200-year rolling mean used in construction of the SPD.

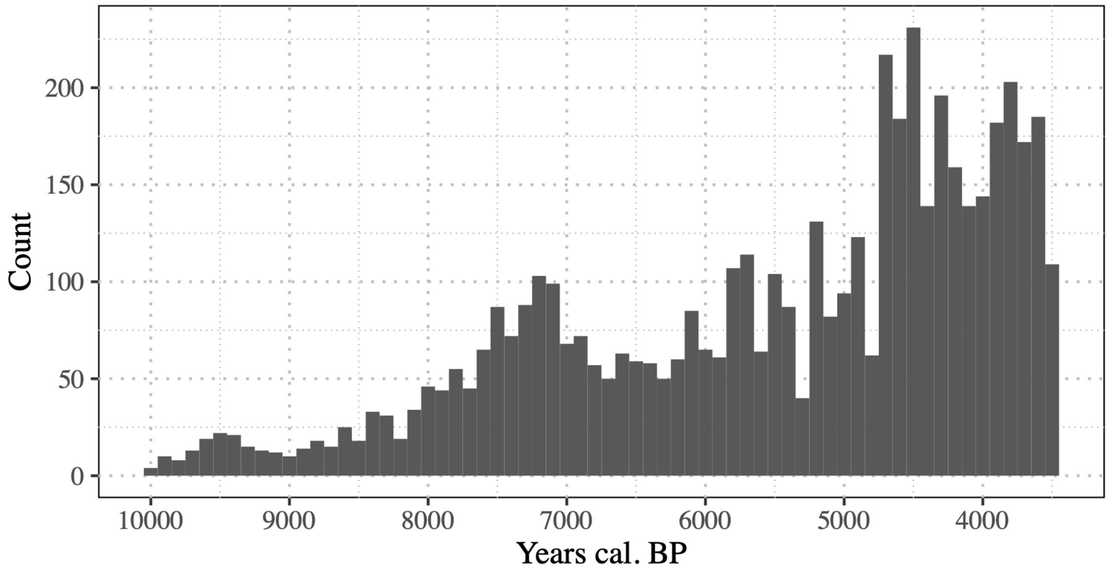

Supplementary Figure 2.4: Number of radiocarbon dated archaeological samples, per 100 year bin. 10,000 to 3,500 cal. BP

S5. Choice of variogram model and kriging interpolated Neolithic surface

The choice of variogram fitted model to inform the kriging interpolated Neolithic surface was in the first instance based on the model standard error.

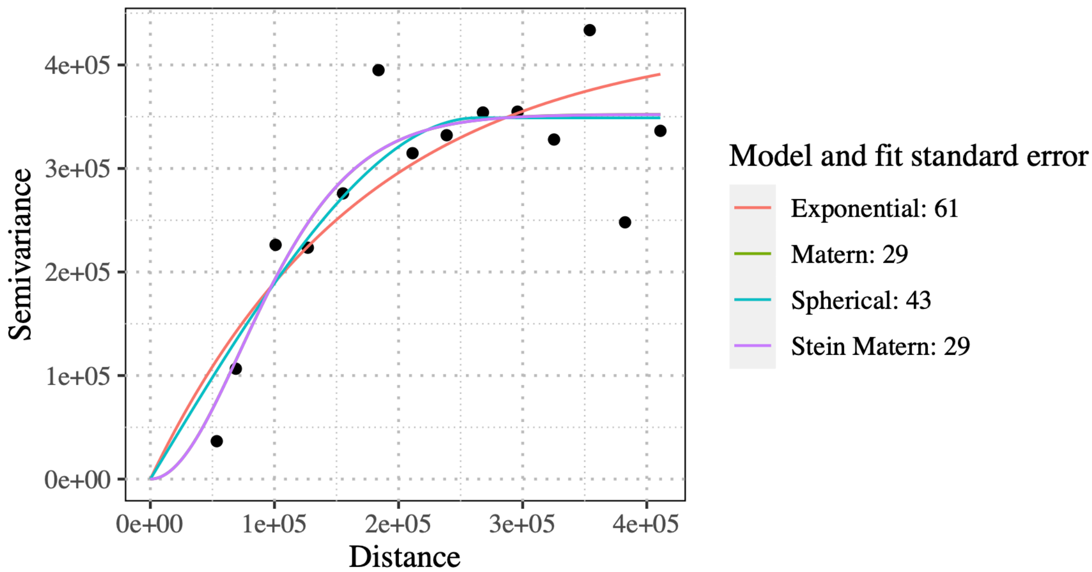

Supplementary Figure 2.5: Variogram and variogram models associated with the Neolithic radiocarbon dates (N.B. Matern and Stein Matern models overlap)

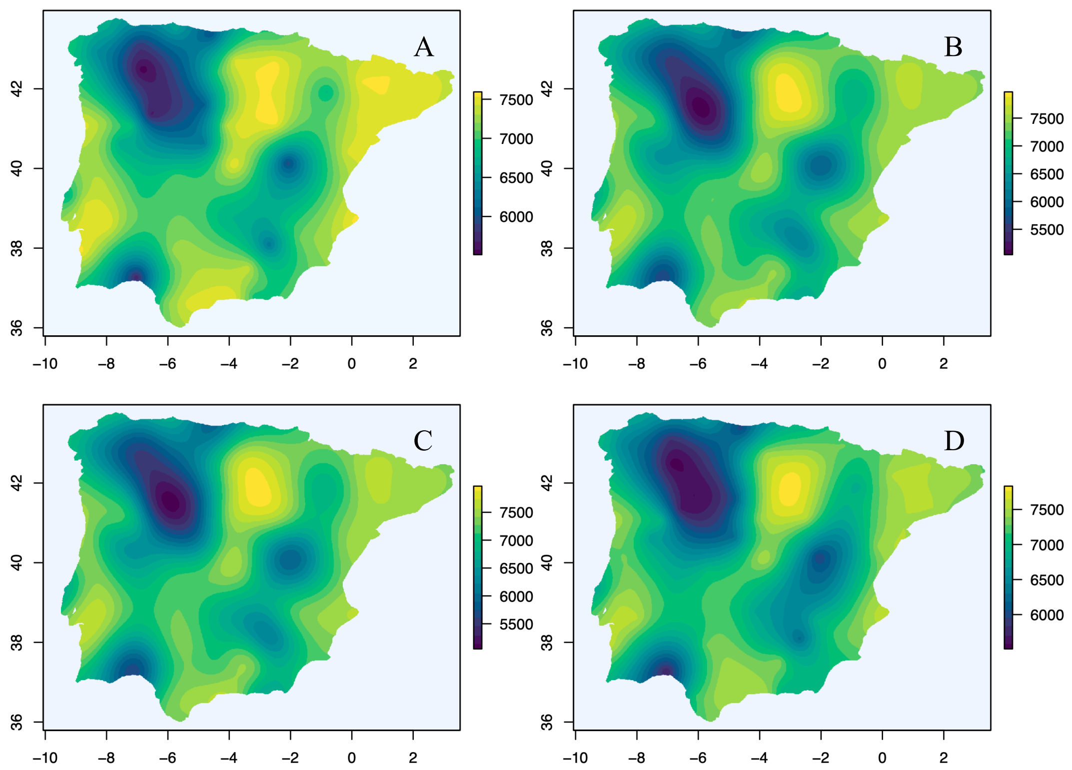

Supplementary Figure 2.6: Kriging interpolated Neolithic surfaces, based on different variogram fitted models: A) Exponential; B) Stein Matern; C) Matern; D) Spherical

However, we applied a further constraint, the earliest accepted date of the Neolithic for Iberia at around 7,600 cal. BP, in choosing the final model. The Exponential model (Sup. Fig. 2.6) was the best model that fulfilled this constraint, although other variogram models had a better fit with the data. The general form of the interpolated surface is relatively consistent irrespective of model specification (Sup. Fig. 2.6).

S6. Influence of the exclusion or inclusion of high elevation sites (>2000m) on charcoal z-score composite

The number of archaeological radiocarbon samples above 2000m is very low throughout the 10,000 to 3,500 cal. BP period, making it difficult to assess the potential influence of humans on fire at high elevations. We excluded the four charcoal sites above 2000m (Table 2.1). There is a difference between the z-score of charcoal accumulation based on sites below 2000m and above 2000m (Sup. Fig. 2.7), implying that fire history may be different in upland regions. However, given the limited amount of data, this needs further testing.

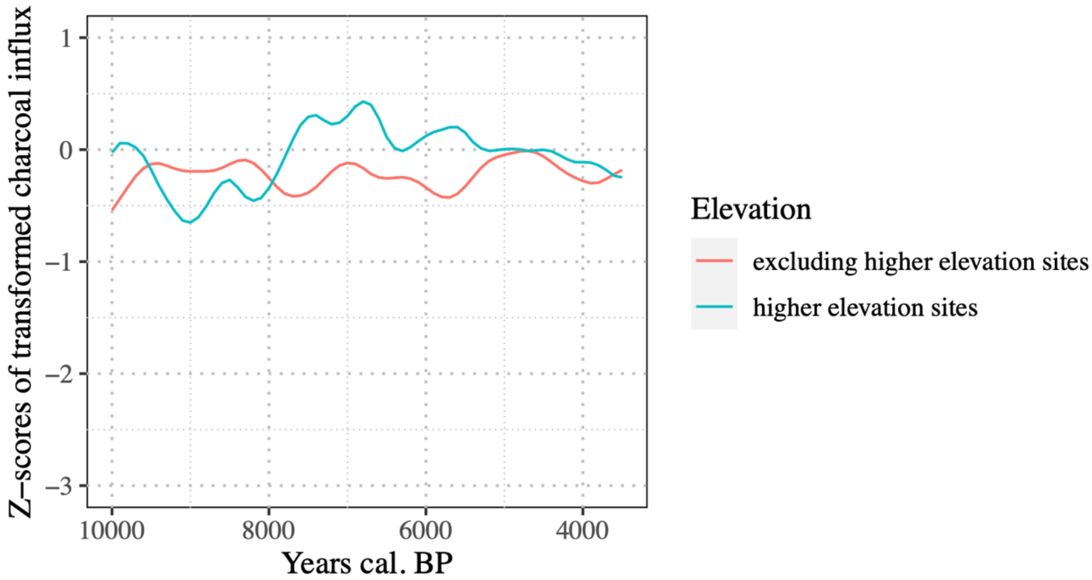

Supplementary Figure 2.7: Z-score composites of charcoal influx for Iberia, 10,000 to 3,500 cal. BP. Curves represent the sites below 2000m (red) or those sites above 2000m (blue)

S7. Number of records contributing to the z-score composite of charcoal influx through time

The number of records that contribute to the z-score composite curve of charcoal influx by 100-year bin generally increases through time (Sup. Fig. 2.8).

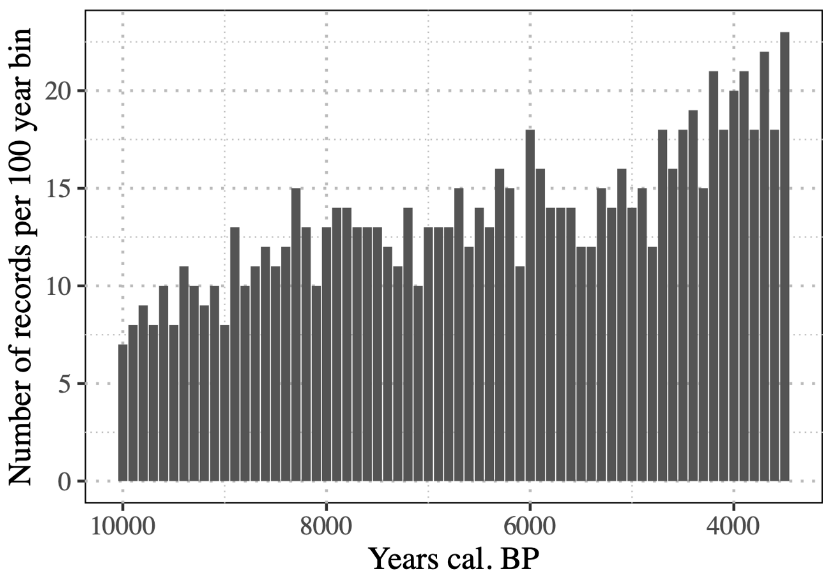

Supplementary Figure 2.8: Number of records contributing to each 100 year bin used in the construction of the z-score composite of charcoal influx, 10,000 to 3,500 cal. BP

S8. Long-term trend in the z-score composite of charcoal influx

Linear regression through the z-score composite of charcoal influx shows that there is a minor increase in fire through time (Sup. Fig. 2.9). By taking the differences between these predicted values to the actual z-score values, variation in charcoal influx excluding this trend can be seen (Sup. Fig. 2.10). The magnitude of the trend and the magnitude of the variation in the composite are comparable.

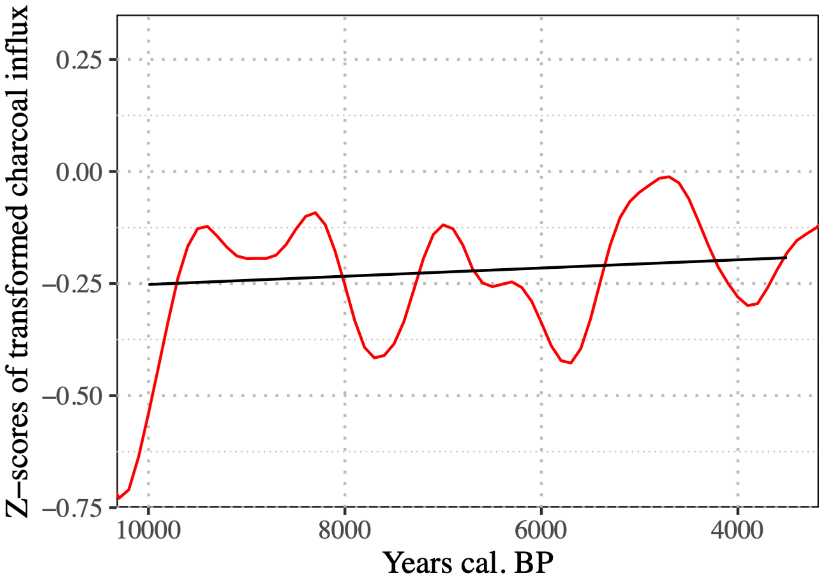

Supplementary Figure 2.9: Z-score composite of charcoal influx for Iberia, 10,000 to 3,500 cal. BP (red) and fitted linear model representing longer-term trend in fire (black)

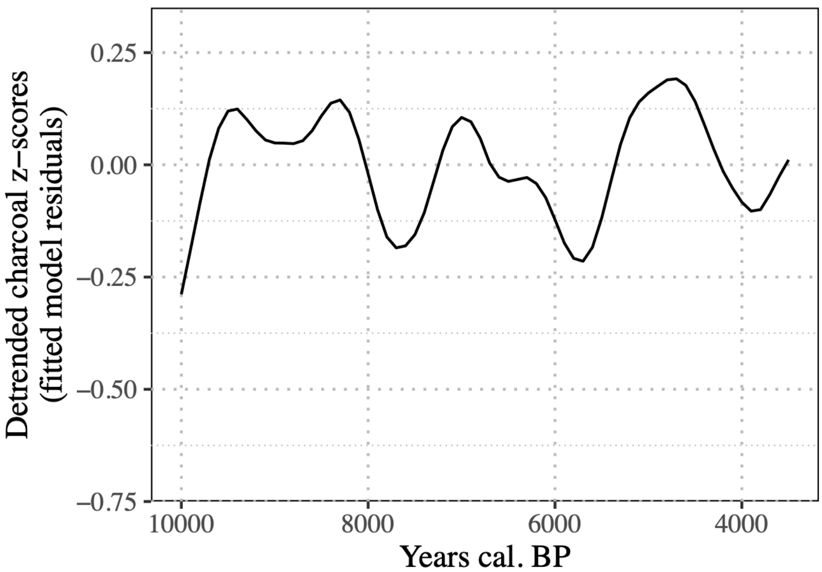

Supplementary Figure 2.10: Detrended z-score composite of charcoal influx for Iberia, 10,000 to 3,500 cal. BP

S9. Implications of exponential compared to logistic model choice in SPD null model selection

The p value for the fit of the exponential or logistic null model associated with SPD data was similar, with the logistic model having a slightly improved fit (p value 0.001 compared to 0.003). However, the choice of a logistic model has more theoretical implications than that of an exponential model, requiring specification of a density dependent maximum. Additionally, as our focus was on deviations from longer-term population change, rather than deviations associated with growth towards a specified population maximum, we used an exponential model. In practice, the specification of key growth periods as shown by periods when the SPD was greater than the envelope of Monte Carlo generated fitted models is very similar irrespective of the model (Sup. Fig. 2.11: A and B). The first period(s) of rapid growth is at the beginning of the record, although this is likely to be an artefact of limited data. The second period of rapid growth based on the exponential model, between ca. 7,400 and ca. 6,880 cal. BP, is almost exactly mirrored with the logistic model as being between ca. 7,410 and ca. 6,830 cal. BP. The subsequent periods of decline in population as identified by the exponential model are likewise identified based on logistic growth, although the periods are longer and wider than in the exponential model. The next period of high population growth identified in the exponential model at ca. 4,750 until ca. 4,460 cal. BP is again mirrored with the logistic model at ca. 4,780 to ca. 4,420 cal. BP. The main difference between the models in the identification of significant periods of change occurs at the end of the record, where a period of decline is indicated by the exponential model but is a period of increase based on the logistic model fit. However, this difference is a function of the logistic model specification. When comparing the exponential and logistic models for the rate of change for the SPD, more differences are apparent (Sup. Fig. 2.11: C and D). There is a significant difference between the rate of change in the SPD and the logistic model at ca. 7,460 cal. BP, which is broadly in line with the significant growth identified with the SPD curve in both the exponential and logistic models. However, the significant increase in the rate of growth in the exponential model from ca. 5,370 to ca. 5,170 cal. BP is also broadly identified in the logistic model between ca. 5,390 and ca. 5,150 cal. BP.

Thus, although there are minor differences in the dates identified as key growth periods between the two models, the importance of the precision of the dates is limited for the comparison with the charcoal z-score composite (see S11).

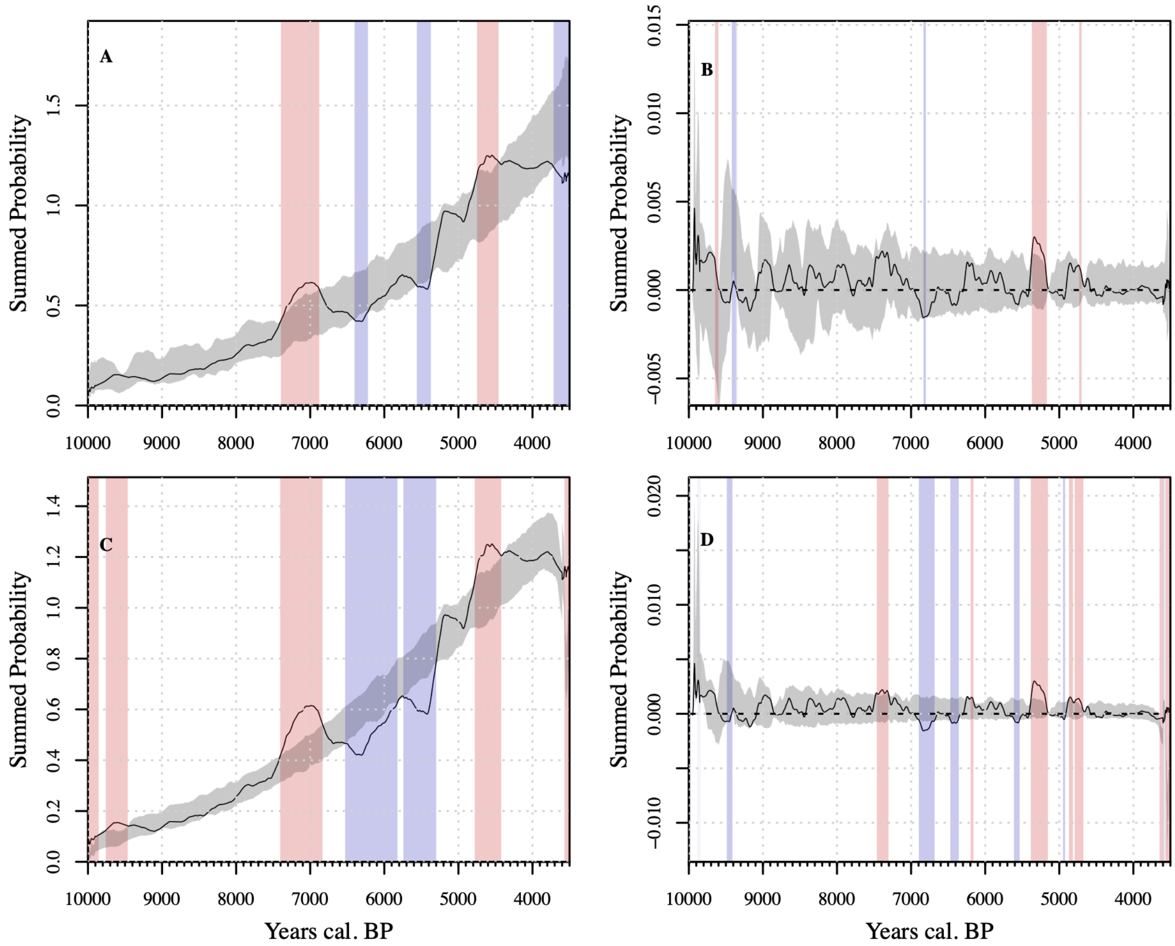

Supplementary Figure 2.11: (A) Summed probability distribution and exponential null model for Iberia (10 – 3.5k cal. BP.) (B) Summed probability distribution rate of change and exponential null model for Iberia (10 – 3.5k cal. BP.); (C) Summed probability distribution and logistic null model for Iberia (10 – 3.5k cal. BP.) (D) Summed probability distribution rate of change and logistic null model for Iberia (10 – 3.5k cal. BP.) Deviations from simulated growth models are shown in red and blue

S10. Detrending the superposed epoch analysis of charcoal z-score composite

To test whether a longer-term trend in the superposed epoch analysis of charcoal z-score composite might influence the potential relationship between key growth periods in population and fire history, we fitted a simple linear regression to the composite curve and extracted the residuals (Sup. Fig. 2.12). As shown, and in common with Figure 5, the detrended analysis shows that fire was increasing ca. 275 years before the intervals of rapid population growth and this increase persists until around ca. 275 after these intervals.

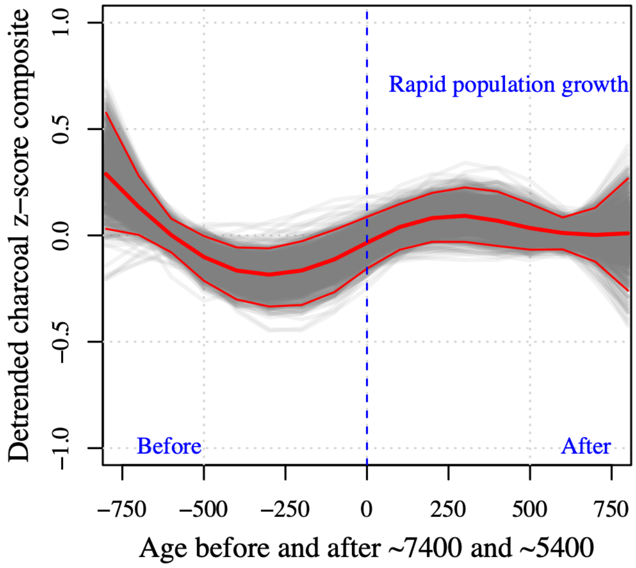

Supplementary Figure 2.12: Superposed epoch analysis of detrended z-score composite of charcoal influx for Iberia, with dates aligned before and after SPD key growth periods at 7,383 and 5,371 cal. BP. Grey lines indicate 1000 bootstrap re-samples of records, with replacement. The solid red lines shows the median z-score values, and the fine red lines are the 95% confidence intervals.

S11. Superposed epoch analysis of charcoal z-score composite with randomly adjusted "key population growth dates"

To test the importance of the precise dates identified as the start of rapid population growth, these "epoch" dates were randomly varied by ± 200 years and a charcoal z-score composite recalculated 1000 times. The 95% confidence intervals of these re-runs (Sup. Fig. 2.13) show that there is limited correspondence between the start of periods of higher population growth and changes in fire, even taking this dating uncertainty into account.

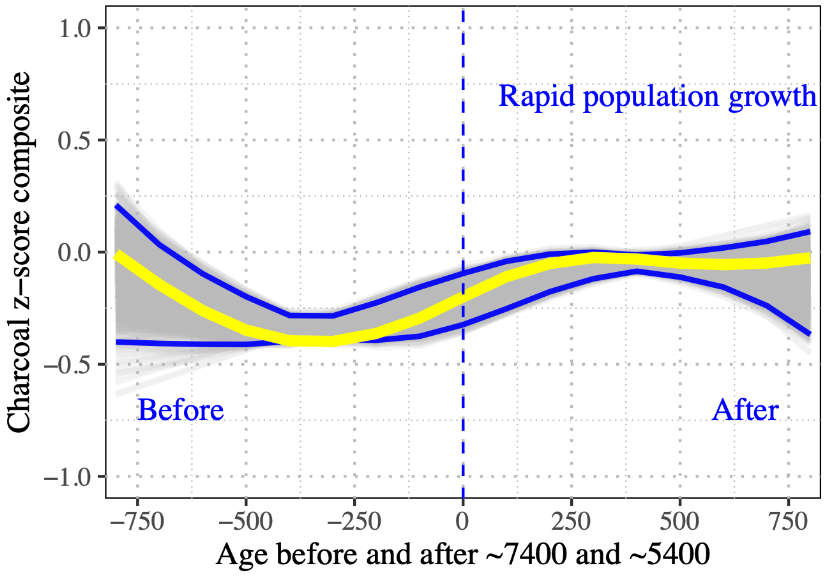

Supplementary Figure 2.13: Superposed epoch analysis of z-score composite of charcoal influx for Iberia, with dates adjusted before and after SPD key growth periods at 7,395 and 5,369 cal. BP. Grey lines indicate 1000 re-runs of the SEA with randomly adjusted key growth periods

S12. Superposed epoch analysis of charcoal z-score composites using AutoRegressive Integrated Moving Average (ARIMA) analysis

To test the influence of the periods of rapid population growth on the SEA charcoal z-score composite, we forecasted the shape of the curve based on trained ARIMA modelling and compared this with the actual composite curve shape (Sup. Fig. 2.14). There is limited variation in the curve compared to the forecasted curve shape (ARIMA model type (1,2,0)), indicating that there is no significant deviation for the subsequent 200 years following the epoch dates.

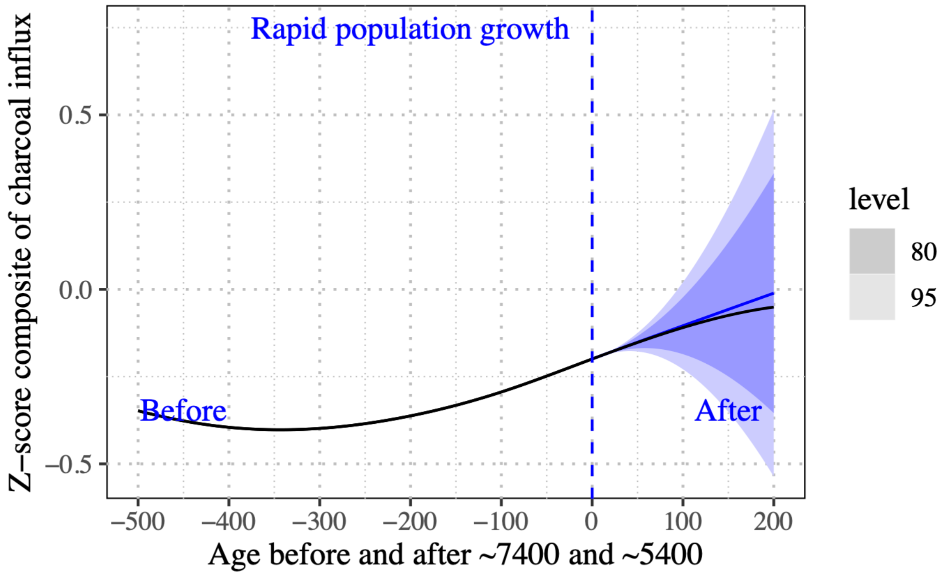

Supplementary Figure 2.14: Superposed epoch analysis of z-score composite of charcoal influx for Iberia, with dates adjusted before and after SPD key growth periods at 7,395 and 5,369 cal. BP. ARIMA model forecast post-epoch dates in blue, with forecast confidence intervals shown

S13. Detrending the Neolithic charcoal z-score composite

To test whether a longer-term trend in the generated Neolithic charcoal z-score composite might influence the potential relationship between key growth periods in population and fire history, we fitted a simple linear regression to the composite curve and extracted the residuals (Sup. Fig. 2.15). As shown, and in common with Figure 7, the detrended analysis shows that fire was increasing ca. 450 years before the spatially heterogenous spread of agriculture and persisted for 750 years afterwards.

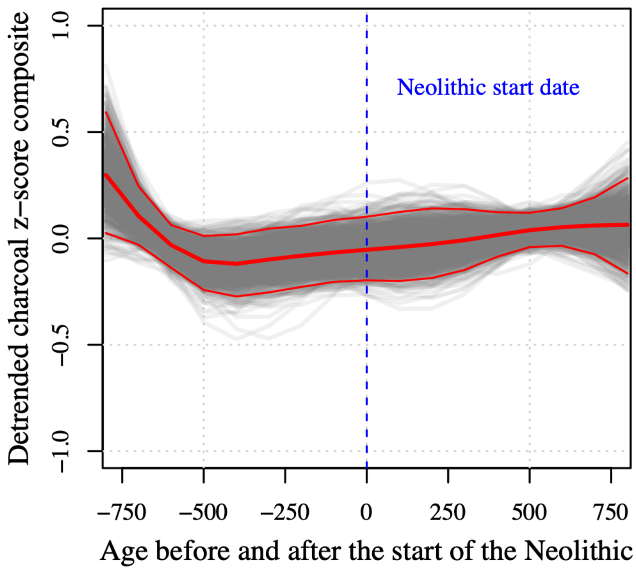

Supplementary Figure 2.15: Superposed epoch analysis of detrended z-score composite of charcoal influx for Iberia, based on spatially heterogenous dates relative to the start of the Neolithic across Iberia. Grey lines indicate 1000 bootstrap re-samples of core sites, with replacement. The solid red line shows the median z-score values, and the fine red lines are the 95% confidence intervals

S14. Neolithic charcoal z-score composite with randomly adjusted radiocarbon Neolithic dates

To test the robustness of the Neolithic charcoal z-score composite analysis to small changes in the interpolated Neolithic surface, we randomly adjusted the calibrated dates of the Neolithic archaeological data by ±200 years, re-constructed the associated variogram and variogram models and re-interpolated the Neolithic surface using kriging. We re-ran these adjusted calibrated dates 1000 times, and each time re-constructed the Neolithic charcoal z-score composite based on the adjusted Neolithic surface. The 95% confidence intervals were calculated based on these 1000 re-runs of this analysis and plotted together with the original composite curve (Sup. Fig. 2.16). The upper and lower bound Neolithic z-score composites share a very similar shape to the original curve, indicating that precise specification of the Neolithic surface does not influence these results.

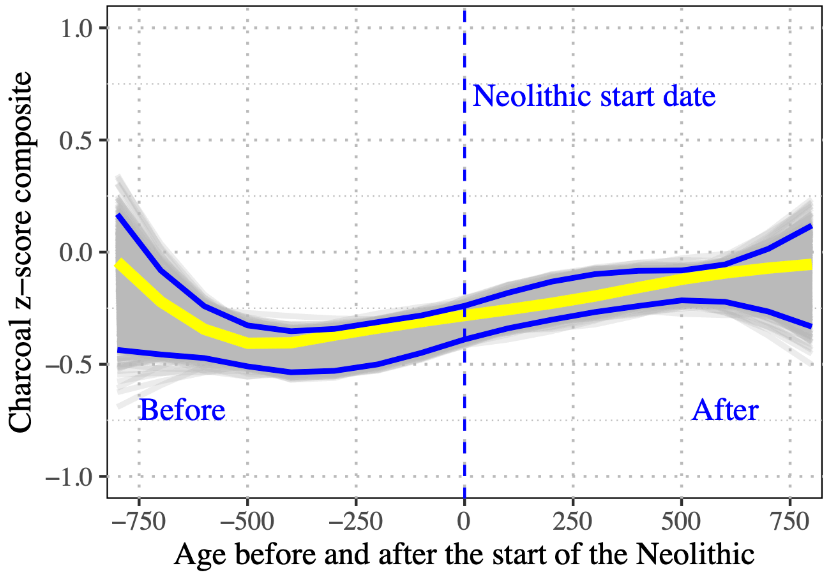

Supplementary Figure 2.16: Neolithic detrended z-score composite of charcoal influx for Iberia, based on spatially heterogenous dates relative to the start of the Neolithic across Iberia. The yellow line represents the detrended adjusted composite; grey lines represent alternative detrended adjusted composites based on randomised changes to the Neolithic interpolation; blue lines represent 95% confidence intervals of the detrended adjusted composite

S15. Neolithic charcoal z-score composite ARIMA analysis

Intervention analysis based on ARIMA modelling of the Neolithic z-score composite curve was used to assess whether the initial impact of the Neolithic could be seen in the fire record. Comparison of the post-Neolithic charcoal z-score composite (ARIMA model type (1, 2, 0)) and the actual shape of the Neolithic charcoal z-score composite shows very little difference for the 200-years following the Neolithic (Sup. Fig. 2.17).

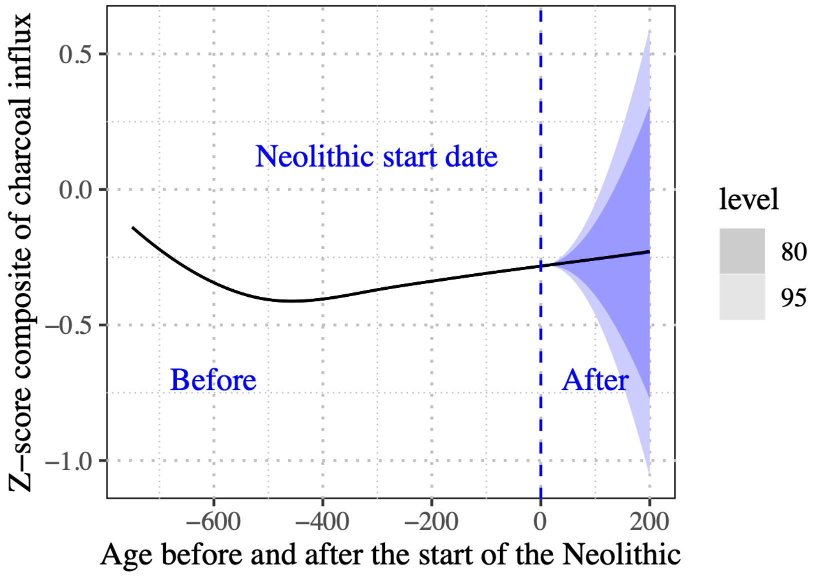

Supplementary Figure 2.17: Neolithic z-score composite of charcoal influx for Iberia, based on spatially heterogenous dates relative to the start of the Neolithic across Iberia. ARIMA model forecast post-Neolithic dates overlayed by actual influx, with forecast confidence intervals shown

S16. Charcoal influx through time of utilised Iberian records

Analysis of regional fire history through time was based on 32 charcoal records. The following figures (Sup. Fig. 2.18, Sup. Fig. 2.19, Sup. Fig. 2.20 and Sup. Fig. 2.21) show the charcoal influx associated with each record through time.

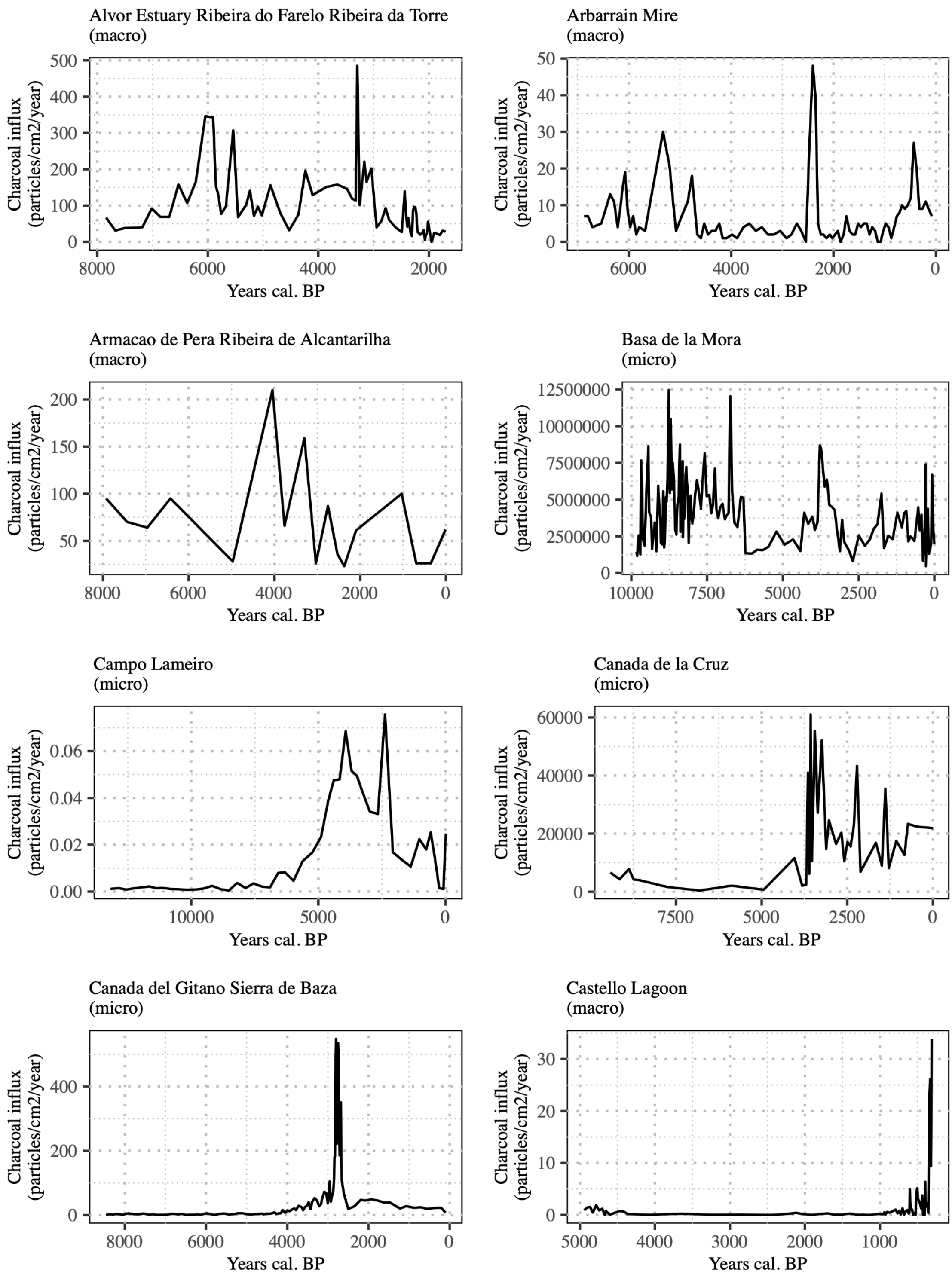

Supplementary Figure 2.18: Charcoal influx associated with records included within the analysis of fire history for Iberia; complete record shown, with macro or micro charcoal type indicated. Records 1-8 of 32

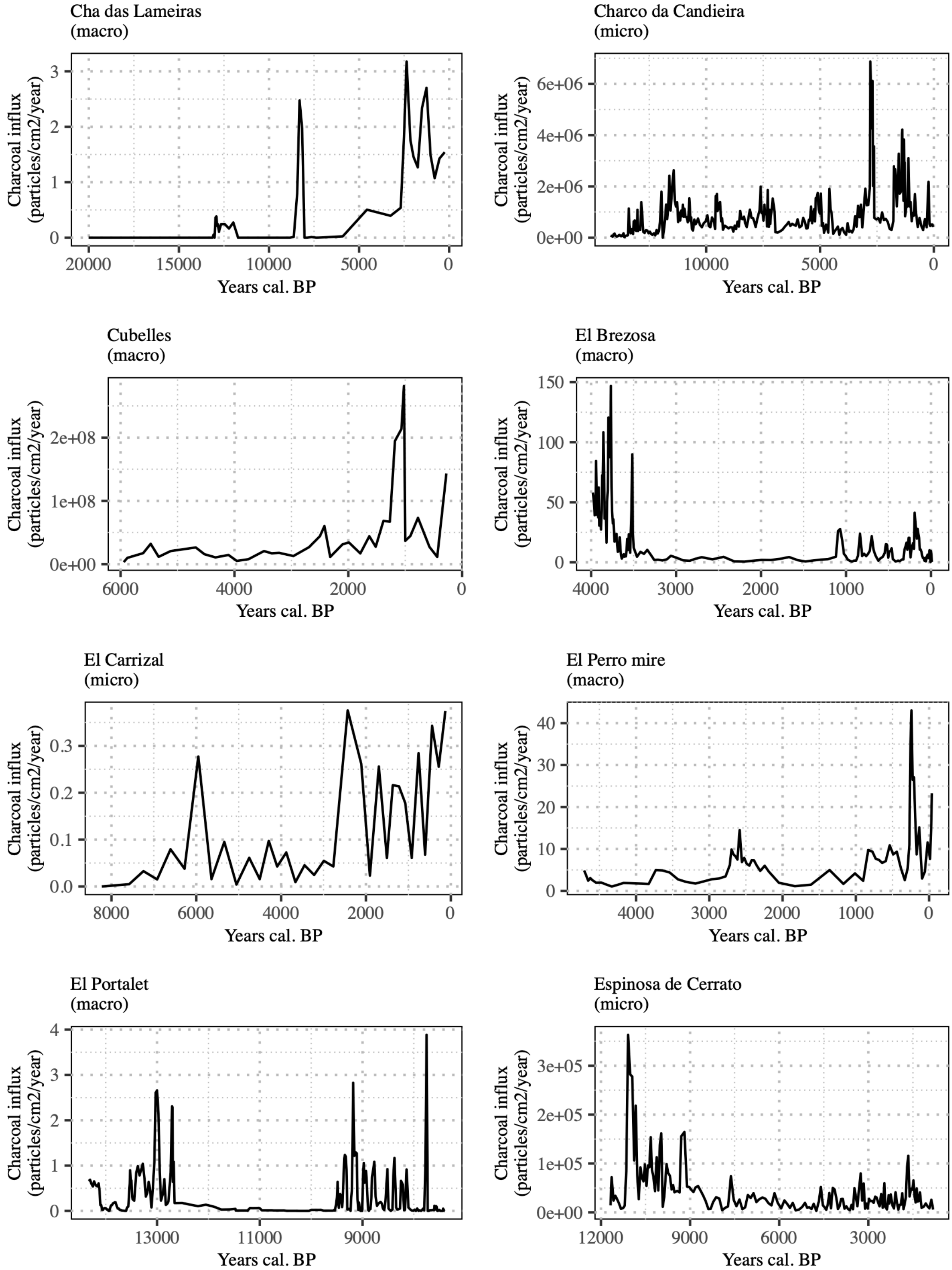

Supplementary Figure 2.19: Charcoal influx associated with records included within the analysis of fire history for Iberia; complete record shown, with macro or micro charcoal type indicated. Records 9-16 of 32

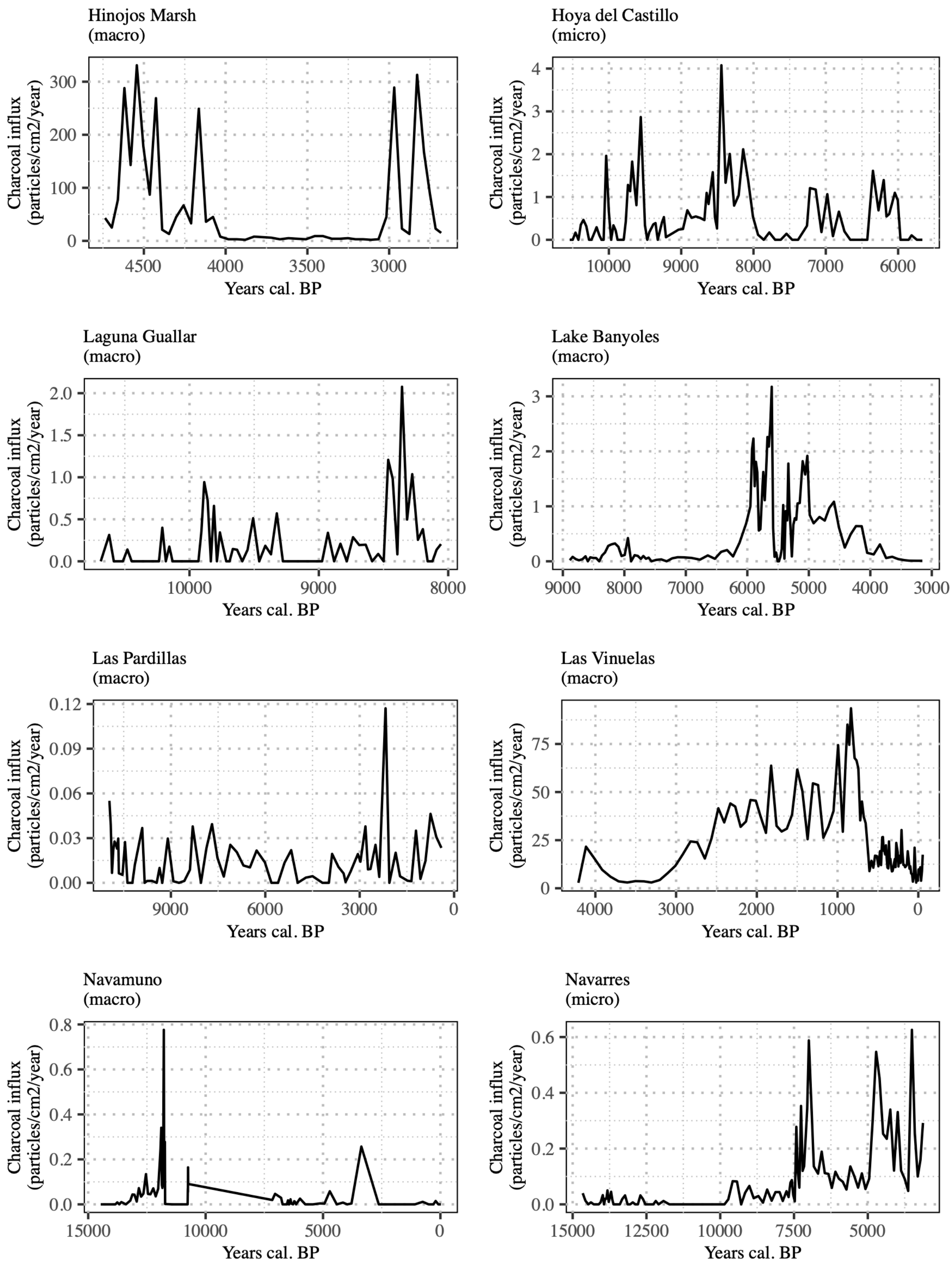

Supplementary Figure 2.20: Charcoal influx associated with records included within the analysis of fire history for Iberia; complete record shown, with macro or micro charcoal type indicated. Records 17-24 of 32

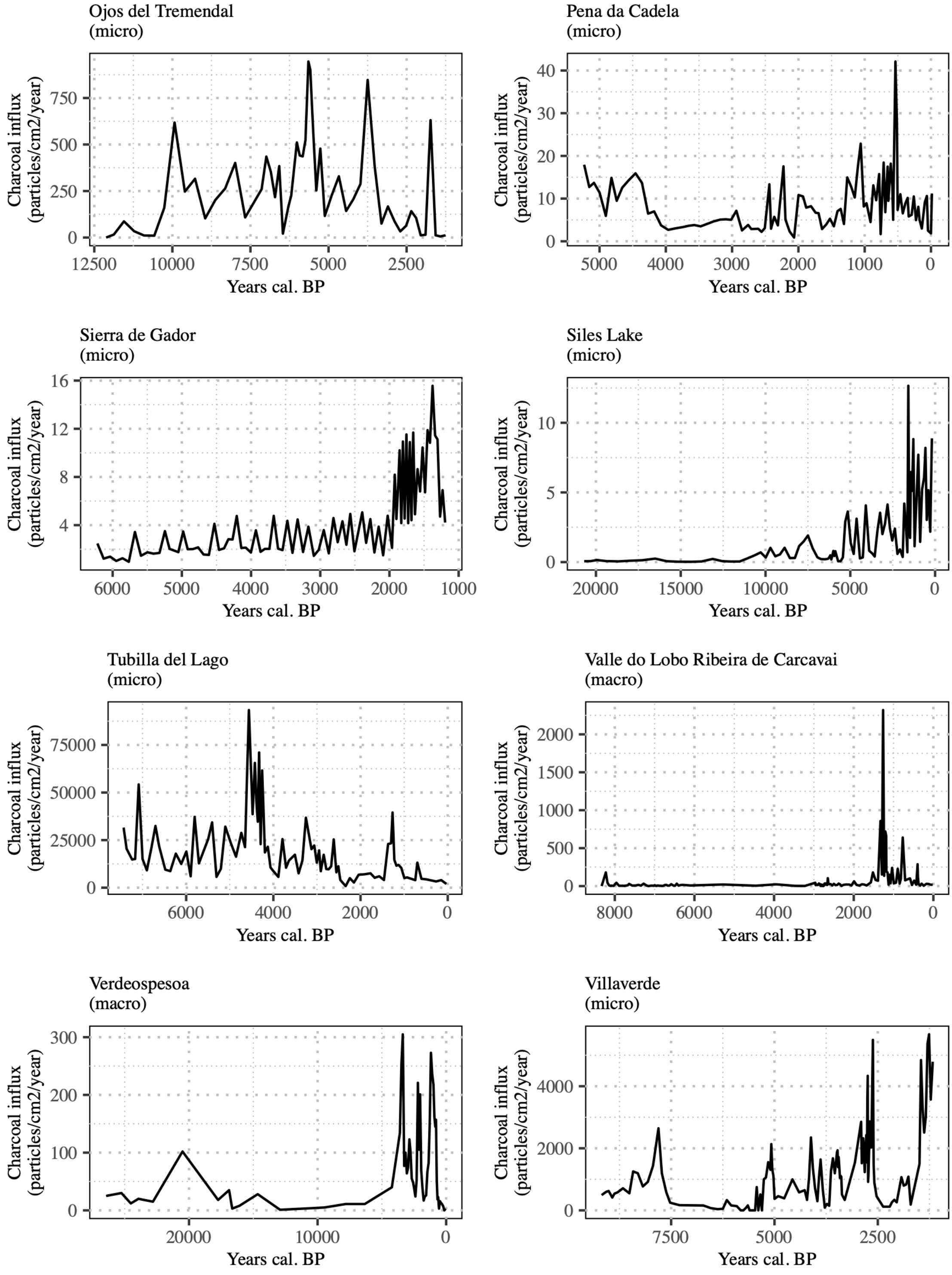

Supplementary Figure 2.21: Charcoal influx associated with records included within the analysis of fire history for Iberia; complete record shown, with macro or micro charcoal type indicated. Records 25-32 of 32

2.9.1. Supplement references

Power, M.J., Marlon, J.R., Ortiz, N., Bartlein, P.J., Harrison, S.P., Mayle, F.E., Ballouche, A., Bradshaw, R.H.W., Carcaillet, C., Cordova, C., Mooney, S., Moreno, P.I., Prentice, I.C., Thonicke, K., Tinner, W., Whitlock, C., Zhang, Y., Zhao, Y., Ali, A.A., Anderson, R.S., Beer, R., Behling, H., Briles, C., Brown, K.J., Brunelle, A., Bush, M., Camill, P., Chu, G.Q., Clark, J., Colombaroli, D., Connor, S., Daniau, A.-L., Daniels, M., Dodson, J., Doughty, E., Edwards, M.E., Finsinger, W., Foster, D., Frechette, J., Gaillard, M.-J., Gavin, D.G., Gobet, E., Haberle, S., Hallett, D.J., Higuera, P., Hope, G., Horn, S., Inoue, J., Kaltenrieder, P., Kennedy, L., Kong, Z.C., Larsen, C., Long, C.J., Lynch, J., Lynch, E.A., McGlone, M., Meeks, S., Mensing, S., Meyer, G., Minckley, T., Mohr, J., Nelson, D.M., New, J., Newnham, R., Noti, R., Oswald, W., Pierce, J., Richard, P.J.H., Rowe, C., Sanchez Goñi, M.F., Shuman, B.N., Takahara, H., Toney, J., Turney, C., Urrego-Sanchez, D.H., Umbanhowar, C., Vandergoes, M., Vannière, B., Vescovi, E., Walsh, M., Wang, X., Williams, N., Wilmshurst, J., Zhang, J.H., 2008. Changes in fire regimes since the Last Glacial Maximum: an assessment based on a global synthesis and analysis of charcoal data. Clim. Dyn. 30, 887–907. https://doi.org/10.1007/s00382-007-0334-x

3. European tree cover during the Holocene reconstructed from pollen records

The following chapter is an amended version of a paper submitted to Biogeosciences, and currently under review. The article pre-print, reviewer and community comments, and author responses are available to read online (https://doi.org/10.5194/egusphere-2024-1523). It has been written and referenced in the style guidelines of this journal. The authors were Luke F. Sweeney, Sandy P. Harrison and Marc Vander Linden. The study was designed by all authors. LS carried out the analyses. The first draft of the manuscript was written by LS and SPH, and all authors contributed to the final article. Estimated contributions are LS: 70%, SPH: 20% and MVL: 10%.

3.1. Abstract

Changes in tree cover influence many aspects of the earth system. Recent regional changes in tree cover, as documented by remote-sensed observations, are insufficient to capture the response to large climate changes or to differentiate the impacts of human activities from natural drivers. Pollen records provide an opportunity to examine the causes of changes in tree cover in response to large climate changes in the past and during periods when human influence was less important than today. Here we reconstruct changes in tree cover in Europe through the Holocene using fossil pollen records, using the modelled relationship between observed modern tree cover and modern pollen samples. At a pan-European scale, tree cover is low at the beginning of the Holocene but increases rapidly during the early Holocene and is maximal at ca. 6,500 cal. BP, after which tree cover declines to present-day levels. The rapidity of the post-glacial increase in tree cover and the timing and length of maximum tree cover varies regionally, reflecting differences in climate trajectories during the early and mid-Holocene. The nature of the subsequent reduction in tree cover also varies, which may be due to differences in climate but may also reflect different degrees of human influence. The reconstructed patterns of change in tree cover are similar to those shown by previous reconstructions, but our approach is relatively simple, only requires readily available data and could therefore be applied to reconstruct tree cover globally.

3.2. Introduction

Tree cover in Europe has been expanding in recent decades (FAO, 2020; Turubanova et al., 2023), with potential implications for land-atmosphere energy exchanges, water and carbon cycles, and ultimately local and global climates (Bonan, 2008; Alkama and Cescatti, 2016). Changes in tree cover may reflect forest or woodland expansion, or the presence of trees in vegetation mosaics and urban settings. Tree cover both affects and is affected by the environment (Moyes et al., 2015; Abis and Brovkin, 2017) and this two-way relationship leads to complex interactions between both. For example, deforestation in the Amazon has been linked to changes in weather patterns, which subsequently affect the moisture available for rainforest maintenance (Staal et al., 2018; Leite-Filho et al., 2020). Similarly, increases in tree cover resulting from farm abandonment has been shown to change fire frequency in the Iberian Peninsula (Moreira et al., 2001; Viedma et al., 2015), which in turn affects vegetation cover and structure and results in further changes to the fire regime. Satellite data can be used to assess the environmental controls on tree cover but, since they only cover the past 20–30 years, are insufficient to look at the response to longer term changes in climate or relationships when the human influence of land-use and vegetation cover was less ubiquitous.

Pollen from sedimentary sequences provides a record of past vegetation changes. The relative abundance of arboreal pollen is commonly used to infer changes in tree abundance at a site (e.g. Hicks, 2001; Kaplan et al., 2016; Adam et al., 2021). The relationship between pollen abundances and vegetation cover is not straightforward however, because it is influenced by differences between species in pollen productivity and transportability, and site characteristics that affect the pollen source area, such as basin size (Bradshaw and Webb, 1985; Prentice and Webb, 1986; Prentice, 1988; Sugita, 1993).

Several different techniques that have been applied to reconstruct regional and sub-regional vegetation in Europe using pollen such as biomization/pseudobiomization (e.g. Fyfe et al., 2015; Binney et al., 2017) or the application of the Modern Analogue Technique using plant functional types (e.g. Davis et al., 2014). Other studies have made reconstructions combining different approaches (e.g. Roberts et al., 2018) and by combining pollen-based reconstructions with simulated potential vegetation (Pirzamanbein et al., 2014). However, the most recent quantitative pan-European pollen-based reconstructions of Holocene vegetation changes have been made using the Regional Estimates of Vegetation Abundance from Large Sites (REVEALS) approach (Sugita, 2007b, a) or the MAT (Overpeck et al., 1985; Guiot, 1990; Jackson and Williams, 2004; Zanon et al. 2018). The REVEALS method calculates regional vegetation cover based on modelled relationships between pollen abundance, estimated differences in species level pollen productivity and pollen transport, and differences in site characteristics. Initially used at individual sites or small regions (e.g. Gaillard et al., 2010; Nielsen et al., 2012; Marquer et al., 2014), REVEALS was first applied at a pan-European scale by Trondman et al. (2015) and later extended with additional sites, taxa and an improved temporal resolution by Githumbi et al. (2022). The most recent analysis by Serge et al. (2023), is based on 1607 records for 500-year intervals before 700 cal. BP and for the subsequent intervals of 700–350 cal. BP, 350–100 cal. BP and 100 cal. BP– present. They tested the impact of including 15 additional taxa (total n=46) on the vegetation reconstructions, producing maps of landcover and species abundance at record-containing 1º grid cells. In contrast, the MAT approach reconstructs past vegetation based on identifying modern analogues of fossil pollen assemblages, on the assumption that samples found in the fossil record that share a similar composition to those found in present-day pollen assemblages will have similar vegetation. Zanon et al. (2018) applied the MAT to 2,526 individual fossil pollen samples from Europe to generate interpolated maps at 250-year intervals at 5 arc-minute resolution through the Holocene.

Each of these approaches presents challenges. The REVEALS approach requires, and is sensitive to, estimates of relative pollen productivity (RPP) and pollen fall speeds (FS) for individual species (Bunting and Farrell, 2022; Githumbi et al., 2022; Serge et al., 2023). Landscape-level reconstructions are problematic if RPP information is not available for relatively common taxa (Harrison et al., 2020). RPP values have been estimated for common taxa in Europe and China, and there are a limited number of studies from North America (see e.g. Wieczorek and Herzschuh, 2020). Studies have been conducted for some ecosystems in South America and Africa, but these only provide RPPs for a very limited number of taxa (e.g. Duffin & Bunting, 2008; Whitney et al, 2018; Gaillard et al., 2021; Hill et al., 2021; Tabares et al., 2021; Piraquive Bermúdez et al., 2022) and even this level of information is not readily available for other regions. The MAT technique requires a large modern pollen data set for training purposes, but such data sets are now available for all regions of the world. However, the application of the MAT involves a number of arbitrary decisions including the choice of analogue threshold (i.e. how similar modern and fossil assemblages must be to be considered analogous), and the number of analogues used (Jackson and Williams, 2004). Techniques designed to minimise the number of samples for which no analogues are found, such as grouping species into plant functional types (PFTs) (see Davis et al., 2003), introduce further uncertainties since the allocation of pollen taxa to PFTs is often ambiguous (Zanon et al., 2018).

In this paper, we develop a simple calibration approach to derive estimates of tree cover at individual sites across Europe, capitalising on an extensive modern pollen data set, new remote-sensed data on tree cover, harmonised age models, and improved information about basin size for fossil records from Europe. We evaluate how well this method reconstructs modern tree cover compared to existing methods. We then reconstruct pan-European changes in tree cover through the Holocene and compare these reconstructions with existing reconstructions.

3.3. Methods

Tree cover during the Holocene was reconstructed by applying a statistical model describing modern tree cover to fossil pollen records from individual sites. There were three steps: 1) selection and treatment of data; 2) development of the predictive model relating modern pollen data to modern tree cover; and 3) application of this model to fossil pollen records (Fig. 3.1). All analyses were performed using the R Statistical Software (R Core Team, 2022).

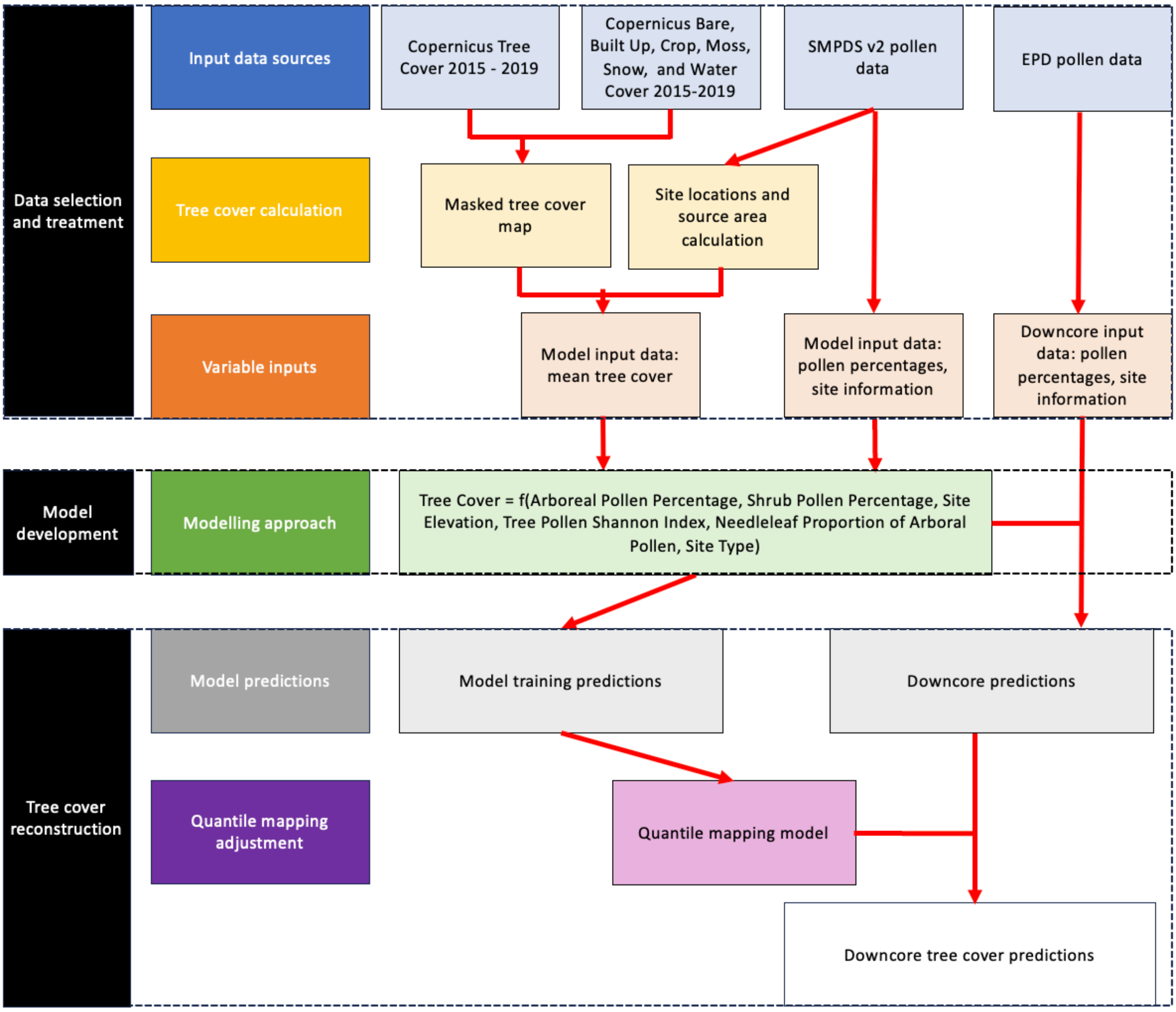

Figure 3.1: Methodology to reconstruct European tree cover during the Holocene

3.3.1. Selection and treatment of data

We used the Copernicus Dynamic Land Cover Dataset to source information on tree cover. This data set provides percentage land cover estimates for individual land-cover classes at a spatial resolution of 100m. We used the land-cover class designated as forest/tree cover, which at this spatial resolution can be regarded as an estimate of actual tree cover. A composite map of modern tree cover for the broadly European region but including the far north of Africa, Turkey and European Russia (12°W to

45°E and 34–73°N) was generated by averaging annual percentage forest/tree cover data from Copernicus annual land cover maps from 2015 to 2019 (Buchhorn et al., 2020a, e, d, c, b), after removing cells dominated (> 50%) by other land-cover classes, including bare ground, built up areas, moss or lichen, permanent water, snow, and crops (Fig. 3.2A). However, the Copernicus maps do not distinguish between natural forests and plantations and so the tree cover target may include planted species. This modern tree cover map has a resolution of 100m.

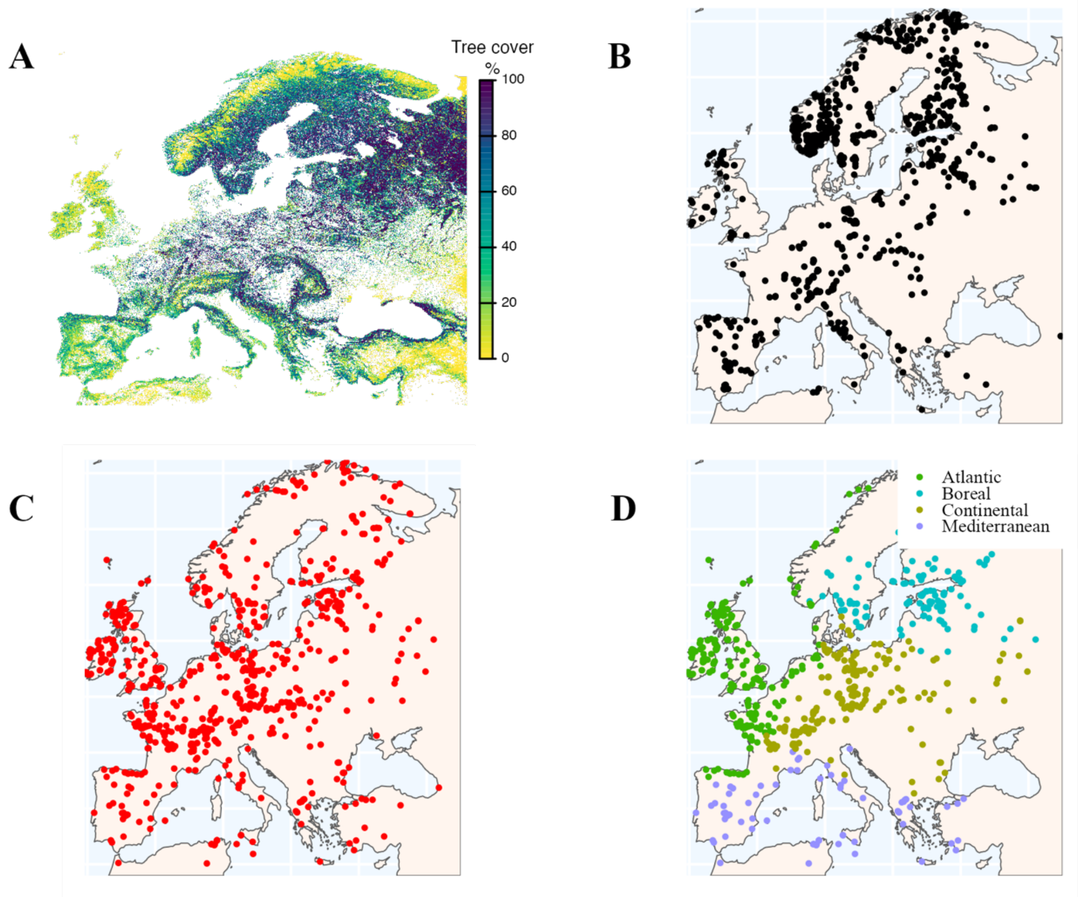

Figure 3.2: A - Observed tree cover based on compositing annual tree cover maps from the Copernicus land cover data sets (2015-2019) and screening out of cells where the dominant land cover was bare ground, built up areas, moss or lichen, permanent water, snow, or crops; B - Modern pollen records used for model fitting; C - Fossil pollen sites used for tree cover reconstructions; D - Classification of the fossil pollen sites into climatic sub-regions

Modern pollen data (Fig. 3.2B) was obtained from version 2 of the SPECIAL Modern Pollen Dataset (Villegas-Diaz and Harrison, 2022). This dataset was created from multiple different published regional datasets, from data repositories (Neotoma, PANGAEA) or directly from data collectors/authors (see *3.9. Supplement: S1* for sources and citations) but employs a standardised taxonomy, and includes improvements to metadata and age models. The data set was further amended for the current analysis by including updated meta information (see *3.7. Code and data availability*). The SMPDS contains pollen samples from the post-industrial era (post-1850 CE). We extracted samples that were explicitly dated to post-1950 and assumed that all samples characterised as modern but without an explicit age assignment also dated to post-1950 CE. We assume that at the regional scale these samples broadly reflect modern (2015–2019) tree cover values. Site metadata (elevation, site type, basin size) from the SMPDSv2, along with the additional metadata updates, were used as explanatory variables in the tree cover model (see section *3.3.2 Model development*). Depauperate samples with Hill's N2 values (Hill, 1973) of < 2 were excluded, following Wei et al. (2021). Wei et al. (2021) found that low taxa diversity produced unreliable estimates of reconstructed variables, in this case temperature via tolerance weighted partial least squares estimation. Pollen counts from cores with multiple modern samples were averaged to prevent over-sampling. Likewise, where there were multiple cores from the same site, pollen counts were averaged so that there was only a single count from each site. Only samples from lakes and bogs were included, to ensure appropriate pollen source areas could be calculated, and samples gathered via moss polsters or pollen traps were excluded as these generally reflect only the very local pollen rain. However, bog records with a radius ≥ 400m were excluded from the analysis because we included taxa that grow on bog surfaces in our analysis (see below), and the exclusion of large bogs reduces the potential for these to bias the regional vegetation reconstructions. Finally, since upslope pollen transport is known to increase the proportion of non-local pollen at high-elevation sites (Fall, 1992; Ortu et al., 2008, 2010), and the complex topography of mountainous areas also impacts pollen transport (Markgraf, 1980; Bunting et al., 2008; Marquer et al., 2020; Wörl et al., 2022), we excluded 236 site records above 1000m. To test the effect of the inclusion of bog sites and the restriction on site elevation, we ran two alternative models excluding bogs and including high elevation sites, and examined summary statistics for each.

The percentage of arboreal pollen (AP%) and shrub pollen (SP%) were calculated based on the Total Terrestrial Pollen Sum (TTPS), and allocation of species into AP/SP or herbaceous (e.g. grass/ herb) pollen types in Europe (see *3.9. Supplement: S2* and *3.7. Code and data availability*). The pollen data were also used to calculate both the needleleaf share of the AP (%needleleaf), and the Shannon Index (SI) of tree species diversity. Species identified as not native to Europe, obligate aquatics and cereals were excluded from the TTPS, but Cyperaceae, Polypodiales and Ericaceae were included as characteristic of more open environments and to prevent the pollen assemblages from these environments being dominated by pollen transported from long distances.

The source area for each record, and hence the appropriate area for the calculation of mean tree cover, was calculated using Prentice's (1985) source area formula for 70% of pollen, and lake or bog area from the SMPDS, noting that the original formula makes no distinction for different site types. The original source area formula used species-specific FS values but, since these were not available for all the taxa used in our analysis, here we used the median FS (0.03) from Githumbi et al. (2022) and Serge et al. (2023) since the tree cover map represents the broad species community around each record location. We assumed basin areas were circular to calculate the radius. For those sites that have no exact information on basin size but were categorised as small (0.1–1km^2), we assumed basin areas of 0.5km^2: there were 30 such sites included in the model construction. Source area radii varied in size from 5,026km to 418,894km for the largest lake, with a median of 28,316km. Mean tree cover was calculated for each site from the tree cover map using the R package *exactextractr (*function*: exact_extract)* (Baston, 2023). There were 263 records where more than half of the contributing grid cells were masked as land-cover classes other than vegetation; these were excluded from the model construction. A total of 852 pollen records were included in the final model training dataset, of which 133 were bog records.

Fossil pollen data were obtained from the SPECIAL-EPD dataset (Harrison et al., 2024), a database of pollen records from Europe, the Middle East and western Eurasia. It builds on a pollen compilation covering the Middle East (EMBSecBIO database: Cordova et al., 2009; Harrison and Marinova, 2017; Marinova et al., 2017; Harrison et al., 2021), data available from public data repositories (NEOTOMA: https://www.neotomadb.org/; PANGAEA: https://www.pangaea.de/) and data provided by the original authors for the Iberian Peninsula (Liu et al., 2023) and other regions. The SPECIAL-EPD dataset includes 1,758 records from 1573 sites, with BACON Bayesian age models, based on the recalibration of radiocarbon ages using INTCAL2020 (Reimer et al., 2020) or Marine20 (Heaton et al., 2020) calibration curve as appropriate, provided for all the records using the *rbacon* R package (Blaauw et al., 2021) in the *ageR* R package (Villegas-Diaz et al., 2021) (for further information see Harrison et al, 2024).We filtered the fossil data in the same way as the modern pollen data, by only using pollen records from lakes and bogs below 1000m in the region 12°W to 45°E and 34-73°N. Where there were multiple records from the same site, we selected a single record, prioritising the record with the maximum number of samples for the period 12,000 cal. BP to present (Fig. 3.2C). The pollen counts were used to calculate AP% and SP%, %needleleaf, and the tree SI, using the species categorisation applied to the modern pollen data (see *3.9. Supplement: S2* and *3.7. Code and data availability*).

3.3.2. Model development

A Beta regression, which is suitable for use with proportional data, was used to model tree cover using the R package *betareg* (Cribari-Neto and Zeileis, 2010). The explanatory variables included AP%, SP%, %needleleaf, site elevation, site type (lake or bog) and arboreal pollen SI values. The AP% and SP% are expected to explain most of the variability in tree cover, but %needleleaf was also included to reflect potential broad differences in pollen productivity and transport between needleleaf and broadleaf species (see Table 1 from Serge et al., 2023). Although records above 1000m were excluded from the data set, site elevation was included as an explanatory variable to capture any residual impacts of elevation on tree cover. Site type (bog, lake) was included because there is a greater potential for pollen mixing prior to sedimentation in lake settings, which means that lakes may be more representative of the regional tree cover (Sugita, 1993; Githumbi et al., 2022). SI was included because species diversity may reflect a more stable (Jactel et al., 2017) or less fragmented landscape (Hill and Curran, 2003). The final model was selected based on the Akaike Information Criteria (AIC: Akaike, 1974) and Cox-Snell R^2 value (Cox and Snell, 1989). We tested the inclusion of interaction effects associated with elevation, since the relationship between AP% and tree cover may be directly influenced by elevation due to upslope transport. In addition, given the potential importance of both RPP and transport, and landscape fragmentation, we tested the inclusion of second and third order polynomial coefficients for %needleleaf and SI. Finally, as Beta regression allows explicit modelling of the precision parameter as well as the mean (i.e. variance does not need to be consistent across observations) (see Simas et al., 2010), we tested the inclusion of regressors describing precision.

The modern tree cover model was tested based on leave one out cross validation (LOOCV), and calculation of root mean squared error (RMSE), mean absolute error (MAE) and R^2 correlation between observed and predicted values. A quantile mapping adjustment, using the R package *qmap* (Gudmundsson et al., 2012) was calculated on the LOOCV model predictions to account for compression of the reconstructions, with overestimation of low tree cover and underestimation of high tree cover values, following Zanon et al. (2018). This decompression was then used to adjust downcore reconstructions generated from the Beta regression.

The final predictions were compared to modern reconstructions of tree cover by Serge et al. (2023) and Zanon et al. (2018), where modern is the interval 100 cal. BP and the present day in Serge et al. (2023) and between 125 cal. BP and present for Zanon et al. (2018). We make comparisons to the Serge et al. (2023) reconstructions based on the 31 taxa originally used by Githumbi et al. (2022) since Serge et al. (2023) show that this produces better results than using the expanded data set of 46 taxa.

For each of the 1° grid cells in Serge et al. (2023), tree cover was calculated from the sum of the appropriate vegetation types. Time series of the change in median tree cover were constructed using median tree cover corresponding to the pollen source area of each of our individual modern reconstructions. As the Serge et al. (2023) and Zanon et al. (2018) data is available in gridded format, comparison with our site-based predictions is not straightforward. Where the site location source areas straddled multiple grid cells, a median was calculated, weighted by the proportion of grid cell coverage using R package *exactextractr (*function*: exact_extract)* (Baston, 2023). The tree cover time series for the Zanon et al. (2018) and Serge et al. (2023) data were initially constructed using all of the extracted tree cover values for each of our model training site locations. However, since there can be multiple sites within some of these grid cells, we tested whether affected the comparisons by taking an average of extracted tree cover values for locations sharing the same grid cell values from Zanon et al. (2018) or from Serge et al. (2023), and using this to create new time series for these two reconstructions.

3.3.3. Application of model to fossil pollen data

The tree cover model, adjusted to deal with the compression bias, was applied to the variables generated from 811 records from the SPECIAL-EPD with data for part or all of the interval between 12,000 cal. BP and the present day. Since the records cover different time periods and have different temporal resolutions, reconstructed tree cover values were binned in 200-year bins. Standard error estimates for site predictions were calculated through the application of a bootstrapping approach, with 1000 resamples of the model training data used to generate models, and equivalent quantile mapping adjustment, which were then applied to the fossil pollen data. We examined temporal trends in tree cover for the European region as a whole and for modern biogeographical regions as defined by the European Environment Agency (EEA) classification (European Environment Agency, 2016). We also produced maps of tree cover through time for 50km^2 grid cells by averaging reconstructed tree cover across all sites in the same cell. These reconstructions were compared with the Serge et al. (2023) and Zanon et al. (2018) reconstructions of Holocene tree cover. As basin size was not available for all record site locations, we extracted tree cover median values using a general 5km^2 buffer to maximise the number of site comparisons and to prevent edge effects.

3.4. Results

3.4.1. Model fit and validation

The final model has a (Cox-Snell) pseudo-R^2 of 0.60, and LOOCV RMSE of 0.14 and MAE of 0.11, indicating a reasonable fit to the data. Variance inflation factor (VIF) scores are not readily interpretable because of the inclusion of interaction terms, but a version of the model with the same variables but excluding the interaction terms has VIF values < 2 for all the explanatory variables, indicating that there is no multicollinearity and that all the explanatory variables represent independent controls on tree cover. The Cox-Snell R^2 for this final model is 0.54.

There is a positive relationship between tree cover and AP% and a negative relationship between tree cover and SP% (Table 3.1), as expected. However, the strength of each relationship is moderated by elevation, with increasing elevation reducing both the positive effect of AP% and the negative effect of SP% on tree cover. There is a negative correlation between %needleleaf and tree cover, although the significant positive quadratic term for needleleaf suggests this relationship becomes positive at higher abundances of %needleleaf. This negative relationship may be a reflection of longer distance pollen transport of needleleaf species (e.g. *Pinus*) to open environments. As tree cover increases, this may imply an increased diversity of species, including broadleaf species. The positive quadratic term indicates that this relationship becomes positive at higher levels of tree cover, potentially reflecting higher tree cover in boreal needleleaf forests. Increased SI is positively related to tree cover, with the effect decreasing with elevation. However, the negative correlation for the quadratic term for the SI suggests that the relationship has less of an effect on tree cover as SI increases. Again, this relationship may be explained in the context of open environments, where tree species diversity may be limited to species with longer distance pollen transport. Tree species diversity may then increase with tree cover, with the negative quadratic term implying that the highest levels of tree cover are represented by relatively uniform species types. Increased SI is positively related to tree cover, with the effect decreasing with elevation. However, the negative correlation for the quadratic term for the SI suggests that the relationship has less of an effect on tree cover as SI increases. There is no significant relationship between site type and tree cover, but the interaction term between them is significant, with a reduction in the effect of elevation on the likelihood of higher tree cover for lake sites. One possible explanation for this relationship is that the increasing likelihood of longer distance pollen transport with elevation affects bog sites more than lake sites in a relative sense, in that bog sites typically have a smaller source area. The Cox-Snell R^2 value increases slightly to 0.62 (from 0.60) if bogs are excluded from the model (*3.9. Supplement: S3*) but this causes a substantial reduction in spatial and temporal coverage. Conversely, including higher elevation sites (>1000 m) within the model reduces the Cox-Snell R^2 to 0.50 (from 0.60) (*3.9. Supplement: S4*). A likelihood-ratio test of the model with the inclusion of variables for precision against a model with a constant precision parameter shows that there is a significant improvement in the model with variable dispersion. Increases in %needleleaf and SI are associated with increased precision of the tree cover reconstructions, whereas lake sites are generally less variable in terms of tree cover than bog sites.

Table 3.1: Modern tree cover model coefficients

Coefficients (mean model with logit link)	Estimate	Standard Error	P Value
(Intercept)	-5.598	0.437	1.54e-37 ***
Tree pollen %	2.374	0.223	1.56e-26 ***
Shrub pollen %	-3.458	0.630	4.06e-08 ***
Needle share of AP%	-1.317	0.456	0.004 **
Needle share of AP%^2	3.009	0.514	4.80e-09 ***
AP Shannon index	5.091	0.458	1.04e-28 ***
AP Shannon index^2	-1.375	0.138	2.09e-23 ***
Lake or bog site	0.031	0.132	0.815
Elevation	0.003	0.001	0.005 **
AP pollen:elevation interaction	-0.001	0.000	0.003 **
SP pollen:elevation interaction	0.004	0.001	0.001 **
AP Shannon:elevation interaction	-0.004	0.001	2.06e-04 ***
AP Shannon^2:elevation interaction	0.002	0.000	2.10e-06 ***
Lake or bog site:elevation interaction	-0.001	0.000	5.57e-04 ***
Precision submodel (log link; after variable selection^)			
(Intercept)	0.407	0.256	0.112
Needle share of AP%	0.798	0.229	5.05e-4 ***
AP Shannon index	0.840	0.121	4.04e-12 ***
Lake or bog site	0.534	0.126	2.17e-5 ***

Significance codes: 0 = '***'; 0.001 = '**'; 0.01 = '*'; 0.05 = .' 0.1; ' ' = 1

^Only significant (at 5% significance) covariates were included

The influence of each variable on the quality of the statistical model is shown in Table 2, with the change in AIC value based on the removal of each variable. These values include the removal of interaction, polynomial and precision terms associated with each variable as applicable. Although AP and SP might be expected to be the most important explanatory variables, the model only using AP and SP has an AIC value 568 greater than the final model, and Cox-Snell R^2 of only 0.27 (Table 2). Thus, the inclusion of the other variables is important in fitting the final model.

Table 3.2: Change in modern model AIC values and Cox-Snell R^2 model values when excluding specific variables (exclusion includes interactions, polynomials and precision variables) and for a model with only arboreal and shrub pollen percentage

Model	**Δ AIC**	**Cox-Snell R^2**
Final model	0	0.60
excluding AP	165	0.51
excluding SP	31	0.58
excluding %needleshare	121	0.55
excluding AP Shannon index	396	0.41
excluding lake or bog site	56	0.57
excluding elevation	204	0.48
AP and SP model	568	0.27

The application of the quantile mapping approach reduced the bias towards the mean, whilst preserving the general structure of the data (*3.9. Supplement: S5*). However, there is still a tendency for under- and over-estimation at low and high observed tree cover respectively in the final model (Fig. 3.3A). There is no obvious spatial patterning in the biases, except for a tendency to overestimate tree cover in northernmost Scandinavia (*3.9. Supplement: S6*). The correlation between the final "decompressed" predictions and observed tree cover values is 0.80 (Fig. 3.3B). This correlation value compares favourably to the correlation between raw AP% and observed tree cover values (0.54): raw AP% values tend to overestimate observed tree cover (*3.9. Supplement: S7*).

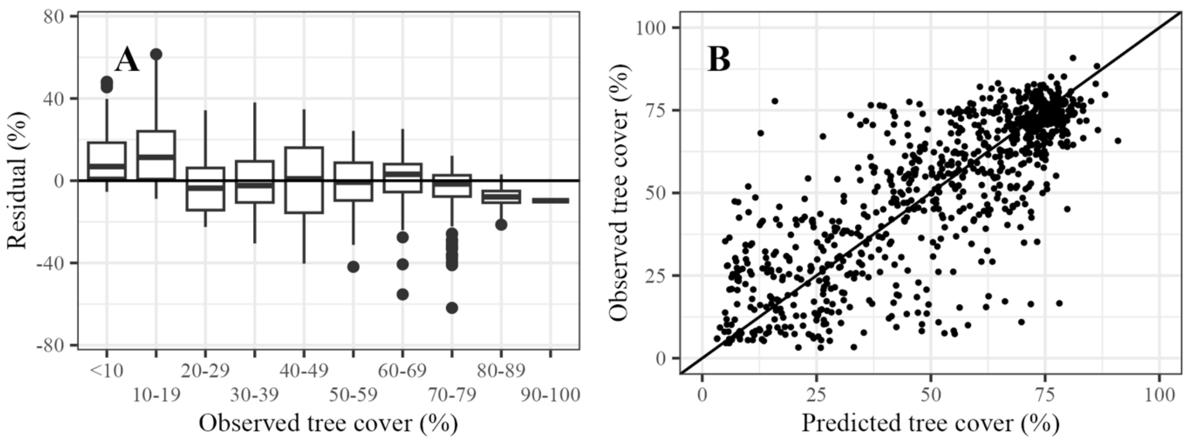

Figure 3.3: Evaluation of final model performance. A – Differences between predictions and observations (residual), in bins of observed tree cover percentage; B – Predictions of tree cover compared to observed tree cover

Our modern predictions differ from those of Serge et al. (2023) and Zanon et al. (2018) (Fig. 3.4). The correlation between the Zanon et al. (2018) reconstructions and observed tree cover is 0.78, which is similar to the correlation between our predictions and observed tree cover (0.8). The Zanon et al.

(2018) reconstructions have fewer outliers, but nevertheless they underestimate tree cover at high levels of observed tree cover (Fig. 3.4A). The correlation between the Serge et al. (2023) predictions and observations is only 0.5. This is partly caused by the use of larger 1º grid cells, but even when taking this into account and comparing with an average value for each grid cell, the correlations between predictions and observations were still lower (0.59) than our predictions and those of Zanon et al. (2018) (*3.9. Supplement: S8*). Zanon et al. (2018) visually compare their interpolated modern tree cover map and the observed tree cover from Hansen et al. (2013), but they do not report a correlation or R^2 value. However, the correlation values for Serge et al. (2023) broadly align with those reported comparing REVEALS tree cover estimates, with observed tree cover derived from Hansen et al. (2013) (R^2 = 0.15; correlation ~ 0.4).

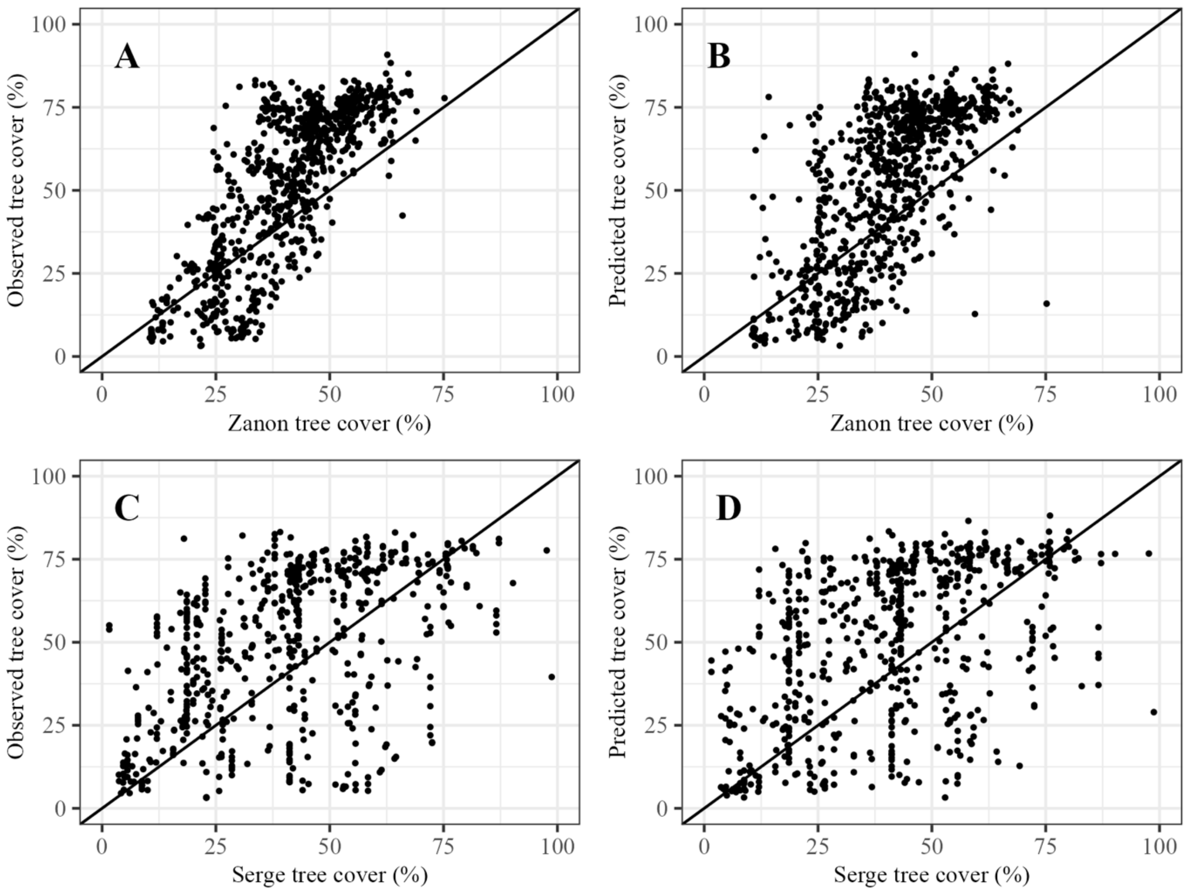

Figure 3.4: Modern tree cover from Zanon et al. (2018) compared to (A) observed tree cover and (B) our predicted tree cover. Modern tree cover from Serge et al. (2023) compared to (C) observed tree cover values and (D) our predicted tree cover.

3.4.2. Holocene changes in tree cover

We applied the tree cover model to reconstruct Holocene changes in tree cover at individual sites (see *3.7 Data and code availability* for binned reconstructions at site level). The median tree cover value, considering Europe as a whole, increased rapidly between 12,000 to ca. 8,500 cal. BP, and then more slowly to a peak at ca. 6,500 cal. BP. Median tree cover declined overall between 6,500 cal. BP and 4,000 cal. BP, albeit with some variability. Median tree cover declined steadily to present-day levels after ca. 4,000 cal. BP (Fig. 3.5A). This same pattern is shown when considering changes in mean tree cover (*3.9. Supplement: S9*), different locally estimated scatterplot smoothing (LOESS) (R package *locfit:* Loader, 2020) of the median tree cover value (Fig. 3.5B), and based on median tree covers reconstructed using the model bootstraps used to generate reconstruction standard errors (*3.9. Supplement: S10*). The rapid warming at the end of the Younger Dryas (Alley, 2000; Cheng et al., 2020), and the changes associated with the 8,200 cal. BP event (Alley et al., 1997; Alley and Ágústsdóttir, 2005) and the 4,200 cal. BP event (e.g. Weiss et al., 1993; Bini et al., 2019) are not apparent at this pan-European scale.

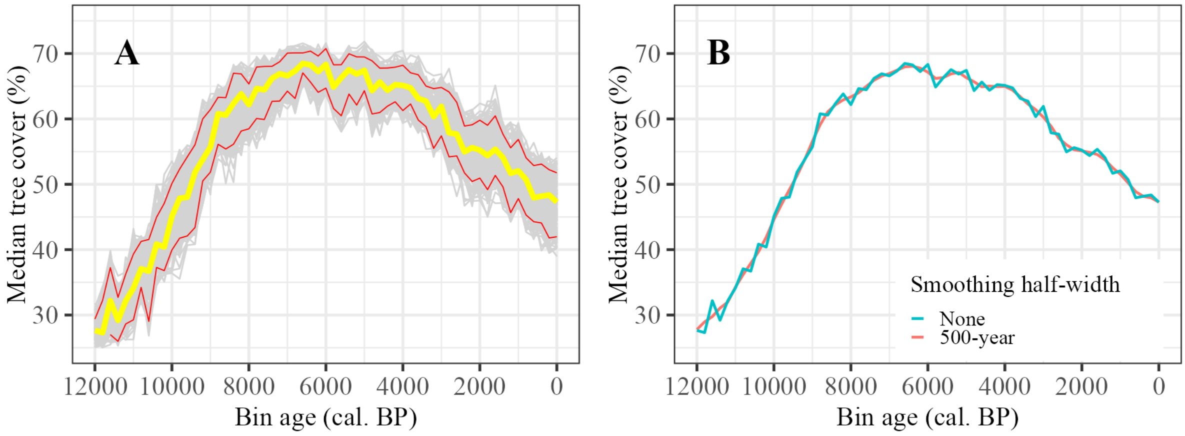

Figure 3.5: A - Median reconstructed tree cover for Europe from 12,000 to 0 cal. BP, with 95% confidence intervals for 1000 bootstrap resampling of records; B - Median reconstructed tree cover for Europe from 12,000 to 0 cal. BP, with differing LOESS regression smoothing half-widths.

These pan-European trends mask considerable regional variability in tree cover at any given time and in trends through time (Fig. 3.6 and see *3.9. Supplement: S11*, for gridded maps of reconstructed tree cover).

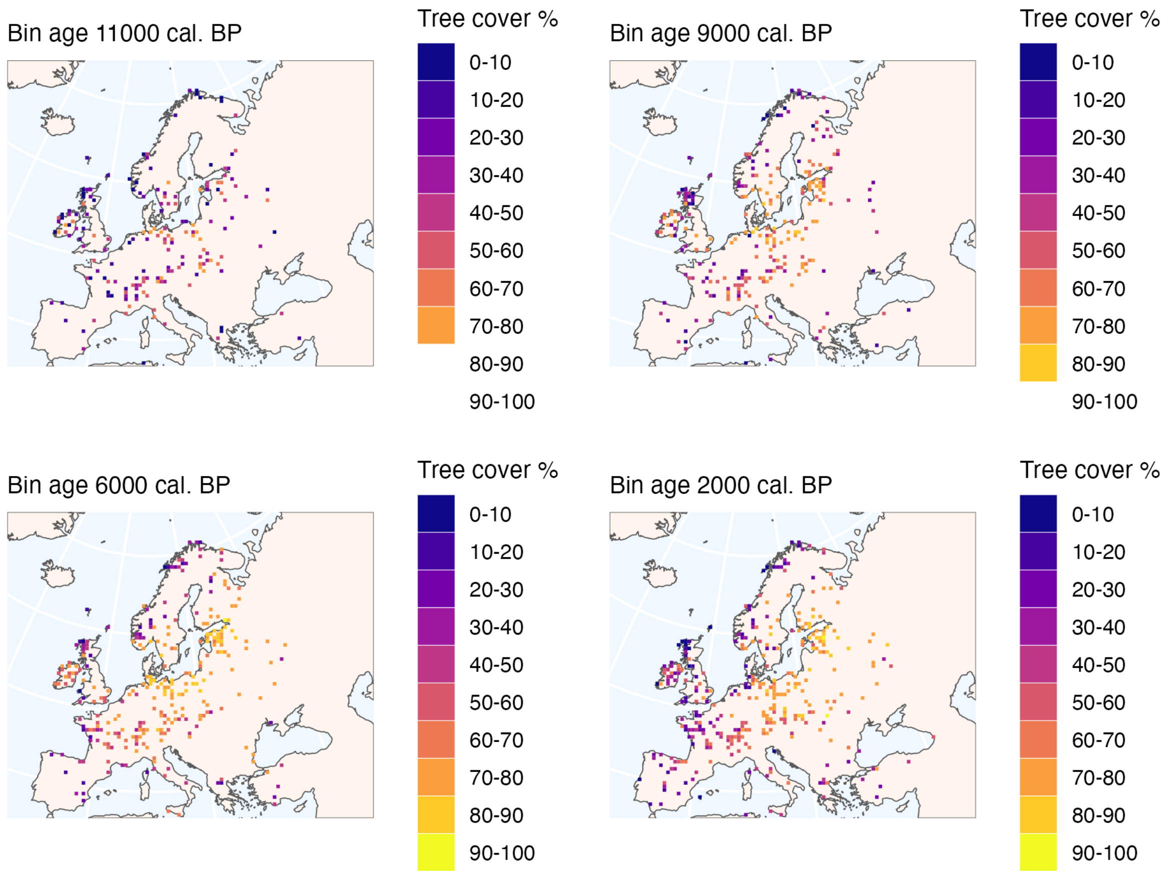

Figure 3.6: Gridded maps of average reconstructed tree cover for selected periods, for 50km² grid cells. Bin ages are 200-years in width, with ages referring to mid-point of each bin.

To examine these trends, we consider four biogeographical regions for which there is sufficient data: the Atlantic, Boreal, Continental and Mediterranean regions (Figure 3.2D; *3.9. Supplement: S12*).

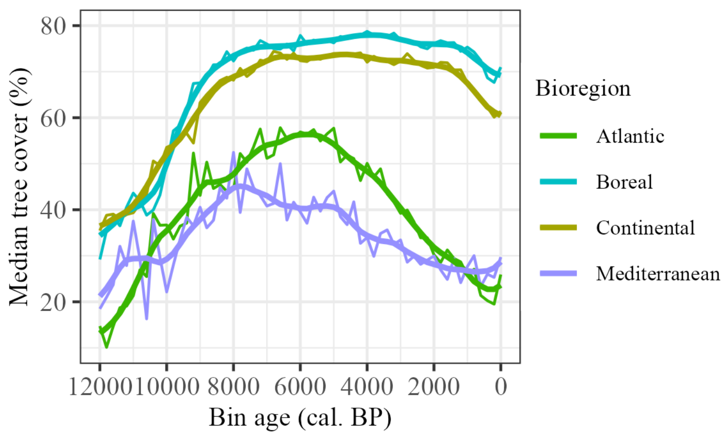

Figure 3.7: Median tree cover values, for selected biogeographical regions. Smoothed lines reflect LOESS fitted regression with 1000-year halfwidth.

The increase in tree cover at the beginning of the Holocene is shown in all four regions, but the trajectories are different (Fig. 3.7). There is an immediate rapid increase in the Atlantic region, but the increase is initially slow in the Boreal and Continental regions and only becomes more rapid after ca. 11,000 cal. BP in the Continental region and after ca. 10,300 cal. BP in the Boreal region. The initial increase in the Mediterranean region is interrupted by a decline between 11,000 and 10,000 cal. BP and only begins to increase again after ca. 9,800 cal. BP. The maximum in tree cover in the Mediterranean region is reached at ca. 8,000 cal. BP. After this there is a decline towards present-day levels, although this is interrupted by intervals of relative stability e.g. between ca. 6,000 and 5,000 cal. BP, again between 4,000 and 3,000 cal. BP and in the most recent millennium. There is also a well-defined maximum in tree cover in the Atlantic region, but this occurs at ca. 6,000 cal. BP. The subsequent decline is gradual until the last ca. 500 years. The maximum in tree cover is broader in the Continental and Boreal regions, with high levels of tree cover characteristic of the entire interval between ca. 8,000 and 1,000 cal. BP although the absolute maximum occurs at ca. 6,400 cal. BP in the Continental region and not until ca. 4,000 cal. BP in the Boreal region. Both regions are characterised by a rapid decline in the last millennium.

This broad pattern of increase, mid-Holocene maximum and then decline to present is consistent with previous reconstructions (Fig. 3.8). Initial levels of tree cover are similar in the three reconstructions (ca. 27.5-30%), but the increase in tree cover is more rapid in the Zanon et al. (2018) and Serge et al. (2023) reconstructions. Our reconstructed maximum cover is slightly lower (ca. 5–10%) than shown by the other reconstructions. However, the mid-Holocene timing of this maximum is broadly consistent across all of the reconstructions (although Zanon et al. (2018) show a double peak in tree cover, with an earlier peak at ca. 9,000 cal. BP) within the limitations of the age models and binning intervals used (see *3.9. Supplement: 13 and 14*). These broad trends are maintained when calculating tree cover from Zanon et al. (2018) and Serge et al. (2023) data such that only a single value per grid cell is permitted in the calculation of the median (*3.9. Supplement: S15*). The biggest difference between our reconstructed tree cover and previous studies is that the decrease post-ca. 2000 cal. BP is less abrupt. Both Zanon et al. (2018) and Serge et al. (2023) show a steep decline to levels (ca. 35%) similar to those at the beginning of the Holocene whereas we show a decline to only ca. 47.5%. Based on pollen record locations and a 5km^2 buffer, observed modern median tree cover is 46%, which suggests our estimated decline is more realistic.

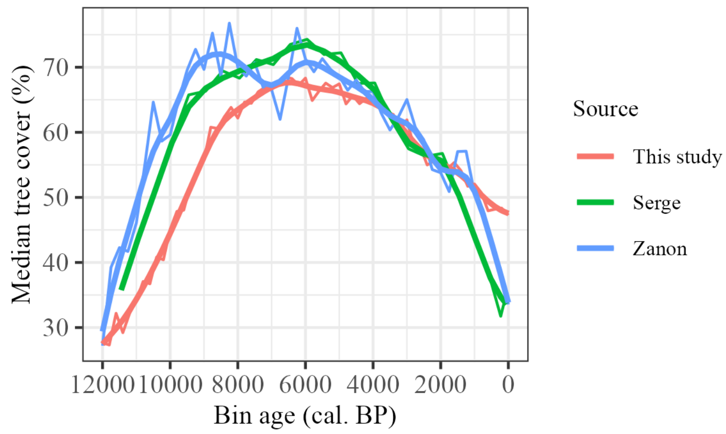

Figure 3.8: Reconstructed median tree cover compared to equivalent extracted tree cover medians for Serge et al. (2023) and Zanon et al. (2018). Smoothed lines reflect LOESS fitted regression with 1000-year halfwidth.

The three reconstructions also show some similarities at a sub-regional scale (Fig. 3.9), although comparison is more difficult because of differences in methodologies and coverage. As is the case for the pan-European comparison, Zanon et al. (2018) and Serge et al. (2023) generally show higher tree cover than our reconstruction. The peak tree cover in the Atlantic region occurs earlier in these reconstructions, and Zanon et al. (2018) also show an earlier peak in the Continental region. The later Holocene decline in tree cover is similar across all three reconstructions in the Atlantic region, but the previous reconstructions show a steeper decline in the Boreal and Continental regions. The biggest differences between the three reconstructions is in the Mediterranean region, where Serge et al. (2023) show a pronounced peak reaching 60% cover at ca. 5,500 cal. BP, whereas the other two reconstructions show comparatively muted changes in tree cover at around 40% throughout the mid- to late Holocene.

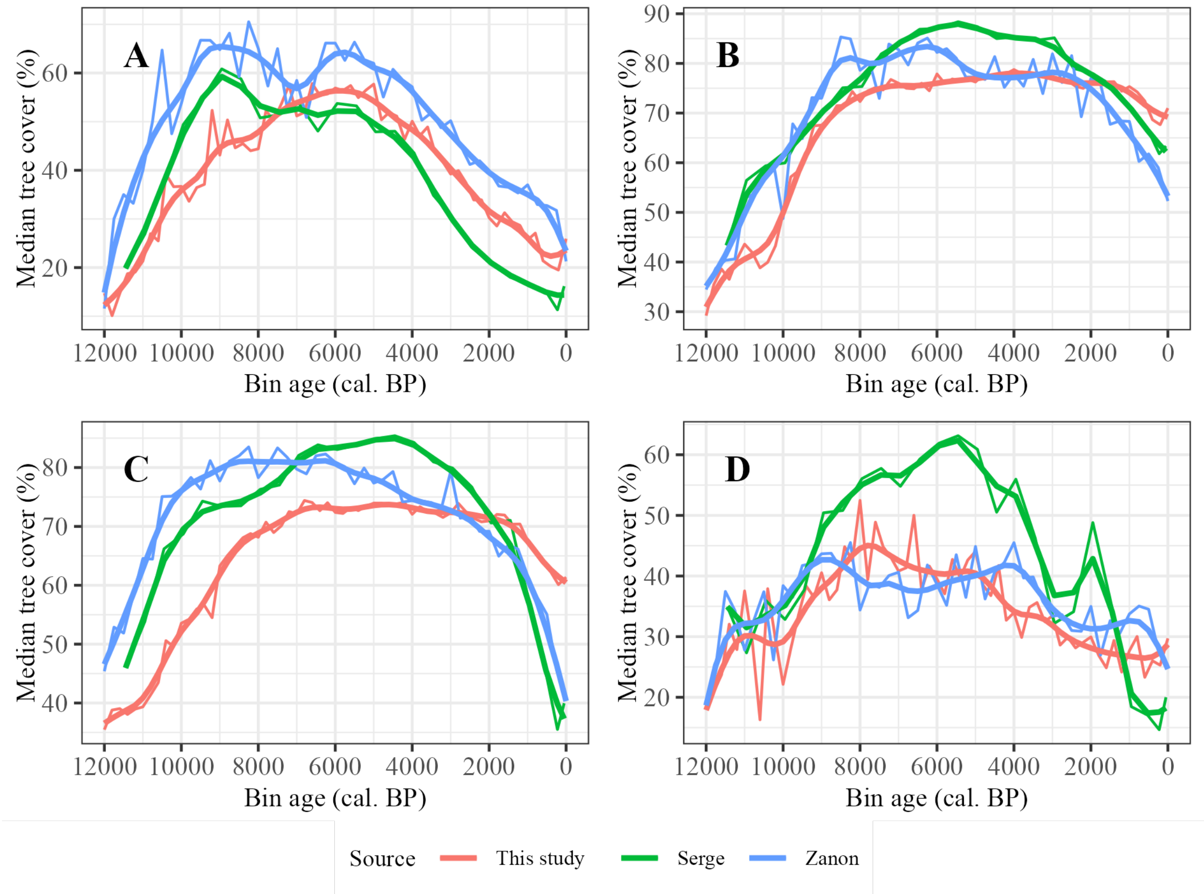

Figure 3.9: Reconstructed median tree cover compared to equivalent extracted tree cover medians for Serge et al. (2023) and Zanon et al. (2018), for selected modern biogeographical regions. Smoothed lines reflect LOESS fitted regression with 1000-year halfwidth. A – Atlantic; B- Boreal; C- Continental; D – Mediterranean.

Although the overall European median tree cover partially reflects the quantity of data for each region, recalculating the European level median tree cover based on just the four biogeographical regions of focus has very little material effect on the overall pattern of median tree cover for each reconstruction (*3.9. Supplement: S16*).

3.5. Discussion

Our reconstructions show that tree cover peaked in the mid-Holocene period, with median tree cover ca. 40% greater than at the beginning of the Holocene. This general pattern is shown by the REVEALS and MAT reconstructions, and is also visible in plant functional type (Davis et al., 2015) and pseudo-biomisation reconstructions of vegetation cover (Fyfe et al., 2015). Despite the similarities in median values between our reconstructions and those calculated from the REVEALS and MAT reconstructions, our site-based estimates are not fully comparable with the gridded estimates provided by the REVEALS reconstruction and the gridded and interpolated values provided by the MAT reconstructions. Nevertheless, the similarities give some support to the overall robustness of our reconstructions. There are differences in the timing and extent of changes between regions, although the general pattern of increase, mid-Holocene peak and subsequent decline is shown everywhere. There are some differences between our reconstructions and those from other studies. Firstly, the maximum tree cover from our reconstructions is around 5–10% less than the maximum calculated from the other reconstructions. This could reflect the conservative nature of our modern-day tree cover model, which underestimates tree cover at the high end despite the application of quantitative mapping adjustment to model predictions. However, Zanon et al. (2018) also underestimate tree cover at high levels of tree cover. Alternatively, the difference may reflect the exclusion of higher elevation records from fossil dataset in order to minimise the impact of upslope pollen transport, which was not done in the other two reconstructions and would tend to reduce overall median tree cover. Secondly, the timings of peak tree cover vary between the reconstructions, with the MAT-based estimate peaking earlier and the REVEALS estimate later than shown in our reconstruction. These differences likely reflect differences in coverage through time and differences in the binning procedure. The major difference at the pan-European scale is the reduction in tree cover from ca. 2000 cal. BP to present, which is less marked in our reconstructions and more consistent with observed tree cover. The observed tree cover values used in the model construction exclude areas dominated by land-cover types such as built areas or areas dominated by crops. We account for this in defining modern source areas in our model. Not accounting for changes in these other land-cover types, which through anthropogenic land use have increased substantially over the past 1000 years (Klein Goldewijk et al., 2017) would result in a steeper decline in tree cover, as seen in the other two reconstructions.

We took an inclusive approach in defining the modern training data and for the fossil records to maximise spatial coverage. The inclusion of bogs, for example, reduced the goodness-of-fit of the model slightly but resulted in much better spatial coverage. Conversely, the exclusion of high-elevation sites did not have a major impact on spatial coverage but was necessary to improve model fit because of the tendency for upslope transport of pollen in mountainous areas. Nevertheless, there are still areas of Europe which lack data, or where there is a mismatch in coverage between the modern and fossil records. Improved sampling of such areas would enhance our confidence in the reconstructions of Holocene tree cover.

Our reconstructions are consistent with understanding of Holocene climate patterns. The rapid increase in tree cover at the beginning of the Holocene shown in the pan-European reconstruction and in most of the sub-regional reconstructions reflects the marked warming after the Younger Dryas. This warming is less pronounced and more gradual in the Mediterranean region, consistent with the fact that the Younger Dryas cool interval is not strongly registered over much of this region (Bottema, 1995; Cruz-Silva et al., 2023). Subsequent pan-European changes in tree cover broadly reflect changes in growing season temperature, which itself is a reflection of orbitally-forced changes in summer insolation. However, modelling studies have shown that the timing of maximum warmth during the Holocene in Europe was delayed compared to the maximum of insolation forcing as a consequence of feedbacks associated with the presence of the Laurentide and Scandinavian ice sheets (Renssen et al., 2009; Blaschek and Renssen, 2013; Zhang et al., 2016, 2018). However, they consistently show that the warming was delayed in the region bordering the Atlantic (and northwest Europe more generally) by ca. 2,000 years compared to more continental regions, consistent with our reconstructions. The more muted changes in tree cover in the Mediterranean region compared to other regions of Europe is consistent with previous reconstructions and is partly explained by the fact that these changes are largely driven by changes in precipitation and precipitation seasonality (Cruz-Silva et al., 2023). The late Holocene decline in tree cover is consistent with the orbitally-driven cooling. However, the more rapid decline in tree cover during the last millennium shown in the Boreal and Continental regions, and shown more dramatically in the Zanon et al. (2018) and Serge et al. (2023) reconstructions, is more difficult to explain as a function of climate changes: transient model simulations of the response to changes in orbital and greenhouse gas forcing (e.g. Liu et al., 2009; Zhang et al., 2016; Braconnot et al., 2019; Dallmeyer et al., 2020) generally indicate muted changes in either summer or winter temperatures during the most recent millennia.

There are several other factors that could have influenced tree cover during the Holocene. Human influence on the landscape has been identified in many regions of Europe from 6,000 cal. BP onwards (e.g. Roberts et al., 2018; Zapolska et al., 2023). Although this may have contributed to the observed decline in tree cover from the mid-Holocene onwards, the most rapid population growth occurred only during the past 2000 years (Klein Goldewijk et al., 2010, 2017). The recent decline in tree cover may therefore reflect this rapid growth and the consequent increasing human influence on the landscape in some regions (see e.g. Marquer et al., 2017; Roberts et al., 2019). Climate-driven changes in disturbance (wildfires, windthrow) may also contribute to the inferred changes in tree cover. Changes in the frequency or intensity of storms has, for example, been shown in maritime Europe (e.g. Pouzet et al., 2018; Sjöström et al., 2024) during the late Holocene; storms are a major cause of widespread forest damage in Europe today (Senf and Siedl, 2020) and could have been important during the Holocene. Changing wildfire regimes could also have been an important influence on tree cover (Marlon et al., 2013; Kuosmanen et al., 2014). Much of the debate about the relative importance of climate and human activities on the environment during the Holocene has been based on local-scale correlations; other contributing factors have been largely ignored. More formal modelling of these relationships, using quantitative information on climate, population size, and disturbance is required to assign the impact of each on tree cover more confidently.

Our simple modelling approach yields a reasonably robust picture of changes in tree cover through the Holocene, largely consistent with known changes in climate. As with other statistical reconstruction techniques, it is predicated on the assumption of stationarity between tree cover and the explanatory variables. This may be problematic for variables such as elevation, where changes in elevational lapse rates (Mountain Research Initiative EDW Working Group, 2015) or atmospheric circulation patterns (Bartlein et al., 2017) could affect the relationship, but is less likely to be an issue for explanatory variables that reflect biophysical controls on pollen transport and deposition such as basin type or proportion of needleleaf trees. Our approach is less data-demanding that the REVEALS approach. Serge et al. (2023) have pointed out that lack of reliable information on species RPP values is likely to lead to less accurate reconstructions. Even in Europe, there is limited RPP data and, as the comparison of reconstructions based on 31 and 46 species shows, some of that data may not be reliable. RPP data is more limited in many other regions of the world (Harrison et al., 2020). Given this, our simple modelling approach provides an alternative method that could be applied to reconstruct tree cover globally. It is difficult to compare our reconstructions with the MAT-based approach of Zanon et al. (2018) since they do not provide individual site estimates and it is therefore not possible to determine the degree to which the patterns are influenced by the spatial and temporal interpolations they applied. Nevertheless, our simple approach overcomes the methodological issues associated with the MAT, such as how to measure the degree of analogy between assemblages, how to deal with non-analogues, and the sensitivity of the reconstructions to the number of analogues used. Thus, given the existence of global modern pollen training data sets and good remote-sensing based modern estimates of tree cover, our approach could be applied to other regions of the world to generate robust reconstructions of tree cover.

3.6. Conclusions

We have made use of modern pollen data and maps of tree cover percentage to build a simple model of tree cover. We then applied this model to fossil pollen records to reconstruct tree cover at a site level during the Holocene across Europe. At a pan-European level, tree cover increased from the early Holocene to the mid-Holocene, and then subsequently declined to the present day. There are regional variations in the speed of the initial increase, the timing of maximum tree cover, and the form of the subsequent decline. Our simple approach produces similar reconstructions of the trends in tree cover during the Holocene reconstructed using more complex methods, and since it only requires readily available data could be used to reconstruct tree cover in other regions of the world.

3.7. Code and data availability

The SMPDSv2 modern pollen database is available from the University of Reading Research Data Archive (https://researchdata.reading.ac.uk/389/) and/or via https://github.com/special-uor/smpds?tab=readme-ov-file
Metadata updates to SMPDSv2, including basin size updates are available at https://doi.org/10.5281/zenodo.13235637
The SPECIAL.EPD fossil pollen database is available from the University of Reading Research Data Archive (https://researchdata.reading.ac.uk/1295/)
The code used in generating tree cover, binned site-based reconstructions of tree cover, the code as cross-analysis of the data, and species categorisation tables are available at https://doi.org/10.5281/zenodo.13235637

3.8. References

Abis, B. and Brovkin, V.: Environmental conditions for alternative tree-cover states in high latitudes, Biogeosciences, 14, 511–527, https://doi.org/10.5194/bg-14-511-2017, 2017.

Adam, M., Weitzel, N., and Rehfeld, K.: Identifying Global-Scale Patterns of Vegetation Change During the Last Deglaciation From Paleoclimate Networks, Paleoceanogr Paleoclimatol, 36, https://doi.org/10.1029/2021PA004265, 2021.

Akaike, H.: A New Look at the Statistical Model Identification, IEEE Trans. Automat. Contr., 19, 716–723, https://doi.org/10.1109/TAC.1974.1100705, 1974.

Alkama, R. and Cescatti, A.: Biophysical climate impacts of recent changes in global forest cover, Science, 351, 600–604, https://doi.org/10.1126/science.aac8083, 2016.

Alley, R. B.: The Younger Dryas cold interval as viewed from central Greenland, Quat. Sci. Rev., 19, 213–226, https://doi.org/10.1016/S0277-3791(99)00062-1, 2000.

Alley, R. B. and Ágústsdóttir, A. M.: The 8k event: Cause and consequences of a major Holocene abrupt climate change, Quat. Sci. Rev., 24, 1123–1149, https://doi.org/10.1016/j.quascirev.2004.12.004, 2005.

Alley, R. B., Mayewski, P. A., Sowers, T., Stuiver, M., Taylor, K. C., and Clark, P. U.: Holocene climatic instability: A prominent, widespread event 8200 yr ago, Geology, 25, 483–486, https://doi.org/10.1130/0091-7613(1997)025<0483:HCIAPW>2.3.CO;2, 1997.

Baston, D.: exactextractr: Fast Extraction from Raster Datasets using Polygons, https://isciences.gitlab.io/exactextractr/, 2023.

Bartlein, P. J., Harrison, S. P., and Izumi, K.: Underlying causes of Eurasian midcontinental aridity in simulations of mid-Holocene climate, Geophys Res Lett, 44, 9020–9028, https://doi.org/10.1002/2017GL074476, 2017.

Bini, M., Zanchetta, G., Perşoiu, A., Cartier, R., Català, A., Cacho, I., Dean, J. R., Di Rita, F., Drysdale, R. N., Finnè, M., Isola, I., Jalali, B., Lirer, F., Magri, D., Masi, A., Marks, L., Mercuri, A. M., Peyron, O., Sadori, L., Sicre, M.-A., Welc, F., Zielhofer, C., and Brisset, E.: The 4.2 ka BP Event in the Mediterranean region: an overview, Clim. Past, 15, 555–577, https://doi.org/10.5194/cp-15-555-2019, 2019.

Binney, H., Edwards, M., Macias-Fauria, M., Lozhkin, A., Anderson, P., Kaplan, J. O., Andreev, A., Bezrukova, E., Blyakharchuk, T., Jankovska, V., Khazina, I., Krivonogov, S., Kremenetski, K., Nield, J., Novenko, E., Ryabogina, N., Solovieva, N., Willis, K., and Zernitskaya, V.: Vegetation of Eurasia from the last glacial maximum to present: Key biogeographic patterns, Quat Sci Rev, 157, 80–97, https://doi.org/10.1016/j.quascirev.2016.11.022, 2017.

Blaschek, M. and Renssen, H.: The Holocene thermal maximum in the Nordic Seas: the impact of Greenland Ice Sheet melt and other forcings in a coupled atmosphere–sea-ice–ocean model, Clim. Past, 9, 1629–1643, https://doi.org/10.5194/cp-9-1629-2013, 2013.

Blaauw, M. and Christen, J. A.: Flexible paleoclimate age-depth models using an autoregressive gamma process, Bayesian Anal, 6, https://doi.org/10.1214/11-BA618, 2011.

Bonan, G. B.: Forests and Climate Change: Forcings, Feedbacks, and the Climate Benefits of Forests, Science, 320, 1444–1449, https://doi.org/10.1126/science.1155121, 2008.

Bottema, S.: The Younger Dryas in the Eastern Mediterranean, Quat. Sci. Rev., 14, 883–891, https://doi.org/10.1016/0277-3791(95)00069-0, 1995.

Braconnot, P., Zhu, D., Marti, O., and Servonnat, J.: Strengths and challenges for transient Mid- to Late Holocene simulations with dynamical vegetation, Clim. Past, 15, 997–1024, https://doi.org/10.5194/cp-15-997-2019, 2019.

Bradshaw, R. H. W. and Webb, T.: Relationships between Contemporary Pollen and Vegetation Data from Wisconsin and Michigan, USA, Ecology, 66, 721–737, https://doi.org/10.2307/1940533, 1985.

Buchhorn, M., Smets, B., Bertels, L., de Roo, B., Lesiv, M., Tsendbazar, N.-E., Li, L., and Tarko, A.: Copernicus Global Land Service: Land Cover 100m: collection 3: epoch 2015: Globe, https://doi.org/https://doi.org/10.5281/zenodo.3939038, 2020a.

Buchhorn, M., Smets, B., Bertels, L., Roo, B. De, Lesiv, M., Tsendbazar, N.-E., Herold, M., and Fritz, S.: Copernicus Global Land Service: Land Cover 100m: collection 3: epoch 2016: Globe, https://doi.org/10.5281/zenodo.3518026, September 2020b.

Buchhorn, M., Smets, B., Bertels, L., Roo, B. De, Lesiv, M., Tsendbazar, N.-E., Herold, M., and Fritz, S.: Copernicus Global Land Service: Land Cover 100m: collection 3: epoch 2017: Globe, https://doi.org/10.5281/zenodo.3518036, September 2020c.

Buchhorn, M., Smets, B., Bertels, L., Roo, B. De, Lesiv, M., Tsendbazar, N.-E., Herold, M., and Fritz, S.: Copernicus Global Land Service: Land Cover 100m: collection 3: epoch 2018: Globe, https://doi.org/10.5281/zenodo.3518038, September 2020d.

Buchhorn, M., Smets, B., Bertels, L., Roo, B. De, Lesiv, M., Tsendbazar, N.-E., Herold, M., and Fritz, S.: Copernicus Global Land Service: Land Cover 100m: collection 3: epoch 2019: Globe, https://doi.org/10.5281/zenodo.3939050, September 2020e.

Bunting, M. J. and Farrell, M.: Do Local Habitat Conditions Affect Estimates of Relative Pollen Productivity and Source Area in Heathlands?, Front. Ecol. Evol., 10, https://doi.org/10.3389/fevo.2022.787345, 2022.

Bunting, M. J., Twiddle, C. L., and Middleton, R.: Using models of pollen dispersal and deposition in hilly landscapes: Some possible approaches, Palaeogeogr. Palaeocl., 259, 77–91, https://doi.org/10.1016/j.palaeo.2007.03.051, 2008.

Cheng, H., Zhang, H., Spötl, C., Baker, J., Sinha, A., Li, H., Bartolomé, M., Moreno, A., Kathayat, G., Zhao, J., Dong, X., Li, Y., Ning, Y., Jia, X., Zong, B., Ait Brahim, Y., Pérez-Mejías, C., Cai, Y., Novello, V. F., Cruz, F. W., Severinghaus, J. P., An, Z., and Edwards, R. L.: Timing and structure of the Younger Dryas event and its underlying climate dynamics, Proc. Natl. Acad. Sci. U.S.A, 117, 23408–23417, https://doi.org/10.1073/pnas.2007869117, 2020.

Cordova, C. E., Harrison, S. P., Mudie, P. J., Riehl, S., Leroy, S. A. G., and Ortiz, N.: Pollen, plant macrofossil and charcoal records for palaeovegetation reconstruction in the Mediterranean-Black Sea Corridor since the Last Glacial Maximum, Quat Int, 197, 12–26, https://doi.org/10.1016/j.quaint.2007.06.015, 2009.

Cox, D. R. and Snell, E. J.: Analysis of Binary Data, 2nd Edition., Chapman & Hall, 1989.

Cribari-Neto, F. and Zeileis, A.: Beta Regression in *R*, J. Stat. Softw., 34, https://doi.org/10.18637/jss.v034.i02, 2010.

Cruz-Silva, E., Harrison, S. P., Prentice, I. C., Marinova, E., Bartlein, P. J., Renssen, H., and Zhang, Y.: Pollen-based reconstructions of Holocene climate trends in the eastern Mediterranean region, Clim. Past, 19, 2093–2108, https://doi.org/10.5194/cp-19-2093-2023, 2023.

Dallmeyer, A., Claussen, M., Lorenz, S. J., and Shanahan, T.: The end of the African humid period as seen by a transient comprehensive Earth system model simulation of the last 8000 years, Clim. Past, 16, 117–140, https://doi.org/10.5194/cp-16-117-2020, 2020.

Davis, B. A. S., Brewer, S., Stevenson, A. C., and Guiot, J.: The temperature of Europe during the Holocene reconstructed from pollen data, Quat Sci Rev, 22, 1701–1716, https://doi.org/10.1016/S0277-3791(03)00173-2, 2003.

Davis, B. A. S., Collins, P. M., and Kaplan, J. O.: The age and post-glacial development of the modern European vegetation: a plant functional approach based on pollen data, Veg. Hist. Archaeobot., 24, 303–317, https://doi.org/10.1007/s00334-014-0476-9, 2015.

Duffin, K. I. and Bunting, M. J.: Relative pollen productivity and fall speed estimates for southern African savanna taxa, Veg Hist Archaeobot, 17, 507–525, https://doi.org/10.1007/s00334-007-0101-2, 2008.

European Environment Agency: Biogeographical regions, https://sdi.eea.europa.eu/catalogue/srv/api/records/11db8d14-f167-4cd5-9205-95638dfd9618, 2016.

Fall, P. L.: Spatial patterns of atmospheric pollen dispersal in the Colorado Rocky Mountains, USA, Rev. Palaeobot. Palynol., 74, 293–313, https://doi.org/10.1016/0034-6667(92)90013-7, 1992.

FAO: Global Forest Resources Assessment 2020, FAO, https://doi.org/10.4060/ca9825en, 2020.

Fyfe, R. M., Woodbridge, J., and Roberts, N.: From forest to farmland: pollen-inferred land cover change across Europe using the pseudobiomization approach, Glob. Chang. Biol., 21, 1197–1212, https://doi.org/10.1111/gcb.12776, 2015.

Gaillard, M.-J., Sugita, S., Mazier, F., Trondman, A.-K., Broström, A., Hickler, T., Kaplan, J. O., Kjellström, E., Kokfelt, U., Kuneš, P., Lemmen, C., Miller, P., Olofsson, J., Poska, A., Rundgren, M., Smith, B., Strandberg, G., Fyfe, R., Nielsen, A. B., Alenius, T., Balakauskas, L., Barnekow, L., Birks, H. J. B., Bjune, A., Björkman, L., Giesecke, T., Hjelle, K., Kalnina, L., Kangur, M., van der Knaap, W. O., Koff, T., Lagerås, P., Latałowa, M., Leydet, M., Lechterbeck, J., Lindbladh, M., Odgaard, B., Peglar, S., Segerström, U., von Stedingk, H., and Seppä, H.: Holocene land-cover reconstructions for studies on land cover-climate feedbacks, Clim. Past, 6, 483–499, https://doi.org/10.5194/cp-6-483-2010, 2010.

Gaillard, M.-J., Githumbi, E., Achoundong, G., Lézine, A.-M., Hély, C., Lebamba, J., Marquer, L., Mazier, F., Li, F., and Sugita, S.: The challenge of pollen-based quantitative reconstruction of Holocene plant cover in tropical regions: A pilot study in Cameroon, in: Quaternary Vegetation Dynamics: the African Pollen Database, edited by: Runge, J., Gosling, W., Lézine, A.-M., and Scott, L., CRC Press, London, 259–279, 2021.

Githumbi, E., Fyfe, R., Gaillard, M.-J., Trondman, A.-K., Mazier, F., Nielsen, A.-B., Poska, A., Sugita, S., Woodbridge, J., Azuara, J., Feurdean, A., Grindean, R., Lebreton, V., Marquer, L., Nebout-Combourieu, N., Stančikaitė, M., Tanţău, I., Tonkov, S., and Shumilovskikh, L.: European pollen-based REVEALS land-cover reconstructions for the Holocene: methodology, mapping and potentials, Earth Syst. Sci. Data, 14, 1581–1619, https://doi.org/10.5194/essd-14-1581-2022, 2022.

Gudmundsson, L., Bremnes, J. B., Haugen, J. E., and Engen-Skaugen, T.: Technical Note: Downscaling RCM precipitation to the station scale using statistical transformations - a comparison of methods, Hydrol. Earth Syst. Sci., 16, 3383–3390, https://doi.org/10.5194/hess-16-3383-2012, 2012.

Guiot, J.: Methodology of the last climatic cycle reconstruction in France from pollen data, Palaeogeogr. Palaeocl., 80, 49–69, https://doi.org/10.1016/0031-0182(90)90033-4, 1990.

Hansen, M. C., Potapov, P. V., Moore, R., Hancher, M., Turubanova, S. A., Tyukavina, A., Thau, D., Stehman, S. V., Goetz, S. J., Loveland, T. R., Kommareddy, A., Egorov, A., Chini, L., Justice, C. O., and Townshend, J. R. G.: High-Resolution Global Maps of 21st-Century Forest Cover Change, Science, 342, 850–853, https://doi.org/10.1126/science.1244693, 2013.

Harrison, S. P. and Marinova, E.: EMBSeCBIO modern pollen biomisation, University of Reading, Dataset, https://doi.org/10.17864/1947.109, 2017.

Harrison, S. P., Gaillard, M.-J., Stocker, B. D., Vander Linden, M., Klein Goldewijk, K., Boles, O., Braconnot, P., Dawson, A., Fluet-Chouinard, E., Kaplan, J. O., Kastner, T., Pausata, F. S. R., Robinson, E., Whitehouse, N. J., Madella, M., and Morrison, K. D.: Development and testing scenarios for implementing land use and land cover changes during the Holocene in Earth system model experiments, Geosci Model Dev, 13, 805–824, https://doi.org/10.5194/gmd-13-805-2020, 2020.

Harrison, S. P., Marinova, E., and Cruz-Silva, E.: EMBSeCBIO pollen database, University of Reading, Dataset, https://doi.org/10.17864/1947.309, 2021.

Harrison, S.P., Egbudom, M.A., Liu, M., Cruz-Silva, E. and Sweeney, L.F.: The SPECIAL EPD Database: an expanded resource to document changes in vegetation and climate from pollen records from Europe, the Middle East and western Eurasia. University of Reading, Dataset, https://doi.org/10.17864/1947.001295, 2024

Heaton, T. J., Köhler, P., Butzin, M., Bard, E., Reimer, R. W., Austin, W. E. N., Bronk Ramsey, C., Grootes, P. M., Hughen, K. A., Kromer, B., Reimer, P. J., Adkins, J., Burke, A., Cook, M. S., Olsen, J., and Skinner, L. C.: Marine20—The Marine Radiocarbon Age Calibration Curve (0–55,000 cal BP), Radiocarbon, 62, 779–820, https://doi.org/10.1017/RDC.2020.68, 2020.

Hicks, S.: The use of annual arboreal pollen deposition values for delimiting tree-lines in the landscape and exploring models of pollen dispersal, Rev Palaeobot Palynol, 117, 1–29, https://doi.org/10.1016/S0034-6667(01)00074-4, 2001.

Hill, J. L. and Curran, P. J.: Area, shape and isolation of tropical forest fragments: effects on tree species diversity and implications for conservation, J. Biogeogr., 30, 1391–1403, https://doi.org/10.1046/j.1365-2699.2003.00930.x, 2003.

Hill, M. O.: Diversity and Evenness: A Unifying Notation and Its Consequences, Ecology, 54, 427–432, https://doi.org/10.2307/1934352, 1973.

Hill, T. R., Duthie, T. J., and Bunting, J.: Pollen productivity estimates from KwaZulu-Natal Drakensberg, South Africa, in: Quaternary Vegetation Dynamics: the African Pollen Database, edited by: Runge, J., Gosling, W., Lézine, A.-M., and Scott, L., CRC Press, London, 259–274, 2021.

Jackson, S. T. and Williams, J. W.: Modern Analogs in Quaternary Paleoecology: Here Today, Gone Yesterday, Gone Tomorrow?, Annu. Rev. Earth Pl. Sc., 32, 495–537, https://doi.org/10.1146/annurev.earth.32.101802.120435, 2004.

Jactel, H., Bauhus, J., Boberg, J., Bonal, D., Castagneyrol, B., Gardiner, B., Gonzalez-Olabarria, J. R., Koricheva, J., Meurisse, N., and Brockerhoff, E. G.: Tree Diversity Drives Forest Stand Resistance to Natural Disturbances, Curr. For. Rep., 3, 223–243, https://doi.org/10.1007/s40725-017-0064-1, 2017.

Kaplan, J. O., Pfeiffer, M., Kolen, J. C. A., and Davis, B. A. S.: Large Scale Anthropogenic Reduction of Forest Cover in Last Glacial Maximum Europe, PLoS One, 11, e0166726, https://doi.org/10.1371/journal.pone.0166726, 2016.

Klein Goldewijk, K., Beusen, A., and Janssen, P.: Long-term dynamic modeling of global population and built-up area in a spatially explicit way: HYDE 3.1, Holocene, 20, 565–573, https://doi.org/10.1177/0959683609356587, 2010.

Klein Goldewijk, K., Beusen, A., Doelman, J., and Stehfest, E.: Anthropogenic land use estimates for the Holocene – HYDE 3.2, Earth Syst. Sci. Data, 9, 927–953, https://doi.org/10.5194/essd-9-927-2017, 2017.

Kuosmanen, N., Fang, K., Bradshaw, R. H., Clear, J. L., and Seppä, H.: Role of forest fires in Holocene stand-scale dynamics in the unmanaged taiga forest of northwestern Russia, Holocene, 24, 1503–1514, https://doi.org/10.1177/0959683614544065, 2014.

Leite-Filho, A. T., Costa, M. H., and Fu, R.: The southern Amazon rainy season: The role of deforestation and its interactions with large-scale mechanisms, Int. J. Climatol, 40, 2328–2341, https://doi.org/10.1002/joc.6335, 2020.

Liu, M., Shen, Y., González-Sampériz, P., Gil-Romera, G., ter Braak, C. J. F., Prentice, I. C., and Harrison, S. P.: Holocene climates of the Iberian Peninsula: pollen-based reconstructions of changes in the west–east gradient of temperature and moisture, Clim Past, 19, 803–834, https://doi.org/10.5194/cp-19-803-2023, 2023.

Liu, Z., Otto-Bliesner, B. L., He, F., Brady, E. C., Tomas, R., Clark, P. U., Carlson, A. E., Lynch-Stieglitz, J., Curry, W., Brook, E., Erickson, D., Jacob, R., Kutzbach, J., and Cheng, J.: Transient Simulation of Last Deglaciation with a New Mechanism for Bølling-Allerød Warming, Science, 325, 310–314, https://doi.org/10.1126/science.1171041, 2009.

Loader, C.: Locfit: Local regression, likelihood and density estimation, http://cran.r-project.org/package=locfit%5Cnpapers2://publication/uuid/E5C68958-7122-4093-A8E2-3108F9DF726A, 2020.

Marinova, E., Harrison, S. P., Bragg, F., Connor, S., de Laet, V., Leroy, S. A. G., Mudie, P., Atanassova, J., Bozilova, E., Caner, H., Cordova, C., Djamali, M., Filipova-Marinova, M., Gerasimenko, N., Jahns, S., Kouli, K., Kotthoff, U., Kvavadze, E., Lazarova, M., Novenko, E., Ramezani, E., Röpke, A., Shumilovskikh, L., Tanţău, I., and Tonkov, S.: Pollen-derived biomes in the Eastern Mediterranean–Black Sea–Caspian-Corridor, J Biogeogr, 45, 484–499, https://doi.org/10.1111/jbi.13128, 2018.

Markgraf, V.: Pollen Dispersal in a Mountain Area, Grana, 19, 127–146, https://doi.org/10.1080/00173138009424995, 1980.

Marlon, J. R., Bartlein, P. J., Daniau, A.-L., Harrison, S. P., Maezumi, S. Y., Power, M. J., Tinner, W., and Vannière, B.: Global biomass burning: a synthesis and review of Holocene paleofire records and their controls, Quat Sci Rev, 65, 5–25, https://doi.org/10.1016/j.quascirev.2012.11.029, 2013.

Marquer, L., Gaillard, M.-J., Sugita, S., Trondman, A.-K., Mazier, F., Nielsen, A. B., Fyfe, R. M., Odgaard, B. V., Alenius, T., Birks, H. J. B., Bjune, A. E., Christiansen, J., Dodson, J., Edwards, K. J., Giesecke, T., Herzschuh, U., Kangur, M., Lorenz, S., Poska, A., Schult, M., and Seppä, H.: Holocene changes in vegetation composition in northern Europe: why quantitative pollen-based vegetation reconstructions matter, Quat. Sci. Rev., 90, 199–216, https://doi.org/10.1016/j.quascirev.2014.02.013, 2014.

Marquer, L., Gaillard, M.-J., Sugita, S., Poska, A., Trondman, A.-K., Mazier, F., Nielsen, A. B., Fyfe, R. M., Jönsson, A. M., Smith, B., Kaplan, J. O., Alenius, T., Birks, H. J. B., Bjune, A. E., Christiansen, J., Dodson, J., Edwards, K. J., Giesecke, T., Herzschuh, U., Kangur, M., Koff, T., Latałowa, M., Lechterbeck, J., Olofsson, J., and Seppä, H.: Quantifying the effects of land use and climate on Holocene vegetation in Europe, Quat. Sci. Rev., 171, 20–37, https://doi.org/10.1016/j.quascirev.2017.07.001, 2017.

Marquer, L., Mazier, F., Sugita, S., Galop, D., Houet, T., Faure, E., Gaillard, M.-J., Haunold, S., de Munnik, N., Simonneau, A., De Vleeschouwer, F., and Le Roux, G.: Pollen-based reconstruction of Holocene land-cover in mountain regions: Evaluation of the Landscape Reconstruction Algorithm in the Vicdessos valley, northern Pyrenees, France, Quat Sci Rev, 228, 106049, https://doi.org/10.1016/j.quascirev.2019.106049, 2020.

Moreira, F., Rego, F. C., and Ferreira, P. G.: Temporal (1958–1995) pattern of change in a cultural landscape of northwestern Portugal: implications for fire occurrence, Landsc. Ecol., 16, 557–567, https://doi.org/10.1023/A:1013130528470, 2001.

Mountain Research Initiative EDW Working Group: Elevation-dependent warming in mountain regions of the world, Nat Clim Chang, 5, 424–430, https://doi.org/10.1038/nclimate2563, 2015.

Moyes, A. B., Germino, M. J., and Kueppers, L. M.: Moisture rivals temperature in limiting photosynthesis by trees establishing beyond their cold-edge range limit under ambient and warmed conditions, New Phytol., 207, 1005–1014, https://doi.org/10.1111/nph.13422, 2015.

Nielsen, A. B., Giesecke, T., Theuerkauf, M., Feeser, I., Behre, K.-E., Beug, H.-J., Chen, S.-H., Christiansen, J., Dörfler, W., Endtmann, E., Jahns, S., de Klerk, P., Kühl, N., Latałowa, M., Odgaard, B. V., Rasmussen, P., Stockholm, J. R., Voigt, R., Wiethold, J., and Wolters, S.: Quantitative reconstructions of changes in regional openness in north-central Europe reveal new insights into old questions, Quat. Sci. Rev., 47, 131–149, https://doi.org/10.1016/j.quascirev.2012.05.011, 2012.

Ortu, E., de Beaulieu, J. L., Caramiello, R., and Siniscalco, C.: Late Glacial and Holocene vegetation dynamics at various altitudes in the Ellero Valley, Maritime Alps, northwestern Italy, Ecoscience, 15, 200–212, https://doi.org/10.2980/15-2-2926, 2008.

Ortu, E., David, F., and Peyron, O.: Pollen-inferred palaeoclimate reconstruction in the Alps during the Lateglacial and the early Holocene: how to estimate the effect of elevation and local parameters, J. Quat. Sci., 25, 651–661, https://doi.org/10.1002/jqs.1335, 2010.

Overpeck, J. T., Webb, T., and Prentice, I. C.: Quantitative Interpretation of Fossil Pollen Spectra: Dissimilarity Coefficients and the Method of Modern Analogs, Quat. Res., 23, 87–108, https://doi.org/10.1016/0033-5894(85)90074-2, 1985.

Piraquive Bermúdez, D., Theuerkauf, M., and Giesecke, T.: Towards quantifying changes in forest cover in the Araucaria forest-grassland mosaic in southern Brazil, Veg Hist Archaeobot, 31, 107–122, https://doi.org/10.1007/s00334-021-00841-2, 2022.

Pirzamanbein, B., Lindström, J., Poska, A., Sugita, S., Trondman, A.-K., Fyfe, R., Mazier, F., Nielsen, A. B., Kaplan, J. O., Bjune, A. E., Birks, H. J. B., Giesecke, T., Kangur, M., Latałowa, M., Marquer, L., Smith, B., and Gaillard, M.-J.: Creating spatially continuous maps of past land cover from point estimates: A new statistical approach applied to pollen data, Ecol Complex, 20, 127–141, https://doi.org/10.1016/j.ecocom.2014.09.005, 2014.

Pouzet, P., Maanan, M., Piotrowska, N., Baltzer, A., Stéphan, P., and Robin, M.: Chronology of Holocene storm events along the European Atlantic coast, Progress in Physical Geography: Earth and Environment, 42, 431–450, https://doi.org/10.1177/0309133318776500, 2018.

Prentice, C.: Records of vegetation in time and space: the principles of pollen analysis, in: Vegetation history, Springer Netherlands, Dordrecht, 17–42, https://doi.org/10.1007/978-94-009-3081-0_2, 1988.

Prentice, I. C.: Pollen Representation, Source Area, and Basin Size: Toward a Unified Theory of Pollen Analysis, Quat. Res., 23, 76–86, https://doi.org/10.1016/0033-5894(85)90073-0, 1985.

Prentice, I. C. and Webb, T.: Pollen percentages, tree abundances and the Fagerlind effect, J. Quat. Sci., 1, 35–43, https://doi.org/10.1002/jqs.3390010105, 1986.

R Core Team: R: A Language and Environment for Statistical Computing, R Foundation for Statistical Computing, Vienna, Austria, 2022.

Reimer, P. J., Austin, W. E. N., Bard, E., Bayliss, A., Blackwell, P. G., Bronk Ramsey, C., Butzin, M., Cheng, H., Edwards, R. L., Friedrich, M., Grootes, P. M., Guilderson, T. P., Hajdas, I., Heaton, T. J., Hogg, A. G., Hughen, K. A., Kromer, B., Manning, S. W., Muscheler, R., Palmer, J. G., Pearson, C., van der Plicht, J., Reimer, R. W., Richards, D. A., Scott, E. M., Southon, J. R., Turney, C. S. M., Wacker, L., Adolphi, F., Büntgen, U., Capano, M., Fahrni, S. M., Fogtmann-Schulz, A., Friedrich, R., Köhler, P., Kudsk, S., Miyake, F., Olsen, J., Reinig, F., Sakamoto, M., Sookdeo, A., and Talamo, S.: The IntCal20 Northern Hemisphere Radiocarbon Age Calibration Curve (0–55 cal kBP), Radiocarbon, 62, 1–33, https://doi.org/10.1017/rdc.2020.41, 2020.

Renssen, H., Seppä, H., Heiri, O., Roche, D. M., Goosse, H., and Fichefet, T.: The spatial and temporal complexity of the Holocene thermal maximum, Nat. Geosci., 2, 411–414, https://doi.org/10.1038/ngeo513, 2009.

Roberts, C. N., Woodbridge, J., Palmisano, A., Bevan, A., Fyfe, R., and Shennan, S.: Mediterranean landscape change during the Holocene: Synthesis, comparison and regional trends in population, land cover and climate, Holocene, 29, 923–937, https://doi.org/10.1177/0959683619826697, 2019.

Roberts, N., Fyfe, R. M., Woodbridge, J., Gaillard, M.-J., Davis, B. A. S., Kaplan, J. O., Marquer, L., Mazier, F., Nielsen, A. B., Sugita, S., Trondman, A.-K., and Leydet, M.: Europe's lost forests: a pollen-based synthesis for the last 11,000 years, Sci. Rep., 8, 716, https://doi.org/10.1038/s41598-017-18646-7, 2018.

Senf, C. and Seidl, R.: Mapping the forest disturbance regimes of Europe, Nat Sustain, 4, 63–70, https://doi.org/10.1038/s41893-020-00609-y, 2020.

Serge, M., Mazier, F., Fyfe, R., Gaillard, M.-J., Klein, T., Lagnoux, A., Galop, D., Githumbi, E., Mindrescu, M., Nielsen, A., Trondman, A.-K., Poska, A., Sugita, S., Woodbridge, J., Abel-Schaad, D., Åkesson, C., Alenius, T., Ammann, B., Andersen, S., Anderson, R., Andrič, M., Balakauskas, L., Barnekow, L., Batalova, V., Bergman, J., Birks, H., Björkman, L., Bjune, A., Borisova, O., Broothaerts, N., Carrion, J., Caseldine, C., Christiansen, J., Cui, Q., Currás, A., Czerwiński, S., David, R., Davies, A., De Jong, R., Di Rita, F., Dietre, B., Dörfler, W., Doyen, E., Edwards, K., Ejarque, A., Endtmann, E., Etienne, D., Faure, E., Feeser, I., Feurdean, A., Fischer, E., Fletcher, W., Franco-Múgica, F., Fredh, E., Froyd, C., Garcés-Pastor, S., García-Moreiras, I., Gauthier, E., Gil-Romera, G., González-Sampériz, P., Grant, M., Grindean, R., Haas, J., Hannon, G., Heather, A.-J., Heikkilä, M., Hjelle, K., Jahns, S., Jasiunas, N., Jiménez-Moreno, G., Jouffroy-Bapicot, I., Kabailienė, M., Kamerling, I., Kangur, M., Karpińska-Kołaczek, M., Kasianova, A., Kołaczek, P., Lagerås, P., Latalowa, M., Lechterbeck, J., Leroyer, C., Leydet, M., Lindbladh, M., Lisitsyna, O., López-Sáez, J.-A., Lowe, J., Luelmo-Lautenschlaeger, R., Lukanina, E., Macijauskaitė, L., Magri, D., Marguerie, D., Marquer, L., Martinez-Cortizas, A., Mehl, I., Mesa-Fernández, J., Mighall, T., Miola, A., Miras, Y., Morales-Molino, C., et al.: Testing the Effect of Relative Pollen Productivity on the REVEALS Model: A Validated Reconstruction of Europe-Wide Holocene Vegetation, Land (Basel), 12, 986, https://doi.org/10.3390/land12050986, 2023.

Simas, A. B., Barreto-Souza, W., and Rocha, A. V.: Improved estimators for a general class of beta regression models, Comput. Stat. Data Anal., 54, 348–366, https://doi.org/10.1016/j.csda.2009.08.017, 2010.

Sjöström, J. K., Gyllencreutz, R., Martínez Cortizas, A., Nylund, A., Piilo, S. R., Schenk, F., McKeown, M., Ryberg, E. E., and Kylander, M. E.: Holocene storminess dynamics in northwestern Ireland: Shifts in storm duration and frequency between the mid- and late Holocene, Quat Sci Rev, 337, 108803, https://doi.org/10.1016/j.quascirev.2024.108803, 2024.

Staal, A., Tuinenburg, O. A., Bosmans, J. H. C., Holmgren, M., van Nes, E. H., Scheffer, M., Zemp, D. C., and Dekker, S. C.: Forest-rainfall cascades buffer against drought across the Amazon, Nat. Clim. Change, 8, 539–543, https://doi.org/10.1038/s41558-018-0177-y, 2018.

Sugita, S.: A Model of Pollen Source Area for an Entire Lake Surface, Quat. Res., 39, 239–244, https://doi.org/10.1006/qres.1993.1027, 1993.

Sugita, S.: Theory of quantitative reconstruction of vegetation I: Pollen from large sites REVEALS regional vegetation composition, Holocene, https://doi.org/10.1177/0959683607075837, 2007a.

Sugita, S.: Theory of quantitative reconstruction of vegetation II: all you need is LOVE, Holocene, 17, 243–257, https://doi.org/10.1177/0959683607075838, 2007b.

Tabares, X., Ratzmann, G., Kruse, S., Theuerkauf, M., Mapani, B., and Herzschuh, U.: Relative pollen productivity estimates of savanna taxa from southern Africa and their application to reconstruct shrub encroachment during the last century, Holocene, 31, 1100–1111, https://doi.org/10.1177/09596836211003193, 2021.

Trondman, A. -K., Gaillard, M. -J., Mazier, F., Sugita, S., Fyfe, R. M., Nielsen, A. B., Twiddle, C., Barratt, P., Birks, H. J. B., Bjune, A. E., Björkman, L., Broström, A., Caseldine, C., David, R., Dodson, J., Dörfler, W., Fischer, E., Geel, B., Giesecke, T., Hultberg, T., Kalnina, L., Kangur, M., Knaap, P., Koff, T., Kuneš, P., Lagerås, P., Latałowa, M., Lechterbeck, J., Leroyer, C., Leydet, M., Lindbladh, M., Marquer, L., Mitchell, F. J. G., Odgaard, B. V., Peglar, S. M., Persson, T., Poska, A., Rösch, M., Seppä, H., Veski, S., and Wick, L.: Pollen-based quantitative reconstructions of Holocene regional vegetation cover (plant-functional types and land-cover types) in Europe suitable for climate modelling, Glob. Chang. Biol., 21, 676–697, https://doi.org/10.1111/gcb.12737, 2015.

Turubanova, S., Potapov, P., Hansen, M. C., Li, X., Tyukavina, A., Pickens, A. H., Hernandez-Serna, A., Arranz, A. P., Guerra-Hernandez, J., Senf, C., Häme, T., Valbuena, R., Eklundh, L., Brovkina, O., Navrátilová, B., Novotný, J., Harris, N., and Stolle, F.: Tree canopy extent and height change in Europe, 2001–2021, quantified using Landsat data archive, Remote Sens. Environ., 298, 113797, https://doi.org/10.1016/j.rse.2023.113797, 2023.

Viedma, O., Moity, N., and Moreno, J. M.: Changes in landscape fire-hazard during the second half of the 20th century: Agriculture abandonment and the changing role of driving factors, Agric. Ecosyst. Environ., 207, 126–140, https://doi.org/10.1016/j.agee.2015.04.011, 2015.

Villegas-Diaz, R., Cruz-Silva, E., and Harrison, S. P.: ageR: Supervised Age Models, https://doi.org/doi:10.5281/zenodo.4636716, 2021.

Villegas-Diaz, R. and Harrison, S.P.: The SPECIAL Modern Pollen Data Set for Climate Reconstructions, version 2 (SMPDSv2), University of Reading, Dataset, https://doi.org/10.17864/1947.000389, 2022

Wei, D., González-Sampériz, P., Gil-Romera, G., Harrison, S. P., and Prentice, I. C.: Seasonal temperature and moisture changes in interior semi-arid Spain from the last interglacial to the Late Holocene, Quat. Res., 101, 143–155, https://doi.org/10.1017/qua.2020.108, 2021.

Weiss, H., Courty, M.-A., Wetterstrom, W., Guichard, F., Senior, L., Meadow, R., and Curnow, A.: The Genesis and Collapse of Third Millennium North Mesopotamian Civilization, Science, 261, 995–1004, https://doi.org/10.1126/science.261.5124.995, 1993.

Whitney, B. S., Smallman, T. L., Mitchard, E. T., Carson, J. F., Mayle, F. E., and Bunting, M. J.: Constraining pollen-based estimates of forest cover in the Amazon: A simulation approach, Holocene, 29, 262–270, https://doi.org/10.1177/0959683618810394, 2019.

Wieczorek, M. and Herzschuh, U.: Compilation of relative pollen productivity (RPP) estimates and taxonomically harmonised RPP datasets for single continents and Northern Hemisphere extratropics, Earth Syst Sci Data, 12, 3515–3528, https://doi.org/10.5194/essd-12-3515-2020, 2020.

Wörl, V., Jetschni, J., and Jochner-Oette, S.: Birch Pollen Deposition and Transport along an Altitudinal Gradient in the Bavarian Alps—A Case Study Using Gravimetric Pollen Traps in the Pollen Season 2020, Atmosphere, 13, 2007, https://doi.org/10.3390/atmos13122007, 2022.

Zanon, M., Davis, B. A. S., Marquer, L., Brewer, S., and Kaplan, J. O.: European forest cover during the past 12,000 years: A palynological reconstruction based on modern analogs and remote sensing, Front. Plant Sci., 9, 1–25, https://doi.org/10.3389/fpls.2018.00253, 2018.

Zapolska, A., Serge, M. A., Mazier, F., Quiquet, A., Renssen, H., Vrac, M., Fyfe, R., and Roche, D. M.: More than agriculture: Analysing time-cumulative human impact on European land-cover of second half of the Holocene, Quat. Sci. Rev., 314, 108227, https://doi.org/10.1016/j.quascirev.2023.108227, 2023.

Zhang, Y., Renssen, H., and Seppä, H.: Effects of melting ice sheets and orbital forcing on the early Holocene warming in the extratropical Northern Hemisphere, Clim. Past, 12, 1119–1135, https://doi.org/10.5194/cp-12-1119-2016, 2016.

Zhang, Y., Renssen, H., Seppä, H., and Valdes, P. J.: Holocene temperature trends in the extratropical Northern Hemisphere based on inter-model comparisons, J. Quat. Sci., 33, 464–476, https://doi.org/10.1002/jqs.3027, 2018.

3.9. Supplement

This supplement contains the following sections:

- S1: Sources for SMPDSv2 data
- S2: Species categorisation
- S3: Coefficients and model fit based on lake sites only
- S4: Coefficients and model fit without exclusion of sites >1000 m
- S5: Quantile mapping influence on model predictions
- S6: Spatial structure of model predictions compared to observations
- S7: Arboreal pollen percentages compared to observed tree cover percentages
- S8: Modern predictions compared with other reconstructions based on grid cell averages
- S9: Mean reconstructed tree cover
- S10: Median reconstructed tree cover, with bootstrapped models
- S11: Gridded maps of reconstructed tree cover through time
- S12: Data by biogeographical region
- S13: Median reconstructed tree cover based on bin-widths from other reconstructions
- S14: Median reconstructed tree cover on upper and lower age model ranges
- S15: Median tree cover reconstructions based on grid cell averages
- S16: Median tree cover reconstructions based on the Atlantic, Boreal, Continental and Mediterranean biogeographical regions only

S1: Sources for SMPDSv2 data

Supplementary Table 3.1 provides the metadata source for the SMPDsv2 data, together with the number of entities/records and citations for each source.

Supplementary Table 3.1: List of SMPDSv2 data sources and references

Source (metadata table)	Number of entities	Publications
AMSS	38	Jolly et al., 1996; Julier et al., 2019, 2018; Lebamba et al., 2009
APD	90	Vincens et al., 2007
Australasian pollen	1540	Adeleye et al., 2021b, 2021a; Beck et al., 2017; Field et al., 2018; Fletcher et al., 2014; Herbert and Harrison, 2016; Luly, 1993; Luly et al., 1986; Mariani et al., 2017; McWethy et al., 2010, 2014; Pickett et al., 2004; Prebble et al., 2019
BIOME6000 Japan	94	Takahara et al., 2000
Blyakharchuk	144	Author: Tatiana A. Blyakharchuk
Bush et al., 2021	636	Bush et al., 2021
CMPD	4208	Chen et al., 2021
Dugerdil et al., 2021	48	Dugerdil et al., 2021
EMBSeCBIO	149	Harrison et al., 2021
EMPDv2	3508	Davis et al., 2020
Gaillard et al., 1992	124	Gaillard et al., 1992
Harrison et al., 2022b	3	Harrison et al., 2022b
Herzschuh et al., 2019	595	Herzschuh et al., 2019
IBERIA	243	Harrison et al., 2022a
Neotoma	6702	Williams et al., 2018
Phelps et al., 2020	106	Phelps et al., 2020
SMPDSv1	6345	Harrison, 2019
Southern Hemisphere pollen	76	Black, 2007; Dodson, 1978; Dodson and Intoh, 1999; Haberle, 1993, 1996; Hope, 2009; Hope et al., 1998, 1999; Macphail, 1975, 1979, 1980; Macphail and McQueen, 1983; Macphail and Mildenhall, 1980; Norton et al., 1986; Prebble et al., 2010; Shulmeister et al., 2003

S2: Species categorisation

Supplementary Table 3.2 lists the higher level groupings of taxa considered native to Europe and included within the Total Terrestrial Pollen Sum. Species are grouped into trees, shrubs and woody vines, and herbaceous pollen (herbs, grasses etc.). Tree species are sub-divided into broadleaf and needleleaf. This data in csv form is downloadable from https://doi.org/10.5281/zenodo.13235637

Supplementary Table 3.2: Classification of taxa included within the Total Terrestrial Pollen Sum

Tree/Shrub/Non-arboreal		**Taxa grouping**
Tree	Broadleaf	Acer, Aesculus, Alnus, Alnus subg. Alnobetula, Anacardiaceae, Arbutus, Arecaceae, Betula, Betula chamaebetula, Buxus, Carpinus, Carpinus betulus, Carpinus orientalis/Ostrya, Castanea, Celtis, Ceratonia, Cercis, Citrus, Clusiaceae, Cornaceae, Cornus, Corylus, Elaeagnaceae, Elaeagnus, Fabaceae, Fagus, Ficus, Fontanesia, Fraxinus, Ilex, Juglandaceae, Juglans, Laburnum, Laurus, Malus, Malus/Pyrus, Moraceae, Moraceae/Urticaceae, Myricaceae, Myrtaceae, Olea, Oleaceae, Pistacia, Platanus, Populus, Prunus, Pyrus, Quercus, Quercus deciduous, Quercus evergreen, Salix, Sapindaceae, Sorbus, Staphyleaceae, Syringa, Tamarix, Thymelaeaceae, Tilia, Ulmaceae, Ulmus, Ulmus/Zelkova, Verbenaceae, Viburnaceae, Viburnum, Vitex
	Needleleaf	*Abies*, *Cedrus*, Cupressaceae, Cupressaceae/Taxaceae, *Larix*, *Larix/Pseudotsuga*, *Picea*, *Pinus*, *Pinus* (diploxylon), *Pinus* (haploxylon), *Taxus*
Shrub and woody vine		Acanthaceae, *Alhagi*, *Andromeda*, Apiaceae, Araliaceae, Aristolochiaceae, *Artemisia*, Asparagaceae, *Astragalus*, Berberidaceae, *Berberis*, *Buddleia*, *Calicotome*, *Calluna*, Capparaceae, Caprifoliaceae, *Cassiope*, *Chamaedaphne*, Cistaceae, *Cistus*, *Citrullus*, *Clematis*, *Clethra*, *Colutea*, Convolvulaceae, *Coriaria*, *Cotinus*, *Cotoneaster*, *Crataegus*, Cucurbitaceae, *Daphne*, *Diapensia*, *Dioscorea*, Dioscoreaceae, *Dryas*, *Empetrum*, *Ephedra*, Ephedraceae, *Erica*, Ericaceae, *Euonymus*, *Flueggea*, *Forsythia*, *Frangula*, Frankeniaceae, Genisteae, *Halimium*, *Hedera*, *Helianthemum*, *Hippophae*, *Kalmia*, *Lavandula*, *Ledum*, *Ligustrum*, *Linnaea*, *Lonicera*, Malvaceae, *Moltkia*, Montiaceae, *Myrica*, *Myricaria*, *Nerium*, Nitrariaceae, *Ononis*, *Osmanthus*, *Paeonia*, *Paliurus*, *Periploca*, *Phillyrea*, *Phlomis*, *Potentilla*, Rhamnaceae, *Rhamnus*, *Rhododendron*, *Rhus*, *Ribes*, Rosaceae, *Rubus*, *Ruscus*, *Salvia*, *Sambucus*, Sapotaceae, *Smilax*, *Styrax*, *Suaeda*, *Vaccinium*, *Ziziphus*
Herbaceous		*Aconitum*, *Actaea*, Aizoaceae, Amaranthaceae, Amaryllidaceae, Apocynaceae, *Aquilegia*, Araceae, Asphodelaceae, Asteraceae, Asteraceae (Liguliflorae), Asteroideae, Balsaminaceae, Boraginaceae, Brassicaceae, Campanulaceae, Cannabaceae, Carduoideae, Caryophyllaceae, Celastraceae, *Chimaphila*, Cichorioideae, Colchicaceae, Commelinaceae, *Consolida*, Crassulaceae, Cyperaceae, *Datisca*, *Delphinium*, Eriocaulaceae, Euphorbiaceae, Fabaceae (herbs), Gentianaceae,

	Geraniaceae, *Helleborus*, Hypericaceae, *Impatiens*, Iridaceae, *Koenigia*, Lamiaceae, Liliaceae, Linaceae, Linderniaceae, *Linum*, *Lysimachia*, Lythraceae, *Malva*, Melanthiaceae, *Mercurialis*, Nartheciaceae, *Nigella*, Onagraceae, Orchidaceae, Oxalidaceae, *Oxyria/Rumex*, Papaveraceae, Penthoraceae, Phyllanthaceae, Plantaginaceae, Plumbaginaceae, Poaceae, Polemoniaceae, Polygalaceae, Polygonaceae, *Polygonum*, Polypodiales, Portulacaceae, Primulaceae, Ranunculaceae, *Ranunculus*, Resedaceae, Rubiaceae, Rutaceae, *Sanguisorba*, Santalaceae, Saxifragaceae, Scrophulariaceae, Solanaceae, *Teucrium*, *Thalictrum*, *Tofieldia*, *Trollius*, Urticaceae, Violaceae, Zygophyllaceae

S3: Coefficients and model fit based on lake sites only

Excluding bog sites from model fit improves the LOOCV RMSE to 0.13 (vs. 0.14), MAE to 0.10 (vs. 0.11) and squared correlation (R^2) of the predictions and observations to 0.69 (vs. 0.63). The model coefficients are shown in Supplementary Table 3.3. Coefficient estimates have the same direction as the model with bogs and lakes. Although the model fit improves, excluding bog sites from the model substantially reduces the applicability of the model to fossil records; lake records only constitute 35% of the total available fossil records.

Supplementary Table 3.3: Modern tree cover model coefficients for lake sites only

Coefficients (mean model with logit link)	**Estimate**	**Standard Error**	**P Value**
(Intercept)	-5.421	0.444	3.05e-34 ***
Tree pollen %	2.169	0.247	1.55e-18 ***
Shrub pollen %	-4.613	0.759	1.25e-09 ***
Needle share of AP%	-1.546	0.529	0.004 **
Needle share of AP%^2	3.241	0.583	2.69e-08 ***
AP Shannon index	5.239	0.483	2.14e-27 ***
AP Shannon index^2	-1.421	0.146	1.65e-22 ***
Elevation	0.001	0.001	0.317
AP pollen:elevation interaction	-0.001	0.001	0.016 *
SP pollen:elevation interaction	0.005	0.002	0.003 **
AP Shannon:elevation interaction	-0.003	0.001	0.005 **
AP Shannon^2:elevation interaction	0.001	0.000	1.02e-04 ***

Precision submodel (log link; after variable selection^)			
(Intercept)	1.089	0.257	2.26e-05 ***
Needle share of AP%	0.751	0.271	0.006 **
AP Shannon index	0.759	0.132	9.28e-09 ***

Significance codes: 0 = '***'; 0.001 = '**'; 0.01 = '*'; 0.05 = '.' 0.1; ' ' = 1

^Only significant covariates were included (at 5% significance)

S4: Coefficients and model fit without exclusion of sites >1000 m

Including higher elevation sites within the model reduces the LOOCV RMSE to 0.15 (vs. 0.14), MAE to 0.12 (vs. 0.11) and squared correlation (R^2) of the predictions and observations to 0.55 (vs. 0.63). The model coefficients are shown in Supplementary Table 3.4. Coefficient estimates have the same direction as the model that excludes higher elevation sites, with the exception of the dummy variable for lake or bog site, which becomes negative and significant (from positive and insignificant), and the interaction between elevation and whether a site was a lake or bog, which becomes positive (but insignificant (from negative and significant). The significance of the coefficients improves in several cases, most notably for elevation which becomes highly significant having been insignificant when excluding higher elevation sites. Although including high elevation records increases the spatiotemporal coverage of the tree cover reconstruction – the number of fossil records increases from 811 to 1050 - the impact on model fit is such that we have much less confidence in the reconstructions.

Supplementary Table 3.4: Modern tree cover model coefficients without exclusion of high (>1000 m) sites

Coefficients (mean model with logit link)	Estimate	Standard Error	P Value
(Intercept)	-5.249	0.346	6.26e-52 ***
Tree pollen %	2.447	0.178	6.58e-43 ***
Shrub pollen %	-3.044	0.495	7.92e-10 ***
Needle share of AP%	-1.599	0.418	1.28e-4 ***
Needle share of AP%^2	2.954	0.453	6.98e-11 ***
AP Shannon index	4.797	0.382	4.27e-36 ***
AP Shannon index^2	-1.214	0.117	2.39e-25 ***
Lake or bog site	-0.349	0.092	1.50e-4 ***
Elevation	0.002	3.74e-4	2.71e-6 ***
AP pollen:elevation interaction	-0.001	1.83e-4	1.76e-6 ***
SP pollen:elevation interaction	0.003	5.14e-4	4.62e-10 ***
AP Shannon:elevation interaction	-0.003	1.39e-4	3.59e-10 ***

AP Shannon^2:elevation interaction	0.003	5.14e-4	1.79e-11 ***
Lake or bog site:elevation interaction	0.000	8.08e-5	0.932
Precision submodel (log link; after variable selection^)			
(Intercept)	1.146	0.228	4.81e-7 ***
Needle share of AP%	0.500	0.271	0.009 **
AP Shannon index	0.473	0.132	4.42e-6 ***
Lake or bog site	0.210	0.098	0.032 *

Significance codes: 0 = '***'; 0.001 = '**'; 0.01 = '*'; 0.05 = '.' 0.1; ' ' = 1

^Only significant covariates were included (at 5% significance)

S5: Quantile mapping influence on model predictions

Supplementary Figure 3.1 (A–D) shows the impact of applying a quantile mapping model to the modern tree cover predictions solely based on the model of modern tree cover. The quantile mapping approach is designed to identify a transformation that matches the distribution of adjusted predictions to that of the observations (Gudmundsson et al., 2012). We used a smoothing spline regression curve to model the transformation, with the resulting calibration curve used to adjust modern and fossil pollen tree cover reconstructions, based on the approach from the R package *qmap* (Gudmundsson et al., 2012) and following Zanon et al. (2018). At the lower and higher levels of observed cover, quantile mapping reduces the respective over- and under-estimation.

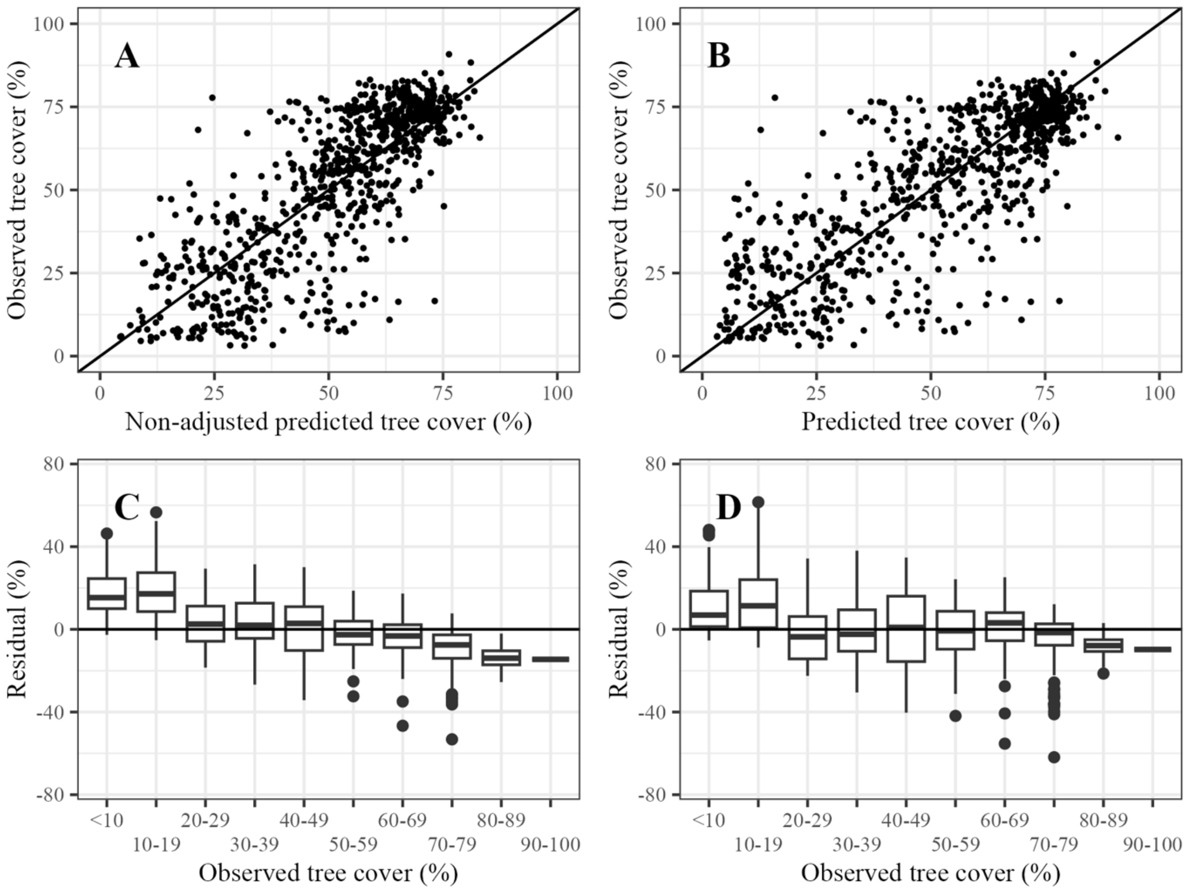

Supplementary Figure 3.1: Model performance: A – Non-adjusted predictions of tree cover compared to observed tree cover; B - Predictions of tree cover compared with observed tree cover; C - Differences between non-adjusted predictions and observations (residual), in bins of observed tree cover percentage; D - Differences between predictions and observations (residual), in bins of observed tree cover percentage

S6: Spatial structure of model predictions compared to observations

Supplementary Figure 3.2 is a 50km^2 map showing the grid cell averaged differences between the model predictions adjusted by quantile mapping, and observations. Difference refers to predictions minus observations. In general, there is no spatial patterning in the location of overestimates, except that there is a tendency for a grouping of cells with overestimates in the far north of Scandinavia and some sites in Ireland.

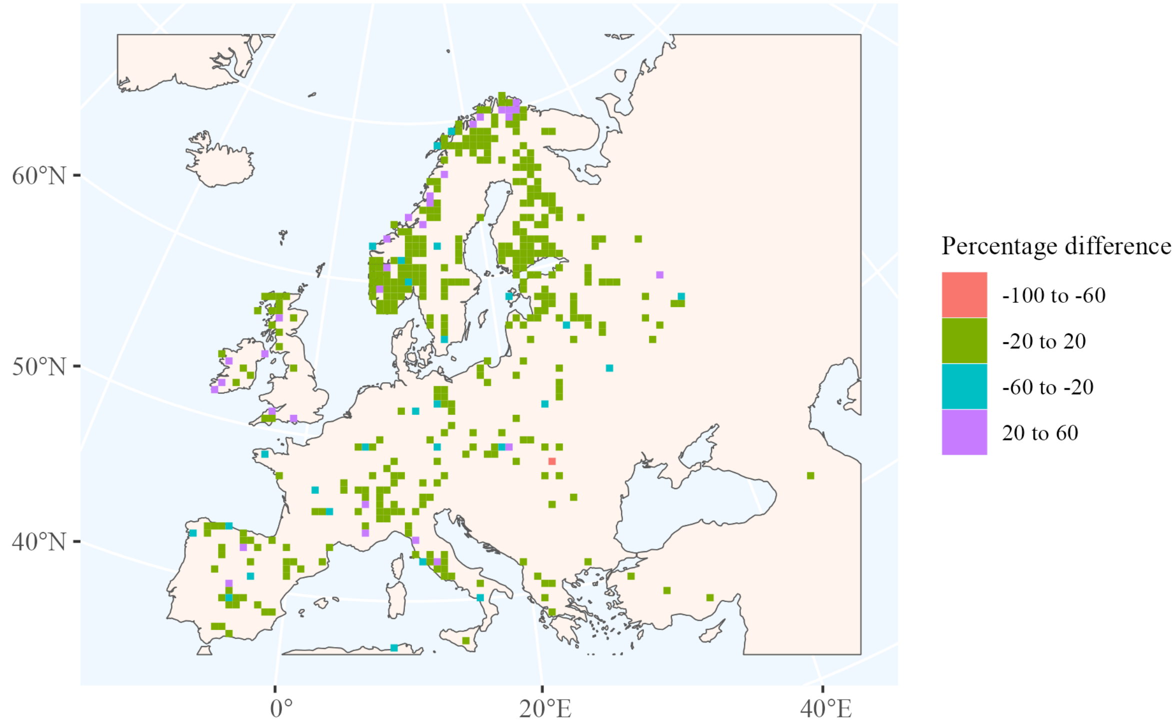

Supplementary Figure 3.2: Spatial structure of differences between predictions and observations.

S7: Arboreal pollen percentages compared with observed tree cover percentages

Raw arboreal pollen percentages tend to overestimate tree cover, with the range in AP% greater for lower observed tree cover groups (Supp. Fig. 3.3).

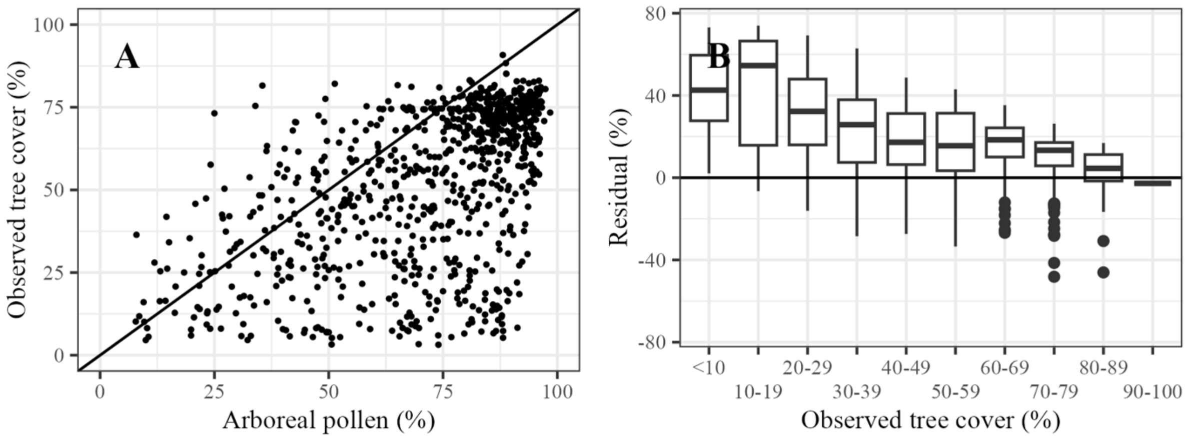

Supplementary Figure 3.3: Arboreal pollen percentage compared to observed tree cover: A - AP% compared to observed tree cover for each record; B - Differences between AP% and observations (residual), in bins of observed tree cover percentage

S8: Modern predictions compared with other reconstructions based on grid cell averages

Supplementary Figure 3.4 (A–D) shows the relationship between observations of tree cover and our predictions of tree cover compared with values extracted from the first bin of Zanon et al. (2018) and Serge et al. (2023) at the same spatial locations. Compared with Fig. 4, Supp. Fig. 3.4 averages tree cover values for each record by grid cell of the other reconstructions. Hence a single point in each panel may represent tree cover value for multiple records, if there were multiple records sharing a grid cell. There are less points within panels C and D compared to A and B because Serge et al. (2023) data is provided at much lower spatial resolution than Zanon et al. (2018) data.

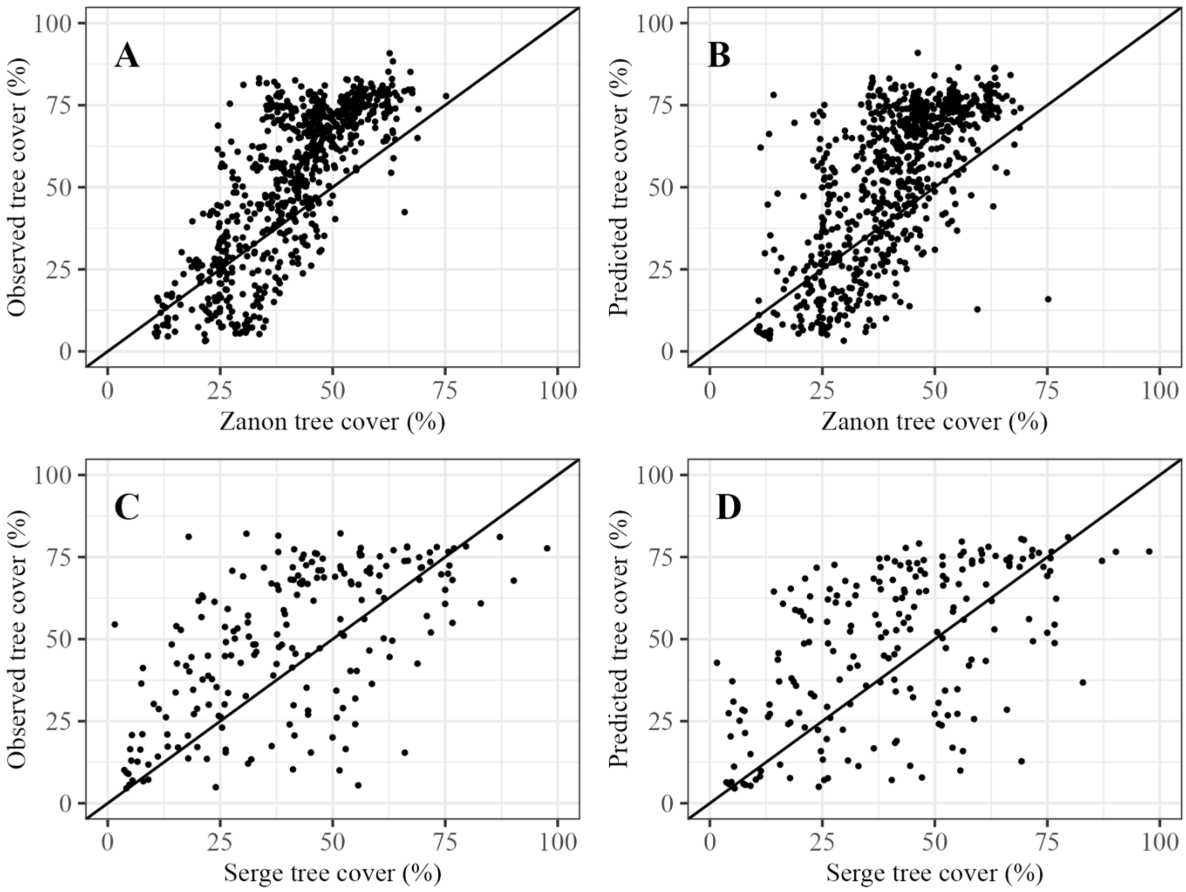

Supplementary Figure 3.4: Modern tree cover from Zanon et al (2018) per grid cell compared to (A) observed tree cover and (B) our predicted tree cover. Modern tree cover from Serge et al. (2023) per grid cell compared to (C) observed tree cover values and (D) our predicted tree cover.

<u>S9: Mean reconstructed tree cover</u>

The influence of using mean tree cover values rather than median values to describe tree cover changes through time is shown in Supp. Fig. 3.5. Compared to the median (Fig. 3.5), the maximum and minimum tree cover values are reduced, and the variation through time is more limited. However, the structure of the trend through time in tree cover remains the same.

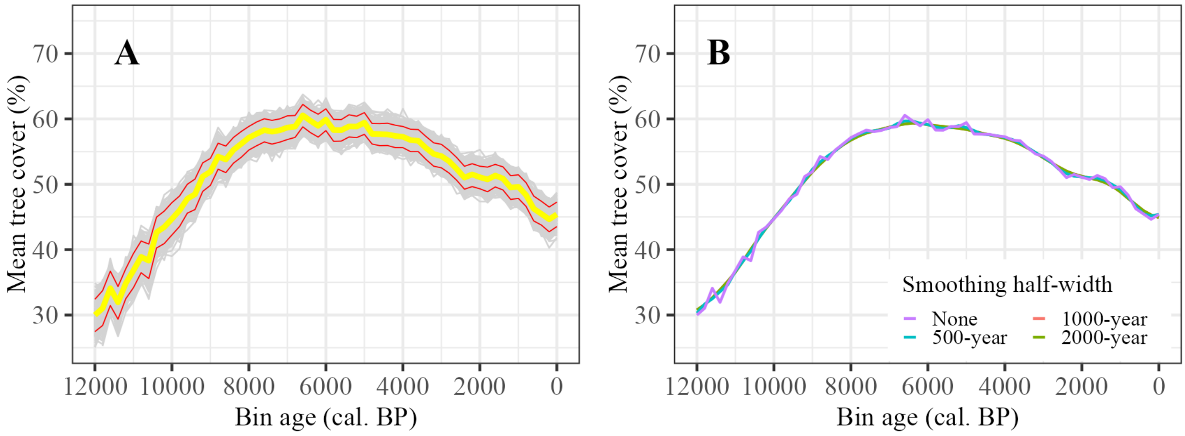

Supplementary Figure 3.5: A - Mean reconstructed tree cover for Europe from 12,000 to 0 cal. BP, with 95% confidence intervals for 1000 bootstrap resampling of records; B - Mean reconstructed tree cover for Europe from 12,000 to 0 cal. BP, with differing LOESS regression smoothing half-widths.

S10: Median reconstructed tree cover, with bootstrapped models

In order to generate reconstruction standard errors, the predictive model that linked observed tree cover to modern pollen data was generated 1000 times by bootstrapping the modern pollen data. These models were also used to generate the equivalent number of quantile mapping adjustments, by relating model predictions using the full dataset to observations. Together these elements were used to produce 1000 different reconstructions of tree cover for each fossil data sample, with prediction standard error calculated by sample and averaged by 200-year bin. As well as using the bootstrapped reconstructions to generate the standard error, we can use the median of these bootstraps as another way of assessing the confidence in the median reconstruction. Supplementary Figure 3.6 shows the median tree cover estimate, together with the bootstrapped medians of tree cover based on the different models and quantile mapping adjustment generated. Although the bootstrapped medians follow the same general pattern as the reconstructed median, maximum tree cover values for the reconstruction are generally on the higher side compared with the bootstrapped medians, implying that some training samples may have a larger influence on the generated model than others.

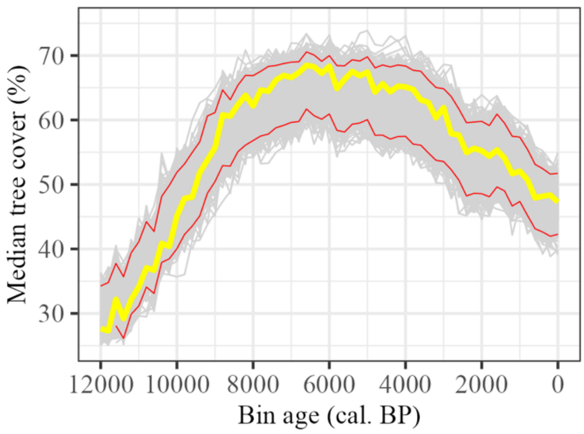

Supplementary Figure 3.6: Median reconstructed tree cover for Europe from 12,000 to 0 cal. BP, with 95% confidence intervals for models generated through 1000 bootstrap resamples of model training data

S11: Gridded maps of reconstructed tree cover through time

Gridded maps of reconstructed tree cover are shown below. The values in each cell are the mean of binned tree cover reconstructions for records located in each 50km^2 grid cell. Bins are 200-years in width, with ages referring to mid-point of each bin (e.g. the bin labelled 12,600 cal. BP represents the interval 12,700–12,500 cal. BP).

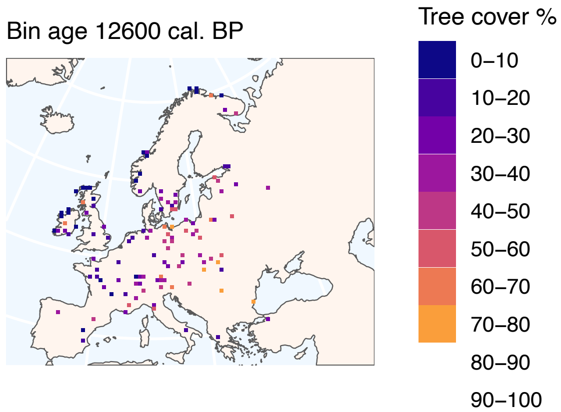

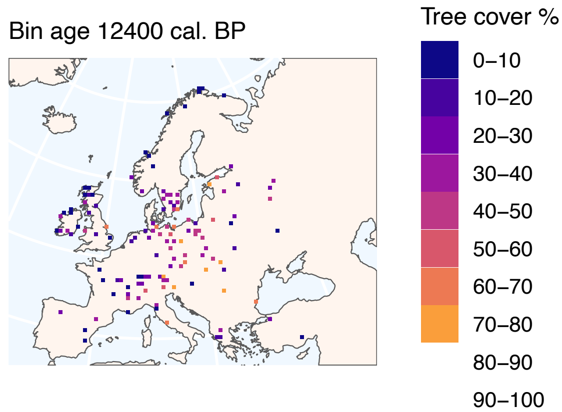

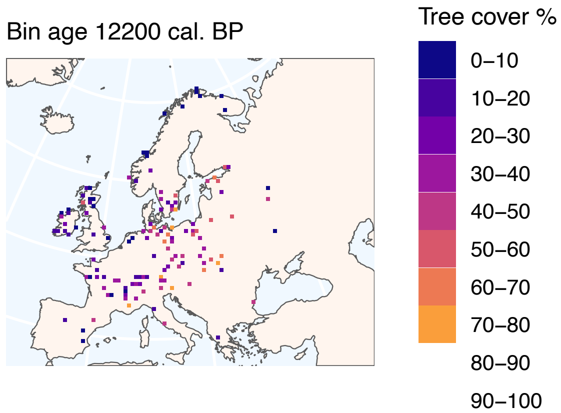

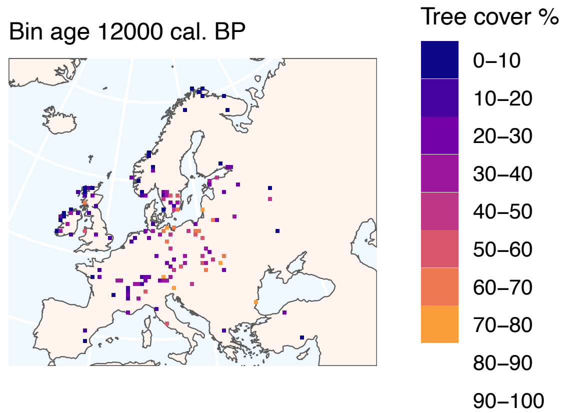

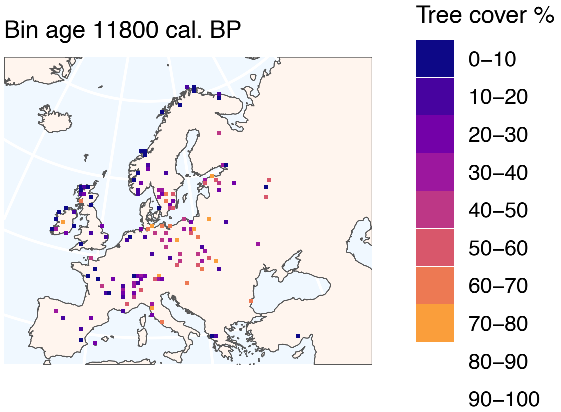
Bin age 11800 cal. BP
Tree cover %
0–10
10–20
20–30
30–40
40–50
50–60
60–70
70–80
80–90
90–100

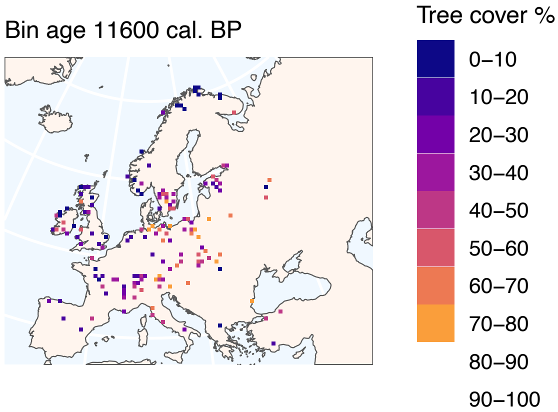
Bin age 11600 cal. BP
Tree cover %
0–10
10–20
20–30
30–40
40–50
50–60
60–70
70–80
80–90
90–100

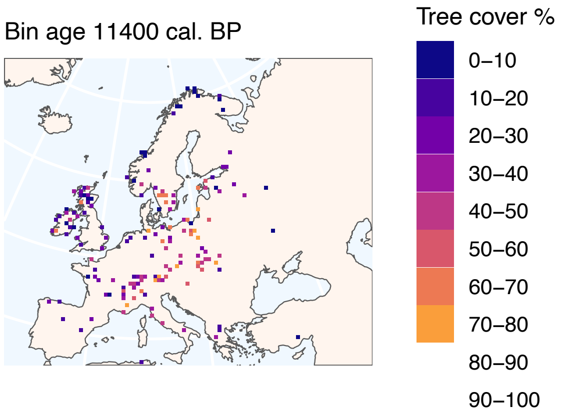
Bin age 11400 cal. BP
Tree cover %
0–10
10–20
20–30
30–40
40–50
50–60
60–70
70–80
80–90
90–100

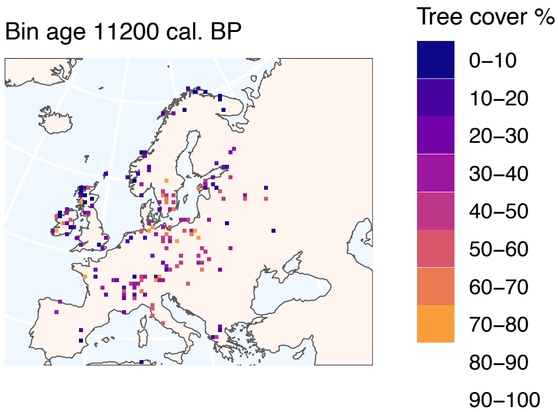
Bin age 11200 cal. BP
Tree cover %
0–10
10–20
20–30
30–40
40–50
50–60
60–70
70–80
80–90
90–100

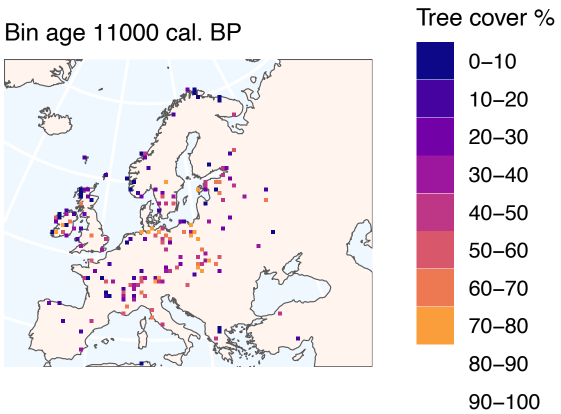
Bin age 11000 cal. BP
Tree cover %
0–10
10–20
20–30
30–40
40–50
50–60
60–70
70–80
80–90
90–100

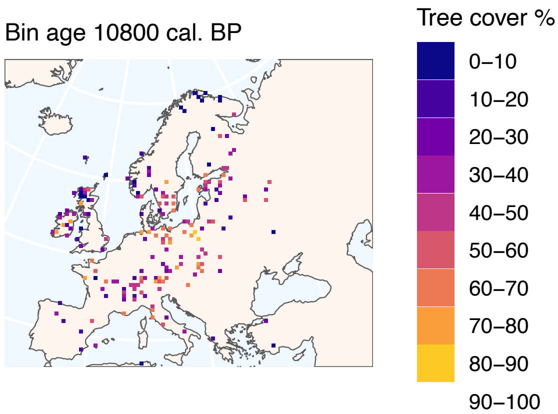
Bin age 10800 cal. BP
Tree cover %
0–10
10–20
20–30
30–40
40–50
50–60
60–70
70–80
80–90
90–100

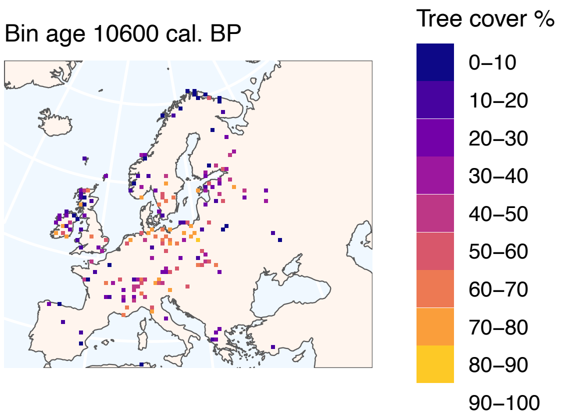
Bin age 10600 cal. BP
Tree cover %
0–10
10–20
20–30
30–40
40–50
50–60
60–70
70–80
80–90
90–100

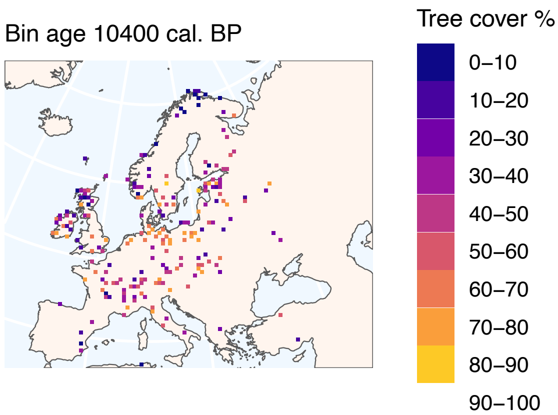
Bin age 10400 cal. BP
Tree cover %
0–10
10–20
20–30
30–40
40–50
50–60
60–70
70–80
80–90
90–100

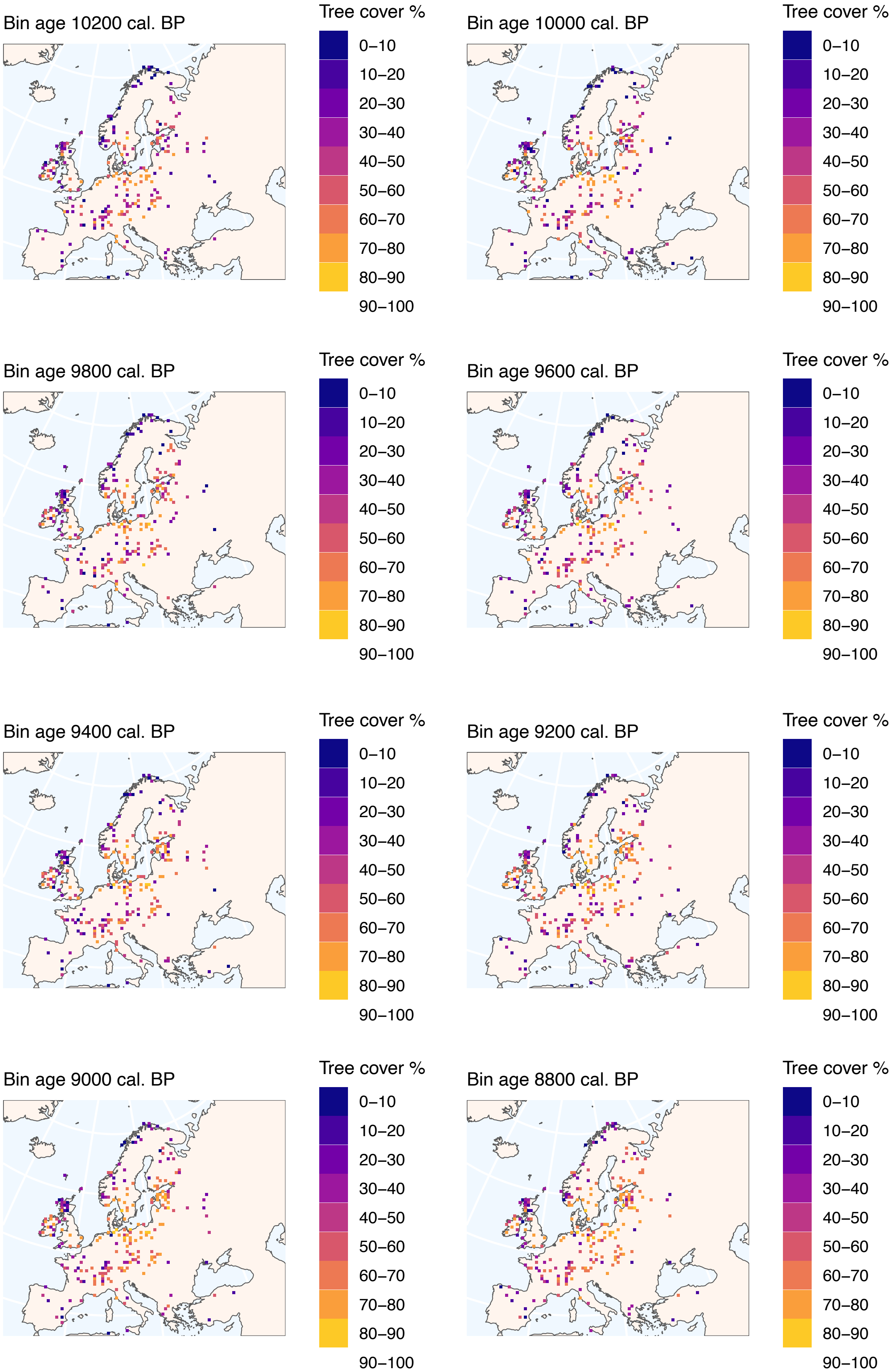
Bin age 10200 cal. BP
Tree cover %
0–10
10–20
20–30
30–40
40–50
50–60
60–70
70–80
80–90
90–100
Bin age 10000 cal. BP
Tree cover %
0–10
10–20
20–30
30–40
40–50
50–60
60–70
70–80
80–90
90–100
Bin age 9800 cal. BP
Tree cover %
0–10
10–20
20–30
30–40
40–50
50–60
60–70
70–80
80–90
90–100
Bin age 9600 cal. BP
Tree cover %
0–10
10–20
20–30
30–40
40–50
50–60
60–70
70–80
80–90
90–100
Bin age 9400 cal. BP
Tree cover %
0–10
10–20
20–30
30–40
40–50
50–60
60–70
70–80
80–90
90–100
Bin age 9200 cal. BP
Tree cover %
0–10
10–20
20–30
30–40
40–50
50–60
60–70
70–80
80–90
90–100
Bin age 9000 cal. BP
Tree cover %
0–10
10–20
20–30
30–40
40–50
50–60
60–70
70–80
80–90
90–100
Bin age 8800 cal. BP
Tree cover %
0–10
10–20
20–30
30–40
40–50
50–60
60–70
70–80
80–90
90–100

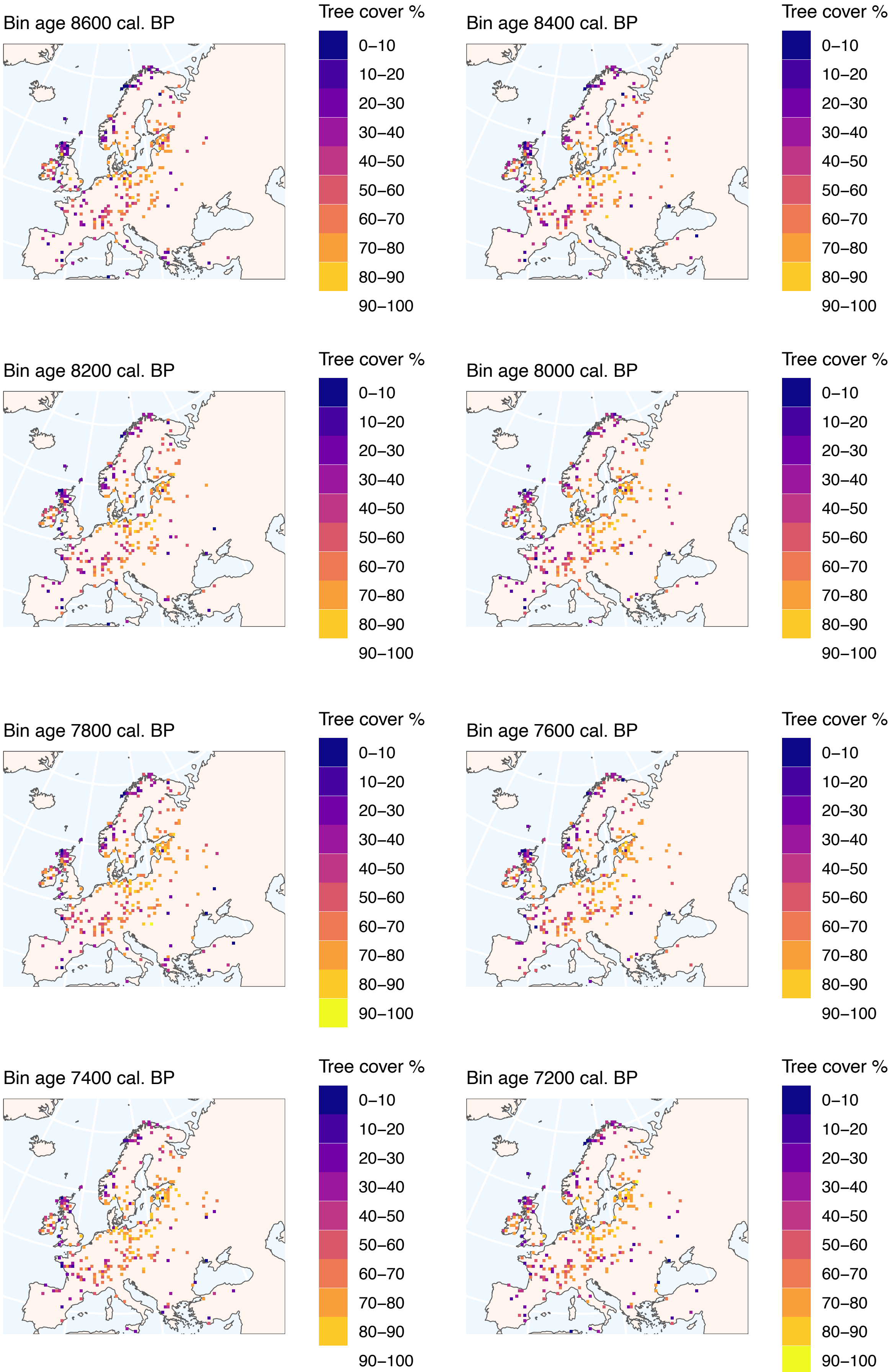
Bin age 8600 cal. BP
Tree cover %
0–10
10–20
20–30
30–40
40–50
50–60
60–70
70–80
80–90
90–100
Bin age 8400 cal. BP
Tree cover %
0–10
10–20
20–30
30–40
40–50
50–60
60–70
70–80
80–90
90–100
Bin age 8200 cal. BP
Tree cover %
0–10
10–20
20–30
30–40
40–50
50–60
60–70
70–80
80–90
90–100
Bin age 8000 cal. BP
Tree cover %
0–10
10–20
20–30
30–40
40–50
50–60
60–70
70–80
80–90
90–100
Bin age 7800 cal. BP
Tree cover %
0–10
10–20
20–30
30–40
40–50
50–60
60–70
70–80
80–90
90–100
Bin age 7600 cal. BP
Tree cover %
0–10
10–20
20–30
30–40
40–50
50–60
60–70
70–80
80–90
90–100
Bin age 7400 cal. BP
Tree cover %
0–10
10–20
20–30
30–40
40–50
50–60
60–70
70–80
80–90
90–100
Bin age 7200 cal. BP
Tree cover %
0–10
10–20
20–30
30–40
40–50
50–60
60–70
70–80
80–90
90–100

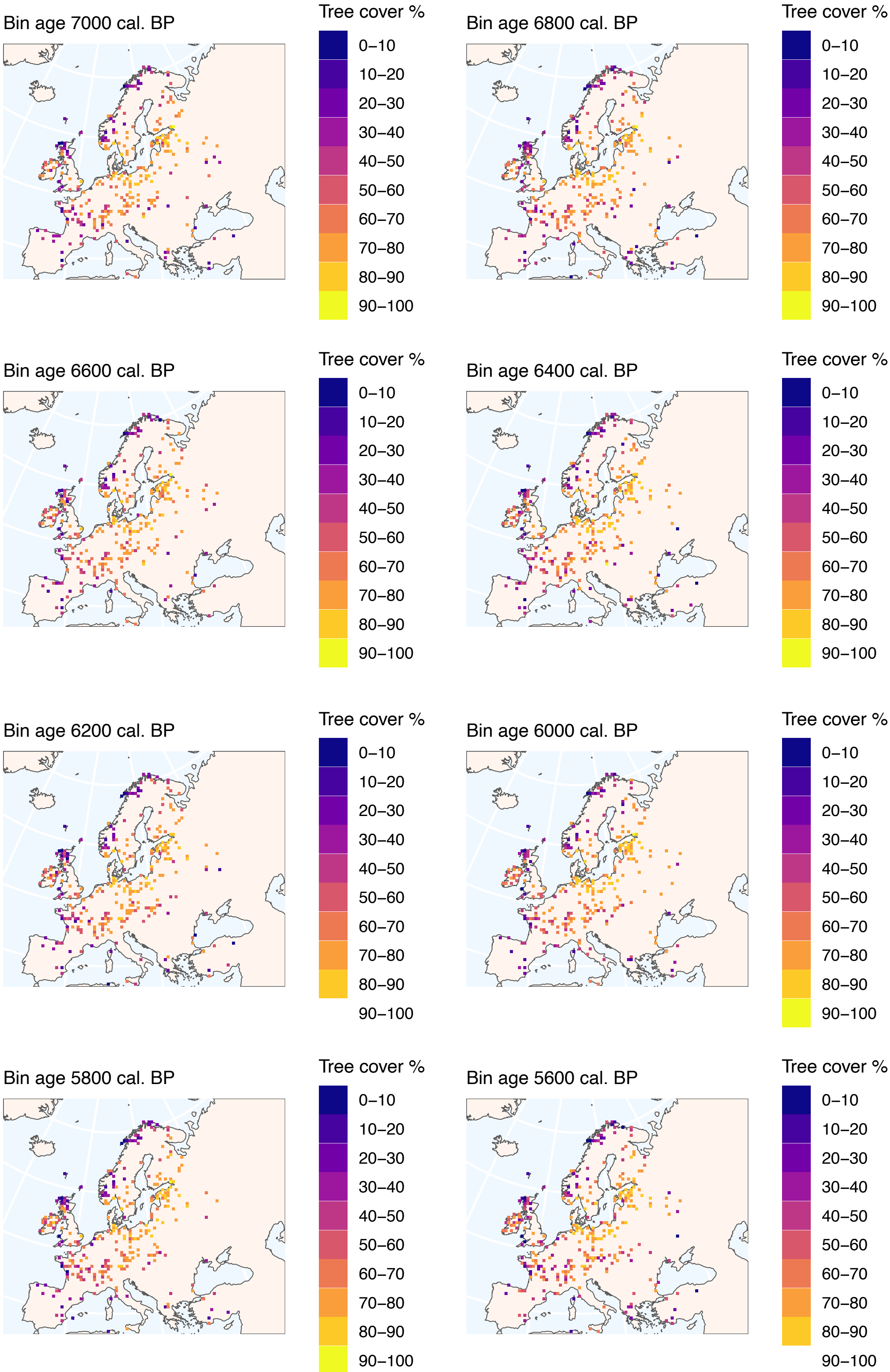
Bin age 7000 cal. BP
Tree cover %
0–10
10–20
20–30
30–40
40–50
50–60
60–70
70–80
80–90
90–100
Bin age 6800 cal. BP
Tree cover %
0–10
10–20
20–30
30–40
40–50
50–60
60–70
70–80
80–90
90–100
Bin age 6600 cal. BP
Tree cover %
0–10
10–20
20–30
30–40
40–50
50–60
60–70
70–80
80–90
90–100
Bin age 6400 cal. BP
Tree cover %
0–10
10–20
20–30
30–40
40–50
50–60
60–70
70–80
80–90
90–100
Bin age 6200 cal. BP
Tree cover %
0–10
10–20
20–30
30–40
40–50
50–60
60–70
70–80
80–90
90–100
Bin age 6000 cal. BP
Tree cover %
0–10
10–20
20–30
30–40
40–50
50–60
60–70
70–80
80–90
90–100
Bin age 5800 cal. BP
Tree cover %
0–10
10–20
20–30
30–40
40–50
50–60
60–70
70–80
80–90
90–100
Bin age 5600 cal. BP
Tree cover %
0–10
10–20
20–30
30–40
40–50
50–60
60–70
70–80
80–90
90–100

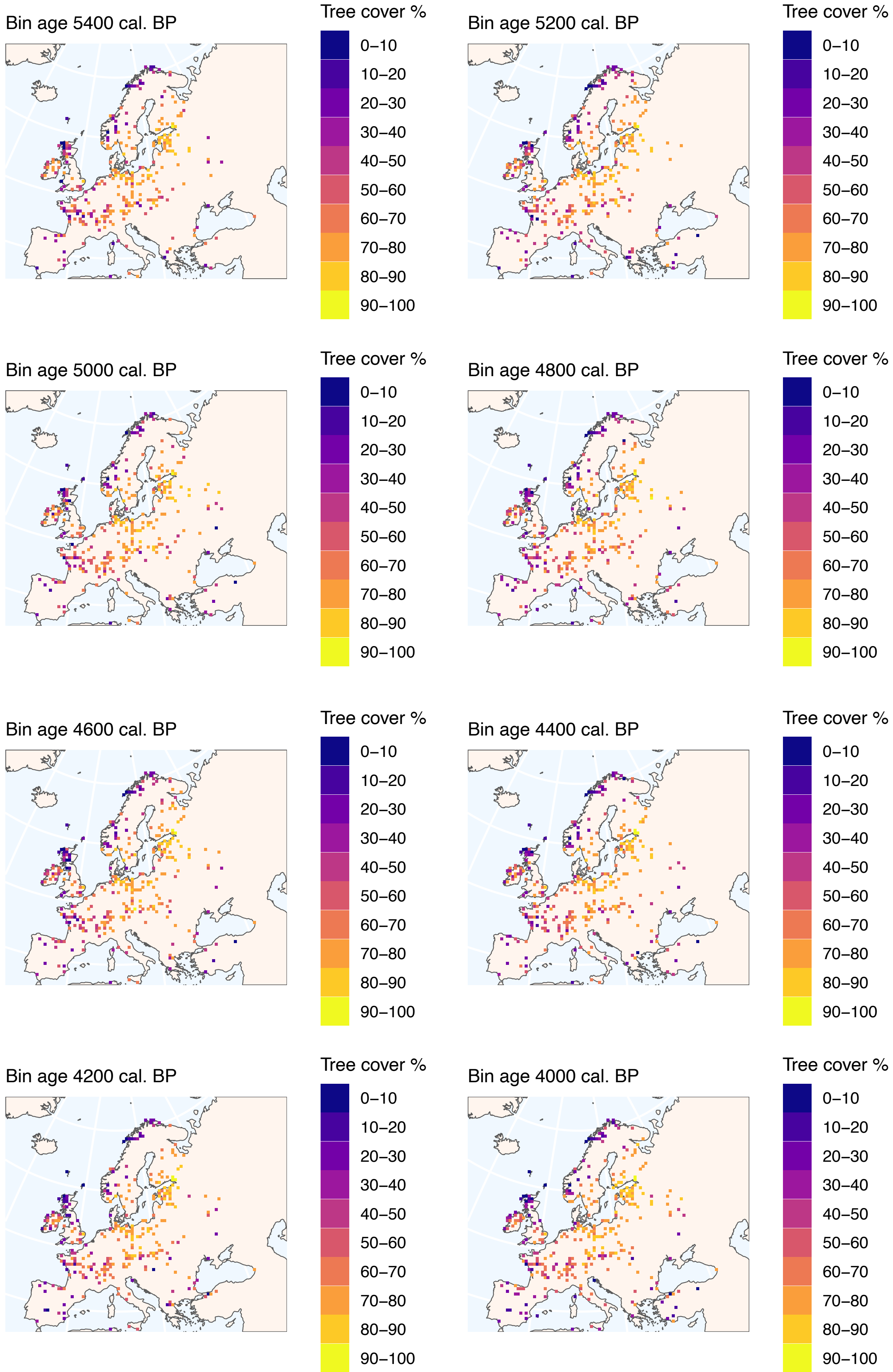
Bin age 5400 cal. BP
Tree cover %
0–10
10–20
20–30
30–40
40–50
50–60
60–70
70–80
80–90
90–100
Bin age 5200 cal. BP
Tree cover %
0–10
10–20
20–30
30–40
40–50
50–60
60–70
70–80
80–90
90–100
Bin age 5000 cal. BP
Tree cover %
0–10
10–20
20–30
30–40
40–50
50–60
60–70
70–80
80–90
90–100
Bin age 4800 cal. BP
Tree cover %
0–10
10–20
20–30
30–40
40–50
50–60
60–70
70–80
80–90
90–100
Bin age 4600 cal. BP
Tree cover %
0–10
10–20
20–30
30–40
40–50
50–60
60–70
70–80
80–90
90–100
Bin age 4400 cal. BP
Tree cover %
0–10
10–20
20–30
30–40
40–50
50–60
60–70
70–80
80–90
90–100
Bin age 4200 cal. BP
Tree cover %
0–10
10–20
20–30
30–40
40–50
50–60
60–70
70–80
80–90
90–100
Bin age 4000 cal. BP
Tree cover %
0–10
10–20
20–30
30–40
40–50
50–60
60–70
70–80
80–90
90–100

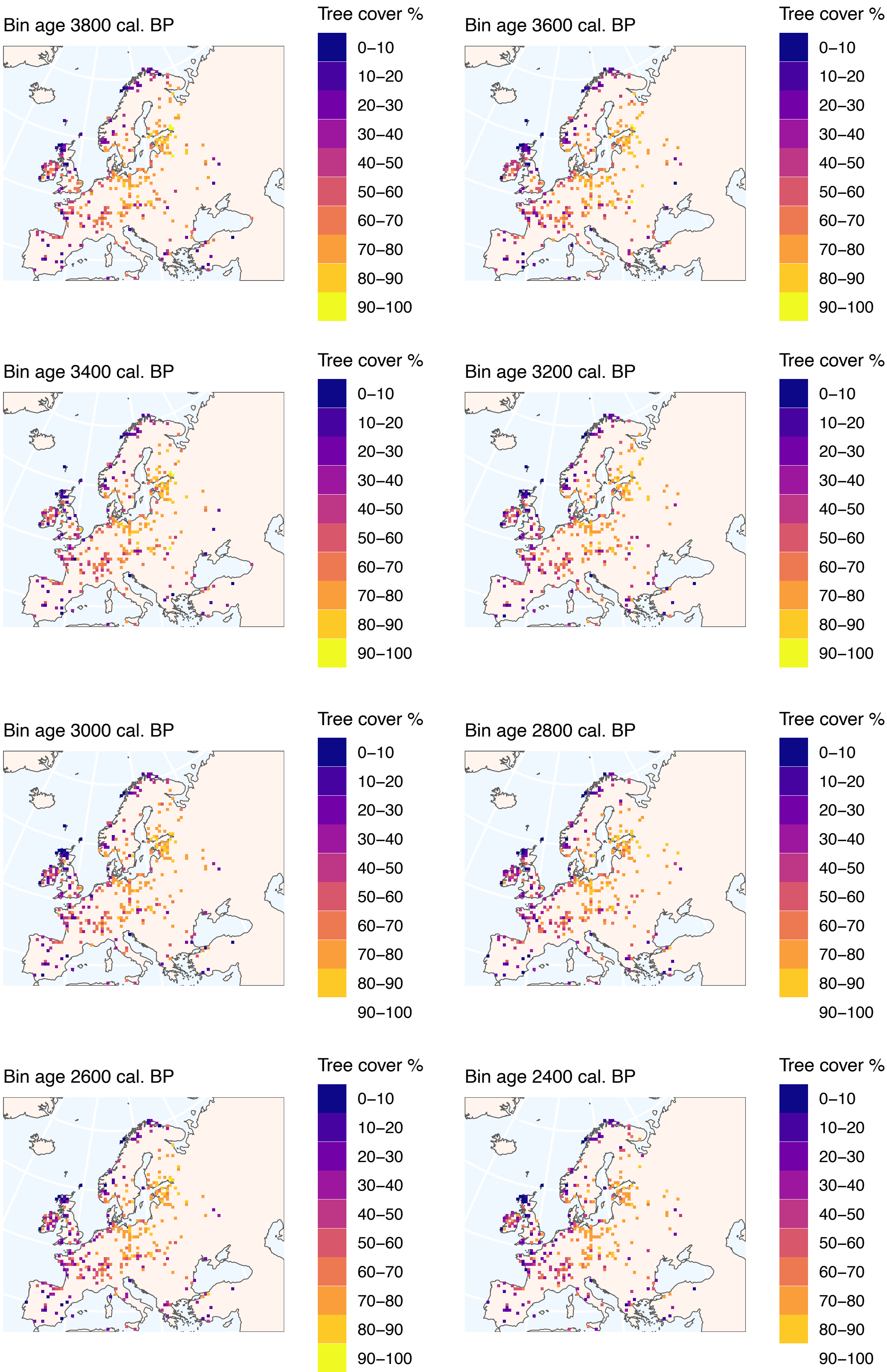
Bin age 3800 cal. BP
Tree cover %
0–10
10–20
20–30
30–40
40–50
50–60
60–70
70–80
80–90
90–100
Bin age 3600 cal. BP
Tree cover %
0–10
10–20
20–30
30–40
40–50
50–60
60–70
70–80
80–90
90–100
Bin age 3400 cal. BP
Tree cover %
0–10
10–20
20–30
30–40
40–50
50–60
60–70
70–80
80–90
90–100
Bin age 3200 cal. BP
Tree cover %
0–10
10–20
20–30
30–40
40–50
50–60
60–70
70–80
80–90
90–100
Bin age 3000 cal. BP
Tree cover %
0–10
10–20
20–30
30–40
40–50
50–60
60–70
70–80
80–90
90–100
Bin age 2800 cal. BP
Tree cover %
0–10
10–20
20–30
30–40
40–50
50–60
60–70
70–80
80–90
90–100
Bin age 2600 cal. BP
Tree cover %
0–10
10–20
20–30
30–40
40–50
50–60
60–70
70–80
80–90
90–100
Bin age 2400 cal. BP
Tree cover %
0–10
10–20
20–30
30–40
40–50
50–60
60–70
70–80
80–90
90–100

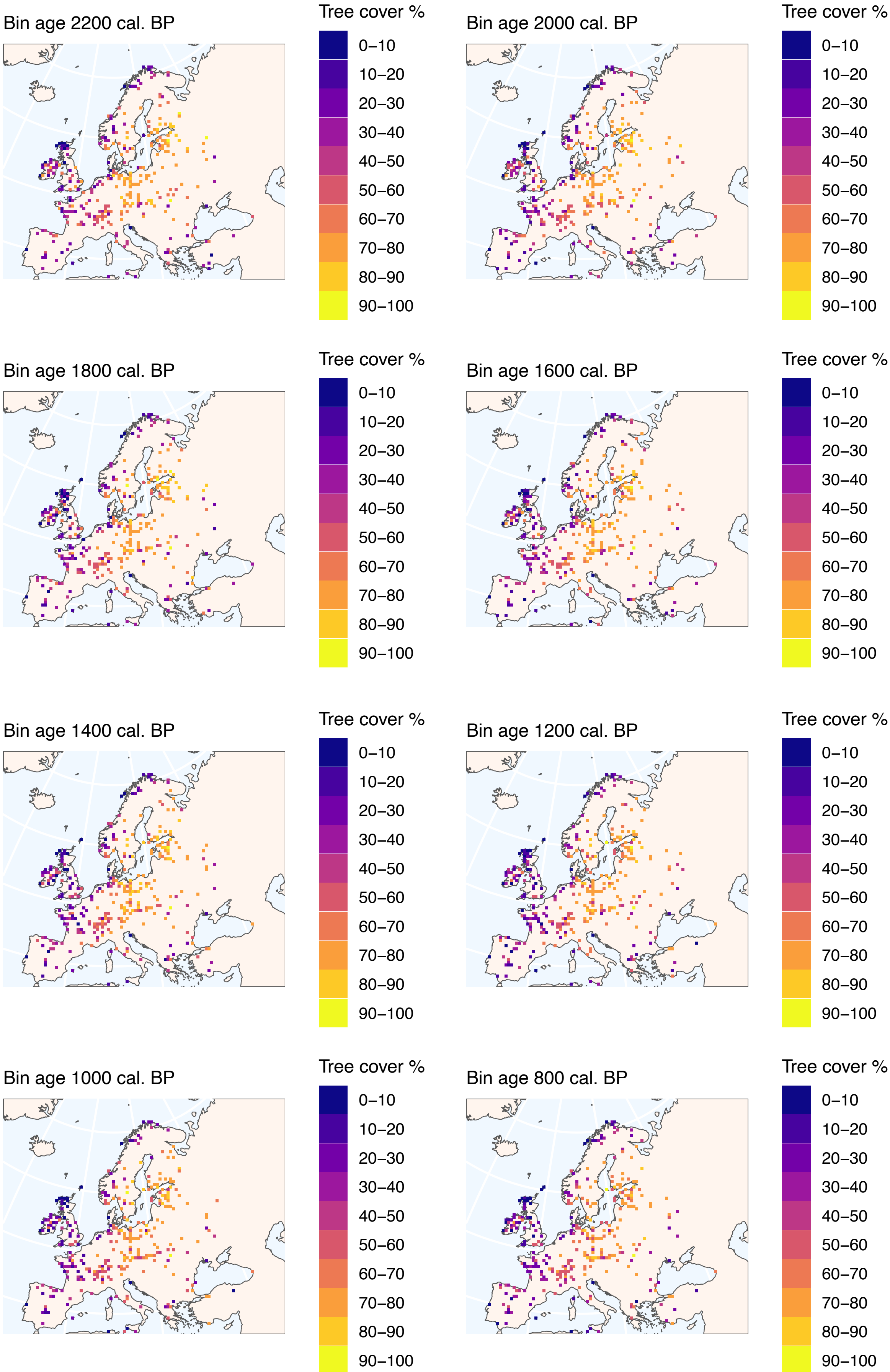
Bin age 2200 cal. BP
Tree cover %
0–10
10–20
20–30
30–40
40–50
50–60
60–70
70–80
80–90
90–100
Bin age 2000 cal. BP
Tree cover %
0–10
10–20
20–30
30–40
40–50
50–60
60–70
70–80
80–90
90–100
Bin age 1800 cal. BP
Tree cover %
0–10
10–20
20–30
30–40
40–50
50–60
60–70
70–80
80–90
90–100
Bin age 1600 cal. BP
Tree cover %
0–10
10–20
20–30
30–40
40–50
50–60
60–70
70–80
80–90
90–100
Bin age 1400 cal. BP
Tree cover %
0–10
10–20
20–30
30–40
40–50
50–60
60–70
70–80
80–90
90–100
Bin age 1200 cal. BP
Tree cover %
0–10
10–20
20–30
30–40
40–50
50–60
60–70
70–80
80–90
90–100
Bin age 1000 cal. BP
Tree cover %
0–10
10–20
20–30
30–40
40–50
50–60
60–70
70–80
80–90
90–100
Bin age 800 cal. BP
Tree cover %
0–10
10–20
20–30
30–40
40–50
50–60
60–70
70–80
80–90
90–100

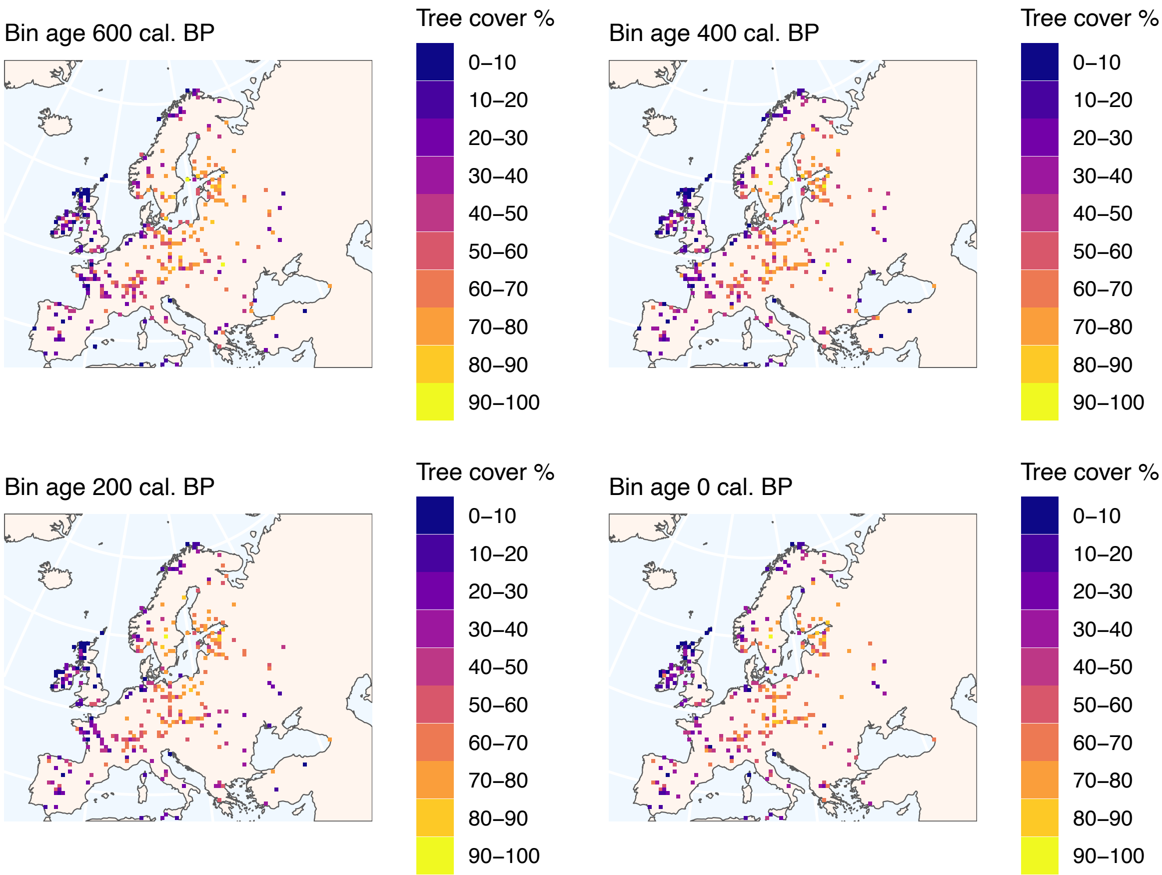

S12: Data by biogeographical region

Supplementary Table 3.5 shows the breakdown of fossil pollen data by biogeographical region, with the number of records and the number of samples by 200-year bin within each region. Biogeographical regions are based on the European Environment Agency modern classification (European Environment Agency, 2016).

Supplementary Table 3.5: Data by biogeographical region

Bioregion	**Number of records**	**Number of temporal bins**
Alpine	67	2377
Anatolian	3	75
Arctic	7	279
Atlantic	284	7117
BlackSea	6	157
Boreal	137	4127

Continental	219	6840
Mediterranean	73	1701
Pannonian	13	368
Steppic	1	38

S13: Median reconstructed tree cover based on bin widths from other reconstructions

The different tree cover reconstructions use different temporal bins, which can have an influence on our reconstructed median tree cover. Supplementary Figure 3.7 shows our median tree cover reconstruction based on a standard 200-year bin, that same reconstruction but based on the bins used by Serge et. al. (2023) and Zanon et al. (2018). Serge et al. (2023) temporal bins cover 500-year intervals before 700 cal. BP and for 700-350 cal. BP, 350-100 cal. BP and 100 cal. BP- present. Zanon et al. (2018) temporal bins cover 250-year intervals. Although the trend in median tree cover remains the same through time, utilising the longer bin widths from Serge et al. (2023) has the effect of reducing both the variability and the range in median tree cover values.

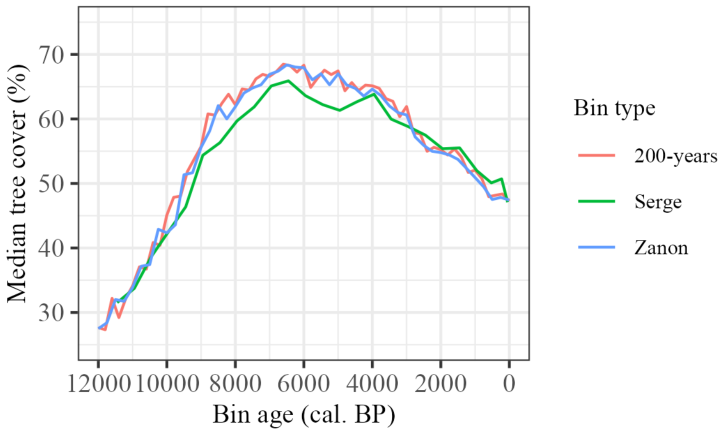

Supplementary Figure 3.7: Median reconstructed tree cover for Europe from 12,000 to 0 cal. BP, based on different bin widths used in other vegetation reconstructions.

S14: Median reconstructed tree cover on upper and lower age model ranges

There is uncertainty associated with the dates used to construct age-depth models for the pollen records, and this is promulgated into uncertainties assigned to the sample ages in the age model. We investigated the implications of this uncertainty on median tree cover through time, by recalculating median tree cover based on the interquartile ranges of age model values (see Supp. Fig. 3.8). The lower quartile median value represents the 25% lower estimate of ages for each sample (older), with the upper quartile representing the 75% upper estimate of ages (younger). Due to the binning approach however, the impact of using different age model values for each sample is minimal. As Zanon et al. (2018) was published prior to the development of INTCAL20 (Reimer et al., 2020) and

Marine20 (Heaton et al., 2020) calibration curves, some differences between our tree cover reconstructions may reflect differences in age models. Similarly, Serge et al. (2023) use the author's original age models, or those published in earlier datasets. Again, this use of different age models may have an impact on the comparison between median tree cover reconstructions.

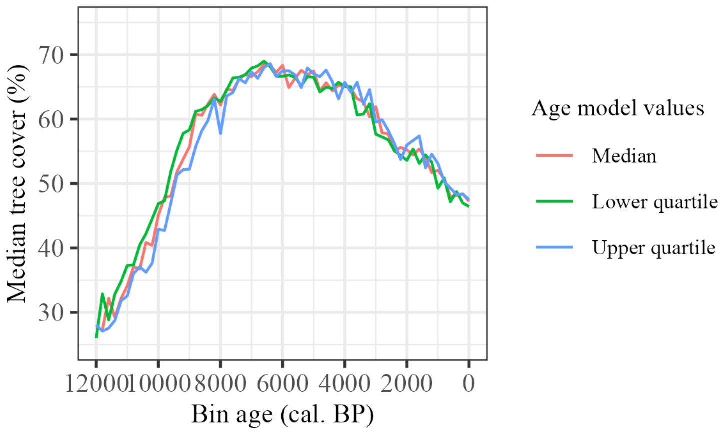

Supplementary Figure 3.8: Mean reconstructed tree cover for Europe from 12,000 to 0 cal. BP, calculated using different fossil sample age model estimates

S15: Median tree cover reconstructions based on grid cell averages

Comparisons of the median tree cover from our reconstructions with those from the Serge et al. (2023) and Zanon et al. (2018) data (Fig. 3.8) are based on individual pollen record locations. However, as the data from the other reconstructions are grid cell averages, the calculation of the median tree cover through time will include multiple instances of individual grid cells, where record locations share a single grid cell. This is more likely for the Serge et al. (2023) data, where reconstructions are based on larger 1° grid cells. To test the potential implications of multiple fossil record locations being within a single grid cell, Supplementary Figure 3.9 shows median tree cover values for these other reconstructions, but based on single values for each overlapping grid cell. Although the general trend of the tree cover medians remains the same, there is a slight increase in median tree cover values for the median reconstructions based on the data from Serge et al. (2023) and Zanon et al. (2018).

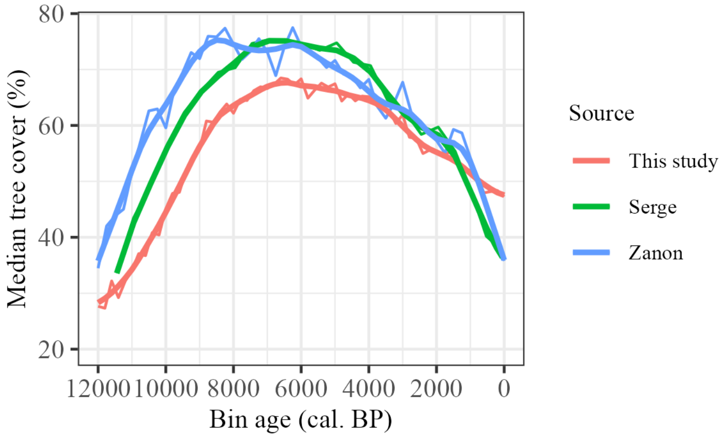

Supplementary Figure 3.9: Mean reconstructed tree cover for Europe from 12,000 to 0 cal. BP, with reconstructions for Serge et al. (2023) and Zanon et al. (2018) data based on grid cell averages rather than record values. Smoothed lines reflect LOESS fitted regression with 1000-year halfwidth.

S16: Median tree cover reconstructions based on the Atlantic, Boreal, Continental and Mediterranean biogeographical regions only

Limiting the data to records within the Atlantic, Boreal, Continental and Mediterranean regions has a limited effect on pan-European median tree cover reconstructions (Supp. Fig. 3.10).

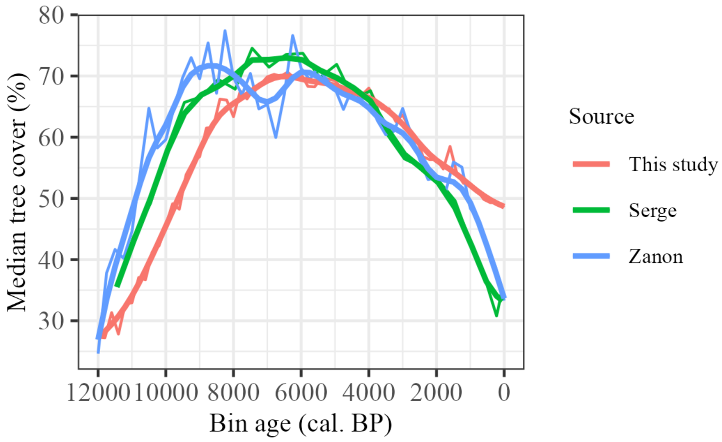

Supplementary Figure 3.10: Mean reconstructed tree cover for Europe from 12,000 to 0 cal. BP, based on records within the Atlantic, Boreal, Continental and Mediterranean biogeographical regions only. Smoothed lines reflect LOESS fitted regression with 1000-year halfwidth.

3.9.1. Supplement references

Adeleye, M. A., Haberle, S. G., McWethy, D., Connor, S. E., and Stevenson, J.: Environmental change during the last glacial on an ancient land bridge of southeast Australia, J Biogeogr, 48, 2946–2960, https://doi.org/10.1111/jbi.14255, 2021a.

Adeleye, M. A., Haberle, S. G., Harris, S., Hopf, F. V., Connor, S., and Stevenson, J.: Holocene heathland development in temperate oceanic Southern Hemisphere: Key drivers in a global context, J Biogeogr, 48, 1048–1062, https://doi.org/10.1111/jbi.14057, 2021b.

Beck, K. K., Fletcher, M.-S., Gadd, P. S., Heijnis, H., and Jacobsen, G. E.: An early onset of ENSO influence in the extra-tropics of the southwest Pacific inferred from a 14, 600 year high resolution multi-proxy record from Paddy's Lake, northwest Tasmania, Quat Sci Rev, 157, 164–175, https://doi.org/10.1016/j.quascirev.2016.12.001, 2017.

Black, M. P., Mooney, S. D., and Haberle, S. G.: The fire, human and climate nexus in the Sydney Basin, eastern Australia, Holocene, 17, 469–480, https://doi.org/10.1177/0959683607077024, 2007.

Bush, M. B., Correa-Metrio, A., van Woesik, R., Collins, A., Hanselman, J., Martinez, P., and McMichael, C. N. H.: Modern pollen assemblages of the Neotropics, J Biogeogr, 48, 231–241, https://doi.org/10.1111/jbi.13960, 2021.

Chen, H.-Y., Xu, D.-Y., Liao, M.-N., Li, K., Ni, J., Cao, X.-Y., Cheng, B., Hao, X.-D., Kong, Z.-C., Li, S.-F., Li, X.-Q., Liu, G.-X., Liu, P.-M., Liu, X.-Q., Sun, X.-J., Tang, L.-Y., Wei, H.-C., Xu, Q.-H., Yan, S., Yang, X.-D., Yang, Z.-J., Yu, G., Zhang, Y., Zhang, Z.-Y., Zhao, K.-L., Zheng, Z., and Ulrike, H.: A modern pollen dataset of China, Chinese Journal of Plant Ecology, 45, 799–808, https://doi.org/10.17521/cjpe.2021.0024, 2021.

Davis, B. A. S., Chevalier, M., Sommer, P., Carter, V. A., Finsinger, W., Mauri, A., Phelps, L. N., Zanon, M., Abegglen, R., Åkesson, C. M., Alba-Sánchez, F., Anderson, R. S., Antipina, T. G., Atanassova, J. R., Beer, R., Belyanina, N. I., Blyakharchuk, T. A., Borisova, O. K., Bozilova, E., Bukreeva, G., Bunting, M. J., Clò, E., Colombaroli, D., Combourieu-Nebout, N., Desprat, S., Di Rita, F., Djamali, M., Edwards, K. J., Fall, P. L., Feurdean, A., Fletcher, W., Florenzano, A., Furlanetto, G., Gaceur, E., Galimov, A. T., Gałka, M., García-Moreiras, I., Giesecke, T., Grindean, R., Guido, M. A., Gvozdeva, I. G., Herzschuh, U., Hjelle, K. L., Ivanov, S., Jahns, S., Jankovska, V., Jiménez-Moreno, G., Karpińska-Kołaczek, M., Kitaba, I., Kołaczek, P., Lapteva, E. G., Latałowa, M., Lebreton, V., Leroy, S., Leydet, M., Lopatina, D. A., López-Sáez, J. A., Lotter, A. F., Magri, D., Marinova, E., Matthias, I., Mavridou, A., Mercuri, A. M., Mesa-Fernández, J. M., Mikishin, Y. A., Milecka, K., Montanari, C., Morales-Molino, C., Mrotzek, A., Muñoz Sobrino, C., Naidina, O. D., Nakagawa, T., Nielsen, A. B., Novenko, E. Y., Panajiotidis, S., Panova, N. K., Papadopoulou, M., Pardoe, H. S., Pędziszewska, A., Petrenko, T. I., Ramos-Román, M. J., Ravazzi, C., Rösch, M., Ryabogina, N., Sabariego Ruiz, S., Salonen, J. S., Sapelko, T. V., Schofield, J. E., Seppä, H., Shumilovskikh, L., Stivrins, N., Stojakowits, P., Svobodova Svitavska, H., Święta-Musznicka, J., Tantau, I., Tinner, W., Tobolski, K., Tonkov, S., Tsakiridou, M., et al.: The Eurasian Modern Pollen Database (EMPD), version 2, Earth Syst Sci Data, 12, 2423–2445, https://doi.org/10.5194/essd-12-2423-2020, 2020.

Dodson, J. R.: A vegetation history from north-east Nelson, New Zealand, N Z J Bot, 16, 371–378, https://doi.org/10.1080/0028825X.1978.10425144, 1978.

Dodson, J. R. and Intoh, M.: Prehistory and palaeoecology of Yap, federated states of Micronesia, Quat Int, 59, 17–26, https://doi.org/10.1016/S1040-6182(98)00068-8, 1999.

Dugerdil, L., Joannin, S., Peyron, O., Jouffroy-Bapicot, I., Vannière, B., Boldgiv, B., Unkelbach, J., Behling, H., and Ménot, G.: Climate reconstructions based on GDGT and pollen surface datasets from Mongolia and Baikal area: calibrations and applicability to extremely cold–dry environments over the Late Holocene, Clim Past, 17, 1199–1226, https://doi.org/10.5194/cp-17-1199-2021, 2021.

European Environment Agency: Biogeographical regions, https://sdi.eea.europa.eu/catalogue/srv/api/records/11db8d14-f167-4cd5-9205-95638dfd9618, 2016.

Heaton, T. J., Köhler, P., Butzin, M., Bard, E., Reimer, R. W., Austin, W. E. N., Bronk Ramsey, C., Grootes, P. M., Hughen, K. A., Kromer, B., Reimer, P. J., Adkins, J., Burke, A., Cook, M. S., Olsen, J., and Skinner, L. C.: Marine20—The Marine Radiocarbon Age Calibration Curve (0–55,000 cal BP), Radiocarbon, 62, 779–820, https://doi.org/10.1017/RDC.2020.68, 2020.

Field, E., Tyler, J., Gadd, P. S., Moss, P., McGowan, H., and Marx, S.: Coherent patterns of environmental change at multiple organic spring sites in northwest Australia: Evidence of Indonesian-Australian summer monsoon variability over the last 14,500 years, Quat Sci Rev, 196, 193–216, https://doi.org/10.1016/j.quascirev.2018.07.018, 2018.

Fletcher, M.-S., Wood, S. W., and Haberle, S. G.: A fire-driven shift from forest to non-forest: evidence for alternative stable states?, Ecology, 95, 2504–2513, https://doi.org/10.1890/12-1766.1, 2014.

Gaillard, M.-J., Birks, H. J. B., Emanuelsson, U., and Berglund, B. E.: Modern pollen/land-use relationships as an aid in the reconstruction of past land-uses and cultural landscapes: an example from south Sweden, Veg Hist Archaeobot, 1, https://doi.org/10.1007/BF00190697, 1992.

Gudmundsson, L., Bremnes, J. B., Haugen, J. E., and Engen-Skaugen, T.: Technical Note: Downscaling RCM precipitation to the station scale using statistical transformations - a comparison of methods, Hydrol. Earth Syst. Sci., 16, 3383–3390, https://doi.org/10.5194/hess-16-3383-2012, 2012.

Reimer, P. J., Austin, W. E. N., Bard, E., Bayliss, A., Blackwell, P. G., Bronk Ramsey, C., Butzin, M., Cheng, H., Edwards, R. L., Friedrich, M., Grootes, P. M., Guilderson, T. P., Hajdas, I., Heaton, T.

J., Hogg, A. G., Hughen, K. A., Kromer, B., Manning, S. W., Muscheler, R., Palmer, J. G., Pearson, C., van der Plicht, J., Reimer, R. W., Richards, D. A., Scott, E. M., Southon, J. R., Turney, C. S. M., Wacker, L., Adolphi, F., Büntgen, U., Capano, M., Fahrni, S. M., Fogtmann-Schulz, A., Friedrich, R., Köhler, P., Kudsk, S., Miyake, F., Olsen, J., Reinig, F., Sakamoto, M., Sookdeo, A., and Talamo, S.: The IntCal20 Northern Hemisphere Radiocarbon Age Calibration Curve (0–55 cal kBP), Radiocarbon, 62, 1–33, https://doi.org/10.1017/rdc.2020.41, 2020.

Haberle, S.: Late quaternary environmental history of the Tari Basin, Papua New Guinea (PhD Thesis), Australian National University, Canberra, 1993.

Haberle, S.: Explanations for palaeoecological changes on the northern plains of Guadalcanal, Solomon Islands: the last 3200 years, Holocene, 6, 333–338, https://doi.org/10.1177/095968369600600307, 1996.

Harrison, S. P.: Modern pollen data for climate reconstructions, version 1 (SMPDS), University of Reading, Dataset, https://doi.org/10.17864/1947.194, 2019.

Harrison, S. P., Marinova, E., and Cruz-Silva, E.: EMBSeCBIO pollen database, University of Reading, Dataset, https://doi.org/10.17864/1947.309, 2021.

Harrison, S. P., Shen, Y., and Sweeney, L.: Pollen data and charcoal data of the Iberian Peninsula (version 3), University of Reading, Dataset, https://doi.org/10.17864/1947.000369, 2022a.

Harrison, S. P., Villegas-Diaz, R., Cruz-Silva, E., Gallagher, D., Kesner, D., Lincoln, P., Shen, Y., Sweeney, L., Colombaroli, D., Ali, A., Barhoumi, C., Bergeron, Y., Blyakharchuk, T., Bobek, P., Bradshaw, R., Clear, J. L., Czerwiński, S., Daniau, A.-L., Dodson, J., Edwards, K. J., Edwards, M. E., Feurdean, A., Foster, D., Gajewski, K., Gałka, M., Garneau, M., Giesecke, T., Gil Romera, G., Girardin, M. P., Hoefer, D., Huang, K., Inoue, J., Jamrichová, E., Jasiunas, N., Jiang, W., Jiménez-Moreno, G., Karpińska-Kołaczek, M., Kołaczek, P., Kuosmanen, N., Lamentowicz, M., Lavoie, M., Li, F., Li, J., Lisitsyna, O., López-Sáez, J. A., Luelmo-Lautenschlaeger, R., Magnan, G., Magyari, E. K., Maksims, A., Marcisz, K., Marinova, E., Marlon, J. R., Mensing, S., Miroslaw-Grabowska, J., Oswald, W., Pérez-Díaz, S., Pérez-Obiol, R., Piilo, S., Poska, A., Qin, X., Remy, C. C., Richard, P. J. H., Salonen, S., Sasaki, N., Schneider, H., Shotyk, W., Stancikaite, M., Šteinberga, D., Stivrins, N., Takahara, H., Tan, Z., Trasune, L., Umbanhowar, C. E., Väliranta, M., Vassiljev, J., Xiao, X., Xu, Q., Xu, X., Zawisza, E., Zhao, Y., Zhou, Z., and Paillard, J.: The Reading Palaeofire Database: an expanded global resource to document changes in fire regimes from sedimentary charcoal records, Earth Syst Sci Data, 14, 1109–1124, https://doi.org/10.5194/essd-14-1109-2022, 2022b.

Herzschuh, U., Cao, X., Laepple, T., Dallmeyer, A., Telford, R. J., Ni, J., Chen, F., Kong, Z., Liu, G., Liu, K.-B., Liu, X., Stebich, M., Tang, L., Tian, F., Wang, Y., Wischnewski, J., Xu, Q., Yan, S., Yang, Z., Yu, G., Zhang, Y., Zhao, Y., and Zheng, Z.: Position and orientation of the westerly jet determined Holocene rainfall patterns in China, Nat Commun, 10, 2376, https://doi.org/10.1038/s41467-019-09866-8, 2019.

Hope, G.: Environmental change and fire in the Owen Stanley Ranges, Papua New Guinea, Quat Sci Rev, 28, 2261–2276, https://doi.org/10.1016/j.quascirev.2009.04.012, 2009.

Hope, G., Gillieson, D., and Head, J.: A Comparison of Sedimentation and Environmental Change in New Guinea Shallow Lakes, J Biogeogr, 15, 603, https://doi.org/10.2307/2845439, 1988.

Hope, G., O'Dea, D., and Southern, W.: Holocene vegetation histories in the Western Pacific: alternative records of human impact, in: The Pacific from 5000 to 2000 BP : colonisation and transformations, edited by: Galipaud, J.-C. and Lilley, I., IRD, Paris, 387–404, 1996.

Jolly, D., R. Bonnefille, S. Burcq, and M. Roux. Représentation pollinique de la forêt dense humide du Gabon, tests statistiques. Comptes rendus de l'Académie des sciences. Série II a, Sciences de la terre et des planètes 322(1):63-70, 1996.

Julier, A. C. M., Jardine, P. E., Adu-Bredu, S., Coe, A. L., Duah-Gyamfi, A., Fraser, W. T., Lomax, B. H., Malhi, Y., Moore, S., Owusu-Afriyie, K., and Gosling, W. D.: The modern pollen–vegetation relationships of a tropical forest–savannah mosaic landscape, Ghana, West Africa, Palynology, 42, 324–338, https://doi.org/10.1080/01916122.2017.1356392, 2018.

Julier, A. C. M., Jardine, P. E., Adu-Bredu, S., Coe, A. L., Fraser, W. T., Lomax, B. H., Malhi, Y., Moore, S., and Gosling, W. D.: Variability in modern pollen rain from moist and wet tropical forest plots in Ghana, West Africa, Grana, 58, 45–62, https://doi.org/10.1080/00173134.2018.1510027, 2019.

Lebamba, J., Vincens, A., Jolly, D., Ngomanda, A., Schevin, P., Maley, J., and Bentaleb, I.: Modern pollen rain in savanna and forest ecosystems of Gabon and Cameroon, Central Atlantic Africa, Rev Palaeobot Palynol, 153, 34–45, https://doi.org/10.1016/j.revpalbo.2008.06.004, 2009.

Luly, J. G.: Holocene Palaeoenvironments Near Lake Tyrrell, Semi-Arid Northwestern Victoria, Australia, J Biogeogr, 20, 587, https://doi.org/10.2307/2845516, 1993.

Luly, J. G., Bowler, J. M., and Head, M. J.: A radiocarbon chronology from the playa Lake Tyrrell, Northwestern Victoria, Australia, Palaeogeogr Palaeoclimatol Palaeoecol, 54, 171–180, https://doi.org/10.1016/0031-0182(86)90123-9, 1986.

Macphail, M. K.: The history of the vegetation and climate in southern Tasmania since the late Pleistocene (ca. 13. 000 - 0 BP) (Doctoral Dissertation), University of Tasmania, 1975.

Macphail, M. K.: Vegetation and Climates in Southern Tasmania since the Last Glaciation, Quat Res, 11, 306–341, https://doi.org/10.1016/0033-5894(79)90078-4, 1979.

Macphail, M. K.: Fossil and modern *Beilschmiedia* (lauraceae) pollen in New Zealand, N Z J Bot, 18, 453–457, https://doi.org/10.1080/0028825X.1980.10425165, 1980.

Macphail, M. K. and McQueen, D. R.: The value of New Zealand pollen and spores as indicators of Cenozoic vegetation and climates, Tuatara, 26, 37–56, 1983.

Macphail, M. K. and Mildenhall, D. C.: *Dactylanthus taylori:* in North-West Nelson, New Zealand?, N Z J Bot, 18, 149–152, https://doi.org/10.1080/0028825X.1980.10427242, 1980.

Mariani, M., Connor, S. E., Fletcher, M., Theuerkauf, M., Kuneš, P., Jacobsen, G., Saunders, K. M., and Zawadzki, A.: How old is the Tasmanian cultural landscape? A test of landscape openness using quantitative land-cover reconstructions, J Biogeogr, 44, 2410–2420, https://doi.org/10.1111/jbi.13040, 2017.

McWethy, D. B., Whitlock, C., Wilmshurst, J. M., McGlone, M. S., Fromont, M., Li, X., Dieffenbacher-Krall, A., Hobbs, W. O., Fritz, S. C., and Cook, E. R.: Rapid landscape transformation in South Island, New Zealand, following initial Polynesian settlement, P Natl Acad Sci USA, 107, 21343–21348, https://doi.org/10.1073/pnas.1011801107, 2010.

McWethy, D. B., Wilmshurst, J. M., Whitlock, C., Wood, J. R., and McGlone, M. S.: A High-Resolution Chronology of Rapid Forest Transitions following Polynesian Arrival in New Zealand, PLoS One, 9, e111328, https://doi.org/10.1371/journal.pone.0111328, 2014.

Norton, D. A., McGlone, M. S., and Wigley, T. M. L.: Quantitative analyses of modern pollen-climate relationships in New Zealand indigenous forests, N Z J Bot, 24, 331–342, https://doi.org/10.1080/0028825X.1986.10412681, 1986.

Phelps, L. N., Chevalier, M., Shanahan, T. M., Aleman, J. C., Courtney-Mustaphi, C., Kiahtipes, C. A., Broennimann, O., Marchant, R., Shekeine, J., Quick, L. J., Davis, B. A. S., Guisan, A., and Manning, K.: Asymmetric response of forest and grassy biomes to climate variability across the African Humid Period: influenced by anthropogenic disturbance?, Ecography, 43, 1118–1142, https://doi.org/10.1111/ecog.04990, 2020.

Pickett, E. J., Harrison, S. P., Hope, G., Harle, K., Dodson, J. R., Peter Kershaw, A., Colin Prentice, I., Backhouse, J., Colhoun, E. A., D'Costa, D., Flenley, J., Grindrod, J., Haberle, S., Hassell, C., Kenyon, C., Macphail, M., Martin, H., Martin, A. H., McKenzie, M., Newsome, J. C., Penny, D., Powell, J., Ian Raine, J., Southern, W., Stevenson, J., Sutra, J., Thomas, I., van der Kaars, S., and Ward, J.: Pollen-based reconstructions of biome distributions for Australia, Southeast Asia and the Pacific (SEAPAC region) at 0, 6000 and 18,000 ^{14}C yr BP, J Biogeogr, 31, 1381–1444, https://doi.org/10.1111/j.1365-2699.2004.01001.x, 2004.

Prebble, M., Kennedy, J., and Southern, W.: Holocene lowland vegetation change and human ecology in Manus Province, Papua New Guinea, in: Altered Ecologies (Terra Australis 32): Fire, climate and human influence on terrestrial landscapes, ANU Press, https://doi.org/10.22459/TA32.11.2010.12, 2010.

Prebble, M., Anderson, A. J., Augustinus, P., Emmitt, J., Fallon, S. J., Furey, L. L., Holdaway, S. J., Jorgensen, A., Ladefoged, T. N., Matthews, P. J., Meyer, J.-Y., Phillipps, R., Wallace, R., and Porch, N.: Early tropical crop production in marginal subtropical and temperate Polynesia, P Natl Acad Sci USA, 116, 8824–8833, https://doi.org/10.1073/pnas.1821732116, 2019.

Serge, M., Mazier, F., Fyfe, R., Gaillard, M.-J., Klein, T., Lagnoux, A., Galop, D., Githumbi, E., Mindrescu, M., Nielsen, A., Trondman, A.-K., Poska, A., Sugita, S., Woodbridge, J., Abel-Schaad, D., Åkesson, C., Alenius, T., Ammann, B., Andersen, S., Anderson, R., Andrič, M., Balakauskas, L., Barnekow, L., Batalova, V., Bergman, J., Birks, H., Björkman, L., Bjune, A., Borisova, O., Broothaerts, N., Carrion, J., Caseldine, C., Christiansen, J., Cui, Q., Currás, A., Czerwiński, S., David, R., Davies, A., De Jong, R., Di Rita, F., Dietre, B., Dörfler, W., Doyen, E., Edwards, K., Ejarque, A., Endtmann, E., Etienne, D., Faure, E., Feeser, I., Feurdean, A., Fischer, E., Fletcher, W., Franco-Múgica, F., Fredh, E., Froyd, C., Garcés-Pastor, S., García-Moreiras, I., Gauthier, E., Gil-Romera, G., González-Sampériz, P., Grant, M., Grindean, R., Haas, J., Hannon, G., Heather, A.-J., Heikkilä, M., Hjelle, K., Jahns, S., Jasiunas, N., Jiménez-Moreno, G., Jouffroy-Bapicot, I., Kabailienė, M., Kamerling, I., Kangur, M., Karpińska-Kołaczek, M., Kasianova, A., Kołaczek, P., Lagerås, P., Latalowa, M., Lechterbeck, J., Leroyer, C., Leydet, M., Lindbladh, M., Lisitsyna, O., López-Sáez, J.-A., Lowe, J., Luelmo-Lautenschlaeger, R., Lukanina, E., Macijauskaitė, L., Magri, D., Marguerie, D., Marquer, L., Martinez-Cortizas, A., Mehl, I., Mesa-Fernández, J., Mighall, T., Miola, A., Miras, Y., Morales-Molino, C., et al.: Testing the Effect of Relative Pollen Productivity on the REVEALS Model: A Validated Reconstruction of Europe-Wide Holocene Vegetation, Land (Basel), 12, 986, https://doi.org/10.3390/land12050986, 2023.

Shulmeister, J., McLea, W. L., Singer, C., McKay, R. M., and Hosie, C.: Late Quaternary pollen records from the Lower Cobb Valley and adjacent areas, North-West Nelson, New Zealand, N Z J Bot, 41, 503–533, https://doi.org/10.1080/0028825X.2003.9512867, 2003.

Takahara, H., Sugita, S., Harrison, S. P., Miyoshi, N., Morita, Y., and Uchiyama, T.: Pollen-based reconstructions of Japanese biomes at 0, 6000 and 18,000 ^{14}C yr bp, J Biogeogr, 27, 665–683, https://doi.org/10.1046/j.1365-2699.2000.00432.x, 2000.

Villegas-Diaz, R. and Harrison, S. P.: smpds: The SPECIAL Modern Pollen Data Set for Climate Reconstructions. Software. 2022.

Vincens, A., Lézine, A.-M., Buchet, G., Lewden, D., and Le Thomas, A.: African pollen database inventory of tree and shrub pollen types, Rev Palaeobot Palynol, 145, 135–141, https://doi.org/10.1016/j.revpalbo.2006.09.004, 2007.

Williams, J. W., Grimm, E. C., Blois, J. L., Charles, D. F., Davis, E. B., Goring, S. J., Graham, R. W., Smith, A. J., Anderson, M., Arroyo-Cabrales, J., Ashworth, A. C., Betancourt, J. L., Bills, B. W., Booth, R. K., Buckland, P. I., Curry, B. B., Giesecke, T., Jackson, S. T., Latorre, C., Nichols, J., Purdum, T., Roth, R. E., Stryker, M., and Takahara, H.: The Neotoma Paleoecology Database, a multiproxy, international, community-curated data resource, Quat Res, 89, 156–177, https://doi.org/10.1017/qua.2017.105, 2018.

Zanon, M., Davis, B. A. S., Marquer, L., Brewer, S., and Kaplan, J. O.: European forest cover during the past 12,000 years: A palynological reconstruction based on modern analogs and remote sensing, Front. Plant Sci., 9, 1–25, https://doi.org/10.3389/fpls.2018.00253, 2018.

4. Assessing relationships between fire, tree cover, climate and population change in Europe during the Holocene

4.1. Introduction

Regional-scale analyses of palaeofire have emphasised the role of climate as the driver of changes during the Holocene (e.g. Marlon et al., 2006; Power et al., 2010; Mooney et al., 2011; Zennaro et al., 2015). However, sub-regional analysis has highlighted the role of vegetation in affecting patterns of fire (e.g. Higuera et al., 2009; Feurdean et al., 2020). While some studies highlighted the role of people in changing fire regimes from the mid Holocene onwards (e.g. Vannière et al., 2016; Dietze et al., 2018; Connor et al., 2019; Zapolska et al., 2023), very few studies have systematically considered all of the drivers in concert. It is against this background that this Chapter investigates different approaches to tease out the relationship between palaeofire and its drivers, looking at the problem holistically across the different controls in a similar way to studies of modern relationships with fire. The focus on Europe during the Holocene period was motivated by the availability of data. The European and sub-regional scale has been considered to identify broad-scale relationships, accepting that this scale may mask local-scale relationships. The different approaches applied include regression analysis of gridded 50km^2 data, Granger causality analysis of time series trends, and Superposed Epoch Analysis associated with changes in reconstructed population, also on time series trends. Each approach is addressed in turn. Prior to this however, the reconstructions of fire and drivers are discussed, with fire and human population reconstructed from available data. Data compilation, and statistical analyses were performed using R (R-core team, 2024).

4.2. Reconstructions of fire and its drivers

This section focusses on reconstructions of fire based on sedimentary charcoal data and human population, inferred from archaeological radiocarbon data. Tree cover reconstructions are based on the output described in Chapter 3, and climate reconstructions from recently updated analysis (Tang et al., in prep.), and are also discussed in turn. Additionally, sub-regions are defined, based on the general availability and overlap between the data.

4.2.1. Reconstructing fire

Reconstructions of fire are based on charcoal data from terrestrial sedimentary records from the Reading Palaeofire Database (RPD) (Harrison et al., 2022). The RPD contains 238 records for the European region (12°W to 45°E and 34–73°N) covering the period from 12,000 cal. BP to the present.

To facilitate inter-site comparisons, the charcoal data were standardised based on the three-step protocol proposed by (Power et al., 2008). After converting charcoal values to influx (i.e. particles/cm^2/year), values were (1) rescaled using a max transformation, (2) transformed and re-scaled with a Box-Cox transformation, (3) then converted to z-scores. A max transformation was preferred over the min-max transformation suggested by Power et al. (2008) to account for zero values of charcoal accumulation. The baseline period from 12,000 cal. BP to 150 cal. BP was chosen to maximise data coverage but excluding the post-industrial period (>1750 CE). Previous work suggests the choice of baseline has a limited impact on z-score determination (Power 2010).

To limit the potential for over-sampling at an individual site, a single charcoal record was selected per site, with records with the greatest amount of data preferred. In the case of records having the same quantity of data for the time period analysed, macro-charcoal records were selected. This reduced the number of records to 201. Records with less than 20 samples and records that had data for less than six 100-year bins were excluded, because these provided a limited record of fire history. In total, there were 192 records included within the analysis (Fig. 4.1A; see chapter supplement for list of included charcoal sites). Figure 4.1A shows that whilst there is a reasonable coverage across Europe, there are clusters in some areas (e.g. Iberia) and other areas with gaps in coverage (e.g. England and the Benelux). Given the differences in sampling resolution between records, and the different calibrated ages associated with each sample per record, data were binned into 100-year bins. This binning procedure helps to prevent highly sampled records from dominating the fire signal, and allows temporal comparison between sites, whilst still maintaining the balance between temporal resolution and site coverage. The number of records increased through time to the present (Fig. 4.1B).

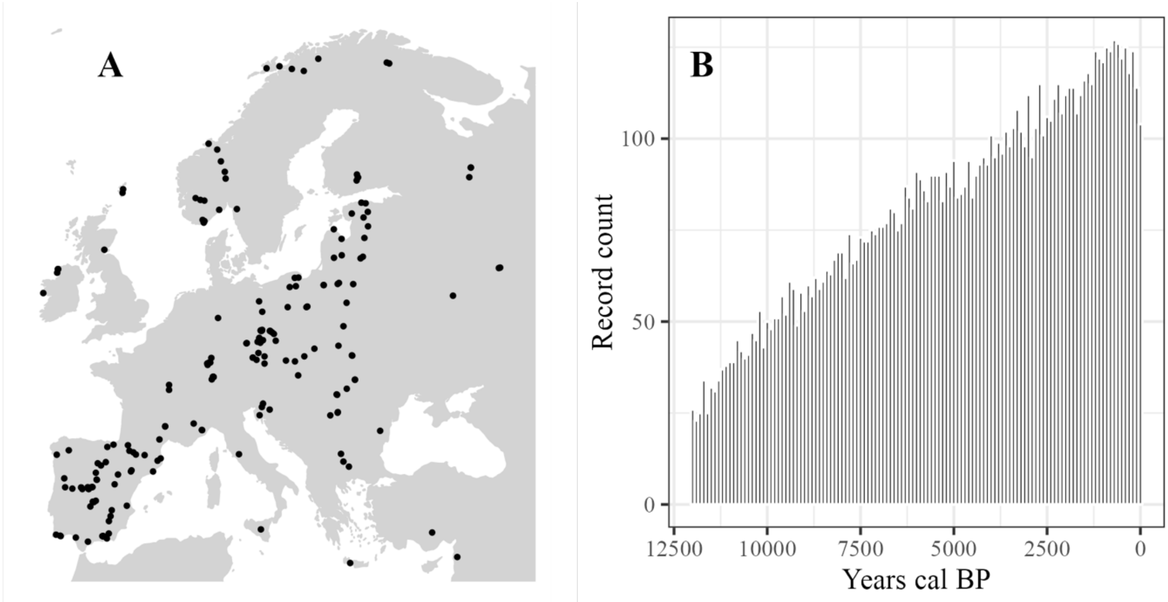

Figure 4.1: A – Charcoal site locations; B – Charcoal record counts through time per 100-year bin

The composite curve of z-score charcoal accumulation for Europe in shown in Fig. 4.2, with a locally fitted regression 500-year smoothing (half) window fitted to the data using R-package *LOCFIT* (Loader, 2020). This smoothing reduces the impact of outliers on the curve (Daniau et al., 2012) and shows millennial trends in the data. Confidence intervals are based on 1000 bootstrap resamples of individual records.

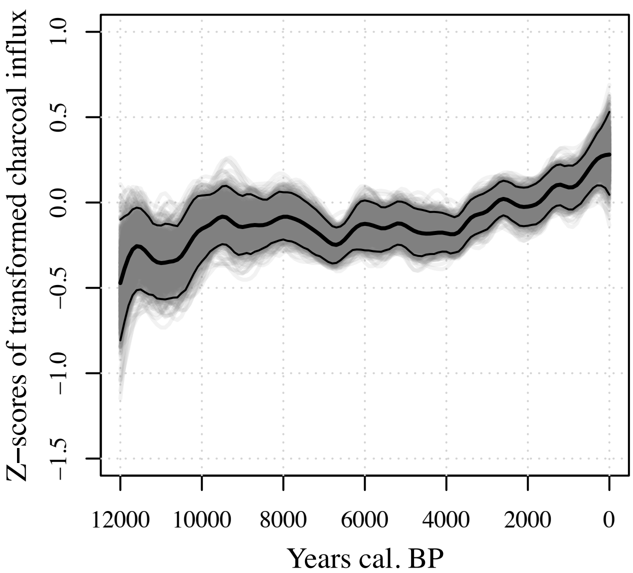

Figure 4.2: Z-score composite of transformed charcoal influx for Europe, 12,000 cal. BP to present. The solid lines show the (smoothed) median value, the thin black lines show the 95% confidence intervals of 1000 bootstrap resample runs.

The composite shows an overall increase in fire through time, but with some periods of decrease or relative stability. Following an increase at the beginning of the Holocene to ca. 11,500 cal. BP, fire declines until ca. 11,000 and remains stable until ca. 10,500 cal. BP. Fire then increases until ca. 9,500 cal. BP and remains relatively stable until ca. 8,000 cal. BP. The curve then declines until ca. 6,500 cal. BP. Fire then increases to 6,000 cal. BP and remains generally stable until ca. 3,750 cal. BP. After this, fire increases to present levels, with a slight pause between ca. 2,500 cal. BP and ca. 2,000 cal. BP. The confidence interval is relatively stable through time, although larger during the earliest intervals because of the reduced number of records. Composite curves of transformed charcoal influx for sub-regions of Europe are shown in section *4.4 Time series analysis*.

At the European level, the choice of binwidth has little impact of the broad-scale patterns (Fig. 4.3). The variation in fire is somewhat greater using a wider binwidth, although as might be expected some of the minor increases and declines are less noticeable. With a narrower smoothing window of 250 years, there is much more variation at smaller time scales.

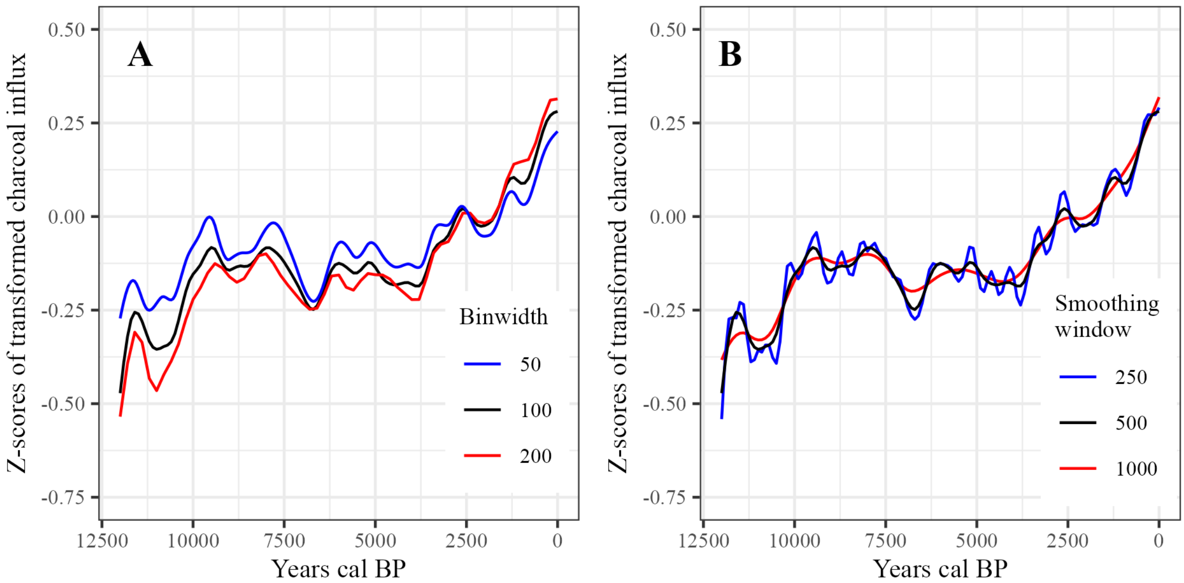

Figure 4.3: Z-score composites of transformed charcoal influx for Europe, 12,000 cal. BP to present: A – Influence of bin width selection, with smoothing window fixed at 500 years; B – Influence of smoothing window half width selection, with bin width fixed at 100 years

4.2.2. Human population

Reconstructions of relative change in human population were used as an index of human influence on the environment. Human population was reconstructed based on radiocarbon dates on archaeological material from a range of sources (Table 4.1) following the "dates as data" approach (Rick, 1987) discussed in the Introduction (see *1.4.4 Reconstructing human influences on fire*).

Table 4.1: Sources of radiocarbon data

Dataset name	**Area**	**No. of 14^C dates***	**Reference**
Balkans Extra	Balkans	4130	Molloy et al. (in prep.)
Bunbury Scandinavia	Scandinavia	20593	Bunbury et al. (2023)
Iberia Extra	Iberia	5988	Sweeney et al. (2021)
p3k14c	Europe	68310	Bird et al., (2022)
XRONOS	Europe	56842	Hinz and Roe (2023)

*The number of 14^C between 12000 and 0 uncal. BP. Note that this may include intra-dataset duplicates. Included dates have a standard error <= 200 years.

The consolidated dataset includes 162,253 radiocarbon dates from 12,000 uncal. BP to present, which excludes dates with a standard error greater than 200 years. Calibration of radiocarbon dates was performed with the R-package *rcarbon* (Crema and Bevan, 2021) using the IntCal2020 calibration curve (Reimer et al., 2020). A summed probability distribution (SPD) was created to represent the cumulative probability distribution of radiocarbon dates. The standard site binning procedure, designed to limit the impact of site oversampling by creating a single probability value per site phase (Shennan et al., 2013; Timpson et al., 2014), also solves the problem of duplicates across the consolidated dataset as duplicates with the same site and dating information will be reduced to single values. This is also the case for site counts, i.e. the number of sites with data at a given time period. Overall, based on a 100-year cut-off value for the binning procedure using hierarchical clustering (Crema et al., 2016; Crema and Bevan, 2021), using the *rcarbon* process for generating an SPD for Europe, there are 48,507 site bins.

However, a European-wide SPD is problematic, as the number of radiocarbon dates can differ dramatically between regions due to differences in research traditions (Crema, 2022), rather than potential differences in underlying populations. This is illustrated by the SPDs and site counts (Fig. 4.4) for the UK (A and B) and Italy (B and C), where the key difference is the scale in summed probability and site counts; combining these two areas together would result in the Italian signal (SPD max ca. 0.6) being overridden by the UK signal (SPD max ca. 3.4). This is also reflected in the gridded ($50km^2$) site counts of radiocarbon data for Europe (Fig. 4.5). The problem is compounded by the fact that the time after which radiocarbon is less used to date archaeological material and is replaced by other methods such as artefact typology, varies between different regions. Radiocarbon dating is used more consistently in the UK than in Italy (Fig. 4.4), so combining these datasets would further bias the population signal towards the UK towards the end of the Holocene.

This suggests that more reliable results would be obtained by using SPDs at a sub-regional level (see *4.2.5 Defining sub-regions*), or to use site-based estimates population change.

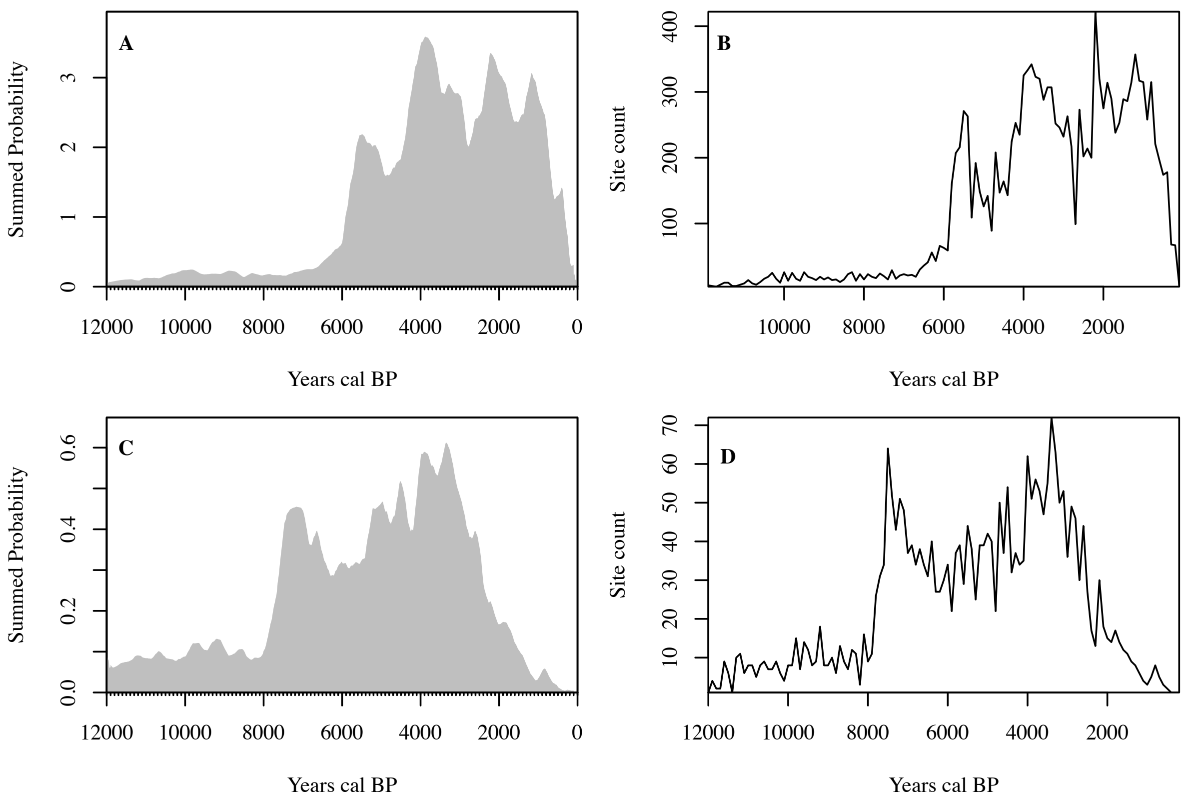

Figure 4.4: SPD and radiocarbon data site count differences for UK and Italy, 12,000 cal. BP to present. A – SPD UK; B – site counts UK; C – SPD; D – site counts Italy

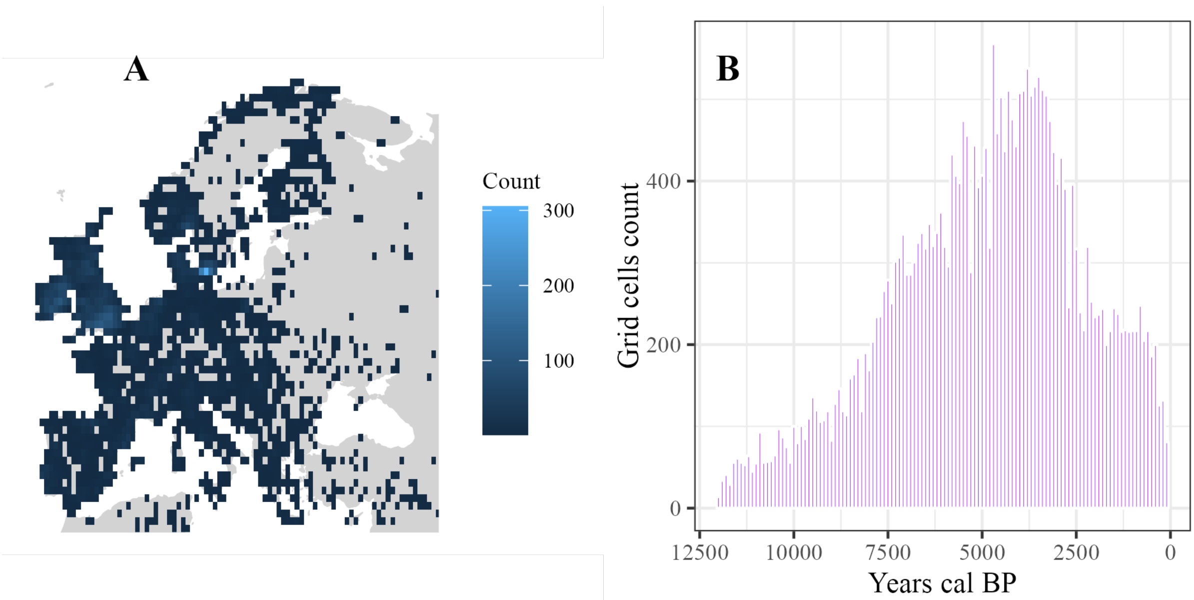

Figure 4.5: A - European site counts of radiocarbon data, from 12,000 cal. BP to present; B – Count of radiocarbon grid cells through time

4.2.3. Tree cover

In a recent global model study based on satellite data, Haas et al. (2020) found that a higher proportion of tree cover is generally associated with reduced burned area and fire size, but with increased fire intensity (Haas et al., 2022). Tree cover reconstructions (Chapter 3) were used in the analysis of relationships between palaeofire and its drivers. Fossil pollen sites for this reconstruction were from the Special version 2 of the SPECIAL Modern Pollen Dataset (Villegas-Diaz and Harrison, 2022), itself created from multiple different published regional datasets, from data repositories (Neotoma, PANGAEA) or directly from data collectors/authors (see Chapter 3 Supplement for further information). This site-based reconstruction of tree cover is based on 808 sites and includes many of the same sites used for reconstructing fire.

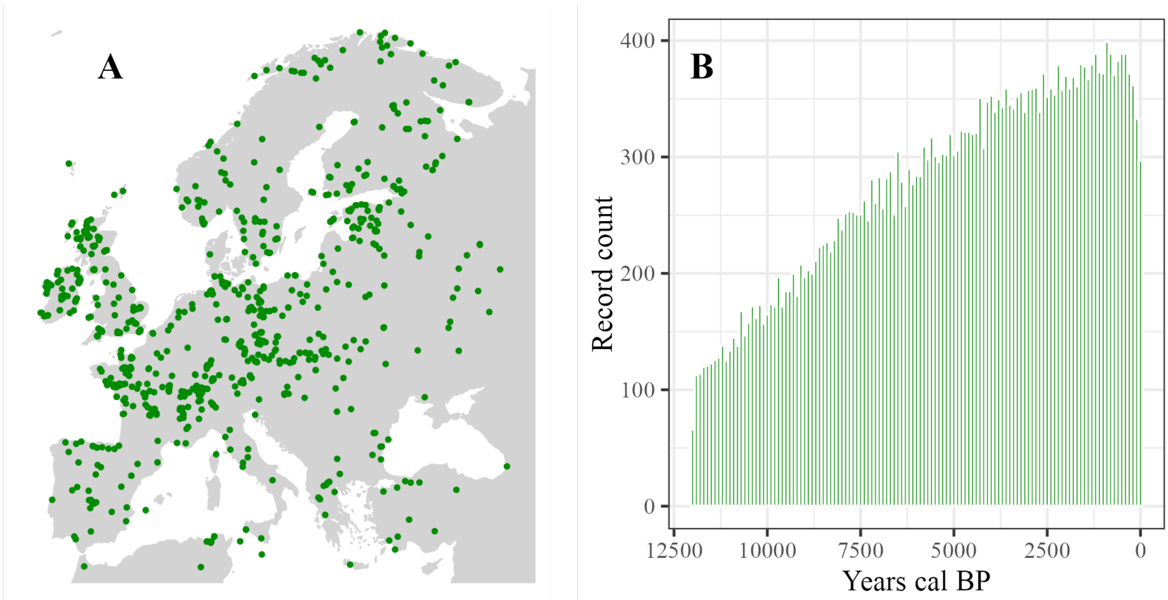

Figure 4.6: A - Tree cover site locations; B – Tree cover record counts through time per 100-year bin

Spatially, there are fewer gaps for the tree cover site locations (Fig. 4.6A) than the charcoal site locations (Fig. 4.1A), reflecting the underlying difference in the number of pollen sites compared to sites where charcoal is (also) measured. This difference is also reflected in the quantity of records through time (Fig. 4.6B).

At the European scale, tree cover increases from the early Holocene to a peak at ca. 6,500 cal. BP, before falling towards present levels (Fig. 4.7). Tree cover shows less short-term variability than fire (Fig. 4.2), which is likely due to the differences in the quantity of records/sites. The overall trend between this tree cover composite and the charcoal composite is quite different.

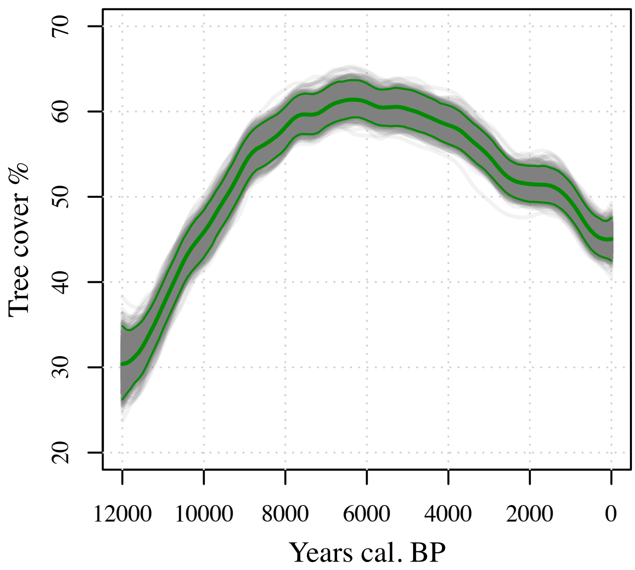

Figure 4.7: Tree cover percentage, for Europe, 12,000 cal. BP to present. The solid lines show the (smoothed) median value, the thin green lines show the 95% confidence intervals of 1000 bootstrap resample runs.

4.2.4. Climate reconstructions

The climate reconstructions were obtained from research performed by Tang (in prep.), using the same modern pollen (SMPDS: Villegas-Diaz and Harrison, 2022) and fossil pollen (SPECIAL-EPD: Harrison et al., 2024) datasets used for the tree cover reconstructions. Mean temperature of the warmest month (MTWA), mean temperature of the coldest month (MTCO), the number of growing degree days above a threshold of 0° (GDD_0) and plant available moisture, represented by the ratio of actual to equilibrium evapotranspiration (α) were calculated via the frequency adjusted, tolerance weighted partial least squares (fxTWA-PLS) approach (Liu et al., 2020, 2021). Summer temperature (MTWA) might be expected to increase the likelihood fire through the effects on fuel moisture (Keeley and Syphard, 2016; Pausas and Keeley, 2021). MTCO is associated with limits on tree growth (Prentice et al., 1992; Körner, 2021) and is expected to have a limited direct impact on fire but may impact fire via effects on fuel loads near the tree line. GDD_0 increases are associated with either an increase in summer temperature (as with MTWA) or with a longer growing season, both of which are expected to lead to increased fire via effects on fuel moisture and productivity. Generally, the relationship between α and fire would be expected to be humpbacked, with fire limited by effects on fuel availability at the low end and, because fuel is too wet to burn, fire limited by too much moisture at the high end (Bond and Keeley, 2005; Pausas and Bradstock, 2007; Pausas and Ribeiro, 2013). Maximum fire would be likely to be found at intermediate levels of α (Fig. 4.8).

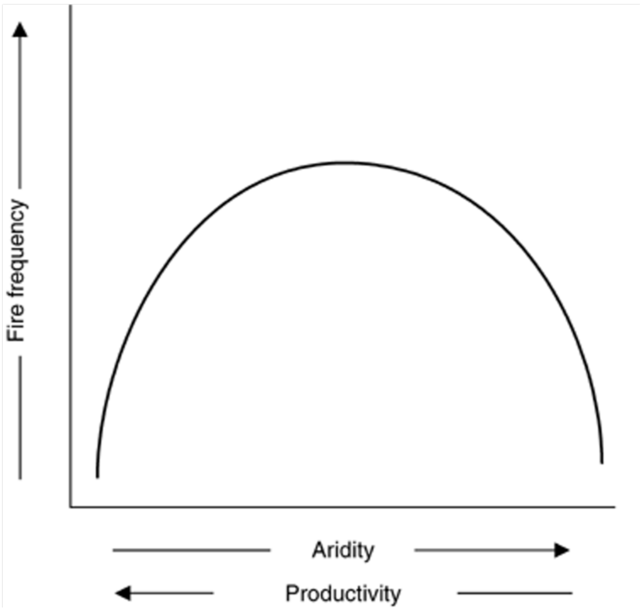

Figure 4.8: Theoretical fire-productivity relationship, moderated by moisture. Adapted from Pausas and Bradstock, (2007: Fig. 5).

There are 1,191 terrestrial pollen sites with reconstructions for each of these variables for the Holocene period (Fig. 4.9A). As with the other sedimentary record data, the quantity of records increase through time (Fig. 4.9B). There are more sites providing climate reconstructions compared to tree cover reconstructions because the latter were screened to remove high-elevation sites and site type other than lakes or bogs (see section *3.2.1: Selection and treatment of data*).

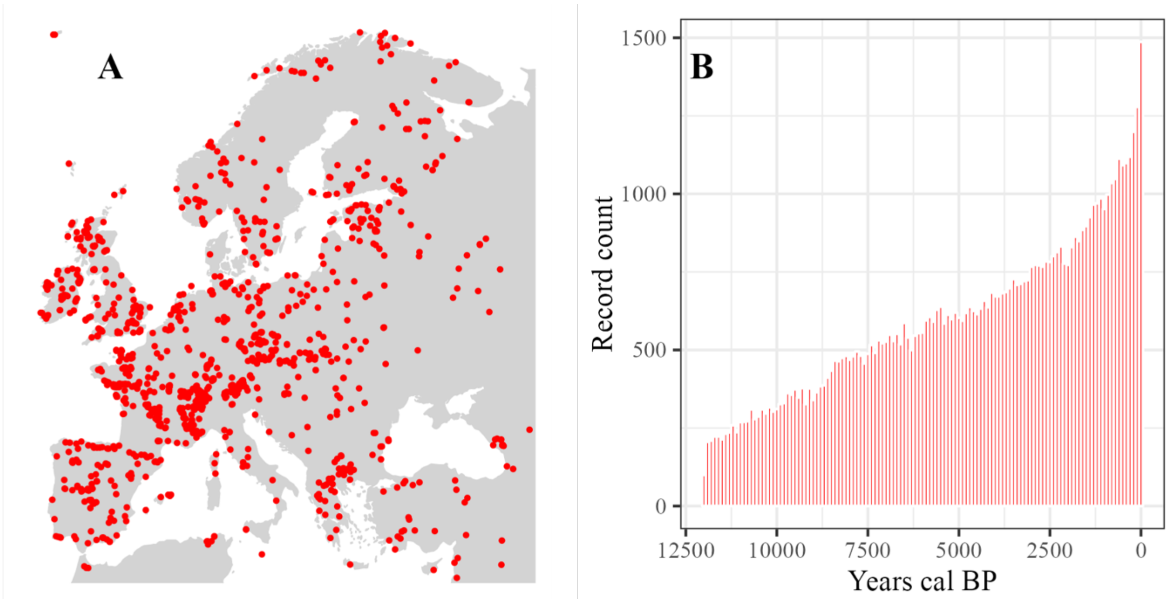

Figure 4.9: A – Climate variable site locations; B – Climate variable record counts through time per 100-year bin

At the European level, these climate variables are very closely correlated (Fig. 4.10). MTWA increases from the start of the Holocene at a decreasing rate until ca. 6,750 cal. BP, after which it remains relatively stable until ca. 1,500 cal. BP and then declines to the present. The composite curve for α is almost a mirror image of MTWA, with a decline in plant available moisture to ca. 6,750 cal. BP, a slight recovery until ca. 5,000 cal. BP, and then slowly declines until ca. 1,000 cal. BP, after which it is relatively stable. MTCO increases during the first part of the Holocene until ca. 9,500 cal. BP, is relatively stable until ca. 7,750 cal. BP, then increases slowly thereafter until ca. 750 cal. BP after which is decreases to present. The trend in GDD_0 shows similarities with both MTWA and MTCO, since it reflects the increasing summer temperatures (MTWA) and increasing growing season length (MTCO).

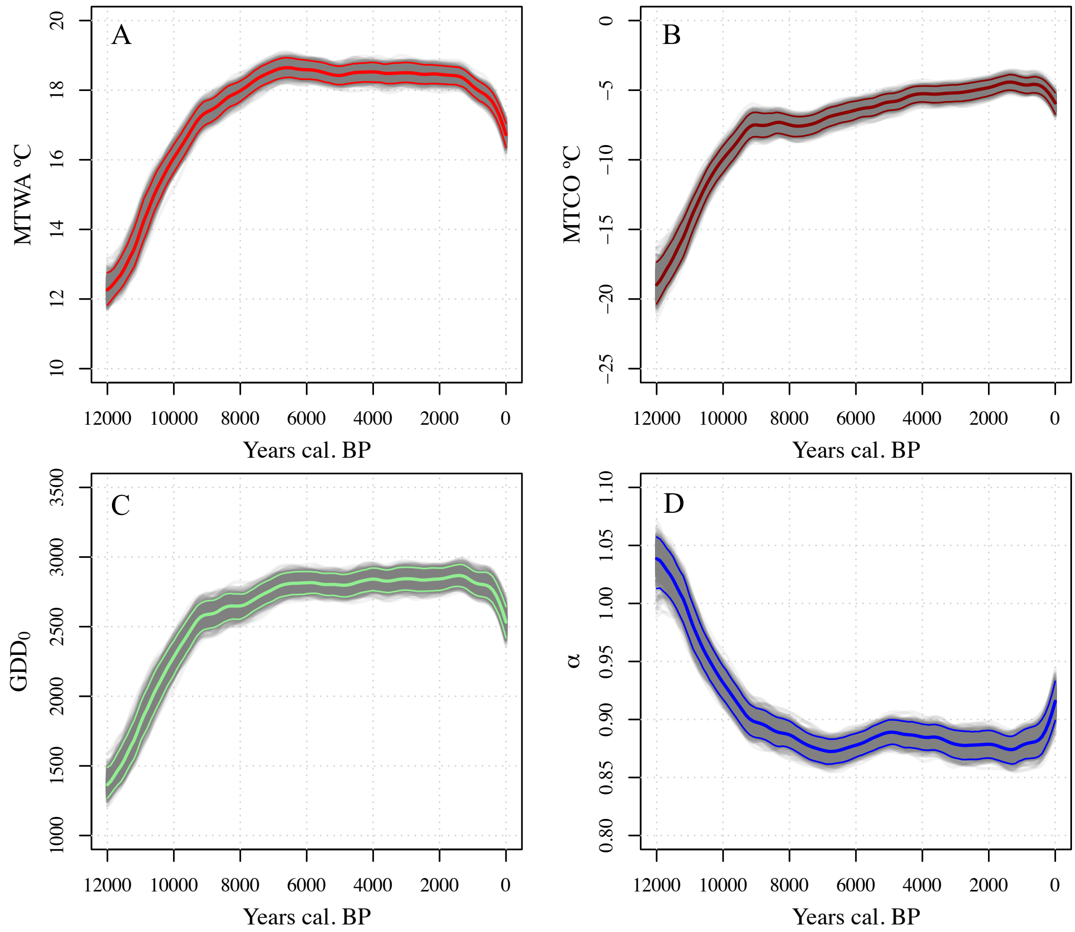

Figure 4.10: Climate reconstructions, for Europe, 12,000 cal. BP to present. The solid lines show the median value, the thin red lines show the 95% confidence intervals of 1000 bootstrap resample runs: A – mean temperature of the warmest month (MTWA); B – mean temperature of the coldest month (MTCO); C – growing degree days above the 0° threshold (GDD_0); D – plant available moisture (α)

4.2.5. Defining sub-regions

Sub-regions of Europe were defined to test whether there were different relationships between reconstructed fire and the other reconstructed variables between regions (Fig. 4.11). This division was based on the spatial structure of the datasets, with coverage of all data types. The charcoal (A) and radiocarbon (D) data are the main constraints in defining sub-regions. The limited charcoal data from the UK, France, Italy, Sweden and Benelux, for example, prevented using these regions of Europe, while the limited availability of archaeological radiocarbon data in eastern Europe and the Baltic prevented defining this as a sub-region. The three sub-regions regions with sufficient coverage of all data sources were central Europe, Iberia and southern Norway.

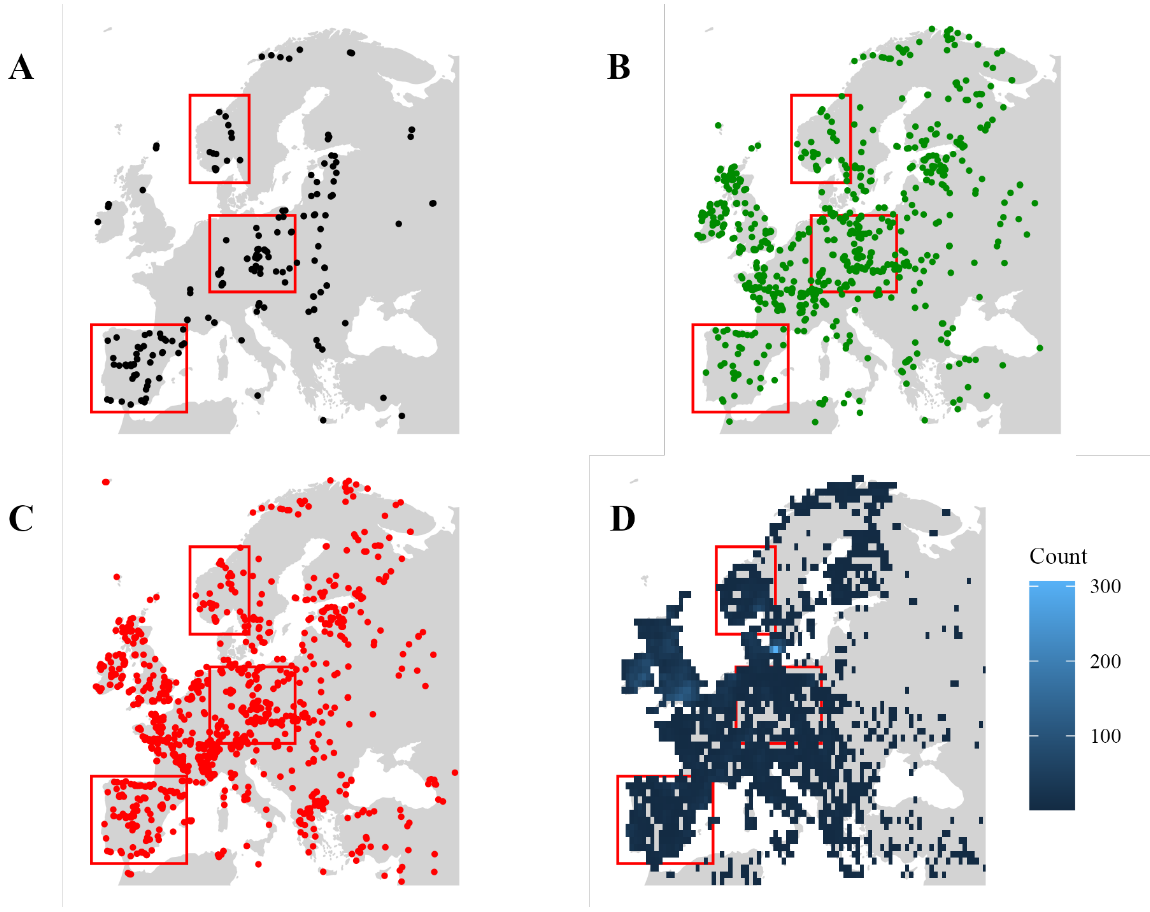

Figure 4.11: Reconstructed data locations, with sub-regions included: A – Sedimentary charcoal record locations; B – Tree cover pollen sedimentary records; C – Climate pollen sedimentary records; D – Gridded (50km²) radiocarbon site locations

4.3. Modelling the relationship between fire and its drivers

Statistical modelling allows the testing of causal relationships between reconstructed variables and reconstructed fire, which may differ from the emergent relationships between fire and individual drivers. Different models were tested, with different functional forms and parameters, after assessing the spatial and temporal overlaps between the different reconstructions to determine the dataset to model.

4.3.1. Reconstruction overlaps

Although the spatial locations of underlying sites were similar (Fig. 4.11), the charcoal and population data had less complete spatial coverage than the other reconstructions. To increase the likelihood over spatial overlaps between data, and to limit the impact of multiple sites in close proximity, reconstructions were spatially binned on a $50km^2$ grid. At a European level, this spatial scale balances the loss of site-level precision with maximising the amount of data and reducing potential oversampling. Temporal binning was necessary to reduce the impact of differences in sampling resolution and to allow comparison across different reconstructions. The choice of temporal resolution was based on pragmatically having sufficient resolution to identify smaller scale changes and maximising the quantity of data available for statistical analysis while limiting the impact of differences in sampling resolution. A 100-year bin width was chosen for this purpose.

Initially, the number of spatiotemporal overlaps included all reconstructions: fire based on charcoal data, tree cover and climate based on pollen data, and population change based on site counts of archaeological radiocarbon data. However, the lack of temporal resolution for the archaeological radiocarbon data was an issue. In total there were only 35 unique grid cells (Fig. 4.12), covering 97 of the 121 temporal bins from 12,000 cal. BP to present. Although there were 435 data points that could be included in a statistical model, the majority (66%) of the grid cells had data in less than 10 temporal bins, which would be problematic for the calculation of z-scores (see *4.3.2 Z-scores*). Furthermore, the SPD and site counts tail off closer to the present day over a large part of the region due to reductions in radiocarbon dating of materials; site counts from the late Holocene are of questionable reliability. Regional differences in when radiocarbon dating is no longer used for dating archaeological material means it is challenging to decide on at time after which these data should not be included in the modelling. In Iberia, for example, the archaeological radiocarbon dates are not considered reliable after 3500 cal. BP (Chapter 2) and if this is used as a cut-off for all regions, the number of grid cells with overlapping data sets would be reduced from 424 to 286.

Based on this challenge, the population data were initially excluded from the regression modelling. This increased the number of grid cells with data to 66, and the number of datapoints/observations to 2757 (Fig. 4.13) and the number of grid cells with data in 10 or less temporal bins was seven (10%).

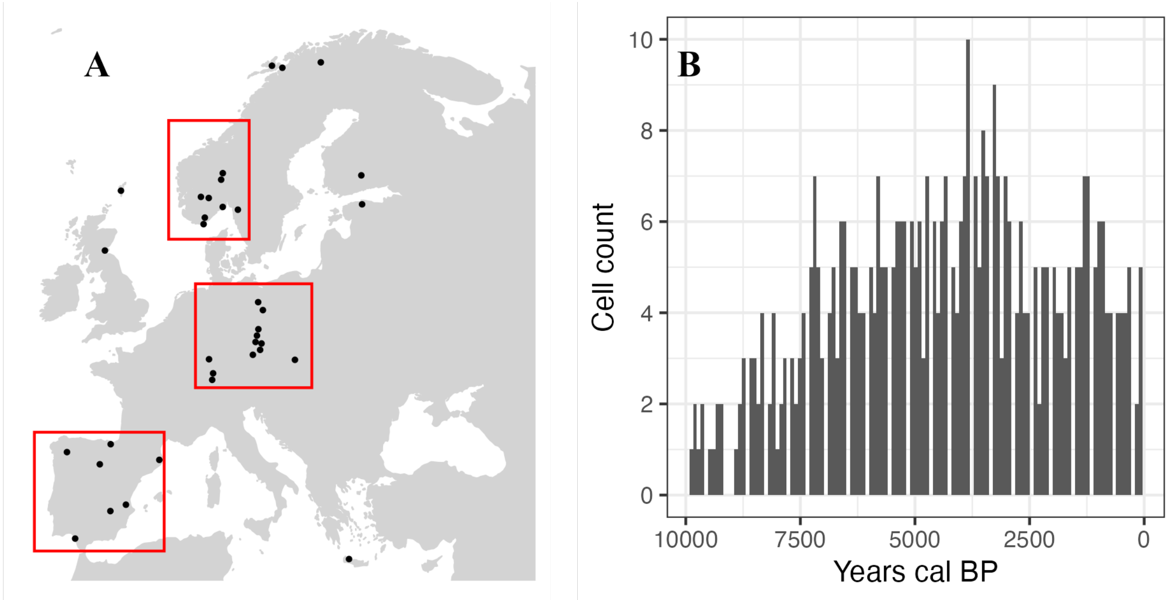

Figure 4.12: Spatiotemporal overlaps between reconstructions of fire, tree cover, climate, and population change: A – Spatiotemporal overlap locations, including sub-regional group demarcation; B – Cell counts for spatiotemporal overlaps through time

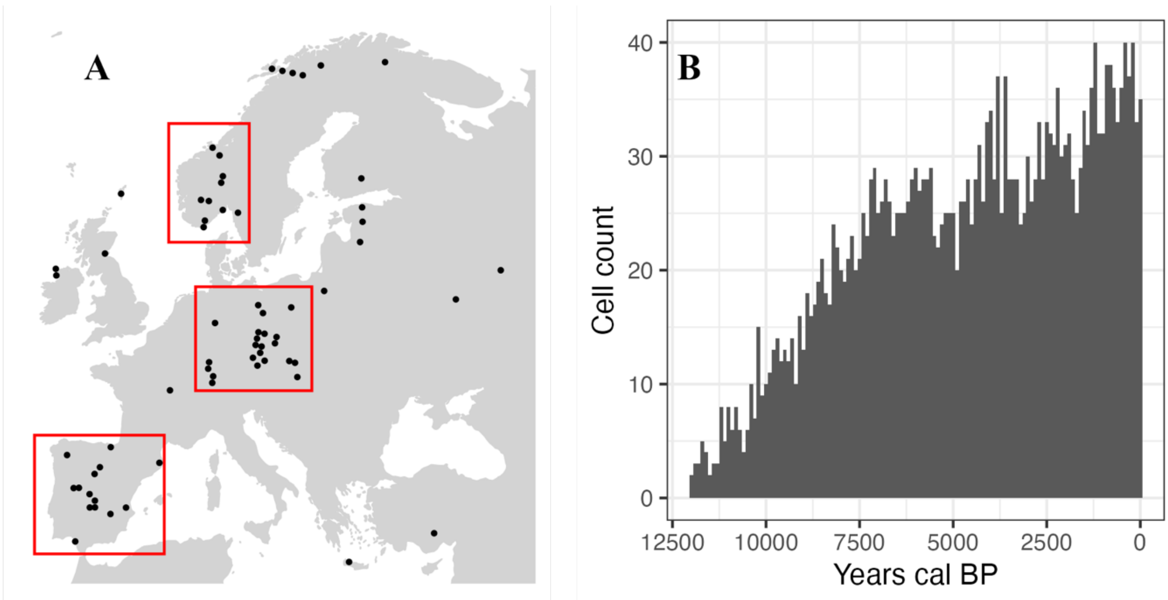

Figure 4.13: Spatiotemporal overlaps between reconstructions of fire, tree cover, and climate: A – Spatiotemporal overlap locations, including sub-regional group demarcation; B – Cell counts for spatiotemporal overlaps through time

4.3.2. Z-scores

One of the key challenges in the statistical analysis of the data is the question of how to treat the charcoal data, given the wide variations the quantities and ranges in charcoal influx values. The approach employed here is to make use of the use of charcoal z-score approach. As these charcoal z-score values are based on relative influx at a site level, these values have no intrinsic meaning compared to the reconstructed values of tree cover and climate variables. However, calculating site-based z-scores for each variable means that, at a site level, changes in fire and its controls can be compared. To ensure as much temporal consistency at the site level as possible, z-scores of charcoal influx, tree cover and climate variables were calculated for the identified overlapping time periods per grid cell. These were then averaged for each grid cell. Note that not all sedimentary records in a single grid cell have data at the same time period, which means that the calculation of z-scores and subsequent averaging may be slightly affected.

4.3.3. Modelling palaeofire as a function of tree cover and climate variables

A simple linear model was tested, with fire a function of tree cover and each of the climate variables. This generated high variance inflation factor (VIF) values, which was expected given the close correlation between some of the predictors (Fig. 4.14). The model was sequentially re-run with fewer variables until VIF values fell below a threshold of 4, resulting in a linear model ("LM1") including only tree cover, MTCO and α. Examination of the partial residual plots for this model suggested there was a non-linear relationship between MTCO and fire (Fig. 4.15), and so a second-degree polynomial for MTCO was also included ("LM2") (Fig. 4.16) resulting in an improvement in the Akaike Information Criteria (AIC) values. There appear to be non-linear relationships for tree cover and α (Fig.4.16) but including these did not improve the AIC values and so were not included in the final model.

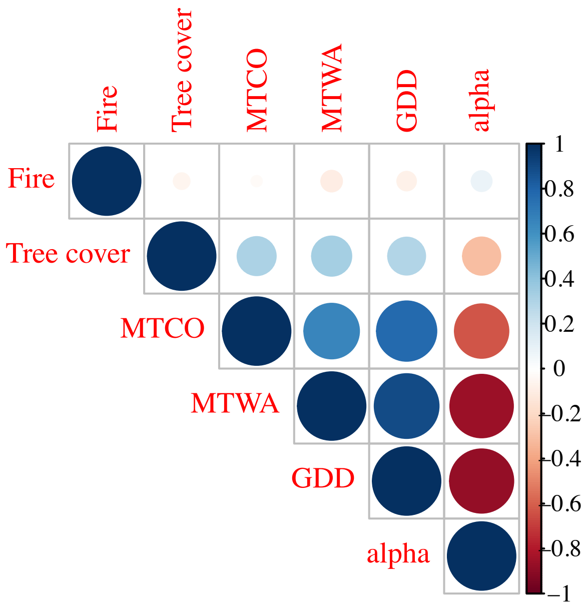

Figure 4.14: Correlation plot for z-score reconstruction values

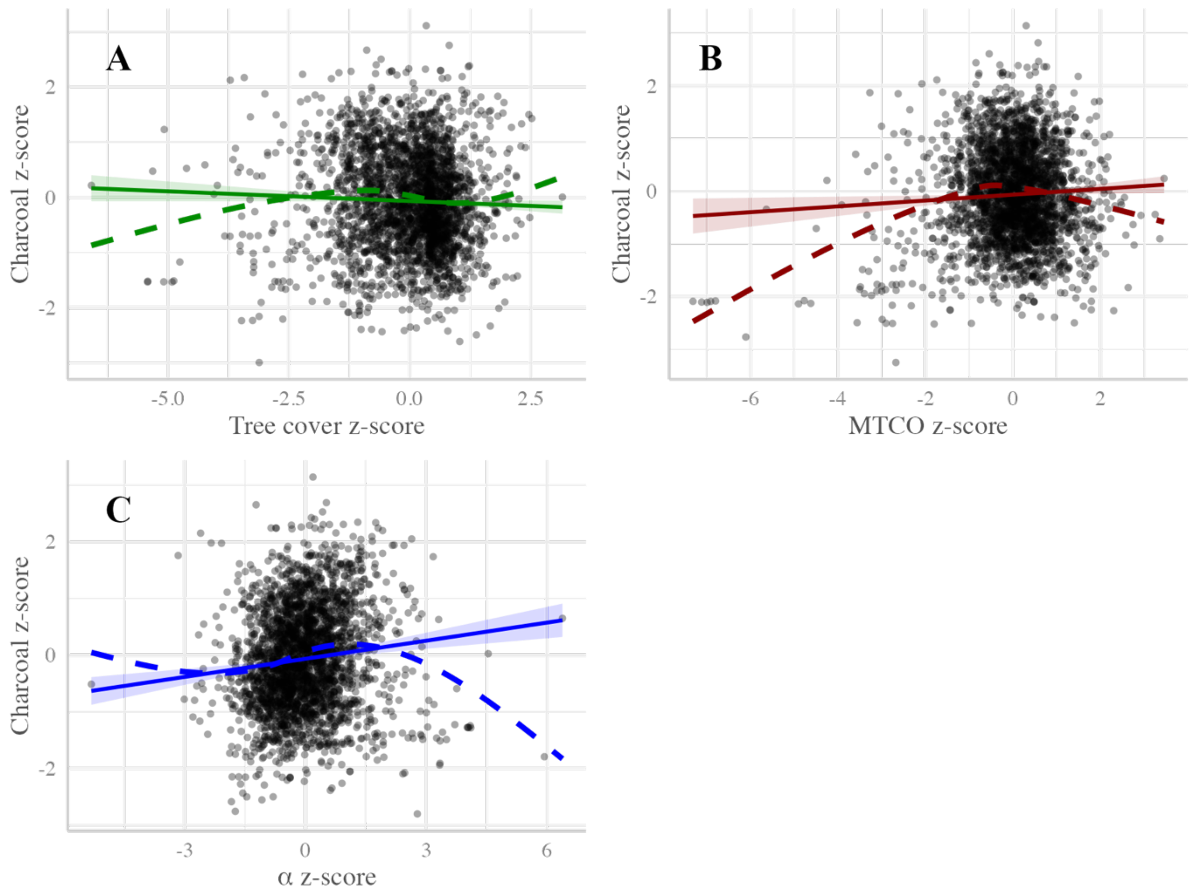

Figure 4.15: Partial residual plots for LM1: charcoal z-score values as a function of: A - tree cover z-scores; B - Mean temperature of the coldest month (MTCO) z-scores; E – Plant available moisture (α) z-scores. Solid lines represent the relationship between the predictor and the charcoal z-score, accounting for the effects of the

other predictors; hashed lines show a loess fitted line showing the model partial residuals plotted against the values of each predictor.

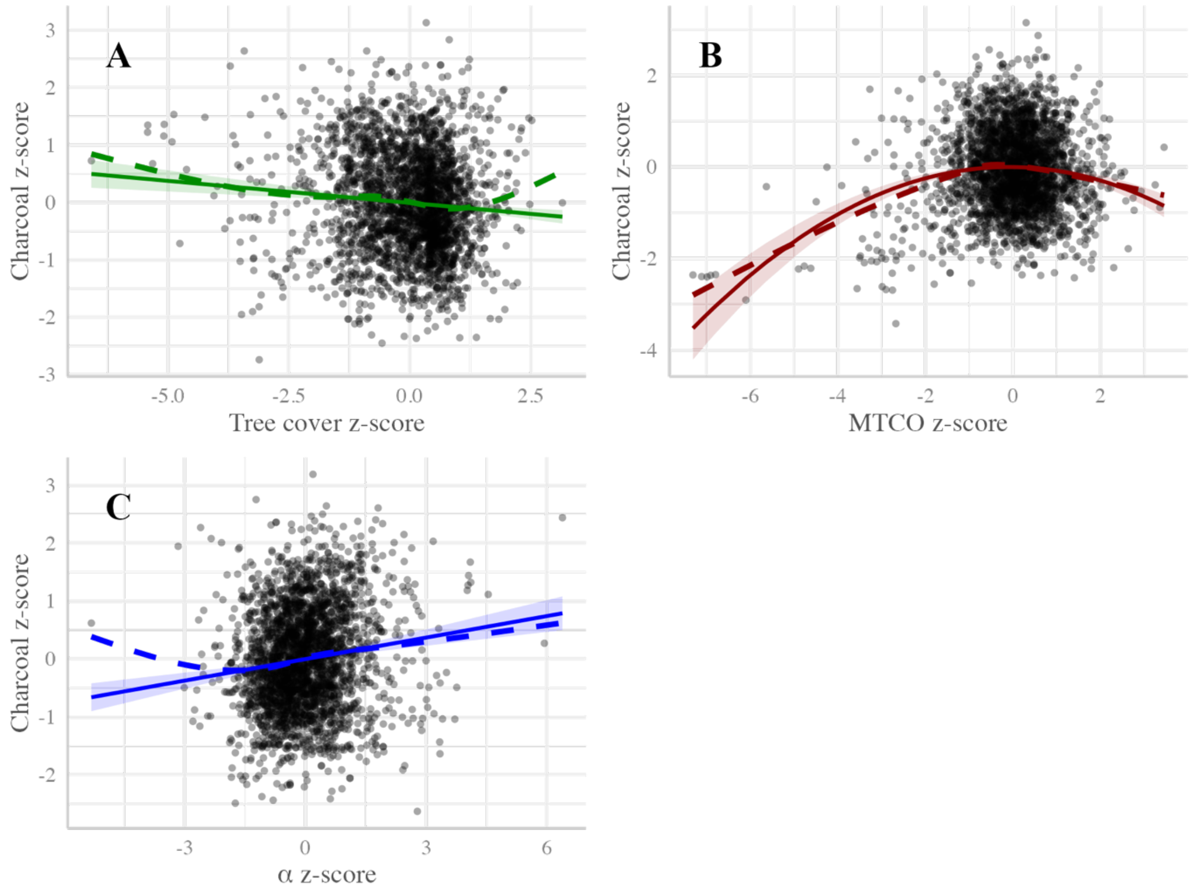

Figure 4.16: Partial residual plots for LM2: charcoal z-score values as a function of: A - tree cover z-scores; B - Mean temperature of the coldest month (MTCO) z-scores (with squared term); E – Plant available moisture (α) z-scores. Solid lines represent the relationship between the predictor and the charcoal z-score, accounting for the effects of the other predictors; hashed lines show a loess fitted line showing the model partial residuals plotted against the values of each predictor.

The model coefficients indicate that tree cover and the polynomial terms for MTCO significantly reduce fire (Table 4.2) while α significantly increases fire. Note that although $MTCO^2$ has negative impact on fire, MTCO itself is significant and positive with respect to fire when performing the regression with orthogonal polynomials (Table 4.3). Given the values for MTCO are generally low in the model due to their conversion to z-scores, this implies the impact of the quadratic term is more relevant to the higher and lower range of MTCO. This relationship can be seen in Fig. 4.16B, where MTCO and fire are mostly positive except at higher values of MTCO. This positive relationship of MTCO on fire may reflect the influence of warming temperatures on fuel availability and fire season lengths, although the negative polynomial value suggests a declining influence with MTCO. However, whilst this European-scale model was significant, it had very poor explanatory power, with an adjusted R^2 value of just 0.04.

Table 4.2: Coefficients for LM2: charcoal z-score values as a function of: tree cover z-scores; mean temperature of the coldest month (MTCO) z-scores (with squared term); plant available moisture (α) z-scores.

Coefficients	**Estimate**	**Standard Error**	**P Value**
(Intercept)	-0.004	0.018	0.806
Tree-cover	-0.077	0.018	3.15e-5 ***
MTCO	-0.012	0.023	0.604
$MTCO^2$	-0.068	0.007	7.35e-23 ***
α	0.124	0.023	8.11e-8 ***

Significance codes: 0 = '***'; 0.001 = '**'; 0.01 = '*'; 0.05 = .' 0.1; ' ' = 1

Table 4.3: Coefficients for LM2: charcoal z-score values as a function of: tree cover z-scores; orthogonal mean temperature of the coldest month (MTCO) z-scores (with squared term); plant available moisture (α) z-scores.

Coefficients	**Estimate**	**Standard Error**	**P Value**
(Intercept)	-0.067	0.017	6.31e-5 ***
Tree-cover	-0.077	0.018	3.15e-5 ***
Orthogonal MTCO	4.020	3.490	4.91e-4 ***
Orthogonal $MTCO^2$	-9.019	0.908	7.35e-23 ***
α	0.124	0.023	8.11e-8 ***

Significance codes: 0 = '***'; 0.001 = '**'; 0.01 = '*'; 0.05 = .' 0.1; ' ' = 1

To test whether this poor performance reflected regional differences, models with the same explanatory variables were run for central Europe, Iberia and southern Norway separately. The adjusted R^2 values for central Europe and Iberia were very poor (adjusted R^2 = 0.01 and 0.02 respectively), but the adjusted R^2 for southern Norway was somewhat better (0.18). In this model, tree cover had a significant positive relationship with fire (Table 4.3), potentially indicating a control on fire based on the availability of vegetation to burn. $MTCO^2$ and α showed negative and positive relationships with fire respectively (Table 4.4). When performing the regression with orthogonal polynomials for MTCO, the linear MTCO value is positive and significant (Table 4.5), in common Europe as a whole. The positive relationship between α and fire is difficult to explain at this latitude, as moisture is unlikely to be a limiting factor for NPP.

Table 4.4: Coefficients for LM2- southern Norway: charcoal z-score values as a function of: tree cover z-scores; mean temperature of the coldest month (MTCO) z-scores (with squared term); plant available moisture (α) z-scores.

Coefficients	**Estimate**	**Standard Error**	**P Value**
(Intercept)	0.215	0.044	1.10e-6
Tree-cover	0.110	0.049	0.026 *
MTCO	0.0329	0.054	0.544
$MTCO^2$	-0.198	0.024	1.29e-15 ***
α	0.399	0.058	1.50e-11 ***

Significance codes: 0 = '***'; 0.001 = '**'; 0.01 = '*'; 0.05 = .' 0.1; ' ' = 1

Table 4.5: Coefficients for LM2- southern Norway: charcoal z-score values as a function of: tree cover z-scores; orthogonal mean temperature of the coldest month (MTCO) z-scores (with squared term); plant available moisture (α) z-scores.

Coefficients	**Estimate**	**Standard Error**	**P Value**
(Intercept)	0.0263	0.372	0.479
Tree-cover	0.110	0.049	0.026 *
Orthogonal MTCO	3.159	1.290	0.015 *
Orthogonal $MTCO^2$	-7.992	0.975	1.29e-15 ***
α	0.399	0.058	1.50e-11 ***

Significance codes: 0 = '***'; 0.001 = '**'; 0.01 = '*'; 0.05 = .' 0.1; ' ' = 1

To test whether there may be a residual cell-based impact – for example, in terms of average elevation of the grid cell – a mixed effect model was run with the unique grid cell as a random effect. Mixed effect models allow for the testing of relationships whilst correcting for potential non-independence in the data structure (e.g. Oberg and Mahoney, 2007). At the European level a linear mixed effect model was run with the grid cell as an intercept random effect, using R package *lmerTest* (Kuznetsova et al., 2017). However, an analysis of variance (ANOVA) test of the inclusion of this random effect was not significant, and the AIC value increased compared to LM2. This test was also run on the sub-regional data, with the same result: none of the models with additional random effect associated with the grid cell were significant improvements on their LM2 variants, with AIC value that were also no better.

To assess whether the temporal bin had an impact on the model, a mixed effect model with an intercept random effect for temporal bin was tested. Temporal trends in the dependent variable will inevitably mean that the time period will significantly impact the model fit. The intraclass correlation (ICC), which represents the proportion of the total model variance explained by between class variance (e.g. Nakagawa and Schielzeth, 2010) was used to determine how important time was in explaining the variance. For the European-level model, the inclusion of temporal bin (linear mixed model 2: LMM2) improved the AIC value (7087 vs 7243 for LM2) and ANOVA testing showed it significantly improved the model. This result probably reflects the fact that the composite curve for z-score charcoal accumulation has an overall upward trend (Fig. 4.2A). However, the ICC value of 0.07, indicating that the difference in time accounted for 7% of the overall variance, is not substantial and the relationships with the drivers was unchanged from the basic model (Table 4.6). This does indicate that predictors still do not explain the pattern of fire well.

Table 4.6: Coefficients for LMM2: charcoal z-score values as a function of: tree cover z-scores; mean temperature of the coldest month (MTCO) z-scores (with squared term); plant available moisture (α) z-scores.

Fixed Effect Coefficients	**Estimate**	**Standard Error**	**P Value**
(Intercept)	-0.072	0.029	0.016 *
Tree-cover	-0.074	0.018	5.75e-05 ***
MTCO	-0.004	0.023	0.866
$MTCO^2$	-0.053	0.007	1.39e-14 ***
α	0.094	0.023	4.89e-05 ***
Random effect	Number	ICC	
Temporal bin	121	0.07	

Significance codes: 0 = '***'; 0.001 = '**'; 0.01 = '*'; 0.05 = .' 0.1; ' ' = 1

The inclusion of time did not significantly improve the model for central Europe and Iberia, nor reduce AIC values. For southern Norway, charcoal accumulation follows a clear trend (Fig. 4.16A), the inclusion of time did significantly improve the model and reduce the AIC value (1400 vs 1455 for LM2 for southern Norway). Here the ICC value was relative substantial – 0.37 – which meant that the conditional Nakagawa R^2 was similarly improved to 0.40. However, the marginal R^2 remained low – 0.05 – indicating that the majority of this R^2 related to the inclusion of time, rather than the impact of explanatory variables. Tree cover was no longer significant in this model, but the negative relationship between the polynomial term for MTCO and fire, and the positive relationship between α and fire, both remained significant.

The predictive ability of the reconstructed drivers using the simple linear modelling approach was poor. Reasons for this are explored in section *4.5 Discussion and conclusions*.

4.4. Time series analysis

An alternative approach to assess the links between fire and its drivers is to investigate changes in the time series. This approach is less rigorous than a full regression analysis, but the composite nature of the curves helps reduce the impact of spatiotemporal noise from the reconstructions. Assessing time series at the sub-regional level also permits the inclusion of population estimates. Granger causality (Granger, 1969) was used to investigate the lagged relationships between the time series, and Superposed Epoch Analysis (SEA) was used to investigate periods of population change and the implications that this had for fire and co-variables.

There are some clear differences in overall trends and millennial fluctuations between sub-regions for the reconstructed variables (Fig. 4.17). The trend in fire for southern Norway appears quite different from the other regions (Fig.4.17A), with a continual increase across the Holocene. Similarly, the population trend appears different in southern Norway (Fig.4.17F), although this is likely to be a reflection of differences in the use of radiocarbon dating by region. These differences highlight the need to investigate changes in fire in relation to the combined influence of variables, rather than focussing on single drivers to explain changes.

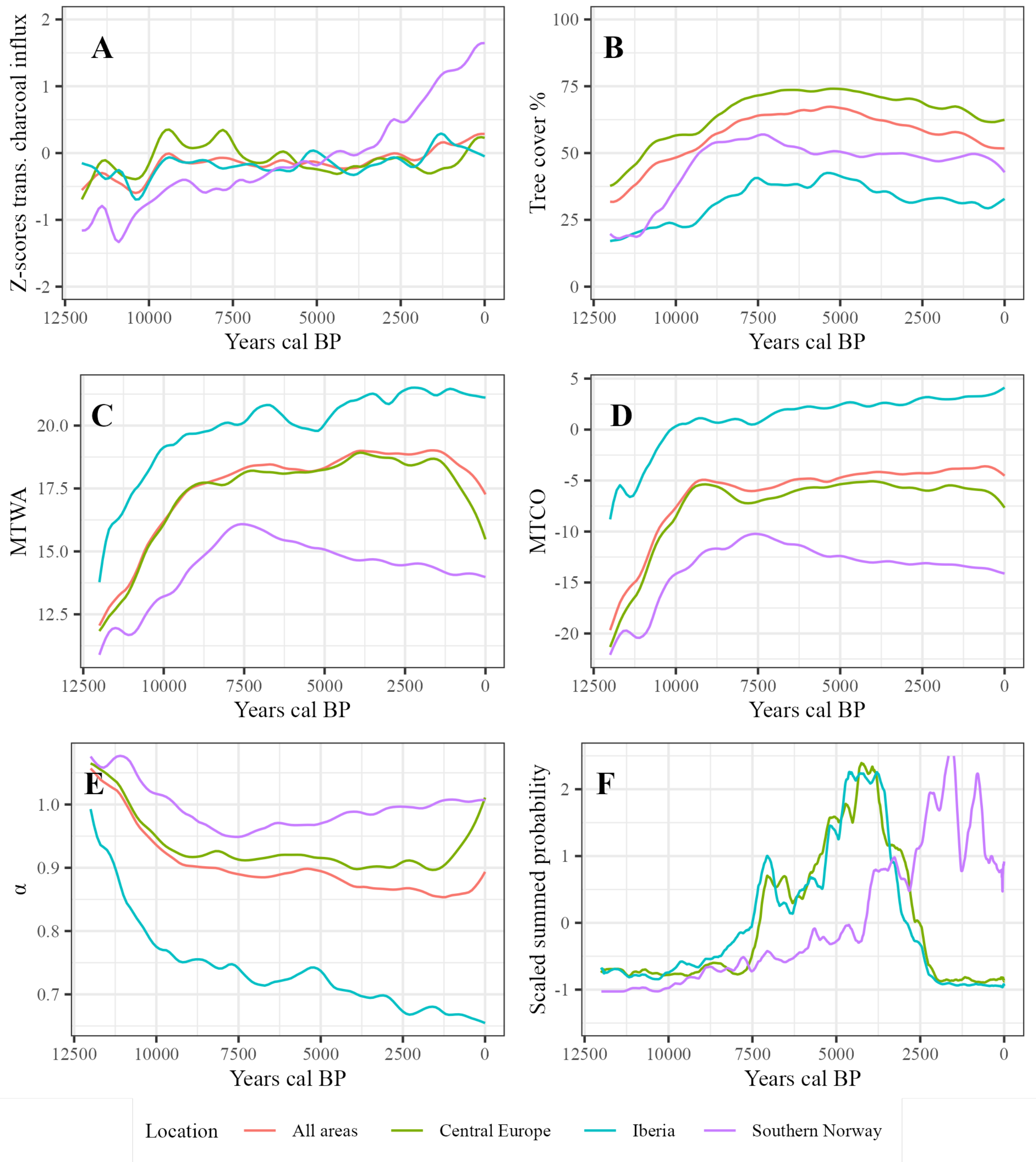

Figure 4.17: Comparison between variables considered by sub-region and all sub-regions combined ("All areas") through time: A – Z-score composite of charcoal accumulation; B – Tree cover; C – Mean temperature of the warmest month (MTWA); D – Mean temperature of the coldest month (MTCO); E – Plant available moisture (α); F – Scaled summed probability distributions

4.4.1. Granger causality testing

Granger causality is one way of testing the relationship between time series. Although originally developed for use with economic data (Granger, 1969), Granger causality has been applied in earth system science (e.g. Kodra et al., 2011; McGraw and Barnes, 2018; Kumar et al., 2023;

Papaspyropoulos and Kugiumtzis, 2024), and in terms of palaeofire (Stivrins et al., 2018; Heidgen et al., 2022). Here, Granger causality is used to test how useful the reconstructed time series for tree cover, human population and climate variables are in explaining reconstructed fire at a sub-regional level.

In the bivariate case, one time series is said to Granger cause another if the lagged values are useful in predicting the other, in addition to lagged values of variable itself (Granger, 1969). This bivariate analysis can be extended to the multivariate case through use of vector autoregressive models (VAR), which are a generalisation of single variable autocorrelation models to incorporate multiple time series (Equation 4.1; Wooldridge, 2005).

$$y_t = \delta_0 + \alpha_1 y_{t-1} + \gamma_1 z_{t-1} + \beta_1 w_{t-1} + \alpha_2 y_{t-2} + \gamma_2 z_{t-2} + \beta_2 w_{t-2} + \cdots$$

Equation 4.1: Vector autoregressive model. Y at time t is modelled as a function of its lagged values Y_{t-1}, Y_{t-2} etc., as well as lagged values for other variables Z and W.

In Equation 4.1, Z Granger causes Y if for the number of lags included within the model, an F-test of this model and a model excluding lagged Z is significant i.e. the lags of Z have explanatory power compared to the lags of Y itself and lags of W. Granger causality is not causality in the strict sense of one variable causing another but implies that a variable (e.g. Z) is useful in predicting future values of another variable (e.g. Y).

The choice of number of lag periods for VAR is typically based on information criteria, with the selection of the fewest lags preferred to prevent over-fitting and false-positive results (Bruns and Stern, 2019). Here lag length selection was based on the Bayesian Information Criterion (BIC: Schwarz, 1978) in the first instance, using the R package *vars* (Pfaff, 2008) to build the VAR models and carrying out the information criteria testing on lag length. Since BIC tends to underfit VAR models (Bruns and Stern, 2019), Portmanteau tests for serial autocorrelation were run on the selected VAR models, and lag numbers increased until serial autocorrelation was removed. Granger causality was tested based on the approach developed by Toda and Yamamoto (1995). After selecting the number of lags in the VAR model based on information criteria, the maximum order of integration for the time series was included as additional lags within the VAR model. The subsequent Wald/F test is run on the VAR model excluding the additional lagged coefficients.

The inclusion of correlated variables, such as some of the climate reconstructions, has implications for the detection of Granger causal relationships because it means the difference between including lagged variable in terms of F/Wald test will be reduced, as the correlated variable will remain with the VAR model. To minimise this problem only one temperature variable, MTCO, was included in the time series analysis. However, α was also retained to represent changed in moisture even though it is correlated with MTCO. The rate of change of the SPD was included, with the underlying assumption that changes in population, rather than the population level itself, would most likely have a short-term impact on fire. The rate of change of the SPD was calculated with a backsight of 200 years and running mean of 100 years, using R package *rcarbon* (Crema and Bevan, 2021). The rate of change population measure was included for the period 12,000 cal. BP to 3,500 cal. BP for central Europe and Iberia, and from 9,500 cal. BP to 500 cal. BP for southern Norway. The later start for southern Norway reflected the paucity of radiocarbon dates from in the early Holocene, which produces distortionary rapid changes in the rate of change, and the later end date reflected the fact that typological dating is less used in this region.

There is considerable variability in each time series curve (Fig. 4.18A, C, and E), and to test the impacts of this, the Granger causality test was also run after smoothing each time series with a 200-year half width (Fig. 4.18B, D and F).

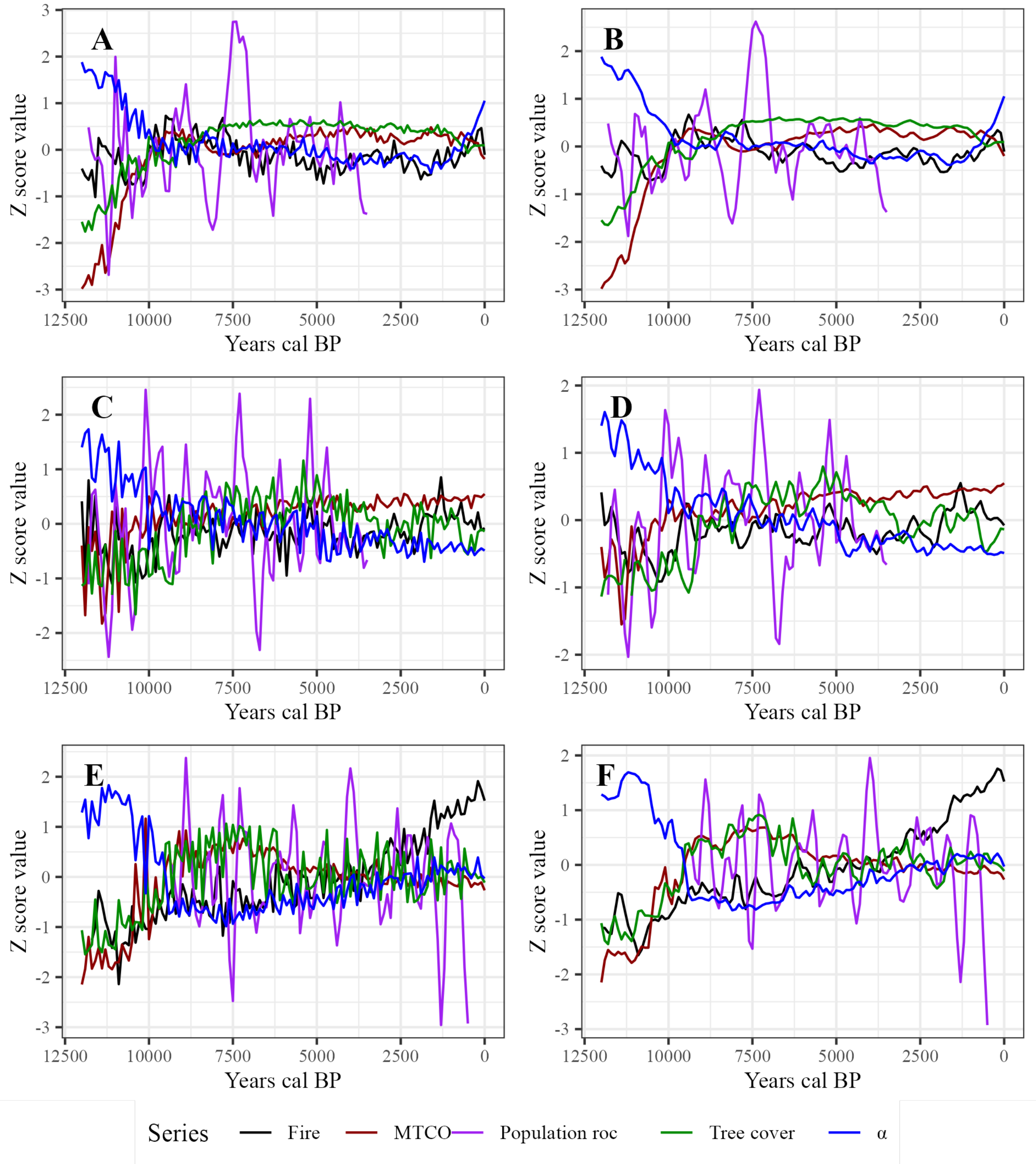

Figure 4.18: Z-score time series for median values of variables for Granger causality analysis. A – central Europe; B – central Europe with 200- year smoothing window; C – Iberia; D – Iberia with 200- year smoothing window; E – southern Norway; F – southern Norway with 200- year smoothing window

The results from the Granger causality test in relation to fire on the unsmoothed data (Table 4.7) shows that in southern Norway, the rate of change of population Granger causes fire. There are no significant Granger causal relationships for fire in Iberia at the 5% significance level, although there are weakly significant relationships (10% significance), also with tree cover and α. There were no VAR models that could be run without significant series autocorrelation for central Europe.

Table 4.7: Granger causality results for non-smoothed time series

Area	Lags	Cause	Chisq	Pvalue
Central Europe	NA	Tree cover	-	-
Central Europe	NA	MTCO	-	-
Central Europe	NA	α	-	-
Central Europe	NA	Population roc	-	-
Iberia	1	Tree cover	4.616	0.099 `
Iberia	1	MTCO	1.095	0.579
Iberia	1	α	4.893	0.087 `
Iberia	1	Population roc	1.488	0.475
Southern Norway	1	Tree cover	2.400	0.301
Southern Norway	1	MTCO	0.136	0.934
Southern Norway	1	α	1.153	0.562
Southern Norway	1	Population roc	7.526	0.023 *

Significance codes: 0 = '***'; 0.001 = '**'; 0.01 = '*'; 0.05 = .' 0.1; ' ' = 1

The results from the Granger causality test for fire on the smoothed data (Table 4.8) shows that tree cover MTCO and the population rate of change Granger cause fire in southern Norway, but with four lag periods (i.e. over 400 years) rather than one lag. At the lower 10% level of significance, α also Granger causes fire. There are no VAR models that do not have series autocorrelation issues for central Europe, and this is also the case for Iberia.

These results suggest an inconsistent picture of Granger causality across the regions. One limitation with the time series is the population time series, which for three of the sub-regions stops at 3,500 cal. BP and therefore limits the VAR models to the 12,000 cal. BP to 3,500 cal. BP range. The analysis was therefore re-run to test the effect of excluding the population rate of change time series. In this case, no VAR models could be found without series autocorrelation for the three sub-regions with unsmoothed time series (central Europe, Iberia and southern Norway). For the smoothed time series case, two VAR models could be run, with southern Norway not having any models without series autocorrelation (Table 4.9). In Iberia, MTCO Granger causes fire, and α may also cause fire, albeit with a low probability. In central Europe, tree cover Granger causes fire at a low significance level.

Table 4.8: Granger causality results for smoothed time series

Area	Lags	Cause	Chisq	Pvalue
Central Europe	NA	Tree cover		
Central Europe	NA	MTCO		
Central Europe	NA	α		
Central Europe	NA	Population roc		
Iberia	NA	Tree cover		
Iberia	NA	MTCO		
Iberia	NA	α		
Iberia	NA	Population roc		
Southern Norway	4	Tree cover	16.723	0.005 **
Southern Norway	4	MTCO	18.513	0.002 **
Southern Norway	4	α	9.845	0.080 `
Southern Norway	4	Population roc	24.502	0.000 ***

Significance codes: 0 = '***'; 0.001 = '**'; 0.01 = '*'; 0.05 = .' 0.1; ' ' = 1

Table 4.9: Granger causality results for smoothed time series, excluding population roc

Area	Lags	Cause	Chisq	Pvalue
Central Europe	4	Tree cover	10.713	0.098 `
Central Europe	4	MTCO	5.273	0.509
Central Europe	4	α	1.625	0.951
Iberia	3	Tree cover	5.411	0.248
Iberia	3	MTCO	11.180	0.025 *
Iberia	3	α	8.185	0.085 `
Southern Norway	NA	Tree cover	-	-
Southern Norway	NA	MTCO	-	-
Southern Norway	NA	α	-	-

Significance codes: 0 = '***'; 0.001 = '**'; 0.01 = '*'; 0.05 = .' 0.1; ' ' = 1

Since α and MTCO are still very closely correlated at the European scale (unsmoothed correlation = -0.93; smoothed correlation = -0.94), the analysis was re-run to test the effect of including only a single climate variable. Including only time series for fire, tree cover, α and population rate of change in the VAR models (Table 4.10) shows that α Granger causes fire in Iberia. In southern Norway, the population rate of change also Granger causes fire, but with weak significance. For smoothed data (Table 4.11), the population rate of change Granger causes fire in southern Norway. There is also weakly significant (at 10%) Granger causality in Iberia for tree cover and the population rate of change.

In southern Norway population change Granger causes fire for models run without series autocorrelation issues. For the other regions the relationships vary with the methodological choices about smoothing, the inclusion of population change and the total number of time periods available for testing, and how many climate variables are included. This limits the credibility of the relationships observed. The consistent Granger causality in southern Norway is difficult to interpret because Granger causality itself says nothing about the nature of any relationship.

Table 4.10: Granger causality results for unsmoothed time series, excluding MTCO

Area	**Lags**	**Cause**	**Chisq**	**Pvalue**
Central Europe	NA	Tree cover		
Central Europe	NA	α		
Central Europe	NA	Population roc		
Iberia	1	Tree cover	5.095	0.078
Iberia	1	α	7.023	0.030 *
Iberia	1	Population roc	2.050	0.359
Southern Norway	2	Tree cover	5.274	0.153
Southern Norway	2	α	1.472	0.689
Southern Norway	2	Population roc	7.431	0.059 `

Significance codes: 0 = '***'; 0.001 = '**'; 0.01 = '*'; 0.05 = .' 0.1; ' ' = 1

Table 4.11: Granger causality results for smoothed time series, excluding MTCO

Area	**Lags**	**Cause**	**Chisq**	**Pvalue**
Central Europe	NA	Tree cover		
Central Europe	NA	α		
Central Europe	NA	Population roc		
Iberia	3	Tree cover	9.009	0.061 `
Iberia	3	α	3.657	0.454
Iberia	3	Population roc	8.282	0.082 `
Southern Norway	3	Tree cover	7.335	0.119
Southern Norway	3	α	2.805	0.591
Southern Norway	3	Population roc	12.319	0.015 *

Significance codes: 0 = '***'; 0.001 = '**'; 0.01 = '*'; 0.05 = .' 0.1; ' ' = 1

Aside from southern Norway, population rate of change did not Granger cause fire except (with weak significance) in the single case of the smoothed time series with only fire, α and population rate of change included in Iberia. This may reflect the limitation of the amount of data but could also be because population changes may have only limited impacts on fire unless they are substantial. This is investigated further in the next section, using Superposed Epoch Analysis (SEA).

4.4.2. Superposed Epoch analysis

<u>Identifying events</u>

SEA is a means of investigating the impact of discrete events on a time series, to test for correlative responses to these events and is used here to investigate the impact of periods of rapid human population growth or declines on fire. To identify periods of rapid population change, exponential growth curves were fitted to the SPD curves for each sub-region. As the focus was on longer-term population trends rather than carrying capacity, exponential growth rates were appropriate. An envelope was defined by Monte Carlo simulations of this fitted growth rate (Crema and Bevan, 2021), and periods when the rate of change of the SPD departed from this envelope were used as periods of rapid population change (following Timpson et al., 2014). The start of these time periods were then used to re-base the charcoal, tree cover and climate data for each sub-region, with a window of +- 500 years around the periods of rapid population change. Composite curves for each time series were then re-drawn for this 1000-year window, to see whether the start of rapid population changes coincided with clear changes to fire, tree cover and climate. This follows the approach used for Iberia (Chapter 2), but extended to include population busts as well as booms, and tree cover and climate variables.

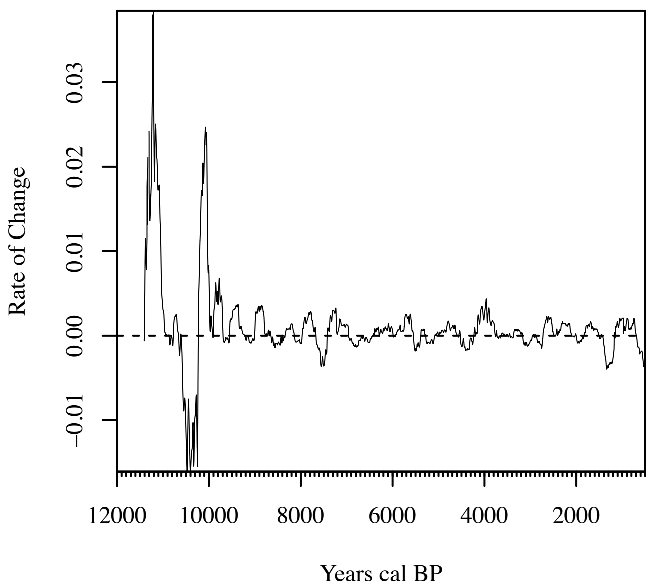

Figure 4.19: Rate of change SPD for southern Norway, with 200-year backsight. 12,000 to 500 cal. BP

Prior to fitting the models, the SPDs and rates of change were investigated to assess the appropriate window of analysis. The availability of radiocarbon data for southern Norway continues much closer to the present than in other areas but was very sparse at the beginning of the Holocene, causing large swings in the rate of change of the SPD with only minor changes in summed probability densities (Fig. 4.19). The window for the analysis, and the generation of the exponential curve, was therefore limited to the period 9,500 cal. BP to 500 cal. BP for this region. The range of data was limited to 10,000 cal. BP to 3,500 cal. BP for the other regions (Fig. 4.20) to avoid similar problems.

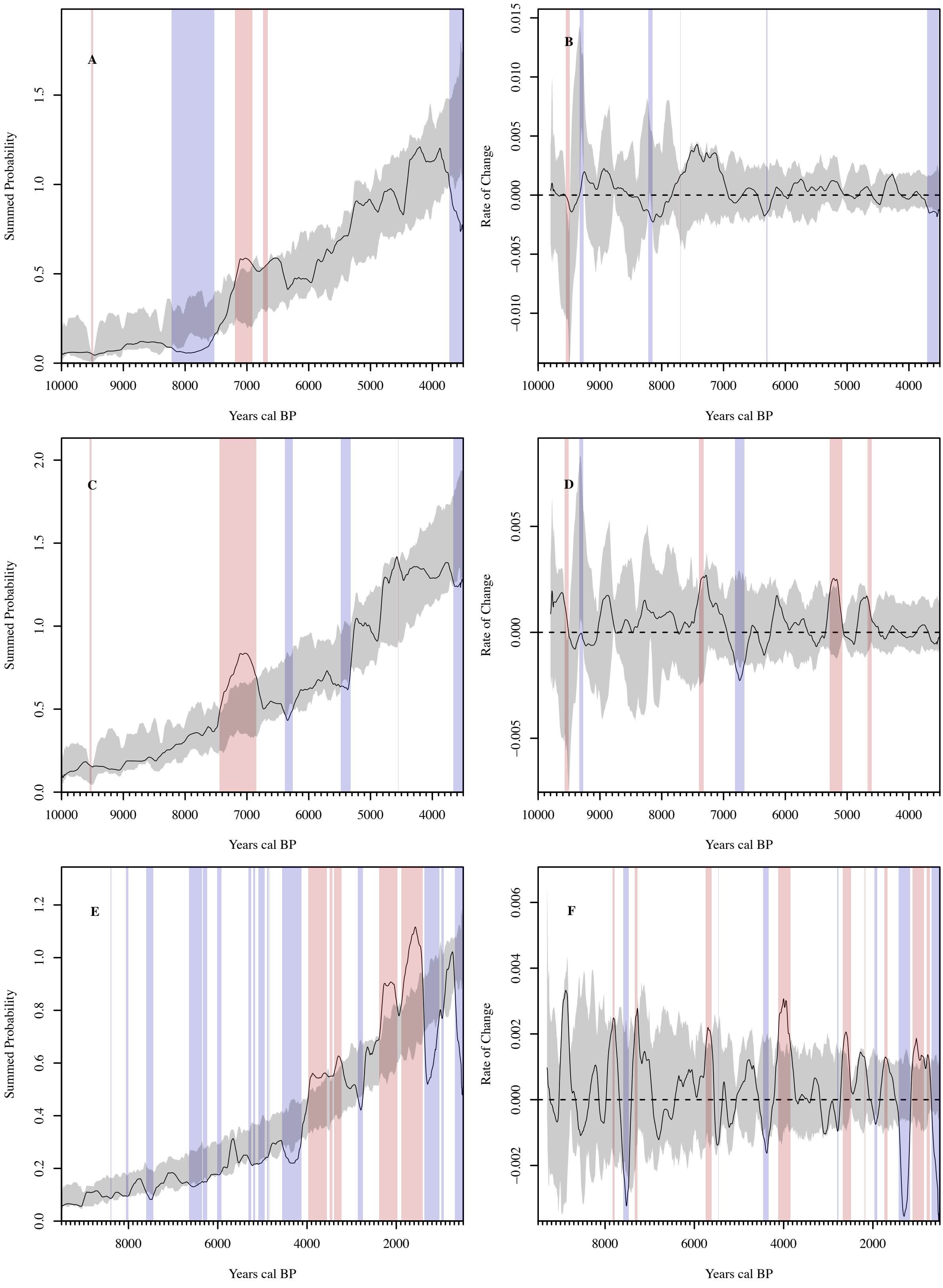

Figure 4.20: SPD and rate of change in SPD, together with exponentially fitted null model. A – SPD for central Europe; B – Rate of change SPD for central Europe; C – SPD for Iberia; D – rate of change SPD for Iberia; E – SPD for southern Norway; F – Rate of change SPD for southern Norway

Although the SPD and fitted null for Iberia identifies clear periods of growth (see section *2.3.1: Fire and population change through time*) and decline in population (in Fig. 4.20A), this is less evident for other sub-regions. In southern Norway, there are many periods of lower population earlier in the SPD, as well as many periods of rapid growth associated with the rate of change exponential null and SPD rate of change. These differences highlight a need for a slightly more nuanced approach than applied in Chapter 2, to enable a consistent approach across regions. Rather than investigating both the SPD and rate of change of the SPD in relation to the fitted null models, focus was placed on the rate of change of the SPD.

After fitting the exponential null model, "events" relating to population growth and decline were identified that (a) were significant local positive and negative deviations from the fitted null that were longer than 50 years, (b) were separated by more than 100 years so as to be regarded as discrete events and (c) continued to increase (or decrease)for 150 years after the initial deviation above (below) the mean population growth for the entire period. The 150-year period was a pragmatic choice, designed to balance exclusivity without restricting event numbers.

An SEA window of 1000-years around each boom or bust event was calculated. This window was used to filter the charcoal, tree cover and climate data, such that only samples occurring within each window for each rub-region were included. This data was then re-based by SEA window, with the boom or bust event set to a date of zero, and then combined, segregating booms and busts into epochs. For each variable, the time series was then re-binned into 100-year bins, and a time series re-calculated with a 200-year smoothing half window. This smoothing window was narrower than applied to the whole series, due to the more limited 1000-year epoch window.

In some instances, the difference in times between booms and busts were not 500-years (i.e. half of the 1000-year window width). In southern Norway, for example, there were several boom-and-bust events in relatively close proximity (4.21C). To prevent the inclusion of overlapping data, where, for example, the same data were used to reflect a boom and a bust epoch, in instances where the events were closer than 500-years, the window was truncated with an equal share of time divided between the two events. In practice this meant that some windows were substantially shorter than 1000 years, with only a short period on one or other (or both) side of the event. Figure 4.21 shows the identified boom and bust events for each sub-region, and the windows either side of each used to define the epoch, for the rate of change of SPD.

The three-step filtering approach resulted in the identification of two boom events identified in Iberia, five in southern Norway, and no events in central Europe. The lack of boom events for central Europe means that an SEA could not be run. For southern Norway, the large number of events effectively reduces the overall SEA window to less than 1000-years. This different specification of events is also visible with the busts in population, with four events in southern Norway, and two events in the other regions.

For central Europe, the lack of identified boom events perhaps points to a more consistent level of growth in the sub-region. For Iberia, the first boom, and following bust in population corresponds with the start of agriculture in the region (Balsera et al., 2015; Drake et al., 2017). The subsequent increase in population at ca. 5000 cal. BP has also been identified and linked with changes to landscapes in some areas (Drake et al., 2017). In southern Norway, the start of continuous arable farming was around 4,000 cal. BP (Solheim, 2021), which corresponds to one of the booms in population. However, it is difficult to attribute other booms and busts to specific events in the population history of this region.

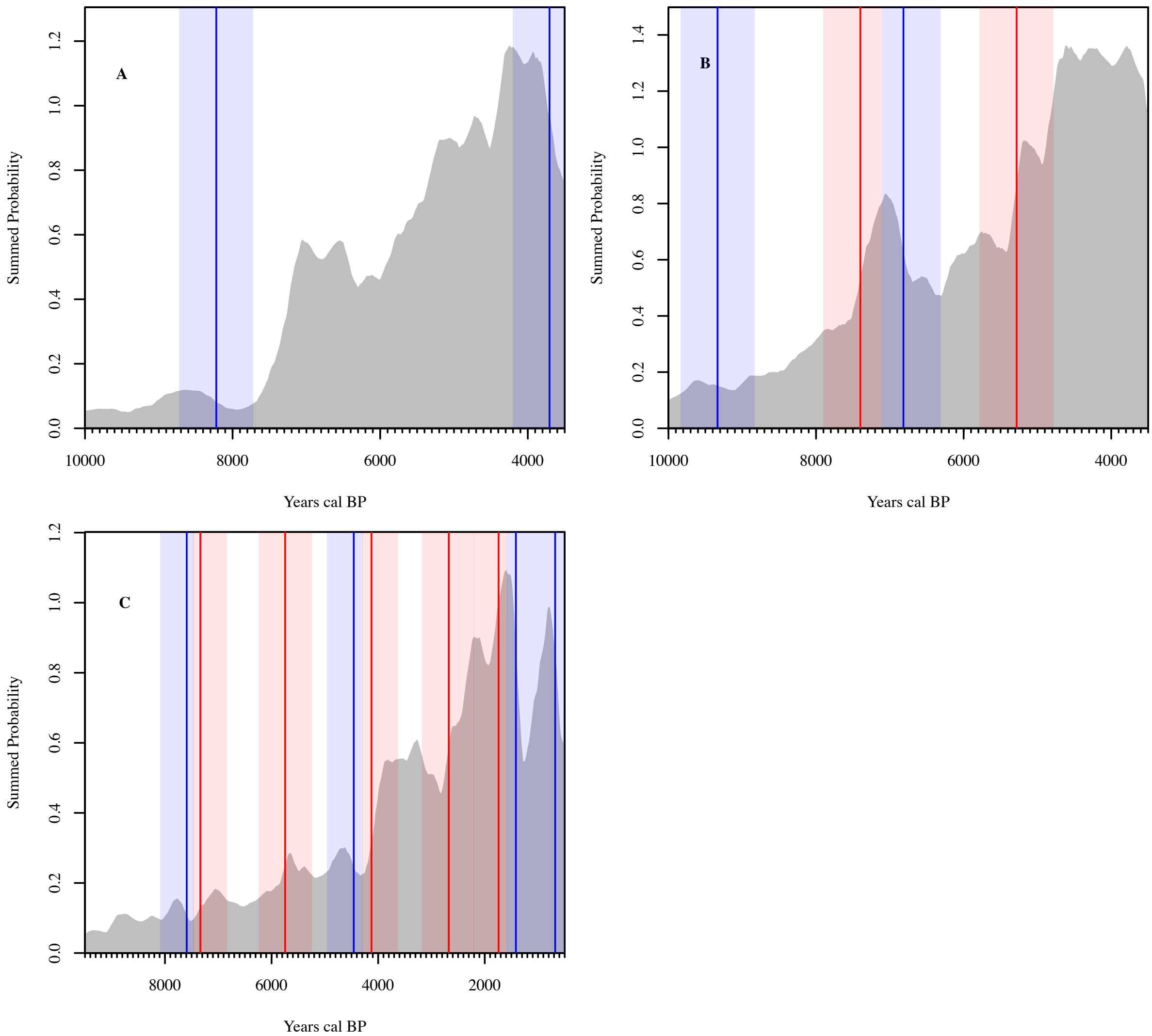

Figure 4.21: SPDs by location, with identified booms (red) and busts (blue) population periods. SEA windows for each boom and bust are shown in light red and blue respectively: A – central Europe; B – Iberia; C – southern Norway

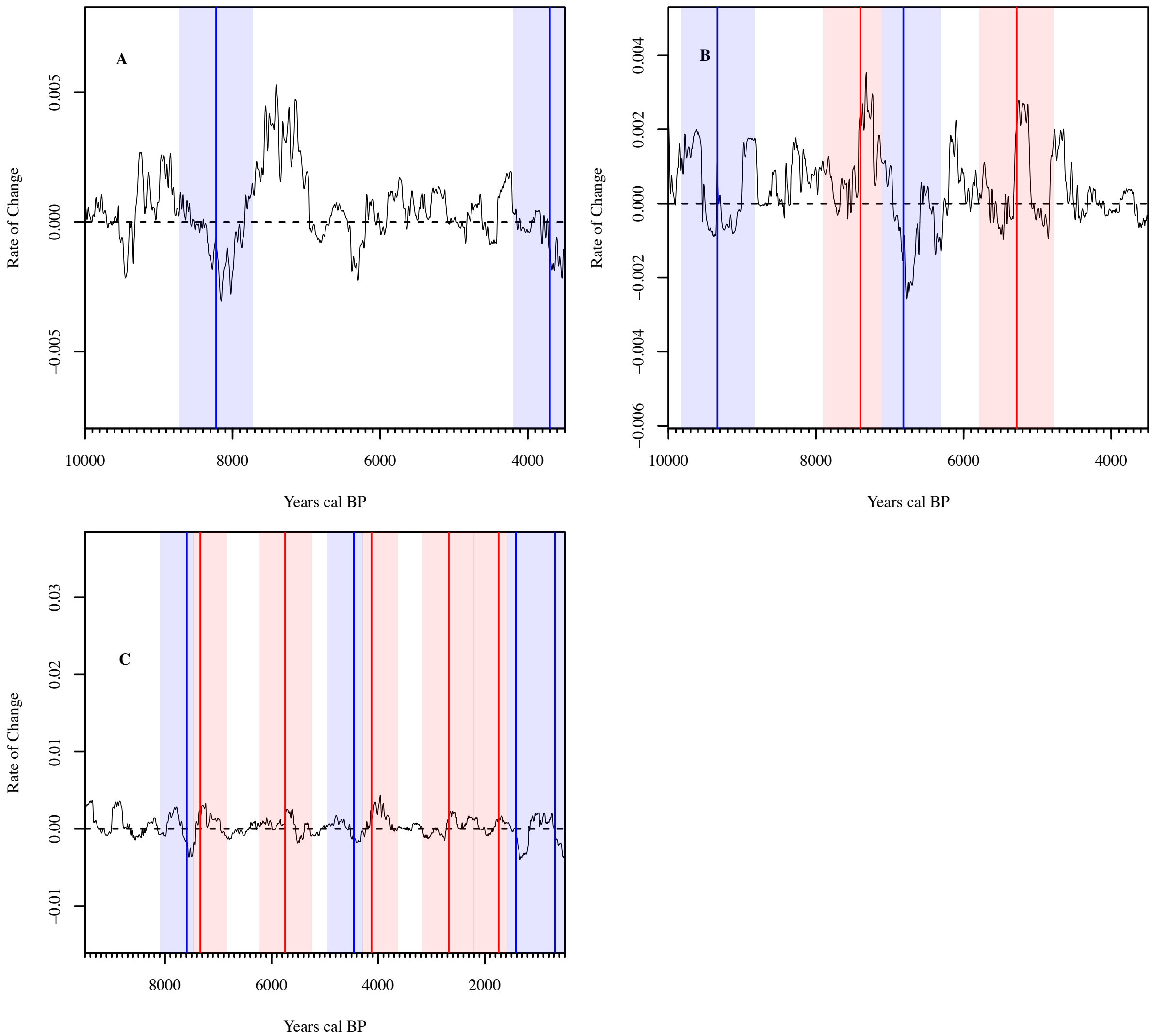

Figure 4.22: Rate of change SPDs, with 200 years backsight by location, with identified booms (red) and busts (blue) population periods. SEA windows for each boom and bust are shown in light red and blue respectively: A – central Europe; B – Iberia; C - southern Norway

<u>SEA results</u>

Population bust events appear to coincide with increases in fire in central Europe (Fig. 4.23). There are only very minor changes in the other variables, which become visible when investigating combined z-score plot (Fig. 4.24). The bust events coincide with a reduction in tree cover and stabilising α, and at the end of the period the increase in MTCO and decline in α coincides with decreases in fire. However, it is difficult to see a consistent climate or tree cover signal associated with fire during this period.

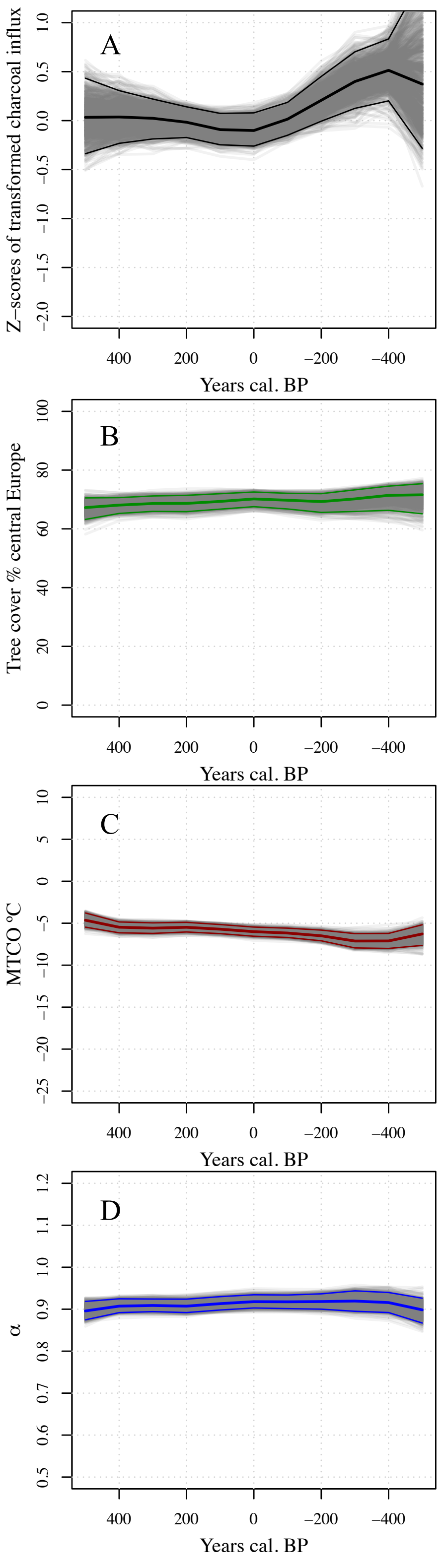

Figure 4.23: SEA figures showing adjusted values for central Europe based on busts in populations: A – SEA busts for z-scores charcoal influx; B – SEA busts for tree cover; C - SEA busts for MTCO; D - SEA busts for α

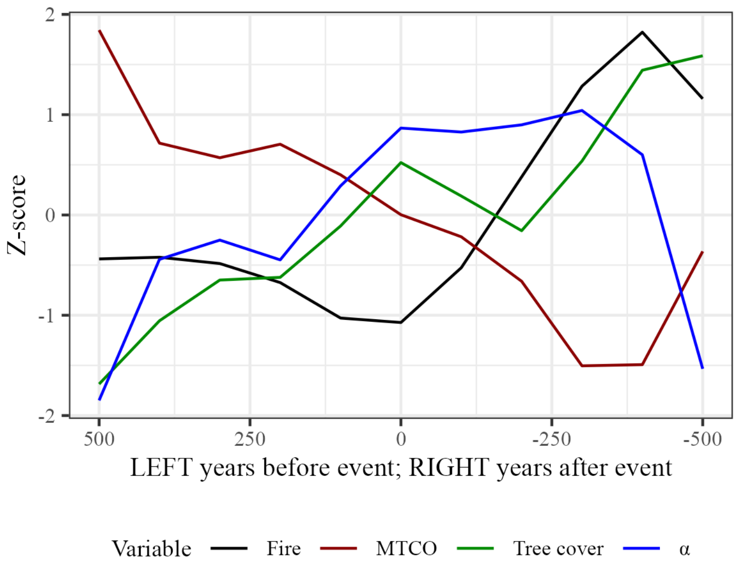

Figure 4.24: Combined SEA plot for central Europe, with variable values for the period -500 to 500 before and after the SEA point converted to z-scores: A – Population booms; B – Population busts

Changes in fire in Iberia appear to coincide with boom events (Fig. 4.25A). This is not consistent with the results from Chapter 2 and most probably reflects methodological differences in terms of window widths, binwidths and smoothing half windows. Again, at the standardised scale, changes in tree cover and climate are barely discernible. For the combined z-score plot, there is no consistent single climate or tree cover signal that explains the changes in fire (Fig. 4.26), although there are consistencies between the signals that suggest a complex interaction of moisture, vegetation coverage and temperature may be at play. There is no clear correlation of population bust effects with fire. The decrease in fire that begins around 300 years prior to the bust events and continues to the end of the SEA window is partially mirrored by the increase in tree cover, although tree cover begins to increase around 100 years earlier. The small-scale changes in MTCO and α visible in the combined plot do not align with changes in fire.

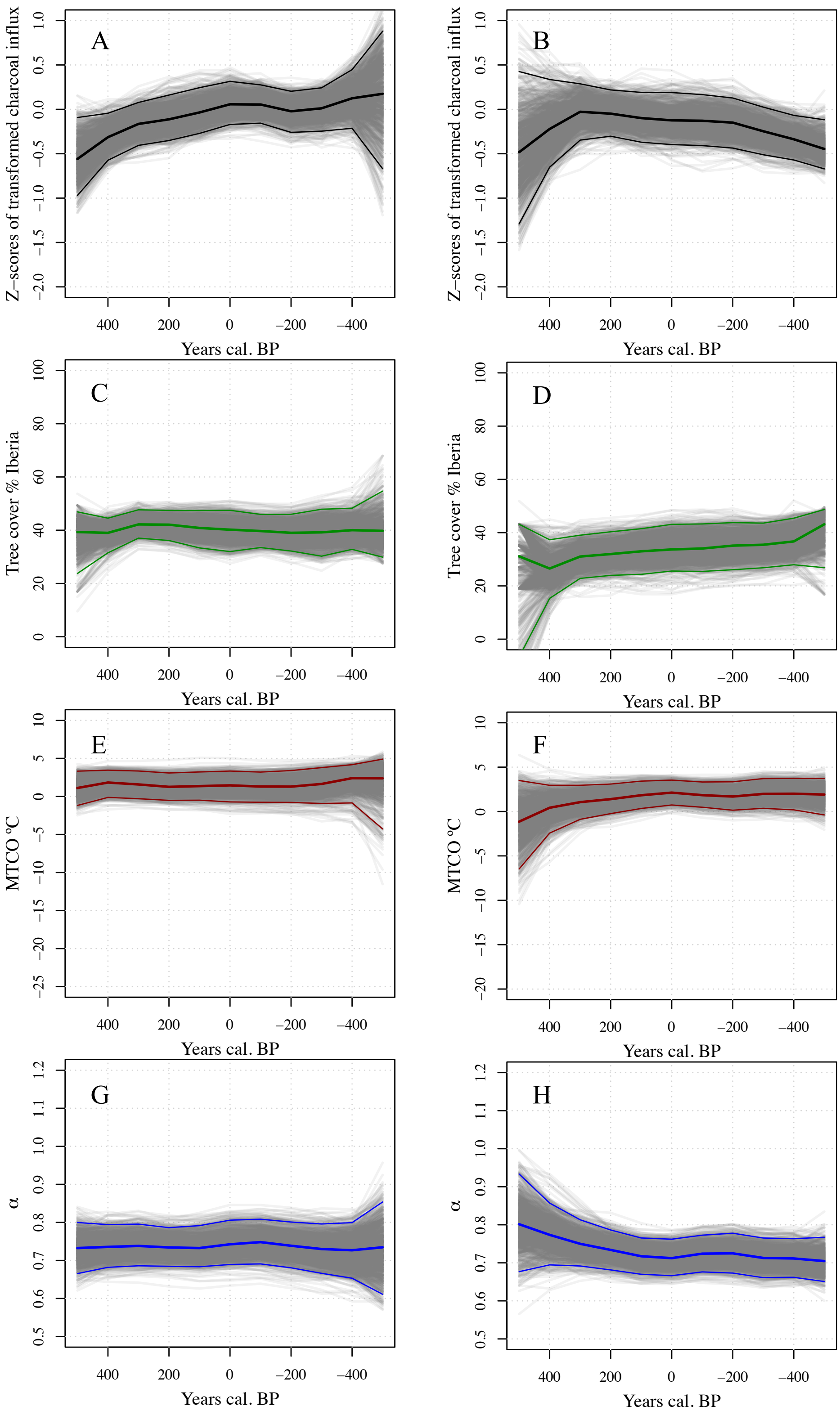

Figure 4.25: SEA figures showing adjusted values for Iberia based on booms and busts in populations: A – SEA booms for z-scores charcoal influx; B – SEA busts for z-scores charcoal influx; C – SEA booms for tree cover; D - SEA booms for tree cover; E - SEA booms for MTCO; F - SEA busts for MTCO; G - SEA booms for α;H - SEA busts for α

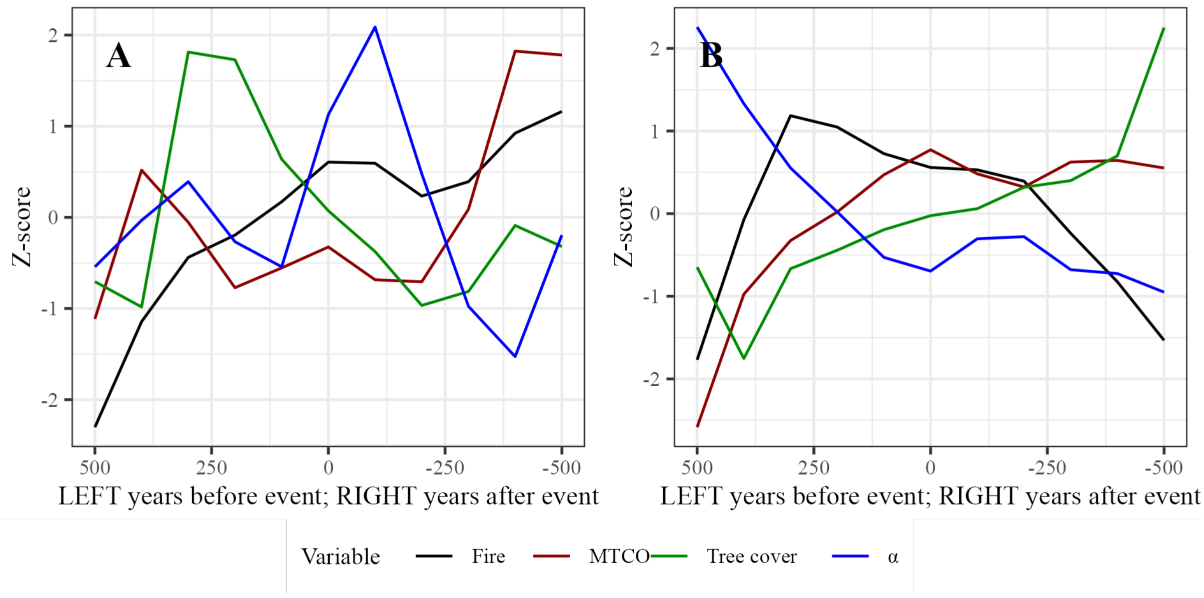

Figure 4.26: Combined SEA plot for Iberia, with variable values for the period -500 to 500 before and after the SEA point converted to z-scores: A – Population booms; B – Population busts

Population booms do not appear to coincide with changes in fire in southern Norway (Fig. 4.27), although there is a minor change in fire 100-years prior to the boom event. For the combined z-score plot (Fig. 4.28), changes in fire appear to be closely associated with those in climate and tree cover. Population busts are correlated with increases in fire. Although the individual curves for tree cover and climate do not show a clear relationship with fire, the combined z-score plot shows a very close correlation between all of the variables, with fire (mostly) positively correlated with α and negatively correlated with MTCO and tree cover. The association of increasing moisture with increasing fire is problematic given that fire is probably not fuel limited in this region. In contrast, increases in MTCO imply increases in tree cover, which is as observed. The mechanism for decreases in fire may then be the expansion of tree cover.

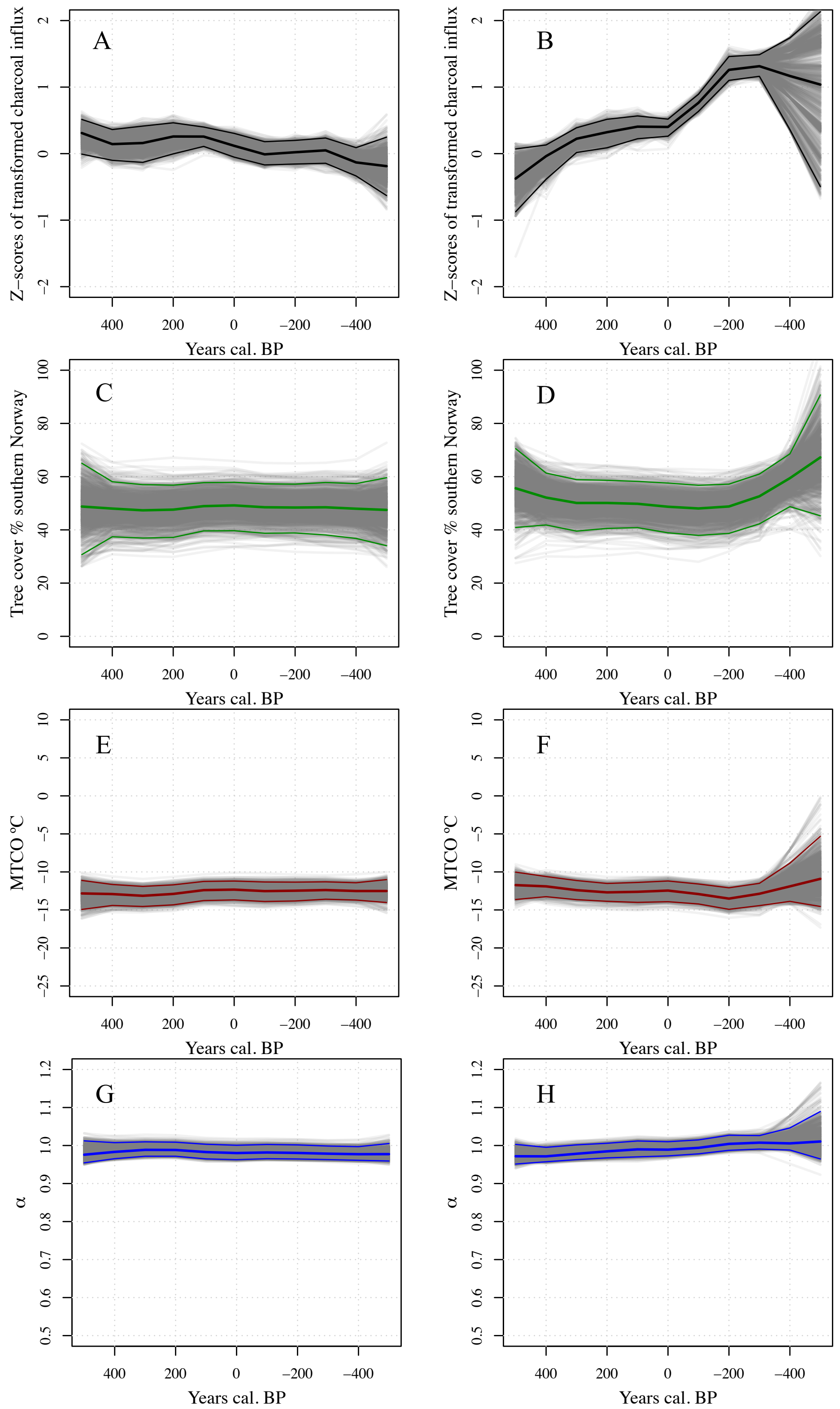

Figure 4.27: SEA figures showing adjusted values for southern Norway based on booms and busts in populations: A – SEA booms for z-scores charcoal influx; B – SEA busts for z-scores charcoal influx; C – SEA booms for tree cover; D - SEA booms for tree cover; E - SEA booms for MTCO; F - SEA busts for MTCO; G - SEA booms for α;H - SEA busts for α

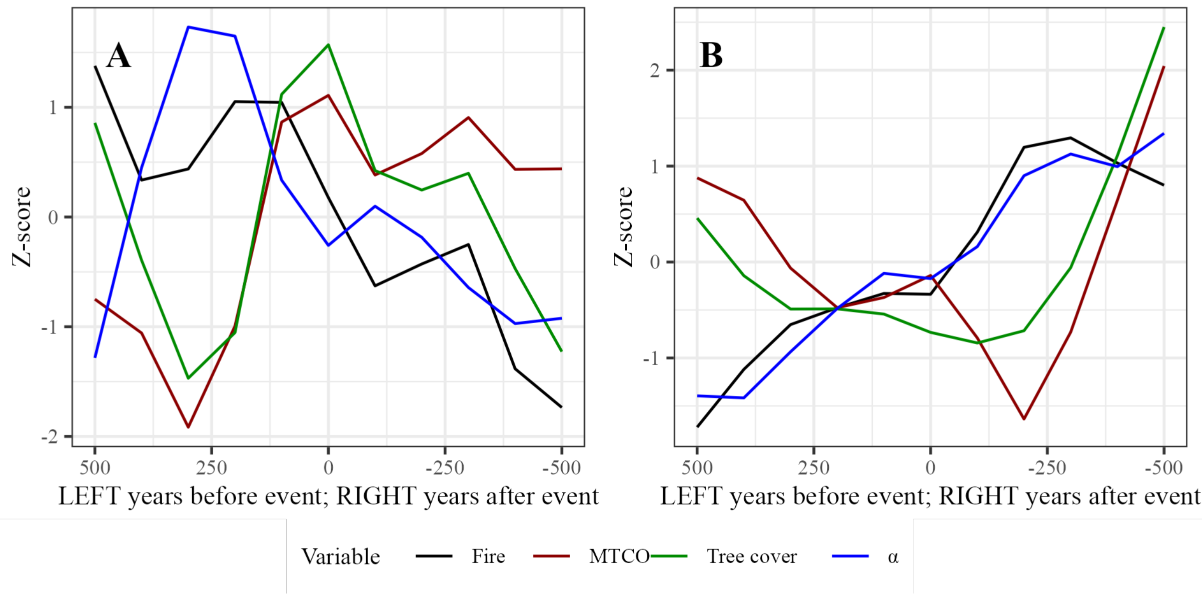

Figure 4.28: Combined SEA plot for southern Norway, with variable values for the period -500 to 500 before and after the SEA point converted to z-scores: A – Population booms; B – Population busts

It is difficult to assess how human population changes have affected fire compared to the influence of other drivers, due to the inconsistencies between regions and between the impacts of booms and busts within regions. A further challenge is separating the different impacts of scale and trend on fire, with climate changes often apparently very stable in scale, but often relating to changes in fire when converted to z-scores. Although there appear to be relationships between some of the population boom periods and bust periods, in most cases a (complex) environmental signal is evident when investigating the micro trends in time series. The boom periods in Iberia appear to coincide with slight reductions in fire, in contradiction to the results presented in Chapter 2, although the resolution of the signal based on the window width, binwidth and smoothing window were different. Again, although the individual signal from the climate variables is complex – the correlation between MTCO and α within the SEA appears less robust than in other sub-regions - the timing of changes appears to align with changes evident in the fire record. The changes in fire in southern Norway during population busts appear very closely related with climate and tree cover, with fire increasing with α and declining with MTCO and tree cover. α also appears to govern changes in fire during population booms in southern Norway, but MTCO and tree cover, and fire are positively correlated. In contrast to these environmental led changes in fire, the SEA for population busts in central Europe is harder to decode. Here, human influence on the fire regime may be evident given the contrasting relationships between fire and other variables before and after the busts.

4.5. Discussion and conclusions

This chapter brought together reconstructions of fire, tree cover, climate and human population change to attempt to assess the drivers of palaeofire in a comprehensive cross-cutting analysis. Evaluation was performed at the European and sub-regional levels, using regression-based and time series analysis.

At the European level, the negative modelled relationship between tree cover and fire is consistent with modern observed relationships at the global scale that link grass cover rather than tree cover to increased fire (e.g. Bistinas et al., 2014; Haas et al., 2022). In contrast, tree cover appears to have positive relationship with fire in the southern Norwegian sub-region. This may be a reflection of vegetation cover more generally, with cooler temperatures limiting overall vegetation cover towards the early Holocene, although this is speculative without information regarding other vegetation cover types. Across all sub-regions, Granger causality tests irrespective of methodological choices regarding smoothing, the inclusion of population rate of change, or MTCO, did not find a relationship between tree cover and fire, with one exception: smoothed curves for southern Norway. In this sub-region, tree cover significantly caused fire, although it should be noted that this was over four lagged periods (400 years) and may be a result of combined trends rather than causality.

Regression modelling also found a significant relationship between MTCO, MTCO^2 and α, and fire at the European scale. For MTCO, this relationship was positive, albeit with a negative quadratic term. This may reflect the close correlation between MTCO and MTWA and the influence that warmer temperatures might have on fire weather (Pausas and Keeley, 2021) and fuel availability at the low rnage of temperatures (Parisien and Moritz, 2009). For α, the positive impact on fire implies an overall dominating impact of increasing fuel on fire, rather than fire being reduced by fuel moisture. However, in southern Norway, the similar relationship between α and fire is difficult to explain in relation to the fire-productivity hypothesis (e.g. Pausas and Bradstock, 2007; Pausas and Ribeiro, 2013), as fire would not be expected to be limited by fuel availability at this latitude. Times series analysis of Granger causality between fire and climate variables for the sub-regions found some limited support for Iberia and southern Norway, albeit for specific methodological cases. In Iberia for example, there was a weakly significant (at 10%) relationship between fire and α for the unsmoothed time series, a significant relationship between fire and α unsmoothed stime series when excluding MTCO, and for both MTCO and α, and fire, when excluding the time series for the population rate of change with smoothed time series. For southern Norway, a significant relationship was observed between fire and MTCO for smoothed time series, providing some limited support for the regression model results. For central Europe, the included fire variable time series did not Granger cause the fire time series in any cases, although it should be noted that VAR models could not be run without series autocorrelation for the most part.

In southern Norway, the availability of the archaeological radiocarbon record until 500 cal. BP, in contrast to the other sub-regions, provides the ability to investigate human influences when they might be expected to be greatest. SEA analysis for southern Norway however does not identify obvious relationships between population boom or bust events and changes in in fire, with fire most closely linked to changes in climate and tree cover. This is in contrast to the Granger causality results for population which are almost uniquely consisent, and to evidence from the literature regarding the noted influence of humans on wildfire in the wider southern Scandinavia region during the later part of the Holocene (e.g. Bradshaw et al., 2010; Cui et al., 2013; Brown and Giesecke, 2014; Clear et al., 2014). Human influence on fire may be variable however, both in terms of land-use patterns (Cui et al., 2013) and in the nature of changes at different periods, with increases in fire associated with earlier landscape changes, and later decreases fire suppression (Bradshaw et al., 2010; Clear et al., 2014). Anthropogenic landscape changes have also been linked to reductions in fire, due to changes in fuel availability (Brown and Giesecke, 2014), further complicating the regional signal. A mixed temporal signal may obscure the pattern of human influence on fire via the SEA analysis but may explain the Granger causal relationship observed.

In central Europe, the population busts appear to explain changes in fire in the absence of a consistent signal from climate or tree cover, although this finding should be treated with caution given timings of the two bust events identified. Unfortunately, there were no boom events identified, limiting the ability to test this finding further. Similarly, the level of series autocorrelation in VAR models (generally) prevented the testing of Granger causality of population in the sub-region.

In Iberia, population booms seemed to coincide with a short interruption of increasing fire for the SEA period, although the magnitude of this signal is more discreet. This difference with the results from Chapter 2 can be explained by methodological differences, particularly in terms of the temporal resolution of the signal investigated. Human influence on fire has been identified for the sub-region from 7000 cal. BP, with increases in fire associated with human induced changes in landscapes (Connor et al., 2019). However, the timings of these changes are not necessarily consistent (Connor et al., 2019), with no obvious spatial coherence that might be expected if the changes were linked to the time-transgressive spread of agriculture (see Chapter 2), but which could be linked to human habitation differences (Gil-Romera et al., 2010). As with southern Norway, the potential difference in timing of human influences may obscure a defined human signal for the sub-regionally identified boom events, although a strong consistent signal of increased fire with human presence might be seen, rather than a stabilisation in increasing fire as observed in this analysis. The climate and tree cover signal in Iberia is difficult to identify for either the SEAs for population busts or booms, due to differences in trends for each time series. This underscores the need to investigate the drivers of fire in tandem.

Although the regression analysis produced models that were themselves significant, with significant relationships describing fire, it is worth re-emphasising that their explanatory power was poor, even when taking into account random effects for time and location. There are a number of potential reasons for this, some of which relate to general issues with palaeodata discussed in depth in Chapter 5. In general, there may be insufficient spatiotemporal resolution in the reconstructions to identify clear relationships, given the noise in the data. The temporal binning procedure was designed to maximise data overlaps and limit the impacts of differences in data temporal resolution, but there may be a case for narrower bins to capture more precise relationships between the reconstructions. The use of z-scores due to the charcoal data affects the information available to the model, with within site values not comparable in absolute terms with each other. The lack of population estimates to feed into the models is an unfortunate omission, especially considering the increased influence of people on fire in Europe towards the present day (e.g. Clear et al., 2014; Robin and Nelle, 2014; Zennaro et al., 2015). The Granger time-series analysis was limited by difficulties in VAR model specifications for some regions, and by inconsistencies in the results based on methodological choices regarding the smoothing of time series and inclusion of reconstructed variables. Additionally, the SEA analysis was hampered by the lack of boom events identified in central Europe. There is arguably space for more nuance in identifying the events, as was applied in Chapter 2 for Iberia. However, a less systematic approach, especially when comparing across sub-regions, is difficult and potentially liable to selective data analysis. In general, the choice of sub-regions was constrained by the availability of overlapping data for the analysis approaches performed. Furthermore, in some sub-regions, clusters of sites contrasted with areas with more limited spatial (and temporal) coverage, which may have implications for the subsequent results.

Overall, despite the different approaches applied, it is difficult to conclude with certainty regarding the relationships between fire and its drivers. Although there are notable exceptions – for example the population rate of change appears to consistently have an impact on fire in southern Norway in terms of the Granger causality analysis, irrespective of methodological choice – the general picture of one of inconsistency. This is discussed further in Chapter 4.

4.6. References

Balsera, V., Díaz-del-Río, P., Gilman, A., Uriarte, A., and Vicent, J. M.: Approaching the demography of late prehistoric Iberia through summed calibrated date probability distributions (7000–2000 cal BC), Quat Int, 386, 208–211, https://doi.org/10.1016/j.quaint.2015.06.022, 2015.

Bird, D., Miranda, L., Vander Linden, M., Robinson, E., Bocinsky, R. K., Nicholson, C., Capriles, J. M., Finley, J. B., Gayo, E. M., Gil, A., d'Alpoim Guedes, J., Hoggarth, J. A., Kay, A., Loftus, E., Lombardo, U., Mackie, M., Palmisano, A., Solheim, S., Kelly, R. L., and Freeman, J.: p3k14c, a synthetic global database of archaeological radiocarbon dates, Sci Data, 9, 27, https://doi.org/10.1038/s41597-022-01118-7, 2022.

Bistinas, I., Harrison, S. P., Prentice, I. C., and Pereira, J. M. C.: Causal relationships versus emergent patterns in the global controls of fire frequency, Biogeosciences, 11, 5087–5101, https://doi.org/10.5194/bg-11-5087-2014, 2014.

Bond, W. J. and Keeley, J. E.: Fire as a global "herbivore": The ecology and evolution of flammable ecosystems, Trends Ecol Evol, 20, 387–394, https://doi.org/10.1016/j.tree.2005.04.025, 2005.

Bradshaw, R. H. W., Lindbladh, M., and Hannon, G. E.: The role of fire in southern Scandinavian forests during the late Holocene, Int J Wildland Fire, 19, 1040, https://doi.org/10.1071/WF09108, 2010.

Brown, K. J. and Giesecke, T.: Holocene fire disturbance in the boreal forest of central Sweden, Boreas, 43, 639–651, https://doi.org/10.1111/bor.12056, 2014.

Bruns, S. B. and Stern, D. I.: Lag length selection and p-hacking in Granger causality testing: prevalence and performance of meta-regression models, Empir Econ, 56, 797–830, https://doi.org/10.1007/s00181-018-1446-3, 2019.

Bunbury, M. M. E., Austvoll, K. I., Jørgensen, E. K., Nielsen, S. V., Kneisel, J., and Weinelt, M.: Understanding climate resilience in Scandinavia during the Neolithic and Early Bronze Age, Quat Sci Rev, 322, 108391, https://doi.org/10.1016/j.quascirev.2023.108391, 2023.

Clear, J. L., Molinari, C., and Bradshaw, R. H. W.: Holocene fire in Fennoscandia and Denmark, Int J Wildland Fire, 23, 781, https://doi.org/10.1071/WF13188, 2014.

Connor, S. E., Vannière, B., Colombaroli, D., Anderson, R. S., Carrión, J. S., Ejarque, A., Gil Romera, G., González-Sampériz, P., Hoefer, D., Morales-Molino, C., Revelles, J., Schneider, H., van der Knaap, W. O., van Leeuwen, J. F., and Woodbridge, J.: Humans take control of fire-driven diversity changes in Mediterranean Iberia's vegetation during the mid–late Holocene, Holocene, 29, 886–901, https://doi.org/10.1177/0959683619826652, 2019.

Crema, E. R.: Statistical Inference of Prehistoric Demography from Frequency Distributions of Radiocarbon Dates: A Review and a Guide for the Perplexed, J Archaeol Method Theory, 29, 1387–1418, https://doi.org/10.1007/s10816-022-09559-5, 2022.

Crema, E. R. and Bevan, A.: Inference from large sets of radiocarbon dates: software and methods, Radiocarbon, 63, 23–39, https://doi.org/10.1017/RDC.2020.95, 2021.

Crema, E. R., Habu, J., Kobayashi, K., and Madella, M.: Summed Probability Distribution of 14C Dates Suggests Regional Divergences in the Population Dynamics of the Jomon Period in Eastern Japan, PLoS One, 11, 1–18, https://doi.org/10.1371/journal.pone.0154809, 2016.

Cui, Q.-Y., Gaillard, M.-J., Lemdahl, G., Sugita, S., Greisman, A., Jacobson, G. L., and Olsson, F.: The role of tree composition in Holocene fire history of the hemiboreal and southern boreal zones of southern Sweden, as revealed by the application of the Landscape Reconstruction Algorithm: Implications for biodiversity and climate-change issues, Holocene, 23, 1747–1763, https://doi.org/10.1177/0959683613505339, 2013.

Daniau, A.-L., Bartlein, P. J., Harrison, S. P., Prentice, I. C., Brewer, S., Friedlingstein, P., Harrison-Prentice, T. I., Inoue, J., Izumi, K., Marlon, J. R., Mooney, S., Power, M. J., Stevenson, J., Tinner, W., Andrič, M., Atanassova, J., Behling, H., Black, M., Blarquez, O., Brown, K. J., Carcaillet, C., Colhoun, E. A., Colombaroli, D., Davis, B. A. S., D'Costa, D., Dodson, J., Dupont, L., Eshetu, Z., Gavin, D. G., Genries, A., Haberle, S., Hallett, D. J., Hope, G., Horn, S. P., Kassa, T. G., Katamura, F., Kennedy, L. M., Kershaw, P., Krivonogov, S., Long, C., Magri, D., Marinova, E., McKenzie, G. M., Moreno, P. I., Moss, P., Neumann, F. H., Norström, E., Paitre, C., Rius, D., Roberts, N., Robinson, G. S., Sasaki, N., Scott, L., Takahara, H., Terwilliger, V., Thevenon, F., Turner, R., Valsecchi, V. G., Vannière, B., Walsh, M., Williams, N., and Zhang, Y.: Predictability of biomass burning in response to climate changes, Global Biogeochem Cycles, 26, 2011GB004249, https://doi.org/10.1029/2011GB004249, 2012.

Dietze, E., Theuerkauf, M., Bloom, K., Brauer, A., Dörfler, W., Feeser, I., Feurdean, A., Gedminienė, L., Giesecke, T., Jahns, S., Karpińska-Kołaczek, M., Kołaczek, P., Lamentowicz, M., Latałowa, M., Marcisz, K., Obremska, M., Pędziszewska, A., Poska, A., Rehfeld, K., Stančikaitė, M., Stivrins, N., Święta-Musznicka, J., Szal, M., Vassiljev, J., Veski, S., Wacnik, A., Weisbrodt, D., Wiethold, J., Vannière, B., and Słowiński, M.: Holocene fire activity during low-natural flammability periods reveals scale-dependent cultural human-fire relationships in Europe, Quat Sci Rev, 201, 44–56, https://doi.org/10.1016/j.quascirev.2018.10.005, 2018.

Drake, B. L., Blanco-González, A., and Lillios, K. T.: Regional Demographic Dynamics in the Neolithic Transition in Iberia: Results from Summed Calibrated Date Analysis, J Archaeol Method Theory, 24, 796–812, https://doi.org/10.1007/s10816-016-9286-y, 2017.

Feurdean, A., Vannière, B., Finsinger, W., Warren, D., Connor, S. C., Forrest, M., Liakka, J., Panait, A., Werner, C., Andrič, M., Bobek, P., Carter, V. A., Davis, B., Diaconu, A.-C., Dietze, E., Feeser, I., Florescu, G., Gałka, M., Giesecke, T., Jahns, S., Jamrichová, E., Kajukało, K., Kaplan, J., Karpińska-Kołaczek, M., Kołaczek, P., Kuneš, P., Kupriyanov, D., Lamentowicz, M., Lemmen, C., Magyari, E. K., Marcisz, K., Marinova, E., Niamir, A., Novenko, E., Obremska, M., Pędziszewska, A., Pfeiffer, M., Poska, A., Rösch, M., Słowiński, M., Stančikaitė, M., Szal, M., Święta-Musznicka, J., Tanţău, I., Theuerkauf, M., Tonkov, S., Valkó, O., Vassiljev, J., Veski, S., Vincze, I., Wacnik, A., Wiethold, J., and Hickler, T.: Fire hazard modulation by long-term dynamics in land cover and dominant forest type in eastern and central Europe, Biogeosciences, 17, 1213–1230, https://doi.org/10.5194/bg-17-1213-2020, 2020.

Gil-Romera, G., Carrión, J. S., Pausas, J. G., Sevilla-Callejo, M., Lamb, H. F., Fernández, S., and Burjachs, F.: Holocene fire activity and vegetation response in South-Eastern Iberia, Quat Sci Rev, 29, 1082–1092, https://doi.org/10.1016/j.quascirev.2010.01.006, 2010.

Granger, C. W. J.: Investigating Causal Relations by Econometric Models and Cross-spectral Methods, Econometrica, 37, 424, https://doi.org/10.2307/1912791, 1969.

Haas, O., Prentice, I. C., and Harrison, S. P.: Global environmental controls on wildfire burnt area, size, and intensity, Environ Res Lett, 17, 065004, https://doi.org/10.1088/1748-9326/ac6a69, 2022.

Harrison, S. P., Villegas-Diaz, R., Cruz-Silva, E., Gallagher, D., Kesner, D., Lincoln, P., Shen, Y., Sweeney, L., Colombaroli, D., Ali, A., Barhoumi, C., Bergeron, Y., Blyakharchuk, T., Bobek, P., Bradshaw, R., Clear, J. L., Czerwiński, S., Daniau, A.-L., Dodson, J., Edwards, K. J., Edwards, M. E., Feurdean, A., Foster, D., Gajewski, K., Gałka, M., Garneau, M., Giesecke, T., Gil Romera, G., Girardin, M. P., Hoefer, D., Huang, K., Inoue, J., Jamrichová, E., Jasiunas, N., Jiang, W., Jiménez-Moreno, G., Karpińska-Kołaczek, M., Kołaczek, P., Kuosmanen, N., Lamentowicz, M., Lavoie, M., Li, F., Li, J., Lisitsyna, O., López-Sáez, J. A., Luelmo-Lautenschlaeger, R., Magnan, G., Magyari, E. K., Maksims, A., Marcisz, K., Marinova, E., Marlon, J. R., Mensing, S., Miroslaw-Grabowska, J., Oswald, W., Pérez-Díaz, S., Pérez-Obiol, R., Piilo, S., Poska, A., Qin, X., Remy, C. C., Richard, P. J. H., Salonen, S., Sasaki, N., Schneider, H., Shotyk, W., Stancikaite, M., Šteinberga, D., Stivrins, N., Takahara, H., Tan, Z., Trasune, L., Umbanhowar, C. E., Väliranta, M., Vassiljev, J., Xiao, X., Xu, Q., Xu, X., Zawisza, E., Zhao, Y., Zhou, Z., and Paillard, J.: The Reading Palaeofire Database: an expanded global resource to document changes in fire regimes from sedimentary charcoal records, Earth Syst Sci Data, 14, 1109–1124, https://doi.org/10.5194/essd-14-1109-2022, 2022.

Harrison, S. P., Egbudom, M.-A., Liu, M., Cruz-Silva, E., and Sweeney, L.: The SPECIAL EPD Database: an expanded resource to document changes in vegetation and climate from pollen records from Europe, the Middle East and western Eurasia, University of Reading, Dataset, https://doi.org/10.17864/1947.001295, 2024.

Heidgen, S., Marinova, E., Nelle, O., Ebner, M., Rotava, T., Tafelmaier, Y., Krauß, R., Bofinger, J., and Junginger, A.: Palaeoecological signals for Mesolithic land use in a Central European landscape?, J Quat Sci, 37, 1164–1179, https://doi.org/10.1002/jqs.3422, 2022.

Higuera, P. E., Brubaker, L. B., Anderson, P. M., Hu, F. S., and Brown, T. A.: Vegetation mediated the impacts of postglacial climate change on fire regimes in the south-central Brooks Range, Alaska, Ecol Monogr, https://doi.org/10.1890/07-2019.1, 2009.

Hinz, M. and Roe, J.: _xronos: Client for the "XRONOS" Chronological Database_, 2023.

Keeley, J. and Syphard, A.: Climate Change and Future Fire Regimes: Examples from California, Geosciences (Basel), 6, https://doi.org/10.3390/geosciences6030037, 2016.

Kodra, E., Chatterjee, S., and Ganguly, A. R.: Exploring Granger causality between global average observed time series of carbon dioxide and temperature, Theor Appl Climatol, 104, 325–335, https://doi.org/10.1007/s00704-010-0342-3, 2011.

Körner, C.: The cold range limit of trees, Trends Ecol Evol, 36, 979–989, https://doi.org/10.1016/j.tree.2021.06.011, 2021.

Kumar, V., Bharti, B., Singh, H. P., and Topno, A. R.: Assessing the interrelation between NDVI and climate dependent variables by using granger causality test and vector auto-regressive neural network model, Physics and Chemistry of the Earth, Parts A/B/C, 131, 103428, https://doi.org/10.1016/j.pce.2023.103428, 2023.

Kuznetsova, A., Brockhoff, P. B., and Christensen, R. H. B.: lmerTest Package: Tests in Linear Mixed Effects Models, J Stat Softw, 82, https://doi.org/10.18637/jss.v082.i13, 2017.

Liu, M., Prentice, I. C., ter Braak, C. J. F., and Harrison, S. P.: An improved statistical approach for reconstructing past climates from biotic assemblages, P Roy Soc A-Math Phy, 476, https://doi.org/10.1098/rspa.2020.0346, 2020.

Liu, M., Shen, Y., González-Sampériz, P., Gil-Romera, G., ter Braak, C. J. F., Prentice, I. C., and Harrison, S. P.: Holocene climates of the Iberian Peninsula: pollen-based reconstructions of changes in the west-east gradient of temperature and moisture, Clim Past Discussions, 2021, 1–30, https://doi.org/10.5194/cp-2021-174, 2021.

Loader, C.: Locfit: Local regression, likelihood and density estimation, http://cran.r-project.org/package=locfit%5Cnpapers2://publication/uuid/E5C68958-7122-4093-A8E2-3108F9DF726A, 2020.

Marlon, J. R., Bartlein, P. J., and Whitlock, C.: Fire-fuel-climate linkages in the northwestern USA during the Holocene, Holocene, 16, 1059–1071, https://doi.org/10.1177/0959683606069396, 2006.

McGraw, M. C. and Barnes, E. A.: Memory Matters: A Case for Granger Causality in Climate Variability Studies, J Clim, 31, 3289–3300, https://doi.org/10.1175/JCLI-D-17-0334.1, 2018.

Molloy, M., Gori, M. and Vander Linden, M. A comprehensive dataset of radiocarbon determinations for the Bronze Age of the Balkans. [Manuscript in preparation].

Mooney, S. D., Harrison, S. P., Bartlein, P. J., Daniau, A.-L., Stevenson, J., Brownlie, K. C., Buckman, S., Cupper, M., Luly, J., Black, M., Colhoun, E., D'Costa, D., Dodson, J., Haberle, S., Hope, G. S., Kershaw, P., Kenyon, C., McKenzie, M., and Williams, N.: Late Quaternary fire regimes of Australasia, Quat Sci Rev, 30, 28–46, https://doi.org/10.1016/j.quascirev.2010.10.010, 2011.

Nakagawa, S. and Schielzeth, H.: Repeatability for Gaussian and non-Gaussian data: a practical guide for biologists, Biol Rev, 85, 935–956, https://doi.org/10.1111/j.1469-185X.2010.00141.x, 2010.

Oberg, A. L. and Mahoney, D. W.: Linear Mixed Effects Models, in: Ambrosius, W. T. (Ed.) Topics in Biostatistics, Humana Totowa: Humana Press, 213–234, https://doi.org/10.1007/978-1-59745-530-5_11, 2007.

Papaspyropoulos, K. G. and Kugiumtzis, D.: On the Validity of Granger Causality for Ecological Count Time Series, Econometrics, 12, 13, https://doi.org/10.3390/econometrics12020013, 2024.

Parisien, M.-A. and Moritz, M. A.: Environmental controls on the distribution of wildfire at multiple spatial scales, Ecol Monogr, 79, 127–154, https://doi.org/10.1890/07-1289.1, 2009.

Pausas, J. G. and Bradstock, R. a.: Fire persistence traits of plants along a productivity and disturbance gradient in mediterranean shrublands of south-east Australia, Global Ecology and Biogeography, 16, 330–340, https://doi.org/10.1111/j.1466-8238.2006.00283.x, 2007.

Pausas, J. G. and Keeley, J. E.: Wildfires and global change, Front Ecol Environ, 19, 387–395, https://doi.org/10.1002/fee.2359, 2021.

Pausas, J. G. and Ribeiro, E.: The global fire-productivity relationship, Global Ecol Biogeogr, 22, 728–736, https://doi.org/10.1111/geb.12043, 2013.

Pfaff, B.: VAR, SVAR and SVEC Models: Implementation Within *R* Package vars, J Stat Softw, 27, https://doi.org/10.18637/jss.v027.i04, 2008.

Power, M. J., Marlon, J. R., Ortiz, N., Bartlein, P. J., Harrison, S. P., Mayle, F. E., Ballouche, A., Bradshaw, R. H. W., Carcaillet, C., Cordova, C., Mooney, S., Moreno, P. I., Prentice, I. C., Thonicke, K., Tinner, W., Whitlock, C., Zhang, Y., Zhao, Y., Ali, A. A., Anderson, R. S., Beer, R., Behling, H., Briles, C., Brown, K. J., Brunelle, A., Bush, M., Camill, P., Chu, G. Q., Clark, J., Colombaroli, D., Connor, S., Daniau, A.-L., Daniels, M., Dodson, J., Doughty, E., Edwards, M. E., Finsinger, W., Foster, D., Frechette, J., Gaillard, M.-J., Gavin, D. G., Gobet, E., Haberle, S., Hallett, D. J., Higuera, P., Hope, G., Horn, S., Inoue, J., Kaltenrieder, P., Kennedy, L., Kong, Z. C., Larsen, C., Long, C. J., Lynch, J., Lynch, E. A., McGlone, M., Meeks, S., Mensing, S., Meyer, G., Minckley, T., Mohr, J., Nelson, D. M., New, J., Newnham, R., Noti, R., Oswald, W., Pierce, J., Richard, P. J. H., Rowe, C., Sanchez Goñi, M. F., Shuman, B. N., Takahara, H., Toney, J., Turney, C., Urrego-Sanchez, D. H., Umbanhowar, C., Vandergoes, M., Vannière, B., Vescovi, E., Walsh, M., Wang, X., Williams, N., Wilmshurst, J., and Zhang, J. H.: Changes in fire regimes since the Last Glacial Maximum: an assessment based on a global synthesis and analysis of charcoal data, Clim Dyn, 30, 887–907, https://doi.org/10.1007/s00382-007-0334-x, 2008.

Power, M. J., Marlon, J. R., Bartlein, P. J., and Harrison, S. P.: Fire history and the Global Charcoal Database: A new tool for hypothesis testing and data exploration, Palaeogeogr Palaeoclimatol Palaeoecol, 291, 52–59, https://doi.org/10.1016/j.palaeo.2009.09.014, 2010.

Prentice, I. C., Cramer, W., Harrison, S. P., Leemans, R., Monserud, R. A., and Solomon, A. M.: Special Paper: A Global Biome Model Based on Plant Physiology and Dominance, Soil Properties and Climate, J Biogeogr, 19, 117, https://doi.org/10.2307/2845499, 1992.

R Core Team, _R: A Language and Environment for Statistical Computing_. R Foundation for Statistical Computing, Vienna, Austria. <https://www.R-project.org/>, 2024.

Reimer, P. J., Austin, W. E. N., Bard, E., Bayliss, A., Blackwell, P. G., Bronk Ramsey, C., Butzin, M., Cheng, H., Edwards, R. L., Friedrich, M., Grootes, P. M., Guilderson, T. P., Hajdas, I., Heaton, T. J., Hogg, A. G., Hughen, K. A., Kromer, B., Manning, S. W., Muscheler, R., Palmer, J. G., Pearson, C., van der Plicht, J., Reimer, R. W., Richards, D. A., Scott, E. M., Southon, J. R., Turney, C. S. M., Wacker, L., Adolphi, F., Büntgen, U., Capano, M., Fahrni, S. M., Fogtmann-Schulz, A., Friedrich, R., Köhler, P., Kudsk, S., Miyake, F., Olsen, J., Reinig, F., Sakamoto, M., Sookdeo, A., and Talamo, S.: The IntCal20 Northern Hemisphere Radiocarbon Age Calibration Curve (0–55 cal kBP), Radiocarbon, 62, 1–33, https://doi.org/10.1017/rdc.2020.41, 2020.

Robin, V. and Nelle, O.: Contribution to the reconstruction of central European fire history, based on the soil charcoal analysis of study sites in northern and central Germany, Veg Hist Archaeobot, 23, 51–65, https://doi.org/10.1007/s00334-014-0438-2, 2014.

Schwarz, G.: Estimating the Dimension of a Model, The Annals of Statistics, 6, https://doi.org/10.1214/aos/1176344136, 1978.

Shennan, S., Downey, S. S., Timpson, A., Edinborough, K., Colledge, S., Kerig, T., Manning, K., and Thomas, M. G.: Regional population collapse followed initial agriculture booms in mid-Holocene Europe, Nat Commun, 4, 2486, https://doi.org/10.1038/ncomms3486, 2013.

Solheim, S.: Timing the emergence and development of arable farming in southeastern Norway by using Summed Probability Distribution of radiocarbon dates and a Bayesian age model, Radiocarbon, 63, 1503–1524, https://doi.org/10.1017/RDC.2021.80, 2021.

Stivrins, N., Liiv, M., Ozola, I., and Reitalu, T.: Carbon accumulation rate in a raised bog in Latvia, NE Europe, in relation to climate warming, Est J Earth Sci, 67, 247, https://doi.org/10.3176/earth.2018.20, 2018.

Sweeney, L., Harrison, S. P., and Vander Linden, M.: Holocene archaeological radiocarbon data of the Iberian Peninsula, University of Reading, Dataset, https://doi.org/10.17864/1947.000340, 2021.

Tang, M., Liu, M., Harrison S. P. and Prentice, I. C. European tree migrations during the Holocene, [Manuscript in preparation].

Timpson, A., Colledge, S., Crema, E. R., Edinborough, K., Kerig, T., Manning, K., Thomas, M. G., and Shennan, S.: Reconstructing regional population fluctuations in the European Neolithic using radiocarbon dates: a new case-study using an improved method, J Archaeol Sci, 52, 549–557, https://doi.org/10.1016/j.jas.2014.08.011, 2014.

Toda, H. Y. and Yamamoto, T.: Statistical inference in vector autoregressions with possibly integrated processes, J Econom, 66, 225–250, https://doi.org/10.1016/0304-4076(94)01616-8, 1995.

Vannière, B., Blarquez, O., Rius, D., Doyen, E., Brücher, T., Colombaroli, D., Connor, S., Feurdean, A., Hickler, T., Kaltenrieder, P., Lemmen, C., Leys, B., Massa, C., and Olofsson, J.: 7000-year human legacy of elevation-dependent European fire regimes, Quat Sci Rev, 132, 206–212, https://doi.org/10.1016/j.quascirev.2015.11.012, 2016.

Villegas-Diaz, R. and Harrison, S. P.: The SPECIAL Modern Pollen Data Set for Climate Reconstructions, version 2 (SMPDSv2), University of Reading, Dataset, https://doi.org/10.17864/1947.000389, 2022.

Wooldridge, J.: Introductory Econometrics, South-Western, Mason, OH, 912 pp., 2005.

Zapolska, A., Serge, M. A., Mazier, F., Quiquet, A., Renssen, H., Vrac, M., Fyfe, R., and Roche, D. M.: More than agriculture: Analysing time-cumulative human impact on European land-cover of second half of the Holocene, Quat Sci Rev, 314, 108227, https://doi.org/10.1016/j.quascirev.2023.108227, 2023.

Zennaro, P., Kehrwald, N., Marlon, J. R., Ruddiman, W. F., Brücher, T., Agostinelli, C., Dahl-Jensen, D., Zangrando, R., Gambaro, A., and Barbante, C.: Europe on fire three thousand years ago: Arson or climate?, Geophys Res Lett, 42, 5023–2033, https://doi.org/10.1002/2015GL064259, 2015.

4.7. Supplement

Supplementary Table 4.1: Charcoal sites included in the reconstruction of fire in the Holocene in Europe

Site name	Lat. (°)	Lon. (°)	Elevation (m a.s.l.)	Depositional context	Citation
Ackgol	37.30	33.44	1000	unknown	Turner et al. (2008)
Ahlequellmoor	51.73	9.51	300	bog sediment	Jahns (2006)
Altar Lough	55.02	-8.40	30	lake sediment	Fossitt (1994)
Alvor Estuary Ribeira do Farelo Ribeira da Torre	37.15	-8.59	0.6	estuarine sediment	Schneider et al. (2010, 2016)
Apsuciems Mire	57.05	23.32	6.6	bog sediment	Gałka et al. (2016)
Arbarrain Mire	43.21	-2.17	1004	bog sediment	Pérez-Díaz et al. (2018)
Arroyo de Valdeconejos	40.86	-4.06	1380	bog sediment	Morales-Molino et al. (2017a)
Arroyo de las Carcavas	40.84	-4.03	1300	small hollow	Morales-Molino et al. (2017a)
Asi Gonia	35.25	24.28	780	bog sediment	Atherden and Hall (1999)
Bagno Serebryskie	51.18	23.53	173	bog sediment	Gałka et al. (2017)
Basa de la Mora	42.55	0.33	1906	lake sediment	Pérez-Sanz et al. (2013)
Bazu bog	57.70	22.45	15	bog sediment	Stivrins, N., unpublished data
Beliya Kanton	41.73	24.14	1547	bog sediment	Marinova, E., unpublished data
Bermu Mire	39.43	-4.15	783	bog sediment	Luelmo-Lautenschlaeger et al. (2018)
Bialowieza forest Site 2	52.75	23.88	165	small hollow	Mitchell and Cole (1998)
Birzulis	55.78	22.47	148	lake sediment	Stančikaitė et al. (2006)
Black Loch	56.32	-3.19	90	lake sediment	Whittington et al. (1991); Edwards and Whittington (2000)
Borreguil de la Caldera	37.05	-3.32	2992	bog sediment	Ramos-Román et al. (2016)
Bricu lake	57.12	25.87	208.4	lake sediment	Steinberga and Stivrins (2021)
Bruckmisse	48.73	8.64	670	bog sediment	Rösch (2009)
Brve	50.07	14.24	362	bog sediment	Pokorný and van der Knaap (2011)
Buchensee	47.77	8.98	614	lake sediment	Rösch and Wick (2019)
Calineasa	46.56	22.83	1300	bog sediment	Feurdean et al. (2009, 2020)
Campo Lameiro	42.53	-8.52	295	soil	Kaal et al. (2008, 2011, 2013); López-Merino et al. (2012)
Canada de la Cruz	38.07	-2.69	1595	lake sediment	Carrión et al. (2001a)
Canada del Gitano Sierra de Baza	37.23	-2.70	1900	bog sediment	Carrión et al. (2007)

Castello Lagoon	42.28	3.10	2.4	other	Ejarque et al. (2016); Feurdean et al. (2017)
Cepicko polje	45.19	14.16	27	lake sediment	Balbo et al. (2006); Feurdean et al. (2020); Balbo, unpublished data
Cepkeliai	54.01	24.62	131	bog sediment	Stančikaitė et al. (2019a)
Cerna Hora	50.66	15.76	1206	bog sediment	Speranza et al. (2000)
Cha das Lameiras	40.94	-7.68	950	soil	López-Sáez et al. (2017)
Charco da Candieira	40.34	-7.58	1409	lake sediment	van der Knaap and van Leeuwen (1995, 1997); Connor et al. (2012)
Cubelles	41.20	-1.67	2	other	Riera-Mora and Esteban-Amat (1994)
Cvitova	49.22	24.47	228	bog sediment	Kołaczek et al. (2016); Feurdean et al. (2020)
Dalane	58.24	8.00	40	lake sediment	Eide et al. (2006)
Dallican Water	60.39	-1.10	56	lake sediment	Bennett et al. (1992)
Dalmutladdo	69.17	20.72	355	lake sediment	Bjune et al. (2004)
Delta del Rio Besos	41.41	2.25	0	soil	Riera-Mora and Esteban-Amat (1994)
Dubrava Wood	48.87	17.10	190	bog sediment	Jamrichová et al. (2017)
Durchenbergried	47.78	8.98	432	bog sediment	Rösch (1986 (1997)
Durnoye	55.09	40.89	118	bog sediment	Novenko et al. (2016b); Feurdean et al. (2020)
El Brezosa	39.35	-4.36	733	bog sediment	Morales-Molino et al. (2018)
El Carrizal	41.32	-4.15	860	lake sediment	Franco-Múgica et al. (2005)
El Payo mire	40.25	-6.77	1000	bog sediment	Silva-Sánchez et al. (2016)
El Perro mire	39.05	-4.76	690	bog sediment	Luelmo-Lautenschlaeger et al. (2019a, b)
El Portalet	42.80	-0.40	1802	bog sediment	González-Sampériz et al. (2006)
El Redondo	40.22	-5.66	1765	bog sediment	López-Sáez et al. (2016b)
El Tiemblo	40.36	-4.53	1250	bog sediment	López-Sáez et al. (2018b)
Espinosa de Cerrato	41.96	-3.94	885	bog sediment	Morales-Molino et al. (2017b)
Etu-Mustajarvi	60.98	25.00	157	lake sediment	Sarmaja-Korjonen (1998)
Eustach	50.89	14.43	387	bog sediment	Bobek et al. (2018b)
Flotatjonn	59.67	7.54	890	lake sediment	Birks (2006)
Fuente de la Leche	40.35	-5.06	1382	bog sediment	Robles-López et al. (2018)
Fuente del Pino Blanco	40.24	-4.98	1343	bog sediment	Robles-López et al. (2018)
Gabarn	43.17	-0.56	310	bog sediment	Rius et al. (2009)
Gammelheimenvatnet	68.48	17.76	290	lake sediment	Bjune et al. (2009)
Gasak II	52.46	19.39	81	bog sediment	Wacnik et al. (2011)
Ghab	35.65	36.25	240	lake sediment	Yasuda et al. (2000)

Ginkunai Lake	55.95	23.34	107	lake sediment	Stančikaitė et al. (2015)
Gleboczek	53.87	18.21	110	bog sediment	Lamentowicz et al. (2019)
Golebiewo I	54.45	18.50	130	bog sediment	Latałowa et al. (2013); Pędziszewska and Latałowa (2016); Święta-Musznicka et al. (2021)
Gorenje jezero	45.74	14.41	550	bog sediment	Andrič and Willis (2003); Andrič (2004); Feurdean et al. (2020); Andrič, unpublished data
Grauthelleren	58.14	7.91	80	lake sediment	Birks (2006)
Griblje	45.57	15.28	160	bog sediment	Andrič (2011; Feurdean et al. (2020)
Grosser Krebssee	52.85	14.10	5	lake sediment	Jahns (2000)
Grosser Treppelsee	52.15	14.45	52.2	lake sediment	Giesecke (2001)
Herrenwieser See	48.67	8.30	830	lake sediment	Rösch (2012)
Hinojos Marsh	36.96	-6.39	1.5	bog sediment	López-Sáez et al. (2018a)
Hoya del Castillo	41.48	-0.16	258	lake sediment	Davis and Stevenson (2007)
Huzenbacher See	48.57	8.35	747	lake sediment	Rösch and Tserendorj (2011b, a)
Jagniecy Potok	50.85	15.36	850	bog sediment	Kajukało et al. (2016)
Jeleni louze	50.89	14.27	460	bog sediment	Pokorný and Kuneš (2005)
Juodonys	55.74	25.44	20	bog sediment	Stančikaitė et al. (2004 (2009)
Kahala	59.49	25.53	33.2	lake sediment	Poska and Saarse (1999)
Kazanie fen	52.46	17.30	101	bog sediment	Czerwiński et al. (2020b, 2021)
Kinnshaugen	61.11	10.36	591	lake sediment	Birks et al. (2012)
Kozcaronliacute	49.38	14.03	460	bog sediment	Pokorný and Kuneš (2009)
Kumata	42.59	23.25	1770	bog sediment	Tonkov and Possnert (2016b, a); Feurdean et al. (2020)
Lac Miroir	44.63	6.79	2214	lake sediment	Carcaillet and Blarquez (2017)
Lagaccione	42.57	11.85	355	lake sediment	Magri (1999, 2004)
Lago di Pergusa	37.51	14.30	674	lake sediment	Sadori et al. (2008)
Laguna Guallar	41.41	-0.23	336	lake sediment	Davis and Stevenson (2007); Davis, unpublished data
Laguna de Rio Seco	37.05	-3.35	3020	lake sediment	Anderson et al. (2011)
Laguna de la Mosca	37.06	-3.31	2889	lake sediment	Manzano et al. (2019)
Laguna de la Mula	37.06	-3.42	2497	lake sediment	Jiménez-Moreno et al. (2013)
Lake Banyoles	42.13	2.75	174	lake sediment	Revelles et al. (2015)
Lake Biale	52.50	19.49	72	lake sediment	Wacnik et al. (2011)
Lake Brazi	45.40	22.90	1740	lake sediment	Finsinger et al. (2018)
Lake Bucura	45.36	22.87	2040	lake sediment	Vincze et al. (2017)

Lake Burg	42.51	1.31	1821	lake sediment	Bal et al. (2011)
Lake Kojle	54.02	22.88	149	bog sediment	Gałka, M., Obremska, M., unpublished data.
Lake Oltina	44.14	27.63	40	lake sediment	Feurdean et al. (2020, 2021)
Lake Pikku Harkajarvi	68.85	28.64	188	lake sediment	Stivrins, N., unpublished data
Lake Rosalia	68.91	28.37	180	lake sediment	Stivrins, N., unpublished data
Lake Ruskowiejskie	53.95	21.31	144	lake sediment	Szal et al. (2017)
Lake Salet	53.94	21.32	132	lake sediment	Szal et al. (2014)
Lake Skogstjern	59.01	9.64	57.2	lake sediment	Wieckowska-Lüth et al. (2017)
Lake Skrzynka	53.81	17.52	121	lake sediment	Apolinarska et al. (2012)
Lake Stiol	47.57	24.81	1670	lake sediment	Haliuc et al. (2016); Feurdean et al. (2020, 2021)
Lake Stiucii	46.97	23.90	240	lake sediment	Feurdean et al. (2013, 2020)
Lake Suchar IV	54.09	23.02	143	lake sediment	Zawisza et al. (2019)
Lake Svarcenberk	49.15	14.71	412	lake sediment	Pokorný and Jankovská (2000); Pokorný (2002)
Lanzahita	40.22	-4.94	588	bog sediment	López-Sáez et al. (2018b)
Larix Hollow	61.85	37.76	155	small hollow	Kuosmanen et al. (2014)
Las Animas Mire	36.69	-5.03	1403	bog sediment	Alba-Sánchez et al. (2019)
Las Pardillas	42.03	-3.03	1850	lake sediment	Goñi and Hannon (1999)
Las Vinuelas	39.37	-4.49	761	bog sediment	Morales-Molino et al. (2019)
Lille Kjelavatn	59.80	7.00	978	lake sediment	Eide et al. (2006)
Litlvatnet	68.53	14.93	106	lake sediment	Bjune et al. (2009)
Litzelsee	47.77	8.93	413	lake sediment	Rösch and Lechterbeck (2016)
Loch of Clickimin	60.15	-1.17	1	other	Edwards et al. (2005)
Lough Maumeen	53.41	-10.02	250	lake sediment	Huang (2002)
Lough Mullaghlahan	54.78	-8.47	40	lake sediment	Fossitt (1994)
Lough Nabraddan	55.02	-8.35	20	lake sediment	Fossitt (1994)
Luka	49.20	24.51	226	bog sediment	Kołaczek et al. (2018a)
Mala niva	48.91	13.82	753	bog sediment	Bobek et al. (2019); Kozáková et al. (2021)
Mala niva	48.91	13.82	753	bog sediment	Svobodová et al. (2001)
Manaderos	40.34	-4.69	1292	bog sediment	Robles-López et al. (2020)
Mannikjarve	58.87	26.25	90	bog sediment	Sillasoo et al. (2007, 2011)
Marbore	42.70	0.04	2612	lake sediment	Leunda et al. (2017)
Masatjornet	61.56	10.27	841	lake sediment	Birks et al. (2012)
Mindelsee	47.76	9.02	406	lake sediment	Rösch (2013; Rösch et al. (2014)
Miticka slatina	48.81	18.11	330	bog sediment	Jamrichová et al. (2018)
Mogielica	49.67	20.28	845	bog sediment	Czerwiński et al. (2020a)
Molhasul Mare	46.59	22.76	1124	bog sediment	Feurdean and Willis (2008); Feurdean et al. (2020)

Morttjern	59.06	11.62	227	lake sediment	Birks et al. (2012)
Mosquito Hollow	61.85	37.77	155	small hollow	Kuosmanen et al. (2014)
Myrvatnet	68.66	16.38	197	lake sediment	Bjune et al. (2009)
Na Bahne	50.20	15.96	240	bog sediment	Pokorný et al. (2000); Pokorný and van der Knaap (2010)
Na mahu	45.97	14.54	290	lake sediment	Andrič et al. (2008); Feurdean et al. (2020)
Nad Dolskym mlynem	50.85	14.34	240	bog sediment	Abraham (2006); Pokorný et al. (2008)
Nakri	57.90	26.27	48.5	lake sediment	Amon et al. (2012)
Nataloup	47.23	4.04	515	bog sediment	Jouffroy-Bapicot (2010); Jouffroy-Bapicot et al. (2013)
Navamuno	40.32	-5.78	1505	bog sediment	Turu et al. (2018); López-Sáez et al. (2020)
Navarres	39.10	-0.68	225	bog sediment	Carrión and Van Geel (1999)
Novoalexandrovskoye	55.12	41.04	113	bog sediment	Novenko et al. (2016b); Feurdean et al. (2020)
Nussbaumersee	47.60	8.81	450	lake sediment	Haas and Hadorn (1998); Hillbrand et al. (2014)
Oberderdingen-Grossvillars	49.04	8.76	207	bog sediment	Rösch (2005)
Ojos del Tremendal	40.54	-2.05	1650	bog sediment	Stevenson (2000)
Olga Hollow	61.20	37.59	200	small hollow	Kuosmanen et al. (2014)
Oygardtjonn	59.63	7.99	665	lake sediment	Birks (2006)
Pancavska louka	50.77	15.54	1336	bog sediment	Speranza (2000)
Parika	58.49	25.77	48.5	bog sediment	Niinemets et al. (2002)
Parizske Mire	47.87	18.47	123	bog sediment	Jamrichová et al. (2014)
Pena Negra	40.33	-5.79	1000	bog sediment	Abel-Schaad and López-Sáez (2013)
Pena da Cadela	42.83	-7.17	970	bog sediment	Martínez Cortizas et al. (2002)
Petresiunai	55.85	25.70	107	lake sediment	Stančikaitė et al. (2019b)
Poiana Stiol	47.59	24.81	1520	bog sediment	Feurdean et al. (2017, 2020)
Pozo de la Nieve	40.35	-4.55	1600	bog sediment	Robles-López et al. (2017)
Prasilske Jezero	49.06	13.40	1079	lake sediment	Carter et al. (2018)
Pravcicky dul	50.88	14.30	382	bog sediment	Bobek et al. (2019)
Puerto de Serranillos	40.31	-4.93	1700	bog sediment	López-Sáez et al. (2018b)
Puerto del Pico	40.32	-5.01	1395	bog sediment	López-Sáez et al. (2016a)
Puklina	50.93	14.44	386	small hollow	Bobek et al. (2019)
Quart du Bois	46.89	4.03	420	bog sediment	Jouffroy-Bapicot (2010); Jouffroy-Bapicot et al. (2013)
Raseliniste Jizery	50.86	15.30	843	bog sediment	Bobek et al. (2019)
Ratasjoen	62.27	9.83	1169	lake sediment	Velle et al. (2005)

Reiarsdalsvatn	58.33	7.79	245	lake sediment	Birks (2006)
Rentukka Hollow	61.19	25.15	150	small hollow	Kuosmanen et al. (2016)
Rifugio Mondovi	44.18	7.73	1760	bog sediment	Ortu et al. (2003, 2008)
Rojkov	49.15	19.16	472	bog sediment	Jamrichová, E., unpublished data
Rynholec	50.13	13.93	478	bog sediment	Pokorný (2005)
Selikhovo	53.23	35.77	209	bog sediment	Feurdean et al. (2020)
Selikhovo	53.23	35.77	209	bog sediment	Novenko et al. (2016a)
Semenic	45.18	22.06	1500	bog sediment	Rösch and Fischer (2000)
Sierra de Gador	36.90	-2.92	1530	lake sediment	Carrión et al. (2003)
Siles Lake	38.40	-2.50	1320	lake sediment	Carrión (2002)
Stara jimka	49.07	13.40	1129	lake sediment	Bobek et al. (2019)
Stazki bog	54.43	18.08	195	bog sediment	Gałka et al. (2013)
Storsandvatnet	63.46	8.45	106	lake sediment	Birks et al. (2012)
Stubno-Naklo	49.86	22.97	186.5	lake sediment	Kołaczek et al. (2018b)
Sudenpesa Hollow	61.18	25.15	167	small hollow	Clear et al. (2015)
Tajga	50.03	12.68	817	bog sediment	Bobek et al. (2019)
Tiavatnet	63.06	9.42	464	lake sediment	Birks et al. (2012)
Tisice	50.24	14.53	160	lake sediment	Dreslerová et al. (2004); Pokorný (2005); Pokorný and Kuneš (2005)
Torbiera del Biecai	44.20	7.70	1920	bog sediment	Ortu et al. (2008)
Tourbiere de La Lande	43.56	2.96	1040	bog sediment	Pulido (2006)
Tourbiere des Narses Morte	44.43	3.60	1400	bog sediment	Pulido (2006)
Tourbiere du Peschio	44.45	3.60	1370	bog sediment	Pulido (2006)
Tubilla del Lago	41.81	-3.57	900	bog sediment	Morales-Molino et al. (2017b)
Valle do Lobo Ribeira de Carcavai	37.06	-8.07	2.3	estuarine sediment	Schneider et al. (2010, 2016)
Vapsko-2	42.07	23.52	2120	bog sediment	Feurdean et al. (2019, 2020)
Velise	58.76	24.46	26.4	bog sediment	Veski (1998)
Verdeospesoa	43.06	-2.86	1015	bog sediment	Pérez-Díaz and López-Sáez (2017); Pérez Díaz and López Sáez (2021)
Vesijako Hollow	61.38	25.03	160	small hollow	Clear et al. (2013)
Viitna Pikkjarv	59.45	26.01	76.5	lake sediment	Heinsalu et al. (1998)
Vilamora Ribeira de Quarteira	37.09	-8.14	3.5	estuarine sediment	Schneider et al. (2010, 2016)
Villaverde	38.80	-2.37	870	bog sediment	Carrión et al. (2001b)
Vlcek	50.04	12.73	769	bog sediment	Bobek et al. (2019)
Vrbka	50.39	14.13	189	bog sediment	Pokorný (2016)
Vuoskkujarvi	68.35	19.10	384	lake sediment	Bigler et al. (2002)

Wildseemoor bei Kaltenbronn	48.72	8.46	909	lake sediment	Rösch (2009)
Zahaji	50.38	14.12	232	bog sediment	Pokorný (2005); Pokorný et al. (2010)
Zofinsky prales	48.66	14.71	785	small hollow	Bobek et al. (2018a)

4.7.1. Supplement references

Abel-Schaad, D. and López-Sáez, J. A.: Vegetation changes in relation to fire history and human activities at the Peña Negra mire Bejar Range, Iberian Central Mountain System, Spain) during the past 4,000 years, Veg Hist Archaeobot, 2 2 (199–214, https://doi.org/10.1007/s00334-012-0368-9, 2013.

Abraham, V.: Přirozená vegetace a její změny v důsledku kolonizace a lesnického hospodaření v Českém Švýcarsku – The natural vegetation of Bohemian Switzerland and its changes as an impact of habitation and forest management MSc Thesis), Charles University, Prague, Czech Republic, 2006.

Alba-Sánchez, F., López-Sáez, J. A., Abel-Schaad, D., Sabariego Ruiz, S., Pérez-Díaz, S., González-Hernández, A., and Linares, J. C.: The impact of climate and land-use changes on the most southerly fir forests *Abies pinsapo*) in Europe, Holocene, 29, 1176–1188, https://doi.org/10.1177/0959683619838043, 2019.

Amon, L., Veski, S., Heinsalu, A., and Saarse, L.: Timing of Lateglacial vegetation dynamics and respective palaeoenvironmental conditions in southern Estonia: evidence from the sediment record of Lake Nakri, J Quat Sci, 27, 169–180, https://doi.org/10.1002/jqs.1530, 2012.

Anderson, R. S., Jiménez-Moreno, G., Carrión, J. S., and Pérez-Martínez, C.: Postglacial history of alpine vegetation, fire, and climate from Laguna de Río Seco, Sierra Nevada, southern Spain, Quat Sci Rev, 30, https://doi.org/10.1016/j.quascirev.2011.03.005, 2011.

Andrič, M.: Paleookolje v Sloveniji in severnemu delu hrvaške Istrev pozni prazgodovini. The vegetation of Slovenia and northern Istria in late prehistory, Arheološki vestnik, 55, 509–525, 2004.

Andrič, M.: Poznoglacialna vegetacija v okolici Blejskega jezera in Gribelj Bela krajina): primerjava v zadnjem stadialu poledenele in nepoledenele pokrajine. Lateglacial vegetation at Lake Bled and Griblje Marsh Slovenia): a comparison of in Last Glacial Maximum) glaciated and non-glaciated landscapes, in: Drobci Ledenodobnega Okolja: Zbornik Ob Življenjskem Jubileju Ivana Turka - Proceedings in Honour of Ivan Turk’s Jubilee, Opera Instituti Archaeologici Sloveniae - Inštitut za arheologijo ZRC SAZU, Ljubljana, 235–249, 2011.

Andrič, M. and Willis, K. J.: The phytogeographical regions of Slovenia: a consequence of natural environmental variation or prehistoric human activity?, Journal of Ecology, 91, 807–821, https://doi.org/10.1046/j.1365-2745.2003.00808.x, 2003.

Andrič, M., Kroflič, B., Toman, M. J., Ogrinc, N., Dolenec, T., Dobnikar, M., and Čermelj, B.: Late quaternary vegetation and hydrological change at Ljubljansko barje Slovenia), Palaeogeogr Palaeoclimatol Palaeoecol, 270, 150–165, https://doi.org/10.1016/j.palaeo.2008.09.008, 2008.

Apolinarska, K., Woszczyk, M., and Obremska, M.: Late <scp>W</scp> eichselian and Holocene palaeoenvironmental changes in northern Poland based on the Lake Skrzynka record, Boreas, 41, 292–307, https://doi.org/10.1111/j.1502-3885.2011.00235.x, 2012.

Atherden, M. A. and Hall, J. A.: Human impact on vegetation in the White Mountains of Crete since AD 500, Holocene, 9, 183–193, https://doi.org/10.1191/095968399673523574, 1999.

Bal, M.-C., Pelachs, A., Perez-Obiol, R., Julia, R., and Cunill, R.: Fire history and human activities during the last 3300cal yr BP in Spain's Central Pyrenees: The case of the Estany de Burg, Palaeogeogr Palaeoclimatol Palaeoecol, 300, 179–190, https://doi.org/10.1016/j.palaeo.2010.12.023, 2011.

Balbo, A. L., Andrič, M., Rubinić, J., Moscariello, A., and Miracle, P. T.: Palaeoenvironmental and Archaeological Implications of a Sediment Core from Polje Čepić, Istria, Croatia, Geologia Croatica, 59, 109–124, https://doi.org/10.4154/GC.2006.08, 2006.

Bennett, K. D., Boreham, S., Sharp, M. J., and Switsur, V. R.: Holocene History of Environment, Vegetation and Human Settlement on Catta Ness, Lunnasting, Shetland, J Ecol, 80, 241, https://doi.org/10.2307/2261010, 1992.

Bigler, C., Larocque, I., Peglar, S. M., Birks, H. J. B., and Hall, R. I.: Quantitative multiproxy assessment of long-term patterns of Holocene environmental change from a small lake near Abisko, northern Sweden, Holocene, 12, 481–496, https://doi.org/10.1191/0959683602hl559rp, 2002.

Birks, H. H., Birks, H. J. B., Bjune, A. E., and Felde, V. A.: Internal report. XXXVI international bog 'moor') excursion of the Institute of Plant Sciences, University of Bern, southern and south-eastern Norway, 8-13 September 2012, Excursion Guide, 2012.

Birks, H. J. B.: Estimating the amount of compositional change in late-Quaternary pollen-stratigraphical data, Veg Hist Archaeobot, 16, 197–202, https://doi.org/10.1007/s00334-006-0079-1, 2006.

Bjune, A., Birks, H. J. B., and Seppä, H.: Holocene vegetation and climate history on a continental-oceanic transect in northern Fennoscandia based on pollen and plant macrofossils, Boreas, 33, 211–223, https://doi.org/10.1080/03009480410001244, 2004.

Bjune, A. E., Seppä, H., and Birks, H. J. B.: Quantitative summer-temperature reconstructions for the last 2000 years based on pollen-stratigraphical data from northern Fennoscandia, J Paleolimnol, 41, 43–56, https://doi.org/10.1007/s10933-008-9254-y, 2009.

Bobek, P., Šamonil, P., and Jamrichová, E.: Biotic controls on Holocene fire frequency in a temperate mountain forest, Czech Republic, J Quat Sci, 33, 892–904, https://doi.org/10.1002/jqs.3067, 2018a.

Bobek, P., Svobodová, H. S., Werchan, B., Švarcová, M. G., and Kuneš, P.: Human-induced changes in fire regime and subsequent alteration of the sandstone landscape of Northern Bohemia Czech Republic), Holocene, 28, 427–443, https://doi.org/10.1177/0959683617729443, 2018b.

Bobek, P., Svobodová-Svitavská, H., Pokorný, P., Šamonil, P., Kuneš, P., Kozáková, R., Abraham, V., Klinerová, T., Švarcová, M. G., Jamrichová, E., Krauseová, E., and Wild, J.: Divergent fire history trajectories in Central European temperate forests revealed a pronounced influence of broadleaved trees on fire dynamics, Quat Sci Rev, 222, 105865, https://doi.org/10.1016/j.quascirev.2019.105865, 2019.

Carcaillet, C. and Blarquez, O.: Fire ecology of a tree glacial refugium on a nunatak with a view on Alpine glaciers, New Phytologist, 216, 1281–1290, https://doi.org/10.1111/nph.14721, 2017.

Carrión, J. S.: Patterns and processes of Late Quaternary environmental change in a montane region of southwestern Europe, Quat Sci Rev, 21, 2047–2066, https://doi.org/10.1016/S0277-379102)00010-0, 2002.

Carrión, J. S. and Van Geel, B.: Fine-resolution Upper Weichselian and Holocene palynological record from Navarrés Valencia, Spain) and a discussion about factors of Mediterranean forest succession, Rev Palaeobot Palynol, 106, https://doi.org/10.1016/S0034-666799)00009-3, 1999.

Carrión, J. S., Munuera, M., Dupré, M., and Andrade, A.: Abrupt vegetation changes in the Segura Mountains of southern Spain throughout the Holocene, Journal of Ecology, 89, https://doi.org/10.1046/j.0022-0477.2001.00601.x, 2001a.

Carrión, J. S., Andrade, A., Bennett, K. D., Navarro, C., and Munuera, M.: Crossing forest thresholds: inertia and collapse in a Holocene sequence from south-central Spain, Holocene, 11, https://doi.org/10.1191/09596830195672, 2001b.

Carrión, J. S., Sánchez-Gómez, P., Mota, J. F., Yll, R., and Chaín, C.: Holocene vegetation dynamics, fire and grazing in the Sierra de Gádor, southern Spain, Holocene, 13, https://doi.org/10.1191/0959683603hl662rp, 2003.

Carrión, J. S., Fuentes, N., González-Sampériz, P., Sánchez Quirante, L., Finlayson, J. C., Fernández, S., and Andrade, A.: Holocene environmental change in a montane region of southern Europe with a long history of human settlement, Quat Sci Rev, 26, https://doi.org/10.1016/j.quascirev.2007.03.013, 2007.

Carter, V. A., Moravcová, A., Chiverrell, R. C., Clear, J. L., Finsinger, W., Dreslerová, D., Halsall, K., and Kuneš, P.: Holocene-scale fire dynamics of central European temperate spruce-beech forests, Quat Sci Rev, 191, 15–30, https://doi.org/10.1016/j.quascirev.2018.05.001, 2018.

Clear, J. L., Seppä, H., Kuosmanen, N., and Bradshaw, R. H. W.: Holocene fire frequency variability in Vesijako, Strict Nature Reserve, Finland, and its application to conservation and management, Biol Conserv, 166, 90–97, https://doi.org/10.1016/j.biocon.2013.06.008, 2013.

Clear, J. L., Seppä, H., Kuosmanen, N., and Bradshaw, R. H. W.: Holocene stand-scale vegetation dynamics and fire history of an old-growth spruce forest in southern Finland, Veg Hist Archaeobot, 24, 731–741, https://doi.org/10.1007/s00334-015-0533-z, 2015.

Connor, S. E., Araújo, J., van der Knaap, W. O., and van Leeuwen, J. F. N.: A long-term perspective on biomass burning in the Serra da Estrela, Portugal, Quat Sci Rev, 55, https://doi.org/10.1016/j.quascirev.2012.08.007, 2012.

Czerwiński, S., Margielewski, W., Gałka, M., and Kołaczek, P.: Late Holocene transformations of lower montane forest in the Beskid Wyspowy Mountains Western Carpathians, Central Europe): a case study from Mount Mogielica, Palynology, 44, 355–368, https://doi.org/10.1080/01916122.2019.1617207, 2020a.

Czerwiński, S., Guzowski, P., Karpińska-Kołaczek, M., Lamentowicz, M., Gałka, M., Kołaczek, P., Izdebski, A., and Poniat, R.: Znaczenie wspólnych badań historycznych i paleoekologicznych nad wpływem człowieka na środowisko. Przykład ze stanowiska Kazanie we wschodniej Wielkopolsce, Studia Geohistorica, 56, https://doi.org/10.12775/SG.2019.04, 2020b.

Czerwiński, S., Guzowski, P., Lamentowicz, M., Gałka, M., Karpińska-Kołaczek, M., Poniat, R., Łokas, E., Diaconu, A.-C., Schwarzer, J., Miecznik, M., and Kołaczek, P.: Environmental implications of past socioeconomic events in Greater Poland during the last 1200 years. Synthesis of paleoecological and historical data, Quat Sci Rev, 259, 106902, https://doi.org/10.1016/j.quascirev.2021.106902, 2021.

Davis, B. A. S. and Stevenson, A. C.: The 8.2 ka event and Early-Mid Holocene forests, fires and flooding in the Central Ebro Desert, NE Spain, Quat Sci Rev, 26, 1695–1712, https://doi.org/10.1016/j.quascirev.2007.04.007, 2007.

Dreslerová, D., Břízová, E., Růžičková, E., Zeman, A.:. Holocene environmental processes and alluvial archaeology in the middle Labe (Elbe) valley, in: Gojda, M. (Ed.), Ancient Landscape, Settlement Dynamics and Non-destructive Archaeology. Academia, Praha, Czech Republic, p. 484.0., 2004.

Edwards, K. J. and Whittington, G.: Multiple charcoal profiles in a Scottish lake: taphonomy, fire ecology, human impact and inference, Palaeogeogr Palaeoclimatol Palaeoecol, 164, 67–86, https://doi.org/10.1016/S0031-018200)00176-0, 2000.

Edwards, K. J., Whittington, G., Robinson, M., and Richter, D.: Palaeoenvironments, the archaeological record and cereal pollen detection at Clickimin, Shetland, Scotland, J Archaeol Sci, 32, 1741–1756, https://doi.org/10.1016/j.jas.2005.06.004, 2005.

Eide, W., Birks, H. H., Bigelow, N. H., Peglar, S. M., and Birks, H. J. B.: Holocene forest development along the Setesdal valley, southern Norway, reconstructed from macrofossil and pollen evidence, Veg Hist Archaeobot, 15, 65–85, https://doi.org/10.1007/s00334-005-0025-7, 2006.

Ejarque, A., Julià, R., Reed, J. M., Mesquita-Joanes, F., Marco-Barba, J., and Riera, S.: Coastal Evolution in a Mediterranean Microtidal Zone: Mid to Late Holocene Natural Dynamics and Human Management of the Castelló Lagoon, NE Spain, PLoS One, 11, https://doi.org/10.1371/journal.pone.0155446, 2016.

Feurdean, A. and Willis, K. J.: The usefulness of a long-term perspective in assessing current forest conservation management in the Apuseni Natural Park, Romania, For Ecol Manage, 256, 421–430, https://doi.org/10.1016/j.foreco.2008.04.050, 2008.

Feurdean, A., Liakka, J., Vannière, B., Marinova, E., Hutchinson, S. M., Mosburgger, V., and Hickler, T.: 12,000-Years of fire regime drivers in the lowlands of Transylvania Central-Eastern Europe): a data-model approach, Quat Sci Rev, 81, 48–61, https://doi.org/10.1016/j.quascirev.2013.09.014, 2013.

Feurdean, A., Florescu, G., Vannière, B., Tanţău, I., O'Hara, R. B., Pfeiffer, M., Hutchinson, S. M., Gałka, M., Moskal-del Hoyo, M., and Hickler, T.: Fire has been an important driver of forest dynamics in the Carpathian Mountains during the Holocene, For Ecol Manage, 389, 15–26, https://doi.org/10.1016/j.foreco.2016.11.046, 2017.

Feurdean, A., Tonkov, S., Pfeiffer, M., Panait, A., Warren, D., Vannière, B., and Marinova, E.: Fire frequency and intensity associated with functional traits of dominant forest type in the Balkans during the Holocene, Eur J For Res, 138, 1049–1066, https://doi.org/10.1007/s10342-019-01223-0, 2019.

Feurdean, A., Vannière, B., Finsinger, W., Warren, D., Connor, S. C., Forrest, M., Liakka, J., Panait, A., Werner, C., Andrič, M., Bobek, P., Carter, V. A., Davis, B., Diaconu, A.-C., Dietze, E., Feeser, I., Florescu, G., Gałka, M., Giesecke, T., Jahns, S., Jamrichová, E., Kajukało, K., Kaplan, J., Karpińska-Kołaczek, M., Kołaczek, P., Kuneš, P., Kupriyanov, D., Lamentowicz, M., Lemmen, C., Magyari, E. K., Marcisz, K., Marinova, E., Niamir, A., Novenko, E., Obremska, M., Pędziszewska, A., Pfeiffer, M., Poska, A., Rösch, M., Słowiński, M., Stančikaitė, M., Szal, M., Święta-Musznicka, J., Tanţău, I., Theuerkauf, M., Tonkov, S., Valkó, O., Vassiljev, J., Veski, S., Vincze, I., Wacnik, A., Wiethold, J., and Hickler, T.: Fire hazard modulation by long-term dynamics in land cover and dominant forest type in eastern and central Europe, Biogeosciences, 17, 1213–1230, https://doi.org/10.5194/bg-17-1213-2020, 2020.

Feurdean, A., Grindean, R., Florescu, G., Tanţău, I., Niedermeyer, E. M., Diaconu, A.-C., Hutchinson, S. M., Nielsen, A. B., Sava, T., Panait, A., Braun, M., and Hickler, T.: The transformation of the forest steppe in the lower Danube Plain of southeastern Europe: 6000 years of vegetation and land use dynamics, Biogeosciences, 18, 1081–1103, https://doi.org/10.5194/bg-18-1081-2021, 2021.

Feurdean, A. N., Willis, K. J., and Astaloş, C.: Legacy of the past land-use changes and management on the 'natural' upland forest composition in the Apuseni Natural Park, Romania, Holocene, 19, 967–981, https://doi.org/10.1177/0959683609337358, 2009.

Finsinger, W., Fevre, J., Orbán, I., Pál, I., Vincze, I., Hubay, K., Birks, H. H., Braun, M., Tóth, M., and Magyari, E. K.: Holocene fire-regime changes near the treeline in the Retezat Mts. Southern Carpathians, Romania), Quaternary International, 477, 94–105, https://doi.org/10.1016/j.quaint.2016.04.029, 2018.

Fossitt, J. A.: Late-Glacial and Holocene Vegetation History of Western Donegal, Ireland, Biology and Environment: Proceedings of the Royal Irish Academy, 94B, 1–31, 1994.

Franco-Múgica, F., García-Antón, M., Maldonado-Ruiz, J., Morla-Juaristi, C., and Sainz-Ollero, H.: Ancient pine forest on inland dunes in the Spanish northern meseta, Quat Res, 63, 1–14, https://doi.org/10.1016/j.yqres.2004.08.004, 2005.

Gałka, M., Miotk-Szpiganowicz, G., Goslar, T., Jęśko, M., van der Knaap, W. O., and Lamentowicz, M.: Palaeohydrology, fires and vegetation succession in the southern Baltic during the last 7500years reconstructed from a raised bog based on multi-proxy data, Palaeogeogr Palaeoclimatol Palaeoecol, 370, 209–221, https://doi.org/10.1016/j.palaeo.2012.12.011, 2013.

Gałka, M., Aunina, L., Tobolski, K., and Feurdean, A.: Development of Rich Fen on the SE Baltic Coast, Latvia, during the Last 7500 Years, Using Paleoecological Proxies: Implications for Plant Community Development and Paleoclimatic Research, Wetlands, 36, 689–703, https://doi.org/10.1007/s13157-016-0779-y, 2016.

Gałka, M., Aunina, L., Feurdean, A., Hutchinson, S., Kołaczek, P., and Apolinarska, K.: Rich fen development in CE Europe, resilience to climate change and human impact over the last ca. 3500 years, Palaeogeogr Palaeoclimatol Palaeoecol, 473, 57–72, https://doi.org/10.1016/j.palaeo.2017.02.030, 2017.

Giesecke, T.: Pollenanalytische und sedimentchemische Untersuchungen zur natürlichen und anthropogenen Geschichte im Schlaubetal, 89–112 pp., 2001.

Goñi, M. F. S. and Hannon, G. E.: High-altitude vegetational pattern on the Iberian Mountain Chain north-central Spain) during the Holocene, Holocene, 9, 39–57, https://doi.org/10.1191/095968399671230625, 1999.

González-Sampériz, P., Valero-Garcés, B. L., Moreno, A., Jalut, G., García-Ruiz, J. M., Martí-Bono, C., Delgado-Huertas, A., Navas, A., Otto, T., and Dedoubat, J. J.: Climate variability in the Spanish Pyrenees during the last 30,000 yr revealed by the El Portalet sequence, Quat Res, 66, 38–52, https://doi.org/10.1016/j.yqres.2006.02.004, 2006.

Haas, J.N., Hadorn, P.:. Die vegetations-und kulturlandschaftsgeschichte des Seebachtals von der Mittelsteinzeit bis zum frühmittelalter anhand von pollenanalysen. Das Seebachtal–Eine archäaologische und paläaokologische bestandesaufnahme. Archäaologie im Thurgau 221–255, 1998.

Haliuc, A., Hutchinson, S. M., Florescu, G., and Feurdean, A.: The role of fire in landscape dynamics: An example of two sediment records from the Rodna Mountains, northern Romanian Carpathians, Catena Amst), 137, 432–440, https://doi.org/10.1016/j.catena.2015.10.021, 2016.

Heinsalu, A., Kaup, E., Poska, A., and Saarse, L.: Holocene Environmental Events in the Viitna Area, North Estonia, Proceedings of the Estonian Academy of Sciences. Geology, 47, 31, https://doi.org/10.3176/geol.1998.1.03, 1998.

Hillbrand, M., van Geel, B., Hasenfratz, A., Hadorn, P., and Haas, J. N.: Non-pollen palynomorphs show human- and livestock-induced eutrophication of Lake Nussbaumersee Thurgau, Switzerland) since Neolithic times 3840 <scp>bc</scp>), Holocene, 24, 559–568, https://doi.org/10.1177/0959683614522307, 2014.

Huang, C. C.: Holocene landscape development and human impact in the Connemara Uplands, Western Ireland, J Biogeogr, 29, 153–165, https://doi.org/10.1046/j.1365-2699.2002.00661.x, 2002.

Jahns, S.: Late-glacial and Holocene woodland dynamics and land-use history of the Lower Oder valley, north-eastern Germany, based on two, AMS14C-dated, pollen profiles, Veg Hist Archaeobot, 9, 111–123, https://doi.org/10.1007/BF01300061, 2000.

Jahns, S.: The later Holocene history of vegetation, land-use and settlements around the Ahlequellmoor in the Solling area, Germany, Veg Hist Archaeobot, 15, 57–63, https://doi.org/10.1007/s00334-004-0055-6, 2006.

Jamrichová, E., Potůčková, A., Horsák, M., Hajnalová, M., Barta, P., Tóth, P., and Kuneš, P.: Early occurrence of temperate oak-dominated forest in the northern part of the Little Hungarian Plain, SW Slovakia, Holocene, 24, 1810–1824, https://doi.org/10.1177/0959683614551225, 2014.

Jamrichová, E., Hédl, R., Kolář, J., Tóth, P., Bobek, P., Hajnalová, M., Procházka, J., Kadlec, J., and Szabó, P.: Human impact on open temperate woodlands during the middle Holocene in Central Europe, Rev Palaeobot Palynol, 245, 55–68, https://doi.org/10.1016/j.revpalbo.2017.06.002, 2017.

Jamrichová, E., Gálová, A., Gašpar, A., Horsák, M., Frodlová, J., Hájek, M., Hajnalová, M., and Hájková, P.: Holocene development of two calcareous spring fens at the Carpathian-Pannonian interface controlled by climate and human impact, Folia Geobot, 53, 243–263, https://doi.org/10.1007/s12224-018-9324-5, 2018.

Jiménez-Moreno, G., García-Alix, A., Hernández-Corbalán, M. D., Anderson, R. S., and Delgado-Huertas, A.: Vegetation, fire, climate and human disturbance history in the southwestern Mediterranean area during the late Holocene, Quat Res, 79, https://doi.org/10.1016/j.yqres.2012.11.008, 2013.

Jouffroy-Bapicot, I.: Évolution de la Végétation du Massif du Morvan Bourgogne-France) depuis la Dernière Glaciation à partir de L'analyse Pollinique. Variations Climatiques et Impact des Activités Anthropiques PhD thesis), Université de Franche-Comté, Besançon, France, 2010.

Jouffroy-Bapicot, I., Vannière, B., Gauthier, É., Richard, H., Monna, F., and Petit, C.: 7000 years of vegetation history and land-use changes in the Morvan Mountains France): A regional synthesis, Holocene, 23, 1888–1902, https://doi.org/10.1177/0959683613508161, 2013.

Kaal, J., Costa-Casais, M., Ferro-Vázquez, C., Pontevedra-Pombal, X., and Martínez-Cortizas, A.: Soil Formation of "Atlantic Rankers" from NW Spain—A High Resolution Aluminium and Iron Fractionation Study, Pedosphere, 18, 441–453, https://doi.org/10.1016/S1002-016008)60035-1, 2008.

Kaal, J., Carrión Marco, Y., Asouti, E., Martín Seijo, M., Martínez Cortizas, A., Costa Casáis, M., and Criado Boado, F.: Long-term deforestation in NW Spain: linking the Holocene fire history to vegetation change and human activities, Quat Sci Rev, 30, 161–175, https://doi.org/10.1016/j.quascirev.2010.10.006, 2011.

Kaal, J., Criado-Boado, F., Costa-Casais, M., López-Sáez, J. A., López-Merino, L., Mighall, T., Carrión, Y., Silva Sánchez, N., and Martínez Cortizas, A.: Prehistoric land use at an archaeological hot-spot the rock art park of Campo Lameiro, NW Spain) inferred from charcoal, synanthropic pollen and non-pollen palynomorph proxies, J Archaeol Sci, 40, 1518–1527, https://doi.org/10.1016/j.jas.2012.09.024, 2013.

Kajukało, K., Fiałkiewicz-Kozieł, B., Gałka, M., Kołaczek, P., and Lamentowicz, M.: Abrupt ecological changes in the last 800 years inferred from a mountainous bog using testate amoebae traits and multi-proxy data, Eur J Protistol, 55, 165–180, https://doi.org/10.1016/j.ejop.2016.04.003, 2016.

van der Knaap, W. O. and van Leeuwen, J. F. N.: Holocene vegetation succession and degradation as responses to climatic change and human activity in the Serra de Estrela, Portugal, Rev Palaeobot Palynol, 89, https://doi.org/10.1016/0034-666795)00048-0, 1995.

van der Knaap, W. O. and van Leeuwen, J. F. N.: Late Glacial and early Holocene vegetation succession, altitudinal vegetation zonation, and climatic change in the Serra da Estrela, Portugal, Rev Palaeobot Palynol, 97, https://doi.org/10.1016/S0034-666797)00008-0, 1997.

Kołaczek, P., Karpińska-Kołaczek, M., Madeja, J., Kalinovych, N., Szczepanek, K., Gębica, P., and Harmata, K.: Interplay of climate-human-vegetation on the north-eastern edge of the Carpathians Western Ukraine) between 7500 and 3500 calibrated years BP, Biological Journal of the Linnean Society, 119, 609–629, https://doi.org/10.1111/bij.12732, 2016.

Kołaczek, P., Gałka, M., Apolinarska, K., Płóciennik, M., Gąsiorowski, M., Brooks, S. J., Hutchinson, S. M., and Karpińska-Kołaczek, M.: A multi-proxy view of exceptionally early postglacial development of riparian woodlands with Ulmus in the Dniester River valley, western Ukraine, Rev Palaeobot Palynol, 250, 27–43, https://doi.org/10.1016/j.revpalbo.2017.12.001, 2018a.

Kołaczek, P., Płóciennik, M., Gałka, M., Apolinarska, K., Tosik, K., Gąsiorowski, M., Brooks, S. J., and Karpińska-Kołaczek, M.: Persist or take advantage of global warming: A development of Early Holocene riparian forest and oxbow lake ecosystems in Central Europe, Quat Sci Rev, 200, 191–211, https://doi.org/10.1016/j.quascirev.2018.09.031, 2018b.

Kozáková, R., Bobek, P., Dreslerová, D., Abraham, V., and Svobodová-Svitavská, H.: The prehistory and early history of the Šumava Mountains Czech Republic) as seen through anthropogenic pollen indicators and charcoal data, Holocene, 31, 145–159, https://doi.org/10.1177/0959683620961484, 2021.

Kuosmanen, N., Fang, K., Bradshaw, R. H., Clear, J. L., and Seppä, H.: Role of forest fires in Holocene stand-scale dynamics in the unmanaged taiga forest of northwestern Russia, Holocene, 24, 1503–1514, https://doi.org/10.1177/0959683614544065, 2014.

Kuosmanen, N., Seppä, H., Alenius, T., Bradshaw, R. H. W., Clear, J. l., Filimonova, L., Heikkilä, M., Renssen, H., Tallavaara, M., and Reitalu, T.: Importance of climate, forest fires and human population size in the Holocene boreal forest composition change in northern Europe, Boreas, 45, 688–702, https://doi.org/10.1111/bor.12183, 2016.

Lamentowicz, M., Kołaczek, P., Mauquoy, D., Kittel, P., Łokas, E., Słowiński, M., Jassey, V. E. J., Niedziółka, K., Kajukało-Drygalska, K., and Marcisz, K.: Always on the tipping point – A search for signals of past societies and related peatland ecosystem critical transitions during the last 6500 years in N Poland, Quat Sci Rev, 225, 105954, https://doi.org/10.1016/j.quascirev.2019.105954, 2019.

Latałowa, M., Pędziszewska, A., Maciejewska, E., and Święta-Musznicka, J.: *Tilia* forest dynamics, *Kretzschmaria deusta* attack, and mire hydrology as palaeoecological proxies for mid-Holocene climate reconstruction in the Kashubian Lake District N Poland), Holocene, 23, 667–677, https://doi.org/10.1177/0959683612467484, 2013.

Leunda, M., González-Sampériz, P., Gil-Romera, G., Aranbarri, J., Moreno, A., Oliva-Urcia, B., Sevilla-Callejo, M., and Valero-Garcés, B.: The Late-Glacial and Holocene Marboré Lake sequence 2612 m a.s.l., Central Pyrenees, Spain): Testing high altitude sites sensitivity to millennial scale vegetation and climate variability, Glob Planet Change, 157, https://doi.org/10.1016/j.gloplacha.2017.08.008, 2017.

López-Merino, L., Silva Sánchez, N., Kaal, J., López-Sáez, J. A., and Martínez Cortizas, A.: Post-disturbance vegetation dynamics during the Late Pleistocene and the Holocene: An example from NW Iberia, Glob Planet Change, 92–93, 58–70, https://doi.org/10.1016/j.gloplacha.2012.04.003, 2012.

López-Sáez, J. A., Alba-Sánchez, F., Robles-López, S., Pérez-Díaz, S., Abel-Schaad, D., Sabariego-Ruiz, S., and Glais, A.: Exploring seven hundred years of transhumance, climate dynamic, fire and human activity through a historical mountain pass in central Spain, J Mt Sci, 13, 1139–1153, https://doi.org/10.1007/s11629-016-3885-7, 2016a.

López-Sáez, J. A., Abel-Schaad, D., Robles-López, S., Pérez-Díaz, S., Alba-Sánchez, F., and Nieto-Lugilde, D.: Landscape dynamics and human impact on high-mountain woodlands in the western Spanish Central System during the last three millennia, J Archaeol Sci Rep, 9, 203–218, https://doi.org/10.1016/j.jasrep.2016.07.027, 2016b.

López-Sáez, J. A., Figueiral, I., and Cruz, D. J.: Palaeoenvironment and vegetation dynamics in Serra da Nave Alto Paiva, Beira Alta, Portugal) during the Late Pleistocene and the Holocene, in: Actas da Mesa-Redonda "A Pré-história e a Proto-história no Centro de Portugal: avaliação e perspectivas de futuro," 2017.

López-Sáez, J. A., Pérez-Díaz, S., Rodríguez-Ramírez, A., Blanco-González, A., Villarías-Robles, J. J. R., Luelmo-Lautenschlaeger, R., Jiménez-Moreno, G., Celestino-Pérez, S., Cerrillo-Cuenca, E., Pérez-Asensio, J. N., and León, Á.: Mid-late Holocene environmental and cultural dynamics at the south-west tip of Europe Doñana National Park, SW Iberia, Spain), J Archaeol Sci Rep, 22, 58–78, https://doi.org/10.1016/j.jasrep.2018.09.014, 2018a.

López-Sáez, J. A., Vargas, G., Ruiz-Fernández, J., Blarquez, O., Alba-Sánchez, F., Oliva, M., Pérez-Díaz, S., Robles-López, S., and Abel-Schaad, D.: Paleofire Dynamics in Central Spain during the Late Holocene: The Role of Climatic and Anthropogenic Forcing, Land Degrad Dev, 29, 2045–2059, https://doi.org/10.1002/ldr.2751, 2018b.

López-Sáez, J. A., Carrasco, R. M., Turu, V., Ruiz-Zapata, B., Gil-García, M. J., Luelmo-Lautenschlaeger, R., Pérez-Díaz, S., Alba-Sánchez, F., Abel-Schaad, D., Ros, X., and Pedraza, J.: Late Glacial-early holocene vegetation and environmental changes in the western Iberian Central System inferred from a key site: The Navamuño record, Béjar range Spain), Quat Sci Rev, 230, 106167, https://doi.org/10.1016/j.quascirev.2020.106167, 2020.

Luelmo-Lautenschlaeger, R., Pérez-Díaz, S., Alba-Sánchez, F., Abel-Schaad, D., and López-Sáez, J. A.: Vegetation History in the Toledo Mountains Central Iberia): Human Impact during the Last 1300 Years, Sustainability, 10, 2575, https://doi.org/10.3390/su10072575, 2018.

Luelmo-Lautenschlaeger, R., Blarquez, O., Pérez-Díaz, S., Morales-Molino, C., and López-Sáez, J. A.: The iberian peninsula's burning heart-long-term fire history in the toledo mountains central Spain), Fire, 2, 1–23, https://doi.org/10.3390/fire2040054, 2019a.

Luelmo-Lautenschlaeger, R., Pérez-Díaz, S., Blarquez, O., Morales-Molino, C., and López-Sáez, J. A.: The Toledo Mountains: A Resilient Landscape and a Landscape for Resilience? Hazards and Strategies in a Mid-Elevation Mountain Region in Central Spain, Quaternary, 2, https://doi.org/10.3390/quat2040035, 2019b.

Magri, D.: Late Quaternary vegetation history at Lagaccione near Lago di Bolsena central Italy), Rev Palaeobot Palynol, 106, 171–208, https://doi.org/10.1016/S0034-666799)00006-8, 1999.

Magri, D.: Two long micro-charcoal records from central Italy, in: Charcoals from the Past: Cultural and Palaeoenvironmental Implications. Proceedings of the Third International Meeting of Anthracology. Cavallino, Lecce, Italy, pp. 265–272, 2004.

Manzano, S., Carrión, J. S., López-Merino, L., Jiménez-Moreno, G., Toney, J. L., Amstrong, H., Anderson, R. S., García-Alix, A., Pérez, J. L. G., and Sánchez-Mata, D.: A palaeoecological approach to understanding the past and present of Sierra Nevada, a Southwestern European biodiversity hotspot, Glob Planet Change, 175, https://doi.org/10.1016/j.gloplacha.2019.02.006, 2019.

Martínez Cortizas, A., García-Rodeja, E., Pontevedra Pombal, X., Nóvoa Muñoz, J. C., Weiss, D., and Cheburkin, A.: Atmospheric Pb deposition in Spain during the last 4600 years recorded by two ombrotrophic peat bogs and implications for the use of peat as archive, Science of The Total Environment, 292, https://doi.org/10.1016/S0048-969702)00031-1, 2002.

Mitchell, F. J. G. and Cole, E.: Reconstruction of long-term successional dynamics of temperate woodland in Białowieża Forest, Poland, Journal of Ecology, 86, 1042–1059, https://doi.org/10.1046/j.1365-2745.1998.00323.x, 1998.

Morales-Molino, C., Colombaroli, D., Valbuena-Carabaña, M., Tinner, W., Salomón, R. L., Carrión, J. S., and Gil, L.: Land-use history as a major driver for long-term forest dynamics in the Sierra de Guadarrama National Park central Spain) during the last millennia: implications for forest conservation and management, Glob Planet Change, 152, 64–75, https://doi.org/10.1016/j.gloplacha.2017.02.012, 2017a.

Morales-Molino, C., Tinner, W., García-Antón, M., and Colombaroli, D.: The historical demise of Pinus nigra forests in the Northern Iberian Plateau south-western Europe), Journal of Ecology, 105, 634–646, https://doi.org/10.1111/1365-2745.12702, 2017b.

Morales-Molino, C., Colombaroli, D., Tinner, W., Perea, R., Valbuena-Carabaña, M., Carrión, J. S., and Gil, L.: Vegetation and fire dynamics during the last 4000 years in the Cabañeros National Park central Spain), Rev Palaeobot Palynol, 253, 110–122, https://doi.org/10.1016/j.revpalbo.2018.04.001, 2018.

Morales-Molino, C., Tinner, W., Perea, R., Carrión, J. S., Colombaroli, D., Valbuena-Carabaña, M., Zafra, E., and Gil, L.: Unprecedented herbivory threatens rear-edge populations of *Betula* in southwestern Eurasia, Ecology, 100, https://doi.org/10.1002/ecy.2833, 2019.

Niinemets, E., Poska, A., and Saarse, L.: Vegetation history and human impact in the Parika area, Central Estonia, Proceedings of the Estonian Academy of Sciences. Geology, 51, 241, https://doi.org/10.3176/geol.2002.4.04, 2002.

Novenko, E. Y., Tsyganov, A. N., Rudenko, O. V., Volkova, E. V., Zuyganova, I. S., Babeshko, K. V., Olchev, A. V., Losbenev, N. I., Payne, R. J., and Mazei, Y. A.: Mid- and late-Holocene vegetation history, climate and human impact in the forest-steppe ecotone of European Russia: new data and a regional synthesis, Biodivers Conserv, 25, 2453–2472, https://doi.org/10.1007/s10531-016-1051-8, 2016a.

Novenko, E. Yu., Tsyganov, A. N., Volkova, E. M., Kupriyanov, D. A., Mironenko, I. V., Babeshko, K. V., Utkina, A. S., Popov, V., and Mazei, Y. A.: Mid- and Late Holocene vegetation dynamics and fire history in the boreal forest of European Russia: A case study from Meshchera Lowlands, Palaeogeogr Palaeoclimatol Palaeoecol, 459, 570–584, https://doi.org/10.1016/j.palaeo.2016.08.004, 2016b.

Ortu, E., David, F., and Caramiello, R.: Rôle de l’homme dans l’histoire de la végétation de la vallée Ellero Alpes maritimes, Italie), C R Biol, 326, 631–637, https://doi.org/10.1016/S1631-069103)00155-0, 2003.

Ortu, E., Peyron, O., Bordon, A., de Beaulieu, J. L., Siniscalco, C., and Caramiello, R.: Lateglacial and Holocene climate oscillations in the South-western Alps: An attempt at quantitative reconstruction, Quaternary International, 190, 71–88, https://doi.org/10.1016/j.quaint.2008.04.004, 2008.

Pędziszewska, A. and Latałowa, M.: Stand-scale reconstruction of late Holocene forest succession on the Gdańsk Upland N. Poland) based on integrated palynological and macrofossil data from paired sites, Veg Hist Archaeobot, 25, 239–254, https://doi.org/10.1007/s00334-015-0546-7, 2016.

Pérez Díaz, S. and López Sáez, J. A.: The Western Pyrenean Northern Iberian Peninsula) during the Upper Paleolithic: A palaeoenvironmental approach, 2021.

Pérez-Díaz, S. and López-Sáez, J. A.: 33. Verdeospesoa mire Basque Country, Northern Iberian Peninsula, Spain), Grana, 56, https://doi.org/10.1080/00173134.2016.1271824, 2017.

Pérez-Díaz, S., López-Sáez, J. A., Núñez de la Fuente, S., and Ruiz-Alonso, M.: Early farmers, megalithic builders and the shaping of the cultural landscapes during the Holocene in Northern Iberian mountains. A palaeoenvironmental perspective, J Archaeol Sci Rep, 18, 463–474, https://doi.org/10.1016/j.jasrep.2018.01.043, 2018.

Pérez-Sanz, A., González-Sampériz, P., Moreno, A., Valero-Garcés, B., Gil-Romera, G., Rieradevall, M., Tarrats, P., Lasheras-Álvarez, L., Morellón, M., Belmonte, A., Sancho, C., Sevilla-Callejo, M., and Navas, A.: Holocene climate variability, vegetation dynamics and fire regime in the central Pyrenees: the Basa de la Mora sequence NE Spain), Quat Sci Rev, 73, https://doi.org/10.1016/j.quascirev.2013.05.010, 2013.

Pokorný, P.: A high-resolution record of Late-Glacial and Early-Holocene climatic and environmental change in the Czech Republic, Quaternary International, 91, 101–122, https://doi.org/10.1016/S1040-618201)00105-7, 2002.

Pokorný, P.: Role of man in the development of Holocene vegetation in Central Bohemia, Preslia, 77, 113–128, 2005.

Pokorný, P.: 29. Vrbka Czech Republic): Pollen record of secondary steppe vegetation development within the Bronze Age agricultural landscape, Grana, 55, 246–249, https://doi.org/10.1080/00173134.2015.1120342, 2016.

Pokorný, P. and Jankovská, V.: Long-term vegetation dynamics and the infilling process of a former lake Švarcenberk, Czech Republic), Folia Geobot, 35, 433–457, https://doi.org/10.1007/BF02803554, 2000.

Pokorný, P. and van der Knaap, W. O.: 10. Na Bahně Czech Republic): Vegetation development over the last 2.5 millennia in the Eastern Bohemian lowland, Grana, 49, 79–81, https://doi.org/10.1080/00173130903435846, 2010.

Pokorný, P. and van der Knaap, W. O.: 15. Brve Czech Republic): Vegetation development over the last about 2.5 millennia in the Bohemian Lowland close to Prague, Grana, 50, 311–313, https://doi.org/10.1080/00173134.2011.645551, 2011.

Pokorný, P. and Kuneš, P.: Holocene acidification process recorded in three pollen profiles from Czech sandstone and river terrace environments, Ferrantia, 44, 107–112, 2005.

Pokorný, P., Kuneš, P., Abraham, V.:. Holocenní vývoj vegetace v Ceském Svýcarsku, in: Bauer, P., Kopecký, V., Smucar, J. (Eds.), Labské pískovce - historie, příroda a ochrana území. Agentura ochrany přírody a krajiny České republiky, Správa CHKO Labské pískovce, Děčín, Czech Republic, pp. 35–49, 2008.

Pokorný, P. and Kuneš, P.: 5. Kožlí S. Bohemia, Czech Republic), Grana, 48, 77–78, https://doi.org/10.1080/00173130902759816, 2009.

Pokorný, P., Klimešová, J., and Klimeš, L.: Late holocene history and vegetation dynamics of a floodplain alder carr: A case study from eastern Bohemia, Czech Republic, Folia Geobot, 35, 43–58, https://doi.org/10.1007/BF02803086, 2000.

Pokorný, P., Sádlo, J., and Bernardová, A.: Holocene history of Cladium mariscus L.) Pohl in the Czech Republic. Implications for species population dynamics and palaeoecology, Acta Palaeobotanica, 50, 65–76, 2010.

Poska, A. and Saarse, L.: Holocene vegetation and land-use history in the environs of Lake Kahala, northern Estonia, Veg Hist Archaeobot, 8, 185–197, https://doi.org/10.1007/BF02342719, 1999.

Pulido, M. G.: Conséquences de L'anthropisation sur la Dynamique Postglaciaire de la Végétation dans le sud du Massif Central, France PhD thesis), Université d'Aix-Marseille, Marseille, France, 2006.

Ramos-Román, M. J., Jiménez-Moreno, G., Anderson, R. S., García-Alix, A., Toney, J. L., Jiménez-Espejo, F. J., and Carrión, J. S.: Centennial-scale vegetation and North Atlantic Oscillation changes during the Late Holocene in the southern Iberia, Quat Sci Rev, 143, 84–95, https://doi.org/10.1016/j.quascirev.2016.05.007, 2016.

Revelles, J., Cho, S., Iriarte, E., Burjachs, F., van Geel, B., Palomo, A., Piqué, R., Peña-Chocarro, L., and Terradas, X.: Mid-Holocene vegetation history and Neolithic land-use in the Lake Banyoles area Girona, Spain), Palaeogeogr Palaeoclimatol Palaeoecol, 435, https://doi.org/10.1016/j.palaeo.2015.06.002, 2015.

Riera-Mora, S. and Esteban-Amat, A.: Vegetation history and human activity during the last 6000 years on the central Catalan coast northeastern Iberian Peninsula), Veg Hist Archaeobot, 3, 7–23, https://doi.org/10.1007/BF00208885, 1994.

Rius, D., Vannière, B., and Galop, D.: Fire frequency and landscape management in the northwestern Pyrenean piedmont, France, since the early Neolithic 8000 cal. BP), Holocene, 19, 847–859, https://doi.org/10.1177/0959683609105299, 2009.

Robles-López, S., Luelmo-Lautenschlaeger, R., Pérez-Díaz, S., Abel-Schaad, D., Alba-Sánchez, F., Ruiz-Alonso, M., and López-Sáez, J. A.: Vulnerabilidad y resiliencia de los pinares de alta montaña de la Sierra de Gredos Ávila, Sistema Central): dos mil años de dinámica socioecológica, Cuaternario y Geomorfología, 31, 51–72, https://doi.org/10.17735/cyg.v31i3-4.55594, 2017.

Robles-López, S., Fernández Martín-Consuegra, A., Pérez-Díaz, S., Alba-Sánchez, F., Broothaerts, N., Abel-Schaad, D., and López-Sáez, J. A.: The dialectic between deciduous and coniferous forests in central Iberia: A palaeoenvironmental perspective during the late Holocene in the Gredos range, Quaternary International, 470, 148–165, https://doi.org/10.1016/j.quaint.2017.05.012, 2018.

Robles-López, S., Pérez-Díaz, S., Ruiz-Alonso, M., Blarquez, O., Luelmo-Lautenschlaeger, R., and López-Sáez, J. A.: Holocene vegetation and fire dynamics in the supra-Mediterranean belt of the Gredos Range central Iberian Peninsula), Plant Biosystems - An International Journal Dealing with all Aspects of Plant Biology, 154, 74–86, https://doi.org/10.1080/11263504.2019.1578281, 2020.

Rösch, M.: Zwei Moore im westlichen Bodenseegebiet als Zeugen prähistorischer Landschaftsveränderungen, Telma, 16, 83–111, 1986.

Rösch, M.: Holocene sediment accumulation in the shallow water zone of Lower Lake Constance, Arch Hydrobiol, 107, 541–562, 1997.

Rösch, M.: Zur Vegetationsgeschichte des südlichen Kraichgaus - Botanische Untersuchungen bei Großvillars, Gemeinde Oberderdingen, Landkreis Karlsruhe, Fundberichte aus Baden-Württemberg, 28, 839–870, 2005.

Rösch, M.: Botanical evidence for prehistoric and medieval land use in the Black Forest, 335–343, https://doi.org/10.1484/M.RURALIA-EB.3.1181, 2009.

Rösch, M.: Vegetation und Waldnutzung im Nordschwarzwald während sechs Jahrtausenden anhand von Profundalkernen aus dem Herrenwieser See. Mitt. Ver. für Forstl, Standortskunde und Forstpflanzenzüchtung, 47, 43–64, 2012.

Rösch, M.: Change of Land Use during the Last Two Millennia as Indicated in the Pollen Record of a Profundal Core from Mindelsee, Lake Constance Region, Southwest Germany, Offa, 69, 355–370, 2013.

Rösch, M. and Fischer, E.: A radiocarbon dated Holocene pollen profile from the Banat mountains Southwestern Carpathians, Romania), Flora, 195, 277–286, https://doi.org/10.1016/S0367-253017)30981-7, 2000.

Rösch, M. and Lechterbeck, J.: Seven Millennia of human impact as reflected in a high resolution pollen profile from the profundal sediments of Litzelsee, Lake Constance region, Germany, Veg Hist Archaeobot, 25, 339–358, https://doi.org/10.1007/s00334-015-0552-9, 2016.

Rösch, M. and Tserendorj, G.: Der Nordschwarzwald–früher besiedelt als gedacht? Pollenprofile belegen ausgedehnte vor-geschichtliche Besiedlung und Landnutzung, Denkmalpflege in Baden-Württemberg, 40, 66–73, 2011a.

Rösch, M. and Tserendorj, G.: Florengeschichtliche Beobachtungen im Nordschwarzwald Südwestdeutschland), Hercynia N.F., 44, 53–71, 2011b.

Rösch, M. and Wick, L.: 43. Buchensee Lake Constance region, Germany), Grana, 58, 308–310, https://doi.org/10.1080/00173134.2019.1569127, 2019.

Rösch, M., Kleinmann, A., Lechterbeck, J., and Wick, L.: Botanical off-site and on-site data as indicators of different land use systems: a discussion with examples from Southwest Germany, Veg Hist Archaeobot, 23, 121–133, https://doi.org/10.1007/s00334-014-0437-3, 2014.

Sadori, L., Zanchetta, G., and Giardini, M.: Last Glacial to Holocene palaeoenvironmental evolution at Lago di Pergusa Sicily, Southern Italy) as inferred by pollen, microcharcoal, and stable isotopes, Quaternary International, 181, 4–14, https://doi.org/10.1016/j.quaint.2007.02.024, 2008.

Sarmaja-Korjonen, K.: Latitudinal differences in the influx of microscopic charred particles to lake sediments in Finland, Holocene, 8, 589–597, https://doi.org/10.1191/095968398666296639, 1998.

Schneider, H., Höfer, D., Trog, C., Busch, S., Schneider, M., Baade, J., Daut, G., and Mäusbacher, R.: Holocene estuary development in the Algarve Region Southern Portugal) – A reconstruction of sedimentological and ecological evolution, Quaternary International, 221, 141–158, https://doi.org/10.1016/j.quaint.2009.10.004, 2010.

Schneider, H., Höfer, D., Trog, C., and Mäusbacher, R.: Holocene landscape development along the Portuguese Algarve coast - A high resolution palynological approach, Quaternary International, 407, 47–63, https://doi.org/10.1016/j.quaint.2016.02.039, 2016.

Sillasoo, U., Mauquoy, D., Blundell, A., Charman, D., Blaauw, M., Daniell, J. R. G., Toms, P., Newberry, J., Chambers, F. M., and Karofeld, E.: Peat multi-proxy data from Männikjärve bog as indicators of late Holocene climate changes in Estonia, Boreas, 36, 20–37, https://doi.org/10.1111/j.1502-3885.2007.tb01177.x, 2007.

Sillasoo, Ü., Väliranta, M., and Tuittila, E.-S.: Fire history and vegetation recovery in two raised bogs at the Baltic Sea, Journal of Vegetation Science, 22, 1084–1093, https://doi.org/10.1111/j.1654-1103.2011.01307.x, 2011.

Silva-Sánchez, N., Martínez Cortizas, A., Abel-Schaad, D., López-Sáez, J., and Mighall, T.: Influence of climate change and human activities on the organic and inorganic composition of peat during the ‘Little Ice Age’ El Payo mire, W Spain), Holocene, 26, 1290–1303, https://doi.org/10.1177/0959683616638439, 2016.

Speranza, A.: Improving the time control of the Subboreal/Subatlantic transition in a Czech peat sequence by 14C wiggle-matching, Quat Sci Rev, 19, 1589–1604, https://doi.org/10.1016/S0277-379199)00108-0, 2000.

Speranza, A., Hanke, J., van Geel, B., and Fanta, J.: Late-Holocene human impact and peat development in the Černá Hora bog, Krkonoše Mountains, Czech Republic, Holocene, 10, 575–585, https://doi.org/10.1191/095968300668946885, 2000.

Stančikaitė, M., Kisielienė, D., and Strimaitienė, A.: Vegetation response to the climatic and human impact changes during the Late Glacial and Holocene: case study of the marginal area of Baltija Upland, NE Lithuania, Baltica, 17, 17–33, 2004.

Stančikaitė, M., Baltrūnas, V., Šinkūnas, P., Kisielienė, D., and Ostrauskas, T.: Human response to the Holocene environmental changes in the Biržulis Lake region, NW Lithuania, Quaternary International, 150, 113–129, https://doi.org/10.1016/j.quaint.2006.01.010, 2006.

Stančikaitė, M., Kisielienė, D., Moe, D., and Vaikutienė, G.: Lateglacial and early Holocene environmental changes in northeastern Lithuania, Quaternary International, 207, 80–92, https://doi.org/10.1016/j.quaint.2008.10.009, 2009.

Stančikaitė, M., Šeirienė, V., Kisielienė, D., Martma, T., Gryguc, G., Zinkutė, R., Mažeika, J., and Šinkūnas, P.: Lateglacial and early Holocene environmental dynamics in northern Lithuania: A multi-proxy record from Ginkūnai Lake, Quaternary International, 357, 44–57, https://doi.org/10.1016/j.quaint.2014.08.036, 2015.

Stančikaitė, M., Gedminienė, L., Edvardsson, J., Stoffel, M., Corona, C., Gryguc, G., Uogintas, D., Zinkutė, R., Skuratovič, Ž., and Taraškevičius, R.: Holocene vegetation and hydroclimatic dynamics in SE Lithuania – Implications from a multi-proxy study of the Čepkeliai bog, Quaternary International, 501, 219–239, https://doi.org/10.1016/j.quaint.2017.08.039, 2019a.

Stančikaitė, M., Simniškytė, A., Skuratovič, Ž., Gedminienė, L., Kazakauskas, V., and Uogintas, D.: Reconstruction of the mid-to Late- Holocene history of vegetation and land-use in Petrešiūnai, north-east Lithuania: Implications from palaeobotanical and archaeological data, Quaternary International, 516, 5–20, https://doi.org/10.1016/j.quaint.2018.09.029, 2019b.

Steinberga, D. and Stivrins, N.: Fire frequency during the Holocene in central Latvia, northeastern Europe, Estonian Journal of Earth Sciences, 70, 127, https://doi.org/10.3176/earth.2021.09, 2021.

Stevenson, A. C.: The Holocene forest history of the Montes Universales, Teruel, Spain, Holocene, 10, 603–610, https://doi.org/10.1191/095968300670543500, 2000.

Svobodová, H., Reille, M., and Goeury, C.: Past vegetation dynamics of Vltavský luh, upper Vltava river valley in the Šumava mountains. Czech Republic, Veg Hist Archaeobot, 10, 185–199, https://doi.org/10.1007/PL00006930, 2001.

Święta-Musznicka, J., Badura, M., Pędziszewska, A., and Latałowa, M.: Environmental changes and plant use during the 5th-14th centuries in medieval Gdańsk, northern Poland, Veg Hist Archaeobot, 30, 363–381, https://doi.org/10.1007/s00334-020-00789-9, 2021.

Szal, M., Kupryjanowicz, M., Wyczółkowski, M., and Tylmann, W.: The Iron Age in the Mrągowo Lake District, Masuria, NE Poland: the Salęt settlement microregion as an example of long-lasting human impact on vegetation, Veg Hist Archaeobot, 23, 419–437, https://doi.org/10.1007/s00334-014-0465-z, 2014.

Szal, M., Kupryjanowicz, M., Tylmann, W., and Piotrowska, N.: Was it ‘ *terra desolata* ’? Conquering and colonizing the medieval Prussian wilderness in the context of climate change., Holocene, 27, 465–480, https://doi.org/10.1177/0959683616660167, 2017.

Tonkov, S. and Possnert, G.: 30. Peat bog Kumata-1, Vitosha Mountain Bulgaria), Grana, 55, 250–252, https://doi.org/10.1080/00173134.2016.1146330, 2016a.

Tonkov, S. and Possnert, G.: A new late Holocene pollen diagram from Vitosha Mountain. Vegetation history and anthropogenic impact, Comptes rendus de l'Académie bulgare des Sciences, 69, 327–337, 2016b.

Turner, R., Roberts, N., and Jones, M. D.: Climatic pacing of Mediterranean fire histories from lake sedimentary microcharcoal, Glob Planet Change, 63, 317–324, https://doi.org/10.1016/j.gloplacha.2008.07.002, 2008.

Turu, V., Carrasco, R. M., Pedraza, J., Ros, X., Ruiz-Zapata, B., Soriano-López, J. M., Mur-Cacuho, E., Pélachs-Mañosa, A., Muñoz-Martín, A., Sánchez, J., and Echeverria-Moreno, A.: Late glacial and post-glacial deposits of the Navamuño peatbog Iberian Central System): Chronology and paleoenvironmental implications, Quaternary International, 470, 82–95, https://doi.org/10.1016/j.quaint.2017.08.018, 2018.

Velle, G., Larsen, J., Eide, W., Peglar, S. M., and Birks, H. John. B.: Holocene environmental history and climate of Ratasjoen, a low-alpine lake in south-central Norway, J Paleolimnol, 33, 129–153, https://doi.org/10.1007/s10933-004-2689-x, 2005.

Veski, S.: Vegetation History, Human Impact and Palaeogeography of West Estonia: Pollen Analytical Studies of Lake and Bog Sediments PhD thesis), Societas Upsaliensis pro geologia quaternaria [Kvartärgeologiska fören], Uppsala,Sweden, 1998.

Vincze, I., Orbán, I., Birks, H. H., Pál, I., Finsinger, W., Hubay, K., Marinova, E., Jakab, G., Braun, M., Biró, T., Tóth, M., Dănău, C., Ferencz, I. V, and Magyari, E. K.: Holocene treeline and timberline changes in the South Carpathians Romania): Climatic and anthropogenic drivers on the southern slopes of the Retezat Mountains, Holocene, 27, 1613–1630, https://doi.org/10.1177/0959683617702227, 2017.

Wacnik, A., Ralska-Jasiewiczowa, M., and Madeyska, E.: Late Glacial and Holocene history of vegetation in Gostynin area, central Poland, Acta Palaeobotanica, 51, 249–278, 2011.

Whittington, G., Edwards, K. J., and Cundill, P. R.: Late- and post-glacial vegetational change at Black Loch, Fife, eastern Scotland – a multiple core approach, New Phytologist, 118, 147–166, https://doi.org/10.1111/j.1469-8137.1991.tb00575.x, 1991.

Wieckowska-Lüth, M., Kirleis, W., and Doerfler, W.: Holocene history of landscape development in the catchment of Lake Skogstjern, southeastern Norway, based on a high-resolution multi-proxy record, Holocene, 27, 1928–1947, https://doi.org/10.1177/0959683617715691, 2017.

Yasuda, Y., Kitagawa, H., and Nakagawa, T.: The earliest record of major anthropogenic deforestation in the Ghab Valley, northwest Syria: a palynological study, Quaternary International, 73–74, 127–136, https://doi.org/10.1016/S1040-618200)00069-0, 2000.

Zawisza, E., Zawiska, I., Szeroczyńska, K., Correa-Metrio, A., Mirosław-Grabowska, J., Obremska, M., Rzodkiewicz, M., Słowiński, M., Woszczyk, M., and et. al.: Dystrophication of lake Suchar IV NE Poland): an alternative way of lake development, Limnetica, 38, 391–416, https://doi.org/10.23818/limn.38.23, 2019.

5. Discussion

The aim of this thesis was to investigate wildfire and its controls during the Holocene across Europe, employing a more statistically rigorous and integrated approach than has typically been the case in previous studies. This final chapter discusses the overall implications of the work under three headings: 1) the need for a robust and holistic approach in assessing palaeofire regimes, as wildfire is influenced by multiple factors; 2) the implications of the results for regional-scale analysis and for the interpretation of findings from prior research; 3) the challenges in working with multiple sets of palaeodata at such spatial and temporal scales. This chapter concludes with proposals for taking this work forward, with suggested potential solutions to some of the challenges faced.

5.1. The need for a robust and holistic approach in assessing palaeofire

Although there is a body of work that has investigated palaeofire at site, sub-region, continental and global scales, there are several issues that could affect the robustness of earlier findings (see discussion in Chapter 1).

Much previous research on palaeofire primarily relies on visual assessment of the synchronicity of reconstructed time series of fire with its drivers (e.g. Blarquez and Carcaillet, 2010; Beffa et al., 2016; Connor et al., 2019; Cui et al., 2020; Bremond et al., 2024). Although this is an intuitive way of identifying first order relationships, this assessment is subjective, and could be affected by noise, outliers, and differences in both the temporal and spatial scale of the records being compared. Furthermore, synchronicity between two events does not identify the direction of causality, which given the multiple two-way interactions between climate, vegetation, fire and human activities can be problematic (Harrison et al., 2023). It can be particularly challenging to identify meaningful correlations when comparing multiple drivers. The analysis of the relationships between fire and human activities in Iberia (Chapter 2) was designed to address this issue, by bringing together datasets and reconstruction techniques from different fields in a robust analytical framework. Reconstructions of fire based on sedimentary charcoal data were paired with archaeological proxies for past population fluctuations, and archaeological data for the timing of the start of agriculture in different parts of Iberia. Rather than direct visual assessment of changes in these time series, a Superposed Epoch Analysis (SEA) was performed to investigate whether there was any human impact on fire between 10,000 and 3,500 cal. BP. Using an archaeological technique based on summed probability distributions (SPDs), periods of rapid population growth were identified, with charcoal data re-based by these time periods and re-constituted into a time series. Changes in fire around these joint events were then investigated. Similarly, the time transgressive spread of agriculture in the region, which was mapped using radiocarbon data and kriging-based interpolation, was used to re-base the charcoal data at the site level, with the influence of this spread of agriculture assessed through times series modelling of charcoal data. The SEA approach, a robust and widely used way of assessing relationships for individual drivers (see e.g. D'Arrigo et al., 1993; Arneth et al., 2010; Blarquez & Carcaillet, 2010; Helama et al., 2021; Higgins et al., 2022), showed that there were no clear relationships between fire and human activities, either as represented by population changes or by the time-transgressive introduction of agriculture, at this scale during this time period.

The work on Iberia led to the recognition of the importance of considering the potential role of other drivers of changes in fire regime alongside human drivers. Much of the research on palaeofire has tended to focus on a limited set of drivers, and then inferred relationships to other drivers based on unexplained changes in fire (e.g. Feurdean et al., 2012; Clear et al. 2014; Iglesias and Whitlock, 2014). This is partly a reflection of the availability of reconstructed variables that are suitable for palaeofire analysis. Analyses using generalised additive models (GAMs) to relate (smoothed) time series of reconstructed past fire based on fire controls (e.g. Daniau et al., 2012; Marlon et al., 2012; Feurdean et al., 2020), for example, have tended to focus on climate and/or vegetation drivers, and to ignore potential human drivers. Analyses of the drivers of fire under modern conditions (e.g. Haas et al., 2022; Haas et al., 2024) show that the relationships between different drivers can change depending on which metrics are included in an analysis; for example, human population changes only have a positive effect on fire when metrics for the negative effect of human-induced landscape fragmentation are also considered. Thus, analyses based on a limited set of drivers may not be adequate or reliable, as the signal could be obscured or enhanced by other factors that were not included. Reconstructions of fire, human influence, vegetation and climate are required to assess the role of the different drivers on wildfire simultaneously.

Fire reconstructions and human population change estimates could be created using the same charcoal and archaeological radiocarbon-based approaches as applied in Iberia, and climate reconstructions were available at the site and temporal resolution required. Although there are reconstructions of European tree cover through the Holocene, they are not suitable for the site-based approach adopted in this thesis. Reconstructions based on the REVEALS approach (Githumbi et al., 2022; Serge et al., 2023) were only available as averages for 1° grid cells, while reconstructions using MAT (Zanon et al., 2018) were interpolated surfaces both in space and time. In addition, the MAT-based reconstructions involve a number of methodological decisions, as discussed in Chapter 1, that can cause further uncertainties. A new reconstruction of tree cover was made (Chapter 3), in order to provide a data set that was more consistent with the site-based fire, climate and population datatesting a novel calibration-based approach that adds to the pantheon of methods for reconstructing vegetation based on pollen data. The alternative approach reduces uncertainties due to differences in spatial (and temporal) scale when comparing across the reconstructions, Furthermore, the new approach is one that could be more appropriate than other approaches in areas because of its relative simplicity and limited data demands.

Unlike modern fire analysis, where simultaneous data coverage of multiple variables lends itself to statistical analysis, the spatiotemporal structure of palaeodata makes the approach to analysing palaeofire less apparent. Different approaches were therefore tried in this thesis. Firstly, multiple regressions were trialled with fire as a function of tree cover and climate, in line with the approaches adopted for modern fire analysis. The inclusion of human population change was not included, given the challenges of incorporating this data due to differences in temporal resolution. In addition, time series were developed based on sub-regional agglomerations of sedimentary records and archaeological data. These were then assessed jointly using Granger causation analysis, to test whether lagged effects of reconstructed tree cover, climate and human population change have any explanatory power in relation to changes in fire through time. These two approaches were designed to tease out individual relationships between fire and drivers. As the results from these analyses were often inconsistent or difficult to interpret (see below), an SEA analysis was performed on reconstructed fire, climate and tree cover time series. However, there were still difficulties in attributing changes in fire to specific variables. In some instances, changes in fire appeared to be closely associated with population fluctuations, but there was also an underlying climate or vegetation signal. In other cases, no clear relationships could be seen with any variables, beyond an apparent cumulative moisture and temperature effect. This joint analysis of multiple data types and variables demonstrates that focussing on a single driver (such as human population) may lead to inaccurate conclusions which overlook the parallel role of other factors in shaping palaeofire and emphasises the need to take a holistic approach to understanding changes in fire regimes..

5.2. Regional scale analysis

The results of the analysis presented in this thesis have implications for future regional-scale analysis of palaeofire beyond the need for a holistic approach in assessing drivers. Key issues include: 1) a lack of consistency in relationships; 2) the importance of methodological choices; and 3) the challenge of identifying a human signal.

Firstly, there were no consistent relationships between palaeofire and its controls across sub-regions, and few significant relationships were evident within sub-regions. Differences between sub-regions may explain the limited explanatory power of the regression analysis at the European level, and at the sub-regional level, any signal was not consistent or strong enough to emerge from variation in the data. As a result, drawing broad conclusions about the drivers of palaeofire at global scale, as done for modern fire, is challenging. Evidence at a site or sub-regional level may not be applicable at larger spatial scales, or in different locations, potentially helping to explain contrasting previous interpretations found in the literature. This lack of consistency could be a reflection of challenges with the data (see below). However, they could reflect inconsistent relationships between fire and its controls through time. A lack of temporal consistency would impact the ability to identify consistent relationships, and may imply the need for temporal segmentation of the data (data coverage notwithstanding). At the same time, it is clear from modern day analysis that the relationships between fire and its controls can vary, with, for example, landscape fragmentation having different impacts on wildfire depending on whether the environment is fire prone already (Harrison, 2021). The lack of consistency may therefore reflect a combination of spatial and temporal variation, which given the interplay of the relationships between drivers and fire may simply reflect this complexity.

Secondly, methodological choices can also directly impact the identification of causal relationships. For the Granger causality analysis, the choice of whether to use smoothed or raw time series sometimes led to contrasting results. In southern Norway, for example, smoothing the data led to the identification of lagged mean temperature of the coldest month (MTCO) and tree cover Granger causing fire in addition to the population change, whereas MTCO and tree cover did not Granger cause fire in the unsmoothed data. Smoothing the data is one way to minimise the impact of noise in identifying relationships by reducing the impact of outliers, but there many different approaches to doing this and it is not always clear which method is the most appropriate to use with a given set of data (Simonoff, 1998; Taylor & Cihon, 2004). . Changes in the window of analysis (and appropriate smoothing half window) can also directly impact results. Such methodological choices explain apparent differences in coincident changes in fire in relation to booms in population between Chapter 2 and Chapter 4. In Chapter 2, the 1500-year window around each identified boom period meant that a 500-year smoothing half width was chosen to identify longer term changes in fire. In Chapter 4, due to the inclusion of bust periods and the narrower 1000-yr (maximum) window of analysis, a 200-year smoothing half width was applied. Shorter-term changes could therefore be identified, with the caveat that noise in the fire signal could obscure possible relationships. Narrower windows and half width smoothing may be necessary to identify direct relationships between population change and fire, if these changes are short lived: for example, dendrochronological data has identified changes in humidity at periods of 100-years (Achterberg et al., 2015). However, across multiple records with different sample depths, identifying legitimate signals with very short windows and half-widths is likely to be challenging. Ultimately, the optimal choice of scale is dependent on the quality of the data and underlying research questions. Whilst it is difficult to assess whether the levelling-off of fire that occurred in Iberia at the boom events represented a legitimate signal, the hypothesised increase in fire from population increases during this period of the Holocene (e.g. Connor et al., 2019) was not evident.

Finally, identifying a clear human influence on palaeofire is difficult at this Europe-wide and sub-regional spatial scale and for this period in the Holocene. Although the SEA analysis (Chapter 4) would seem to suggest that population changes were coincident with changes in palaeofire in some regions for either population booms or busts, in most cases a climate signal could also be discerned. For example, for Iberia, population change did not appear to Granger cause fire (in central Europe Granger causality analysis was hampered by series autocorrelation issues). The sole exception is southern Norway, where based on the Granger causality test the population rate of change appears to cause fire. However, this relationship does not appear apparent in the subsequent SEA analysis for boom periods of growth, with climate seemingly driving fire during these episodes of population change. It may be that, while population change contributes to fire, this relationship is less dependent on particularly rapid periods of change. Alternatively, this may reflect multiple drivers working in concert. Finally, one cannot rule out the possibility of mixed human signals in relation to fire, with increases in fire in some regions or at some time periods counteracted by opposing signals during other periods or in other locations. For example, both increases and decreases in burned area during the middle of the Holocene resulting from anthropogenic land clearance have been observed in different areas of southern Europe (e.g. Tinner et al., 2016; Vannière et al., 2016). However, the lack of archaeological radiocarbon data for regions other than southern Norway after 3,500 cal. BP, meant that is was not possible to analysis relationships during periods with high population size and density.

5.3. The challenges associated with palaeodata

As well as general issues associated with palaeodata highlighted in Chapter 1, there were several additional challenges associated with combining different types of data which may have impacted the ability to draw strong conclusions relating to fire and its controls in this thesis.

Fundamentally this analysis tries to draw together multiple categories of data, collected for different purposes and originating from different disciplines. The most obvious implication lies in the general lack of spatiotemporal overlap between different types of data, which hampers cross-comparison for many regions. The limited number of sedimentary charcoal records available for the British Isles and France precluded any investigation of wildfire there, although there is abundant information that could be used to reconstruct changes in human populations. Although the site-focussed approach followed here, with some adjustment for proximate site locations, means that data from sedimentary records can be spatially aligned, archaeological data used for reconstructing population change are often not at the same location at other records. Spatial overlap of the sedimentary records and radiocarbon data for regression analysis was thus more limited, affecting the ability to include site-based measurements of population influence. In terms of temporal resolution, the nature of the sedimentary records and archaeological radiocarbon data is such that there are differences in the timings of samples. Irrespective of dating uncertainty, temporal comparability of the data is limited due to the requirements of data binning. Although a relatively narrow binwidth of 100 years was used in the analysis of palaeofire and its multiple controls (Chapter 4) to try and minimise this potential temporal congruence, at the extreme, changes in variables in close temporal proximity could be separated by bins, whilst changes further apart in time – up to 100 years – could be combined in a single bin. Again, if broad patterns at millennial timescales are the focus, this may not be important, but it could still limit the ability to identify legitimate relationships. Lastly, this relatively narrow 100-year bin raises potential issues with noisy data, and differences in sampling resolutions between sites.

Although the dating of palaeodata can be inaccurate as discussed in Chapter 1, with radiocarbon data for example sometimes subject to wide error margins, such uncertainty places limits on the ability to compare records at the finer temporal scale that may be needed to identify relationships. To a certain extent, the inclusion of large numbers of records or radiocarbon dates may mitigate these issues with uncertainty, especially if millennial and regional-scale relationships are the focus. But this also can lead to over smoothing, minimising the ability to detect legitimate relationships or reducing regression model effectiveness due to wide variances. As well as issues with data resolution, differences in data sample range also affects the ability to assess relationships across the Holocene. This is most clearly seen in reference to the archaeological radiocarbon data which, due to cultural dating approaches of material later in the Holocene, places a constraint on how far towards the present that the joint analysis of data could be performed. The reduction in the availability of sedimentary charcoal and pollen data samples through time also affects the representativeness of the data temporally, reducing the quality of the signal further back in time for the time series analyses, and biasing the modelling analysis more towards the present day.

Charcoal is a broad measure of landscape burning, reflecting a combination of fire regime elements. Changes in charcoal accumulation then may reflect different factors within the fire regime: charcoal production varies depending on fire size, intensity and vegetation types (e.g. Patterson et al., 1987; Higuera et al., 2011), even at a site level. This can be problematic when assessing the controls on palaeofire, which have been shown to affect different elements of the fire regime in modern day conditions (Haas et al., 2022). The challenge of cross-site comparison of charcoal accumulation rates also affects the ability to model palaeofire as a function of its drivers. Although the conversion of charcoal influx to z-scores facilitates comparison, in a modelling framework this reduces the information within the data, especially when other variables are similarly treated. Although sedimentary charcoal data provides an unmatched record of fire through time, there is a clear challenge in terms of interpreting the signal which is compounded by vastly different measurements of accumulation across sites.

5.4. Proposals for future work

Despite the challenges faced in identifying consistent region-wide or sub-regional relationships between palaeofire and its drivers, this research has shown the merits in developing this research approach further. From a practical point of view there are a number of directions worth exploring.

Future research should incorporate additional variables within the analysis. Assessments of the drivers of modern fire can draw on a range of detailed variables that focus on particular aspects of fire regimes. By contrast, this thesis has drawn on a more limited range of variables, which themselves may not have the necessary explanatory power. For example, although plant available moisture may be relevant for describing fire in broad terms, it is the number of dry days and the vapour pressure deficit that have been identified as key drivers for burned area (Haas et al., 2022). The multivariate nature of pollen data, with different plant responses to different bioclimatic variables, should allow the reconstruction of additional variables. Similarly, the use of tree cover to measure the influence of the vegetation control on fire may not fully capture the specific effects of vegetation on fire. Analyses of modern relationships include shrub and grass cover, and gross or net primary production as additional predictors (Haas et al, 2022; Haas et al., 2024). Pollen data has been used to reconstruct different vegetation types (see e.g. Cruz-Silva et al., 2022; Cruz-Silva et al., 2024), and in combination with modelling to reconstruct changes in vegetation productivity through time (e.g. Chen et al., 2023). An exercise to map both the range of appropriate variables to reconstruct and the feasibility of these reconstructions, and a subsequent concerted effort to extend the availability of reconstructions across multiple variables would greatly enhance the ability to test the drivers of palaeofire.

Multiple types of palaeodata have been used to reconstruct past climate and vegetation, as discussed in Chapter 1. Future research could investigate the use of multiple sources of evidence for different variables to increase the confidence in the reconstructions and improve their spatiotemporal coverage. Reconstructions of changes in fire based on charcoal data, for example, could be supplemented with fire scar data (e.g. Marlon et al., 2012; Clear et al., 2014), or with biomarker data from ice cores, increasing resolution, as well as increase overall confidence in the fire signal. A similar approach could be used for climate reconstructions, by combining reconstructions based on pollen with other biotic records. It would also be useful to use multiple reconstruction approaches for specific variables, The tree cover reconstructions based on the technique employed in this thesis could, for example, be composited in an ensemble with reconstructions based on different techniques (e.g. the MAT, REVEALS). For population reconstructions, archaeological radiocarbon data could be combined with site counts (e.g. Roberts et al., 2019; Kolář et al., 2022), to extend the temporal range of the data into other sub-regions. For human influence more generally, multiple sources of evidence such as indicator species, or land cover changes could be combined with population reconstructions, to generate a wider measure of human impact on the environment, taking inspiration from measures of human influence in the modern day (e.g. Sanderson et al., 2002). Finally, modelled climate, vegetation and population data could be used in conjunction with reconstructions, to enhance overlaps and potentially improve the ability to identify relationships.

Modern day statistical analysis shows the importance of accounting for multiple factors when identifying the controls on fire. Although there are many challenges in applying a multivariable analysis of palaeofire, this is necessary to avoid possible misleading interpretations of relationships. Coupled with the application of statistical approaches to enhance confidence in observed relationships, the extension of the work developed within this thesis to include additional variables based on a methodologically diverse approach could provide further clarity on the controls of fire in past, present and future.

5.5. References

Achterberg, I., Bauerochse, A., Giesecke, T., Metzler, A., and Leuschner, H. H.: Contemporaneousness of Trackway Construction and Environmental Change: a Dendrochronological Study in Northwest-German Mires, Interdisciplinaria Archaeologica - Natural Sciences in Archaeology, VI, 19–29, https://doi.org/10.24916/iansa.2015.1.2, 2015.

Arneth, A., Harrison, S. P., Zaehle, S., Tsigaridis, K., Menon, S., Bartlein, P. J., Feichter, J., Korhola, A., Kulmala, M., O'Donnell, D., Schurgers, G., Sorvari, S., and Vesala, T.: Terrestrial biogeochemical feedbacks in the climate system, Nat Geosci, 3, 525–532, https://doi.org/10.1038/ngeo905, 2010.

Beffa, G., Pedrotta, T., Colombaroli, D., Henne, P. D., van Leeuwen, J. F. N., Süsstrunk, P., Kaltenrieder, P., Adolf, C., Vogel, H., Pasta, S., Anselmetti, F. S., Gobet, E., and Tinner, W.: Vegetation and fire history of coastal north-eastern Sardinia (Italy) under changing Holocene climates and land use, Veg Hist Archaeobot, 25, 271–289, https://doi.org/10.1007/s00334-015-0548-5, 2016.

Blarquez, O. and Carcaillet, C.: Fire, fuel composition and resilience threshold in subalpine ecosystem, PLoS One, 5, https://doi.org/10.1371/journal.pone.0012480, 2010.

Bremond, L., Aleman, J. C., Favier, C., Blarquez, O., Colombaroli, D., Connor, S. E., Cordova, C. E., Courtney-Mustaphi, C., Dabengwa, A. N., Gil-Romera, G., Gosling, W. D., Hamilton, T., Montade, V., Razafimanantsoa, A. H. I., Power, M. J., Razanatsoa, E., Yabi, I., and Vannière, B.: Past fire dynamics in sub-Saharan Africa during the last 25,000 years: Climate change and increasing human impacts, Quat Int, https://doi.org/10.1016/j.quaint.2024.07.012, 2024.

Chen, W., Zhang, Z., Ciais, P., Tan, L., Kemp, D. B., and Viovy, N.: Enhanced Mid-Holocene Vegetation Growth and Its Biophysical Feedbacks in China, Geophys Res Lett, 50, https://doi.org/10.1029/2023GL104702, 2023.

Clear, J. L., Molinari, C., and Bradshaw, R. H. W.: Holocene fire in Fennoscandia and Denmark, Int J Wildland Fire, 23, 781, https://doi.org/10.1071/WF13188, 2014.

Connor, S. E., Vannière, B., Colombaroli, D., Anderson, R. S., Carrión, J. S., Ejarque, A., Gil Romera, G., González-Sampériz, P., Hoefer, D., Morales-Molino, C., Revelles, J., Schneider, H., van der Knaap, W. O., van Leeuwen, J. F., and Woodbridge, J.: Humans take control of fire-driven diversity changes in Mediterranean Iberia's vegetation during the mid–late Holocene, Holocene, 29, 886–901, https://doi.org/10.1177/0959683619826652, 2019.

Cruz-Silva, E., Harrison, S. P., Marinova, E., and Prentice, I. C.: A new method based on surface-sample pollen data for reconstructing palaeovegetation patterns, J Biogeogr, 49, 1381–1396, https://doi.org/10.1111/jbi.14448, 2022.

Cruz-Silva, E., Harrison, S. P., Prentice, I. C., and Marinova, E.: Holocene vegetation dynamics of the Eastern Mediterranean region: Old controversies addressed by a new analysis, J Biogeogr, 51, 294–310, https://doi.org/10.1111/jbi.14749, 2024.

Cui, Q. Y., Gaillard, M. J., Vannière, B., Colombaroli, D., Lemdahl, G., Olsson, F., Benito, B., and Zhao, Y.: Evaluating fossil charcoal representation in small peat bogs: Detailed Holocene fire records from southern Sweden, Holocene, 30, 1540–1551, https://doi.org/10.1177/0959683620941069, 2020.

D'Arrigo, R. D., Cook, E. R., Jacoby, G. C., and Briffa, K. R.: Nao and sea surface temperature signatures in tree-ring records from the North Atlantic sector, Quat Sci Rev, 12, 431–440, https://doi.org/10.1016/S0277-3791(05)80007-1, 1993.

Daniau, A.-L., Bartlein, P. J., Harrison, S. P., Prentice, I. C., Brewer, S., Friedlingstein, P., Harrison-Prentice, T. I., Inoue, J., Izumi, K., Marlon, J. R., Mooney, S., Power, M. J., Stevenson, J., Tinner, W., Andrič, M., Atanassova, J., Behling, H., Black, M., Blarquez, O., Brown, K. J., Carcaillet, C., Colhoun, E. A., Colombaroli, D., Davis, B. A. S., D'Costa, D., Dodson, J., Dupont, L., Eshetu, Z., Gavin, D. G., Genries, A., Haberle, S., Hallett, D. J., Hope, G., Horn, S. P., Kassa, T. G., Katamura, F., Kennedy, L. M., Kershaw, P., Krivonogov, S., Long, C., Magri, D., Marinova, E., McKenzie, G. M., Moreno, P. I., Moss, P., Neumann, F. H., Norström, E., Paitre, C., Rius, D., Roberts, N., Robinson, G. S., Sasaki, N., Scott, L., Takahara, H., Terwilliger, V., Thevenon, F., Turner, R., Valsecchi, V. G., Vannière, B., Walsh, M., Williams, N., and Zhang, Y.: Predictability of biomass burning in response to climate changes, Global Biogeochem Cycles, 26, 2011GB004249, https://doi.org/10.1029/2011GB004249, 2012.

Feurdean, A., Spessa, A., Magyari, E. K., Willis, K. J., Veres, D., and Hickler, T.: Trends in biomass burning in the Carpathian region over the last 15,000 years, Quat Sci Rev, 45, 111–125, https://doi.org/10.1016/j.quascirev.2012.04.001, 2012.

Feurdean, A., Vannière, B., Finsinger, W., Warren, D., Connor, S. C., Forrest, M., Liakka, J., Panait, A., Werner, C., Andrič, M., Bobek, P., Carter, V. A., Davis, B., Diaconu, A.-C., Dietze, E., Feeser, I., Florescu, G., Gałka, M., Giesecke, T., Jahns, S., Jamrichová, E., Kajukało, K., Kaplan, J., Karpińska-Kołaczek, M., Kołaczek, P., Kuneš, P., Kupriyanov, D., Lamentowicz, M., Lemmen, C., Magyari, E. K., Marcisz, K., Marinova, E., Niamir, A., Novenko, E., Obremska, M., Pędziszewska, A., Pfeiffer, M., Poska, A., Rösch, M., Słowiński, M., Stančikaitė, M., Szal, M., Święta-Musznicka, J., Tanţău, I., Theuerkauf, M., Tonkov, S., Valkó, O., Vassiljev, J., Veski, S., Vincze, I., Wacnik, A., Wiethold, J., and Hickler, T.: Fire hazard modulation by long-term dynamics in land cover and dominant forest type in eastern and central Europe, Biogeosciences, 17, 1213–1230, https://doi.org/10.5194/bg-17-1213-2020, 2020.

Githumbi, E., Fyfe, R., Gaillard, M.-J., Trondman, A.-K., Mazier, F., Nielsen, A.-B., Poska, A., Sugita, S., Woodbridge, J., Azuara, J., Feurdean, A., Grindean, R., Lebreton, V., Marquer, L., Nebout-Combourieu, N., Stančikaitė, M., Tanţău, I., Tonkov, S., and Shumilovskikh, L.: European pollen-based REVEALS land-cover reconstructions for the Holocene: methodology, mapping and potentials, Earth Syst Sci Data, 14, 1581–1619, https://doi.org/10.5194/essd-14-1581-2022, 2022.

Haas, O., Prentice, I. C., and Harrison, S. P.: Global environmental controls on wildfire burnt area, size, and intensity, Environ Res Lett, 17, 065004, https://doi.org/10.1088/1748-9326/ac6a69, 2022.

Haas, O., Keeping, T., Gomez-Dans, J., Prentice, I. C., and Harrison, S. P.: The global drivers of wildfire, Front Environ Sci, 12, https://doi.org/10.3389/fenvs.2024.1438262, 2024.

Harrison, S. P., Cruz-Silva, E., Haas, O., Liu, M., Parker, S., Qiao, S., and Sweeney, L.: Tools and approaches to addressing the climate-humans nexus during the Holocene. Proceedings of the 12th International Congress on the Archaeology of the Ancient Near East *(ICAANE) Congress*, *Volume 1: Environmental Archaeology, Hammering the Material World, Cognitive Archaeology, Modeling the Past, Networked Archaeology, Endangered Cultural Heritage*, edited by: Marchetti, N., Campeggi, M., Cavaliere, F., D'Orazio, C., Giacosa, G., and Mariani, E., Harrassowitz Verlag, https://doi.org/10.13173/9783447118736, 2023.

Helama, S., Stoffel, M., Hall, R. J., Jones, P. D., Arppe, L., Matskovsky, V. V., Timonen, M., Nöjd, P., Mielikäinen, K., and Oinonen, M.: Recurrent transitions to Little Ice Age-like climatic regimes over the Holocene, Clim Dyn, 56, 3817–3833, https://doi.org/10.1007/s00382-021-05669-0, 2021.

Higgins, P. A., Palmer, J. G., Turney, C. S. M., Andersen, M. S., and Johnson, F.: Do Southern Hemisphere tree rings record past volcanic events? A case study from New Zealand, Climate of the Past, 18, 1169–1188, https://doi.org/10.5194/cp-18-1169-2022, 2022.

Higuera, P. E., Whitlock, C., and Gage, J. A.: Linking tree-ring and sediment-charcoal records to reconstruct fire occurrence and area burned in subalpine forests of Yellowstone National Park, USA, Holocene, 21, 327–341, https://doi.org/10.1177/0959683610374882, 2011.

Iglesias, V. and Whitlock, C.: Fire responses to postglacial climate change and human impact in northern Patagonia (41–43°S), Proceedings of the National Academy of Sciences, 111, E5545–E5554, https://doi.org/10.1073/pnas.1410443111, 2014.

Kolář, J., Macek, M., Tkáč, P., Novák, D., and Abraham, V.: Long-term demographic trends and spatio-temporal distribution of past human activity in Central Europe: Comparison of archaeological and palaeoecological proxies, Quat Sci Rev, 297, 107834, https://doi.org/10.1016/j.quascirev.2022.107834, 2022.

Marlon, J. R., Bartlein, P. J., Gavin, D. G., Long, C. J., Anderson, R. S., Briles, C. E., Brown, K. J., Colombaroli, D., Hallett, D. J., Power, M. J., Scharf, E. A., and Walsh, M. K.: Long-term perspective on wildfires in the western USA, P Natl Acad Sci USA, 109, E535–E543, https://doi.org/10.1073/pnas.1112839109, 2012.

Patterson, W. A., Edwards, K. J., and Maguire, D. J.: Microscopic charcoal as a fossil indicator of fire, Quat Sci Rev, 6, 3–23, https://doi.org/10.1016/0277-3791(87)90012-6, 1987.

Roberts, C. N., Woodbridge, J., Palmisano, A., Bevan, A., Fyfe, R., and Shennan, S.: Mediterranean landscape change during the Holocene: Synthesis, comparison and regional trends in population, land cover and climate, Holocene, 29, 923–937, https://doi.org/10.1177/0959683619826697, 2019.

Sanderson, E. W., Jaiteh, M., Levy, M. A., Redford, K. H., Wannebo, A. V, and Woolmer, G.: The Human Footprint and the Last of the Wild: The human footprint is a global map of human influence on the land surface, which suggests that human beings are stewards of nature, whether we like it or not, Bioscience, 52, 891–904, https://doi.org/10.1641/0006-3568(2002)052[0891:THFATL]2.0.CO;2, 2002.

Serge, M., Mazier, F., Fyfe, R., Gaillard, M.-J., Klein, T., Lagnoux, A., Galop, D., Githumbi, E., Mindrescu, M., Nielsen, A., Trondman, A.-K., Poska, A., Sugita, S., Woodbridge, J., Abel-Schaad, D., Åkesson, C., Alenius, T., Ammann, B., Andersen, S., Anderson, R., Andrič, M., Balakauskas, L., Barnekow, L., Batalova, V., Bergman, J., Birks, H., Björkman, L., Bjune, A., Borisova, O., Broothaerts, N., Carrion, J., Caseldine, C., Christiansen, J., Cui, Q., Currás, A., Czerwiński, S., David, R., Davies, A., De Jong, R., Di Rita, F., Dietre, B., Dörfler, W., Doyen, E., Edwards, K., Ejarque, A., Endtmann, E., Etienne, D., Faure, E., Feeser, I., Feurdean, A., Fischer, E., Fletcher, W., Franco-Múgica, F., Fredh, E., Froyd, C., Garcés-Pastor, S., García-Moreiras, I., Gauthier, E., Gil-Romera, G., González-Sampériz, P., Grant, M., Grindean, R., Haas, J., Hannon, G., Heather, A.-J., Heikkilä, M., Hjelle, K., Jahns, S., Jasiunas, N., Jiménez-Moreno, G., Jouffroy-Bapicot, I., Kabailienė, M., Kamerling, I., Kangur, M., Karpińska-Kołaczek, M., Kasianova, A., Kołaczek, P., Lagerås, P., Latalowa, M., Lechterbeck, J., Leroyer, C., Leydet, M., Lindbladh, M., Lisitsyna, O., López-Sáez, J.-A., Lowe, J., Luelmo-Lautenschlaeger, R., Lukanina, E., Macijauskaitė, L., Magri, D., Marguerie, D., Marquer, L., Martinez-Cortizas, A., Mehl, I., Mesa-Fernández, J., Mighall, T., Miola, A., Miras, Y., Morales-Molino, C., et al.: Testing the Effect of Relative Pollen Productivity on the REVEALS Model: A Validated Reconstruction of Europe-Wide Holocene Vegetation, Land (Basel), 12, 986, https://doi.org/10.3390/land12050986, 2023.

Simonoff, J. S.: Smoothing Methods in Statistics, Springer New York, New York, NY, https://doi.org/10.1007/978-1-4612-4026-6, 1996.

Taylor, J. K. and Cihon, C.: Statistical techniques for data analysis, 2nd ed., Chapman & Hall/CRC, Philadelphia, PA, 294 pp., 2004.

Tinner, W., Vescovi, E., van Leeuwen, J. F. N., Colombaroli, D., Henne, P. D., Kaltenrieder, P., Morales-Molino, C., Beffa, G., Gnaegi, B., van der Knaap, W. O., La Mantia, T., and Pasta, S.: Holocene vegetation and fire history of the mountains of Northern Sicily (Italy), Veg Hist Archaeobot, 25, 499–519, https://doi.org/10.1007/s00334-016-0569-8, 2016.

Vannière, B., Blarquez, O., Rius, D., Doyen, E., Brücher, T., Colombaroli, D., Connor, S., Feurdean, A., Hickler, T., Kaltenrieder, P., Lemmen, C., Leys, B., Massa, C., and Olofsson, J.: 7000-year human legacy of elevation-dependent European fire regimes, Quat Sci Rev, 132, 206–212, https://doi.org/10.1016/j.quascirev.2015.11.012, 2016.

Whitlock, C. and Larsen, C.: Charcoal as a Fire Proxi. In: Smol J.P., Birks H.J.B., Last W.M., Bradley R.S., Alverson K. (eds) Tracking Environmental Change Using Lake Sediments. Developments in Paleoenvironmental Research, vol 3., 5, 75–97, https://doi.org/10.1007/0-306-47668-1, 2001.

Zanon, M., Davis, B. A. S., Marquer, L., Brewer, S., and Kaplan, J. O.: European forest cover during the past 12,000 years: A palynological reconstruction based on modern analogs and remote sensing, Front Plant Sci, 9, 1–25, https://doi.org/10.3389/fpls.2018.00253, 2018.